2014 RCBJSF FM&NT
SEPTEMBER 29 - OCTOBER 2
RIGA • LATVIA

Joint 12th Russia/CIS/Baltic/Japan Symposium on Ferroelectricity

and 9th International Conference Functional Materials and Nanotechnologies

Institute of Solid State Physics,
University of Latvia
September 29 – October 2
Riga, 2014

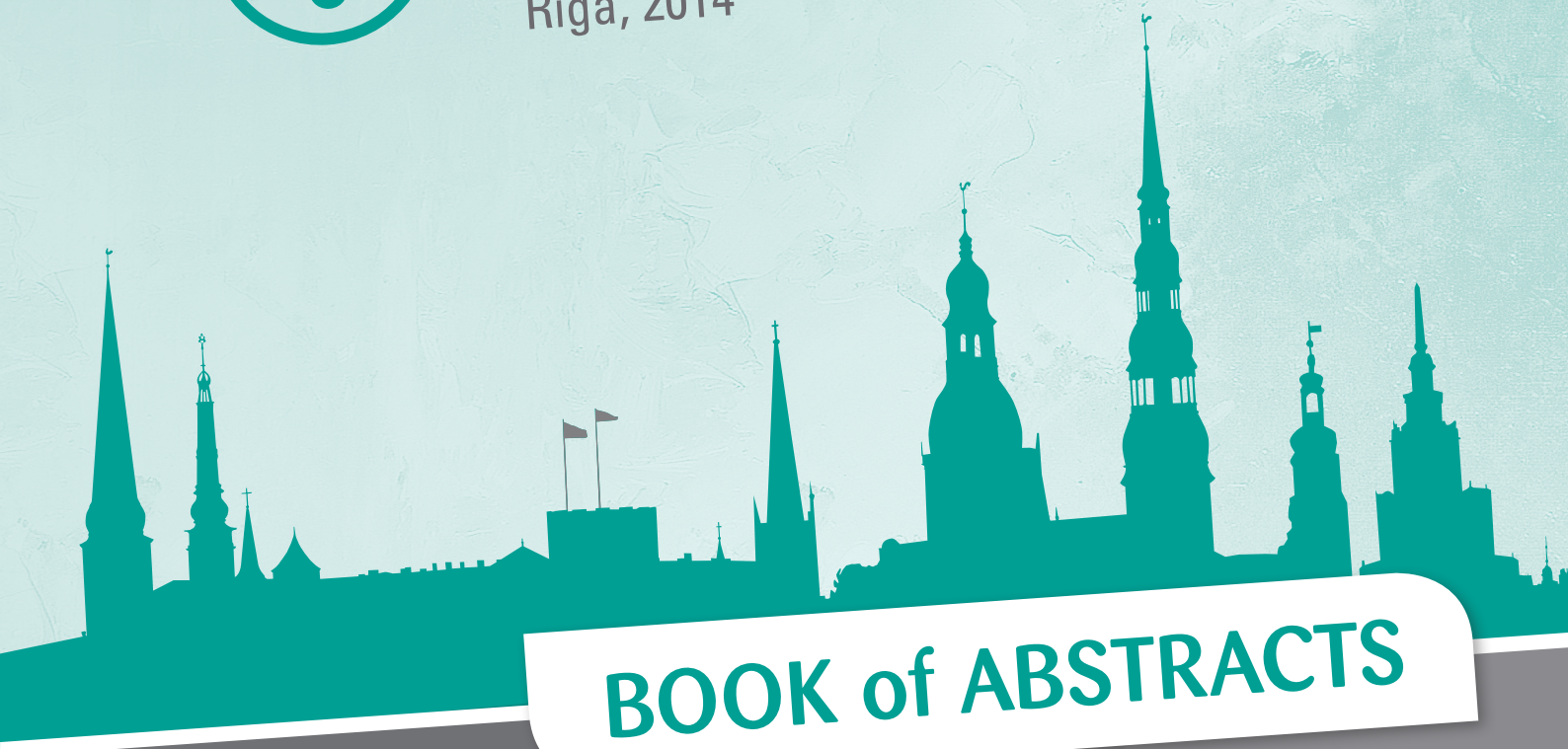

BOOK of ABSTRACTS

Edited by: Andris Sternbergs (ISSP UL), Liga Grinberga (ISSP UL)
Typesetting: Jurgis Grube (ISSP UL), Anatolijs Sarakovskis (ISSP UL)
Cover Design: Ainars Gromskis
ISBN: 978-9984-45-875-5
Institute of Solid State Physics, University of Latvia
8 Kengaraga Street, LV-1063, Riga, Latvia
Phone: +371-67187816
Fax: +371-67132778
e-mail: issp@cfi.lu.lv
web: http://www.cfi.lu.lv
Riga, 2014

Welcome Message to **RCBJSF–2014–FM&NT** Participants

Welcome to Latvia, welcome to Riga, the European Capital of culture in 2014!

It is my great pleasure to welcome you at the Joint International **RCBJSF–2014–FM&NT** Symposium combining 12th Russia/CIS/Baltic/Japan Symposium on Ferroelectricity (**RCBJSF-12**) and 9th annual International Conference Functional Materials and Nanotechnologies (**FM&NT**).

The **RCBJSF-12** symposium is a continuation of series of meetings on ferroelectricity, first of which took place in Novosibirsk (USSR) in 1976. **FM&NT** Conferences since 2006 has been organized by Institute of Solid State Physics, University of Latvia in Riga. Nevertheless the FM&NT–2013 was held in the Dorpat conference centre in Tartu, organized by the Institute of Physics, University of Tartu. In this year the joint international symposium **RCBJSF–2014–FM&NT** is organized as an event of Riga – 2014, the European Capital of culture.

Advanced materials, being central to the economic growth, prosperity and quality of life of humans, are general topic that thematically joins both meetings – **RCBJSF** and **FM&NT**. Materials science is an enabling technology, forming a bridge between basic science and applied engineering. It ranges from understanding and controlling atoms in materials to making numerous innovative products, devices and services. Ferroelectrics, e.g. perovskite-type oxides exhibiting a broad variable spectrum of structural, electronic and magnetic properties are on large scale multifunctional materials. These and other actual topics will be discussed within the frames of work program.

The purpose of the Symposium is to bring together materials scientists, physicists, chemists, research staff, engineers, as well as experts in of a wide range of the most demanding application areas. We anticipate having high scientific quality presentations at the Symposium: 5 plenary talks, 42 invited talks, 82 oral presentations and over 200 posters. The Symposium will also provide a platform for the future collaboration promoting interdisciplinary research.

The **RCBJSF–2014–FM&NT** symposium will take place in the new National Library of Latvia building. The pyramidal structure which rises 68 meters high on the Daugava riverbank opposite the historic city centre has been the most significant investment in cultural infrastructure since the establishment of the Latvian State and is one of the largest cultural buildings in Northern Europe in the 21st century. On 29 August 2014, which is the 95th -anniversary of the National Library, the building was officially opened for public access.

I wish to thank International Organizing and Program Committees, as well as Local Committee members for hard work preparing the joint international symposium **RCBJSF–2014–FM&NT.**

I am looking forward to welcome and see you in Riga!

Andris Sternberg,
Chairman of **RCBJSF–2014–FM&NT**
Institute of Solid State Physics, University of Latvia, Riga, Latvia

Scientific Topics of the Symposium

Ferroelectricity:

Ferroelectrics and multiferroics, pyroelectrics, piezoelectrics and actuators, integrated ferroelectrics, relaxors, phase transitions and critical phenomena

Multifunctional Materials:

Theory, multiscale and multiphenomenal material modeling and simulation, advanced inorganic, organic and hybrid materials

Nanotechnologies:

Progressive methods, technologies and design for production, investigation of nano - particles, composites, structures, thin films and coatings

Energy:

Perspective materials and technologies for renewable and hydrogen energy, fuel cells, photovoltaics, LEDs, OLEDs

List of Previous Events

RCBJSF

1.	Novosibirsk (USSR)	1976
2.	Kyoto (Japan)	1980
3.	Novosibirsk (USSR)	1984
4.	Tsukuba (Japan)	1988
5.	Moscow (Russia)	1994
6.	Noda (Japan)	1998
7.	St. Petersburg (Russia)	2002
8.	Tsukuba (Japan)	2006
9.	Vilnius (Lithuania)	2008
10.	Yokohama (Japan)	2010
11.	Ekaterinburg (Russia)	2012

FM&NT

1.	Riga (Latvia)	2006
2.	Riga (Latvia)	2007
3.	Riga (Latvia)	2008
4.	Riga (Latvia)	2009
5.	Riga (Latvia)	2010
6.	Riga (Latvia)	2011
7.	Riga (Latvia)	2012
8.	Tartu (Estonia)	2013

Joint International Symposium RCBJSF – 2014 - FM&NT

Symposium Chairman: Dr.habil.phys. Andris Sternberg

RCBJSF Organizing Committee

- J. Kobayashi (Honorary chairmen), Japan
- Y. Ishibashi (Honorary chairmen), Japan
- B.A. Strukov (Honorary chairmen), Russia
- J. Grigas (Honorary chairmen), Lithuania
- Y. Akishige (Chairmen), Japan
- S. Kojima (Vice-chairmen), Japan
- A.S. Sigov (Vice-chairmen), Russia
- J. Banys (Vice-chairmen), Lithuania
- N. Ikeda, Japan
- M. Itoh, Japan
- M. Iwata, Japan
- S. Mori, Japan
- M. Shimizu, Japan
- H. Suzuki, Japan
- S. Wada, Japan
- E. Birks, Latvia
- V. Samulionis, Lithuania
- V.M. Fridkin, Russia
- S.G. Lushnikov, Russia
- V.Ya. Shur, Russia
- A.S. Sidorkin, Russia
- O.G. Vendik, Russia
- Yu.M. Vysochanskii, Ukraine

FM&NT Organizing Committee

- M. Rutkis (Chairman), Latvia
- J. Banys, Lithuania
- G. Borstel, Germany
- N.E. Christensen, Denmark
- R.A. Evarestov, Russia
- C.G. Granqvist, Sweden
- D. Hovik, Norway
- M. Kirm, Estonia
- E. Nommiste, Estonia
- J. Kulda, France
- W. Lojkowski, Poland
- I. Thorbjornsson, Iceland

RCBJSF Program Committee

- N. Ikeda (Chairmen), Japan
- E. Kotomin (Chairmen), Latvia
- J. Kano, Japan
- H. Mashiyama, Japan
- S. Mori, Japan
- K. Ohwada, Japan
- M. Takesada, Japan
- H. Taniguchi, Japan
- S. Tsukada, Japan
- R. Wang, Japan
- H. Yokota, Japan
- E. Klotins, Latvia
- R. Grigalaitis, Lithuania
- E. Tornau, Lithuania
- I.N. Flerov, Russia
- S.A. Gridnev, Russia
- V.P. Sakhnenko, Russia
- S. Vakhrushev, Russia
- T.R. Volk, Russia
- V.I. Zinenko, Russia
- M.D. Glinchuk, Ukraine
- R. Vlokh, Ukraine

FM&NT Program Committee

- A. Sarakovskis (Chairman), Latvia
- L. Berzina-Cimdina, Latvia
- J. Grabis, Latvia
- L. Grinberga, Latvia
- E. Kotomin, Latvia
- L. Skuja, Latvia
- M. Springis, Latvia
- J. Zicans, Latvia

Local Committee

Liga Grinberga (Chairlady), Anatolijs Sarakovskis, Jurgis Grube, Maris Kundzins, Raitis Siatkovskis, Andris Sivars, Anastasija Jozepa, Anna Grube, Liga Klebaha.

The Organizing Committee sincerely hopes that the symposium will give all the participants new insights into the wide spread development of functional materials and nanotechnologies and will enhance the circulation of information released at the meeting.

Thank you all for coming and we wish you the most successful and enjoyable event!

Useful Contact phones

Symposium Chairman: Dr.habil.phys. Andris Sternberg (mobile)	+371 26183061
Secretary of Organizing Committee (mobile)	+371 27038016
Hotels:	
Radisson Blu Daugava Hotel	+371 67061111
Maritim Park Hotel	+371 67069000
Hanza Hotel	+371 67796040
Taxi:	
BalticTAXI	+371 20008500

Organizers:

Publishers:

Sponsors and Exhibitors:

RCBJSF–2014–FM&NT Program

September 29	
16:00	Registration
17:00 18:30	Excursion to the top of LNB Welcome party

Colour legend RCBJSF-12
Theory and modelling
New materials, thin films and nanostructures
Bulk materials: crystals and ceramics
Characterisation of materials

Colour legend FM&NT-2014
Theory and modelling
Nanomaterials and nanostructures
Multifunctional materials and technologies
Energy

September 30				
Ziedoņa hall				
8:00	Registration			
9:00	Opening			
9:50	Technical information/ Conference photo			
Coffee break 10:20 - 10:50				
10:50	Introductory talk - O. Spārītis, Latvian Academy of Sciences			
11:10	Itoh			
11:50	Sigov			
Lunch 12:30 - 13:40				
Conference halls, -1 floor				
	RCBJSF-12		FM&NT-2014	
	Hall 1	Hall 2	Hall 3	Hall 4
13:40	Banys	Fridkin	Spohr	Brik
14:10	Tornau	Kholkin	Merkle	Fuks
14:40	Ishibashi	Takesada	Kotomin	Krack
14:55	Moriwake		Yaremchenko	
15:10	Mamedov	Rybyanets	Macías	Bjoerheim
15:25	Zhukovskii	Glinchuk	Niklasson	Bandura
Coffee break 15:40 - 16:10				
16:10	Tsujimi	Shur	Schwartz	Evarestov
16:40	Roleder	Lushnikov	Chang	Galdikas
16:55			Pishtshev	
17:10	Tsukada	Ehara	Kuzmin	Shunin
17:25	Burkovsky	Yashchyshyn	Shalapska	Porsev
17:40	Chezganov	Delimova	Smits	Høvik
Refreshments 18:00 - 18:30				
Poster session 18:30- 20:30				

October 1				
Conference halls, -1 floor				
8:00	Registration			
9:00	Technical information			
9:10	Purans			
9:50	Schweizer			
10:30	Laurila			
Coffee break 11:10 - 11:40				
	RCBJSF-12		FM&NT-2014	
	Hall 1	Hall 2	Hall 3	Hall 4
11:40	Flerov	Volk	Oberhofer	Bellucci
12:10	Suchaneck	Tanaka	Kulkova	Bianconi
12:40	Rappe	Kuroiwa	Krunks	Chen
12:55	Bussmann-Holder		Mere	
13:10	Bujakiewicz-Korońska	Kojima	Aquilanti	Plyushch
13:25	Politova		Eglitis	Dovbeshko
Lunch 13:40 - 14:50				
15:00 - 23:00 Excursion and conference dinner				

October 2			
Conference halls, -1 floor			
8:30	Registration		
	RCBJSF-12		FM&NT-2014
	Hall 1	Hall 2	Hall 3
9:00	Iwata	Kimura	Hermansson
9:30	Ikeda	Yoneda	Fursikov
9:45			Polyakov
10:00	Akishige	Vlokh	Vahtrus
10:15	Pryakhina		Erts
10:30	Krylov	Bondarev	Andzane
10:45	Samulionis	Vtyurin	Oras
11:00			Boiko
Coffee break 11:15 - 11:45			
11:45	Noguchi	Ogawa	Popova M.
12:15	Skaliukh	Taniguchi	Nihei
12:30	Molak		Azamat
12:45	Yokota	Li	Österlund
13:00	Nuzhnyy	Zhu	Kirchner
13:15	Macutkevic	Bagdzevičius	Mannsberger
Lunch 13:30 - 14:50			
14:50	Laguta	Tsuda	Rutkis
15:05	Grigalaitis		
15:20	Ivanov	Trepakov	Bogdanov
15:35	Ovchinnikov		Ozols
15:50	Starkov	Svirskas	Saldan
16:05	Popova E.	Anspoks	Vembris
Closing 16:30 - 17:00			
17:00 - 18:30 Farewell refreshments			

RCBJSF-12 Program

September 29	
16:00	Registration
17:00 18:30	Excursion to the top of LNB Welcome party

Colour legend
Theory and modelling
New materials, thin films and nanostructures
Bulk materials: Crystals and Ceramics
Characterisation of materials

Plenary - 40 min
Invited (Inv) - 30 min
Oral (Or) - 15 min

Ziedoņa hall, 0 floor
Conference hall, -1 floor

September 30			
Ziedoņa hall			
8:00	Registration		
9:00	Opening		
9:50	Technical information/ Conference photo		
Coffee break 10:20 - 10:50			
10:50	Introductory talk - O. Spārītis, Latvian Academy of Sciences		
11:10	Itoh		
11:50	Sigov		
Lunch 12:30 - 13:40			
Conference halls, -1 floor			
	Hall 1		Hall 2
13:40	Banys	13:40	Fridkin
14:10	Tornau	14:10	Kholkin
14:40	Ishibashi	14:40	Takesada
14:55	Moriwake		
15:10	Mamedov	15:10	Rybyanets
15:25	Zhukovskii	15:25	Glinchuk
Coffee break 15:40 - 16:10			
16:10	Tsujimi	16:10	Shur
16:40	Roleder	16:40	Lushnikov
17:10	Tsukada	17:10	Ehara
17:25	Burkovsky	17:25	Yashchyshyn
17:40	Chezganov	17:40	Delimova
Refreshments 18:00 - 18:30			
Poster session 18:30- 20:30			

October 1			
Conference halls, -1 floor			
8:00	Registration		
9:00	Technical information		
9:10	Purans		
9:50	Schweizer		
10:30	Laurila		
Coffee break 11:10 - 11:40			
	Hall 1		Hall 2
11:40	Flerov	11:40	Volk
12:10	Suchaneck	12:10	Tanaka
12:40	Rappe	12:40	Kuroiwa
12:55	Bussmann-Holder		
13:10	Bujakiewicz-Korońska	13:10	Kojima
13:25	Politova		
Lunch 13:40 - 14:50			
15:00 - 23:00 Excursion and conference dinner			

October 2			
Conference halls, -1 floor			
8:30	Registration		
	Hall 1		Hall 2
9:00	Iwata	9:00	Kimura
9:30	Ikeda	9:30	Yoneda
10:00	Akishige	10:00	Vlokh
10:15	Pryakhina		
10:30	Krylov	10:30	Bondarev
10:45	Samulionis	10:45	Vtyurin
Coffee break 11:15 - 11:45			
11:45	Noguchi	11:45	Ogawa
12:15	Skaliukh	12:15	Taniguchi
12:30	Molak		
12:45	Yokota	12:45	Li
13:00	Nuzhnyy	13:00	Zhu
13:15	Macutkevic	13:15	Bagdzevičius
Lunch 13:30 - 14:50			
14:50	Laguta	14:50	Tsuda
15:05	Grigalaitis		
15:20	Ivanov	15:20	Trepakov
15:35	Ovchinnikov		
15:50	Starkov	15:50	Svirskas
16:05	Popova E.	16:05	Anspoks
Closing 16:30 - 17:00			
17:00 - 18:30 Farewell refreshments			

RCBJSF-12 Plenary presentations (in alphabetic order)

Pl – 1	**M. Itoh**	Strategy for the New Ferroelectric Materials in Tetrahedral System
Pl – 3	**J. Purans**	Beyond the Quasiharmonic Approximation: Local Structure of Perovskites with Negative Thermal Expansion
Pl – 5	**A. Sigov**	Charge Transport Mechanisms in Ferroelectric Heterostructures

RCBJSF-12 Invited presentations (in alphabetic order)

In - 1	**J. Banys**	Cooperation of Latvian and Lithuanian Scientists in Studies of Ferroelectrics and Related Materials
In - 2	**I. Flerov**	Phase Transitions and Caloric Effects in Ferroics and Multiferroics
In - 3	**V. Fridkin**	Ferroelectricity and the Bulk Photovoltaic Effect at the Nanoscale
In - 4	**N. Ikeda**	Ferroelectric and Electronic Property of RFe_2O_4
In - 5	**M. Iwata**	Electric Field Effects in $Pb(Zn_{1/3}Nb_{2/3})O_3$-7%$PbTiO_3$ Solid Solutions
In - 6	**A. Kholkin**	Nanoscale Piezoelectricity due to Symmetry Breaking: an Atomic Force Microscopy Study
In - 7	**H. Kimura**	Neutron Diffraction Study of Magnetism and Ferroelectricity in RMn_2O_5 (R = rare-earth, Bi, Y) Multiferroics
In - 8	**S. Kojima**	Broadband Terahertz Time-Domain Spectroscopy of Ferroelectric Crystals
In - 9	**Y. Kuroiwa**	Valence Electron Distributions of Ferroactive Ions in Perovskite Oxides and Polar Lattice Distortions
In - 10	**S. Lushnikov**	Central Peak and Quasi-Elastic Light Scatering in Cubic Relaxor Ferroelectrics
In - 11	**Y. Noguchi**	Defect-Polarization Control for Enhancing Piezoelectric Properties of $BaTiO_3$-Based Single Crystals and Ceramics
In - 12	**T. Ogawa**	Evaluation of Elastic Constants in Piezoelectric Ceramics by Measuring Acoustic Wave Velocities
In - 13	**K. Roleder**	Do We Understand Why Antiferroelectric Order is Realized in $PbZrO_3$ and $PbHfO_3$?
In - 14	**V. Shur**	Domain Shape Instabilities and Fractal Domain Growth in Uniaxial Ferroelectrics in Highly Non-equilibrium Switching Conditions
In - 15	**G. Suchaneck**	Materials and Device Concepts for Electrocaloric Refrigeration
In - 16	**M. Takesada**	Broadband Light Scattering and Second Harmonic Generation in Ferroelectric Nanocrystals
In - 17	**H. Tanaka**	Valence Electron Density and Electrostatic Potential in Ferroelectric Materials Evaluated by MEM Analysis of X-ray Diffraction

In - 18	**H. Taniguchi**	Ferroelectricity Driven by Twisting of Silicate Tetrahedral Chains
In - 19	**E. Tornau**	Phase Transitions in Antiferromagnetic Triangular Blume-Capel Model with Hard Core Exclusions
In - 20	**V. Trepakov**	Electronic Structure, Optical and Dielectric Spectroscopy of $TbMnO_3$ Multiferroic
In - 21	**K. Tsuda**	Study of Nanoscale Local Structural Fluctuations in Ferroelectrics Using Convergent-Beam Electron Diffraction
In - 22	**Y. Tsujimi**	Broad Doublet Spectra in the Quantum Paraelectric State of $SrTiO_3$
In - 23	**R. Vlokh**	Generation of Optical Vortices via Electro- and Piezo-Optic Effects in Ferroelectric-Type Crystalline Materials
In - 24	**T. Volk**	Planar Microdomain Patterns for Nonlinear-Optical Applications Fabricated in Ferroelectric Crystals by Microscopic Methods (AFM and SEM).
In - 25	**Y. Yoneda**	Atomic Pair-Distribution Function (PDF) Analysis on Ferroelectric Materials Using Synchrotron X-ray

RCBJSF-12 Oral presentations (in alphabetic order)

Or - 1	**Y. Akishige**	Dielectric Properties and Phase Diagram of $(Sr_{1-x}Ba_x)_2Nb_2O_7$ Single Crystals
Or - 2	**A. Anspoks**	Local Structure Studies of Ti for $SrTi^{16}O_3$ and $SrTi^{18}O_3$ by Advanced X-ray Absorption Spectroscopy Data Analysis
Or - 3	**Š. Bagdzevičius**	Structural and Electrical Characterization of Epitaxially Strained $Ba_{0.7}Sr_{0.3}TiO_3$ Thin Films Deposited by PLD
Or - 4	**V. Bondarev**	Cooling Method Based on Electrocaloric Effect Realized in Periodically Switching Electric Field in Triglycinesulphate
Or - 5	**R. Bujakiewicz-Korońska**	Searching of New Multiferroics on the Base of Co-Doped $BaTiO_3$
Or - 6	**R. Burkovsky**	Lattice Dynamics and Incommensurate Phase in $PbHfO_3$
Or - 7	**A. Bussmann-Holder**	Revisiting the Fascinating Properties of $EuTiO_3$ and Its Mixed Crystals with $SrTiO_3$: Possible Candidates for Novel Functionalities and Multiferroicity
Or - 8	**D.V. Chezganov**	Temperature Dependence of Isolated Domain Shape in Lithium Tantalate Single Crystals
Or - 9	**L. Delimova**	Electrophysical Properties of Integrated Ferroelectric Capacitors Based on Sol-gel PZT Films
Or - 10	**Y. Ehara**	True Operational Range of Lead-Free and Lead-Based Piezoelectric Actuators
Or - 11	**M.D. Glinchuk**	New Room Temperature Multiferroics on the Base of Single-Phase Nanograined Ceramics with Perovskite Structure

Or - 12	**R. Grigalaitis**	Dielectric Properties of Barium Titanate and Nickel-Zinc Ferrite Multiferroic Composites
Or - 13	**Y. Ishibashi**	On the Conical Point Crossing
Or - 14	**M. Ivanov**	Dielectric Properties of $BaTiO_3$-$KNbO_3$ Composites
Or - 15	**A. Krylov**	Temperature Phase Transitions in $CsScF_4$ Crystal
Or - 16	**V.V. Laguta**	Multiferroicity and Superparamagnetism in the New Magnetoelectric $Pb(Fe_{1/2}Sb_{1/2})O_3$
Or - 17	**D. Li**	Research on Electromagnetic Interference Resistance of Piezoelectric Vibration Acceleration Sensor with Printed Circuit Board
Or - 18	**J. Macutkevic**	Dielectric Properties of $AgLiNbO_3$
Or - 19	**A. Mamedov**	Optical Properties of the Narrow-Band Ferroelectrics: First Principle Calculations
Or - 20	**A. Molak**	Electric Current Relaxation and Resistance Switching in Non-Homogeneous Bismuth Manganite
Or - 21	**H. Moriwake**	First-principles Calculations of Ferroelectricity in Wurtzite Structured Simple Chalcogenides
Or - 22	**D. Nuzhnyy**	Porous $Pb(Mg_{1/3}Nb_{2/3})O_3$ Ceramics: Experiment, Modelling and Simulation
Or - 23	**S. Ovchinnikov**	Giant Lattice Expansion in $GdCoO_3$ due to the Multiplicity Fluctuation Contributions
Or - 24	**E.D. Politova**	New Multiferroic Oxides with Corundum-Related Structure
Or - 25	**E. Popova**	Ferroelectricity in Minerals
Or - 26	**V.I. Pryakhina**	Formation of Charged Domain Walls in Lithium Niobate Crystals with Inhomogeneous Bulk Conductivity
Or - 27	**A. Rappe**	Ferroelectric Oxides for Visible-Light Photovoltaics and Engineering of Shift Current
Or - 28	**A. Rybyanets**	Nanoparticles Transport in Ceramic Matrices
Or - 29	**V. Samulionis**	Ultrasonic Studies of Piezoelectric Response in Ferroelectric; Crystals of $Sn_2P_2P_6$ Family
Or - 30	**A. Skaliukh**	The Construction of Domains Density Distribution in the Simulation of Process Polarization in the Ceramics
Or - 31	**A. Starkov**	Giant Piezocaloric Effect in PZT Ceramics
Or - 32	**Š. Svirskas**	Dielectric, IR and Raman Spectroscopies of $(0.4\text{-}y)Na_{0.5}Bi_{0.5}TiO_3$-$0.6SrTiO_3$-$yPbTiO_3$ Solid Solutions
Or - 33	**S. Tsukada**	Critical Points in KF-Substituted $BaTiO_3$
Or - 34	**A. Vtyurin**	Structural and Magnetic Phase Transitions in Rear Earth Ferroborate Crystals – Raman Scattering Study

Or - 35	**Y. Yashchyshyn**	Prospects of Ferroelectric Ceramic-Polymer Composites in Sub-Terahertz Applications
Or - 36	**H. Yokota**	The Evidence of Monoclinic Structure on Zr-Rich $PbZr_{1-x}Ti_xO_3$
Or - 37	**X. Zhu**	Characterization of Extruded Ferroelectric Film P(VDF-TrFE)
Or - 38	**Y. Zhukovskii**	First Principles Simulations on Stoichiometric $SrTiO_3$ Nanowires

RCBJSF-12 Poster presentations

Theory and Modelling		
R-1	**A. Soloviev**	Modeling of Piezoelectric Elements with Inhomogeneous Polarization in ACELAN
R-2	**E. Petrova**	A Novel Approach for Optimization of Finite Element Models of Lossy Piezoelectric Elements
R-3	**J. Timoshenko**	Local Structure of Multiferroic $Mn_{1-c}Co_cWO_4$ Solid Solutions Revealed by the Evolutionary Algorithm
R-4	**A. Mamedov**	Dynamic Nonlinear Optical Processes in Some Oxygen-Octahedra Ferroelectrics: First Principle Calculations
R-5	**R.I. Eglitis**	First Principles Calculations of the Diffusion and Aggregation of F Centers, as Well as Bulk and Nano-Surface H Centers in CaF_2, BaF_2 and SrF_2
R-6	**R.I. Eglitis**	First Principles Calculations of $SrTiO_3$, $BaTiO_3$, $PbTiO_3$ and $CaTiO_3$ (001), (011) and (111) Surfaces
R-7	**P. Konsin**	Semi-Microscopic Vibronic Theory of the Properties of Quantum Paraelectrics and Ferroelectrics of $SrTiO_3$-type
New materials, thin films and nanostructures		
R-8	**A. Rybyanets**	New Piezoelectric Materials and Transducer Designs for Energy Harvesting Devices
R-9	**R. Grechishkin**	Surface Relief And Domain Structure Of Ferromagnetic Shape Memory Alloys
R-10	**N. Hasegawa**	Dielectric Behavior in A-site Ordered Perovskite $CaCu_3Ti_4O_{12}$: Effect of A'-site Doping
R-11	**E. Mikhaleva**	Multicaloric Efficiency of Ferroelectric-Ferromagnetic Volume Composites $(x)La_{0.7}Pb_{0.3}MnO_3$-$(1-x)PbTiO_3$
R-12	**I. Bochkov**	The Nickel and Cobalt Ferrite Nanopowders and it Composites with Polycarbonate
R-13	**R. Mackeviciute**	Dielectric Properties of Diammonium Hypodiphosphate $(NH_4)_2H_2P_2O_6$
R-14	**E. Pawlikowska**	Influence of Powder Milling on Properties of Barium Strontium Titanate Particles and the Ferroelectric Ceramic-Polymer Composites
R-15	**A. Naumenko**	Losses and Dispersion in Ceramic Matrix Composites
R-16	**A. Sigov**	Porous PZT Films Prepared by PVP Assisted Sol-gel Process
R-17	**S. Aplesnin**	Magnetodielectric Properties of $Bi_{1-x}La_xFeO_3$ Films
R-18	**D. Jablonskas**	Microwave Dielectric Measurements of Mn-Doped Perovskite-Type $SrTiO_3$ Nanopowders

R-19	**A. Popov**	Effects of Long Term Annealing on the Nanostructures Formed in CdI_2 Crystals

Characterisation of materials

R-20	**A. Popov**	Cathodoluminescence Characterization of Polystyrene–$BaZrO_3$ Hybrid Composites
R-21	**A. Badalyan**	An Observation of Nano Sized Effect on EPR of Mn^{4+} and Cr^{3+} in $SrTiO_3$ Powders
R-22	**W. Zapart**	Phase Transitions in Li-Doped $KSc(MoO_4)_2$
R-23	**S. Tsuge**	X-ray Diffraction Intensity Influenced by Transverse Electric Field in TGS
R-24	**M.B. Zapart**	Optical Studies and Birefringence of $K_{1-x}Rb_xSc\ (MoO_4)_2$
R-25	**A. Ivanova**	Optical Anisotropy and Domain Structure of Multiferroic Ni-Mn Based Heusler Alloys
R-26	**M. Fukunaga**	Dielectric Behavior of Monoclinic $Rb(H_{0.7}D_{0.3})_2PO_4$ Under Constant Hydrostatic Pressure
R-27	**S.N. Kallaev**	Thermal Diffusion and Heat Conductivity of $BiFeO_3$ and $Bi_{0.95}La_{0.05}FeO_3$ Multiferroics at High Temperatures
R-28	**I. Sluchinskaya**	Local Structure and Oxidation State of 3d Impurities in Cubic $(Ba,Sr)TiO_3$
R-29	**M. Antonova**	Photoelectric Current and Dielectric Properties of Barium-Strontium Niobate Ceramics under UV and Visible Irradiation
R-30	**M. Antonova**	Preparation and Electric Properties of Barium Zirconium Titanate Ceramics
R-31	**K. Godziszewski**	Characterization of Ferroelectric Ceramic-Polymer Composites in Sub-Terahertz Frequency Range
R-32	**M. Livinsh**	Electrical Characterization of Fe Doped $BaTiO_3$ Ceramic by Impedance Spectroscopy
R-33	**B. Garbarz-Glos**	AC Impedance Spectroscopy Study of Barium Titanate Based Electroceramics
R-34	**D. Sitko**	Study of Dielectric Properties of Europium Doped Barium Titanate Ceramics by Impedance Spectroscopy
R-35	**S. Ilyashenko**	Heat Losses and Thermal Imaging of Piezoelectric Elements
R-36	**M. Dunce**	Interpretation of the Electrocaloric Effect in NBT-ST-PT Solid Solutions

Bulk materials: Crystals and Ceramics

R-37	**A. Akhmatkhanov**	Polarization Reversal and Domain Kinetics in MgO Doped Congruent and Stoichiometric Lithium Tantalate Crystals
R-38	**A. Akhmatkhanov**	Time-Dependent Conductivity and Dielectric Permittivity in Lithium Niobate Crystals with Charged Domain Walls

R-39	**E. Dul'kin**	Relaxor Behavior of the Surface Layer of $BaTiO_3$ Crystals, Grown by Remeika Method
R-40	**M.A. Helal**	Critical Slowing Down and Elastic Anomaly in Relaxor-Based Ferroelectric PMN-53PT Crystals Proved by Broadband Brillouin Scattering
R-41	**V. Lisitsin**	The Pyroelectric Properties of Calcium Barium Niobate Crystals of Different Composition
R-42	**E. Palaimiene**	Conductivity Investigations of PMT-PT Single Crystals
R-43	**S. Pavlov**	Phenomenological Model of Phase Transitions in $[N(C_2H_5)_4]_2MnCl_4$ Crystals
R-44	**N.V. Sidorov**	Raman Studies of Stoichiometric and Congruent Lithium Niobate Crystals at Temperatures Within the 100 - 450 K Range
R-45	**N.V. Sidorov**	Structural and Optical Homogeneity in Lithium Niobate Crystals of Low Photorefractivity
R-46	**D.S. Petukhova**	As-Grown Domain Structure of β-glycine Single Crystal
R-47	**P.S. Zelenovskiy**	In Situ Observation of Polymorphic Phase Transformation in Glycine Crystal
R-48	**M.N. Palatnikov**	Electrical Properties of Congruent $LiTaO_3$ Single Crystals
R-49	**M.N. Palatnikov**	Synthesis, Structure, Electrical and Mechanical Characteristics of Ceramic $Nb_{2(1-y)}Ta_{2y}O_5$
R-50	**K. Bormanis**	Thermal Properties of Relaxor $PbNi_{1/3}Nb_{2/3}O_3$ Solid Solution Ceramics
R-51	**K. Bormanis**	The Slow Relaxation of Polarization in $(K_{0,5}Na_{0,5})(Nb_{1-x}Sb_x)O_3$+0,5mol%$MnO_2$ Ferroelectric Ceramics
R-52	**A. Kalvane**	Electronic Properties of Hexagonal $SrMnO_3$ Ceramic
R-53	**D. Karpinski**	Phase Coexistence in $Bi_{1-x}Pr_xFeO_3$ Ceramics
R-54	**A.H. Segalla**	Development of Ceramics for High Temperature Applications
R-55	**J. Suchanicz**	Influence of Compressive Stress and Aging on Dielectric Properties of $BiFeO_3$ Ceramics
R-56	**W. Bąk**	Dielectric Behaviour of $(Ba_{1-x}Na_x)(Ti_{1-x}Nb_x)O_3$ Ceramics Obtained by Conventional and Mechanochemical Synthesis
R-57	**D. Gabrielaitis**	Dielectric Relaxation Processes in $Ba_2NdFeNb_4O_{15}$ and $Ba_2EuFeNb_4O_{15}$ Ceramics
R-58	**M.S. Shashkov**	Dielectric Properties of Cromium-Containing Bismuth Titanate Ceramics with the Layered Perovskite Type Structure
R-59	**O. Malyshkina**	Effect of Bismuth Oxide Dispersivity on the Dielectric Properties of Zinc Oxide Ceramics
R-60	**E.V. Barabanova**	Pore Effect on the Switching Processes in PZT Ceramics

R-61	**M. Lugovaya**	Porous Piezoelectric Ceramics: Complex Representation of Material Properties
R-62	**W. Smiga**	Mechanical and Electrical Properties of Li Doped Sodium Niobate Ceramic System
R-63	**V. Dimza**	Aging and Memory Effects in Electro-Optical PLZT 8/65/35 Ceramics Modified with 3d Transition-Metal Ions
R-64	**E.I. Gerzanych**	p,T,x – Diagram Ferrielectric Crystals $CuInP_2(Se_xS_{1-x})_6$ in the Range $0 \leq x \leq 1.0$
R-65	**A. Salnik**	Dynamics in Incommensurate Phase Transition in C and 2C Polytypes of $TlInS_2$ Ferroelectric
R-66	**A. Salnik**	On Photoinduced Phase Transition in Ferroelectric Ag_3AsS_3
R-67	**O.V. Shusta**	Investigation of $CuInP_2S_6$ Family Layered Crystals Under High Hydrostatic Pressure
R-68	**A.I. Susla**	The Influence of an External Electric Field and Uniaxial Pressure on the Dielectric Properties of Co- and Cu-Doped TGS Crystals
R-69	**Y. Vysochanskii**	Ab Initio Characterization of Pressure-Induced Metallic State in Ferroelectric $Sn_2P_2S_6$
R-70	**Y. Vysochanskii**	Tricritical Point and Virtual Ferroelectricity in $(Pb_ySn_{1-y})_2P_2S_6$

FM&NT-2014 program

September 29	
16:00	Registration
17:00 18:30	Excursion to the top of LNB Welcome party

Colour legend
Theory and modelling
Nanomaterials and nanostructures
Multifunctional materials and Technologies
Energy

Plenary - 40 min
Invited (Inv) - 30 min
Oral (Or) - 15 min

Ziedoņa hall, 0 floor
Conference hall, -1 floor

September 30			
Ziedoņa hall			
8:00	Registration		
9:00	Opening		
9:50	Technical information/ Conference photo		
Coffee break 10:20 - 10:50			
10:50	Introductory talk - O. Spārītis, Latvian Academy of Sciences		
11:10	Itoh		
11:50	Sigov		
Lunch 12:30 - 13:40			
Conference halls, -1 floor			
	Hall 3		Hall 4
13:40	Spohr	13:40	Brik
14:10	Merkle	14:10	Fuks
14:40	Kotomin	14:40	Krack
14:55	Yaremchenko		
15:10	Macías	15:10	Bjoerheim
15:25	Niklasson	15:25	Bandura
Coffee break 15:40 - 16:10			
16:10	Schwartz	16:10	Evarestov
16:40	Chang	16:40	Galdikas
16:55	Pishtshev		
17:10	Kuzmin	17:10	Shunin
17:25	Shalapska	17:25	Porsev
17:40	Smits	17:40	Høvik
Refreshments 18:00 - 18:30			
Poster session 18:30- 20:30			

October 1			
Conference halls, -1 floor			
8:00	Registration		
9:00	Technical information		
9:10	Purans		
9:50	Schweizer		
10:30	Laurila		
Coffee break 11:10 - 11:40			
	Hall 3		Hall 4
11:40	Oberhofer	11:40	Bellucci
12:10	Kulkova	12:10	Bianconi
12:40	Krunks	12:40	Chen
12:55	Mere		
13:10	Aquilanti	13:10	Plyushch
13:25	Eglitis	13:25	Dovbeshko
Lunch 13:40 - 14:50			
15:00 - 23:00 Excursion and conference dinner			

October 2	
Conference hall, -1 floor	
8:30	Registration
	Hall 3
9:00	Hermansson
9:30	Fursikov
9:45	Polyakov
10:00	Vahtrus
10:15	Erts
10:30	Andzane
10:45	Oras
11:00	Boiko
Coffee break 11:15 - 11:45	
11:45	Popova M.
12:15	Nihei
12:30	Azamat
12:45	Österlund
13:00	Kirchner
13:15	Mannsberger
Lunch 13:30 - 14:50	
14:50	Rutkis
15:20	Bogdanov
15:35	Ozols
15:50	Saldan
16:05	Vembris
Closing 16:30 - 17:00	
17:00 - 18:30 Farewell refreshments	

FM&NT-2014 Plenary presentations (in alphabetic order)

Pl – 2	**T. Laurila**	Hybrid Carbon Nanomaterials for Electrochemical Detection of Biomolecules
Pl – 4	**S. Schweizer**	Multi-functionality of Luminescent Glasses for Energy Applications

FM&NT-2014 Invited presentations (in alphabetic order)

In - 1	**S. Bellucci**	Heat Resistant Unfired Phosphate Ceramics with Carbon Nanotubes and Boron Compounds for Electromagnetic and Ionizing Shielding Applications
In - 2	**A. Bianconi**	Nanoscale Phase Separation in Two-dimensional Layers in the Limit of a Few Unit Cells Controlling Material Functionalities Unveiled by Scanning Submicron XRD
In - 3	**M. Brik**	A Review of The Structural, Electronic and Elastic Properties of Spinels
In - 4	**R. Chen**	Surface-controlled Transport Properties in 1D and 2D Nanocrystals
In - 5	**R. Evarestov**	Theoretical Study of Single- and Multi-Walled Nanotubes Rolled-up from Group IV Metal Disulfides
In - 6	**D. Fuks**	Controlling the Figure of Merit in TiNiSn Half-Heusler Alloy: DFT Study
In - 7	**A. Galdikas**	Diffusion Processes in Nanostructured Three-Way Automotive Powder Catalysts
In - 8	**K. Hermansson**	Ceria Chemistry at the Nano-scale
In - 9	**M. Krack**	Electronic Structure Simulation of Uranium Dioxide
In - 10	**S. Kulkova**	Influence of Interstitial Impurities on the Griffith work in Ti-based Alloys
In - 11	**R. Merkle**	Mixed Conducting Perovskites as Solid Oxide Fuel Cell Cathode Materials: Insight from Experiments and Theory
In - 12	**H. Oberhofer**	A Theoretical Description of Photo-Catalytic Water Splitting on Metal Decorated Oxide Surfaces
In - 13	**M. Popova**	Materials for Optical Quantum Memory
In - 14	**M. Rutkis**	Development of NLO Active Organic Molecular Glasses for Photonic Applications
In - 15	**K. Schwartz**	Irradiation Induced Nanostructures in LiF Crystals and Possible Applications
In - 16	**E. Spohr**	Simulation of Oxide Nanostructures for Energy Conversion

FM&NT-2014 Oral presentations (in alphabetic order)

Or - 1	**J. Andzane**	Fabrication of Bismuth Chalcogenide Nanoribbons by Catalyst-Free Solid-Vapor Technique
Or - 2	**G. Aquilanti**	In-operando XAFS Analysis of Li-sulfur Batteries
Or - 3	**D. Azamat**	Spin-Phonon Relaxation Processes of Transition Metal Ions in ZnO
Or - 4	**A. Bandura**	Phonon Spectra of Single-Walled TiO_2 Nanotubes
Or - 5	**T. Bjoerheim**	Defect Thermodynamics of $BaZrO_3$ from First Principles Phonon Calculations
Or - 6	**V. Bogdanov**	Water-Like Anomaly of Elastic Properties of Inorganic Glasses and Their Melts
Or - 7	**V. Boiko**	New Materials for Nanobiophotonics Based on Photonic Crystals
Or - 8	**L. Chang**	Nonpolar ZnO Epilayers and $ZnO/Zn_{1-x}Mg_xO$ Multiple Quantum Wells Grown on $LiGaO_2$ by Molecular Beam Epitaxy
Or - 9	**G. Dovbeshko**	Graphene Sheets Versus Carbon Nanotubes: Synthesis, Properties, Applications
Or - 10	**R. Eglitis**	Towards a Practical Rechargeable 5 V Li Ion Battery
Or - 11	**D. Erts**	Space Charge Limited Current in Bi_2S_3 Nanowires
Or - 12	**P. Fursikov**	Nanostructural Properties of Holmium Oxide Prepared by the Thermal Decomposition of Organic and Inorganic Precursors
Or - 13	**D. Høvik**	Impact of Nanotechnology on Green and Sustainable Growth: Micro- and Nanofibrillated Cellulose. A Nordic Case Study to the OECD
Or - 14	**M. Kirchner**	An Innovative EBL Writing Strategy for High Speed and Precision Lithography of Large Circle Arrays for Microfiltration and Photonics in Solar Cells
Or -15	**E.A. Kotomin**	Challenges in Energy Applications of Non-stoichiometric Complex Perovskites
Or - 16	**M. Krunks**	Transition Metal Doped Indium Sulfide Films by Chemical Spray Method
Or - 17	**A. Kuzmin**	High-pressure X-ray Absorption Spectroscopy Study of Tin Tungstates
Or - 18	**J. Macías**	Electrical Properties and Redox Stability of Nb-substituted $SrVO_3$ as Prospective SOFC Anode Material
Or - 19	**M. Mannsberger**	XPS Depth Profiling of Organic and Organic/Inorganic Multilayer Systems
Or - 20	**A. Mere**	Plasmonic Solar Cells by Low-Cost Chemical Spray Method
Or - 21	**H. Nihei**	Optimization of Optical Parameters for Qubit Operation in Photonic Crystals
Or - 22	**G. Niklasson**	Electrochemical Measurements of the Electronic Density of States

Or - 23	**S. Oras**	Manipulation of Nanoparticles With Different Morphology Inside a Scanning Electron Microscope
Or - 24	**L. Österlund**	Precise Tuning of the Photonic Band Gap Using Multilayered Inverse Opals
Or - 25	**A. Ozols**	Dark Relaxation of Holographic Gratings in Azobenzene and Chalcogenide Films
Or - 26	**A. Pishtshev**	Electronic and Optical Properties of Magnesium and Calcium Hydroxides: The role of Covalency and Many-Body Effects
Or - 27	**A. Plyushch**	Electromagnetics of Tannin-based Carbon Foams
Or - 28	**B. Polyakov**	Silver and Gold Nanodumbbells for Tribological Experiments
Or - 29	**V. Porsev**	First-Principles Calculations of V_2O_5 Nanotubes
Or - 30	**I. Saldan**	GaAs and $Ga_{1-x}Al_xAs$ Overlayer Formation on GaAs (111) Sbstrate Plane by Organometallic Vapor Phase Epitaxy
Or - 31	**T. Shalapska**	Luminescence, Energy Migration and Energy Transfer Processes in Gd_2SiO_5 and $(LuGd)_2SiO_5$ Single Crystals Doped with Ce^{3+}, Eu^{3+} and Tb^{3+} ions
Or - 32	**Y. Shunin**	Electromechanics and Electromagnetics of CNT- and Graphene-Based Nanoporous Materials: Interconnects and Nanosensoring
Or - 33	**K. Smits**	Praseodymium Luminescence in Zirconia Nanocrystals and Single Crystals
Or - 34	**M. Vahtrus**	Shape Restoration Effect And Enhanced Fracture Resistance of Ag/SiO_2 Core-Shell Nanowires
Or - 35	**A. Vembris**	Energy Levels of Glass Forming Low Molecular Weight Organic Compounds in Thin Amorphous Film
Or - 36	**A. Yaremchenko**	Phase Stability and Thermochemical Expansion of $Ba_{0.5}Sr_{0.5}Co_{0.8}Fe_{0.2}O_{3-\delta}$ Mixed-Conducting Ceramics Under Oxidizing Conditions

FM&NT-2014 Poster presentations

Theory and Modelling		
F-1	**T. Plank**	Technet_nano: The Cooperation Network of Clean Room Facilities in BSR
F-2	**A. Abuova**	Ab Initio Modelling of Ag Adsorption on the MnO_2- and LaO-terminated LMO[001] Surfaces
F-3	**A. Chesnokov**	Ab Initio Simulations on N and S Co-doped Titania Nanotubes for Photocatalytic Applications
F-4	**D. Zablotsky**	Numerical Simulation of Thermo-Magneto-Osmotic Flow of Ferrocolloid Through Ordered and Disordered Permeable Structures
F-5	**E. Trutnev**	The Consideration of Virial Corrections in the Diffusion Equations
F-6	**A. Usseinov**	Electronic Effects on Hydrogen-Adsorbed Surfaces of ZnO: First Principles Study
F-7	**D. Sergeyev**	Calculation of the Excess Current and the Pseudogap in Cuprate High-Temperature Superconductors by the Monte Carlo Method
F-8	**E. Shidlovskaya**	Theoretical Modeling of Nanodevices Using Embedded Molecular Cluster Method
F-9	**A. Platonenko**	Ab Initio Simulations on Frenkel Pairs of Radiation Defects in Corundum
F-10	**S. Lukyanov**	First-Principles Calculations of TiO_2-based Consolidated Single-Walled Nanotubes
F-11	**S. Kulkova**	The Peculiarities of Halogens Adsorption on A^3B^5(001) Surface
F-12	**E. Klotins**	Relativistic Time-resolved Approach for Phonon Assisted Interaction Between Electron and Intensive Radiation Field
F-13	**A. Gopejenko**	Ab Initio Calculations of Interactions between Y and O Impurity Atoms and Vacancies in bcc- and fcc-iron Lattices
F-14	**D. Bocharov**	R and M Mode Softness in Cubic ScF_3: Predictions From First Principles
F-15	**A. Bakulin**	Ab-Initio Study of Cation-rich InP(001) and GaP(001) Surface Reconstructions and Iodine Adsorption
F-16	**M. Wessel**	Quantum Chemical Investigations of Oxide Nanostructures for Energy Conversion in Aqueous Solution
Nanomaterials		
F-19	**B. Polyakov**	Plasmonic Photoluminescence Enhancement by Silver Nanowires
F-21	**A. Chodosovskaja**	Silver Nanoprisms Self-Assembly on Differently Functionalized Silica Surface
F-22	**E. Abkhalimov**	A New Preparation Method of Size Controllable Gold Nanoparticles Using Hydrogen

F-23	**D.W. Kim**	Self-Assembly of Gold Nanoparticles and Poly(diphenylamine): A Versatile Approach to One-Step Synthesis of Poly(diphenylamine) and Gold Nanoparticles
F-24	**S. Čornaja**	The Novel Au/TiO_2 and Au/CeO_2 Nanocomposites Synthesis. The Study of Their Physical Properties and Catalytic Activity
F-25	**J. Grabis**	Microwave Synthesis of Nanocomposites in ZnO-ZnO_2SnO_4/Ag System and Their Photocatalytic Activity
F-26	**T. Tamulevičius**	Layers of Two and Three Dimensional Metal Nanoparticle Assemblies for Plasmonic Sensor Applications
F-27	**J. Prikulis**	Polarization Effects in Layers Of Dense Short-Range Ordered Plasmonic Nanoparticles
F-28	**R. Poplausks**	Dense Arrays Of Nanometer Holes in Thin Metal Films on Anodized Aluminum Oxide Membranes
F-29	**V.I. Pryakhina**	Colloid of Metal Nanoparticles Produced by Laser Ablation in Liquid
F-30	**I. Oja Acik**	Ultra Thin TiO_2 Films with Gold Nanoparticles by the Chemical Spray Pyrolysis Method
F-31	**R. Drunka**	Microwave Assisted Synthesis and Photocatalytic Properties of Sulfur and Platinum Modified TiO_2 Nanofibers
F-32	**A. Knoks**	Synthesis and Photocatalytic Activity of TiO_2 Nanotubes
F-33	**D. Kuruch**	Water Adsorption on $SrTiO_3$ Single-Walled Nanotubes
F-34	**I. Zalite**	Hydrothermal Synthesis of Cobalt Ferrite Nanosized Powders
F-35	**I. Gromyko**	ZnO Nanorods Grown Electrochemically on Different Metal Oxide Underlays
F-36	**V. Teil**	Structure and Stability of WC Nanorods
F-37	**J. Kalnacs**	Graphene Nanosheets Grown on Ni Particles
F-38	**I. Reinholds**	Structure and Properties of Functionalized Carbon Nanotube/Polypropylene Composites
F-39	**U. Kanders**	Investigation of Hard Wear Resistant Nanostructured Carbonitride Coatings Based on Ti-(Nb,Hf)-C-N Quarternary System Deposited by DC Magnetron Sputtering
F-40	**U. Kanders**	Tribological and Mechanical Properties of Sputter Deposited Carbon-Copper Composite Films and their Structure
F-41	**R. Meija**	Humidity Induced Resistive Response Behavior of Bismuth Sulfide Nanowires
F-42	**V. Serga**	Synthesis and Properties of Magnetic Iron Oxide/platinum Nanocomposites
F-43	**I. Segal**	Magnetite Based Nanoparticles with Immobilized Heterocyclic Choline Derivatives as Potential Anti-Infective Agents
F-44	**L. Puķina**	Optical Forcing of Magnetostatic Patterns in Ferrofluid Layers

F-45	**A. Jarmola**	Enhancement of the Optical Signal from Nitrogen-vacancy Centers by Coupling to Surface Plasmons in Nanostructures
F-47	**F. Muktepavela**	Structure, Nanohardness and Photoluminiscence of ZnO Ceramics Based on Nanopowders
F-48	**A. Moskina**	Cathodoluminescence Studies of Nanostructured AlN and AlN/CsI
F-49	**A. Fomin**	Induction Heat Treatment and Technique of Nano-Bioceramic Coatings Production on Titanium
F-50	**J. Zicans**	Dielectric and Mechanical Relaxation in the Modified Carbon Nanofillers Containing Polyvinyl Alcohol Composites
F-51	**R. Merijs Meri**	Structure, Rheological and Mechanical Properties of Melt Compounded Polypropylene Nanocomposites
F-52	**J. Macutkevic**	Dielectric Properties of Graphene Like/Polyurethane Composites
F-53	**I. Kranauskaite**	Dielectric Properties of Composites with Carbon Nanotubes in PMMA Matrix
F-54	**S. Stepina**	Detecting VOC with Diferent Polymer-Nanostructured Carbon Composites
F-55	**A. Volperts**	Highly Porous Wood Based Carbon Materials for Supercapacitors
F-56	**M. Petrenec**	Nanostructure Characterization of Fatigued IN738LC Superalloy at Elevated Temperature
F-57	**O.I. Davarashvili**	Control of Thickness and Residual Deformation in Lead Selenide Nanolayers

Multifunctional materials and Technologies

F-58	**K. Shunkeyev**	Multifunctional Properties of KI Crystal at Lattice Symmetry Lowering by Low Temperature Elastic Stress
F-59	**K. Vanyukhin**	Sheet Resistance Parameter Optimization of Light Transmitting Welding Electrodes Made of Indium Tin Oxide
F-60	**K. Smits**	Comparative Studies of Alumina Coatings on Aluminum Prepared with Electrochemical and Plasma Electrolytic Oxidation Routes
F-61	**A. Mamedov**	SbSI Based Photonic Crystal Superlattices: Band Structure and Optics
F-62	**L. Maksimov**	Comparative Study of Nanoscaled Fluctuation Inhomogeneities in Main Glass Forming Oxides
F-63	**L. Maksimov**	Electrooptical Fibers
F-64	**M. Baitimirova**	Fabrication and Properties of Graphene/Bismuth Chalcogenide Layered Structures
F-65	**A. Gerbreders**	Optical Properties of the Low-Molecular Amorphous Azochromophores
F-66	**M. Reinfelde**	Kinetics of Diffraction Efficiency During the Holographic Recording of Surface Relief Gratings

F-67	**K. Klismeta**	Recording of Surface Relief in Azobenzene Containing Low Molecular Weight Organic Glasses
F-68	**E.A. Kotomin**	Analysis of Excitonic Mechanism of Defect Formation in Insulating Materials - Generalization of Rabin-Klick Diagram for a Whole Family of Alkali Halides
F-69	**R. Trukša**	Integrating Sphere Produced by 3D Printing and CNC Milling
F-70	**M. Manins**	Study of Performance of Hybrid Fiber (Hemp/Polypropylene/Glass) Woven Reinforcements
F-71	**E. Pentjuss**	Properties of Carbonized Na-Al-Si Glass Fiber Fabrics
F-72	**A. Lusis**	A Comparative Study of Natural Fiber and Glass Fiber Fabrics Properties with Metal or Oxide Coatings
F-73	**S. Vihodceva**	Durable Hydrophobic Sol-Gel Finishing for Textiles
F-74	**K. Ozols**	Mechanical Pressure Induced Capacitance Changes of Polyisoprene/Nanostructured Carbon Black Composite Samples
F-75	**G. Kaptagay**	Research of Interaction Fluorine-Doped Co_3O_4 (100) and (111) Surfaces with Water
F-76	**P. Rubin**	Insulator-Metal Transition in $FeAs_2$ Caused by Substitutions
F-77	**S. Zazubovich**	Low-Temperature Delayed Recombination in Y_2SiO_5:Ce and Lu_2SiO_5:Ce
F-78	**R. Zabels**	Depth Profiles of Indentation Hardness and Dislocation Mobility in MgO Single Crystals Irradiated with Swift Kr and N Ions
F-79	**L. Wang**	New Insights into Charge Transfer Transitions in $CdWO_4$: Covalency, Polarizability and Charge Effects on Energy Positions
F-80	**N. Mironova-Ulmane**	Template-Based Synthesis of Nickel Oxide
F-81	**A. Dindune**	Synthesis, Structure and Electrical Properties of $Li_{4x}Ti_{1-x}P_2O_7$ (x = 0; 0.1) Pyrophosphates
F-82	**E. Sproge**	Production of Glycolic Acid from Glycerol Using Novel Fine-Disperse Platinum Catalysts
F-83	**B.E. Park**	Fabrication and Electrical Characteristics of P(VDF-TrFE) Films on Si(100) Substrates using Cyanoethyl Pullulan Buffer Layers;
F-84	**G. Chikvaidze**	Method for Purifying Silicon Using Electron Beam Technology
F-85	**A. Brangule**	Importance of FTIR Spectra Deconvolution in Amorphous Calcium Phosphate Analysis
F-86	**J. Belovickis**	Ultrasonic Wave Propagation in PDMS with ZnO Nanoparticles
F-87	**A. Fedotovs**	Angular Dependence of Recombination Luminescence Detected EPR in ZnO Crystal
F-88	**A. Antuzevics**	EPR Spectra of ScF_3
F-89	**D. Jakovlevs**	Gallstones Studies by Raman, EPR and EDX Spectroscopes

F-90	**M. Oja**	EPR Spectroscopy of C3A
F-91	**M. Polakovs**	Determination of Methemoglobin in Human Blood After Ionising Radiation by EPR
F-92	**M. Baizhumanov**	Color Center Creation in LiF Irradiated with 12C and 130Xe MeV Ions: Dependence on Energy Loss and Absorbed Energy
F-93	**I. Jonane**	EXAFS Study of the Local Structure of Crystalline and Nanocrystalline Y_2O_3 Using Evolutionary Algorithm Method
F-94	**K. Lazdins**	Local Structure and Lattice Dynamics of Cubic Y_2O_3: an X-ray Absorption Spectroscopy Study
F-95	**A. Cintins**	ODS Steel Raw Material Local Structure Analysis Using X-ray Absorption Spectroscopy
F-96	**J. Gabrusenoks**	Vibrational Spectra of Tungsten Oxytetrachloride
F-97	**R. Grants**	Kinetic Properties of Grain Boundary with Ridges in Zn Bicrystal
F-98	**A. Kuzmin**	Preparation and Characterization of Tin Tungstate Thin Films
F-99	**P. Ščajev**	Electronic Properties of Polar and Nonpolar ZnO Films on $LiGaO_2$
F-100	**P. Ščajev**	Optical Properties of Polar and Nonpolar ZnO Thin Films Grown on $LiGaO_2$ Substrate
F-101	**V. Karitans**	Measuring the Brightness of the Retinal Reflex to Study the Accommodative Response of Stimuli with Various Spectral Distribution
F-102	**S. Fomins**	Adaption of Liquid Crystal Shutters for Infrared Binocular Eye Pupil Tracking
F-103	**M. Ozolinsh**	Smart Model Eye on Base of PDLC for Continued Stage Cataract Studies
F-104	**E. Butanovs**	HOPG Patterning Methods for Graphene Transferring onto the Substrate
F-105	**A. Dravniece**	Optimization of Deposition and Characterization of Graphene Oxide Monolayers and Films Obtained by Langmuir-Blodgett Technique
F-106	**V. Kampars**	Thermal Deoxygenation of Graphite Oxide at Low Temperature
F-107	**K. Pudzs**	TTT Thin Film Morphology and Electrical Properties
F-108	**V. Skvortsova**	Optical Properties of Natural and Synthetic Beryl Crystals
F-109	**M. Zubkins**	Optical and Structural Studies of Zn-Ir-O Thin Films Deposited by Reactive DC Magnetron Sputtering
F-110	**J. Grube**	Examining Temperature Influence on Er^{3+} Luminescence in $NaLaF_4$ Matrix
F-111	**A. Sarakovskis**	Influence of Different Crystal Field Environments on the Luminescence of $NaLaF_4$:Er^{3+}
F-112	**S.H. Kwon**	Synthesis and Luminescent Properties of Blue Emitting $CaAl_2Si_2O_8$:Eu^{2+} Phosphor

F-113	**A. Zolotarjovs**	Thermally Stimulated Luminescence of Undoped and Ce^{3+} Doped Gd_2SiO_5 and $(LuGd)_2SiO_5$ Single Crystals
F-114	**G. Yue**	Luminescent Properties of Tb^{3+}-Doped $SrLaMgTaO_6$ Phosphor for White Light-Emitting Diodes
F-115	**A. Trukhin**	Luminescence of Coesite
F-116	**D. Spassky**	Luminescence and Energy Transfer in $RE(Nb_xTa_{1-x})O_4$, RE = Y or Gd
F-117	**U. Rogulis**	Luminescence of Eu Ions in Oxyfluoride Glasses and Glass-Ceramics
F-118	**L. Grigorjeva**	Luminescence of Er/Yb Doped HAp-FAp Nanocrystals and Ceramics
F-119	**Y.W. Seo**	Synthesis and Photoluminescence Properties of $Sr_3Y(PO_4)_3$: Dy^{3+}
F-120	**V. Pankratov**	Excitation Luminescence Spectroscopy of Rare-Earth Doped $NaLaF_4$
F-121	**J.H. Oh**	Enhanced Up-Conversion Emission of Core-Shell Structured α-$NaYF_4$:Yb^{3+}/Er^{3+}@SiO_2
F-122	**E. Elsts**	Luminescence of Terbium Activated $NaLaF_4$ in Oxyfluoride Ceramics
F-123	**D. Millers**	Radioluminescence and Cathodoluminescence of TlCl:Bi Crystals
F-124	**B. Berzina**	AlN Based Composite - White Light Emitter
F-125	**K. Chernenko**	Photoluminescence Properties of Bi^{3+} Centers in Yttrium Oxide
F-126	**E.O. Kim**	Improved Optical Photoluminescence by Bi^{3+} Co-Doped in $CaMoO_4$:Eu^{3+}
F-127	**I. Kudryavtseva**	Luminescence of Complex Terbium Centres in $CaSO_4$
F-128	**T. Koketai**	Thermally Stimulated Luminescence of KPO_3-NO_3-doped Tl^+ Ions
F-129	**V. Levushkina**	Thermostimulated Luminescence (TSL) and Temperature Studies of the $Lu_xY_{1-x}PO_4$:Ce^{3+} Solid Solutions
F-130	**V. Korsaks**	Hexagonal Boron Nitride Luminescence Intensity Dependent on Ambient Vacuum Level
F-131	**R.R. Rosul**	The Study of the High-Pressure Phase of $TlInS_2$ Crystal

ENERGY

F-132	**An. Kravtsov**	Novel Method for Feedstock Production For High Efficiency FZ c-Si Photovoltaics
F-133	**Al. Kravtsov**	New Feedstock for c-Si Photovoltaics
F-134	**I. Kaulachs**	Sequentially Deposited Perovskite Solar Cell Employing $CH_3NH_3PbI_{(3-x)}Cl_x$ Light Absorber
F-135	**J. Kleperis**	Research on Controlled Porosity Composite Thin Layers and Systems for Energy Storage and Conversion Applications
F-136	**I. Dimanta**	Bacteria Produced Hydrogen Storage Possibilities in Metal Hydride Alloy

F-137	**I. Rundane**	Structural Studies of Graphite-Containing Divertor Materials by Raman Spectroscopy and by Quantum Chemical Calculations
F-138	**M. Halitovs**	Floor Tile Tritium Accumulation at Various JET Fusion Device Divertor Configurations
F-139	**L. Avotina**	Thermal Treatment of JET Carbon Dust Mixtures Containing Long-Chain Hydrocarbons
F-140	**I. Liepiņa**	Structure and Photocatalytic Properties of TiO_2-WO_3 Composites Prepared by Electrophoretic Deposition
F-141	**M. Vanags**	Yttrium Doped Hematite Nanograin Thin Films as Anode Material for Solar Water Splitting
F-142	**A. Zvyagintseva**	Possibility of the Doping of Electrochemical Systems with Deuterium
F-143	**O. Morozov**	Effects of Concentration Ti, Zr, V, Fe on Deuterium Desorption Temperature Range from Mg-based Composite
F-144	**I. Saldan**	Synthesis of $Mg(BH_4)_2$–TMO (TMO=TiO_2; ZrO_2; Nb_2O_5; MoO_3) Composites and Their Hydrogen Desorption
F-145	**K. Kaprans**	Electrophoretic Graphene Film Electrode for Lithium Ion Battery
F-146	**G. Kučinskis**	Deposition and In-Depth Electrochemical Analysis of $LiFePO_4$ Thin Films
F-147	**A. Ukshe**	Investigation of Electrochemical Noise in the Cells with Advanced Superionic
F-148	**P. Fursikov**	Experiment and Quantum Chemical Calculations in Studying the H Sorption Behavior of Nanostructured Composites and Light Metal Clusters
F-149	**P. Lesnicenoks**	Studies of Hydrogen Bonding to Graphitic Nanosheet Structures
F-150	**J. Hodakovska**	Composite Organic-Inorganic Membranes for Fuel Cells
F-151	**G. Vaivars**	SPEEK Polymer Composites with 1-butyl-2,3-dimethyl-imidazolium dimethylphosphate Ionic Liquids for Fuel Cell Membranes
F-152	**E. Sprugis**	Mechanical Properties and XRD of Composite SPEEK Polymer Membranes Modified by Acidic Ionic Liquids
F-153	**Q. Ying**	Function of Titanium Oxide Coated on Carbon Nanotubes as Support for Platinum Catalysts
F-154	**Q. Ying**	Investigation of Activities for Pt_3-M Bimetallic Nanoparticles Catalysts on the Oxygen Reduction Reaction
F-155	**Y. Dobrovolsky**	New Proton Conductors: the Calix(aren)sulfonic Acids

Labochema Company Group operating in the Baltic States for over 10 years is one of the biggest company groups in the Baltic States selling the top quality chemical reagents, consumables, laboratory equipment, furniture, and implementing individual laboratory installation projects. Labochema Company Group is offering a very large assortment of laboratory equipment, which consists of just world known and recognized company's products. We offer only high quality and reliable equipment for your laboratory as

TESCAN PERFORMANCE IN NANOSPACE  **scanning electron microscopes**	JPK Instruments  **atomic force microscopes**
ThermoFisher SCIENTIFIC  **microanalysis, electron microscopy and other analytical equipment**	Leica MICROSYSTEMS  **stereo/digital/light and confocal microscopes**
TA Instruments  **thermal analysis and thermophysical property measurement systems**	 LakeShore **probe stations, Hall Effect systems and electromagnets**
hielscher Ultrasound Technology  **ultrasonic homogenizers**	Mecmesin testing to perfection  **force and torque measuring systems**

Labochema Company Group - The reliable supplier for your laboratory in the Baltic States

Elpa Research Institute and Pilot Line JSC

Elpa Research Institute and Pilot Line JSC is one of the oldest Russian companies involved in the development and manufacturing of piezoelectric materials, piezoelectric elements, piezo technique products and acoustic electronics for electronic equipment, control systems and monitoring mechanisms and structures

COMPANY PROFILE - RESEARCH, DEVELOPMENT AND PRODUCTION OF:

- piezoelectric materials;
- piezoelectric elements;
- piezoelectric devices;
- acoustic electronic devices.

A number of new high-performance piezoelectric materials for the following applications was developed and produced:

- emitting and transceiver emitting hydroacoustic antenna;
- multi-layered and flexural piezo actuators;
- high temperature piezo actuators and vibration sensors.

In recent years, a family of high performance piezoelectric materials for general and specialized applications was developed: PZT-43, PZT-46, PZT-47, PZT-48, PZT-50, all of them exhibit high dielectric, piezoelectric, and elastic characteristics. A specialized piezoceramic material NPZT-2 having d_{33} = 800 pC/N , $\varepsilon_{33}^{T}/\varepsilon_0$ = 4600, T_C= 140 °C and exhibiting low sintering temperature was developed.

Unique piezoceramic material TCVC-2 with d_{33} = 340 pC/N, d_{15} = 520 pC/N was developed, its working temperature equals 320°C.

JSC Research Institute "Elpa" is the only Russian research and production company, owning piezoelectric film casting technology and having the full manufacturing cycle for multilayer piezoceramic actuators and sensors.

Contacts:
Address: Russia, 124460, Moscow, Zelenograd, Panfilovskiy prospect, b.10.
Phone: +7 499 710-13-10;
Fax: +7 499 710-13-02;
e-mail: ddd@elpapiezo.ru
internet: www.elpapiezo.ru

2014 RCBJSF FM&NT

SEPTEMBER 29 - OCTOBER 2

RIGA • LATVIA

INVITED SPEAKERS

Jūras **BANYS**

WORK EXPERIENCE

2012	Acting Rector of Vilnius University
2007	Vice Rector for research of Vilnius University
2003	Dean of the Physics Faculty, Vilnius University
2003	Professor, Department of Radiophysics, Faculty of Physics, Vilnius University
2000	Associated professor, Department of Radiophysics, Faculty of Physics, Vilnius University

EDUCATION AND TRAINING

2000	Defended habilitated doctor thesis
1993 - 1995	A.Humboldt scholarship and research in Leipzig University in Prof.G.Voelkel laboratory.
1990	PhD thesis and obtained doctor degree.
1989 - 1990	Soros scholarship and research in Oxford University, England in Prof.A.M.Glazer laboratory.
1985	Graduated Vilnius University

SCIENTIFIC DIRECTION

Main directions of the research are: lattice dynamics, ferroelectrics, structural phase transitions, dipolar glasses, relaxors, dielectric spectroscopy.

Publications	More than 240 ISI published papers from 1990.
Presentations	Participated in conferences in Germany, Russia, France, Italy, USA, England, Czech Republic, Poland, Spain, Brazil, Japan, China etc., and have more than 400 contributions to the conferences.
Projects	Received the Lithuanian National Prize in Science 2002. P. Brazdžiūnas Award in Experimental Physics of the Lithuanian Academy of Sciences in 2003.
Memberships	Member of the Lithuanian Physical Society Member of the Lithuanian Materials Research Society Member of the Lithuanian Academy of Sciences Foreign member of the Latvian Academy of sciences Foreign member of the Saxony Academy of sciences Member of the international advisory board of ECAPD (European Conference on Applications of Polar Dielectrics) Member of the international advisory board of EMF (European Meeting on Ferroelectrics). Chair and Organizing and Program Committee Member in Lithuanian national and international conferences. Coordinated numerous projects of Lithuanian Research Council, had FP6, FP7 projects, coordinated NATO, European Defense Agency projects.

RCBJSF In-1

Cooperation of Latvian and Lithuanian Scientists in Studies of Ferroelectrics and Related Materials

J. Banys[1], A. Sternberg[2], M. Antonova[2], Š. Bagdzevičius[1], E. Birks[2], K. Bormanis[2], M. Dunce[2], R. Grigalaitis[1], K. Kundzins[2], and J. Macutkevič[1]

[1]Faculty of Physics, Vilnius University, Lithuania

[2]Institute of Solid State Physics, University of Latvia, Latvia

e-mail: juras.banys@ff.vu.lt; stern@latnet.lv

Recent years have witnessed the fruitful collaboration between Lithuanian and Latvian researchers in the field of ferroelectricity. Two main institutions were involved in the scientific work – Faculty of Physics, Vilnius University and the Institute of Solid State Physics of University of Latvia.

Lithuanian team is concentrated on the broadband dielectric spectroscopy techniques which extend from milihertz range up to 120 gigahertz frequency. These experimental methods allow to investigate the dipolar relaxation which gives crucial contribution to the properties of ferroelectrics and related materials.

On the other hand, Latvian team in the framework of this cooperation is focused on the synthesis of high quality ferroelectric ceramics and basic characterization of the material – crystallographic structure by means of x-ray diffractometry and microstructure by TEM and AFM. Furthermore polarization, dielectric, electromechanical, electrocaloric parameters are studied. As a result, phase diagrams of complex solid solution systems were determined.

A lot of effort was devoted to the relaxors, including canonic relaxor lead magnium niobate (PMN), lead scandium niobate (PSN) and their solid solutions and other materials possessing B-site chemical disorder. Afterwards it was extended to the A-site substituted relaxors which had sodium bismuth titante (NBT) as a main component. Furthermore, the collaboration involving additional experimental and theoretical investigations were developed [1, 2].

Subsistent presentation will shed the light on the previous work which have been done as well on the current status and future perspectives. The presentation is dedicated to commemorate the 10th anniversary of Lithuania's and Latvia's EU membership.

References

1. S. Svirskas, M. Ivanov, S. Bagdzevicius, J. Macutkevic, A. Brilingas, J. Banys, J. Dec, S. Miga, M. Dunce, E. Birks, M. Antonova, and A. Sternberg, Acta Materialia 64, 123 (2014).
2. J. Macutkevic, S. Kamba, J. Banys, A. Brilingas, A. Pashkin, J. Petzelt, K. Bormanis, and A. Sternberg, Phys. Rev. B 74, 104106 (2006).

Stefano **BELLUCCI**

Dr. Stefano Bellucci obtained in 1986 his Ph.D. in Physics of elementary particles at SISSA, Trieste. He worked as Research Associate at Brandeis Univ., Waltham, MA, USA (1983-1985); as visiting researcher at M.I.T., Cambridge, MA, USA (1985-1986), at Univ. of Maryland, USA (1986-1987), at Univ. of California at Davis, USA (1987-1988). He was appointed as a Tenured Researcher (Research Staff) at INFN (Istituto Nazionale di Fisica Nucleare) Laboratori Nazionali di Frascati (LNF) in 1987. He was appointed as INFN First Researcher (Senior Research Staff) in 2005. He coordinates all LNF theoretical physics activities. His research interests include theoretical physics, condensed matter, nanoscience and nanotechnology, nanocarbon based composites, biomedical applications. His lab cultivated over 20 between PhD and master students in theoretical physics, condensed matter, nanoscience and nanotechnology. He published over 400 papers in peer-reviewed journals with $h = 40$, http://scholar.google.com/citations?hl=en&user=mOq8urEAAAAJ, and more than 10 invited book chapters. He is the Editor and/or co-author of 10 books with Springer. He appears in the list of Top Italian Scientists published by the VIA Academy.

He received the B.W. Lee Prize at Erice School of Subnuclear Physics (Erice, Italy) 1982. In 1980 he was selected as Summer student at CERN (Geneva).

He is Series Editor of Springer Lecture Notes in Nanoscale Science and Technology, and biannual (2012-2014) Associate Editor of Nanoscience and Nanotechnology Letters. He is Editorial Board Member of the many scientific journals.

He is Director of the NATO Emerging Security Challenges Division, SPS Programme project "Development of Biosensors using Carbon Nanotubes". He is INFN scientist in charge of EU projects "BY-NanoERA–Institutional Development of Applied Nanoelectromagnetics: Belarus in ERA Widening", "NAmiceMC–Nano-thin and micro-sized carbons: Toward electromagnetic compatibility application", and "FAEMCAR–Fundamental and Applied Electromagnetics of Nano-Carbons". He is LNF Spokesperson of GSS Supersymmetry project and INFN National Spokesperson of SEMS Condensed Matter Theory project.

Heat Resistant Unfired Phosphate Ceramics with Carbon Nanotubes and Boron Compounds for Electromagnetic and Ionizing Shielding Applications

A. Plyushch[1], D. Bychanok[1], P. Kuzhir[1], S. Maksimenko[1], K. Lapko[2], A. Sokol[2], J. Macutkevic[3], J. Banys[3], F. Micciulla[4], A. Cataldo[4], S. Bellucci[4]

[1]Research Institute for Nuclear problems of Belarusian State University, Belarus

[2]Research Institute for Physical-Chemical problems of Belarusian State University, Belarus

[3]Vilnius University (VU), Lithuania

[4]INFN-Laboratori Nazionali di Frascati, Italy

e-mail: Stefano.Bellucci@lnf.infn.it

Many modern industrial applications ranging from electromagnetic (EM) interference shielding to nuclear energetics require the design and fabrication of new materials with controlled physical properties, including hardness, mechanical strength, high thermal stability, electrical conductivity, *etc*. Because of their advanced physical properties phosphate based composites could be very interesting for different practical uses, e.g. as a matrix for effective EM and/or ionizing radiation shields. Phosphates working temperatures could reach 1600-1700 °C, whereas the curing can be done at room temperature. Some of the developed phosphate composites have been used as thermal insulation plates in Energiya-Buran spacecraft [1]. Filled with boron compounds, phosphate/boron composites were proved as effective materials for slow neutrons absorption and collimation [2]. Here we report the fabrication of phosphate ceramics filled with multi-walled carbon nanotubes (MWCNT) of different diameter by energy-efficient method. It has been observed that the percolation threshold shifts into the lower concentration range for MWCNT with smaller diameter together with increase of the absolute values of electrical conductivity.

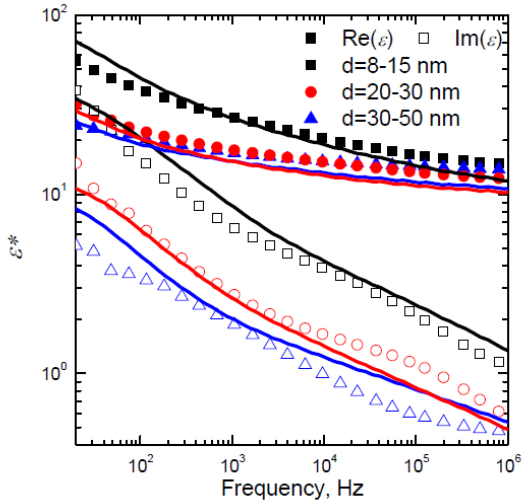

Fig.1. Comparison of experimentally measured dielectric spectra (dots) and its modeling (solid lines) for composites containing MWCNTs of various diameter at the constant concentration 1.5 wt. %

References

1. Ph. Krylova, et al, High-temperature glue composition, *Patent* 2066335. RU. Bulletin No 25, September 10 (1996)
2. P. P. Kuzhir, et al, Nanoscience and Nanotechnology Letters 4(11), 1104 (2012).

Antonio **BIANCONI**

Prof. Antonio Bianconi graduated in Physics in Rome university in 1969.
Full professor of Physics since 1986 in l'Aquila University and Rome University in Italy.
Has held the Chair of Biophysics at the La Sapienza University of Roma (1992-2012).
Visiting Professor in the Stanford University in USA, Univ of Paris VI in France, Tokyo University in Japan.
Antonio Bianconi is Director of the Rome International Center for Materials Science Superstripes.
President of the association for scientific culture Superstripes, associated at the Institute of Crystallography of Italian National Research Council.
He has been member of the Scientific Committees of various international institutions, and of many international conferences. He is in the editorial board member of several international journals.
He has been main lecturer in many international conferences.
His main scientific interests are in local lattice fluctuations in complex materials.
He is a pioneer of synchrotron radiation research first at Frascati syncrotron 1972-1975; Stanford SSRL 1976-1980; Frascati Adone storage ring 1980-1987; and later at the synchrotron facilities of Lure (Paris), Photon-Factory (Tsukuba), ESRF (Grenoble), and Elettra (Trieste). He has invented the name XANES spectroscopy in 1980, having identified the key role of shape resonances in x-ray absorption spectra near the absorption edge. He has identified many body effects in core excitations of correlated electronic systems. He has resolved the local structure of active sites in metalloproteins, of complex oxides and of high temperature superconductor. In the field of high temperature superconductors he has first identified the charge carriers as holes in the oxygen orbital and the stripes scenario of local lattice fluctuations.
He is chairman of the Series Int. Conferences on Stripes, and director of the Superstripes schools at the E. Majorana Center in Erice.
Recently has showed the key role of nanoscale phase phase separation in unconventional high temperature superconductors developing a new experimental method: scanning micro x-ray diffraction.
Quantitative valuation:

- following ISI: **Researcher_ID:** J-3997-2013; author of 424 Articles;
- H-index = 53,
- Sum of the Times Cited: **9213**
- http://www.researcherid.com/ProfileView.action?returnCode=ROUTER.Unauthorized&queryString=KG0UuZjN5WkAbUEghFfNvmNOSHWiWER6H9y7k6%252F0pLs%253D&SrcApp=CR&Init=Yes

Following google scholar profile:

- http://scholar.google.it/citations?user=98JhlmQAAAAJ&hl=it

He has a total of 13706 citations, h-index=56

FM&NT In-2

Nanoscale Phase Separation in Two-Dimensional Layers in the Limit of a Few Unit Cells Controlling Material Functionalities Unveiled by Scanning Submicron XRD

A. Bianconi

RICMASS, Rome International Center for Materials Science Superstripes Via dei Sabelli 119A, 00185 Roma, Italy

e-mail: antonio.bianconi@ricmass.eu

The emergent functionalities in two-dimensional layers in the limit of a few unit cells is becoming a hot topic both for fundamental new low energy physics and for new exciting applications. Novel heterostructures at atomic limit show unconventional ferroelectrics, magnetic and superconducting properties which can be tuned by strain and photo-induced effects. Recent breakthroughs have led to intense research into these ferroelectrics and more generally ferroic materials. Understanding the ferroelectric properties of such engineered thin film systems requires taking into account the interfaces with electrodes, substrates, or atmosphere1, the use of piezo-effets allows nanoscale domain writing [2,3] and strain engineering allows significantly change values of remnant polarization, coercive field, or the Curie temperature [4,5]. The scientific interest is now focusing to networks where superconducting, magnetic and ferro-electric nano-domains compete. New materials made of atomic layers intercalated by different atomic layers show nanoscale phase separation with co-existence of ferroelectric, magnetic and superconducting phases, where defects, and strain tune the material functionality. We have addressed our interest to develop a new method to get the spatial imaging of the fluctuating order in the k-space: scanning micro x-ray diffraction (SμXRD) [6-11] in these multi-phase materials. We have developed statistical methods of data analysis of SμXRD to get new information on the statistical physics of the complex nanoscale phase separation taking place in these novel functional materials [6-11]. Using SμXRD we have shown that statistical physics of the spatial distribution of the grains controls the material functionality, in the case of unconventional granular superconductors with the key role of percolation.

References

1. M. Dawber, K. M. Rabe, and J. F. Scott, Rev. Mod. Phys. 77, 1083 (2005).
2. S. V. Kalinin, et al. Rep. Prog. Phys. 73, 056502 (2010).
3. I. Infante, et al. Phys. Rev. Lett. 105, 057601 (2010).
4. D. G. Schlom, et al. Annu. Rev. Mater. Res. 37, 589 (2007).
5. K. J. Choi, et al. , Science 306, 1005 (2004).
6. M. Fratini, et al. Nature 466, 841-844 (**2010**)
7. N. Poccia, et al.Nature Materials, 10, 733-736 (**2011**)
8. N. Poccia, et al Proc. of the Nat. Acad. of Sciences 109, 15685 (**2012**)
9. A. Ricci, et al. Scientific Reports 3, 2383 (2013).
10. A. Bianconi Nature Physics 9, 536–537 (2013)
11. Ricci et al. New Journal of Physics 16 053030 (2014)

Mikhail **G. BRIK**

Professor Mikhail G. Brik received his PhD degree from Kuban State University (Krasnodar, Russia) in 1995 and his Doctor of Science (habilitation) degree from the Institute of Physics, Polish Academy of Sciences (Warsaw, Poland) in 2012. Since 2007 he has been taking a Professor position in the Institute of Physics, University of Tartu, Estonia. Before that, he had been working in Kyoto University (Kyoto, Japan), 2003-2007; Weizmann Institute of Science (Rehovot, Israel), 2002; Asmara University (Asmara, Eritrea), 2000-2001; Kuban State University (Krasnodar, Russia), 1995-2000. His area of scientific interests covers theoretical spectroscopy of transition metal and rare earth ions in optical materials, crystal field theory, ab initio calculations of physical properties of pure and doped functional compounds. He is a co-editor of two books, author of 10 book chapters and about 250 papers in the international journals. According to Google Scholar, he has more than 1900 citations with h-index=23. In 2006 he received the Dragomir Hurmuzescu Award of Romanian Academy; in 2013 he received the State Prize of Republic of Estonia in the field of exact sciences. He is also an Honorary Professor of the Hong Kong Institute of Education.

FM&NT In-3

A Review of the Structural, Electronic and Elastic Properties of Spinels

M.G. Brik

Institute of Physics, University of Tartu, Riia 142, Tartu 51014, Estonia

e-mail: brik@fi.tartu.ee

The crystals with the spinel structure form a large group of technologically important materials. The spinels with the halogen atoms as the anions are typical semiconductors with a narrow band gap, whereas the oxygen-based spinels possess considerably wider band gaps, which make them suitable for doping with rare earth and transition metal ions. In the present work a review of the structural, electronic, optical and elastic properties of a large group consisting of 185 ternary and binary spinel compounds is given. At first, a simple empirical model based on the ionic radii and electronegativities of the constituting ions was developed [1]. The average relative error between the experimental and modeled lattice constants is less than 1 %. The model allowed for a prediction of the lattice constants of new spinels [1]; moreover, the criteria of stability of spinel structure were suggested that can be used for narrowing the search space when looking for new spinels. As a further step, the ab initio and semi-empirical methods were used to analyze the electronic, optical and elastic properties of pure and doped spinels, like $ZnAl_2S_4$, $ZnGa_2O_4$ [2-4], $CdIn_2S_4$ [5]. Special attention was paid to the location of the impurities energy levels within the host band gap; suggested combination of the semi-empirical and ab initio techniques gives a complementary description of doped materials.

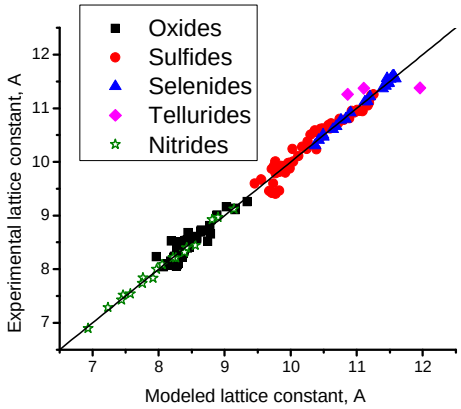

Fig.1. Correlation between the modeled and experimental lattice constants in the group of 185 cubic spinels, which were classified according to the anions (oxides with O, sulfides with S, selenides with Se, tellurides with Te, nitrides with N).

References

1. M.G. Brik, A. Suchocki, A. Kamińska, Inorg. Chem. (2014, in press).
2. M.G. Brik, J. Phys. Chem. Solids **71**, 1435 (2010).
3. M.G. Brik, M. Nazarov, M.N. Ahmad-Fauzi, L. Kulyuk, S. Anghel, K. Sushkevich, G. Boulon, J. Lumin.**132**, 2489 (2012).
4. M.G. Brik, M. Nazarov, M.N. Ahmad Fauzi, L. Kulyuk, S. Anghel, K. Sushkevich, G. Boulon, J. Alloys Compds. **550**, 103 (2013).
5. V. Krasnenko, M.G. Brik, Mat. Res. Express **1**, 015905 (2014).

Ruei-San CHEN

Prof. Ruei-San Chen, of Graduate Institute of Applied Science and Technology, National Taiwan University of Science and Technology (Taiwan Tech), Taiwan and his group have special expertise in the formation of single nanostructure device of metal-oxides and III-V nitride semiconductors. He is also experienced in crystallographic structural analysis and structure property correlation in measuring as well as understanding optoelectronic properties of single nanostructures and extracting various device properties meticulously. Additionally, he was one of the pioneers in the studies of the surface photoconductivity and high-gain transport in III-nitride nanowires when he was a postdoc working with Dr. Kuei-Hsien Chen (Academia Sinica) and Dr. Li-Chyong Chen (National Taiwan University). His acumen in the understanding of nanoelectronics has helped the group laurel with number of very important publications. Over the past decade, he has published near 40 papers, two review articles, and one book chapter.

FM&NT In-4

Surface-controlled Transport Properties in 1D and 2D Nanocrystals

R.S. Chen[1], K.H. Chen[2], L.C. Chen[3]

[1]National Taiwan University of Science and Technology (Taiwan Tech), Taiwan

[2]Institute of Atomic and Molecular Sciences, Academia Sinica, Taiwan

[3]Center for Condensed Matter Sciences, National Taiwan University, Taiwan

e-mail: rsc@mail.ntust.edu.tw

We give an overview to the surface effects on electronic transport properties in the low-dimensional material systems. For one-dimensional (1D) systems, photoconduction (PC) properties are dominantly controlled by the surface depletion regions in group-III nitrides (e.g. GaN, InN, and AlN) and metal-oxide (e.g. ZnO, SnO_2, TiO_2, WO_3, etc.) nanowires. Electron-hole spatial separation and oxygen sensitization PC mechanisms are two major causes resulting in the several orders of magnitude higher PC gains and carrier lifetimes in the nanowires in comparison to their bulk counterparts. In addition, a remarkable thickness-dependent conductivity was generally observed in quasi-2D layer semiconductors such as MoS_2, $MoSe_2$, and WS_2. A probable higher surface conductivity and electron surface accumulation are proposed to explain the anomalous dimension effect.

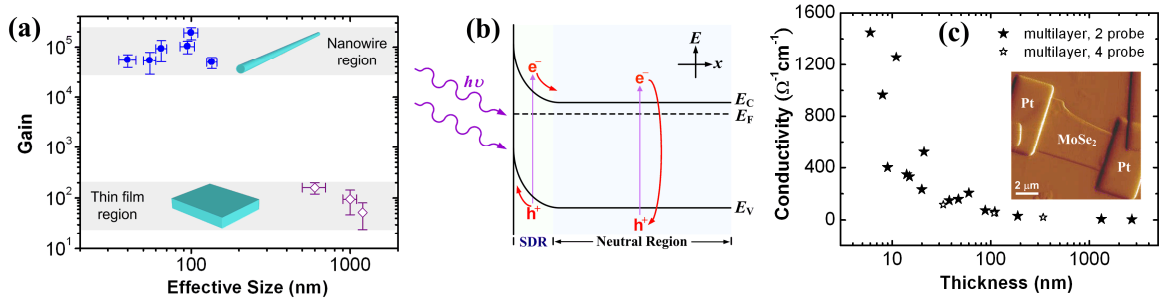

Fig. 1 (a) The photoconductive gain as a function of size for the GaN NWs (solid circles) and thin films (open diamonds) at 400 V/cm applied field and 4.0 eV excitation with 10–12 W/m^2 power density. The "effective size" is defined by the values of the NW diameter and the film thickness.[1,2] (b) The schematic band diagram shows the spatial separation and direct recombination of *ehp* in the SDR and neutral region, respectively.[3] (c) The electrical conductivities for the $MoSe_2$ multilayers with different thicknesses ranged from 6 to 2700 nm measured by two-probe (black solid star) and four-probe (black open star) methods. Inset: The AFM image of a $MoSe_2$ multilayer device with a thickness at ~60 nm fabricated by focused-ion beam (FIB) approach.

References

1. R. S. Chen, H. Y. Chen, C. Y. Lu, K. H. Chen, C. P. Chen, L. C. Chen, Y. J. Yang, *Appl. Phys. Lett.* **91**, 223106 (2007)

2. R. S. Chen, S. W. Wang, Z. H. Lan, J. T. H. Tsai, C. T. Wu, L. C. Chen, K. H. Chen, Y. S. Huang, C. C. Chen, *Small* **4**, 925 (2008).

3. R. S. Chen, W. C. Wang, M. L. Lu, Y. F. Chen, H. C. Lin, K. H. Chen, L. C. Chen, *Nanoscale* **5**, 6867 (2013).

Robert
A. EVARESTOV

Robert A. Evarestov graduated St. Petersburg State University as theoretical physicsist in 1960. He obtained his PhD in the Department of Theoretical Physics at St. Petersburg State University in 1964 (supervisor Prof. Marija Petrashen), Habilitation degree -in the same Department in 1977 "Molecular models in the electronic structure theory of crystals". From 1968 he woks at the Department of Quantum Chemistry of St. Petersburg State University (Professor – from 1979). In 1990-1994 he was Director of the Chemistry Institute of St. Petersburg State University, in 1994-1998 he was First Vice Rector of St. Petersburg State University. Since 1999 till present time he is Head of Department of Quantum Chemistry of St. Petersburg State University. His research interest cover symmetry of crystalline solids (the monograph "Site Symmetry in crystals" has been published by Springer in 1993, second edition in 1997). He is interested also by the application of quantum chemistry methods to perfect and defective crystals (the monograph "Quantum Chemistry of Solids" has been published by Springer in 2007, second edition in 2012). Now his interests cover symmetry and quantum chemical study of monoperiodic nanostructures (nanotubes, nanowires). He is Foreign Member of Latvian Academy of Science (from 2005), Humboldt Foundation Awardee (1998). His publication list includes over 260 papers indexed in WOS and cited more than 2600 times, his Hirsh index is 24 (Web of Science data, March 2014).

FM&NT In-5

Theoretical Study of Single- and Multi-Walled Nanotubes Rolled-up from Group IV Metal Disulfides

R. Evarestov, A. Bandura

Institute of Chemistry, Quantum Chemistry Division, St. Petersburg State University, Russia

e-mail: re1973@re1973.spb.edu

In recent years, nanometer-sized dichalcogenides are intensively studied as they are promising building blocks for engineering and for tailoring nanoscale structures. Among the dichalcogenides, group IV metal disulfides have attracted a great attention and the corresponding nanotubes (NTs), nanowires, and nanobelts have been synthesized.

The structure and properties of single-walled TiS_2- and ZrS_2-based NTs have been studied in [1, 2] using the first-principles calculations. In this work we consider the structure and stability of the single-, double- and triple-walled rolled up NTs constructed via folding of hexagonal layers of ZrS_2 and SnS_2. Choice of these two crystals allows us to compare the properties of the NTs formed by sulfides of *p*- and *d*-elements. Calculations have been made within the density functional theory using the hybrid exchange-correlation functional and localized atomic basis set.

The obtained results show that the atomic structure of ZrS_2 and SnS_2 NTs is very similar; however, the electronic structure is different. Moreover, the formation and strain energies of tin disulfide NTs are 1.5-3 times greater than those of zirconium disulfide NTs, thus demonstrating the lower stability of the SnS_2 tubes.

It is known [3] that some inorganic multiwalled nanotubes can exhibit the polygonal cross-section. Our analysis of the relaxed shape of double- and triple-walled ZrS_2 and SnS_2 NTs indicates a noticeable deviation from the completely cylindrical shape. This deviation is negligible in the case of zigzag NTs, but it becomes significant in the outmost shells of the armchair NTs and it is enhanced with the shell radius increasing.

Acknowledgements

Authors are grateful to St. Petersburg State University for the financial support (Grant No. 12.38.273.2014) and for the computer center facilities.

References

1. D. Teich, T. Lorenz, J.-O. Joswig, G. Seifert, D.-B. Zhang, T. Dumitrică, J. Phys. Chem. C **115**, 6392 (2011)
2. R. A. Evarestov and A. V. Bandura, Phys. Scr. **89**, 044001 (2014)
3. R. Tenne and G. Seifert, Annu. Rev. Mater. Res. **39**, 387 (2009)

Igor
N. FLEROV

Since 1966 Dr. Sc., Professor Igor N. Flerov works at L.V. Kirensky Institute of Physics, Siberian Department of RAS, Krasnoyarsk, Russia. He has occupied successively the following positions: engineer, junior scientist, senior scientist, leading scientist, a head of laboratory.

At the moment Prof. Igor Flerov is a main scientist of the Crystal Physics Laboratory.

He received the Ph. D and Dr. Sc. degrees in 1978 and 1994, respectively.

The main field of his interests is concentrated on the physics of ferroics including structure and thermodynamic properties. Other fields are associated with the solid state chemistry and materials science. Investigations are aimed at the studies of the mechanism and nature of phase transitions in the oxygen, fluorine, oxygen-fluorine ferroics and multiferroics. Recently his research activities cover also caloric and multicaloric effects in solids especially in connection with seeking for the ways of caloric efficiency elevating in solid refrigerants.

He has authored about 250 journal articles.

Starting in 1984 (the Third RCBJSF in Novosibirsk, Russia), Professor Igor Flerov took part in the Symposium as a member of the Organizing Committee.

He is also a member of the Scientific Council on Condensed Matter Physics of RAS (Division of Ferroelectrics, Dielectrics and Liquid Crystals).

Prof. Igor Flerov is responsible for the teaching of the thermal properties substances theory and technical thermodynamics at Siberian Federal University (Krasnoyarsk, Russia).

RCBJSF In-2

Phase Transitions and Caloric Effects in Ferroics and Multiferroics

I. Flerov[1,2], M. Gorev[1,2], E. Mikhaleva[1], A. Kartashev[1]

[1]Kirensky Institute of Physics, Siberian Department of RAS, Krasnoyarsk, Russia

[2]Siberian Federal University, Krasnoyarsk, Russia

e-mail: flerov@iph.krasn.ru

In recent years much attention has been focused on ferroelectrics, ferromagnets and ferroellastics showing monocaloric effects (CE) associated with the reversible change of entropy or/and temperature under external field (magnetic, electric, mechanical stress). The main reason is that such materials are highly promising to be used as working bodies in thermodynamic cycles of the effective alternative solid-state refrigeration technologies. The greatest CE in ferroics can be realized in the temperature region near phase transitions close to the tricritical point and characterized by large values of entropy change and susceptibility to external field. Electro(ECE)- and magneto(MCE)-caloric effects are the most extensively studied compared to baro(BCE)-caloric one. However the latter effect associated with a heat emission or absorption at changing external pressure is the most universal because it can be realized in solids in spite of their physical nature.

In this paper, we present a short review of some recent studies results evidently showing that along with a searching for new effective solid refrigerants, it is profitable also to seek for the ways of caloric efficiency elevating in known ferroics not only by the increase of external field. Because phase transitions in many ferroelectrics and ferromagnets are followed by the unit cell deformation (do not obligatory associated with the symmetry change), one of the most efficient directions is to use a twofold CE (ECE + BCE, MCE + BCE) generated in the same ferroic material by two distinct external fields. Another way is associated with using the CE effects in multiferroics. Owing to magnetoelectric coupling between two monoferroic subsystems there is possibility to realize the multicaloric effect (ECE + MCE) by one of the external fields. But the monophase ferromagnet-ferroelectric materials are characterized not infrequently by rather low values of magnetoelectric coefficient. That is why it is worth to give much attention to compositional materials, especially when the transformation temperatures in ferroelectric and ferromagnetic components are close to each other. In such a case, using magnetic or electric field, one can generate the total multicaloric effect consisting of ECE, MCE and BCE. The latter effect results from the elastic mechanical interaction between magnetostrictive and piezoelectric phases introducing stress in each other.

Vladimir M. FRIDKIN

Vladimir M. Fridkin

011-70-95-135 1500 (office)
011-70–95-135 1011 (FAX)
011-70-95-137 6470 (home)

Head of the Laboratory of Electronic Materials
Institute for Crystallography
Russian Academy of Sciences
Leninsky Prospect 59, Moscow 117333

EXPERIENCE

1967–present	Head of the Laboratory of Electronic Materials, Institute of Crystallography
1970–1975	Professor of the Physics Department of the Moscow Lomonosov State University
1965–1967	Senior Scientist of the Institute of Crystallography
1960–1965	Research Scientist of the Institute of Crystallography

EDUCATION

1969	Habilitation "Doctor of Science in Physics and Mathematics", Institute of Crystallography. Thesis: "Physics of the Electrophotographic Process"
1965	Ph.D. in "Physical and Mathematical Sciences", Institute of Crystallography. Thesis: "New Materials for Electrets"
1959	Master's Degree from Physics Department of Moscow State University

VISITING APPOINTMENTS

1993–present	Visiting Professor, Department of Physics and Astronomy, U. of Nebraska
1993–99	Visiting Professor, Department of Physics, University of Trento, Italy
1990	Visiting Professor, Laboratory of Materials Sciences, Pennsylvania State U.
1989	Visiting Professor, Tokyo Institute of Technology, Japan
1979	Visiting Professor, Solid State Institute, Tokyo University, Japan

SYNERGISTIC ACTIVITIES

1989–present	Secretary of the Organizing Committee, US–Soviet Ferroelectricity Meetings
1973–present	Member of the Editorial Board of Ferroelectrics and Ferroelectric Letters
1964–present	Member of the Russian (formerly USSR) Academy of Sciences

Honorary Member of the Society for Technology and Photographic Science of Japan (1985)
Kozar Memorial Award of the American Photographic Society (1984)

RESEARCH ACTIVITIES

Current Fields of Interest: Pyroelectric and Ferroelectric Phenomena, Electroactive Polymers, Phase Transformations in Electronic Materials, Nonconventional Photographic Processes

Discovered Two-Dimensional Ferroelectricity (1997)
Discovered Optical Sensitization of Polymer Ferroelectrics (1990)
Discovered the Bulk Photovoltaic Effect in Ferroelectric and Piezoelectric Materials (1969)
Discovered the Tricritical Point in a Ferroelectric Crystal (1968)
Discovered and investigated the Photostimulated Phase Transitions in Ferroelectrics (1966)
Developed Electrophotography using photo-electrets (1954)
Developed Infrared Photography using photoactive materials

RCBJSF In-3

Ferroelectricity and the Bulk Photovoltaic Effect at the Nanoscale

V. Fridkin

Shubnikov Institute of Crystallography of the Academy of Sciences, Russia

e-mail: fridkin@crys.ras.ru

Ferroelecric films at the nanoscale (1- 10nm) show very peculiar properties, including switching kinetics and coercive field scaling. These properties could be successfully explained by the Ginzburg-Landau phenomenology for the homogeneous (without domains) medium.

One of the most remarkable properties of the ferroelectrics at the nanoscale is high efficiency of the bulk photovoltaic effect.

The experimental results are obtained for polymeric and perovskite ferroelectric films at the nanoscale.

References:

1. Vladimir Fridkin and Stephen Ducharme. Ferroelectricity at the Nanoscale (Springer, Berlin-Heidelberg, 2014)
2. Boris Sturman and Vladimir Fridkin. The Photovoltaic and Photorefractive Effects in Noncentrosymmetric Materials (Gordon and Breach Science Publishers, Philadelphia, 1992)

David **FUKS**

1971 - MSc- Odessa State University - Department of Theoretical Physics - Odessa, USSR
1975 - Ph.D.-Tomsk State University - Department of Solid State Physics - Tomsk, USSR
Dr of Sc./Dr. Habil.-1984-Moscow State University - Department of Solid State Physics - Moscow, USSR

Currently **Professor** in Department of Materials Engineering, Ben-Gurion University of the Negev, Beer-Sheva, Israel; Stephen and Edith Berger Chair in Physical Metallurgy.
Author of monograph and more than 250 papers in scientific journals.
Research is devoted to the study of different aspects of application of quantum mechanical and statistical thermodynamics approaches to the analysis of the properties of solid bulk materials, surfaces and the interfaces. The research is based mainly on the Density Functional Theory (DFT) which is considered nowadays as one of the most powerful tools in the study of the nature of bonding in materials.
The topics that are intensively investigated nowadays are:
a) Structure and properties of the interfaces; b) Stability of intermetallic compounds;
c) Thermodynamics and kinetics of phase transitions in metallic alloys and perovskites;
d) theoretical aspects of wetting phenomena; e) adsorption in catalysis;
f) growth of thin metallic films; g) refining of the structure and understanding the nature of new uranium-based multi-component compounds.

FM&NT In-6

Controlling the Figure of Merit in TiNiSn Half-Heusler Alloy: DFT Study

D. Fuks, K. Kirievsky, M. Shlimovich, Y. Gelbstein

Materials Engineering Department, Ben Gurion University of the Negev, Beer Sheva, Israel

e-mail: fuks@bgu.ac.il

TiNiSn half-Heusler (HH) alloys are considered as promising materials for application in thermoelectric devices. Improving their figure of merit may be achieved by increasing the Seebeck coefficient and/or by reduction of thermal conductivity. The magnitude of Seebeck coefficient depends on the shape of the electron Density of states (DOS) in the vicinity of Fermi energy, therefore engineering of DOS may improve thermoelectric figure of merit. Morphology of material influences the thermal conductivity, and this is an additional way to manage the thermoelectric efficiency. The promising method is to reduce the thermal conductivity by varying the average grain size in the sintering of nano-particles. The important question in this context is how the nanocrystalline structure influences their electronic properties. The aim of this presentation is to examine the improving thermoelectric figure of merit by Density Functional theory (DFT) calculations and statistical thermodynamics.

Investigation of different types of antisite defects shows that Ni antisite defects are more preferable energetically in comparison with other antisite defects. Influence of this defect on DOS is studied. Changes of DOS due to doping with iron and copper are presented pointing that alloying element may change the type of conductivity.

The analysis of the stability of TiNiSn with growing Ni contents is carried out for $T \neq 0$ by combining the DFT calculations with statistical thermodynamics. The approach bridges the gap between the quantum mechanical calculations of the phase stability in the ground state and the behavior of the alloys at elevated temperatures. The quasi-binary phase diagram beyond T=0K for TiNiSn-$TiNi_2Sn$ solid solutions is calculated with the energy parameters extracted from the calculations of the ordered structures on the Ni sublattice.

It is shown that the decomposition of the off-stoichiometric Ni-rich HH alloy in the stoichiometric phase and $TiNi_2Sn$ with the deficiency of Ni occurs at elevated temperatures – an effect which is confirmed by recent experimental data. Existence of the miscibility gap between TiNiSn and $TiNi_2Sn$ leads to phase separation in the nano-scale and to reduction of thermal conductivity recently found in experiments. It is discussed also how the formation of TiNiSn compound with grain boundaries may influence the conductivity of this material.

Arvaidas **GALDIKAS**

Arvaidas Galdikas is full professor in Kaunas University of Technology and in Lithuanian Health Sciences University. He was born in 1963 Lithuania. PhD in physics he obtained at 1994 and doctor habilitus degree in Materials Engineering at 2000. He did research work in Thessaloniki Aristotle University, Greece, Poitiers University, France. He published over 60 scientific papers in ISI referred journals, two scientific monographs published in Lithuania and USA, and 6 textbooks for university students. His research interest is the modeling of mass transport processes on the surfaces of solids under interaction of atomic and molecular beams. Recently his research is focusing into three main fields: 1) analysis of mass transport processes taking place during plasma nitriding of stainless steels and cobalt chromium alloys (it was proposed novel mechanism and model based in barrodiffusion phenomenon), 2) modeling of phase separation and encapsulation processes in growing films (formation of nanoclusters during plasma deposition) and 3) modeling of mass transport processes in nanostructured powder catalysts for automotive exhaust gas (three way automotive catalysts). Recently, the novel model which involvs grain boundary diffusion process in polycrystalline particles of powder was proposed and verified for perovkite catalyst.

FM&NT In-7

Diffusion Processes in Nanostructured Three-Way Automotive Powder Catalysts

A. Galdikas

Institute Physics Department, Kaunas University of Technology, Lithuania

e-mail galdikas@ktu.lt

Catalytic properties of nanosized perovskite $LaCoO_3$ and $LaMnO_3$ powders are considered experimentally and theoretically. For the purpose of the use of those catalysts in automotive exhaust gas conversion the kinetics of oxygen atom transport processes from/to gas phase and catalyst are experimentally analyzed by isotopic oxygen exchange method. Molecular oxygen isotope $^{18}O_2$ gas is introduced into reactor with powder of catalyst. The process of exchange is performed at temperature 400^{o}C. As a result of oxygen exchange between gas as catalyst the molecular species of oxygen $^{18}O_2$, $^{18}O^{16}O$ and $^{16}O_2$ appears in gas phase which kinetics is registered by mass spectrometer. Monocrystalline and polycrystalline powder particles are prepared [1,2] are considered.

The obtained experimental kinetic curves of partial pressures of oxygen species are fitted by proposed real time kinetic model based on rate equations. Model includes processes of chemical reactions (complex and simple heteroexchange) and diffusion of oxygen inside powder nanoparticles. The diffusion process is introduced considering the bulk diffusion adapted for powder catalysts [3] and diffusion in grain boundaries for polycrystalline particles. The main attention is paid on grain boundary diffusion.

Calculated curves are in a good agreement with experimental points for all three types of catalysts. In the case of polycrystalline powder particles both bulk and grain boundary diffusion takes place, while in monocrystalline case only bulk diffusion occurs. This assumption is realized in model. From the calculated results the kinetic (exchange rate constants, diffusion coefficients of bulk and grain boundary diffusion) and thermodynamic (activation energies of exchange reactions and diffusion) parameters are obtained.

References:

1. S. Royer, F. Berube, H. Alamdari, R. Davidson, S. McIntyre, S. Kaliaguine, Appl. Catal. A 282 (2004) 273.
2. S. Royer, D. Duprez, S. Kaliaguine, J. Catal., 234 (2005) 364.
3. A. Galdikas, D. Duprez, C. Descorme, Appl. Surf. Sci., 236 (2004) 342.

Kersti **HERMANSSON**

Kersti Hermansson is strongly involved in e-science for materials chemistry, namely the development of multiscale methods to bring chemical modelling closer to the complex dynamical systems of the real world, using various types of electronic structure and force-field approaches. Her current applications focus on dynamical phenomena on metal oxide surfaces and nanoparticles, and in aqueous media, including computational vibrational spectroscopy and hydrogen bonding. She is a Professor of Inorganic Chemistry at the Ångström Laboratory of Uppsala University. She is actively involved in the new European Modelling Council and a member of the Royal Swedish Academy of Sciences. Webpage: www.teoroo.kemi.uu.se.

FM&NT In-8

Ceria Chemistry at the Nano-Scale

K. Hermansson

Department of Chemistry, The Ångström Laboratory, Bpx 531, S-75121 Uppsala, Sweden

e-mail: kersti@kemi.uu.se

The chemistry of CeO_2 (ceria) is rich and intriguing, and has important technical applications, for example in solid oxide fuel cells and for the purification of exhaust gases in vehicle emissions control – all of this largely a consequence of ceria's exceptional reduction-oxidation properties enabled by the duality of cerium, which easily toggles between Ce^{4+} and Ce^{3+} thanks to its 4*f* electron.

In this talk we will discuss ceria clusters and nanoparticles in reducing, oxidative and humid environments and the powerful analyses and predictions that can be achieved though computational materials modelling. Realistic materials modelling calculations need to be able to mimic these intricate details and at the same time treat large (and dynamic) systems. This is a challenge.

We have used a range of theoretical methods to study ceria, including DFT, DFTB (DFT-based tight-binding), as well as force-field calculations with a newly parameterized reactive force-field – all within a multi-scale simulation environment.[1-4] Based on the quantum-chemical calculations, we find that small ceria nanoparticles of certain shapes (such as perfect octahedra) under low-temperature conditions can be stabilized through the adsorption of oxygen molecules in the form of superoxo species (in agreement with experimental studies; blue in *the figure*), and water in the form of hydroxo species. Moreover, based on force-field simulations we can predict the relative stabilities of very large ceria nanoparticles of different shapes. These and other examples will be discussed.

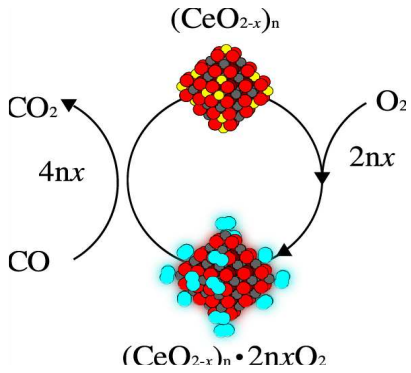

References

1. J. Kullgren, K. Hermansson, and P. Broqvist, J. Phys. Chem. Lett. **4**, 604−608 (2013)
2. J. Kullgren, K. Hermansson, and P. Broqvist, SPIE Solar Energy and Technology (2013).
3. J. Kullgren, K. Hermansson, and P. Broqvist, P hys. Status Solidi RRL (2014) / DOI 10.1002/pssr.201409099
4. J. Kullgren, P. Broqvist, A.C.T. van Duin and K. Hermansson. To be published.

Naoshi **IKEDA**

Graduate School of Natural Science and Technology, Okayama University
3-1-1 Tsushima-naka, Kita-ku, Okayama-city, Okayama 700-8530, Japan
Phone: +81-86-251-7810, FAX: +81-86-251-7810, E-mail: ikedan@science.okayama-u.ac.jp

Professional Preparation:

B.S. in Physics, 1985,	Waseda University
M.S. in Physics, 1988,	Waseda Univeristy
Dr. Sci., 1995,	Waseda University

Appointments:

2009 - present	Director, Energy Device Center, Okayama University
2005 - present	Professor, Okayama University
1998 - 2005	Team Leader, Dynamical Structure Team, JASRI
1996 - 1998	Lecturer, Waseda University
1990 - 1993	Research Associate, Waseda University

Publications: (From over 110 publications)

1. *Magnetoelectric Effect Driven by Magnetic Domain Modification in $LuFe_2O_4$*, Takashi Kambe, Yukimasa Fukada, Jun Kano, Tomoko Nagata, Hiroyuki Okazaki, Takayoshi Yokoya, Shuichi Wakimoto, Kazuhisa Kakurai, and Naoshi Ikeda *Phys. Rev. Lett.* **110**, 117602 (2013).
2. *Superconductivity in alkali-metal-doped picene*, R. Mitsuhashi, Y. Suzuki, Y. Yamanari, H. Mitamura, T. Kambe, N. Ikeda, H. Okamoto, A. Fujiwara, M. Yamaji, N. Kawasaki, Y. Maniwa & Y. Kubozono *Nature* **464**, 76 (2010).
3. *Ferroelectric properties of triangular charge-frustrated $LuFe_2O_4$*, N. Ikeda *J. Phys. Cond. Mat.* **20** (2008) 434218 pp6.
4. *Spontaneous formation of vanadium "molecules" in a geometrically frustrated compound: AlV_2O_4*, Y. Horibe, M. Shingu, K. Kurushima, H. Ishibashi, N. Ikeda, K. Kato, Y. Motome, N. Furukawa, S. Mori and T. Katsufuji *Phys. Rev. Lett.* **96**, 086406 (2006).
5. *An organic thyristor*, F. Sawano, I. Terasaki, H. Mori, T. Mori, M. Watanabe, N. Ikeda, Y. Nogami and Y. Noda *Nature* **437**, 522-524 (2005).
6. *Ferroelectricity from iron valence ordering in the charge-frustrated system $LuFe_2O_4$*, N. Ikeda, H. Ohsumi, K. Ohwada, K. Ishii, T. Inami, K. Kakurai, Y. Murakami, K. Yoshii, S. Mori, Y. Horibe and H. Kitô *Nature* **436**, 1136-1138 (2005).
7. *Ferro-type orbital state in Mott transition system $Ca_{2-x}Sr_xRuO_4$ studied by the resonant X-ray scattering interference technique*, M. Kubota, Y. Murakami, M. Mizumaki, H. Ohsumi, N. Ikeda, S. Nakatsuji, H. Fukazawa and Y. Maeno *Phys. Rev. Lett.* **95**, 026401/1-4 (2005).

Membership of Academic Societies:

The Physical Society of Japan
The Crystallographic Society of Japan
The Japanese Society of Synchrotron Radiation Research

Activities of Academic Society:

Member of Councilor of SPring-8 Users Society

RCBJSF In-4

Ferroelectric and Electronic Property of RFe_2O_4

N. Ikeda[1], T. Nagata[2], M. Fukunaga[1], T. Kambe[1], J. Kano[1], H. Kimura[3], P.E. Janolin[4], J.M. Kiat[4]

[1]Department of Physics, Okayama University, Japan

[2]Departmet of Electronic Engineering, Nihon University, Japan

[3]Institute of Multidisciplinary Research for Advanced Materials, Tohoku University, Japan

[4]Laboratoire Structures, Propriétés, Modélisation des Solides, Ecole Centrale Paris, France

e-mail: ikedan@okayama-u.ac.jp

RFe$_2$O$_4$ (R=Y, Ho-Lu) [1,2] consists of the stacking of triangular lattice of rare earth and iron ions as shown in figure 1. The equal amount of Fe^{2+} and Fe^{3+} existing in the iron double triangular layer drives a kind of charge frustrated state. It is considered that the charge frustration realizes a ordering of Fe^{2+} and Fe^{3+} in the triangular plane, where the charge arrangement become polar [1,2].

There is long discussion for the presence of the ferroelectricity in this material[3,4]. We report our recent experimental results as, high quality single crystal growth, measurement of the Fermi level, Magneto Electric response detection[5], precise pyroelectric current measurement and succession of the *P-E* loop measurement[6].

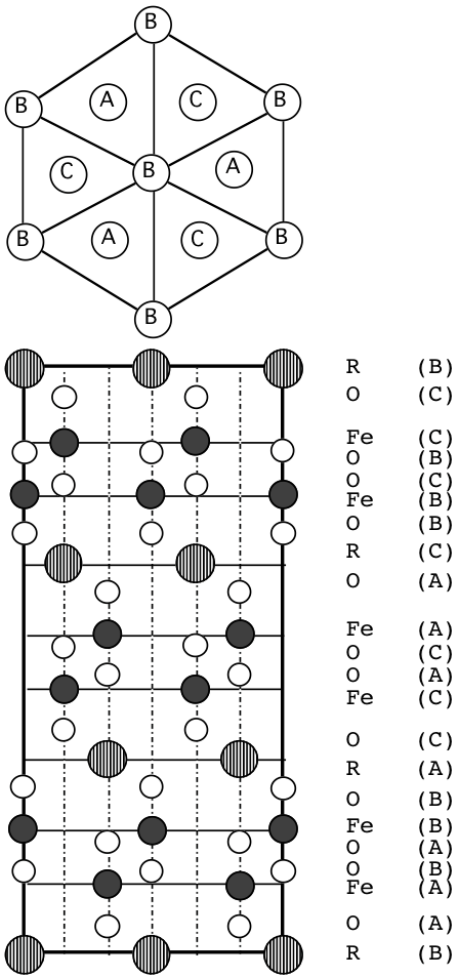

Fig.1 Crystal structure of RFe_2O_4

References

1. N. Ikeda, *et al.*: Nature 436 (2005) 1136.
2. N. Kimizuka, *et al.*, (Handbook on the Physics and Chemistry of Rare Earths **13**, 283 (Elsevier, 1990).
3. M. Angst, *et al.* :*Phys. Rev. Lett.*, **101** (2008) 227601.
4. A. M. Mulders, *et al.*: *Phys. Rev. Lett.*, **103** (2009) 077602.
5. T. Kambe, *et al.*: *Phys. Rev. Lett.* **110**, 117602 (2013).
6. M. Fukunaga and Y. Noda. J. Phys. Soc. Jpn. **77**, 064706 (2008)

Mitsuru **ITOH**

Education:

B.S. in Technology, 1977, Nagoya Institute of Technology
M.S in Materials Science, 1979, Tokyo Institute of Technology
Dr. in Eng., 1982, Tokyo Institute of Technology

Academic carrier:

1982- Assistant professor, Osaka University
1988- Associate professor, Materials and Structures Laboratory, Tokyo Institute of Technology
1999- Professor, Materials and Structures Laboratory, Tokyo Institute of Technology
2013- Director, Materials and Structures Laboratory, Tokyo Institute of Technology

Recent Publications: (From over 420 publications)

1. **Hierarchical Dielectric Orders in Layered Ferroelectrics Bi_2SiO_5**, Younghun Kim, Jungeun Kim, Akihiko Fujiwara, Hiroki Taniguchi, Sungwng Kim, Hiroshi Tanaka, Kunihisa Sugimoto, Kenichi Kato, Mitsuru Itoh, Hideo Hosono, and Masaki Takata, IUCrJ, vol.1, part3(2014), pp.160-164.
2. **Ferroelectric Quantum Criticality**, S. E. Rowley, L. J. Spalek, R. P. Smith, M. P. M. Dean, M. Itoh, J. F. Scott, G. G. Lonzarich, and S. S. Saxena, Nature Phys., vol.10, No.5 (2014), pp367-372.
3. **Epitaxial Growth of Metastable Multiferroic $AlFeO_3$ Film on $SrTiO_3$ (111) Substrate**, Yosuke Hamasaki, Takao Shimizu, Hiroki Taniguchi, Tomoyasu Taniyama, Shintaro Yasui, and Mitsuru Itoh, Appl. Phys. Lett., vol.104, No.8 (2014), pp082906 1-5.
4. **Ferroelectricity Driven by Twisting of Silicate Tetrahedral Chains**, Hiroki Taniguchi, Akihide Kuwabara, Jungeun Kim, Younghun Kim, Hiroki Moriwake, Sungwng Kim, Takuya Hoshiyama, Tsukasa Koyama, Shigeo Mori, Masaki Takata, Hideo Hosono, Yoshiyuki Inaguma, and Mitsuru Itoh, Angewandte Chem. Int. Ed., vol.52, No.31 (2013), pp8088-8092.
5. **Structural Modification and Domain Structure in a $BaTiO_3$ Film on (110) $SrTiO_3$**, Takao Shimizu, Dai Suwama, Hiroki Taniguchi, Tomoyasu Taniyama, and Mitsuru Itoh, Appl. Phys. Express, vol.6 (2013), pp015803 1-3.
6. **Elastic and Anelastic Properties of Ferroelectric $SrTi^{18}O_3$ in the kHz-MHz Regime**, J. F. Scott, J. Bryson, M. A. Carpenter, J. Herrero-Albillos, and M. Itoh, Phys. Rev. Lett., vol.106, No.10 (2011), pp105502 1-4.
7. **Relaxor $Pb(Mg_{1/3}Nb_{2/3})O_3$: A Ferroelectric with Multiple Inhomogeneities**, Desheng Fu, Hiroki Taniguchi, Mitsuru Itoh, Shin-ya Koshihara, N. Yamamoto, and Shigeo Mori, Phys. Rev. Lett., vol.103, No.20 (2009), pp207601 1-4.
8. **Low-Driving-Voltage Electroluminescence in Perovskite Films**, Hiroshi Takashima, Kohei Shimada, Noboru Miura, Tetsuhiro Katsumata, Yoshiyuki Inaguma, Kazushige Ueda and Mitsuru Itoh, Adv. Mat., vol.21, No.36 (2009), pp3699-3702.
9. **Positive and Negative Magnetodielectric Effects in *A*-Site Ordered $(BiMn_3)Mn_4O_{12}$ Perovskite**, Naoki Imamura, Maarit Karppinen, Teruki Motohashi, Desheng Fu, Mitsuru Itoh, and Hisao Yamauchi, J. Am. Chem. Soc., vol.130, No.45 (2008), pp14948-14949.

Membership of Academic Societies

American Chemical Society, Physical Society of Japan, Ceramics Society of Japan, Chemical Society of Japan, Applied Physics Society of Japan

Pl-1

Strategy for the New Ferroelectric Materials in Tetrahedral System

M. Itoh

Materials and Structures Laboratory, Tokyo Institute of Technology, Japan

e-mail: itoh.m.aa@m.titech.ac.jp

Recent our summary on the stability diagram of perovskites ABO_3 with octahedral system [Fig.1] has pointed out the importance of chemical bonds of A-O as well as B-O in perovskites[1]. Tolerance factor, which is a useful parameter to consider the structure and the stability of the perovskite, gives an intuitive image of deformation of BO_6 system from cubic (e.g. $SrTiO_3$, $BaZrO_3$) to tetragonal (e.g. $BaTiO_3$, $KNbO_3$, $PbTiO_3$) in the region $t>1$. $GdFeO_3$-type orthorhombic (*Pnma*) distortion is generally known to appear in the region $t<1$ due to the tilting of BO_6. Most important result of Fig.1 is ferroelectric materials appear both in regions $t<1$ and $t>1$. The ferroelectricity of ABO_3 in $t>1$ is intuitively clear from the uniaxially elongated oxygen octahedra.

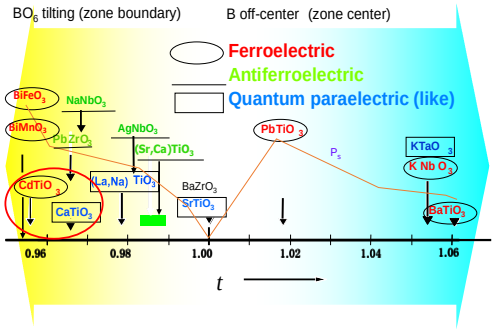

Fig.1 Tolerance factor *t vs.* dielectric/ferroelectric properties of perovskites.

Famous and important ferroelectric materials such as $BiFeO_3$, $BiMnO_3$ (metastable), $BiCoO_3$ (metastable), $PbVO_3$ (metastable), and $CdTiO_3$[2], some of which have larger electric polarization comparable to that of $PbTiO_3$, also exist in the region $t<1$. Chemical bonds between A-O triggers the ferroelectricity in the materials with $t<1$ and the caused polarization is not small compared to the materials in the region $t>1$, as clearly seen in Fig.1. These results encourage us to consider new materials with distorted polyhedra of other coordination numbers, different from perovskites, four[3], five, and seven. Recently we have reported $FeAlO_3$[4] with mixed coordination numbers of 4 and 6. More recently we have just begun the evaluation of the potential of wurtzite system, which was first studied by prof. Sawada's group [5]. Moriwake *et al.*[6] have calculated the possibility of polar materials, including wurtzite materials, switching to ferroelectric by the applied electric field. Detailed calculated data will be presented at the presentation to explore the possibility to get new ferroelectric in the tetrahedral system.

References

1. Rowley *et al.*, Nature Phys., vol.10, No.5 (2014), pp367-372.
2. Moriwake *et al.*, vol.84, No.10 (2011), pp104114 1-8.
3. Taniguchi *et al.*, Angewandte. Chem. Int, Ed., vol.52, No.31 (2013), pp8088-8092. Kim *et al.*, IUCrJ, vol.1, part 3 (2014), pp160-164.
4. Sawada *et al.*, JPSJ, vol.35, No.6 (1973), 946.
5. Hamasaki *et al.*, APL, vol.104, No.8 (2014), pp082906 1-5.
6. Moriwake *et al.*, Meeting Abstracts of Phys. Soc. Jpn., 2014.

Makoto **IWATA**

Nationality: Japanese

Address:
Department of Engineering Physics, Electronics and Mechanics, Graduate School of Engineering, Nagoya Institute of Technology, Nagoya 466-8555, Japan

E-mail: miwata@nitech.ac.jp

Education:
1994 Nagoya University (PhD)
1989 Shinsyu University (Bachelor)

Employment:
1994-2001 Nagoya University, Research Associate
2001-2002 Nagoya Institute of Technology, Research Associate
2002- present Nagoya Institute of Technology, Associate Professor

Selected publications:

1) "Temperature–field phase diagrams in $Pb(Mg_{1/3}Nb_{2/3})O_3$–29.5%$PbTiO_3$", Makoto Iwata and Ryuta Yokoi, Yusuke Sugiyama, Maeda Masaki, Yoshihito Tchi, and Yoshihiro Ishibashi: Feroelectrics **462** (2014) pp. 19–27.
2) "Dielectric Tunability near the Critical End Point in $Pb(Zn_{1/3}Nb_{2/3})O_3$-9%$PbTiO_3$", Makoto Iwata, K. Tanaka, Maeda Masaki, and Yoshihiro Ishibashi: Japanese Journal of Applied Physics **53** (2014) pp. 038004/1-3.
3) "Coexistence States near the Morphotropic Phase Boundary: II. The Scaling of the Free Energy in $PbZr_{1-x}Ti_xO3$", Makoto Iwata and Yoshihiro Ishibashi: Japanese Journal of Applied Physics **52** (2013) pp. 09KF07/1-5.
4) "Temperature–field phase diagrams in $Pb(Zn_{1/3}Nb_{2/3})O_3$–4.5%$PbTiO_3$ II", Makoto Iwata, Naoya Iijima, Msaki Maeda, and Yoshihiro Ishibashi: Ceramics International **39** (2013) S75-S79.
5) "Structural Phase Transition and Symmetry Change in $Bi_4Ti_3O_{12}$", Makoto Iwata, Kenichiro Ando, Masaki Maeda, and Yoshihiro Ishibashi: Journal of Physical Society of Japan **82** (2013) pp. 025001/1-2.
6) "Possible Commensurate Phases in $LuFe_2O_4$", Makoto Iwata and Yoshihiro Ishibashi: Journal of Physical Society of Japan **81** (2012) pp. 035003/1-2.

RCBJSF In-5

Electric Field Effects in $Pb(Zn_{1/3}Nb_{2/3})O_3$-7%$PbTiO_3$ Solid Solutions

M. Iwata[1], A. Amano[1], R. Nagahashi[1], M. Maeda[1], and Y. Ishibshi[2]

[1]I Department of Engineering Physics, Electronics and Mechanics Nagoya Institute of Technology, Japan

[2]Department of Applied Physics, Nagoya University, Japan

e-mail: miwata@nitech.ac.jp

Solid solution systems such as (1-*x*)$Pb(Zn_{1/3}Nb_{2/3})O_3$-*x*$PbTiO_3$ (PZN-*x*PT) are known as relaxor ferroelectrics. Among them, PZN-*x*PT having the morphotropic phase boundary (MPB) is a technologically important material mainly due to the giant dielectric and piezoelectric responses. A theoretical model for such physical properties near MPB was proposed on the basis of the Landau-type free energy function.[1)] It was also reported that temperatute(T)-field(E) phase diagrams including the critical end point(CEP) can be qualitatively reproduced using the Landau-type free energy function.[2)]

In our previous work, we investigted T-E phase diagrams in PZN-9%PT near MPB, and found that the diffuseness of the phase transition in (1-*x*)PZN-*x*PT considerably decreases when the dc biasing field is applied, implying that decrease of heterogeneity owing to the applied electric field may make the phase transition sharp.[3)]

To clarify the bulk property related to an avarage structure, we investigated the phase transition by using such an electric field effect. Fig. 1 shows the T-E phase diagram with the electric field along the $[111]_c$-direction in PZN-7%PT, where the measurment is carried out on heating or on changing the dc field after field cooling in PZN-7%PT. The stable region of the orthorhombic phase under the electric field was clarified.

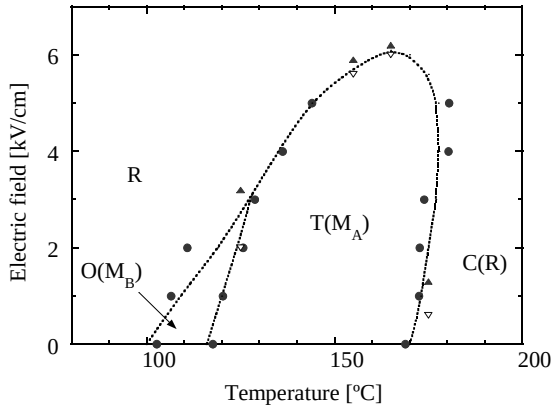

Fig. 1. Temperature-field phase diagram under the dc biasing field along the $[111]_c$-direction in PZN-7%PT.

References

1. Y. Ishibashi and M. Iwata: Jpn. J. Appl. Phys. **37**, L985 (1998).
2. M. Iwata, Z. Kutnjak, Y. Ishibashi and R. Blinc: J. Phys. Soc. Jpn. **77**, 034703 (2008).
3. M. Iwata, K. Tanaka, M. Maeda, and Y. Ishibashi: Ferroelectrics **440**, 67 (2012).

Andrei **KHOLKIN**

Dr. Andrei Kholkin received his B.Sc. and M.Sc. degrees in Physics from St. Petersburg State University and Ph.D. degree in Solid State Physics from the A. F. Ioffe Physical-Technical Institute (Russia), respectively. Since 1993, he has been working outside Russia and held research positions in Leibniz Institute for Solid State and Materials Research (Germany), Swiss Federal Institute of Technology (Switzerland) and Rutgers University (USA). He is currently a research coordinator and head of the functional imaging and nanocharacterization laboratory of the Center for Research in Ceramic and Composite Materials of the University of Aveiro (Portugal). His group develops multifunctional materials (including ferroelectrics and multiferroics) and scanning probe microscopy techniques. He is a coauthor of more than 400 technical papers in this area including numerous reviews and book chapters. He was a coordinator of three European projects on multifunctional materials and currently serves as an Associate Editor-in-Chief for the IEEE Transactions on Ultrasonics, Ferroelectrics and Frequency Control (TUFFC). He is a member of editorial boards of several scientific journals and serves in advisory boards of international conferences on ferroelectrics. He is a member of the Ferroelectric Committee of IEEE and was a recipient of the "Excellency" award from the Portuguese Foundation for Science and Technology. He has been a Technical Committee member of several international conferences and cofounded a new conference series "Piezoresponse Force Microscopy and Nanoscale Phenomena in Polar Materials" (proceedings published yearly in J. Appl. Phys.). He was a guest editor of the special issues on ferroelectrics published in TUFFC, Journal of Applied Physics and Materials Research Society Bulletin. Dr. Kholkin is a Fellow of IEEE (class 2012), and holds membership in IEEE, Materials Research Society and Portuguese Materials Society.

RCBJSF In-6

Nanoscale Piezoelectricity Due to Symmetry Breaking: an Atomic Force Microscopy Study

A.L. Kholkin

Department of Materials and Ceramics Engineering and Center for Research in Ceramic and Composite Materials (CICECO), University of Aveiro, Portugal

e-mail: kholkin@ua.pt

Electromechanical coupling is ubiquitous in nature and directly underpins sensing/actuating functionalities of various systems. Rapidly developing Piezoresponse Force Microscopy (PFM) and Electromechanical Strain Microscopy (ESM) techniques offer an amazing opportunity to explore electromechanical activity at the nanoscale with a few nm resolution that allows to uncover fundamental mechanisms of the local piezoelectric phenomena. Piezoelectric coupling may arise locally due to symmetry breaking in small dimensions and at the interfaces. In this presentation, I will briefly overview the new features in PFM and ESM as of today and present our recent results on nanoelectromechanical imaging in several novel materials to be used in multifunctional devices. The materials range will include centrosymmetric perovskites (such as $SrTiO_3$ and manganites with charge order states), hydroxyapatite thin films, and deformed graphene. The results are interpreted in light of the possible symmetry breaking induced by the highly inhomogeneous electric field and mechanical stress.

Hiroyuki **KIMURA**

PRESENT ADDRESS
Institute of Multidisciplinary research for Advanced Materials, Tohoku University
Katahira 2-1-1, Aoba, Sendai, Miyagi 980-8577, Japan
Tel: +81-22-217-5354
Email: kimura@tagen.tohoku.ac.jp

OBJECTIVE
Neutron and X-ray scattering study of structural physics on Multiferroics, Ferroelectrics, Transition metal oxides, and High-Tc superconductivity

EDUCATION
Tohoku University, Sendai, Japan
Ph. D. Physics, March 1999

EXPERIENCE
April, 1999 Research Associate in Institute of Multidisciplinary Research for Advanced Materials (IMRAM), Tohoku University
April, 2007 Assistant Professor in IMRAM, Tohoku University
April, 2008 Associate Professor in IMRAM, Tohoku University
April, 2013 Professor in IMRAM, Tohoku University

SELECTED PUBLICATIONS

- Control of magnetic interaction and ferroelectricity by nonmagnetic Ga substitution in multiferroic YMn2O5
  H. Kimura, et al. Phys. Rev. B **87**, (2013) 104414. **(Editor's Suggestion)**
- Magnetic-Field-Induced Magnetic Phase Transitions Associated with Ferroelectricity in Multiferroic ErMn2O5
  H. Kimura, et al. J. Phys. Soc. Jpn. **78**, (2009) 034718.
- Magnetically Induced Ferroelectricity in Multiferroic Compounds of RMn2O5
  H. Kimura, et al. Ferroelectrics **354**, (2007) 77. **(Invited review paper)**
- Ferroelectricity induced by an incommensurate commensurate magnetic phase transition in mutiferroic HoMn2O5
  H. Kimura, et al. J. Phys. Soc. Jpn. **75**, (2006) 113701. **(Editor's Choice)**
- Novel In-Gap Spin State in Zn-Doped La1:85Sr0:15CuO4
  H. Kimura, et al. Phys. Rev. Lett. **91**, (2003) 067002.

HOBBIES
Free climbing, Bicycle

RCBJSF In-7

Neutron Diffraction Study of Magnetism and Ferroelectricity in $R\mathrm{Mn_2O_5}$ (R = Rare-Earth, Bi, Y) Multiferroics

H. Kimura and Y. Noda

Institute of Multidisciplinary Research for Advanced Materials, Tohoku University, Sendai, Japan

e-mail: kimura@tagen.tohoku.ac.jp

$R\mathrm{Mn_2O_5}$ (R = rare-earth, Bi, Y) is one of the most famous and prototypical mutiferroics. In this system, ferroelectricity or magnetism can be controlled by external field such as magnetic field or electric field, which is called as a magnetoelectric effect. Since electric polarization can be induced only in antiferromagnetic phase, magnetic order has been thought to be a primary order parameter for ferroelectricity.

We have carried out neutron diffraction study under magnetic fields for many types of $R\mathrm{Mn_2O_5}$ single crystals to elucidate microscopic mechanism of magnetically induced ferroelectricity. The study have shown that ferroelectric phase transitions simultaneously occur with magnetic phase transitions induced by magnetic field, suggesting that the magnetic structure consisting of R^{3+} spin, Mn^{3+} spin, and Mn^{4+} spin induces the electric polarization in this system. Our magnetic structure analysis using neutron diffraction clarified that the arrangement of Mn^{3+} and Mn^{4+} spins commonly seen regardless of the type of R^{3+} ions essentially contributes to the electric polarization. On the contrary, the direction of 4*f* magnetic moment on R^{3+} site strongly depends on the type of rare-earth elements (electronic state, single ion anisotropy, and so on), indicating that the 4*f* magnetic moment plays an important role for a rich variety of magnetoelectric effects in this system.

We recently have found in $\mathrm{EuMn_2O_5}$ that magnetic phase transition is induced by applying hydrostatic pressure, where the ferroelectric transition occurs and the electric polarization enhanced. Magnetic structure analysis under pressure have revealed that the suppression of cycloidal magnetic structure increases the electric polarization in this material.

Acknowledgment

This study has been supported by “KAKENHI” programs of Scientific Research (B) (24340064), Scientific Research (A) (21244051), Challenging Exploratory Research (23654098), and of Scientific Research on Priority Areas “Novel States of Matter Induced by Frustration” (19052001).

Seiji KOJIMA

Name and Date of Birth: Seiji Kojima
April 22, 1951

Nationality Japanese

Position Professor, Division of Materials Scinece, University of Tsukuba

Address 1-1-1, Tennoudai, Tsukuba, Ibaraki 305-8573, Japan
Tel: +81-(029)-853-4967, 5307, Fax: +81-(029)-853-4490, kojima@ims.tsukuba.ac.jp

Education: 1979, University of Tokyo (PhD)
1974, University of Tokyo (Bachelor)

Employment 1979-1980 JSPS PD Fellow, University of Tokyo
1980-1981 Research associate, University of Tsukuba
1981-1994 Assistant professor, University of Tsukuba
1994-2002 Associate Professor, University of Tsukuba
2002- Professor, University of Tsukuba 2011-Chair, Division of Materials Science

Professional Societies: American Physical Society
American Ceramic Society
IEEE

Committees Chairman of organizing committee, Ultrasonic Electronics Symoposium, Tokyo, 2014
Vice-Chairman of organizing committee, 12th Russia/CIS/Baltic/Japan Symposium on Ferroelectricity, Riga, 2014
Topical editor, Current Applied Physics
Editorial board, Ferroelectrics

Awards and Honors: JJAP Editorial Award (Japan Society of Applied Physics)

Publications: Over 300 publications.

Some recent ones:

1. S. Tsukada, T. H. Kim, and S. Kojima, APL Mater. **1**, 032114-1-7 (2013), "Large acoustic thermal hysteresis in relaxor ferroelectric Pb(Zn1/3Nb2/3)O3-PbTiO3"
2. J. Zushi, T. Ariizumi, S. Kojima, and R. Wang, and H. Bando, Jpn. J. Appl. Phys. **52** (2013) 07HB02, "Formation of morphotropic phase boundary in (Na0.5K0.5)NbO3-BaZrO3(Bi0.5Li0.5)TiO3 lead-free piezoelectric ceramics"
3. M. Maczka, A. Majchrowski, J. Hanuza, and S Kojima, J. Phys.:Cond. Matt. **25** (2013) 025901. "Temperature-dependent IR and Raman scattering studies of phase transitions in K2MgWO2(PO4)2"
4. S. Tsukada, Y. Hidaka, S. Kojima, A. A. Bokov, and Z.-G. Ye, Phys. Rev. B **87** (2013) 014101. "Development of nanoscale polarization fluctuations in relaxor-based (1-x) Pb(Zn1/3Nb2/3)O3 -xPbTiO3 ferroelectrics studied by Brillouin scattering"
5. T.-H. Kim, J.-H. Ko, and S. Kojima, Jpn. J. Appl. Phys. 52 (2013), "Ferroelectric phase transition behaviors in Pb(In1/2Nb1/2)O3-Pb(Mg1/3Nb2/3)O3-PbTiO3 single crystals studied by Micro-Brillouin light scattering"

RCBJSF In-8

Broadband Terahertz Time-Domain Spectroscopy of Ferroelectric Crystals

S. Kojima and T. Mori

Division of Materials Science, University of Tsukuba Tennodai 1-1-1, Tsukuba, Ibaraki 305-8573, Japan

e-mail: kojima@ims.tsukuba.ac.jp

The far-IR spectroscopy has been extensively applied to various kinds of ferroelectric materials to investigate IR active soft optic phonon and relaxation process of polarization fluctuations. By using the incoherency of light sources, the many far-IR studies were reported on the frequency-dependent absorption, but not the real and imaginary parts of dielectric constants. The new technique of coherent terahertz generation enabled to determine real and imaginary parts of dielectric constant uniquely, and terahertz time domain spectroscopy (THz-TDS) attracted much attention. However, the most of the THz spectra until now were measured between 0.5 and 3 THz, where 3 THz is equivalent to 100 cm^{-1}(wavenumbers) [1]. Recently widely tunable monochromatic Cherenkov phase-matched terahertz (THz) wave generator was developed recently, and the frequency range of THz-TDS has been extended up to 6 THz in organic materials [2,3]. In this study, broadband THz-TDS was applied to various kinds of ferroelectric crystals from 0.2 to 6.5 THz. Both transmission and reflection spectra were measured to determine real and imaginary parts of dielectric constants in the far-IR range, and the results were shown on technologically important ferroelectric crystals such as $LiTaO_3$, $LiNbO_3$[4], $SrTiO_3$[5], and β-$Gd_2(MoO_4)_3$.

References

1. S. Kojima, N. Tsumura, M. Wada Takeda, and S. Nishizawa, Phys. Rev. B **67**, 035102 (2003).
2. S. Kojima, T. Shibata, H. Igawa, and T. Mori, IOP Conf. Series: MSE. **54**, 012001 (2014).
3. T.Shibata, H. Igawa, T.H. Kim, T. Mori, and S. Kojima, J. Mol. Struct. **1062**, 185 (2014).
4. H. Igawa, T. Mori, and S. Kojima, Jpn. J. Appl. Phys. **53**, 05FE01 (2014).
5. T. Mori, H. Igawa, and S. Kojima, IOP Conf. Series: MSE. **54**, 012006 (2014).

Matthias KRACK

Personal Data:

Name: Matthias Krack, Dr. rer. nat.,
born on August 24, 1963 in Hannover, Germany
Nationality: German
Official address: Paul Scherrer Institute (PSI)
Nuclear Energy and Safety Research Department (NES)
Laboratory for Reactor Physics and Systems Behaviour (LRS)
OHSA/D07
5232 Villigen PSI
Switzerland
Phone: +41 (0)56 310 58 56
FAX: +41 (0)56 310 23 27
E-Mail: matthias.krack@psi.ch

Academic Education:

- Pre-Diploma in chemistry, University of Hannover, 1985
- Diploma in chemistry, University of Hannover, 1989
- Dr. rer. nat. in Theoretical Chemistry, University of Hannover, 1993

Employment History:

- Research assistant (Analytical Chemistry), University of Hannover, 1986–1987
- Research assistant (Theoretical Chemistry), University of Hannover, 1988–1989
- Research associate (Theoretical Chemistry), University of Hannover, 1990–1998
- Research associate at the Max Planck Institute for Solid State Research Stuttgart (Department Parrinello), 1998–2001
- Senior research associate (Oberassistent) at the Swiss Federal Institute of Technology (ETH Zurich), Department of Chemistry and Applied Biosciences, 2001–2007
- Materials scientist at the Paul Scherrer Institute (PSI), since September 1, 2007

Main Research Activities:

- Atomistic simulation of nuclear materials especially fuel materials like uranium dioxide
- Development and application of empirical potential and electronic structure methods especially density functional theory (DFT) based methods
- Development of the open source code CP2K (http://www.cp2k.org)
- Study of transition metal compounds (e.g. pyrite) and phase-change materials (e.g. GST)
- New techniques for accelerated (*ab initio*) molecular dynamics simulations

FM&NT In-9

Electronic Structure Simulations of Uranium Dioxide

M. Krack

Paul Scherrer Institute, Switzerland

e-mail: matthias.krack@psi.ch

Reliable simulations for actinide materials are important as a complementary alternative to experimental investigations, because experiments with such usually hazardous materials are difficult and costly. During the recent decades density functional theory (DFT) has proven to be such a method for condensed phase actinide systems. However, the accurate description of the strong correlation of the 5f electrons still poses a challenge for current density functionals and in fact a plain DFT method predicts uranium dioxide (UO_2) to be metallic. As a remedy Anisimov *et al.* [1] proposed the addition of a Hubbard-like U term to the DFT functional. This term introduces an energy penalty for the delocalized 5f electrons which "encourages" the 5f electrons to localize. This so-called DFT+U method improves indeed many physical properties with respect to the experiment, but, unfortunately, it creates also a manifold of possible localization patterns for the 5f electrons at each uranium site which causes the occurrence of metastable states. Several recipes have been devised in the literature to tackle this problem to ensure a convergence to the true electronic ground state for a given atomic configuration [2-5]. In this work fully unconstrained cell optimizations of UO_2 bulk model systems are presented using the DFT+U implementation in the CP2K code [5,6]. Different effective U_{eff} values are employed in the framework of the DFT+U approach proposed by Dudarev [7] for various electronic density guesses. The detected low-lying states are presented and their properties are analyzed.

References

1. V. I. Anisimov et al., Phys. Rev. B 44, 943 (1991)
2. B. Dorado et al.,, Phys. Rev. B **79**, 235125 (2009)
3. B. Meredig et al., Phys. Rev. B **82**, 195128 (2010)
4. H. Y. Geng et al., Phys. Rev. B **82**, 094106 (2010)
5. J. Rabone, M. Krack, Comput. Mat. Sci. **71**, 157-164 (2013)
6. CP2K developers group 2000-2014, http://www.cp2k.org
7. S. L. Dudarev et al., Philos. Mag. B **75**, 613 (1997)

Svetlana **KULKOVA**

Affiliation

Head scientists of the Institute of Strength Physics and Materials Science, Siberian Branch of the Russian Academy of Sciences, Laboratory of physics of non-linear media, pr. Akademichesky 2/4, Tomsk, 634021, Russia,Tel.: +7 (3822) 286952, Fax.: +7 (3822) 492576

Prof. of the Department of Theoretical Physics of the Physical Faculty, National Research Tomsk State University, pr. Lenina 36, Tomsk, 634050, Russia

Education

1997 – Doctor of Science in Physics and Mathematics, Institute of Strength Physics and Materials Science, SB RAS, Tomsk. Thesis: "The investigation of the electronic properties of advanced materials"

1984 – Candidate of Physical and Mathematical Sciences, Tomsk State University. Thesis: "Electronic structure of transition metal alloys NiMn, TiNi, FeV, etc."

1976-1978 – Post-graduate student of Physical Dept. of Tomsk State University

1970-1975 – Student of Physics Faculty of Tomsk State University.

Current research projects:

1. Hydrogen storage materials and hydrogen diffusion
2. First-principles study of the formation of oxides layers on Ti-based alloys and the oxide-matrix interface
3. Investigation of halogen interaction with A3B5 semiconductor low-index surfaces and their influence on the surface reconstruction transformations
4. Ab-initio investigations of the electronic structure of surface and grain boundaries in metals and alloys.
5. Ab-initio study of adhesion at the metal-ceramics interfaces.
6. Physics and chemistry of advanced materials.
7. Martensitic transformations in the Heusler alloys.

Academic Honors, Awards and Prizes

Special worship award of SB RAS (veteran SB RAS), Veteran of RAS, Silver sigma award, Siberian Branch of RAS Prize, Soros and USAID grants, diplomas of many national conferences.

Scientific activity was supported by numerous grants of the Russian Foundation for Basic Researches (14-02-91150a_NSCF, 13-02-98017r_a, 09-03-00523a, 09-02-01045a, 08-02-92201a_NSFC, 07-02-01452a, 05-02-16074a, 04-02-17221a, 04-02-39009a_NSCF, 02-02-16336a, etc.) and international grants (DFG Schm 746/133-1, 111-1, 87-1, 81-1, INTAS, CRDF, NATO, KOSEF, etc.).

Visiting professor of Institute for Materials Testing, Materials Science and Strength of Materials of University of Stuttgart, Stuttgart, Germany (2007-2014), Donostia International Physical Centre, San-Sebastian, Spain (2009), EMAT, Antwerp RUCA University (2003), Pohang University of Science and Technology (2000-2002), etc. Collaborators from Germany (Prof. S. Schmauder, Dr. Hocker), Belgium (Prof. D. Schryvers), China (Prof. R.Yang, Dr. Q.M. Hu), Japan (Prof. T. Kakeshita), etc.

FM&NT In-10

Influence of Interstitial Impurities on the Griffith Work in Ti-based Alloys

A. Bakulin[1,2], S. Kulkov[2], S. Kulkova[1,2], S. Hocker[3], S. Schmauder[3]

[1]Institute of Strength Physics and Materials Science SB RAS, Tomsk, Russia

[2]National Research Tomsk State University, Russia

[3]Institute of Materials Testing, Materials Science and Strength of Materials, University of Stuttgart, Germany

e-mail: kulkova@ispms.tsc.ru

It is known that segregated impurities can induce embrittlement of materials. For example, even small concentration of H reduces the mechanical strength and may limit some industrial applications of advanced materials. In order to understand the grain boundary (GB) cohesion it is necessary to find general rules for the description of the relationship between microscopic features and macroscopic material properties. In this work we investigate the influence of the interstitial (H, B, C) and substitutional (Co, Ni, Pd, Al) impurities on the chemical bonds at the GB and surface in the series of the B2-TiMe alloys, where Me=Fe, Co, Ni, Pd. The atomic and electronic structures of TiMe alloys with Σ5(310) GB and (310) surface were investigated by the plane-wave pseudopotential method. The change of the Griffith work (GW) due to an interstitial impurity was calculated as the difference in GW for impurity doped and undoped systems or the difference between segregation energies of the impurity to surface and GB. The influence of impurities on H sorption properties was also studied. It was shown that hydrogen sorption energies at the grain boundary and surface depend strongly on the H local environment. The most preferential sites for both B and C segregation are the same as for H. The analysis of the electronic properties allows us to establish the microscopic nature of the chemical bonding of interstitial impurities at the interfaces. It was found that H decreases the surface energies more significantly than the GB energy, which results in decrease of the Griffith work and indicates also the decrease of the strength of the grain boundary. The segregation of H at the GB makes intergranular fracture much easier because the bonding between metal atoms, which are neighbors of H, is weakened. In contrast to H other impurities (B or C) lead to opposite effect on the Griffith work. Our estimation of the Griffith work for the alloy containing both B and H atoms gives its increase in comparison with undoped alloy but the effect of carbon on the GB strengthening during hydrogenation seems to be negligible. The contributions of the chemical and elastic mechanisms to the binding energies and GW are discussed.

Yoshihiro **KUROIWA**

Affiliation: Department of Physical Science, Graduate School of Science, Hiroshima University
Address: 1-3-1 Kagamiyama, Higashi-Hiroshima, Hiroshima 739-8526, JAPAN
Phone: +81-82-424-7397, Fax: +81-82-424-7398, E-mail: kuroiwa@sci.hiroshima-u.ac.jp

Date of Birth: July, 1962

Education: BS of Engineering in Physics, Osaka University, March, 1985, MS of Engineering in Physics, Osaka University, March, 1987, and PhD of Engineering, University of Tsukuba, March, 1990

Employment: Research Associate, Chiba University, April, 1990, Associate Professor, Okayama University, April, 1998, and Professor, Hiroshima University, October, 2005

Current Areas of Research Interest: (1) Phase transitions of solids (ferroelectrics, strongly correlated materials, and layered materials), (2) Synchrotron radiation science (powder & single-crystal diffraction, charge density study, and time-resolved crystal structure analysis)

Awards: Scientific Award in the Crystallographic Society of Japan (2005), and the Japan Society of Applied Physics Paper Award (2012)
Current Membership of Editorial Boards: Japanese Journal of Applied Physics and Membership Journal of the Physical Society of Japan
Current Membership of International Committees: Chair of organization committee in 10th Japan-Korea Conference on Ferroelectrics (2014)

Publication: Listed below are representative for current research interest in over 200 original papers.

1) Y. Kuroiwa, S. Aoyagi, A. Sawada, J. Harada, E. Nishibori, M. Takata and M. Sakata, Phys. Rev. Lett. **87**, 217601 (2001), "Evidence for Pb-O Covalency in Tetragonal $PbTiO_3$."
2) H. Tanaka, Y. Kuroiwa and M. Takata, Phys. Rev. B **74**, 172105 (2006), "Electrostatic Potential of Ferroelectric $PbTiO_3$: Visualized Electron Polarization of Pb Ion"
3) C. Moriyoshi, S. Hiramoto, H. Ohkubo, Y. Kuroiwa, H. Osawa, K. Sugimoto, S. Kimura, M. Takata, Y. Kitanaka, Y. Noguchi and M. Miyayama, Jpn. J. Appl. Phys. **50**, 09NE05 (2011), "Synchrotron Radiation Study on Time-resolved Tetragonal Lattice Strain of $BaTiO_3$ under Electric Field"

RCBJSF In-9

Valence Electron Distributions of Ferroactive ions in Perovskite Oxides and Polar Lattice Distortions

Y. Kuroiwa

Department of Physical Science, Hiroshima University, Japan

e-mail: kuroiwa@sci.hiroshima-u.ac.jp

The polar lattice distortion and the lattice stability of perovskite-type oxides with the chemical formula ABO_3 are strongly influenced by substituting other ions for the *A*- and/or *B*-site ions. For example, primal 2nd-order (pseudo) Jahn-Teller distortions are caused in $BaTiO_3$ by the octahedrally coordinated high-valent d^0-ness Ti ion at the *B*-site, whereas a structure with a large tetragonal distortion is stabilized up to higher temperature in $PbTiO_3$ by cooperation of the Ti ion at the *B*-site and the Pb ion with lone pair electrons at the *A*-site. Most of valence electrons in perovskite-type oxides are distributed in shells of oxygen ions in general, while a small part of valence electrons of such ferroactive ions remains at the *A*- and/or *B*-sites to form covalent bonding with oxygen ions. The chemical bonding between the ferroactive ions and the oxygen ions is a clue for understanding phase transitions in perovskite-type oxides.

Our group has been devoted to visualizing the electron density distributions of perovskite-type oxides by analyzing the synchrotron-radiation x-ray powder diffraction (SXRD) data measured at SPring-8 using the maximum entropy method (MEM)/Rietveld method [1, 2]. In this study, the distributions of valence electrons in the outer shells of atoms are derived accurately from the SXRD data of various perovskite-type oxides to prove the characteristic chemical bonds which govern the ferroelectric phase transition. The obtained results provide direct experimental evidence that the hybridization of orbitals forming the *B*-O bonds weakens the short-range repulsion force, and causes the polar lattice distortion on the BO_6 octahedron.

References

1. Y. Kuroiwa, S. Aoyagi, A. Sawada, J. Harada, E. Nishibori, M. Takata, and M. Sakata, Phys. Rev. Lett. **87**, 217601 (2001)
2. H. Tanaka, Y. Kuroiwa, and M. Takata, Phys. Rev. B**74**, 172105 (2006)

Tomi **LAURILA**

Professor Tomi Laurila received the D.Sc. degree (with honours) in electronics production technology from the Helsinki University of Technology in 2001. The thesis was focused on the solid-state reactions in different metal/silicon systems and development of feasible diffusion barriers to be used in Cu metallized IC's. At the moment he is Associate Professor in the field of Microsystem technology and holds an adjunct professorship on Electronics Reliability and Manufacturing.

Presently his research involves the study of interfacial reactions between dissimilar materials used in microsystems, biocompatibility issues related to different types of materials and electrochemical measurements of neurotransmitters from the brain. He has published extensively on the thermodynamic-kinetic analysis of interfacial reactions, electrochemical detection of biomolecules and issues related to reliability testing of electronic devices. Prof. Laurila is also responsible for the teaching of material science, electronics reliability and bioadaptive technology to under- and post-graduate as well as postdoctoral students.

Pl-2

Hybrid Carbon Nanomaterials for Electrochemical Detection of Biomolecules

T. Laurila

Department of Electronics, School of Electrical Engineering, Aalto University, Finland

e-mail: tomi.laurila@aalto.fi

It has been estimated that currently up to 27 % of the adult population in Europe are affected by mental and neurological disorders [1]. Many of these disorders are directly related to different neurotransmitters, specifically to the amount of neurotransmitters present in different parts of brain.

Carbon based materials have frequently been used in *in vitro* experiments for detecting neurotransmitters. Recently, promising results in the field of electrochemical detection of neurotransmitters have been achieved by using different types of electrodes coated with thin films of diamond-like carbon (DLC) [2-4] DLC is a metastable form of amorphous carbon of which properties are determined by the ratio of sp2 and sp3 bonds, the amount of hydrogen and the deposition method of DLC [5]. All the different DLC types display some of the typical properties of diamond, such as stability, good biocompatibility and resistance to bacterial adhesion [2], making them feasible materials for biomedical applications. However, the sensitivity of the DLC electrodes is typically not high enough to detect the very low concentrations of neurotransmitters present in *in vivo* conditions.

Thus, there is a clear need to combine DLC thin films with other more electrocatalytic forms of carbon or to induce enhanced reactivity to the DLC surface by some other means. In this communication we will present three methods to realize the required higher sensitivity: (i) carbon nanotubes (CNT's) grown directly on top of DLC electrode, (ii) chemically reduced graphene oxide combined with DLC electrode and (iii) introduction of surface topography to DLC by using Ti adhesion layer underneath the electrode material. We will show that all of the three approaches can provide the much increased sensitivity towards our benchmark molecule, which is dopamine, over plain DLC electrodes. However, there are also clear differences among the three types of thin film materials with respect to stability and electron transfer rate, for instance. Finally, we will discuss about further possibilities to fabricate other hybrid nanocarbon materials.

References

1. Wittchen, H., Jacobi, F., Rehm, J., Gustavsson, A., Svensson, M., Jönsson, B., Olesen, J.,Allgulander, C., Alonso, J., Faravelli, C., Fratiglioni, L., Jennum, P., Lieb, R., Maercker A., van Os, J., Preisig, M., Salvador-Carulla, L., Simon, R. and Steinhausen, H-C., "Cost of disorders of the brain in Europe 2010", European Neuropsychopharmacology, 21, 655-679, (2011)

2, Kaivosoja, E., Sainio, S., Lyytinen, J., Palomäki, T., Laurila, T., Kim, S., Han, J., and Koskinen, J., "Carbon Thin Films as Electrode Material in Neural Sensing", Surface and Coatings Technology, (in print), (2014)

3. Laurila T., Rautiainen A., Sintonen S., Jiang H., Kaivosoja E., and Koskinen J., "Diamond-like carbon (DLC) thin film bioelectrodes: Effect of thermal post treatments and the use of Ti adhesion layer ", *Materials Science and Engineering C: Materials for biological applications*, **34,** pp. 446-454, (2014).

4. Kaivosoja, E., Berg, E., Rautiainen, A., Palomäki, T., Koskinen, J., Paulasto-Kröckel, M. and Laurila, T., " Improving the Function of Dopamine Electrodes with Novel Carbon Materials", Conf Proc IEEE Eng Med Biol Soc. 632-634, 2013

5. J. Robertson, "Diamond-like amorphous carbon", Materials Science and Engineering R, 129-281, 2002

Sergey LUSHNIKOV

Ferroelectricity and Magnetism Laboratory
A.F. Ioffe Physical Technical Institute
26, Politekhnicheskaya
St. Petersburg, 194021
Russia

Phone: +7(812) 515-9234
Fax: +7(812) 515-6747

e-mail: sergey.lushnikov@mail.ioffe.ru

Date and Place of Birth: October 22, 1959, Leningrad, USSR

Education:

MD, Physical Department, Leningrad State University, 1985
Ph.D. in Physics, A.F.Ioffe Physical Technical Institute, St.Petersburg, 1992, advisor Dr. I.G. Siny
Dr.Sci. in Physics, A.F.Ioffe Physical Technical Institute, St.Petersburg, 2004

Permanent Positions:

Head of Laboratory of Ferroelectricity and Magnetism, 2009 to present;
Professor, leader scientist, 2005 to 2009;
Senior Scientist, 1998 to 2004;
Researcher Scientist, 1992 to 1998;
Researcher, 1987 to 1992;
Graduate Student, 1985 to 1987; Department of Ferroelectricity and Magnetism, A.F.Ioffe Physical Technical Institute, Russian Academy of Sciences, St.Petersburg.

Area of expertise:

Optic (Brillouin and Raman) and Neutron Spectroscopy, Phase Transitions, Ferroelectrics and Ferroelastic, Multiferroics, Lattice Dynamics, Superionic Conductors, Glass-like State, Dynamic of Biopolymers.

Memberships Fellow, Section of Ferroelectrics and Dielectrics of Committee of Condense Matter Physics Russian Academy of Sciences
American Physical Society

Professional service Member of Organized or Program Committee:
Russian Ferroelectrics Conference (1996 to present);
2 and 3^{d} International Seminar on Relaxor Ferroelectrics (Dubna, 1998, 2000)
Japan-CIS/Baltic-Russian Conference on Ferroelectrics (Petersburg, 2002; Tsukuba 2006, Vilnius 2008, Yokohama, 2010; Ekaterinburg 2012, Riga 2014);
Head of Organizing Committee "**Quantitative Imaging and Spectroscopy in Neuroscience"** (QISIN), 16-19 September 2012, Saint-Petersburg, Russia.
Co-chairman of Program Committee "International Workshop on Relaxor Ferroelectrics", 1-6 July 2013, Saint-Petersburg, Russia.
Head of State Selection Committee of St.Petersburg State Politekchnikal University, Biophysics Department.
Member of State Selection Committee of St.Petersburg State University, Crystallograpgy Department.

PhD Thesis adviser –
E.A. Rogacheva (2000), "Phase transition dynamics of relaxor ferroelectrics in light scattering spectra"
S.N. Gvasaliya (2001), "Features of the lattice dynamics of complex perovskites"
Anna V. Svanidze (2007), "Light and neutron scattering at phase transformations in the lysozyme"

Teaching: Lecture for undergraduate students "Lattice dynamic in ferroelectrics" Tokyo Institute of Technology, 2008.
Lecture for undergraduate students "Lattice dynamic in crystals" St.Petersburg State University, 2011 to present.

RCBJSF In-10

Central Peak and Quasi-Elastic Light Scatering in Cubic Relaxor Ferroelectrics

S. Lushnikov[1], and S. Kojima[2]

[1]A.F. Ioffe Physical Technical Institute of RAS, 194021, St.Petersburg, Russia

[2]Insitute Materials Science, University of Tsukuba, Tsukuba, Ibaraki 305-8573, Japan

e-mail: sergey.lushnikov@mail.ioffe.ru

In our report results of studying of $PbMg_{1/3}Nb_{2/3}O_3$ (PMN), $PbMg_{1/3}Ta_{2/3}O_3$ (PMT), $PbSc_{1/2}Ta_{1/2}O_3$ (PST), and $Na_{1/2}Bi_{1/2}TiO_3$ (NBT) crystals by Raman and micro-Brillouin light scattering are presented. Need to note, that PMN, PMT, PST and NBT crystals are cubic relaxor ferroelectrics.

It is clearly seen in temperature behavior of the low-frequency vibration spectra: the velocity anomaly and corresponding broad maximum of damping in relaxors well correlate with the main dielectric maximum in the vicinity of a diffuse phase transition temperature. The anomalies are absent in $BaMg_{1/3}Ta_{2/3}O_3$ crystals where the acoustic response is determined by anharmonicity. Unusual frequency dispersion of the longitudinal acoustic phonons (LA) in PMN and PMT crystals was observed in our experiments that were in a good agreement with mode-coupling phenomena in neutron scattering. Investigation of the Brillouin scattering by Sandercock type tandem system gives possibility for correct analysis of the low frequency part of the vibration spectra of the crystals. We observed quasielastic light scattering and separated this addition contribution from the scattering spectra of the studied crystals vs. temperature. It was found that quasielastic light scattering in relaxors has a complicate structure and temperature behavior.

Presence of the quasielastic scattering with such properties (relaxation mode) shows that despite previous expectations order-disorder behaviour plays an important role in the dynamics of the diffuse phase transition.

In present report we would like to discuss: *(1)* Our results of broadband light scattering studies *(2)* Relation of our observation with previously published neutron and light scattering data [1-4].

References

1. I.G.Siny, S.G.Lushnikov, R.S.Katiyar and E.A.Rogacheva Phys.Rev.B **56**, 7962 (1997).
2. I.G. Siny, et.al., Physica B, 293, 382 (2001).
3. S.G. Lushnikov, F.M. Jiang and S. Kojima Sol.State Commun.122, 3-4 129 (2002).
4. S.N. Gvasaliya, S.G. Lushnikov, B. Roessli Phys.Rev. B, **69**, 092105, (2004).
5. R.A. Cowley, et.al., Advances in Physics, **60**, 229 (2011).
6. Akitoshi Koreeda et.al. Phys.Rev.Let., **109**, 197601 (2012).

Rotraut **MERKLE**

Rotraut Merkle received her PhD in Physical Chemistry and then joined the department of Physical Chemistry at the Max-Planck Institute for Solid State Research in Stuttgart. Research interests range from fundamental aspects of point defect formation and transport in ionic solids to detailed investigations of reaction kinetics at oxide surfaces and properties of grain boundaries and heterointerfaces. The experimental studies are complemented by phenomenological or ab-initio modelling. These research intereststs are closely related to applications such as solid oxide fuel cells (based on proton as well as oxide ion conducting electrolytes), gas sensors and heterogeneous catalysis.

FM&NT In-11

Mixed Conducting Perovskites as Solid Oxide Fuel Cell Cathode Materials: Insight from Experiments and Theory

R. Merkle[1], D. Poetzsch[1], D. Gryaznov[2], E. Kotomin[1,2], J. Maier[1]

[1]Max Planck Institute for Solid State Research, Stuttgart, Germany

[2]Institute of Solid State Physics, University of Latvia, Latvia

e-mail: r.merkle@fkf.mpg.de

Slow kinetics of the oxygen reduction reaction at the cathode is one of the main limiting factors for the performance of solid oxide fuel cells. The cathode material should not only conduct electronic carriers, but also transport ions between the electrolyte and the interface to the gas phase allowing the reaction to extend beyond the electrolyte/electrode/gas triple phase boundary. Thus, for fuel cells based on proton conducting oxides such as Y-doped $BaZrO_3$, mixed proton/hole conducting oxides are highly desired. The defect chemistry of such materials will be discussed on the example of $Ba_{0.5}Sr_{0.5}Fe_{0.8}Zn_{0.2}O_{3-\delta}$ (BSFZ) perovskite based on thermogravimetry experiments [1] and numerical simulations. Trends concerning water incorporation into related perovskites will further be analyzed with the help of ab initio calculations.

The kinetics of the oxygen exchange reaction for BSFZ on $Ba(Zr,Y)O_{3-\delta}$ electrolytes is investigated on dense thin film microelectrodes by impedance spectroscopy [2]. The results indicate that the proton conductivity of BSFZ indeed suffices to transport protons from the $Ba(Zr,Y)O_{3-\delta}$ electrolyte through the dense BSFZ film to the gas interface, where O_2 is reduced to water. This also means that oxygen is not necessarily incorporated into the perovskite to perform the reduction reaction. The results are compared to cathode materials on oxide ion conducting electrolytes (YSZ, CGO). For perovskites such as $(La,Sr)MnO_{3-\delta}$ or $Ba_{0.5}Sr_{0.5}Co_{0.8}Fe_{0.2}O_{3-\delta}$ on YSZ, the reaction mechanism is quite well-understood based on experimental correlations [3] and ab initio calculations [4].

References

1. D. Poetzsch, R. Merkle, J. Maier, in revision
2. D. Poetzsch, R. Merkle, J. Maier, J. Power Sources 242 (2013) 784
3. L. Wang, R. Merkle, Y. A. Mastrikov, E. A. Kotomin, J. Maier, J. Mater. Res. 27 (2012) 2000
4. Y. A. Mastrikov, R. Merkle, E. Heifets, E. A. Kotomin, J. Maier, J. Phys. Chem. C 114 (2010) 3017

Yuji **NOGUCHI**

Yuji Noguchi was born in 1970 in Japan. He received a bachelor's degree, an M.S degree in electrical engineering, and a Ph.D. degree in materials science from Nagaoka University of Technology, Japan. He is an Associate Professor of the Research Center for Advanced Science and Technology at The University of Tokyo, Japan. His research interests are electronic materials, especially dielectric and ferroelectric crystals and ceramics with defect-induced functions. Associate Professor Noguchi received the Ikeda Award in 2005 (award for the outstanding paper by a Japanese young scientist published in 2005), the Young Investigator Award of the Ceramic Society of Japan, for "research on the ferroelectric characteristics of Bi-layered ferroelectrics," and the JCerSJ (Journal of the Ceramic Society of Japan) Award for the outstanding papers or review papers, for "New intergrowth Bi_2WO_6-Bi_3TaTiO_9 ferroelectrics," *J. Ceram. Soc. Jpn.,* vol. 109, no. 1, pp. 29–32, and the Ferroelectrics Young Investigator award of the IEEE Ultrasonics, Ferroelectrics, and Frequency Control Society in 2012, The Richard M. Fulrath Awards (The American Ceramic Society) "Enhanced properties in Bi-based ferroelectrics by defect engineering" in 2013.

RCBJSF In-11

Defect-Polarization Control for Enhancing Piezoelectric Properties of $BaTiO_3$-Based Single Crystals and Ceramics

Y. Noguchi[1], Y. Ichikawa[1], R. Inoue[1], Y. Kitanaka[1], M. Miyayama[1] and Y. Yoneda[2]

[1]Research Center for Advanced Science and Technique, The University of Tokyo. 4-6-1 Komaba, Meguro-ku, Tokyo 153-8904, Japan

[2]Reaction Dynamics Research Division, Japan Atomic Energy Agency, Sayo-cho, Sayo-gun, Hyogo 679-5148, Japan

e-mail: ynoguchi@crm.rcast.u-tokyo.ac.jp

The properties of ferroelectric materials are governed by domain (polarization) structures and their dynamics with respect to external stimuli. It has been reported that engineered domain configurations with a fine domain structure enhance piezoelectric and dielectric properties.[1-3] These enhanced properties are suggested to originate from a large response with electric field (E) around domain-wall (DW) regions.[2] It has been reported that charged DWs show a giant dielectric and piezoelectric response with E.[4]

One of the other intriguing characteristics of ferroelectrics is a photovoltaic effect. The photovoltaic charge separation has been reported to operate near the ferroelectric DWs with a distance of 1–2 nm. [5]

The defect-polarization control is defined as the domain engineering based on defect chemistry. This concept originates from the strong attractive interaction between ferroelastic DWs and oxygen vacancies ($V_O^{\bullet\bullet}$). [6-8] Our DFT calculations show that the energy of 90° DWs in $PbTiO_3$ is largely reduced by introducing $V_O^{\bullet\bullet}$ from 37 mJ/m^2 (perfect crystal) to 11 mJ/m^2 ($PbTiO_{2.833}$). In this study, $BaTiO_3$ (BT) single crystals are chosen as model materials and the doping of an acceptor of Mn is selected as a means for introducing $V_O^{\bullet\bullet}$ into BT.

Figure 1 (a) shows the piezoelectric strain coefficients (d) (the slope of S at low E's along <110>) as a function of Mn content (x). Mn (0.1 %)-BT showed a d of 630 pm/V, which was much larger than that of undoped BT (69 pm/V) and single domain BT crystals (86 pm/V[7]).

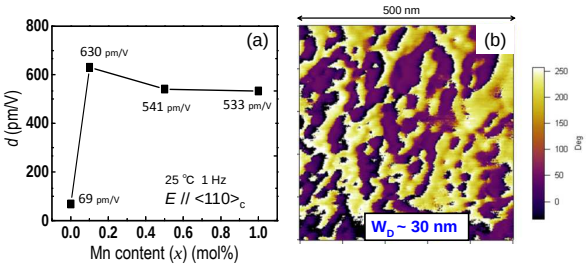

Fig.1. (a) Piezoelectric strain coefficient (d) as a function of Mn content (x) and (b) PFM phase image (in-plane) of Mn(0.1 %)-BT crystals poled along the <110> direction.

Figure 1 (b) shows the piezoresponse-force microscope (PFM) image (RCBJSF In-plane, phase) of Mn (0.1 %)-BT crystals poled along <110>. Mn-BT had a peculiar domain structure with a size of 20 ~ 40 nm. This domain size was much smaller than that of undoped BT poled along <110> (0.02 ~ 0.03 mm). These results show that the domain size of BT-based crystals became much smaller by the Mn doping.

References

1. S. E. Park. *et al*., *J. Appl. Phys*. **86**, 2746 (1999)
2. S. Wada. *Ferroelectrics*, **389**, 3 (2009).
3. T. Hoshina. *et al*., *Jpn. J. Appl. Phys*., **47**, 7607 (2008).
4. S.E.Park *et al*., *J. Appl. Phys*. **82**, 1804 (1997)
5. Yang *et al*., *Nature Nanotechnology*, **5**, 143 (2010)
6. Y. Kitanaka and Noguchi. *et al*., *Phys. Rev. B* **81**, 094114 (2010).
7. Y. Ichikawa and Noguchi. *et al*., *J. Ceram. Soc. Jpn.* (2014), in press.
8. Y. Kitanaka and Noguchi. *et al*., *Phys. Rev. B* (2014), in press.

Harald OBERHOFER

Personal Details

Nationality	Austria
Birthplace	Vienna, Austria
Date of birth	20.08.1980
Affiliation	Group leader (Habilitand), Chair for Theoretical Chemistry, TU Munich

Education

Feb. 2008	**PhD in Physics,** *University of Vienna,* Austria, with Prof. Christoph Dellago. *(graduation with distinction)*
July 2005	**Master des Sciences de la MatiŽre (MSc),** *Ecole Normale Supérieure Lyon,* France.
Oct. 2004	**Diploma in Physics (MSc),** *University of Vienna,* Austria. *(graduation with distinction)*

Work History

Feb. 2011 –	**Group leader (Habilitand),** *with Prof. Karsten Reuter,* Chair for Theoretical Chemistry, Technical University Munich.
Feb. 2012 – Jan. 2014	**von Humboldt Foundation post-doctoral research fellow,** *with Prof. Karsten Reuter,* Chair for Theoretical Chemistry, Technical University Munich.
Feb. 2008 – Jan. 2011	**Post-Doctoral research associate,** *with Dr. Jochen Blumberger,* Department of Chemistry, University of Cambridge.
Dec. 2004 – Jan. 2008	**Research assistant,** *with Prof. Christoph Dellago,* Faculty of Physics, University of Vienna.

Research Interests

Charge transfer	Theoretical description of charge transfer reactions in energy relevant materials (e.g. solar cells & photocatalysts).
Photocatalysis	Development of computational methods for the study and improvement of photocatalytic materials.
Free energy	Improvement of currently available methods for the calculation of free energy profiles.

Theoretical Chemistry, Dept. of Chemistry
TU Munich, Lichtenbergstr. 4, 85747 Garching, Germany
✉ *harald.oberhofer@tum.de* • *www.th4.ch.tum.de*

FM&NT In-12

A Theoretical Description of Photo-Catalytic Water Splitting nn Metal-Decorated Oxide Surfaces

H. Oberhofer, D. Berger, M. Sinstein, K. Reuter

Chair for Theoretical Chemistry, Technical University Munich, Germany

e-mail: harald.oberhofer@tum.de

Efficient, sustainable production of molecular hydrogen---a promising alternative to batteries in terms of energy storage---is still an unsolved problem. Implementation of direct water splitting using only sunlight and suitable metal-oxide photo-catalysts so far has been hampered by poor photon absorption properties of the materials and low reaction efficiencies. To understand the microscopic processes involved in photo-catalytic hydrogen production we implemented an implicit solvent model and a solid state QM/MM embedding scheme based on ChemShell into the all electron DFT code FHI-aims.[1] This allows us to study defects and charged systems---as occurring in electron-hole driven water splitting---without any spurious interaction between periodic images, while at the same time yielding the correct electrostatic potential and solvent screening in the QM region.

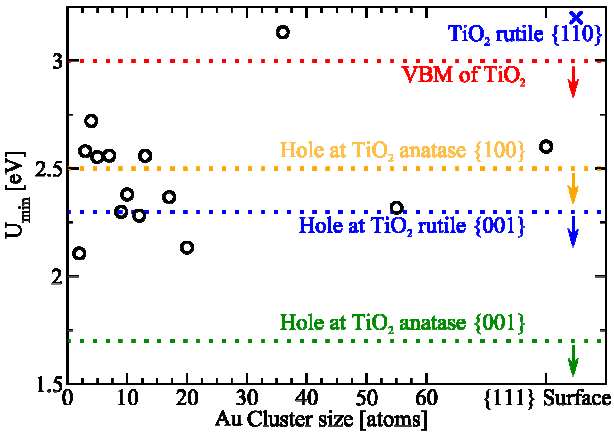

Fig 1: First screening results for TiO2 nano-patterned with Au nano-clusters. Clusters lying below a certain dotted line are predicted to be catalytically active on that surface.

In order to overcome the limitations of current water splitting setups we study the use of small metal clusters as co-catalysts, the microscopic effect of which is still poorly understood in literature. We develop an enhanced version of the thermodynamic approach pioneered by Nørskov and Rossmeisl,[2] of water oxidation reactions on metal clusters in the non-scalable size regime (less than 55 atoms) and compare with the bare extended oxide surface.[3]

References

1. V. Blum *et al.*, Comp. Phys. Commun. **180**, 2175 (2009)
2. A. Valdes *et al.*, J. Phys. Chem. C **112**, 9872 (2008)
3. H. Oberhofer, K. Reuter, J. Chem. Phys. **139**, 44710 (2013)

Toshio **OGAWA**

Toshio Ogawa is professor and professional engineer (“Gijyutsushi” since 1986) of electronic materials science and engineering in the department of electrical and electronic engineering, and head in the graduate school, Shizuoka Institute of Science and Technology, Japan.

He joined Murata Mfg. Co., Ltd. during 19 years in the fields of piezoelectric ceramics and thin films. Since 1992 he works at Shizuoka Institute of Science and Technology. Ogawa’s research focuses on functional materials such as ferroelectric ceramics, thin films and single crystals, and their applications.

He has authored over 100 journal articles and 170 patents. He received awards from the Japan Society of Powder & Powder Metallurgy (Award of Engineering Progress in 1985), from the American Ceramic Society (Fulrath Pacific Award in 1990), from Hamamatsu Electronic Engineering Organization (Takayanagi Memorial Award in 1993: Dr. Kenjiro Takayanagi is called "The Father of Modern Television"), from the Organizing Committee of the International Korea-Japan Seminar on Ceramics, 25th Anniversary (Distinguished Service Award in 2008), and from the Fulrath Okazaki Memorial Association (7th Okazaki Distinguished Service Award in 2012: Dr. Okazaki is called “The Father of Electronic Ceramics in Japan”). He becomes the Fellow of the American Ceramic Society (ACerS) since 2011. His current interests are a fundamental understanding of dielectric and piezoelectric properties in ceramics and single crystals from the viewpoints of ferroelectric domain structures by measuring acoustic wave velocities.

He is an organizing committee member of International Japan-Korea Seminar on Ceramics and an editorial board member of Ceramics International. He belongs to Electronics Division of ACerS.

RCBJSF In-12

Evaluation of Elastic Constants in Piezoelectric Ceramics by Measuring Acoustic Wave Velocities

T. Ogawa, T. Ikegaya

Department of Electrical and Electronic Engineering, Shizuoka Institute of Science and Technology, Japan

e-mail: ogawa@ee.sist.ac.jp

Piezoelectric ceramics including lead-free were investigated from viewpoints of relationships between piezoelectricity and elastic constants such as Young's modulus (Y^E_{33}) and Poisson's ratio (σ). Recently, we developed a method to be convenient to measure acoustic wave velocities suitable for disk samples (dimensions of 10-15 mm diameter and 1.0-1.5 mm thickness) by an ultrasonic thickness gauge (Olympus Co., Model 35DL) with high-frequency (30 MHz and 20 MHz) pulse generation [1, 2]. Figure 1 shows the relationships between planar coupling factors (k_p) vs Young's modulus (Y_{33}^E) and Poisson's ratio (σ) in alkali niobate (abbreviated to "SZ"), alkali bismuth titanate ("KBT" and "BT") lead-free ceramics compared with "hard PZT" and "soft PZT", and with lead titanate ("PLT" and "PT") ceramics after fully DC poling. It was confirmed that higher k_p values appeared at lower Y_{33}^E and higher σ values. The origin of high piezoelectricity was due to the mechanical softness of materials in the direction perpendicular as well as parallel to the poling field. This work was partially supported by a Grant-in-Aid for Scientific Research C (No. 21560340) and a Grant of Strategic Research Foundation Grant-aided Project for Private Universities 2010-2014 (No. S1001032) from the Ministry of Education, Culture, Sports, Science and Technology, Japan.

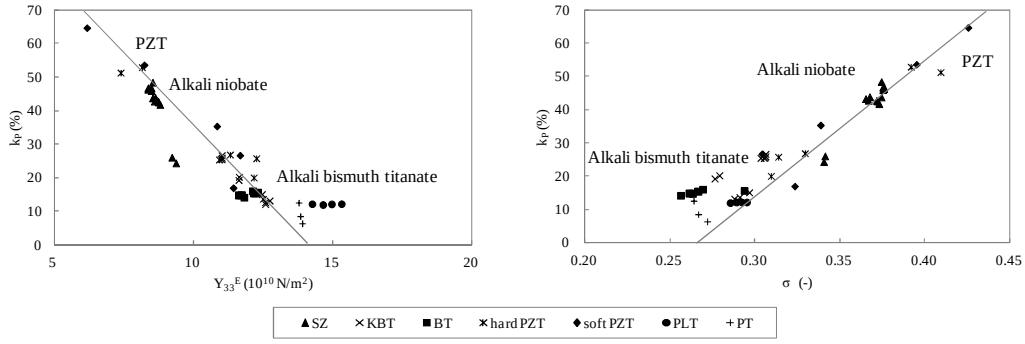

Fig. 1 Relationships between k_p vs Y_{33}^E and σ in piezoelectric ceramics.

References

1. T. Ogawa, Piezoelectric Materials and Devices -Practice and Applications-, Ed. F. Ebrahimi, INTECH, 2013, pp. 35-55.
2. T. Ogawa, K. Ishii, T. Matsumoto and T. Nishina, Jpn. J. Appl. Phys. **51**, 09LD03-1 (2012).

Marina **POPOVA**

Marina Popova graduated from the Moscow Institute of Physics and Technology (MIPT) in 1964. She worked as PhD student in the Laboratory of Luminescence of the Lebedev Physical Institute, USSR Academy of Sciences, under the supervision of Prof. M.D. Galanin and Dr. A.M. Leontovich, creators of the first laser in the USSR. She received her PhD from the Lebedev Physical Institute in 1968, after defending her PhD thesis "Dynamics of ruby laser". During 1968-1975, she worked as researcher in the Problem Laboratory of Semiconductor Physics of the Latvian State University in Riga. She has made a ruby laser there (the first one in Baltic states) and studied multiphoton absorption in crystals. Since 1975, she is with the Institute of Spectroscopy, Russian Academy of Sciences, were she also got her Doctor of physical and mathematical sciences degree (1992) after defending her second thesis: "High-resolution Fourier-transform spectroscopy of rare earth containing crystals". Since 2001, she has the title of professor in optics. At present, she is head of the Laboratory of Fourier Spectroscopy in the Department of Solid State Spectroscopy in the Institute of Spectroscopy. Her main research interests are physics of impurity centers in crystals, Fourier-transform spectroscopy, spectra of rare-earth ions, solid-state lasers, spectroscopy of magnetic insulators. Her laboratory concentrates on studies of new functional materials for quantum and optoelectronics, quantum informatics.

FM&NT In-13

Materials for Optical Quantum Memory

M. Popova

Institute of Spectroscopy, Russian Academy of Sciences, Moscow, Troitsk, Russia

e-mail: popova@isan.troitsk.ru

Much effort is given at present to implementation of optical quantum memory (OQM) which is supposed to be an essential part of different quantum informatics devices, in particular, of quantum repeaters intended for increasing the length of already functioning quantum cryptographic communication lines [1]. Any scheme of optical quantum memory is based on a so-called three-level Λ system. Among different systems investigated so far, the ground-state hyperfine levels of rare-earth (RE) ions in a crystal, combined with a third (metastable) level in optical frequency region are considered as the most promising candidates to realize an efficient three-level Λ system.

I'll briefly discuss what requirements should be met by materials for OQM and what characteristics of particular materials should be studied. Those are precise level positions, the optical density, coherence times of hyperfine levels, life times of metastable optical levels, hyperfine structure (HFS) of the energy levels, inhomogeneous broadening of spectral lines. A resent successful demonstration of the gradient echo type optical memory where the bandwidth limitations come from the HFS being unresolved [2] has put forward a task to search for crystals with resolved HFS in optical spectra.

My group, in collaboration with other institutions in Russia and abroad, studies spectroscopic properties of RE-doped crystals, relevant for applications in OQM. I'll review our recent results on the HFS studies in different crystals [3-5] and on specific peculiarities of an inhomogeneous broadening which have to be taken into account when considering applications in OQM [3,6,7].

Acknowledgement

Support by the Russian Foundation for Basic Research (Grant No 13-02-01091a) is acknowledged.

References

1. N. Sangouard, C. Simon, H. de Riedmatten, N. Gisin, Rev. Modern Phys. **83**, 33 (2011).
2. B. Lauritzen, N. Timoney, N. Gisin, M. Afzelius, H. de Riedmatten, et al., Phys. Rev. B **85**, 115111 (2012).
3. S. A. Klimin, D. S. Pytalev, M. N. Popova, B. Z. Malkin, et al., Phys. Rev. B, 81, 045113 (2010).
4. D. S. Pytalev, E. P. Chukalina, M. N. Popova, et al., Phys Rev B 86, 115124 (2012).
5. M. N. Popova, Optical Materials, **35**, 1842 (2013).
6. B. Z. Malkin, D. S. Pytalev, M. N. Popova, et al., Phys Rev B 86, 134110 (2012).
7. M. Popova, Journal of Rare Earths, 32, 278 (2014).

Juris **PURANS**

Juris Purans received his PhD from the University of Latvia (UL) in 1980 "EPR of disordered solid state materials" and his habilitation from the ISSP UL in 1993 "XAFS Spectroscopy of Transition Metal Oxides". Since 1993, he is a head of the EXAFS laboratory at the ISSP UL in Riga (www.dragon.lv/exafs). J. Purans was qualified to the list of Professors of Universities of France and Italy. He worked for many times at the synchrotron radiation facilities ADONE/DAFNA (ITALY), LURE-SOLEIL (France) as a beam-line scientist, as well as invited professor – Universities of France, Italy and Switzerland. J. Purans has 30 years of experience and published more than 200 papers on studies of functional materials using synchrotron radiation at the ESRF (Grenoble), LURE-SOLEIL (Orsay), HASYLAB (Hamburg), ADONE/DAFNA – ELLETRA (ITALY). He is the author/coauthor of 270 papers and 2 review articles on synchrotron radiation EXAFS studies, as well as RAMAN, EPR and XRD. His H-index is 23, with 1500 citations (http://www.researcherid.com/rid/E-8443-2010). His laboratory has recently developed EXAFS experiments with unprecedented (femtometer 10^{-5} Å) accuracy and nanometer scale (50 nm) lateral resolution (FP6 STRP project "X-TIP"). 2013-2016 – head of Latvian National grant "XAFS studies of functional materials with femtometer accuracy" Latvian Council of Science; 2010-2013 – Head of Latvian EU regional development grant ERAF-088 "Innovative glass coatings" VIAA. Since 2013, he is a Full member of the Latvian Academy of Sciences.

FOREIGN LANGUAGES – Italian, English, French, Russian, German.

Pl-3

Beyond The Quasiharmonic Approximation: Local Structure of Perovskites with Negative Thermal Expansion

J. Purans

Institute of Solid State Physics, University of Latvia

e-mail: purans@cfi.lu.lv

The interest towards ReO_3-type perovskites has been recently renewed by the discovery of large negative thermal expansion (NTE) in cubic ScF_3 structure in a wide temperature range [1], to be compared with a much less intense effect measured for the cubic ReO_3 [2]. At present, the great difference between the isostructural compounds is not yet explained, but it is found that the materials correspond to cases of strong anharmonic effects.

Anharmonicity is of general importance in condensed matter in relation to thermal expansion, structural phase transitions, soft modes in ferroelectrics, melting and related phenomena. Usually anharmonicity in crystals is weak enough and thus so called *implicit* anharmonisity can be described in the framework of Quasiharmonic approximation (QHA) as variations of the phonon frequency due to the change in volume with temperature or pressure. However, this might be not the case for strongly *explicit* anharmonic systems, like perovskites with NTE. The explicit anharmonic effect links the phonon frequencies to the amplitude of the atomic vibrations.

Synchrotron radiation EXAFS studies of local structure with femtometer accuracy [3] offer the possibility to study implicit and explicit anharmonic effects for perovskites with NTE. The temperature dependent EXAFS measurements include both anharmonic effects. The relative contributions of these two effects can be estimated by the extent to which quasiharmonic calculations of amplitude of the atomic vibrations reproduce the experimental EXAFS data. In my talk a description will be made of the most important achievements.

References

1. B.K. Greve, K.L. Martin, P.L. Lee, P.J. Chupas, K.W. Chapman and A .P. Wilkinson J. Am. Chem. Soc. 132 154962 (2010).
2. J. Purans, G. Dalba, P. Fornasini, A. Kuzmin, S. D. Panfilis,and F. Rocca, AIP Conf. Proc. 882, 422 (2007) and J. Timoshenko, A. Kuzmin, J. Purans, J. Phys.: Condens. Matter 26 (2014) 055401.
3. J.Purans, N. D.Afify, G.Dalba, R.Grisenti, S.De Panfilis, A.Kuzmin, V.I.Ozhogin, F.Rocca, A.Sanson, S. I. Tiutiunnikov, P.Fornasini, Phys.Rev.Lett., 100, 00055901 (2008)

Krystian ROLEDER

1977-1981: doctoral studies at the Institute of Physics, University of Silesia, Katowice, Poland
1981: defence of doctoral thesis in Physics
1990: *habilitation* in the Adam Mickiewicz University in Poznań in the field of ferroelectrics and experimental physics
1994: associate professor of the Institute of Physics, University of Silesia
1999: professor, permanent position at the Institute of Physics, University of Silesia

SCIENTIFIC ACTIVITIES

Dielectric, electrostrictive, piezoelectric and optical properties of ABO_3 perovskites
98 papers published in the international journals, e.g.:
Phase Transitions, Ferroelectrics, Journal of Physics: Condensed Matter, Solid State Communications, Journal of Physics E: Science Instruments, Acta Crystallographica, Japanese Journal of Applied Physics, Physica Status Solidi, Physical Review B, Nature Communications.
According to the ISI Web of Knowledge: 950 citations, h-index = 20

80 posters and/or oral presentations at international conferences, e.g.:
ECAPD European Conference on Application of Polar Dielectrics, Metz, France 2006
ECAPD Aveiro, Portugal 2012
EMF-10 European Meeting on Ferroelectricity, Cambridge 2003;
EMF-11 Bled, Slovenia 2007
EMF-12 Bordeaux, 2011
IMF-7 International Meeting on Ferroelectricity, Saarbrücken, Germany 1989
IMF-10 Madrid, Spain, 2001
IMF-11 Iguassu Falls, Brazil 2005
IMF-12 Xi'an, China, 2009

General Chair of the IMF-13 in Kraków, Poland, 2013
Member of Steering Committees: EMF, IMF & ECAPD

Associate Editor of the multinational journal *Phase Transitions*
Founding Editor: A.M. Glazer, University of Oxford
Editor-in-Chief: Jens Kreisel, France
Associate Editor Peter Gehring, USA
http://www.tandf.co.uk/journals/journal.asp?issn=0141-1594&linktype=5

ORGANISATIONAL ACTIVITIES

1990-1996: vice-dean for physics studies in the University of Silesia
1992-1995: co-ordinator of the European Mobility Scheme for Physics Students (under the auspices of the European Physical Society)
1996-2002: vice-rector of the University of Silesia
2005-2012: head of the Institute of Physics
2003-2014: head of the Department of Ferroelectric Physics

RCBJSF In-13

Do We Understand Why Antiferroelectric Orderis Realized in $PbZrO_3$ and $PbHfO_3$?

K. Roleder[1], A. Bussmann-Holder[2], J.H. Ko[3], A. Majchrowski[4]

[1]University of Silesia, Institute of Physics, 40-007 Katowice, ul. Uniwersytecka 4, Poland

[2]Max-Planck-Institute for Solid State Research, Heisenbergstr. 1, D-70569 Stuttgart, Germany

[3]Department of Physics, Hallym University, 1 Hallymdaehakgil, Chuncheon, Gangwondo, Korea

[4]Institute of Applied Physics, Military University of Technology, ul. Kaliskiego 2, Warsaw, Poland

e-mail: Krystian.Roleder@us.edu.pl

In spite of over 60 years of investigations concerning antiferroelectricity in oxidic perovskites ABO_3, it cannot be claimed that we understand the phase transition mechanism(s) leading to this state. Lead zirconate PbZrO3 and lead hafnate $PbHfO_3$ belong to the so called *classical* aniferroelectrics. While the latter has been intensively studied in the last few years, the former one suffered for long time from the lack of systematic investigations. The most important reason was certainly a lack of good quality single crystals and their large enough sizes.

After intense investigations of single crystals of these antiferroelectrics, a hypothesis has been put forward that an antiferroelectric state (order) in ABO_3 perovskites is not realised directly but only through a transient phase of polar (ferroelectric) properties spreading out through a temperature range of few degrees below T_C. It is due to strongly competing zone center and zone boundary instabilities being induced by strong anharmonic lattices. These two instabilities, i.e. softening of the long wave length transverse optic mode of almost displacive type and the accompanying softening of a zone boundary related to transverse acoustic mode are the origin of precursor effects in the form of static (stable) clusters/domains of non-centrosymmetric symmetry. As a result, an anomalous temperature dependence of the elastic stiffness coefficients has been observed before the transition point at T_C [1], and the structure of the paraelectric phase can no longer be considered as a pure paraelectric one [2]. The following results will be presented: the the polarizability model used for calculations, the birefringence in single PbZrO3 and PbHfO3 crystal, structural data, temperature dependencies of dielectric and electromechanical properties, and elastic stiffness coefficients determined by Brillouin spectroscopy.

All the statements above would not have been considered, if earlier investigations on the pre-transitional phenomena in BaTiO3 [3] and $SrTiO_3$ [4] had not been detected. While the stable (static) and non-centrosymmetric (birefringent) microregions were visible above T_C in BaTiO3, which is entirely ferroelectric below T_C, considerably different behaviour was observed in case of $SrTiO_3$, in which precursor effects are related to long wavelength and zone boundary acoustic modes instabilities, and exist even 80K above the transition point at 105K.

References

1. A. Bussmann-Holder, J-H. Ko, A. Majchrowski, M. Górny, K. Roleder *Precursor dynamics, incipient ferroelectricity and huge anharmonicity in antiferroelectric $PbZrO_3$*J. Phys.: Condens. Matter 25 212202 (2013)

2. N. Zhang, H. Yokota, A. M. Glazer, P. A. Thomas *The not so simple cubic structure of $PbZr_{1-x}Ti_xO_3$(PZT): complex local structural effects in perovskites* Acta Cryst. B67 461–466 (2011)

3. A. Ziębińska, D. Rytz, K. Szot, M. Górny, K. Roleder *Birefringence above T_C in single crystals of barium titanate* J. Phys.: Condensed Matter 20 142202 (2008)

4. K. Roleder, A. Bussmann-Holder, M. Górny, K. Szot, A.M. Glazer *Precursor dynamics to the structural instability in $SrTiO_3$* Phase Transition 85, No. 11, 939–948 (2012)

Martins **RUTKIS**

Data Of Birth: August 8, 1957, Riga, Latvia

Nationality: Latvian

Occupation:

- Deputy Director for Research, Head of Laboratory of Organic materials and Senior Researcher at Institute of Solid State Physics University of Latvia;
- Member of Expert Commission of Natural Sciences and Mathematics at Latvian Council of Science;
- Associated member of the Latvian Academy of Sciences.

Education:

- 1992 Dr.phys from the Institute of Physical Energetics, Latvian Academy of Sciences;
- 1990 Candidate of Science (equivalent of Ph.D.) from the University of Latvia;
- 1982 - 1987 Post Graduate Student at University of Latvia, Department of Physics;
- 1975 - 1982 Student at University of Latvia, Department of Physics.

Number of Publications: 188 Publications in scientific journals and proceedings of conferences.

Research Interests:

- Optical and Electrical Properties of Organic Substances;
- Nonlinear Optical Properties of Organic Substances;
- Photonics of polymer composites;
- Structure and Spectroscopy of Organic Substances;
- Quantum chemical and molecular mechanical modelling.

Member of:

- Optical Society of America (OSA);
- American Chemical Society (ACS);
- Royal Society of Chemistry (RSC);
- Editorial board of “Optics and Photonics Journal”.

FM&NT In-14

Development of NLO Active Organic Molecular Glasses for Photonic Applications

M. Rutkis[1], K. Traskovskis[2], A. Tokmakovs[1], V. Kokars[2]

[1]Institute of Solid State Physics, University of Latvia, Riga, Latvia
[2]Institute of Applied Chemistry, Riga Technical University, Latvia
e-mail: martins.rutkis@cfi.lu.lv

Over the last two decades increased interest in the development of organic photonics and optoelectronics is driven by demand for new cost effective high performance materials which are easy to process. Most of attention is focused on such application areas as photovoltaic, lighting and optical data processing. The key process in manufacturing organic photonic device for above mentioned applications is preparation of uniform thin films. In general there are two methods to prepare such films – thermal vacuum vapor deposition and solution based methods like spin coating. For the first one high cost of equipment and processing are characteristic. Solution based thin film production processes are less demanding therefore became more and more popular among researchers in field of organic optoelectronics and photonics. Nowadays polymers and polymer composites are most intensively employed in attempts to create devices via solution based technology. Among them there has also been increasing interest in so called "organic molecular glasses" as photonic thin film materials[1,2]. Compared to polymeric systems, organic molecular glasses do not need complicated chemical synthesis or purification processes and has a well-defined structure.

Within last decade our attention is paid to develop organic materials for nonlinear optical (NLO) applications. During our research it came to our attention that the presence of triphenylmethyl and triphenylsilyl substitutes noticeably enhances amorphous phase formation of low molecular weight molecules[3]. Exploiting this molecular motif large amount of glass forming structures with different active chromophores, are synthesized at RTU.

With scope of above mentioned applications thermal, optical and NLO properties of these compounds are intensively investigated at ISSP UL. In this contribution we would like to present our investigation results and discus possible structure property relations within this new class of low molecular glasses.

Acknowledgement

This work has been supported by the European Social Fund within the Project No. 2013/0045/1DP/1.1.1.2.0/13/APIA/VIAA/018

References

1. P. Strohriegl, J. V. Grazulevicius. Adv. Mater., **14**, 1439 (2002).
2. S.-H. Jang and A. K.-Y. Jen. Chem. Asian J., **4**, 20–31 (2009)
3. K. Traskovskis, I. Mihailovs, A. Tokmakovs, A.Jurgis, V. Kokars, M. Rutkis. J. Mater. Chem., **22** 11268-11276 (2012).

Kurt SCHWARTZ

Kurt Schwartz, born 27.04.1930 in Riga, Latvia. From 1949 to 1954 physics studies at the Latvian State University.Ph.D.1969 at the University of Tartu (Luminescence efficiency of doped alkali halides). Habilitation in 1970 at the P. Lebedev Physical Institute (FIAN), Academy of Sciences, Moscow (Radio-luminescence and radiation damage of alkali halides). Member of Latvian Academy of Sciences (1991; Award of the Latvian Academy of Sciences for radiation damage studies (2010))

Scientific and pedagogical activities

From 1957 to 1961 assistant professor at the Department of Physics, Latvian State University. From 1961 to 1991 head of the Radiation Physics Labor, Institute of Physics, Latvian Academy of Sciences. From 1974 to1985 also professor at the Department of Physics of the Engineering Institute of Civil Aviation (Riga).

From 1992 in Germany. From 1992 to 1994 visiting professor at the University of Heidelberg. From 1994 up to now senior scientist at the GSI Helmholtzzentrum für Schwerionenforschung, Materials Research Department.

Scientific cooperation

Institute of Solid State Physics, University of Latvia; Institute o Physics, University of Tartu; Institute of Nuclear Physics, Astana, Kazakhstan; L. N. Gumilyov Eurasian National University, Astana, Kazakhstan; Kurchatov Institute, Moscow, Russia; Technical University Darmstadt, Germany..

Research Interests: solid state physics, optical spectroscopy, radiation damage in dielectric materials, optical recording materials, radiation detectors.

Publications: more than 250 including 5 monographs.

FM&NT In-15

Irradiation Induced Nanostructures in LiF Crystals and Possible Applications

K. Schwartz[1], I. Manika[2], J. Maniks[2]

[1]GSI Helmholtzzentrum für Schwerionenforschung, Planckstr. 1, 64291 Darmstadt, Germany

[2]Institute of Solid State Physics, University of Latvia, Latvia

e-mail: k.schwartz@gsi.de

Lithium flouride crystals with simple ionic binding and a large band gap (14.6 eV) played an important role on understanding of radiation damage processes in dielectric materials [1 – 4]. A detailed study of heavy ion irradiation in LiF crystals (from ^{4}He up to ^{238}U) shows that after creation of single Frenkel pairs ((*F*-*H*) and (*α*–*I*)) the concentration of single F centers saturates ($N_F \approx 10^{19}$ cm^{-3}) and at higher absorbed energy (fluences) complex color centers F_n and larger aggregates (dislocation loops, vacancy and fluorine clusters, colloids etc.) are produced [1-3]. The formation of nanodefects depends on density of the absorbed energy and/or ion energy loss (dE/dx). The nanodefects are produced both in single ion tracks (above the threshold of dE/dx) as well us under of ion track overlapping. Irradiation with heavy ions leads to a large absorbed energy in the central part of the track (core) with a strong gradient of the absorbed energy and defect concentration around the ion path (halo). At high absorbed energy the concentration of nanodefects is comparable to the concentration of color centers [1-3]. Nanoclusters are observed also under ion induced sputtering [5]. The role of self-trapped holes during the electron-hole relaxation in ion tracks in LiF crystals is analyzed [4]. Applications of color centers and nanoclusters are discussed [6].

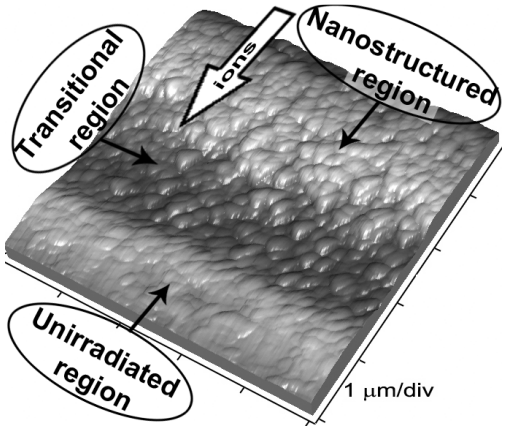

Fig.1. AFM image of nano-crystallites in LiF sample irradiated with 15 MeV Au ions at fluence 5x10^{13} Au/cm^2 after chemical etching.

References

1. K. Schwartz, A. E. Volkov, M. V. Sorokin et al., Phys. Rev. B **82**, 144116 (2010)
2. J. Maniks, I. Manika, R. Zabels et al., Nucl. Instr. Meth. B **282**, 81 (2012)
3. M.V. Sorokin, K. Schwartz, C. Trautmann et al., Nucl. Instr. Meth. B (2014) - in print
4. N. Medvedev, A. E. Volkov, K. Schwartz, C. Trautmann, Phys. Rev. B **87**. 104103 (2013)
5. H. Hijazi, L.S. Farenzena, H. Rothard et al., Eur. Phys. J. D **63**, 391 (2011)
6. R. M. Montereali, F. Bonfigli, G. Dietler et. al., Phys. Stat. Sol. (c) **2**, 298 (2005)

Stefan **SCHWEIZER**

Stefan Schweizer obtained his physics diploma from the University of Giessen, Germany, in 1994. Subsequently, he moved to the University of Paderborn where he obtained a PhD in 1997 and his habilitation in 2000 for his work in the field of radiation detectors. After long-term research appointments as visiting professor at MIT and Argonne National Laboratory, both in the USA, he returned to Germany in 2006 joining the Fraunhofer Institute for Mechanics of Materials IWM in Halle. In addition, he headed a research group at the Martin Luther University of Halle. Since March 2012 he is a professor for "Physics and Energy Technologies" at the South Westphalia University of Applied Sciences and director of the Fraunhofer Application Center for Inorganic Phosphors in Soest.

Pl-4

Multi-Functionality of Luminescent Glasses for Energy Applications

S. Loos[1], F. Steudel[2], B. Ahrens[1,2], and S. Schweizer[1,2]

[1]Department of Electrical Engineering, South Westphalia University of Applied Science, Lübecker Ring 2, 59494 Soest, Germany

[2]Fraunhofer Institute for Mechanics of Materials IWM, Walter-Hülse-Str. 1, 06120 Halle (Saale), Germany

e-mail: schweizer.stefan@fh-swf.de

Luminescent glasses gain increasing importance in optical devices, such as fibre lasers or light emitting diodes. In this work, series of rare-earth doped glasses are investigated for their potential application as photon converters for photovoltaic (PV) and solid state lighting (SSL) applications.

Solar modules have a poor response in the blue and near ultraviolet (UV) spectral range due to thermalization losses and absorption in the cover glass and the front contact layer. To overcome this problem, luminescent glasses are used as cover, which down-shift the incident blue and UV photons to photons of a wavelength more effectively absorbed by the solar cell. Apart from photon down-shifting, rare-earth doped glasses can also be used for photon up-conversion, where a high-energy photon is emitted after sequential absorption of two (or more) low-energy photons. Here, a practical application is in concentrated PV systems where the efficiency can be further improved by using an up-converting layer on the backside to up-convert the far-infrared photons to a more suitable wavelength in the near infrared or even in the visible spectral range.

In light emitting diode (LED) applications, luminescent glasses have the potential as encapsulating material for the generation of white light. There are two possibilities how white light can be produced by using commercial LEDs: In the early days of the LED lightning technology, white light was generated by the primary colours red, green and blue. Another possibility can be achieved with a phosphor or a luminescent glass, which converts a part of the blue light from the LED into yellow light. Mixing the two complementary colours blue and yellow in the correct ratio yields to the emission of white light.

Vladimir **SHUR**

Vladimir Ya. Shur graduated at the Ural State University, Ekaterinburg, Russia in 1967. He received the M.S. degree in physics in 1967, the Ph.D. degree in 1974, and the Dr. Phys.-Math. Sci. degree in 1990, all from the Ural State University. He founded the Ferroelectric Laboratory of USU in 1982 and director of the Ural Center of Shared Use "Modern Nanotechnology", Ural Federal University. He is President of the Ural Branch of Optical Society of Russia. He is currently engaged in research of the kinetics and statics of the domain structure in ferroelectrics, and micro- and nanodomain engineering in lithium niobate and lithium tantalate for nonlinear optical applications. He is an author or coauthor of more than 260 publications in peer-reviewed journals and 6 book chapters.

RCBJSF In-14

Domain Shape Instabilities and Fractal Domain Growth in Uniaxial Ferroelectrics in Highly Non-Equilibrium Switching Conditions

V. Shur[1,2]

[1]Ferroelectrics Laboratory, Institute of Natural Science, Ural Federal University, Russia

[2]Labfer Ltd., Russia

e-mail: Vladimir.Shur@urfu.ru

The kinetic approach to evolution of the ferroelectric domain structure, based on the analogy with the first order phase transition, allows to explain the formation of the metastable domain structures with energy essentially exceeding the equilibrium ones. The screening of the depolarization field stabilizes any non-equilibrium domain pattern. It was shown that the screening retardation changes drastically the domain structure evolution. The highly non-equilibrium switching conditions characterized by ineffective bulk screening lead to formation and evolution of the self-assembled nanodomain structures [1,2]. The domain structure evolution has been studied by joint application of optical microscopy, confocal Raman microscopy, scanning electron microscopy and piezoelectric force microscopy for domain visualization in the uniaxial ferroelectrics lithium niobate $LiNbO_3$, lithium tantalate $LiTaO_3$, lead germanate $Pb_5Ge_3O_{11}$, and relaxor ferroelectric strontium-barium niobate $Sr_xBa_{1-x}Nb_2O_6$. The role of the residual depolarization field in formation of the self-assembled fractal micro- and nanodomain structures have been demonstrated [1-3]. The effects of domain wall shape instabilities and formation of the nanodomains in front of the moving walls have been discussed. The special attention has been paid to formation of the self-assembled nanoscale and dendrite domain structures in highly non-equilibrium switching conditions [3]. All obtained results have been considered in framework of the described kinetic approach to the domain structure evolution.

The equipment of the Ural Center for Shared Use “Modern Nanotechnology”, Ural Federal University has been used. The research was made possible in part by RFBR and the Government of Sverdlovsk region (Grant 13-02-96041-r-Ural-a), by RFBR (Grants 13-02-01391-a, 14-02-01160-a).

References

1. V.Y. Shur, A.R. Akhmatkhanov, D.S. Chezganov, A.I. Lobov, I.S. Baturin, and M.M. Smirnov, Appl. Phys. Lett. **103**, 242903 (2013).
2. V. Shur, V. Shikhova, A. Ievlev, P. Zelenovskiy, M. Neradovskiy, D. Pelegov, and L. Ivleva, J. Appl. Phys., **112**, 064117 (2012).
3. V.Ya. Shur, D.S. Chezganov, M.S. Nebogatikov, I.S. Baturin, and M.M. Neradovskiy, J. Appl. Phys., **112**, 104113 (2012).

Alexander **SIGOV**

Alexander S. Sigov (born May 31st, 1945 in Donetsk)- President of the University, Fellow Member of the Russian Academy of Sciences (RAS), Honored Scientist of the Russian Federation, Doctor of Physics and Mathematics, Full Professor.

Alexander Sigov is one of the most influential Russian specialists in solid state physics, solid state electronics and materials research.

He is best known for the research of defect contributions to the anomalies of various physical quantities near second order phase transition points. His monograph co-published with A.P. Levanyuk "Defects and Structural Phase Transitions" (New York, 1987) became an encyclopedia for all researchers in this field.

A. Sigov was educated at Moscow State University, Chair of Quantum Theory of the Faculty of Physics and graduated with honors in 1968. He works at the Moscow State University of Radioengineering, Electronics and Automation (MIREA) since 1972. Same year, he defended his PhD thesis, and in 1985 he became a Doctor of Sciences. In 1987 he had attained the rank of full professor, in 2006 he was elected a Corresponding Member (and in 2011, a Fellow Member) of the Russian Academy of Sciences, the Nanotechnology and IT Division.

He held the position of the Dean of the Department of Electronics and Opto-electronic engineering from 1985 to 1998, and was a Rector of MIREA since May 1998 up to June 2013. Now he serves as the President of the University. He also is the Head of the Chair of Condensed State Physics.

A. Sigov is the author and co-author of more than 300 scientific papers, six monographs, nine textbooks and over thirty inventions. He supervised more than 25 PhD students, while 17 of his colleagues became doctors of sciences and full professors under his supervision.

Alexander Sigov is a member of the Security Council Scientific Committee of the Russian Federation, member of Bureau of the Joint Council of the RAS on condensed matter physics, member of a number of Boards and Councils of the Ministry for Education and Science of the Russian Federation, member of the European Physical Society, Institution of Engineering and Technology, IEEE, MRS, as well as member of editorial boards of "the RAS News (physics series)", "Microsystems Engineering", "Integrated Ferroelectrics" and many others.

The 4-th degree Order of Service to Motherland and several state honorary medals have been conferred to Alexander Sigov. He is a winner of the State Award of the Russian Federation, and 3 governmental awards for sciences, engineering and education.

He is married, has two children and 3 grandchildren.

Pl-5

Negative Conductivity in Thin Ferroelectric Films

A. Sigov, Y. Podgorny, P. Lavrov, and K. Vorotilov

Moscow State Technical University of Radioengineering, Electronics and Automation, Russia

e-mail: sigov@mirea.ru

The current-voltage (*I-V*) characteristics of some ferroelectric thin films frequently exhibit regions with an apparent negative differential conductivity as it is shown at Fig. 1. To describe this phenomenon Dawber and Scott have suggested the diffusion current model [1]. However this model does not fully describe real *I-V* characteristics [2].

In this report we consider *I-V* dependences taking into account the polarization relaxation. The polarization relaxation in thin ferroelectric films can reach about tens percent. Thus, in spite of the pre-polarization of the ferroelectric structure before the measurement, the total current in the structure consists of the leakage current and the polarization recovery current components.

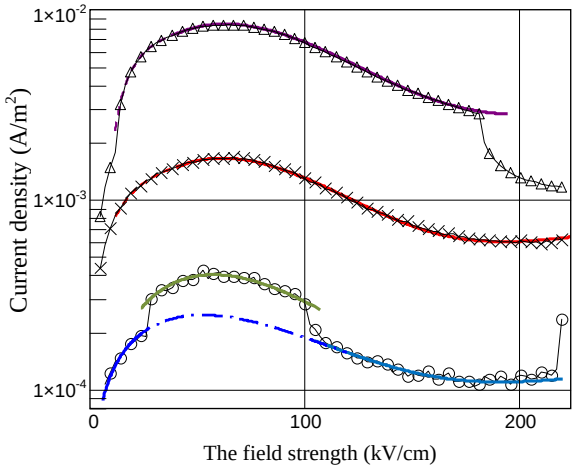

Fig.1 Experimental I-V dependencies (points) of PZT films with the negative differential conductivity region and the fitting curves taking into account the recovery polarization current.

We have shown that the probability density of the Weibull distribution simulates well the polarization recovery current. A maximum value of the polarization recovery current is observed in the vicinity of the coercive field.

A technique is proposed that enables to exclude a polarization recovery current component from the *I-V* data. A method of recovery charge determination at different voltage ramp speed is discussed as well.

References

1. M. Dawber, J.F. Scott . J Phys: Condens Matter. **16**, L515-L521 (2004).
2. Yu. Podgorny, A. Sigov, A. Vishnevskiy, K. Vorotilov. Ferroelectrics. in press (2014).

Eckhard **SPOHR**

1. Curriculum vitae

2007 -	W3-Professor for Theoretical Chemistry, University of Duisburg-Essen
2003 - 2007	Group Leader "Physical Chemical Fundamentals", Institute for Energy Research, Research Center Jülich
2001 - 2002	Scientic coworker, Institute for Energy Research, Research Center Jülich
1996 - 2000	Scientic Assistant, University of Ulm
1995	Habilitation in Theoretical and Computational Chemistry, University of Ulm
1991 - 1996	Scientic Coworker, University of Ulm
1989 - 1990	Feodor Lynen fellow of the Alexander von Humboldt foundation at the University of California in Irvine
1986 - 1988	Scientic coworker, Max Planck Institute for Chemistry, Mainz
1986	Ph.D. in Physical Chemistry, Johannes-Gutenberg University of Mainz
1983	Diploma of Chemistry, Johannes-Gutenberg University of Mainz
09.02.1960	born

2. Five most relevant publications

1. Florian Wilhelm, Renat R. Nazmutdinov, Eckhard Spohr, andWolfgang Schmickler, *A model for proton transfer to metal electrodes,* J. Phys. Chem. C 112, 10814 (2008).
2. F. Wilhelm, W. Schmickler, and E. Spohr, *Proton transfer to charged platinum electrodes. a molecular dynamics trajectory study,* J. Phys.: Condens. Matter, 22, 175001 (2010).
3. F. Wilhelm, W. Schmickler, R. Nazmutdinov, and E. Spohr, *Modeling proton transfer to charged silver electrodes,* Eletrochim. Acta 56 10632 (2011).
4. W. Schmickler, F. Wilhelm, and E. Spohr, *Probing the temperature dependence of proton transfer to charged platinum electrodes by reactive molecular dynamics trajectory studies,* Electrochim. Acta, doi: 10.1016/j.electacta.2013.01.146 (2013).
5. A. A. Kornyshev, A. M. Kuznetsov, E. Spohr and J. Ulstrup, *Kinetics of Proton Transport in Water,* J. Phys. Chem. B 107, 3351 (2003).

FM&NT In-16

Simulation of Oxide Nanostructures for Energy Conversion

E. Spohr[1], M. Wessel[1], D. Bocharov[2], S. Piskunov[2]

[1]Faculty of Chemistry, University Duisburg-Essen, Essen, Germany

[2]Institute of Solid State Physics, University of Latvia, Latvia

e-mail: eckhard.spohr@uni-due.de

The design of usable and photocatalysts for efficient conversion of sunlight to hydrogen from water is a formidable task that has been approached at various levels in recent years. Conventional photocatalyst electrodes such as titanium dioxide can operate with high efficiency under ultraviolet irradiation, but it remains a challenge to drive them with visible light. Many attempts at adjusting the semiconductor band gap, generally through doping, have been made in the past, but this often leads to electron and hole trapping. One possible approach to overcome this challenge is the synthesis of nanostructured electrodes in which photon propagation and charge transport are orthogonalized, which can be realized through wire arrays or other nanostructures with large surface-to-volume ratios.

In our work we have performed hybrid density functional theory calculations of hollow $SrTiO_3$ nanotubes with the goal to identify the most stable single- and multi-walled structures. We found, e.g., that stable single-walled nanotubes, which show a widened band gap relative to the bulk, can be folded from $SrTiO_3$(110) nanosheets of rectangular morphology[1]. We recently extended this study to an investigation of various defect structures with cationic and anionic dopants[2] and found that the electronic structure of both TiO_2 and $SrTiO_3$ nanotubes can be modulated remarkably by substitutional impurity defects. These and other related results pertaining to inhomogeneous oxide systems in one and two dimensions will be discussed in this presentation in more detail.

References

1. S. Piskunov and E. Spohr, J. Phys. Chem. Lett. **2**, 2566 (2011)

2. S. Piskunov, D. Bocharov, O. Lisovski, J. Begens, Z. F. Zhukovskii, M. Wessel and E. Spohr, submitted to PCCP

Gunnar SUCHANECK

Scientific Career

Since 1997	Senior Researcher at TU Dresden, Electrical and Computer Engineering department.
1984-1997	Assistant at TU Dresden, Electrical and Computer Engineering department.
1980-1983	PhD student at Leningrad Electrotechnical University (LETI), Cand. phys.-math. sci., PhD thesis: Crystal growth and polytypism of tetrahedral compound semiconductors.
1974-1980	Studies in Electronic Technology at Leningrad Electrotechnical University (LETI), Diploma engineer degree (with distinction – red diploma) Diploma work: Electronic structure and crystal lattice structure of tetrahedral compound semiconductors.

Scientific Focus

Solid state sensor technology: ferroelectric thin film sensor materials, metal oxide thin films, silicon oxide and silicon nitride, thin film deposition by reactive sputtering, plasma enhanced chemical vapor deposition.

Characterization of thin films by optical and electrical measurements, evaluation of the thin-film properties by means of intensity modulated laser beams.

Scientific Activities

- Member of the Working Group "Plasma Germany" of the Association of German Engineers (VDI), http://www.plasmagermany.org.
- Referee of numerous scientific journals of Elsevier B.V., Taylor&Francis, AVS Publications and IEEE.
- Project referee of FP6, FP7 and Horizon 2020 of the European Union.
- Project referee for the subject "Thin film technology" of the Grant Agency, Academy of Science of the Czech Republic.

Scientific Indexing

- H-factor: 15
- ≥ 130 refereed journal publications
- 15 patents awarded

Publications

Cp. http://rcswww.urz.tu-dresden.de/~suchanec/scipub.htm

RCBJSF In-15

Materials and Device Concepts for Electrocaloric Refrigeration

G. Suchaneck

Solid State Electronics Laboratory, TU Dresden, Germany

e-mail: Gunnar.Suchaneck@tu-dresden.de

Electrocaloric (EC) basic research is mostly focused on materials with a first-order phase transition providing a large EC temperature change ΔT_{EC}. However, near the Curie temperature T_C in the ferroelectric phase, the spontaneous and induced polarization contributions to the EC effect partially cancel each other out. Additionally, there is a peak of dielectric losses in this temperature region. Dielectric losses affect not only the heat balance, but they also make the temperature change of adiabatic heating larger than that of adiabatic cooling. This is not suitable for devices subjected to repeated thermodynamic cycles.

This work considers EC device operation above the temperature T_m of the dielectric permittivity peak $\varepsilon(T_m)$. The complex physics of ferroelectrics and relaxors close to T_m is replaced by considering a modified Curie-Weiss law predicting $\partial\varepsilon/\partial T$ as a function of four parameters: $\varepsilon(T_m)$, the intercept of the $\varepsilon(T)^{-1}$ vs T line with the T-axis, T_0, the parameter Ω characterizing the distribution of local Curie temperatures of materials which exhibit a diffuse phase transition (DPT), and the DPT diffuseness γ. The requirements to electrocaloric materials derived on this base ($\varepsilon(T_m)$ > 3000, Ω = 20-50 K, γ = 1.2...2), are fulfilled by relaxor single crystals, relaxor ceramics and ferroelectric or relaxor thin films deposited by advanced technologies. Refrigerators using reverse Brayton, Ericsson and Stirling cycles are compared.

The field dependence of ΔT_{EC} is shown to be determined by the field dependence of ε. Perovskites with a nearly ideal close-packed structure possess field induced paralectric-ferroelectric (above T_C) or antiferroelectric-ferroelectric phase transitions. This results in a Clausius-Clapeyron contribution to ΔT_{EC} due to the latent heat of the field induced first-order phase transition. The critical field of field-induced phase transitions is in the order of a few V/µm. Therefore, the Clausius-Clapeyron contribution is of relevance only for bulk ceramic-based EC refrigerators.

Since the cooling power density dq/dt characterizes a thermal flux determined by the ratio of the temperature span to the total thermal resistance of the device, a comparable to bulk ceramics dq/dt may be realized also using thin film devices which are operated with higher cycle frequency employing the lower thin film thermal relaxation times.

Masaki **TAKESADA**

NAME: Masaki TAKESADA
AFFILIATION: Department of Physics, Hokkaido University
ADDRESS: Sapporo, 060-0810, Japan
PHONE: +81-11-706-4418
DATE OF BIRTH: February, 1967
EDUCATION: BS in Physics, Yamaguchi University, 1990, MS in Physics, Yamaguchi University 1992, and Dr. Sc. in Physics, Hokkaido University 1995.
EXPERIENCE: Associate Professor in Department of Physics, Hokkaido University from 2013, Lecturer in Department of Physics, Hokkaido University from 2004 to 2012, Research Associate in Research Institute for Electronic and Science, Hokkaido University from 2001 to 2004, Research Scientist in Kanagawa Academy of Science and Technology from 1998 to 2001, JSPS PD fellow in Hokkaido University from 1996 to 1998, and Research Scientist in Colorado State University in 1995.
RESEARCH INTEREST: Phase transition and photoinduced cooperative phenomena in electronic materials such as low dimensional dielectrics, ferroelectrics and multiferroics studied by highresolution broadband light scattering.
MENBERSHIP OF EDITRIAL BOARDS: Journal of Physical Society of Japan.
PUBLICATION: (1) "Perfect Softening of Ferroelectric Mode in the Isotope-exchanged Strontium Titanate of $SrTi^{18}O_3$ studied by Light Scattering", M. Takesada, M. Itoh and T. Yagi, Phys. Rev. Lett. 96 (2006) 226702, (2) "A Gigantic Photoinduced Dielectric Constant of Quantum Paraelectric Perovskite Oxides Observed under a Weak DC Electric Field", M. Takesada, T. Yagi, M. Itoh and S. Koshihara, J. Phys. Soc. Jpn. 72 (2003) 37-40, (3) "Structural Study of a-b Phase Transition in K_2ZnBr_4", M. Takesada and H. Mashiyama, J. Phys. Soc. Jpn. 63 (1994) 2618-2626.

RCBJSF In-16

Broadband Light Scattering and Second Harmonic Generation in Ferroelectric Nanocrystals

M. Takesada[1], Y. Hakuta[2], H. Takashima[2] A. Onodera[1]

[1]Department of Physics, Hokkaido University, Japan

[2]National Institute of Advanced Industrial Science and Technology, Japan

e-mail: mt@phys.sci.hokudai.ac.jp

A stability of ferroelectricity is important in the practical application with reduced spatial dimensions in the nanometer size regime. Much interest has focused in recent years on ferroelectric nanostructure crystals, because of the clarification of the physical origin in the size effect of ferroelectricity and the technological development in the miniaturization of multilayer ceramic capacitors (MLCC) and ferroelectric non-volatile memory devices. The correlation length of polarization fluctuation was estimated as 10-50 nm above the ferroelectric phase transition point.[1] From the viewpoint of the polarization fluctuation the size effect should be remarkable below the correlation length. Furthermore, as a new topics of ferroelectric nanocrystals the toroidal like ferroelectrisity has recently been proposed in $BaTiO_3$ and related materials from ab initio study by Naumov and Bratkovsky.[2,3] In the present study, the property of polarization fluctuation and symmetry breaking has been studied in $BaTiO_3$ nanocrystals with sizes of 17 nm and 30 nm using broadband light scattering and second harmonic generation (SHG). The temperature dependence of broadband light scattering spectra on a log-log plot was obtained in Figure 1. The spectra have a central peak component. The line width of central peak shows anomaly around 350 K at which the temperature dependence of SHG signal also shows anomaly. The dynamical behavior of the ferroelectric phase transition will be discussed in $BaTiO_3$ nanocrystals in comparison with one of a bulk $BaTiO_3$ sample.

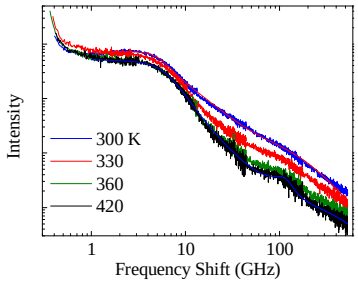

Figure 1. The broadband light scattering spectra in $BaTiO_3$ nanocrystals.

References

1. M. E. Lines and A. M. Glass, Principles and Applications of Ferroelectrics and Related Materials, Oxford 1977.
2. I. Naumov et al., Nature **432**, 737 (2004)
3. I. Naumov and A. M. Bratkovsky, Phys. Rev. Lett. **101**, 107601 (2008)

Hiroshi **TANAKA**

Title: Valence electron density and electrostatic potential in ferroelectric materials evaluated by MEM analysis of X-ray diffraction

Prof. Hiroshi Tanaka
Dept. of Materials Science, Shimane University,
1060, Nishi-kawatsu-cho, Matsue, Shimane 690-8504, JAPAN

Education:
1987 MS of Engineering from Dept. of Applied Physics, University of Tokyo
1993 PhD of Engineering from Dept. of Applied Physics, Graduate School of Engineering, University of Tokyo.

Employment:
1987-1996 IBM Research, Tokyo Research Lab.
1995-1996 Japan Atomic Energy Research Institute
1996- Dept. of Materials Science, Shimane University

Research Interests:
Theoretical Physics, Mathematical Physics, Computational Physics

RCBJSF In-17

Valence Electron Density and Electrostatic Potential in Ferroelectric Materials Evaluated by MEM Analysis of X-ray Diffraction

H. Tanaka

Department of Materials Science, Shimane University, Japan

e-mail: h.tanaka@riko.shimane-u.ac.jp

The maximum entropy method (MEM) analysis of X-ray diffraction data is a powerful tool, which enables us to reproduce *total* electronic charge density in detail from a limited number of experimental data [1]. Kuroiwa and coworkers applied the method to $PbTiO_3$, and showed the first experimental evidence for covalency between Pb and O ions [2]. The *valence* charge density is, however, more informative in many cases from the viewpoint of materials design. Then we have proposed a smart method evaluating valence charge density, and shown an example for crystalline Si [3]. It is now improved, and applicable to any crystal structures consisting of most kind of atoms in the periodic table.

We also developed a method evaluating the electrostatic potential and electric field on the basis of MEM, and applied it to $PbTiO_3$. Visualized electrostatic potential and electric field on the isosurface of charge density distribution give a direct evidence for the dipolar polarization of the Pb ion. They show close agreement with results by *ab initio* calculations [4]. We extended the scheme in order to deal with materials showing large anisotropic thermal vibrations.

In this talk, we explain how to evaluate the valence charge density and electrostatic potential from the synchrotron radiation data by using MEM, and show some new results for $PbTiO_3$ and $BaTiO_3$. They are compared with those obtained by *ab initio* calculations, and reliabilities of the method will be discussed.

References

1. M. Takata, E. Nishibori, and M. Sakata, Z. Kristallogr. **216**, 71 (2001), and references there in.
2. Y. Kuroiwa, S. Aoyagi, A. Sawada, J. Harada, E. Nishibori, M. Takata, and M. Sakata, Phys. Rev. Lett. **87**, 217601(2001).
3. H. Tanaka, M. Takata, and M. Sakata, J. Phys. Soc. Jpn. **71**, 2595 (2002).
4. H. Tanaka, Y. Kuroiwa, and M. Takata, Phys. Rev. B74, 172105 (2006).

Hiroki **TANIGUCHI**

Prof. Hiroki Taniguchi
Department of Physics, Nagoya University
Furo-cho, Chikusa, Nagoya 464-8602
e-mail: hiroki_taniguchi@cc.nagoya-u.ac.jp

Hiroki Taniguchi received a bachelor's degree in Department of Physics, Osaka University (2001) and a M.S degree in Department of Physics, Kyushu University (2003). Subsequently, he moved to Hokkaido University as a doctoral course student. After two and half years in Hokkaido University, he joined the Materials and Structures laboratory, Tokyo Institute of Technology as an assistant professor. During working at the Materials and Structures laboratory, he obtained a Ph.D. degree from Hokkaido University (2006). Since 2013, he is an associate professor in Department of Physics, Nagoya University. His research covers solid state physics, inorganic chemistry, materials science, and light scattering spectroscopy. He currently focuses on the development of eco-friendly functional oxides, including ferroelectric and thermoelectric materials.

RCBJSF In-18

Ferroelectricity Driven by Twisting of Silicate Tetrahedral Chains

H. Taniguchi

Department of Physics, Nagoya University, Furo-cho, Chikusa, Nagoya 464-8602, Japan

e-mail: hiroki_taniguchi@cc.nagoya-u.ac.jp

To date, ferroelectric materials have been widely applied in various electronic devices, including actuators, non-volatile memory, and sensors. Ferroelectric materials traditionally comprise oxygen octahedral units, such as those found in perovskite-type oxides. The strong covalency of the cations in the perovskite structures plays an important role for achieving robust ferroelectricity with a high-T_c and a large spontaneous polarization. With this in mind, recent ferroelectric devices typically rely on the use of lead-based compounds such as $Pb(Zr,Ti)O_3$ (PZT) to achieve such robust ferroelectricity. Mindful of the toxicity of Pb, there is an increasing demand for sustainable and environmentally friendly electronic devices, free from toxic elements. As such, a new guiding principle for designing ferroelectric materials is necessary.

In the present study, we demonstrate the occurrence of ferroelectricity in a silicate-based compound, Bi_2SiO_5, by direct observation of polarization switching. The novel mechanism of ferroelectricity in Bi_2SiO_5 has been elucidated from comprehensive studies employing Raman scattering, transmission electron microscopy, X-ray powder diffraction, and first principles calculations. The obtained experimental results and calculations clarified that the observed ferroelectricity in Bi_2SiO_5 stems from twisting of the one-dimensional SiO_4 tetrahedral chain.[1] This recent discovery opens up a new frontier for designing functional oxides based on "tetrahedra-engineering", as opposed to conventional "octahedra-engineering". Furthermore, it also provides a guiding principle for the development of sustainable and environmentally friendly electronic and electro-mechanical devices, as compounds comprising tetrahedral chains are widely found in rock-forming oxides, which are abundant in the earth's crust.

Acknowledgement

A. Kuwabara and H. Moriwake (Japan Fine Ceramics Center), J. Kim, Y. Kim, and M. Takata (Spring-8, RIKEN), S. Kim (Sungkyunkwan Univ.), S. Mori (Osaka Pref. Univ.), Y. Inaguma (Gakushuin Univ.), and H. Hosono and M. Itoh (Tokyo Inst. Tech.).

References

1. H. Taniguchi *et al*., Angew. Chem. Int. Ed. **52** (2013) 1-6.

Evaldas **TORNAU**

Dr. habil. Evaldas E. Tornau, leading scientific researcher of Semiconductor Physics Institute of Center for Physical Sciences and Technology, Vilnius, Lithuania. Published close to 100 papers on models of phase transitions, phase transitions in ferroelectrics, magnetics and high-temperature superconductors, ordering of atoms and molecules on surfaces.

Title of a talk:
Phase transitions in antiferromagnetic triangular Blume-Capel model with hard core exclusions.

RCBJSF In-19

Phase Transitions in Antiferromagnetic Triangular Blume-Capel Model with Hard Core Exclusions

M. Simenas, A. Ibenskas, E.E. Tornau

Semiconductor Physics Institute, Center for Physical Sciences and Technology, Gostauto 11, LT-01108 Vilnius, Lithuania

e-mail: et@et.pfi.lt

Using Monte Carlo simulation we analyze phase transitions of three triangular Blume-Capel (BC) models with antiferromagnetic (AFM) interactions. First model is a standard BC model with AFM interactions between nearest neighbours (1NN). Two other models have AFM interactions between third nearest neighbors (3NN). One of them has hard core exclusions between the 1NN particles (3NN1 model) and the other - between 1NN and second-neighbour particles (3NN12 model). Finite-size scaling analysis reveals that in these models, as in the 1NN AFM BC model, the transition from paramagnetic to long-range order (LRO) AFM phase is either of the first-order or goes through intermediate phase which might be attributed to Berezinskii-Kosterlitz-Thouless (BKT) type. We show that properties of the low-temperature phase transition to the AFM phase of 1NN, 3NN1 and 3NN12 models are very similar in all interval of a normalized single-ion anisotropy parameter, δ, except the first order phase transitions region. Due to different entropy of the 3NN12 and 3NN1 models, their higher temperature behaviour is different from that of the 1NN model. Three phase transitions are observed for the 3NN12 model: (i) from paramagnetic phase to the phase with domains of the LRO AFM phase at T_c ; (ii) from this structure to diluted frustrated BKT- type phase at T_2 (high-temperature limit of the critical line of the BKT- type phase transitions) and (iii) from this frustrated phase to the AFM LRO phase at T_1 (low-temperature limit of this line). For the 3NN12 model $T_c > T_2 > T_1$ at $0 < \delta < 1.15$ (range I), $T_c = T_2 > T_1$ at $1.15 < \delta < 1.3$ (range II) and $T_c = T_2 = T_1$ at $1.3 < \delta < 1.5$ (range III). For 3NN1 model $T_c = T_2 > T_1$ at $0 < \delta < 1.2$ (range II) and $T_c = T_2 = T_1$ at $1.2 < \delta < 1.5$ (range III). In range III there is only first order phase transition. In range II the transition at $T_c = T_2$ is of the first order, too. In range I the transition at T_c is either a weak first-order or a second-order phase transition.

Vladimir **TREPAKOV**

Vladimir Trepakov graduated at St.-Petersburg Polytechnical Institute in 1972. From 1972 he has been working in Ioffe Physical-Technical Institute, St-Petersburg, Russia, where in 1980 he obtained his PhD degree (supervisor Professor G.A. Smolensky); during 2001-2003 – Professor at the University of Osnabrueck, Germany; from 2003 he joined the Institute of Physics AS CR, Prague, Czech Republic. V. Trepakov is a well known scientist successfully working in physics of ferroelectrics, incipient ferroelectrics, highly polarizable advanced oxides and multiferroics, crystals, ceramics, thin films, nano-powders and structures. His research activities cover phase transitions, zero- and low-T phase transitions, electronic processes and ordering phenomena, photoinduced phenomena, structural and spectroscopic active impurities in highly polarizable materials, confine geometry and nano-size effects; strongly correlated systems. His publication list includes over 250 papers. V. Trepakov is the co-author of the several important fundamental pioneer results, e.g.: i) experimental discovery of the family of the kinetic dielectric thermo-polarization effects (dielectric analogs of Seebeck, Peltier and Thomson effects in semiconductors) awarded the First prize of the International Thermoelectric Society; ii) first observation of the reentrant polar glass state, iii) photoinduced local configuration instability of impurity ions in matrix with soft-modes iv) direct observation of the soft electronic modes, v) experimental observation of polaronic excitons, etc.

RCBJSF In-20

Electronic Structure, Optical and Dielectric Spectroscopy of $TbMnO_3$ Multiferroic

V.A. Trepakov[1,2], A.G. Dejneka[1], O.E. Kvyatkovskii[2], Z. Potucek[1], M.E. Savinov[1], L. Jastrabik[1], X. Wang[3] and S.-W. Cheong[3]

[1]Institute of Physics, ASCR, Na Slovance 2, 182 21 Prague 8, Czech Republic

[2]Ioffe Physical-Technical Institute of the RAS, 194 021 St.-Petersburg, Russia

[3]Rutgers Centers for Emergent Materials and Department of Physics and Astronomy Rutgers University, NJ 08854

e-mail: trevl@fzu.cz

Remarkable family of orthorhombically distorted perovskite-like rare earth manganites *R*MnO_3 (R = La, Pr, Nd, Sm, Eu, Gd, Tb, Dy) has been attracting a plenty of attention exhibiting new diverse properties, of high fundamental academic and application interests (e.g. colossal magnetoresistance). Among of them, magnetoelectric multiferroics (or ferroelectromagnets) manganites with R = Eu, Gd, Tb, Dy are turned out to be the objects of the peculiar interest now. At room temperature they are paramagnetic ones. In the temperature region of T < 30- 40 K they obey magnetic ordering followed by induced long order ferroelectric phase transitions. Close proximity of ferroelectric and magnetic phase transitions provides strong coupling magnetic and ferroelectric degree of freedom, intricate interplay of the lattice, charge, orbital, and spin, emergence of unique properties and effective magnetic control of a spontaneous polarization. In this regard, orthorhombic $TbMnO_3$ has attracted a special considerable attention. Namely studies this material led to discovery of a new class of multiferroics with spin-spiral driven ferroelectricity (new mechanism of ferroelectricity), and efficient switching phenomena. In this report we present recent results of spectral ellipsometry, thermooptics, luminescence, and low-frequency dielectric permittivity studies of $TbMnO_3$ single crystals. The main attentions was paid to determination of electronic structure, elucidation of the nature of main optical transitions, phase transitions related properties, obtaining experimental evidences of electronic contribution in ferroelectric phase transitions of $TbMnO_3$ and nature of an unusual dielectric dispersion was found in the region of ferroelectric phase transition. It was shown that observed dispersion is caused by pronounced magneto-electric coupling.

Kenji **TSUDA**

Research Interests

- Development of a method to refine crystal structural parameters and electrostatic potential using Convergent-Beam Electron Diffraction (CBED)
- Nano-scale local electrostatic potential analysis of ferroelectrics and multiferroics
- Electrostatic potential analysis of charge-/orbital-ordering materials
- Structural study of phase transformation materials

Education / Employment

- Apr. - Jul. 2004: Visiting researcher at Triebenberg lab, TU Dresden, Germany
- Nov. 2001 - present: Associate professor, Institute of Multidisciplinary Research for Advanced Materials (IMRAM), Tohoku University.
- Apr. 2001 - Oct. 2001: Research associate, IMRAM, Tohoku University.
- Apr. 1992 - Mar. 2001: Research associate, Research Institute for Scientific Measurements (RISM), Tohoku University.
- Apr. 1991 - Mar. 1992: JSPS Fellowships for Japanese Junior Scientists.
- Nov. 1991: Ph. D., Physics, Tohoku University.
- Mar. 1989: M.C., Physics, Tohoku University.
- Mar. 1987: B.S., Physics, Tohoku University.

Awards

- Research Award of the Crystallographic Society of Japan (2010)
- Award of the Society of promotion of Scientific measurements (2009)
- Seto Award, The Japanese Society of Microscopy (2004)
- Harada Research Award (1993)
- Reserch Award of Inoue Foundation for Science (1992)

Publication listi s available at
http://www.tagen.tohoku.ac.jp/labo/terauchi/personal/tsuda/KTpub.html

RCBJSF In-21

Study of Nanoscale Local Structural Fluctuations in Ferroelectrics Using Convergent-Beam Electron Diffraction

K. Tsuda[1], R. Sano[1], A. Yasuhara[2] and M. Tanaka[1]

[1]Institute of Multidisciplinary Research for Advanced Materials, Tohoku University, Japan

[2]JEOL Ltd., Japan

e-mail: k_tsuda@tagen.tohoku.ac.jp

It is well known that $BaTiO_3$ undergoes successive phase transformations from the cubic paraelectric phase to three ferroelectric phases: tetragonal, orthorhombic and rhombohedral ones. Coexistence of the displacive and order-disorder characters in the phase transformations of $BaTiO_3$ was pointed out from many experiments and theories. However, local structures related to the order-disorder character were discovered neither in crystal structure analyses using neutron and X-ray diffraction nor by TEM observations. In the present study, the convergent-beam electron diffraction (CBED) method [1] was applied to examine nanometer-scale local structures of $BaTiO_3$.

Rhombohedral nanostructures were observed in the orthorhombic and tetragonal phases of $BaTiO_3$ using CBED [2]. It was found that the symmetry of the orthorhombic phase is formed as the average of two rhombohedral variants with different polarizations, and that of the tetragonal phase is formed as the average of four rhombohedral variants. These results indicate an order-disorder character in their phase transformations.

Similar rhombohedral nanostructures were also found in the ferroelectric orthorhombic phase of $KNbO_3$ [3], while it was confirmed that the ferroelectric tetragonal phase of $PbTiO_3$ does not have such rhombohedral nanostructures [4].

We also proposed a combined use of STEM and CBED methods (STEM-CBED method) to observe the nanostructures of polarizations [5]. Using the method, two-dimensional distributions of the rhombohedral nanostructures, or nanoscale fluctuations of the polarization clusters, were successfully visualized in the tetragonal phase of $BaTiO_3$. We are also planning to apply this method to the orthorhombic and cubic phases.

References

1. Tanaka and Tsuda, J. Electron Microsc. **60(Suppl. 1)**, S245 (2011).
2. Tsuda, Sano and Tanaka, Phys. Rev. B **86**, 214106 (2012).
3. Tsuda, Yasuhara and M. Tanaka, Appl. Phys. Lett. **102**, 051913 (2013).
4. Tsuda and Tanaka, Appl. Phys. Express **6**, 101501 (2013).
5. Tsuda, Sano and Tanaka, Appl. Phys. Lett. **102**, 051913 (2013).

Yuhji
TSUJIMI

Title of my talk:
Broad Doublet Spectra in the Quantum Paraelectric State of $SrTiO_3$

Short CV:
Professional Experiences:
1978-1993: Hokkaido University of Education
(1987-1988 IBM Research-Zurich: Invited scientist)
1993-present: Research Institute for Electronic Science, Hokkaido University

RCBJSF In-22

Broad Doublet Spectra in the Quantum Paraelectric State of $SrTiO_3$

Y. Tsujimi and S. Nakamura

Research Institute for Electronic Science, Hokkaido University, Sapporo 001-0020, Japan

e-mail: yts@es.hokudai.ac.jp

In 1995, Hehlen *et al*. discovered the strange spectral peak called "Broad doublet" (BD) appearing only in the quantum paraelectric state (QPS) of $SrTiO_3$.[1] The frequency of the BD is lower than that of the transverse acoustic mode (TA) of lowest frequency. This fact is very interesting, because any excitation should not exist in the frequency region lower than TA mode's frequency. Hehelen *et al*. proposed that the physical origin of the BD is a second sound, and Koreeda *et al*. supported their proposal.[2] On the other hand, some negative reports for the second sound scenario have been published.[3]

In order to clarify the physical origin of the BD, we have performed the light scattering experiment with a scattering vector of $\boldsymbol{q}$ // $[001]_c$ and observed the BD under the uniaxial stress σ (along the $[010]_c$ direction). Figure shows the results of the polarization analyses (VV, VH, HV, and HH 180° light scattering spectra) performed under σ = 19.4 kgf/mm^2 at 16.5 K. The intensity of the LA mode is almost the same both in the VV and HH spectra, whereas the intensity of the BD is much stronger in the HH spectrum than in the VV spectrum. If the BD is the second sound, it should behave like a LA mode (the second sound is the density wave of phonons) and should not show any anisotropic behavior in the polarization analyses. We can conclude without any assumption that the physical origin of the BD is not the second sound. In this conference, we are going to discuss what the real physical origin is.

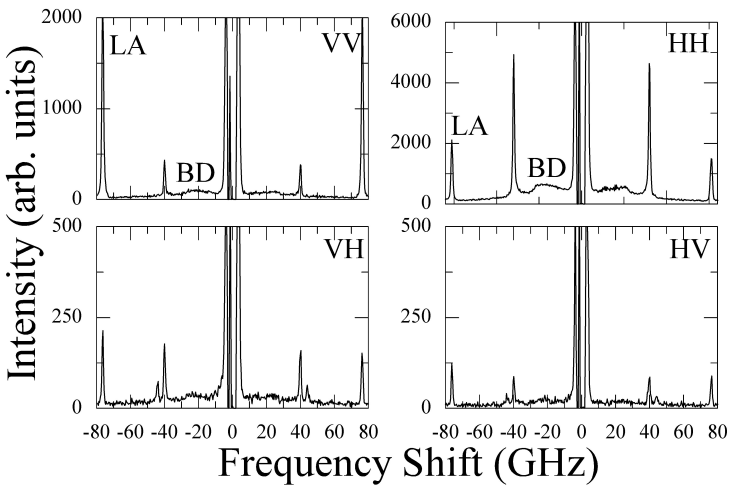

References

1. K.A. Müller and H.Burkard, PRB 19 (1979) 3593. [2] A. Koreeda, R. Takano, and S. Saikan, Phys. Rev. Lett. **99**, 265502 (2007). [3] e. g. : Y. Tsujimi and M. Itoh, J. Korean Phys. Soc. **51**, 819 (2007).

Rostyslav **VLOKH**

Professor, Habilitated Doctor, Director of the Institute of Physical Optics of the Ministry of Education and Science of Ukraine

Rostyslav Vlokh has obtained his MS Degree at the Lviv National University in 1987, the PhD Degree at the Uzhgorod National University in 1990, and his Habilitation at the Institute of Physical Optics in 1996. Up to 2000, he has occupied a position of Professor at the Lviv National Polytechnic University. During 2001–2009 he has been the Deputy Director and, beginning from 2010, the Director of the Institute of Physical Optics.
The scientific activities by Professor R. Vlokh are concerned with the optical properties of crystals in the course of structural phase transitions, the methods for studying the optical phenomena, the optical materials, the effects of parametric optics, the crystal optics, and the singular optics.

RCBJSF In-23

Generation of Optical Vortices via Electro- and Piezo-Optic Effects in Ferroelectric-Type Crystalline Materials

R. Vlokh, I. Skab, Y. Vasylkiv, and M. Smyk

Institute of Physical Optics, Ukraine

e-mail: vlokh@ifo.lviv.ua

The aim of this work is to report the recent achievements in generation of optical vortices that bear an orbital angular momentum, using the crystalline materials subjected to inhomogeneous electric fields and mechanical stresses [1–6]. It is shown that the optical vortices with different topological charges can be generated as a result of the following factors: (i) the torsion and bending stresses, via the piezo-optic effect, (ii) the 'conically' shaped electric fields, via the Pockels and Kerr electro-optic effects, and (iii) the acousto-optic diffraction in crystals possessing the optical activity effect. The conditions of generation of the optical vortices are analyzed for the crystals of different point symmetry groups. The singularities of optical wave fronts and the induced optical vortices are revealed experimentally for a number of crystalline materials. The efficiency of optical vortices generation is analyzed for different crystalline materials. It is found that the ferroelectric crystals are among the most efficient materials used for this aim (see [7]). The results obtained are discussed, considering the fact that the angular momentum linked to optical beams represents one of their fundamental properties, which have been widely studied in the recent years. There is a great interest in 'spinning' and 'twisting' of light as manifestations of the two rotational degrees of freedom of any photonic flux, in the spin and orbital angular momentums associated with the quantum properties of light. They can be used in a number of novel areas of application, e.g. information processing, quantum cryptography, quantum teleportation, manipulation of microparticles and creation of non-diffractive beams [8].

References

1. I. Skab, Yu. Vasylkiv, I. Smaga, and R. Vlokh, Phys. Rev. A. **84**, 043815 (2011).
2. I. Skab, Yu. Vasylkiv, and R. Vlokh, Appl. Opt., **51**, 5797 (2012).
3. I. Skab and R. Vlokh R., Ukr. J. Phys. Opt., **13**, 1 (2012).
4. I. Skab, Yu. Vasylkiv, B. Zapeka, V. Savaryn, and R. Vlokh. J. Opt. Soc. Am. A. **28**, 1331 (2011).
5. I. Skab, Yu. Vasylkiv, V. Savaryn, and R. Vlokh, J. Opt. Soc. Am. A. **28**, 633 (2011).
6. Yu. Vasylkiv, I. Skab, and R. Vlokh, Appl. Opt., **53**, B60 (2014).
7. Yu. Vasylkiv, I. Skab, and R. Vlokh, Opt. Mater. **35**, 2496 (2013).
8. Yu. Vasylkiv, M. Smyk, I. Skab, and R. Vlokh, Ukr. J. Phys. Opt. **15**, 9 (2014).

Tatyana **VOLK**

Tatyana R. Volk graduated from Moscow University in 1965. Starting in 1968 till nowadays she has been working in Shubnikov Institute of Crystallography of the Russian Academy of Sciences (IC RAS), where she obtained her PhD in 1972 and doctoral degree in 1995. Since 1998 she is the Head of the Laboratory of crystal optics in IC RAS. Her main research interests belong to the ferroelectricity (phase transitions, domain structure), nonlinear – optical phenomena (photorefraction, optical frequency conversion) and point defects (radiation induced effects in ferroelectrics). She has published in co-authorship more than 150 papers and two monographs: "Lithium Niobate (Defects, Photorefraction, Vibrational Spectrum and Polaritons)" by N. V. Sidorov, T. R. Volk, B. N. Mavrin and V. T. Kalinnikov, 2003, Nauka (in Russian) and "Lithium Niobate (Defects, Photorefraction and Ferroelectric Switching)" by T. Volk and M. Woehlecke, 2008, Springer. She is the vice-chairman of the Russian National Council in the Physics of Ferroelectrics and Dielectrics and a member of the Steering Committee of European Meeting on Ferroelectricity.

RCBJSF In-24

Planar Microdomain Patterns for Nonlinear-Optical Applications Fabricated in Ferroelectric Crystals by Microscopic Methods (AFM and SEM)

T.R. Volk[1], L.S. Kokhanchik[2], R.V. Gainutdinov[1], and E.D. Mishina[3]

[1]Shubnikov Institute of Crystallography of the Russian Academy of Sciences, Russia

[2]Institute of Microelectronics Technology and High Purity Materials of the Russian Academy of Sciences, Russia, Russia

[3]Moscow State Institute of Radio Engineering, Electronics and Automation, Russia

e-mail: volk@crys.ras.ru

1D and 2D microdomain patterns of specified design have attracted increased attention in view of their applicability for nonlinear-optical frequency conversion. We summarize our results on recording planar microdomain patterns by means of the AFM method and electron-beam of SEM. Experiments were performed in $Sr_xBa_{1-x}Nb_2O_6$ (SBN) and $LiNbO_3$ crystals and He-implanted planar optical waveguides.

In the AFM method, the local polarization reversal occurs under standard AFM dc-voltages applied to the tip. In SEM method it is caused by space-charge fields induced by local e-beam irradiation. We investigated the regularities and specificity of the domain formation under these conditions. Shaping of domain gratings and other 2D patterns with specified parameters was elaborated. Stable domain gratings with spatial periods 3 - 7 μm, several microns in thickness and dimensions up to 500 x 300 μm^2 were recorded. The recorded patterns were examined using the nonlinear-optical methods such as SHG microscopy and nonlinear diffraction.

The results obtained are promising for development of the domain engineering by microscopic methods, in particular in optical waveguides.

References

1. T. R. Volk, L. V. Simagina, R. V. Gainutdinov, et al, J. Appl. Phys., 108, 042010, 2010
2. L. V. Simagina, E. D. Mishina, S. V. Semin, et al. J. Appl. Phys., 110, 052015, 2011
3. L. S. Kokhanchik, T. R. Volk, Appl. Phys. B, 110, 367, 2013

Yasuhiro **YONEDA**

Nationality: Japanese

Address:
Japan Atomic Energy Agency (JAEA), 1-1-1 Kouto, Sayo-cho, Sayo-gun, Hyogo 679-5148, Japan

E-mail: yoneda@spring8.or.jp

Education:

1997 Kwanse-Gakuin University (PhD)
1992 Kwansei-Gakuin University (Bachelor)

Employment:

1997-1998 Japan Atomic Energy Agency, Postdoctoral researcher
1998- present Japan Atomic Energy Agency, Researcher

Selected publications:

1) "Local structure analysis of $BaTiO_3$ nanoparticles",
Y. Yoneda, S. Kohara, and K. Kato:
Japanese Journal of Applied Physics **62** (2013) 09KF01/1-5.

2) "Local structure analysis of $SmFe_2$ and $TbFe_2$",
Yasuhiro Yoneda, Shinji Kohara, Masayoshi Ito, Hiroshi Abe, Mitsuaki Takeuchi, Hirohisa Uchida, and Yoshihito Matsumura:
Trans. Mat. Res. Soc. Japan **38** (2013) pp. 109-112.

3) "Electronic and local structures of Mn-doped $BiFeO_3$ crystal",
Y. Yoneda, Y. Kitanaka, Y. Noguchi, and M. Miyayama:
Phys. Rev. B **86** (2012) pp. 184112/1-10.

4) "Local structure analysis of $NaNbO_3$",
Yasuhiro Yoneda, Desheng Fu, and Shinji Kohara:
Journal of Physics: Conference Series **502** (2014) pp. 012022/1-4.

5) "Phase Transition of Bi_2WO_6 below 300 K",
Yasuhiro Yoneda, Hiroaki Takeda, and Takaaki Tsurumi:
Journal of Physical Society of Japan Conf. Proc. **1** (2014) pp. 012103/1-4.

RCBJSF In-25

Atomic Pair-Distribution Function (PDF) Analysis on Ferroelectric Materials using Synchrotron X-ray

Y. Yoneda

Japan Atomic Energy Agency (JAEA) 1-1-1 Kouto, Sayo-cho, Sayo-gun, Hyogo 679-5148, Japan

e-mail: yoneda@spring8.or.jp

Since the domain structure exists in a ferroelectric material, there is a difference in average structure and local structure inside a domain. In the solid solution system from which average structure tends to be cubic structure, in order to understand a ferroelectric mechanism, local structure analysis is required. We performed atomic pair-distribution function (PDF) analysis of BaTiO3 – KNbO3 solid solutions as an example of the local structure analysis. The characteristic local structure, which appears in a phase boundary was found out.

RCBJSF-12 Oral Presentation Abstracts

RCBJSF Or-1

Dielectric Properties and Phase Diagram of $(Sr_{1-x}Ba_x)_2Nb_2O_7$ Single Crystals

Y. Akishige, M. Kamada, and S. Tsukada

Faculty of Education Shimane University, Japan

e-mail: akishige@edu.shimane-u.ac.jp

$Sr_2Nb_2O_7$ (SN) is one of the high T_C ferroelectrics with the perovskite slab structure. The crystal structure is orthorhombic-*Cmcm* in the paraelectric phase above T_C (=1615 K) (pase I) and it becomes orthorhombic-$Cmc2_1$ in the ferroelectric phase below T_C (phase II): the spontaneous polarization along the *c*-axis is ca. 9 $\mu C/cm^2$ at room temperature [1]. An Incommensurate phase transition occurs at T_2 (=488 K) accompanying with a weak dielectric anomaly in dielectric constant ε'_c along the *c*-axis. In the incommensurate phase, the modulation wave propagates along the *a*-axis with a wave vector of $q = (1/2-\delta)a^*$. If the misfit parameter δ is zero, the space group becomes $Pbn2_1$. The dielectric constant ε'_b along the *b*-axis exhibits a large anomaly at T_3 (=100 K) and the ferroelectric polarization vector somewhat tilts to the *b*-axis. Below T_3 the space group is probably *Pb*11. As for Ba doped SN, $(Sr_{1-x}Ba_x)_2Nb_2O_7$, the T_C decreases with *x* [2]. For *x*=0.32 crystals, the low temperature ferroelectric transition at T_3 disappears and a new ferroic phase transition occurs at 465 K [3].

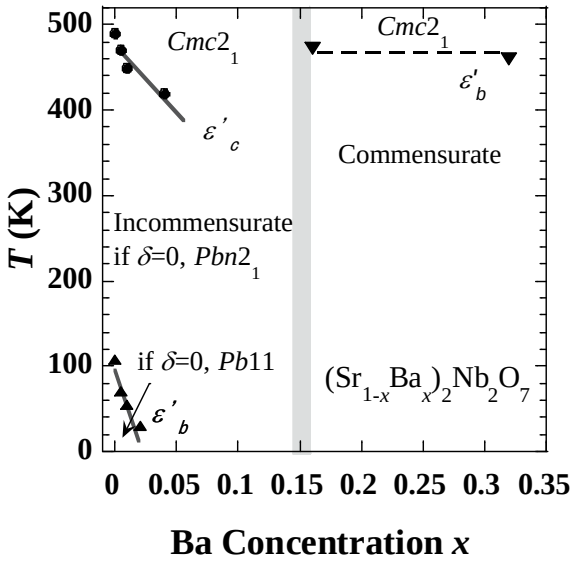

Fig. 1 Phase diagram of $(Sr_{1-x}Ba_x)_2Nb_2O_7$

In order to reveal the phase diagram of the Ba-doped SN, we prepared single crystals with different *x* up to *x* = 0.32 by a floating zone method and measured the dielectric constant in a temperature range from 10 K to 600 K. As shown in Fig. 1, both of the phase transition temperatures T_2 and T_3 decrease monotonously with *x*, and the incommensurate phase disappears at around *x* = 0.15. Above this Ba concentration, ε'_b shows anomaly at ca. 465 K.

References

1. S. Nanamatsu *et al.* J. Phys. Soc. Jpn. **30**, 300 (1971).
2. S. Nanamatsu *et al.* J. Phys. Soc. Jpn. **38**, 817 (1975).
3. Y. Akishige *et al.* J. Korea. Phys. Soc. **42**, S1187 (2003).

RCBJSF Or-2

Local Structure Studies of Ti for $SrTi^{16}O_3$ and $SrTi^{18}O_3$ by Advanced X-ray Absorption Spectroscopy Data Analysis

A. Anspoks[1], D. Bocharov[1], J. Purans[1], F. Rocca[2], A. Sarakovskis[1], J. Timoshenko[1], V. Trepakov[3,4], A. Dejneka[3] and M. Itoh[5]

[1]Institute of Solid State Physics, University of Latvia

[2]IFN-CNR, Institute for Photonics and Nanotechnologies, Unit 'FBK-Photonics' of Trento, Povo (Trento), Italy

[3]Institute of Physics, AS CR, Prague, Czech Republic

[4]Ioffe Physical-Technical Institute RAS, St-Petersburg, Russia

[5]Tokyo Institute of Technology, Japan

e-mail: andris.anspoks@cfi.lu.lv

Strontium titanate ($SrTiO_3$) is a model quantum paraelectric in which in the region of dominating quantum statistics the ferroelectric (FE) instability is inhibited due to nearly complete compensation of the harmonic contribution into FE soft mode frequency by the zero-point motion [1]. The enhancement of atomic masses by the substitution of ^{18}O for ^{16}O decreases the zero-point atomic motion and low-T ferroelectricity in $SrTi^{18}O_3$ is realized [2].

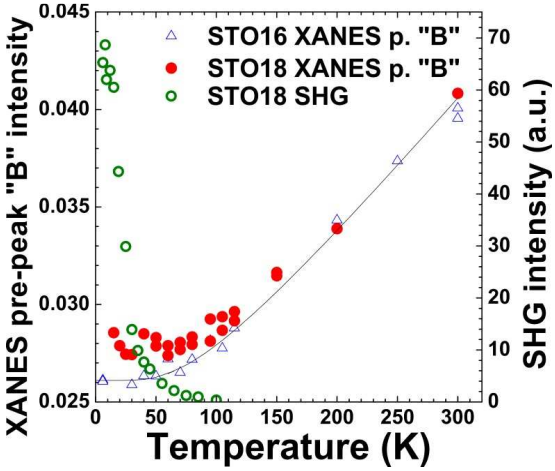

Fig.1 Temperature dependence of the XANES pre-peak "B" for STO18 (red dots) compared with that of STO16 (blue triangles) and optical second harmonic generation signal from STO18 (green circles).

We report on the local structure studies of Ti in $SrTi^{16}O_3$ (STO16) and $SrTi^{18}O_3$ (STO18) by Ti K-edge extended x-ray absorption fine structure (EXAFS) and x-ray absorption near edge structure (XANES) spectroscopy, supplemented by optical second harmonic generation (SHG) measurements at low temperature (6 – 300 K). Advanced methods of EXAFS analysis [3] and *ab initio* XANES modeling allowed us to reveal the local atomic structure and dynamics around Ti near the ferroelectric (25 K) and antiferrodistortive (105 K) phase transitions.

References

1. Muller K A and Burkard H *Phys. Rev.* **B 19,** 3593 (1979)
2. M. Itoh, R. Wang, Y. Inaguma, et.al., *Phys. Rev Letters*. **82**, 3540 (1999).
3. J. Timoshenko, A. Kuzmin, J. Purans, *J. Phys.: Condens. Matter* **26**, 055401 (2014).

RCBJSF Or-3

Structural and Electrical Characterization of Epitaxially Strained $Ba_{0.7}Sr_{0.3}TiO_3$ Thin Films Deposited by PLD

Š. Bagdzevičius[1, 2], R. Mackevičiūtė[1], N. Setter[2], J. Banys[1]

[1]Faculty of Physic, Vilnius University, Vilnius, Lithuania

[2]Ceramics Laboratory, Swiss Federal Institute of Technology (EPFL), Lausanne, Switzerland

e-mail: sarunas.bagdzevicius@ff.vu.lt

The aim of this work was to investigate processing conditions and deposit epitaxially strained BST70/30 ($Ba_{0.7}Sr_{0.3}TiO_3$) thin films with smooth and well defined interfaces. Depositted thin films were analysed by structural and electrical characterization techniques. Influence of deposition temperature, laser fluence and repetition rate, ambient pressure on growth mode, film crystalinitty and electrical properties were studied.

BST70/30 thin films were deposited on 001 oriented $SrTiO_3$ single crystal substrates with LSMO ($La_{0.8}Sr_{0.2}MnO_3$) electrode by pulsed laser deposition with KrF excimer laser (λ=248 nm). BST and LSMO ceramics were used as the targets. Substrates were etched in buffered HF acid and annealed in oxygen flow at 935°C [1] to get atomically smooth surface. Best quality BST films were obtained at 750–800°C deposition temperature range, with 3 Hz laser repetition rate and 40–42 mJ energies. The oxygen pressure was 0.15 mBar during deposition and was raised to 1 mBar during cool down. Both LSMO electrode and BST thin films showed good epitaxy (Fig. 1) and crystallinity, XRD BST 002 reflex rocking curve FWHM was 0.12° (BST film thickness 76 nm, LSMO electrode thickness 13 nm).

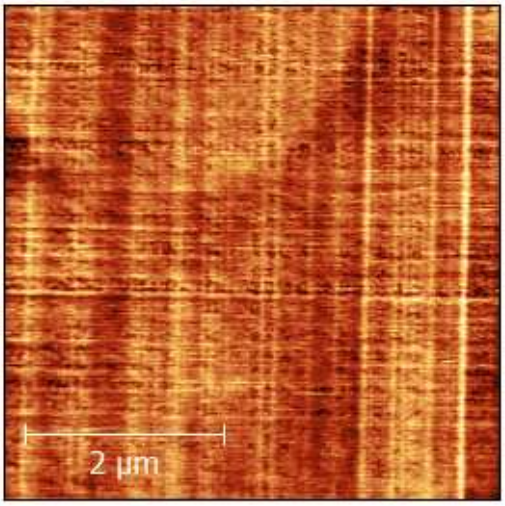

Fig.1 AFM images of BST thin film BST/LSMO//STO (BST thickness - 76 nm, LSMO – 13 nm). Vertical scale is 1.5 nm.

Acknowledgements

This work has been financed by the Lithuanian-Swiss cooperation programme "Research and development" joint research project "SLIFE", project code LSP-12 007

References

1. T. Ohnishi, K. Shibuya, M. Lippmaa, D. Kobayashi, H. Kumigashira, Appl. Phys. Lett. **85**, 272 (2004).

RCBJSF Or-4

Cooling Method Based on Electrocaloric Effect Realized in Periodically Switching Electric Filed in Triglycinesulphate

V.S. Bondarev[1, 2], M.V. Gorev[1, 2], E.A. Mikhaleva[1], I.N. Flerov[1, 2]

[1]L.V. Kirensky Institute of Physics, Krasnoyarsk, Russia

[2]Siberian Federal University, Krasnoyarsk, Russia

e-mail: vbondarev@yandex.ru

Recently there was suggested a cooling method based on electrocaloric effect (ECE) realized in periodically switching electric filed in nonequilibrium thermal conditions [1]. It was pointed out, that optimal cooling process takes place at proper selection of working temperature point on non-linear $\partial\chi/\partial T(T)$ dependence because of nonequality of absorbed and emitted heat amounts induced by applying and removing electric field, respectively [2, 3]. In this work, the experimental data concerning ECE in triglycinesulphate (TGS) in nonequilibrium (Fig.1) and adiabatic conditions are presented. Applying an electric field in the adiabatic conditions to TGS crystal causes temperature increase. This effect is highly reversible, because an equal and opposite temperature change is observed upon subsequent removal of the electric field. However, it has been found, that in the nonequilibrium conditions of both para- and ferroelectric phases the temperature gradient of the sample leads to the appearance of polarization which was detected by thermopolarization current. Due to both ECE and the temperature gradient, periodically switching electric field leads to periodical heating and cooling of the sample and directional heat flux appears as the result of such influence. Such effect causes insignificant cooling of the sample in the nonequilibrium temperature conditions.

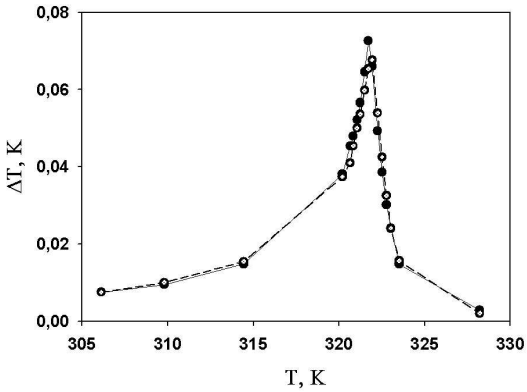

Fig.1 Electrocaloric effect in crystal TGS at different temperatures in field at 2000V/cm. The open and closed circles represent the adiabatic temperature change upon applying and removing the electric field.

Acknowledgment

This work was supported in part by the Council on Grants from the President of the Russian Federation for Support of Leading Scientific Schools (project no. Nsh- 924.2014.2).

References

1. A.S. Starkov, S.F. Karmanenko, O.V. Pakhomov et al. Phys. Sol. State, **51**, 7, p. 1510 (2009)
2. A.L. Kholkin, V.A. Trepakov and G.A. Smolenskii. JETP Lett, **35**, p. 124 (1982)
3. A.K. Tagantsev. Sov. Phys. Usp. **30**, p. 588 (1987)

RCBJSF Or-5

Searching of New Multiferroics on the Base of Co-Doped $BaTiO_3$

R. Bujakiewicz-Korońska

Institute of Physics, Pedagogical University, Cracow, Poland

e-mail: rbk@up.krakow.pl

New ceramics material $Ba_{0.95}Pb_{0.05}TiO_3$:Co_2O_3 (BPTC) has been prepared by the conventional hot-sintering method in the aim of looking for new multiferroics which could be useful for the electronic industry. The experimental results showed that substituting Pb^{2+} ions in A—site is very useful tool to control the Curie temperature [1]. The co-doping with Co^{3+} ions reduces high dielectric losses related to the structural phase transition in BPTC. The Pb^{2+} and Co^{3+} doping ions diffuse the ferroelectric-paraelectric phase transition. The BPTC exhibits relaxor-like behaviour in the temperature range from 125 to 225 K, checked by dielectric test. It shows the existence of the polar nanoregions, which originate from the presence of acceptor-oxygen vacancy Co^{3+}-V_O^{1-} dipoles in highly polarizable lattice [2].

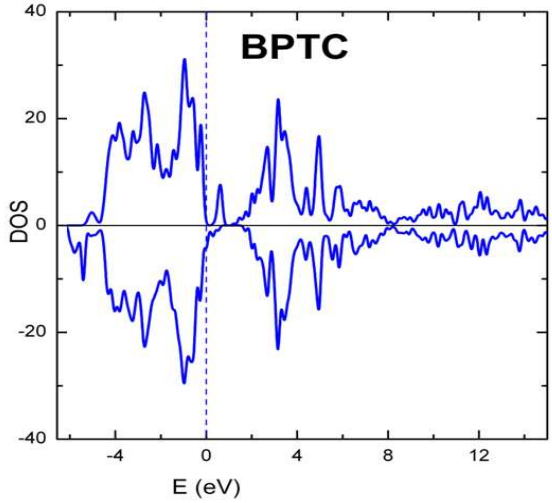

Fig.1 Diagram DOS with spin polarization. There are differences visible between spin down and spin up.

Ab initio calculations were performed within DFT using GGA and LCAO with localized basis set in the form of spherical functions as implemented in SIESTA 3.2 code together with spin polarization (Fig 1). The results of DOS calculations and magnetic measurements allow to classify BPTC as a multiferroic of I type, since weak coupling between ferroelectric and magnetic properties occurs.

Acknowledgments

The authors acknowledge the CPU time allocation at Academic Computer Centre CYFRONET AGH in Cracow. This work was supported in part by PL-Grid Infrastructure.

References

1. R. Bujakiewicz-Korońska, A. Kalvane, Y. Zhydachevskii, B. Garbarz-Glos, W. Śmiga, L. Vasylechko, J. Czerwiec, A. Suchocki, A. Kamińska, and W. Piekarczyk, Ferroelectrics **436**, 62 (2012).
2. E. Markiewicz, R. Bujakiewicz-Korońska, D. Majda, L. Vasylechko, A. Kalvane, and M. Matczak, J Electroceram **32**, 92 (2014).

RCBJSF Or-6

Lattice Dynamics and Incommensurate Phase in $PbHfO_3$

R. Burkovsky[1,2]

[1]European Synchrotron Radiation Facility, Grenoble, France

[2]St.-Petersburg State Polytech. University, St.-Petersburg, Russia

e-mail: burkovsk@esrf.fr

We report the results of a combined diffraction and inelastic X-ray scattering study of lead hafnate. We find that this crystal is a first chemical-disorder-free and non-magnetic perovskite with an incommensurate (IC) phase. The IC phase is characterized by transverse modulations with a wavevector $\mathbf{q}_I=[q,q,0]$, where q is a temperature dependent parameter of magnitude slightly larger than 1/7. The formation of IC phase is preceded by the softening and increase of damping constant for a hybridized anharmonic transverse phonon branch along almost the whole <110> direction of the Brillouin zone. This branch is a continuation of the small-q acoustic branch and is thus marked simply as TA in Fig. 1. The TO mode, on the other hand, is temperature independent in the whole range where it can be clearly distinguished. It cannot be distinguished close to the zone center, where it is expected to be soft in accord with the observed growth of dielectric permittivity, and badly distinguished close to M-point, where it is heavily damped with damping constant being increased on cooling. Notably, the anisotropy of the TO dispersion is the opposite with respect to the anisotropy of the TA mode. In other words, it is stiffer in directions where the incommensurate modulations are going to be formed. Among the yet reported low-energy spectra in perovskites the one corresponding to <110> direction in $PbHfO_3$ hast the most similarity with the one corresponding to <100> direction in $KNbO_3$ [2]. This might suggest that despite a lot of differences the mechanisms of phase transitions in lead-based and lead-free perovskites can be indeed very similar.

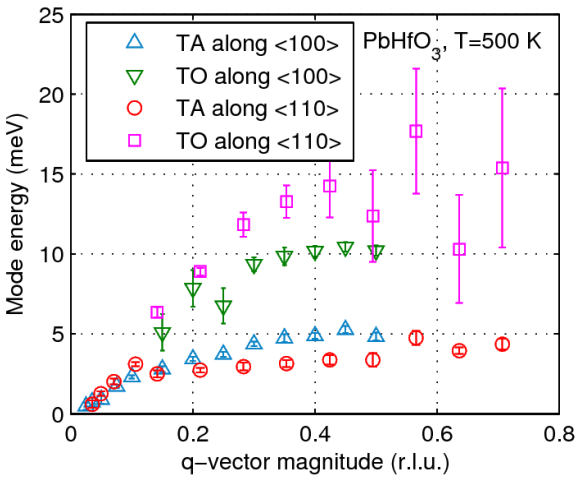

Fig.1 Dispersion relations for the two lowest energy transverse phonons polarized and propagating in {001} plane, T=500 K. The data are obtained at ESRF ID28.

RCBJSF Or-7

Revisiting the Fascinating Properties of $EuTiO_3$ and Its Mixed Crystals with $SrTiO_3$: Possible Candidates for Novel Functionalities and Multiferroicity

A. Bussmann-Holder and J. Köhler

Max-Planck-Institute for Solid State Research, Heisenbergstr. 1, D-70569 Stuttgart, Germany

e-mail: a.bussmann-holder@fkf.mpg.de

The research in perovskite oxides is ever increasing since their discovery in 1945. The number of compounds with this rather simple structure is growing continuously since then and fascinating properties ranging from magnetic via dielectric and superconducting have been reported for them. While an extreme research activity has been devoted to $SrTiO_3$ from its discovery on, its analogue $EuTiO_3$ has attracted rather little interest until recently. Here we concentrate on the recent results from studies of this perovskite and its mixed crystals with $SrTiO_3$ and demonstrate that novel interesting properties are related to it. Specifically we provide evidence for the existence of hybrid-paramagnon-phonon coupling at elevated temperatures and its manifestations in bulk sensitive experiments. In addition, the phase diagram of the mixed crystal series is presented where pressure and temperature effects are included. A novel hidden magnetic order is discovered which is tightly bound to the oxygen octahedral rotation and follows the temperature dependence of the soft acoustic mode.

RCBJSF Or-8

Temperature Dependence of Isolated Domain Shape in Lithium Tantalate Single Crystals

V.Ya. Shur[1,2], A.R. Akhmatkhanov[1,2], D.S. Chezganov[1], A.I. Lobov[1], I.S. Baturin[1,2], and M.M. Smirnov[1]

[1]Ferroelectric Laboratory, Institute of Natural Sciences, Ural Federal University, Russia

[2]Labfer Ltd., Russia

e-mail: dmit.chezganov@gmail.com

The temperature dependence of the shape of isolated domains and its evolution after merging during polarization reversal in uniform electric field have been studied in lithium tantalate crystals (congruent CLT and stoichiometric SLT) in temperature range up to 250^{O}C. The obtained shape evolution has been analyzed in terms of kinetic approach [1].

The domain patterns revealed after partial polarization reversal by HF selective etching after removal of metal electrodes were visualized by optical microscopy and scanning electron microscopy. The observed change of the growing domain shape with temperature increase in CLT from triangular with X oriented walls (3X) to circular through hexagonal (6X) has been attributed to increase of the relative input of isotropic ionic conductivity [2]. This fact leads to increase of the role of stochastic nucleation of the steps at the walls and to more effective screening of depolarization field. It was shown that X orientation of the domain walls existing in CLT at temperatures below 190^{O}C results in their nonstop motion and independent domain growth after merging in contrast to jerky wall motion and the domain shape stability effect obtained in SLT and lithium niobate with Y oriented walls [3].

The computer simulation of the domain growth taking into account the competition between determined and stochastic nucleation mechanisms and incomplete screening of depolarization field has been successfully used for explanation of the domain shape change with temperature increase. The obtained results confirmed the applicability of the kinetic approach to explanation of the domain shape.

Acknowledgment

The equipment of the Ural Center for Shared Use “Modern Nanotechnology” UrFU has been used. The research was made possible in part by RFBR and the Government of Sverdlovsk region (Grant 13-02-96041-r-Ural-a), by RFBR (Grants 13-02-01391-a, 14-02-01160-a, 14-02-31255-mol_a, 14-02-31864-mol_a), by OPTEC LLC, by Ural Federal University development program with the financial support of young scientists.

References

1. V.Ya. Shur, J. Mat. Science. **41**, 199 (2006).
2. V.Ya. Shur, A.R. Akhmatkhanov, D.S. Chezganov, I.S. Baturin, and M.M. Smirnov , Appl. Phys. Lett. **103**, 242903 (2013).
3. V.Ya. Shur, “Handbook of advanced dielectric, piezoelectric and ferroelectric materials. Synthesis, properties and applications”, edited by Zuo-Guang Ye, Woodhead Publishing Ltd, pp.622-669 (2008).

RCBJSF Or-9

Electrophysical Properties of Integrated Ferroelectric Capacitors Based on Sol-gel PZT Films

L. Delimova[1], E. Guschina[1], V. Yuferev[1], I. Grekhov[1], D. Seregin[2], K. Vorotilov[2], A. Sigov[2]

[1]Ioffe Physicotechnical Institute, Saint Petersburg, Russia

[2]Moscow State Technical University of Radioengineering, Electronics and Automation, Russia

e-mail: ladel@mail.ioffe.ru

We study Pt/Pb($Zr_{0.53}Ti_{0.47}$)O_3(PZT)/Pt/Ti/SiO_2/Si capacitors, where PZT films were prepared with 15% excess of Pb by sol-gel deposition. The capacitors C1 and C2 differ with annealing conditions and type of Si substrate. The (111) textured polycrystalline films are shown by scanning spreading resistance microscopy to have nonconductive PZT grain boundaries, the current flows inside the grains. Ferroelectric hysteresis loops, transient current-voltage characteristics, short-circuited photocurrent under illumination of the films by light with the quantum energy of 2.7 eV are measured. To control a preliminary polarization of the film, before each measurement the film is depolarized by application of the external prolonged decaying sinusoidal voltage, after that it is poled in a certain direction.

With the external bias decay upon depolarizing the capacitors C1, the measured polarization is found to tend not to zero, but to the stable value of P_{dep} = -16μC/cm^2, directed from the top to the bottom electrode. We explain this result in terms of flexoelectricity and assume that substrate downward bending generates a strain gradient across the film thickness which creates the downward self-polarization [1]. Application to the films a positive bias of ~2 V together with a sinusoidal one or illumination of negatively poled film in a short-circuit state can switch the negative self-polarization into a state with positive or zero P_{dep}. Capacitors C2 do not show initial self-polarization.

In transient current-voltage curves all the capacitors show peaks near values of coercive strength, the current is larger in case the directions of the bias and polarization coincide. This result agrees with the current behavior in epitaxial PZT films [2] and is the opposite to the current behavior in polycrystalline PZT films with conductive grain boundaries, where current is larger when the directions of the bias and polarization are opposite to each other [3].

References

1. Z. Wang, X.X. Zhang, X. Wang, W. Yue, J. Li, J. Miao, W. Zhu, Adv. Funct. Mater. **23**, 124 (2013)
2. L. A. Delimova, E. V. Gushchina, V. S. Yuferev, I. V. Grekhov, MRS Fall Meeting, Symp. P, P1.09 (2013).
3. L. A. Delimova, V. S. Yuferev, A. V. Ankudinov, E. V. Gushchina, I. V. Grekhov, MRS Proc. **1292**, mrsf10- 1292-k03-31 (2011).

RCBJSF Or-10

True Operational Range Of Lead-Free and Lead-Based Piezoelectric Actuators

Y. Ehara, J. Koruza, D. Franzbach, F. Schneider, and K.G. Webber

Institute of Materials Science, Technische Universität Darmstadt, Germany

e-mail: yoshitaka.ehara@gmail.com

Strong electromechanical coupling makes ferroelectric ceramics ideal candidates for high precision, fast response, and high force actuator application [1]. Among the most important actuator figures of merit, which also define their operational range, are the free displacement that can be achieved at a given electric field without an external load and the maximal force that the actuator can produce in a fully clamped state (blocking force). Due to nonlinear electrical and mechanical constitutive behavior of ferroelectrics [2] the operational range, as it is currently defined, strongly depends on the loading history and is, therefore, path-dependent, which is not taken into account by the currently utilized measurement methods [3]. This may result in inaccurate prediction of the actuator´s complex operational range and considerable performance decrease, e.g., due to deviations in impedance matching of the actuator to the external load [4].

In order to determine the true operational range of piezoelectric actuators we present a novel experimental procedure utilizing the proportional loading method, which enables full characterization of a piezoelectric material under actual operating conditions. The method was used to investigate well-established lead-based materials, such as $Pb(Zr,Ti)O_3$, as well as selected $BaTiO_3$- and $(Bi,Na)TiO_3$-based lead-free compositions. The determined operational ranges will be compared and discussed with respect to different mechanisms responsible for the unipolar strains. Moreover, the materials will be evaluated in terms of electromechanical conversion efficiency, showing large room temperature values of some lead-free compositions, making them promising candidates for actuation applications [5].

References

1. K. Uchino, Ferroelectric Devices, Marcel Dekker (2000)
2. T. Fett, D. Munz, G. Thun, Ferroelectrics 274, **67** (2002)
3. K. G. Webber, D. Franzbach, J. Koruza, J. Am. Ceram. Soc., submitted (2014)
4. L. D. Mauck, C. S. Lynch, J. Intell. Mater. Syst. Struct. 758, **11** (2000)
5. D. R. J. Brandt, M. Acosta, J. Koruza, K. G. Webber, J. Appl. Phys., submitted (2014)

RCBJSF Or-11

New Room Temperature Multiferroics on the Base of Single-Phase Nanograined Ceramics with Perovskite Structure

M.D. Glinchuk[1], E.A. Eliseev[1], A.N. Morozovska[1,2]

[1]Institute for Problems of Materials Science, NAS of Ukraine, Kiev, Ukraine

[2]Institute of Physics, NAS of Ukraine, Kiev, Ukraine

e-mail: glin@ipms.kiev.ua

The search of room temperature magnetoelectric multiferroics is known to be a hot topic for researchers and engineers working in the field of novel functional devices fabrication [1]. For the majority of these devices operation at room temperature and significant magnetoelectric coupling are especially vital. Until recently such characteristics were demonstrated on multiferroic heterostructures. The discovery of single phase room temperature magnetoelectrics on the basic of solid solutions of ferroelectric antiferromagnets $Pb(Fe_{1/2}Ta_{1/2})O_3$ and $Pb(Fe_{1/2}Nb_{1/2})O_3$ with $Pb(Zr_{1/2}Ti_{1/2})O_3$ seems to be very important.

However the magnitude of the magnetoelectric (ME) coupling in conventional ceramics appeared to be a few orders smaller than that for heterostructures. Investigations for $Pb(Fe_{1/2}Ta_{1/2})_x$–$(Zr_{1/2}Ti_{1/2})_{1-x}O_3$ nanograined ceramics [2] revealed the value of effective ME coefficient close enough to that obtained for heterostructures. The physical reason of this important for applications phenomenon stays unexplained up to now. To find out this intriguing phenomenon physical reasons it is necessary to clear up the mechanisms of ferromagnetic, ferroelectric phases appearance and their dependence on temperature, solid solution composition x for given value of nanograined average radius R. Therefore the description of phase diagram will be given and compared with observed one. The proposed theory appeared possible to be applied to the bulk materials in some cases, e.g. for $x = 1$, due to our approach generality, since it took into account polarization, magnetization, elastic and magnetoelectric properties. The comparison of the developed theory with experiments establishing the boundaries between paraelectric, paramagnetic, antiferromagnetic, ferroelectric, ferromagnetic and magnetoelectric phases, as well as characteristic features of the observed ferroelectric domain switching by magnetic field are performed and discussed.

References

1. J. F. Scott, J. Mater. Chem. **22**, 4567 (2012)
2. D. M. Evans, A. Schilling, A. Kumar, D. Sanchez, N. Ortega, M. Arredondo, R. S. Katiyar, J. M. Gregg and J. F. Scott. Nature Communications **4**, 1534 (2013)

RCBJSF Or-12

Dielectric Properties of Barium Titanate and Nickel-Zinc Ferrite Multiferroic Composites

R. Grigalaitis[1], A. Sakanas[1], J. Banys[1], L. Mitoseriu[2], V. Buscaglia[3]

[1]Faculty of Physics, Vilnius University, Lithuania

[2]Faculty of Physics, University "Al. I. Cuza", Romania

[3]Institute of Energetics & Interphases IENI-CNR, Italy

e-mail: robertas.grigalaitis@ff.vu.lt

In recent years, there is a tendency to search for novel multifunctional materials. It is not surprising that multifunctional multiferroic materials have gained a lot of attention and are being intensively studied. Due to restrictions of *d*-orbital occupancy the synthesis of new single-phase multiferroic materials is not very promising and efforts are made to search for a new two-phase multiferroic composites, being nowadays the most extensively studied multifunctional materials.

The present work is dedicated to the comparison of broadband dielectric spectroscopy results of $x BaTiO_3$-$(1-x)Ni_{0.5}Zn_{0.5}Fe_2O_4$ composite ceramics synthesized from powders prepared by using two different methods – co-precipitation and core-shell. Particle morphology and composite microstructure was confirmed in each case by XRD, SEM and other devices [1, 2]. Various devices and broadband dielectric spectroscopy methods were used in experiments to cover the wide range of temperatures and frequencies, spanning from 100 K to 500 K and from 20 Hz up to 50 GHz.

The samples prepared by co-precipitation method display significantly higher values of dielectric permittivity than those having core-shell structure. Moreover, three peeks visible in the temperature dependencies of co-precipitation samples can be associated with phase transitions occurring in pure barium titanate, while in core-shell samples such behavior is not present anymore. The behavior at low frequencies is primarily determined by more conductive low-permittivity material (nickel-zinc ferrite). At higher frequencies, a nearly Debye-type relaxation process can be observed. This shows that the preparation methodology is able to modify dielectric properties significantly in a very broad frequency range.

References

1. A. Testino, L. Mitoseriu, V. Buscaglia et al., J. Eur. Ceram. Soc. **26**, 3031-3036 (2006)
2. M. T. Buscaglia, V. Buscaglia, L. Curecheriu et al., Chem. Mater. **22**, 4740-4748 (2010)

RCBJSF Or-13

On the Conical Point Crossing

Y. Ishibashi[1] and M. Iwata[2]

[1]Department of Applied Physics, Nagoya University, Japan

[2]I Department of Engineering Physics, Electronics and Mechanics Nagoya Institute of Technology, Japan

e-mail: miwata@nitech.ac.jp

The conical point crossing is a form of the energy level crossing, where the level crossing occurs two-dimensionally.[1, 2)] It has been concretely exemplified by using a simple lattice vibration model of the hexagonal lattice only with two atoms in a unit cell, each atom interacting with the nearest neighbor atoms (Fig. 1), that the conical point crossing occurs in the K-point denoted by $\boldsymbol{k}$ = (1/3, 1/3, 0) *inside* the Brillouin zone of the hexagonal lattice (Fig. 2). Near the K-point, the dispersion relation is given as[1)]

$$\omega^2 - \omega_0^2 = \pm \frac{K}{M}\left[|\Delta| + O\left(|\Delta|^2 \right) \right],$$

where M is the mass of atoms, K the force constant, ω_0^2 the ω^2-value at the K-point, $|\Delta|$ the distance (non-dimensional) from the K-point in the reciprocal lattice, and $O(|\Delta|^2)$ implies the terms higher than the second order in Δ.

It has been shown that the conical point crossing appearing in the hexagonal lattice remains even in the orthorhombic and monoclinic lattices induced by the proper or improper ferroelastic transition, where a small strain is involved[3)]. In the present paper we discuss how the conical point crossing will change according to lowering symmetry.

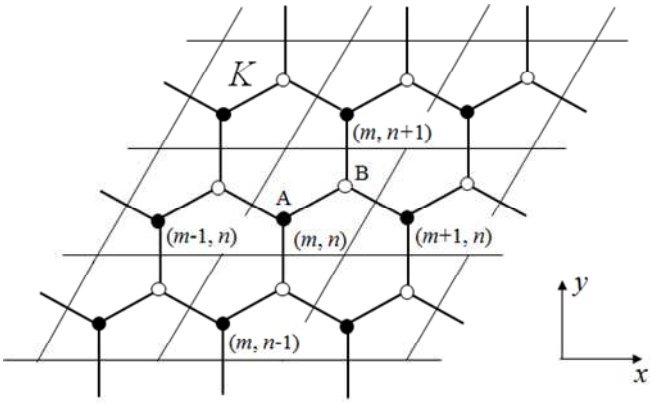

Fig. 1. The hexagonal lattice.

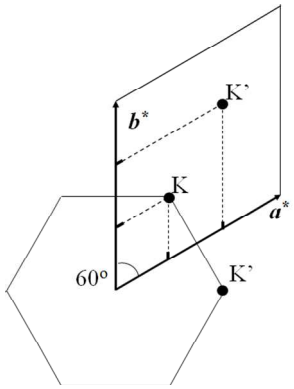

Fig. 2. The reciprocal lattice vectors.

References

1. Y. Ishibashi and V. Dvorak: J. Phys. Soc. Jpn. **45** (1978) 1119.
2. Y. Ishibashi and M. Iwata: Ferroelectrics 459 (2014) 107.
3. Y. Ishibashi and M. Iwata: To be published in J. Phys. Soc. Jpn.

RCBJSF Or-14

Dielectric Properties of $BaTiO_3$-$KNbO_3$ Composites

M. Ivanov[1], S. Balčiūnas[1], J. Banys[1], S. Wada[2]

[1]Faculty of Physics, Vilnius University, Sauletekio 9/3 817k., LT10222 Vilnius, Lithuania

[2]Interdisciplinary Graduate School of Medical and Engineering, University of Yamanashi, Kofu,Yamanashi 400-8510, Japan

e-mail: maksim.ivanov@ff.vu.lt

Barium titanate (BT) is a classic ferroelectric with average properties. Inserting potassium niobate to BT structure creates stresses that increases domain wall count and in result piezoelectric coefficient [1]. Although ferroelectric PZT has taken a substantial share of piezoelectric market due to its high piezoelectric characteristics, KNBT has comparable piezoelectric coefficient, thus making it a great substitute. The fact that KNBT is lead free ceramic makes it of high interest for both researchers and engineers due to environmental concerns.

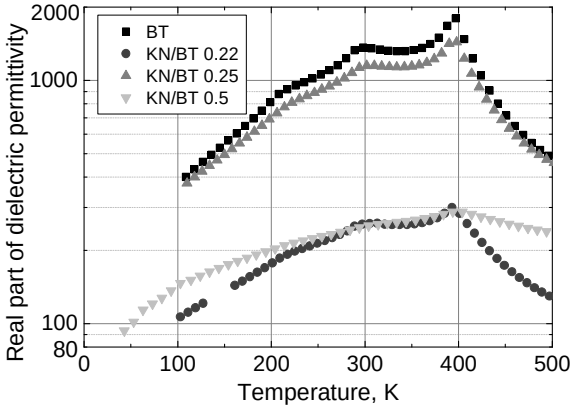

Fig 1. Temperature dependence of real part of dielectric permittivity for:
BT with 60% relative density.
KN/BT 0.22 with 53% relative density
KN/BT 0.25 with 79% relative density
KN/BT 0.5 with 60% relative density

Composites were prepared in two steps: compact BT particles were heated to 1000^0C for 2h to create low-density ceramics, then KN were epitaxially deposited to BT structure. [2]

In this presentation dielectric properties of KNBT with different KN molar ratios will be presented. From Figure 1 we can observe that the bigger the KN/BT ratio is, the more obscured phase transitions of BaTiO3 become. Low dielectric permittivities in KN/BT with molar ratios of 0.22 and 0.5 can be explained by its low relative density.

References

1. T. Higuchi, *Journal of mechanical science and technology*, vol. 24, pp. 13-18, (2010).
2. I. Fujii, S. Shimizu, K. Yamashita, K. Nakashima, N. Kumada, C. Moriyoshi, *et al.*, *Applied Physics Letters*, vol. 99, p. 202902, (2011).

RCBJSF Or-15

Temperature Phase Transitions in $CsScF_4$ Crystal

A. Krylov[1], M. Molokeev[1], A. Ivanenko[1], V. Popova[2], Y. Ivanov, A. Vtyurin[1], A. Oreshonkov[1] and S. Krylova[1]

[1]L.V. Kirensky Institute of Physics SB RAS, Russia

[2]Institute of Automation and Electrometry SB RAS, Russia

e-mail: shusy@iph.krasn.ru

The aim of this work is to a comprehensive study of the temperature of phase transitions in the $CsScF_4$ crystal. The $CsScF_4$ crystal presents a typical example of a layered perovskite structure. It is formed by square layers of ScF_6 octahedra connected via common F atoms, and separated with Cs ions in interlayer holes. According to x-ray data and macroscopic measurements, the space group of its high-temperature phase is *P4/mmm*, the highest symmetry for such an arrangement. Cooling below $T_1 = 475$ K results in a new phase with *P4/mbm* symmetry. A second phase transition appears at $T_2 = 317$ K leading to a phase with *P4/mmn* space group.

At the first phase transition ScF_6 octahedrons with are rotated with jump on φ~η which accounts for a first-order transition. There are no any other rotations or heavy atom displacement. At the second phase transition two new rotations are appeared: around $\bar{a}+\bar{b}$ axis on angle ψ_1 and around $\bar{a}-\bar{b}$ axis on angle ψ_2. Atoms Cs1 and Cs2 move along c. Mechanism of all phase transitions have displacive distortion nature.

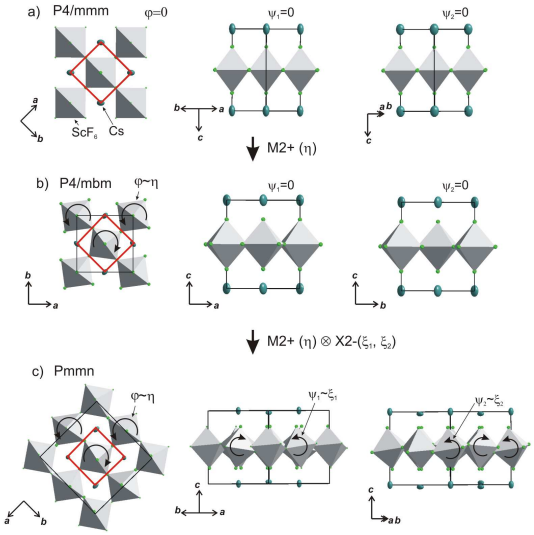

Fig.1 Fig.5. Different projection of crystal structure: a) tetragonal *P4/mmm* parent phase, b) tetragonal *P4/mbm* distorted phase; c) orthorhombic *Pmmn* distorted phase,

Phase transitions are accompanied by condensation of soft modes in Raman spectra, one at first phase transition T_1 and two at second phase transition T_2.

The results of investigations by powder X-ray diffraction, Raman and IR vibrational spectroscopy, Brillouin scattering and NMR will be presented.

RCBJSF Or-16

Multiferroicity and Superparamagnetism in the New Magnetoelectric $Pb(Fe_{1/2}Sb_{1/2})O_3$

V.V. Laguta[1,2], M. Marysko[1], M. Savinov[1], R.O. Kuzian[2], V.A. Stephanovich[3], N.M. Olekhnovich[4], A.V. Pushkarev[4], Yu.V. Radyush[4], I.P. Raevski[5], S.I. Raevskaya[5], S.A. Prosandeev[5,6]

[1]Institute of Physics, AS CR, Czech Republic

[2]Institute for Problems of Materials Science NASU, Ukraine

[3]Institute of Physics, Opole University, Poland

[4]Scientific-Practical Materials Research Centre, NASB, Belarus

[5]Research Institute of Physics, Southern Federal University, Russia

[6]Department of Physics, University of Arkansas, USA

e-mail: laguta@fzu.cz

Multiferroics are materials having two or more order parameters (for instance, magnetic, electric or elastic) coexisting in the same phase. Among them, magnetoelectric (ME) materials that exhibit coupling of electric polarization and magnetization are very promising for spintronic and magnetic random access memory applications.

In the present study we report a detailed study of magnetic, dielectric and ME properties of new magnetoelectric multiferroic $PbFe_{1/2}Sb_{1/2}O_3$ (PFS). It belongs to the rich family of Fe-based double perovskites $A(Fe_{1/2}M_{1/2})O_3$ with nonmagnetic ions A=Pb,Ca,Sr,Ba, and M=Nb,Ta,Sb. In these compositions, Fe^{3+} and M^{5+} cation positions may be ordered or disordered within simple cubic B-sublattice of the perovskite structure ABO_3. By employing high-pressure high-temperature synthesis we obtained PFS ceramics possessing a high degree (up to 0.9) of chemical ordering of the Fe^{3+} and Sb^{5+} cations. This results in several interesting properties. In particular, PFS shows unexpectedly strong high-temperature magnetic relaxation. We explain this relaxation by the creation, at high temperatures, not less than 250 K, of giant superspins, owing, curiously, to the antiferromagnetic (AFM) superexchange interaction between Fe^{3+} spins. These superspins are capable of strong magnetic relaxation down to about 150 K, where they transform into a superspin glass phase, and, on further cooling, the material experience transition into the ordinary AFM phase at $T_N \approx 30$ K. We have also found that PFS undergoes ferroelectric phase transition at 195 K. Its remanent polarization experiences substantial (almost 20%) variations below the Neel temperature indicating extremely strong direct ME coupling.

RCBJSF Or-17

Research on Electromagnetic Interference Resistance of Piezoelectric Vibration Acceleration Sensor with Printed Circuit Board

D. Li, C. Hao

School of Automation, Beijing Information Science and Technology University, China

e-mail: haocui0433234@163.com

Because of the importance of the electromagnetic interference resistance in the modern life, the electromagnetic shielding of the piezoelectric vibration acceleration sensor with printed circuit board(PCB) is analyzed in this paper. The shell of the piezoelectric vibration acceleration sensor is taken as a rectangular cavity with aperture. The shielding effectiveness of the shell irradiated by plane electromagnetic wave is modelled using transmission line theory. In the modeling process, incident angle and polarization angle of the plane electromagnetic wave are introduced, and the scattering voltage produced on the aperture is taken as the radiation source. The aperture is taken as the asymmetrical coplanar stripline and the rectangular cavity is taken as a rectangular waveguide with one end completely open and another end completely closed. The PCB is taken as a dielectric slab with certain dielectric constant and electrical conductivity. The shielding effectiveness of any point in the cavity is calculated using transmission line theory. Compared to the others before, this method improved the completeness of the model and the computation speed which supplied good reference for engineering practice.

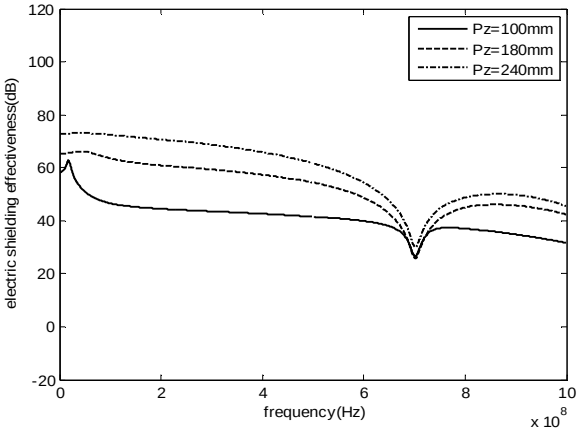

Fig. 1 The shielding effectiveness curves when the position of point P gets different value

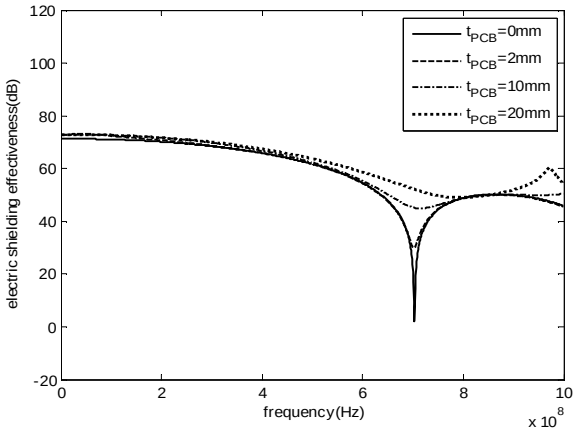

Fig. 2 The shielding effectiveness curves when the thickness of PCB gets different value

RCBJSF Or-18

Dielectric Properties of $AgLiNbO_3$

J. Macutkevic[1], J. Banys[1], I. Gruszka[2] and A. Kania[2]

[1]Faculty of Physics, Vilnius university, Sauletekio al. 9, LT-10222 Vilnius, Lithuania

[2]Institute of Physics, University of Silesia, ul. Uniwersytecka 4, PL-40-007 Katowice, Poland

e-mail: jan.macutkevic@gmail.com

X-ray, electron diffraction, dielectric, Raman, and domain structure studies showed that in silver niobate ($AgNbO_3$) the following phase transitions are observed at temperatures: 340 K—from the orthorhombic M_1 to the orthorhombic M_2, 540 K—from the orthorhombic M_2 to the orthorhombic M_3, 626 K—from the orthorhombic M_3 to the orthorhombic O_1, 634 K—from the orthorhombic O_1 to the orthorhombic O_2, 660 K—from the orthorhombic O_2 to the tetragonal T, 852 K—from the tetragonal T to the cubic C [1]. The M_1 phase exhibits ferroelectric properties, the phases M_2 and M_3 are antiferroelectric and phases O_1, O_2, T and C are paraelectric. All phase transitions are mostly related with Nb ions dynamics, however the role of Ag and O ions should be also not neglected. Therefore it is very interesting to investigate dielectric properties of various mixed systems like $Ag_{1-x}Li_xNbO_3$ in wide frequency range [2]. In this work results of dielectric investigations of $Ag_{1-x}Li_xNbO_3$ (ALN) solid solutions for Li concentration range $0<x<0.1$ are reported in very wide frequency range (20 Hz -3 THz). They show a perovskite structure and exhibit the orthorhombic symmetry at room temperature. Three predominant aspects of Li substitution were found (Fig. 1). The first one is associated with a shift of M_1-M_2 dielectric anomaly to the low temperatures, the anomaly completely vanishes for $x \geq 0.6$. The second one is related to a gradual increase of the broad $\varepsilon(T)$ maximum associated with the transition between disordered antiferroelectric M_2 and M_3 phases. The third one is related with dipolar glass phase appearance for compositions with $0.01<x<0.6$. The dipolar glass behaviour completely vanishes together with disappearance of M_1-M_2 phase transition. The Li substitution influence is discussed in terms of the appearance of electric dipole moments linked with the occupation of the off-centre positions by Li ions.

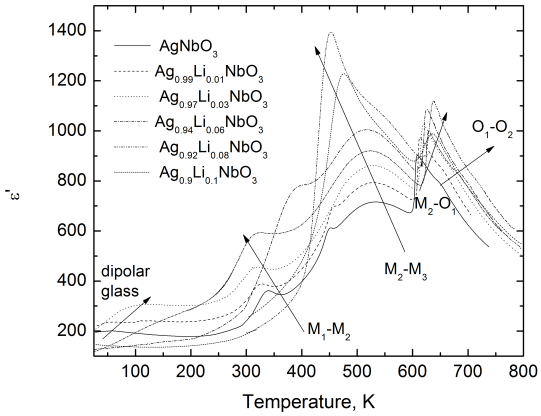

Fig.1 Temperature dependence of the static dielectric permittivity of $Ag_{1-x}Li_xNbO_3$.

Acknowledgment

This research is funded by the European Social Fund under the Global Grant measure.

References

1. I. Levin, V. Krayzman, J. C. Wojcik, J. Karapetrova, T. Proffen, M. Tucker, I. M. Reaney, Structural changes underlying the diffuse dielectric response in $AgNbO_3$, Phys. Rev. B, 79, 104113 (2009).

2. H. U. Khan, I. Sterianou, S. Miao, J. Pokorny and I. M. Reaney, The effect of Li substitution on the M-phases of $AgNbO_3$. J. Appl. Phys. 111, 024107 (2012).

RCBJSF Or-19

Optical Properties of the Narrow-Band Ferroelectrics: First Principle Calculations

H. Koc[1], A.M. Mamedov[2,3], E. Ozbay[2]

[1]Department of Physics, Faculty of Science and Letters, Siirt University, Siirt Turkey

[2]Nanotechnology Research Center, Bilkent University, Ankara Turkey

[3]International Scientific Center, Baku State University, Baku, Azerbaijan

e-mail: mamedov@bilkent.edu.tr

Based on density functional theory, we have studied the structural, mechanical, electronic, and optical properties of narrow-band ferroelectric compounds – (Ge,Sn)Te. Local density approximation has been used for modeling exchange-correlation effects. The lattice parameters, bulk modulus, and the first derivate of bulk modulus (to fit to the Murnaghan's equation of state) of considered compounds have been calculated. The second-order elastic constants have been calculated, and the other related quantities such as the Young's modulus, shear modulus, Poisson's ratio, anisotropy factor, sound velocities, Debye temperature, and hardness have also been estimated in the present work. The calculated electronic band structure shows that GeTe and SnTe compounds have an direct forbidden band gap of 0.18 eV and 0.35 eV. The real and imaginary parts of dielectric functions and hence the optical constant such as energy-loss function, the effective number of valance electrons and the effective optical dielectric constant are calculated. We also calculated some nonlinearities (tensors of elasto-optical coefficients) under pressure. Our structural estimation and some other results are in agreement with the available experimental and theoretical data.

RCBJSF Or-20

Electric Current Relaxation and Resistance Switching in Non-Homogeneous Bismuth Manganite

A. Molak, A. Leonarska, and A. Szeremeta

Institute of Physics, University f Silesia, ul. Uniwersytecka 4, 40-007 Katowice, Poland

e-mail: andrzej.molak@us.edu.pl

The bismuth manganite ceramics has been obtained by high temperature sintering [1]. The X-ray pattern analysis has shown that the ceramics consists of centro-symmetric orthorhombic *Pbam* and cubic *I23* phases. Such result is consistent with former electron microprobe analysis of the chemical composition [1] and non-ferroelectric features of $BiMnO_3$ compound [1, 2]. Impedance has been measured at radio-frequencies (f = 100 Hz – 1 MHz) in 85-570 K range in the parallel circuit mode C_p-G_p. The resistance $R_{dc}(T)$ temperature dependence was checked repeatedly after electroformation procedure carried out at 800 K, at ambient air, for several hours [1].

The marked step-like anomaly in the $\varepsilon'(T,f)$ occurres in 100-250 K range and it corresponds to a peak anomaly, both in dielectric loss coefficient $tan\delta(T,f)$ and imaginary part of electric modulus $M''(T,f)$. This anomaly has been assigned to electric current dispersion or relaxation since it moves with frequency and temperature [3, 4]. The relaxation times τ temperature dependences have been fitted to Arrhenius law. Estimated activation energy value E_τ = 0.20 eV corresponds to the semiconductor-type electric conductivity activation energy E_a = 0.20 eV [1]. Estimated value of relaxation characteristic time $\tau_0 \sim 10^{-11}$ s indicates polaronic mechanism of conduction. The other anomaly distingushed in the $tan\delta(T,f)$ and $M''(T,f)$ dependences, in 270-320 K range, relates to longer relaxation times ($\tau_0 \sim 10^{-8}$ s) and it can be assigned to an ionic process, which contributes to the electric conduction [3].

The high temperature electroformation induced the resistance switching to metallic-like state, which was stable for several weeks at room temperature. The resistance temperature dependence has been fitted to formula $M''(T,f)$. $R_{dc}(T) = R_0(1 + \alpha T + \beta T^2)$. Recently proposed model for the resistance switching induced in the aged and rejuvenated crystals, which is related to vortices at ferroelectric domains structure [5, 6], is not applicable due to non-ferroelectric features of the ceramics studied herein. Hence, we propose to relate the resistance switching in bismuth manganite ceramics to extended defects, which occur in vicinity of interfaces [7] formed in the bismuth manganite ceramics studied herein.

References

1. A. Molak, Z. Ujma, M. Pilch, I. Gruszka, and M. Pawełczyk, *Ferroelectrics* **462,** *pp.1-13* (2014); DOI: 10.1080/00150193.2014.892815
2. V. Goian, S. Kamba, M. Savinov, D. Nuzhny, F. Borodavka, P. Vanek, A.A. Belik, *Journal of Applied Physics* **112,** 074112-1-6 (2012).
3. F. Kremer, A. Schonhals, 2003, *Broadband Dielectric Spectroscopy*, (Berlin Heidelberg New York: Springer).
4. A. Molak, M. Paluch, and S. Pawlus, Physical Review B 78, 34207-1-14 (2008).
5. N. Balke, B. Winchester, W. Ren, Y.H. Chu, A.N. Morozovska, E.A. Eliseev, M. Huijben, R.K. Vasudevan, P. Maksymovych, J. Briston, S. Jesse, I. Kornev, R. Ramesh, L. Bellaiche, L.Q. Chen, S.V. Kalinin, *Nature Physics* **8,** 81 (2012).
6. M. Pilch and A. Molak, *Journal of Alloys and Compounds* **586**, 488 (2014).
7. J. Maier, *Nature Materials* **4**, 805 (2005).

RCBJSF Or-21

First-Principles Calculations of Ferroelectricity in Wurtzite Structured Simple Chalcogenides

H. Moriwake[1], A. Konishi[1], T. Ogawa[1], K. Fujimura[1], C.A.J. Fisher[1], A. Kuwabara[1], T. Shimizu[2], S.Yasui[2], M. Itoh[2]

[1]Nanostructures Research Laboratory, Japan Fine Ceramics Center, Japan

[2]Materials and Structure Laboratory, Tokyo Institute of Technology, Japan

e-mail: moriwake@jfcc.or.jp

Binary compounds with the wurtzite structure (S.G.: $P6_3mc$) have a polar crystal structure due because the system is non-centrosymmetric. Such crystals have been assumed to be non-ferroelectric because of the rigid tetrahedral units held together by strong covalent bonding, so that its electric polarization cannot be switched by an electric field. For this reason, wurtzite structured compounds are categorized as consisting of non-ferroelectric polar crystals. However, if we consider the relative displacement of the cation relative to the anion along the c axis, as illustrated in Figure 1, a centrosymmetric paraelectric state corresponding to space group $P6_3/mmc$ is found to exist between two polar states (the original P63mc symmetry of wurtzite). If the potential barrier of this displacement is sufficiently low, the direction of electric polarization can be switched between these two equivalent polar states ($P6_3mc$) via this paraelectric state. If this is the case, the wurtzite structure should represent a new class of ferroelectric materials. The possibility of ferroelectricity in the wurtzite structure was not examined. It is thus still an unanswered question whether wurtzite structured compounds can exhibit ferroelectricity or not. In this study we report a series of first-principles calculation of wurtzite structured phases of MX chalcogenides (where M = Zn, and Be, X = O, S, Se, and Te), in an attempt to answer this question. The calculation results of the potential surface of poralization switching will be presented.

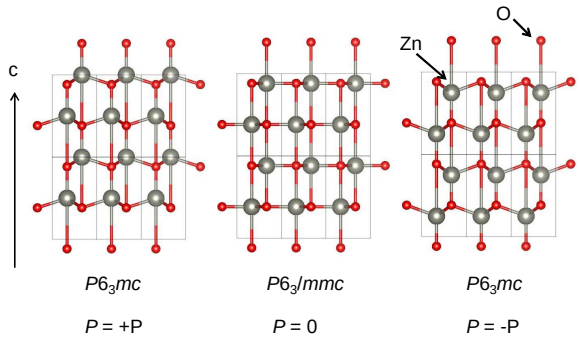

Figure 1. Wurtzite structure ZnO in two polar states (left and right), corresponding to space group $P6_3mc$, compared with ZnO in a non-polar state (center), corresponding to space group $P6_3/mmc$. If the potential barrier is suffiiciently low, the electric polarization can be switched between the two polar states via the non-polar structure.

RCBJSF Or-22

Porous $Pb(Mg_{1/3}Nb_{2/3})O_3$ Ceramics: Experiment, Modelling and Simulation

D. Nuzhnyy[1], J. Petzelt[1], I. Rychetsky[1], G. Trefalt[2,3]

[1]Institute of Physics, Academy of Sciences of the Czech Republic, Czech Republic

[2]Jozef Stefan Institute, Slovenia

[3]Center of Excellence NAMASTE, Slovenia

e-mail: nuzhnyj@fzu.cz

We produced a set of $Pb(Mg_{1/3}Nb_{2/3})O_3$ (PMN) relaxor ceramics with different porosities from a pure perovskite PMN powder [1] by varying the sintering temperature and isostatic pressure. We measured the room temperature infrared (IR) reflectivity of corresponding 7 polished ceramics. Several IR reflectivity spectra are shown in Fig.1. We fitted experimental data and obtained the effective dielectric response, which was discussed using several effective medium models. The best results were obtained using the Lichtenecker model [2]

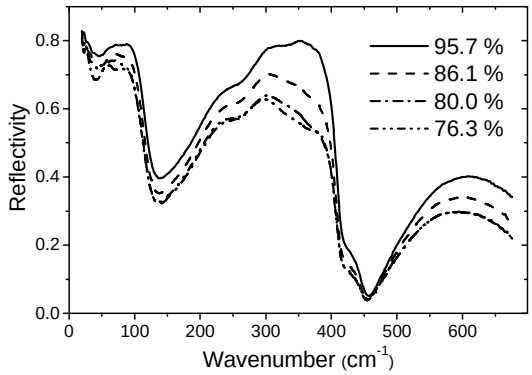

Fig.1 Room temperature IR reflectivities of PMN ceramics with different porosities.

$$\varepsilon_{eff}^{\alpha} = (1-x)\varepsilon_1^{\alpha} + x\varepsilon_2^{\alpha},\ -1 \le \alpha \le 1$$

for the positive α both components are partially percolated for all compositions *x* and for the negative α neither of the components is percolated, again independently of *x*. The simulation using the finite element method supported the same model.

We found that the Lichtenecker model with α = 0.2 produced reliable values of low-frequency permittivity for all samples and confirmed the independence of the degree of porosity. It indicates that the different sintering conditions yield the same topology and shape of pores in the ceramics.

References

1. G. Trefalt, B. Malic, D. Kuscer, J. Holc and M. Kosec, J. Am. Ceram. Soc. **94**, 2846 (2011)
2. K. Lichtenecker, Phys. Z. **27**, 115 (1926)

RCBJSF Or-23

Giant Lattice Expansion in $GdCoO_3$ due to the Multiplicity Fluctuation Contributions

S.G. Ovchinnikov[1], V.A. Dudnikov[1], Yu.S. Orlov[1], A.A. Kuzubov[1], L.A. Soloviev[2], S.N. Vereshagin[2], A.G. Anshits[2]

[1]L.V.Kirensky Institute of Physics, Siberian Branch of RAS, Krasnoyarsk, 660036, Krasnoyarsk, Russia

[2]Institute of Chemistry and Chemical Technology, Siberian Branch of RAS, Krasnoyarsk, 660036, Krasnoyarsk, Russia

e-mail: sgo@iph.krasn.ru

We have investigated the X-ray diffraction (XRD), magnetic susceptibility and head capacity of $GdCoO_3$ in a wide temperature range. Two phases of the same symmetry with different lattice parameters corresponding to the low spin (LS) and high spin (HS) states of Co^{3+} ion have been revealed based on the analysis of XRD peak shape anomalies at 200K<T<800K. From magnetic measurements we have obtained the temperature dependent spin gap between HS and LS states and the thermal occupation numbers for HS and LS states. We found a smooth spin crossover at 800K.

By *ab initio* DFT-GGA method we have calculated the volumes of the LS and HS unit cells. We have model the unit cell volume at arbitrary temperature as the average between HS and LS with temperature dependent occupation numbers. We have reproduced the measured thermal expansion and found the giant thermal expansion coefficient $\sim 10^{-4}$ contrary to the anharmonicity contribution $\sim 10^{-5}$. The origin of this large multiplicity fluctuation contribution is the 10% difference in the HS and LS ionic radii of Co^{3+} ion.

The other effect of the temperature induced LS-HS crossover is a smooth insulator – metal transition. Our multielectron LDA+GTB energy structure calculations have found the insulated bands with the activation energy for conductivity decreasing with temperature due to increasing HS concentration. The insulator gap tends to zero at 780K, and the measure heat capacity has a maximum at this temperature.

Acknowledgment

We are thankful to the FRRI grant 13-02-00358 and SB RAS integration project 38 for financial support of this work.

RCBJSF Or-24

New Multiferroic Oxides with Corundum-Related Structure

G.M. Kaleva[1], S.A. Ivanov[1], E.D. Politova[1], A.V. Mosunov[1], S.Yu. Stefanovich[1], R. Mathieu[2], P. Nordblad[2], R. Tellgren[2], C. Ritter[3], M.Weil[4]

[1]L.Ya. Karpov Institute of Physical Chemistry, Moscow, Russia

[2]University of Uppsala, Uppsala, Sweden

[3]Institute Laue-Langevin, Grenoble, France

[4]University of Technology, Vienna, Austria

e-mail: politova@cc.nifhi.ac.ru

Intensively studied transition metals containing oxides with multiferroic properties mainly have perovskite-related structure. However, the search for compositions with other structural types in which multiferroic behaviour may occur, is still of fundamental importance.

In this work, single crystals of Ni_3TeO_6 and Ni_2InSbO_6 prepared by the gas-transport reactions and complex oxides Ni_2BSbO_6 (B - Sc, In) and $(Cu,Ni)_3TeO_6$ solid solutions prepared by the solid state reaction method were studied. Crystal structure and properties of ceramics were studied using X-ray and Neutron powder diffraction, calorimetric, second harmonic generation (SHG) and magnetic measurements. Dielectric properties of sintered ceramics were measured at frequencies 100 Hz – 1 MHz in temperature range 300 - 1000 K.

Antiferromagnetic (AFM) ordering was found in Ni_3TeO_6 with corundum-related structure. This oxide has a noncentrosymmetric structure which suggests that ferroelectric ordering above room temperature is possible. At room temperature Ni_2BSbO_6 (B - Sc, In) compounds have a trigonal structure. The magnetic susceptibilities showed AFM behavior for both compounds with T_N=60 K (Sc) and 76 K (In). Neutron diffraction patterns confirmed a long-range magnetic ordering below T_N. SHG measurements at room temperature confirmed that these compounds possess a noncentrosymmetric crystal structure. The pronounced dielectric peaks were observed for Ni_3TeO_6 samples near 1000 K. These peaks may correspond to ferroelectric phase transition. It should be also noted that dielectric properties of all ceramics studied revealed typical relaxor behavior at lower temperatures.

Dielectric anomalies related to structural phase transitions were revealed at ~800 K, and AFM ordering was determined at temperatures 50-70 K in the $(Cu,Ni)_3TeO_6$ ceramics. The factors governing the observed structural and magnetic properties of Ni-based compounds will be discussed and possible role of structural distortions of the Ni-cation sublattices on dielectric and magnetic properties will be considered.

Acknowledgment

The work was supported by Sweden Academy of Sciences and Russian Fund for Basic Research (Grant 12-03-00132).

RCBJSF Or-25

Ferroelectricity in Natural Minerals

E.A. Popova[1,2], S.G. Lushnikov[1,2], S.V. Krivovichev[2]

[1]Ioffe Physical Technical Institute RAS

[2]Saint Petersburg State University, Department of Crystallography, Russia

e-mail: elena.popova566@gmail.com

One of the novel and quickly developing directions of research in the physics of condensed matter is the investigation of the relations between the phase transition dynamics and the processes that occur in the Earth's crust and mantle. It has been shown that the olivine-spinel phase transition can be a trigger mechanism for the Earth's deepest earthquakes that occur in the subducting oceanic lithosphere[1]. Investigations of the dynamics of phase transitions in minerals as natural compounds help to understand different phenomena in the Earth's mantle, such as the anomalies in the behavior of elastic waves detected in seismic investigations.

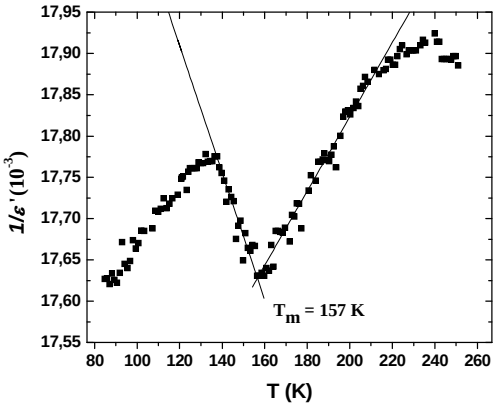

Fig.1 The temperature dependence of the inverse static permittivity in loparite-(Ce). Dashed line is a result of approximation by the Curie–Weiss law.

On this report we will discuss the phase transitions into the ferroelectric state in naturally occurring minerals of the order-disorder and displacement types. Ferroelectric transition of loparite-(Ce) (the mineral of perovskite family with complex composition (Ce,Ca,Na)(Ti,Nb)O_3) according to our results of dielectric and Raman spectroscopy and X-ray single crystal diffraction investigations is the phase transition of displacement type. The origin of ferroelectricity in lawsonite $CaAl_2(Si_2O_7)(OH)_2*H_2O$ and colemanite $Ca[B_3O_4(OH)_3]*H_2O$ is related to the dynamical ordering of protons[2,3].

References

1. Alexandre Schubnel, F. Brunet, N. Hilairet, J. Gasc,Y. Wang, H. W. Green, Science **341**, 1377 (2013).
2. P. Sondergeld, W. Schranz et al., Phys. Rev. B **64**, 024105 (2001).
3. M.E. Lines and A.M. Glass, Principal and application of ferroelectrics and related materials. (Clarendon Press, Oxford 1977).

RCBJSF Or-26

Formation of Charged Domain Walls in Lithium Niobate Crystals with Inhomogeneous Bulk Conductivity

V.Ya. Shur, D.O. Alikin, V.I. Pryakhina, I.S. Palitsyn, N.A. Besedina, S.A. Negashev

Ferroelectrics Laboratory, Institute of Natural Sciences, Ural Federal University, 51 Lenin Ave., 620000, Ekaterinburg, Russia

e-mail: victoria.pryahina@labfer.usu.ru

Formation of the charged domain walls (CDW) during polarization reversal has been studied in lithium niobate (LN) single crystals with inhomogeneous bulk conductivity produced by irradiation of the polar surface by glow discharge in plasma of Ar^+ ions and high temperature annealing in vacuum.

The conductivity of the thick surface layers of congruent and MgO doped LN have been increased by annealing at 700-850°C or polar surface irradiation by glow discharge in plasma of Ar^+ ions (energy 2-5 keV, time 2-8 min) in vacuum [1]. The spatial distribution of the bulk conductivity has been extracted from the surface conductivity values measured by two-probe method using repeated removal of 10 to 100 μm-thick surface layers by polishing. The electric field distribution in the bulk had been measured by optical interferometry [2]. The local change of the interference pattern is proportional to the local value of the applied electric field due to linear electro-optical effect. The analysis of the recorded interference patterns allowed to extract the electrical field distribution.

The polarization reversal in the bulk leading to formation of CDW has been *in situ* visualized by optical microscopy under application of the field pulses using liquid electrodes. CDW have been studied by optical microscopy on cross-sections after selective chemical etching and by analysis of the domain images obtained at different depth by Raman confocal microscopy [3]. The main stages of CDW formation in the crystal bulk have been separated. The field dependence of CDW parameters have been revealed.

Acknowledgment

The equipment of the Ural Center of Share Use “Modern Nanotechnology”, Institute of Natural Sciences, Ural Federal University has been used. The research was made possible in part by RFBR (Grant 13-02-01391-a), the Government of Sverdlovsk region (Grant 13-02-96041-r-Ural-a) and UrFU development program with the financial support of young scientists.

References

1. V.I. Pryakhina, V.Ya. Shur, D.O. Alikin and S.A. Negashev, Ferroelectrics **439**, 20 (2012)
2. V.Ya. Shur, A.L. Gruverman, N.V. Korovina, M.Z. Orlova and L.V. Sherstobitova, Sov. Phys. Solid State **30**, 299 (1988)
3. V.Ya. Shur, M.S. Nebogatikov, D.O. Alikin, P.S. Zelenovskiy, M.F. Sarmanova, A.V. Ievlev, E.A. Mingaliev, D.K. Kuznetsov, J. Appl. Phys. **110** (5), 052013 (2011)

RCBJSF Or-27

Ferroelectric Oxides for Visible-Light Photovoltaics and Engineering of Shift Current

F. Wang[1], F. Zheng[1], I. Grinberg[1], H. Takenaka[1], A.M. Rappe[1]

[1]The Makineni Theoretical Laboratories, Department of Chemistry, University of Pennsylvania, Philadelphia, PA 19104-6323 USA

e-mail: rappe@sas.upenn.edu

Ferroelectric oxides have recently attracted much attention as photovoltaics because they can separate the photo-excited charge carriers well due to the strong inversion symmetry breaking. They can generate above band gap photovoltages which may enable power conversion efficiencies beyond the maximum possible in a conventional *p-n* junction solar cell. However, further improvements in photovoltaic efficiency have been inhibited by their wide band gaps (>2.7 eV). We design and make [1] a family of single-phase oxides using conventional solid-state methods: $[KNbO_3]_{1-x}$ $[BaNi_{1/2}Nb_{1/2}O_{3-\delta}]_x$. These oxides exhibit both ferroelectricity and a wide variation of direct band gaps in the range 1.1-3.8 eV. In particular, the x=0.1 composition is polar, has a direct band gap of 1.39 eV, and has a photocurrent density 50 times larger than that of the classic ferroelectric (Pb,La)(Zr,Ti)O_3 material. This provides strong benefits for solar energy absorption, conversion and other applications.

In a homogeneous noncentrosymmetric single-phase material, the charge can be separated spontaneously by the bulk through the shift current mechanism. Here we also study the effects of vacancy, composition and cation arrangement on the shift current response using a simpler material $Pb(Ni_xTi_{1-x})O_{3-x}$. [2] As the electronic transitions at the band edges involve more of the Ti 3*d* and Pb 6*p* orbitals, the shift vector direction flips, allowing the shift current from different *k* regions to propagate along the same direction.

In addition to ferroelectric perovskites, we also report the properties of polar rocksalt structure materials. Inversion symmetry breaking can arise from strain due to lattice mismatch. Heteroepitaxial superlattice materials can induce interlayer strain, leading to symmetry breaking. We therefore study sulfide rocksalt superlattices for new photovoltaic materials, since binary sulfides form rocksalt structures more readily than oxides and since the band gaps of sulfides are lower than those of oxides. We calculate various combinations of (Ag,Bi,Pb)S superlattices using first-principles calculations.

References

1. I. Grinberg *et al.*, Nature **503**, 509 (2013).
2. J. W. Bennett *et al.*, JACS **130,** 17409 (2008); G. Y. Gou *et al.*, PRB **83**, 205115 (2011).

RCBJSF Or-28

Nanoparticles Transport in Ceramic Matrices

A. Rybyanets, A. Naumenko, M. Lugovaya, G. Konstantinov

Institute of Physics, Southern Federal University, Russia

e-mail: arybyanets@gmail.com

The results of practical implementation of a new method for porous piezoceramics, and ceramic matrix piezocomposites fabrication were presented. The method was based on nanoparticles transport in ceramic matrices using a polymer nanogranules coated or filled with a various chemicals, with successive porous ceramics fabrication processes.

Different types of polymer microgranules filled and coated by metal-containing nanoparticles were used for a pilot samples fabrication. Polymer microgranules were examined using transmission and scanning electron microscopy as well as by EXAFS and X-ray emission spectroscopy. Pilot samples of nano- and microporous ceramics and composites were fabricated using different piezoceramics compositions (PZT, lead-potassium niobate and lead titanate) as a ceramic matrix bases.

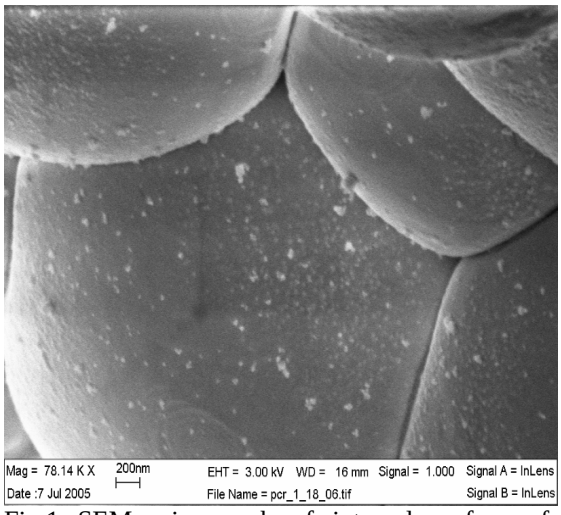

Fig.1 SEM micrograph of internal surface of closed pore in PZT piezoceramics covered by Pd nanoparticles.

Resulting ceramic matrix piezocomposites were composed by super lattices of closed or open pores filled or coated by nanoparticles of metals, oxides, ferromagnetics etc. embedded in piezoceramic matrix. Dielectric and piezoelectric parameters of a pilot samples were measured using piezoelectric resonance analysis method. New family of nano- and microporous piezoceramics and ceramic matrix piezocomposites are characterized by a unique spectrum of the electrophysical properties unachievable for standard PZT ceramic compositions and fabrication methods.

References

1. A.N. Rybyanets and A.A. Rybyanets, IEEE Trans. UFFC. **58**, 1757, (2011),
2. A.N. Rybyanets, IEEE Trans. UFFC. **58,** 1492, (2011),
3. A.N. Rybyanets**.** Ferroelectrics. **419,** 90, (2011).

RCBJSF Or-28

Ultrasonic Studies of Piezoelectric Response in Ferroelectric Crystals of $Sn_2P_2P_6$ Family

V. Samulionis[1], J. Macutkevic[1], J. Banys[1] and Y. Vysachanskii[2]

[1]Faculty of Physics, Vilnius University, Sauletekio 9/3, LT-10222 Vilnius, Lithuania

[2]Institute of Solid State Physics and Chemistry, Uzhgorod University, Ukraine

e-mail: vytautas.samulionis@ff..vu.lt

The ferroelectric crystals of $Sn_2P_2S_6$ family are promising multifunctional materials for functional piezo-electronics. In this contribution we present applications of ultrasonic method for characterization of these piezoelectric crystals. For this purpose we applied pulse-echo ultrasonic method for detecting of piezoelectric sensitivity [1]. In conventional transmission ultrasonic system, the receiving ultrasonic transducer is replaced by plate of material under investigation. Piezoelectric signal which appears on the plate under ultrasonic excitation is proportional to appropriate piezoelectric constant. In this case the temperature and DC electric field dependencies of piezoelectric effect can be measured. Ultrasonically detected piezoelectric signal revealed clear step-like anomalies at the ferroelectric phase transitions. Field-induced piezosensitivity in the ferroelectric phase increases with bias DC field then saturates, and after reversion of voltage the piezoelectric signal decreases, at field near coercive, changes sign, and saturates again at high voltage of opposite polarity (hysteresis loop is observed). In the paraelectric nonpolar phase due to electrostriction there is only linear dependence of piezoelectric signal on DC electric field. Therefore using our ultrasonic method we could study the polar state of the crystal and measure the values of coercive field. By means of this electroacoustic method we investigated piezoelectric state of new $(Sn,Pb)_2P_2S_6$ crystals and solid solutions, obtained after substitution Sn to Pb, Sn to CuBi, or S to Se [2]. The phase diagrams were constructed for these systems. It was shown that at room temperature electromechanical coupling constant K^2 as high as > 30 % could be obtained in $(Sn,Pb)_2P_2S_6$ family crystals after appropriate poling. The application of our method for studies of other multiferroic materials, using ultrasonic detection of piezoelectric sensitivity on a surface barrier of crystal or ceramic, also is discussed.

Acknowledgment

This research is funded by the European Social Fund under the Global Grant measure.

References

1. V. Samulionis, J. Banys and Yu Vysochanskii, Materials Science Forum. **636-637**, 398-403 (2011)
2. V. Samulionis, J. Banys, A. Dziaugys, et al. Ferroelectrics. **419,** 97-102 (2011)

RCBJSF Or-30

The Construction of Domains Density Distribution in the Simulation of Process Polarization in the Ceramics

A. Skaliukh

Southern Federal University, Russia

e-mail: a.s.skaliukh@gmail.com

To describe the nonlinear properties of irreversible polarization processes in polycrystalline material we have to use such a model where in a representative volume it is considered complete information about the mechanical and electrical fields, about the distribution of domains, about the size of the crystallites, their influence on each other, on the impact of charges on domain walls, etc. For example [1], in the models that uses mathematical methods of plasticity we have to store the information about the surface polarization. In Preisach methods we have to store- the information about the boundaries of the region of integration in the half plane of intensive and coercive fields. In the method of Jiles - Atherton is used a domains distribution function based on Boltzmann statistical laws, and moreover, in this model we must only store information about the residual polarization.

In this study we attempted to create a mathematical model, in which had to be taken into account at least the information about the remnant polarization, on the one hand, and functional way to describe distribution of the domains in a representative volume on the other hand. We used the energy criterion of domain switching and simple mathematical mapping all domains to a spherical shell. With every domain we bind not only the one vector but triple of vectors that define its vector of spontaneous polarization and its possible directions for switching after polarization. The domains distribution function was constructed as function of two parameters: electric field intensity and the angle between the direction of vector of the spontaneous polarization and the direction of the electric field. To describe this function, depending on the module of the electric field, was used the law of population dynamics described by a logistic curve. The developed method is designed to further finite element analysis of nonhomogeneously polarized ceramic elements.

Acknowledgment

The work was supported by the Russian Foundation for Basic Research (grant 12-01-00829-a, grant 13-08-01094-a).

References

1. A.V. Belokon, A.S. Skaliukh, Mathematical modeling of irreversible processes of polarization. M.: Fizmatlit, 328 pp., (2010).

RCBJSF Or-31

Giant Piezocaloric Effect in PZT Ceramics

A. Starkov[1], O. Pakhomov[1], I. Starkov[2]

[1]Institute of Refrigeration and Biotechnology, University ITMO, St. Petersburg, Russia

[2]SIX Research Centre, Brno University of Technology, Brno, Czech Republic

e-mail: ferroelectrics@ya.ru

The lack of progress in the realization of cooling devices based on classical caloric effects (CE) provides a strong incentive for a move towards a more effective use of these phenomena. One such an option is the employment of interaction of various caloric effects [1], i.e. the multicaloric effect (MultiCE). According to thermodynamics, any temperature dependent coefficient of the Gibbs free energy of a multiferroic system contributes to MultiCE. Moreover, the interaction of the electromagnetic and elastic fields in this type of materials is described using magnetoelectric, piezomagnetic and piezoelectric coefficients. In addition to these coefficients, terms responsible for the interaction of the fields with their gradients, e.g. flexoelectric, are usually included in the free energy as well. The total number of terms induced by the interplay of the fields is large. As a consequence, the temperature dependence of the coefficients in these terms leads to the corresponding caloric effects. From the above effects, according to our estimates, only piezoelectrocaloric effect (PECE) can reach significant values. This fact can be explained by the temperature dependence of the piezomodulus. Results of the theoretical calculation of PECE for the PZT ceramics are presented in Fig.1. We can conclude that magnitudes of electrocaloric effect (ECE) [2] and PECE are approximately equal. Hence, in this sense PECE might be called gigantic. It should be noted that the existence region of PECE is substantially narrower than of ECE. In addition, these effects have different points of maxima - 509K for PECE and 515K ECE. Thus, the interaction of the electric and elastic fields may result in a doubling of the isothermal entropy change and adiabatic temperature change at CE. Such fascinating findings appear to be promising for the improvement of the solid-state refrigerators on caloric effects.

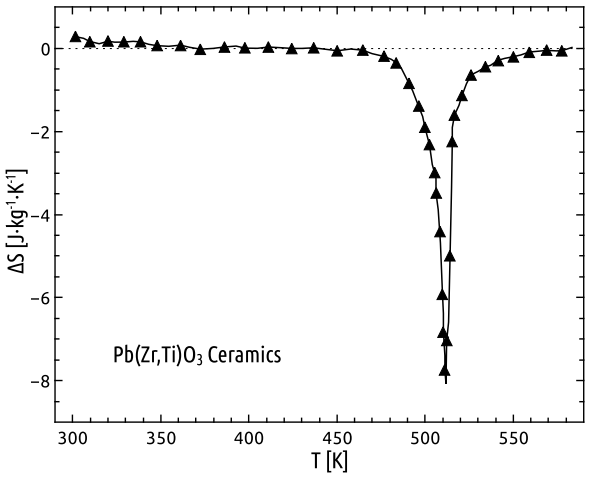

Fig.1 The temperature dependence of the isothermal entropy change at piezoelectrocaloric effect for PZT ceramics. The calculations were performed for an electric field of 480kV/cm and pressure of 0.3GPa.

References

1. A. S. Starkov, O. V. Pakhomov, I. A. Starkov Ferroelectrics. **430**, 108 (2012)
2. A. Mischenko, Q. Zhang, J. F. Scott, R. W. Whatmore, and N.D. Mathur . Appl. Phys. Lett. **89**, 242912 (2006)

RCBJSF Or-32

Dielectric, IR and Raman Spectroscopies of $(0.4\text{-}y)Na_{0.5}Bi_{0.5}TiO_3\text{-}0.6SrTiO_3\text{-}yPbTiO_3$ Solid Solutions

Š. Svirskas[1], T. Ostapchuk[2], M. Ivanov[1], J. Pokorny[2], M. Dunce[3], E. Birks[3], M. Antonova[3], J. Banys[1], S. Kamba[2], A. Sternberg[3]

[1]Vilnius University, Faculty of Physics, Saulėtekio av. 9, III b., LT-10222 Vilnius, Lithuania

[2]Institute of Physics, Academy of Sciences of the Czech Republic, Na Slovance 2, 182 21 Prague 8, Czech Republic

[3]Institute of Solid State Physics, University of Latvia, Kengaraga street 8, LV-1063 Riga, Latvia

e-mail: sarunas.svirskas@ff.vu.lt

Lead-free solid solutions which exhibit morphotropic phase boundary have drawn much attention due to their enhanced piezoelectric properties and demand for high performance materials in order to replace the outstanding lead zirconate titanate (PZT) [1, 2]. Despite of the progress, there are still many challenges concerning not only technology, but also fundamental science.

In this work we present broadband dielectric spectroscopic measurements from 1 mHz to 45 THz at temperatures ranging from 30 K to 500 K. In addition to this, Raman scattering spectra taken between 80 and 600 K will be presented.

The dielectric relaxation of polar nanoregions (PNRs) in the samples containing 0, 10, 20, 30 % of lead titanate in the relaxor phase shows gradual shift to the higher frequencies and the distribution of relaxation times narrows with increasing temperature. The insight to the relaxor-ferroelectric phase transition from the point of view of infrared and Raman spectra will be presented as well. Finally, the system will be compared with the 0.4NBT-(0.6-x)ST-xPT solid solutions which show rich behavior and a crossover from glassy/relaxor state to the ferroelectric phase [3].

References

1. J. Roedel, W. Jo, K. T. P. Seifert, E. M. Anton, T. Granzow, D. Damjanovic, J. Am. Ceram. Soc, **92**(6), pp. 1153-1177 (2009);
2. I. Coondoo, N. Panwar, A. Kholkin, J. Adv. Dielect. **3**(2), 1330002 (2013);
3. S. Svirskas, M. Ivanov, S. Bagdzevicius, J. Macutkevic, A. Brilingas, J. Banys, J. Dec, S. Miga, M. Dunce, E. Birks, M. Antonova, A. Sternberg, Acta Mater., **64**, pp. 123-132 (2014).

RCBJSF Or-33

Critical Points in KF-Substituted $BaTiO_3$

S. Tsukada, T. Moriyama, Y. Akishige

Shimane University, Matsue city, Shimane 609-8504, Japan

e-mail: tsukada@edu.shimane-u.ac.jp

The origin of large ferroelectricity in of $BaTiO_3$ is attributed to be the strong Ti-O covalency. Therefore, the substitution of O by F which has the largest electronegativity can control the ferroelectricity. We have fabricated $Ba_{1-x}K_xTiO_{3-x}F_x$ (KF-BT/x) single crystals and have reported the critical slowing down [1], the large annealing effect on T_C [2], and the enhanced piezoelectric and dielectric properties at x =0.10 [3]. The reason why these properties are enhanced at x =0.10 is interpreted so far as a result of the existence of tricritical point (TCP), however, the details are still unclear. As is known today, understanding of materials property by connecting them with critical phenomena is essential to develop materials science [4].

In the present paper, the x-E-T phase diagram of KF-BT/x is established by measuring dielectric constant under an electric field. Figure 1 shows the temperature dependence of dielectric constant under an electric field at x=0.023. Judging from the peak height in FIG. 1, CEP is placed at 380 K and 4 kV/cm. The electric field is smaller than that of $BaTiO_3$. The x-E-T phase diagram indicates that electric fields necessary for polarization rotations significantly decrease as the CEP approaches usage environment (0 V/cm, 300 K), thus showing that not only the existence of the TCP but also that of CEP are at the heart of the enhanced piezoelectric and dielectric properties in KF-BT/x at x=0.10.

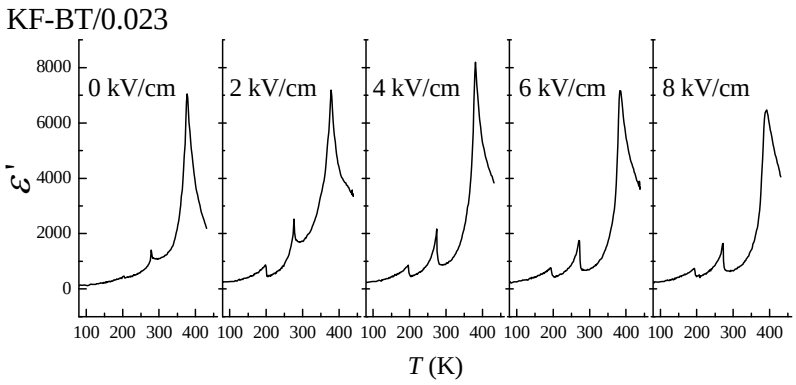

FIG. 1 Temperature dependence of the dielectric constant along $[001]_C$-direction, ε', obtained in a KF-BT/0.023 single crystal at various external electric fields along $[001]_C$-direction. The probe frequency is 20 Hz. The measurement is performed on heating.

References

1. S. Tsukada, Y. Hiraki, Y. Akishige, and S. Kojima, Phys. Rev. B **80**, 012102 (2009).
2. S. Tsukada and Y. Akishige, Scripta Materialia **64**, 268 (2011).
3. Y. Akishige, J. Phys. Soc. Jpn. **75**, 073704 (2006).
4. Z. Kutnjak, R. Blinc, and Y. Ishibashi, Phys. Rev. B **76**, 104102 (2007).

RCBJSF Or-34

Structural and Magnetic Phase Transitions in Rear Earth Ferroborate Crystals – Raman Scattering Study

A. Vtyurin[1,2], A. Krylov[1], S. Sofronova[1], J. Gerasimova[1], I. Gudim[1]

[1]Kirensky Institute Physics, Russia

[2]Siberian Federal University, Russia

e-mail: vtyurin@iph.krasn.ru

Crystals of the $RFe_3(BO_3)_4$ family (R is rare earth ion) were reported to possess multiferroic features, demonstrating both structural and magnetic phase transitions [1-4], where transition points may be varied by rare earth composition. In this work we used Raman spectroscopy to study $Ho_{(1-x)}Nd_xFe_3(BO_3)_4$ (x = 0, 0.22, 0.38, 0.75) crystals. Measurements were performed in the temperature range 10–400 K. The aim of this study is to investigate possible existence of a soft mode related to structural order parameter and effects of magnetic transitions on Raman spectra. Structural transitions manifest clearly by soft mode restoration and new Raman lines appearance below 366 K and 203 K for $x = 0$ и $x = 0.22$ compositions respectively. In Nd-doped crystals significant modification of Raman scattering was induced by magnetic ordering below the Neel temperature (about 40 K), that include both magnon scattering and strong intensity redistribution of high frequency lattice modes. Analysis of vibrational spectra and its numerical simulation demonstrate that bigger cell volume of Nd-containing solid solutions provides bigger displacements of oxygen ions in a BO_3 groups below the Neel temperature that results in stronger magnetoelastic interactions. This leads to the appearance of additional lines in the Raman spectra and rapid increase of their intensity with increasing magnetic order.

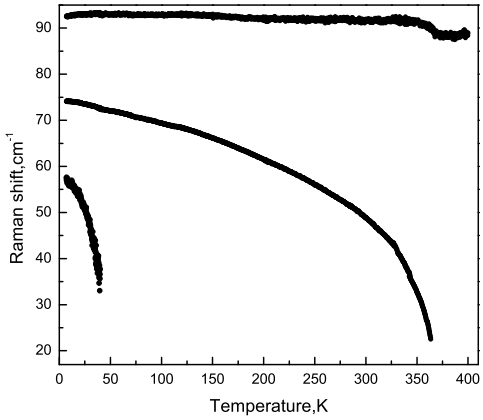

Fig. 1. Soft modes restoration below magnetic and structural phase transitions in $Ho_{0.78}Nd_{0.22}Fe_3(BO_3)_4$ crystal.

References

1. Zvezdin A. K. et al. JETP Lett. **81**, 272 (2005).
2. Fausti D. et al. Phys. Rev. **B74**, 024403 (2003).
3. Kuz'menko A. M. et al. JETP Lett. **94**, 294 (2011).
4. A. S. Krylov et al. Solid State Commun. **174**, 26 (2013).

RCBJSF Or-35

Prospects of Ferroelectric Ceramic-Polymer Composites in Sub-Terahertz Applications

Y. Yashchyshyn[1], K. Godziszewski[1], E. Pawlikowska[2], M. Szafran[2]

[1]Institute of Radioelectronics, Warsaw University of Technology, Poland

[2]Faculty of Chemistry, Warsaw University of Technology, Poland

e-mail: E.Jaszczyszyn@ire.pw.edu.pl

Tunable ferroelectric ceramic-polymer composites are very promising in sub-terahertz applications. Thanks to the possibility of changing the permittivity they may be used in, e.g. antennas with electrically controlled parameters, phase shifters and tunable filters [1]. In [2] the concept of microstrip scan antenna on a ferroelectric substrate without phase shifters was presented. Another possible application is a combination with other materials, e.g. liquid crystal polymers (LCP) or low temperature co-fired ceramics (LTCC) to form multilayer structures in which one of the layers could be electrically tuned. It is also possible to achieve flexible, durable as well as environmentally friendly composites. In this case, it is very important that developed composites should be characterized by high tunability, low losses and good mechanical properties.

In [1] was shown that materials with desired permittivity values can be synthesized by suitable selection of the proportions of ingredients and the use of appropriate technology process. Presented composites consisted of barium strontium titanate (BST) and polymeric binder have high tunability (up to 100%) and low losses in sub-THz range and as a result they are competitive to other state-of-the-art tunable materials.

Designing of tunable devices based on ferroelectric ceramic-polymer composites needs to resolve problem connected with the deposition of conductors on the surface of the composite. It is possible by using e.g. ink jet printing technology. This technology is based on deposition of ink containing metallic nanoparticles without using photolithography. In [3] was shown that good quality conductive structures can be made on the surface of composite material using this low cost and simple technology.

References

1. Y. Yashchyshyn, J. Modelski, K. Godziszewski, P. Bajurko, E. Pawlikowska, B. Bogdanska, E. Bobryk and M. Szafran, Proc. of Asia-Pacific Microwave Conference, 206 (2013)
2. Y. Yashchyshyn and J. Modelski, IEEE Trans. Microw. Theory Tech. **52**, 427 (2005)
3. J. Weremczuk, G. Tarapata, R. Jachowicz, Y. Yashchyshyn, K. Godziszewski, P. Bajurko, M. Szafran and E. Pawlikowska, Proc. of SPIE **890201**, 89021V (2013)

RCBJSF Or-36

The Evidence of Monoclinic Structure on Zr-rich $PbZr_{1-x}Ti_xO_3$

H. Yokota[1], N. Zhang[2], P. Thomas[3], Z.G. Ye[2], M. Glazer[3,4]

[1]Depatrment of Physics, Chiba University, Japan

[2]Department of Chemistry, Simon Fraser University, Canada

[3]Department of Physics, University of Warwick, U. K.

[4]Department of Physics, University of Oxford, U. K.

e-mail: yokota@physics.s.chiba-u.ac.jp

A true crystal structure of $PbZr_{1-x}Ti_xO_3$ (PZT-*x*) is still in a mystery in spite of a vast research. Our current understanding of PZT is the mixture phase of more than two phases ina whole area of the phase diagram. High resolution neutron diffraction experiments showed the existence of monoclinic phase even at the Zr-rich region [1,2] which had been considered as a single rhombohedral phase. However, there still has been argument whether the monoclinic phase is a real phase or an artifact. Here, local structure of PZT with Zr-rich concentrations was studied by pair distribution function analysis (PDF). Time of flight neutron powder diffraction data were collected by GEM at ISIS. Reverse Monte Carlo modelling was carried out with 10 by 10 by 10 rhombohedral unit cells based on the Reitveld refinement. The comparisons for experimental and simulated Bragg profile, PDF and total structure factor show good agreement for whole range. Figure 1 shows the Pb atom displacement of PZT-0.3 on a stereographic projection. A large intensity of Pb atom displacement is observed along [111] rhombohedral direction. Additionally, a triangle shape distribution around [111] direction can be seen in Fig.1. It suggests the existence of local monoclinic displacement which is averaged out to a long-range rhombohedral structure. The same tendency is obtained for PZT-0.2 and PZT-0.4 instead the ratio between M_A and M_B changes with Ti concentration. The details of PDF analysis will be discussed in the presentation.

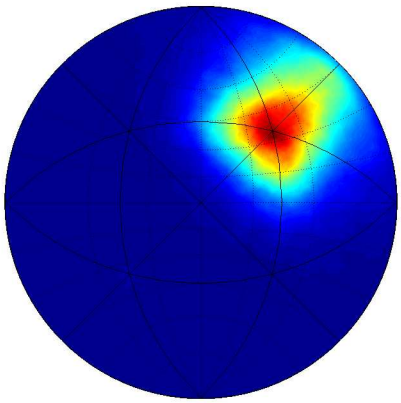

Figure 1 Stereographic projection of Pb atom displacements for PZT-0.3 measured at r.t.

References

1. H. Yokota, N. Zhang, A. E. Taylor, P. Thomas, and M. Glazer, Phys. Rev. B **80**, 104109 (2009)
2. N. Zhang, H. Yokota, M. Glazer, and P. Thomas, Acta Crystal. B **67**, 386-398 (2011)

RCBJSF Or-37

Characterization of Extruded Ferroelectric Film P(VDF-TrFE)

X. Zhu[1,2], E. Bilotti[1,3], X. Meng[2], and M. Reece[1,3]

[1]School of Engineering and Material Science, Queen Mary University of London, London, E1 4NS, UK

[2]Shanghai Institute of Technical Physics(SITP), Chinese Academy of Sciences (CAS), Shanghai 200083, China

[3]Nanoforce Technology Limited, London, E1 4NS, UK

e-mail: x.zhu@qmul.ac.uk

Ferroelectric copolymer poly(vinylidene fluoride and trifluoroethylene) [P(VDF-TrFE)] have been attracted much attention for its advantages of flexibility over ferroelectric ceramics. The ferroelectric performance of P(VDF-TrFE) derived from spin-coating, Langmuir-Blodgett and cast-stretching has been comprehensively investigated[1]. However no ferroelectric performance of extruded P(VDF-TrFE) films has been reported yet. In this work, P(VDF-TrFE) films was extruded from melt and was hot pressed at different temperatures up to 120℃ to obtain smooth and uniform films. Morphology results show that the P(VDF-TrFE) films have compact banded structures where the crystal grains stack closely together, suggesting the structure was not disturbed by the hot-pressing process. The film is highly crystallized in the ferroelectric low temperature (LT) phase and confirmed by the X-ray diffraction (XRD). The extruded film with a hot-pressed processing at 120℃ achieved higher crystallinity than that without a hot-pressed process, as shown in Fig.1. The films show good ferroelectricity with a remnant polarization around 0.07C/m2. Our research presents that the extruded-film technique is a simple way to prepare P(VDF-TrFE) thin films with a good performance.

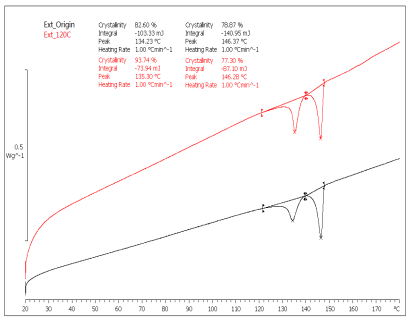

Figure 1 DSC results of extruded films (black) without hot-pressing and (red) hot-pressed at 120℃.

Reference

1. R. V. Gaynutdinov, et al.Polarization switching at the nanoscale in ferroelectric copolymer thin films.Applied Physics Letters.99.14: 142904(2011)

RCBJSF Or-38

First Principles Simulations on Stoichiometric $SrTiO_3$ Nanowires

Yu.F. Zhukovskii[1], R.A. Evarestov[2] and A.V. Bandura[2]

[1]Institute of Solid State Physics, University of Latvia, Riga, Latvia

[2]St. Petersburg State University, Chemistry Faculty, Petrodvorets (St. Petersburg), Russian Federation

e-mail: quantzh@latnet.lv

The increasing demands to reduce the sizes of microelectronic ferroelectric devices motivated synthesis of $SrTiO_3$ (STO) nanowires (NWs) and their theoretical simulations. Meanwhile, the only *ab initio* study of STO NWs has been reported so far [1], configuration of which has been considered to be symmetric non-stoichiometric described by D_{4h} point group. Unlike those non-stoichiometric STO NW configurations, we have simulated for the first time the properties of stoichiometric $SrTiO_3$ nanowires (Fig. 1) of different thicknesses with a lower symmetry as compared to the former and described by point group C_{2v}. To generate them, the cubic $SrTiO_3$ crystal has been cut along the [001] crystallographic axis, the lateral size of which has been equal to a period of bulk. STO NWs contain {100} and {010} facets, with two possible terminations by the SrO and TiO_2 atomic layers, respectively.

For optimization of equilibrium STO NW structures and simulation of their numerous properties, we have performed large-scale DFT LCAO calculations within the hybrid PBE0 exchange-correlation functional using CRYSTAL14 code [2]. The computational details of the method applied are the same as in recent $SrTiO_3$ bulk calculations [3]. The dependence of 1D lattice parameter, the energy gap, the formation and surface energies on the NW thickness is studied for the stoichiometric nanowires consisting of 5, 20, 45, 80 atoms in 1D unit cell. All the calculations have been performed in the Computer Center of St. Petersburg State University.

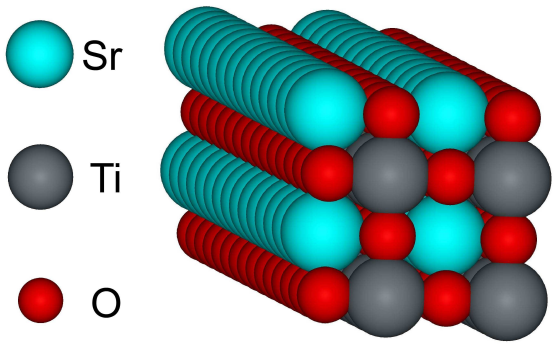

Fig. 1. Axonometric image of stoichiometric [001]-oriented $SrTiO_3$ NW terminated by both SrO and TiO_2 facets with 2×2 extension of the thinnest possible nanowire (5 atoms *per* UC). Left panel contains labels of constituent atoms.

References

1. Q. Fu, T. He, J. L. Li, and G. W. Yang, *J. Appl. Phys.* **112**, 104322 (2012)
2. R. Dovesi, V. R. Saunders, C. Roetti, R. Orlando, C. M. Zicovich-Wilson, F. Pascale, B. Civalleri, K. Doll, N. M. Harrison, I. J. Bush, P. D'Arco, M. Llunell, M. Causà and Y. Noël, *CRYSTAL14 User's Manual* (University of Torino, Torino, 2014)
3. D. Gryaznov, E. Blokhin, A. Sorokine, E. A. Kotomin, R. A. Evarestov, A. Bussmann-Holder, J. Maier, *J. Phys. Chem.* C, **117**, 13776 (2013)

RCBJSF-12 Poster Presentation Abstracts

R-1

Modeling of Piezoelectric Elements with Inhomogeneous Polarization in ACELAN

A.N. Soloviev[1, 2, 3], P.A. Oganesyan[1, 3], A.S. Skaliukh[2]

[1]Department of Theoretical and Applied Mechanics, Don State Technical University, Russia

[2]Department of Mathematics, Mechanics and Computer Sciences, Southern Federal University, Russia

[3]Department of Mechanics of Active Materials, Southern Scientific Centre of Russian Academy of Sciences, Russia

e-mail: solovievarc@gmail.com

The paper presents the results of the calculation of harmonic oscillations nonuniformly polarized transducers using the finite element program ACELAN. As an example, we considered the two-dimensional problem of longitudinal rod vibrations with the transverse inhomogeneous polarization and taking into account the damping. It is shown that the nature of the distribution of vector residual polarization is closely associated with vibration modes, that it is shown in Figure 1. In particular, for the second vibration mode electromechanical coupling coefficient can be increased more than three times, if the nature of the field of residual polarization is selected as shown in the same figure.

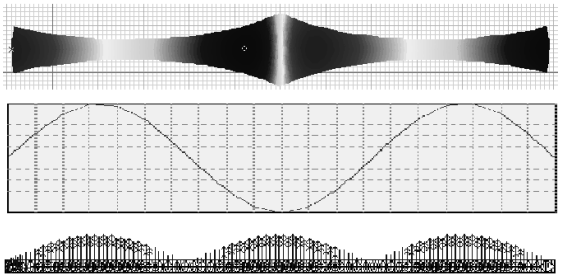

Fig.1 The displacement, longitudinal strain and field of polarization on the second eigenmodes.

Acknowledgment

This work was partially supported by RFBR (grant number 13-01-00196 A, 13-01-00943 A, 12-01-00829-a, 13-08-01094-a).

R-2

A Novel Approach for Optimization of Finite Element Models of Lossy Piezoelectric Elements

E. Petrova, A. Naumenko, M. Lugovaya, A. Rybyanets

Institute of Physics, Southern Federal University, Russia

e-mail: harigamypeople@gmail.com

In recent years low-Q piezoceramics and piezocomposite materials are widely used for wide-band medical and NDT ultrasonic transducers with high sensitivity and resolution. The majority of these advanced materials are lossy and direct use of IEEE Standards for material constant determination leads to significant errors.

The modeling and design of piezoelectric devices by finite element methods, among others, relies on the accuracy of the dielectric, piezoelectric and elastic coefficients of the active material used, commonly an anisotropic ferroelectric polycrystals. The accurate description of piezoceramics must include the evaluation of the dielectric, piezoelectric and mechanical losses, accounting for the out-of-phase material response to the input signal [1].

Standard finite element modeling (FEM) packages that are widely used for modeling of piezoelements and devices don't take into account losses (mechanical losses can be included in calculations by implicit manner). Sets of material constants used for FEM calculations also do not contain losses data, except for Q_M for radial mode of vibrations. As a result, FEM calculations of real piezoelements and devices can give inadequate results for lossy materials (composites, porous ceramics etc.) [2].

In this work, a novel approach for optimization of finite element modeling (FEM) of lossy piezoceramic elements has been proposed.

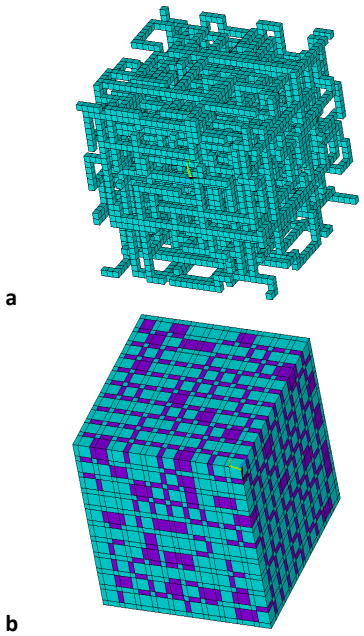

Fig.1. Examples of representative volumes used for FEM calculations of porous piezoceramics: a) 3-3 connectivity, porosity 80%; b) 3-0 connectivity, porosity 20%.

In this paper, a novel approach for optimization of finite element modeling (FEM) of lossy piezoelectric elements has been proposed. Procedure of optimization has consisted in sequential and iterative application of FEM and piezoelectric resonance analysis to complex electric impedance spectra of piezoceramic elements. For validation of proposed optimization procedure, FEM calculations of standard shape piezoelements (disks, shear plates, bars, and rods) made from porous PZT-type piezoceramics were fulfilled using FEM ANSYS software package.

References

1. A.N. Rybyanets, IEEE Trans. UFFC. **58,** 1492, (2011),
2. A.N. Rybyanets, A.A. Naumenko, N.A. Shvetsova. In.: " Nano- and Piezoelectric Technologies, Materials and Devices", Ivan A. Parinov Ed. Nova Science Publishers Inc., 2013. Chapter 1. – P. 275-308.

R-3

Local Structure of Multiferroic $Mn_{1-c}Co_cWO_4$ Solid Solutions Revealed by the Evolutionary Algorithm

J. Timoshenko[1], A. Anspoks[1], A. Kalinko[1,2], I. Jonane[1], A. Kuzmin[1]

[1]Institute of Solid State Physics, University of Latvia, Latvia

[2]Synchrotron SOLEIL, France

e-mail: janis.timoshenko@gmail.com

Manganese tungstate $MnWO_4$ is a multiferroic material with wolframite-type structure, isomorphic to the antiferromagnetic $CoWO_4$ [1]. At low temperatures $MnWO_4$ undergoes three successive magnetic phase transitions to antiferromagnetically (AF) ordered states. In the AF2 state, existing in the temperature range between 7.6 K and 12.7 K, $MnWO_4$ has also a simultaneous ferroelectric polarization. It is known that the presence of Co ions in the $MnWO_4$ lattice allows one to tune its magnetic properties [2]. However, the relation between multiferroic properties of $Mn_{1-c}Co_cWO_4$ solid solutions and their structure is still debatable.

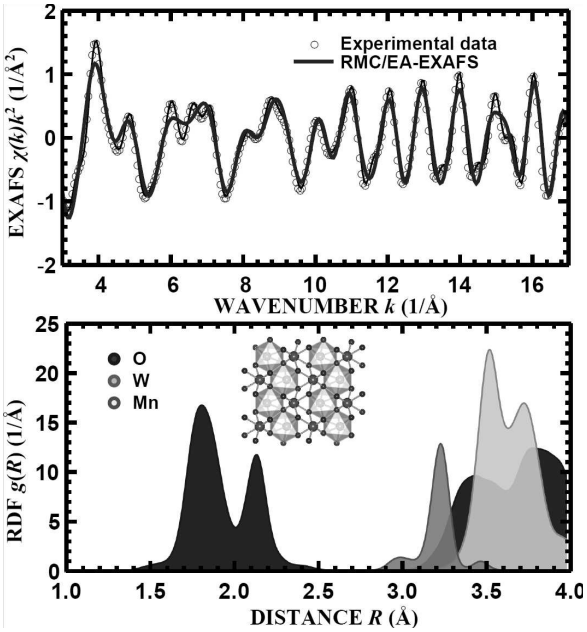

Fig.1. Experimental (T=6 K) and calculated by the RMC/EA method W L_3-edge EXAFS spectra for $MnWO_4$ and the radial distribution function (RDF) around tungsten, calculated from the RMC/EA results.

Recently we have addressed this question using the Mn(Co) K-edge and W L_3-edge extended X-ray absorption fine structure (EXAFS) spectroscopy [3]. However, the conventional EXAFS data analysis does not allow extracting information beyond the first coordination shell due to complex structure of the material. Therefore, in this study we report on the results of the local structure reconstruction (Fig. 1) using the advanced approach based on the reverse Monte Carlo (RMC) and evolutionary algorithm (EA) techniques [4].

References

1. O. Heyer, N. Hollmann, I. Klassen, et al., J. Phys.: Condens. Matter **18**, L471 (2006).
2. Y.S. Song, J.H. Chung, J. Park and Y.N. Choi, Phys. Rev. B **79**, 224415 (2009).
3. A. Kuzmin, A. Anspoks, A. Kalinko and J. Timoshenko, J. Phys.: Conf. Ser. **430**, 012109 (2013).
4. J. Timoshenko, A. Kuzmin and J. Purans, J. Phys.: Condens. Matter **26**, 055401 (2014).

R-4

Dynamic Nonlinear Optical Processes in Some Oxygen-Octahedra Ferroelectrics: First Principle Calculations

S. Simsek[1], A.M. Mamedov[2,3], E. Ozbay[2]

[1]Department of Material Science and Engineering, Hakkari University, Hakkari, Turkey

[2]Nanotechnology Research Center, Bilkent University, Ankara, Turkey

[3]International Scientific Center, Baku State University, Baku, Azerbaijan

e-mail: mamedov@bilkent.edu.tr

The nonlinear optical properties and electro-optic effects of some oxygen-octahedric ferroelectrics are studied by the density functional theory (DFT) in the local density approximation (LDA) expressions based on first principle calculations without the scissor approximation. We present calculations of the frequency- dependent complex dielectric function and the second harmonic generation response coefficient $\chi(2)(-2\omega,\omega,\omega)$ over a large frequency range in tetragonal and rhombohedral phases. The electronic linear electrooptic susceptibility $\chi(2)$ $(-\omega,\omega,0)$ is also evaluated below the band gap. These results are based on a series of the LDA calculation using DFT. Results for $\chi(2)$ $(-\omega,\omega,0)$ are in agreement with the experiment below the band gap and those for $\chi(2)(-2\omega,\omega,\omega)$ are) compared with the experimental data where available.

R-5

First Principles Calculations of the Diffusion and Aggregation of *F* Centers, as Well as Bulk and Nano-Surface *H* Centers in CaF_2, BaF_2 and SrF_2

R.I. Eglitis[1], H. Shi[2] and R. Jia[3]

[1]Institute of Solid State Physics, University of Latvia, Latvia

[2]School of Science, Beijing Institute of Technology, 100081, Beijing, PR China

[3]Institute of Theoretical Chemistry, State Key Laboratory of Theoretical and Computational Chemistry, Jilin University, 130023 Changchun, PR China

e-mail: rieglitis@gmail.com

Our hybrid B3PW calculations show that the *F*-center diffusion barrier is equal to 1.84, 1.67 and 1.83 eV in SrF_2, CaF_2 and BaF_2 crystals [1-3]. During the *F* center diffusion, the trapped electron is more delocalized than that in the regular *F* center case, and the gap between the defect level and CB in the alpha spin state decreases. The *F* center in CaF_2, BaF_2 and SrF_2 is strongly localized inside vacancy, it contrasts with *F* centers in ABO_3 perovskites, for example $KNbO_3$, where two *F* center electrons are considerably delocalized [4]. The calculation of total energies of different nano-surface *H* center configurations in BaF_2 implies that *H* centers have a trend to locate near the surface [5]. The energy difference between *H* centers with different orientations show that the *H* centers oriented in the [111] direction in SrF_2, CaF_2 and BaF_2 crystals are the most stable configuration [6].

References

1. H. Shi, L. Chang, R. Jia and R. I. Eglitis, Comput. Mater. Sci. **79**, 527 (2013)
2. H. Shi, L. Chang, R. Jia and R. I. Eglitis, J. Phys. Chem. C **116**, 4832 (2012)
3. H. Shi, R. Jia and R. I. Eglitis, Solid State Ionics **187**, 1 (2011)
4. R. I. Eglitis, Int. J. Mod. Phys. B **28**, 1430009 (2014)
5. H. Shi, R. Jia and R. I. Eglitis, Phys. Rev. B **81**, 195101 (2010)
6. L. Yue, R. Jia, H. Shi, X. He and R. I. Eglitis, J. Phys. Chem. A **114**, 8444 (2010)

R-6

First Principles Calculations of $SrTiO_3$, $BaTiO_3$, $PbTiO_3$ and $CaTiO_3$ (001), (011) and (111) Surfaces

R.I. Eglitis[1]

[1]Institute of Solid State Physics, University of Latvia, Latvia

e-mail: rieglitis@gmail.com

While the (001) surfaces of $SrTiO_3$, $BaTiO_3$, $PbTiO_3$ and $CaTiO_3$ have been extensively studied during the last decade, much less is known about the (011) and (111) surfaces [1-3]. For the (011) surfaces, I consider three types of surfaces, terminating on a TiO layer, a Ba (Pb, Sr or Ca) layer and O layer. The surface relaxation energies for $BaTiO_3$, $PbTiO_3$, $CaTiO_3$ and $SrTiO_3$ (011) surfaces for all terminations are considerably larger than for (001) surfaces. I predict a considerable increase of the Ti-O chemical bond covalency near the $ATiO_3$ (011) surfaces as compared to both the bulk and the (001) surfaces. My calculated $SrTiO_3$, $BaTiO_3$, $PbTiO_3$ and $CaTiO_3$ (111) surface energies are considerably larger than the (001) and (011) surface energies [4-6].

References

1. R. I. Eglitis and D. Vanderbilt, Phys. Rev. B **76**, 155439 (2007)
2. R. I. Eglitis and D. Vanderbilt, Phys. Rev. B **77**, 195408 (2008)
3. R. I. Eglitis and D. Vanderbilt, Phys. Rev. B **78**, 155420 (2008)
4. R. I. Eglitis, Ferroelectrics **424**, 1 (2011)
5. R. I. Eglitis, Phase Transitions **86**, 1115 (2013)
6. R. I. Eglitis, Int. J. Mod. Phys. B **28**, 1430009 (2014)

R-7

Semi-Microscopic Vibronic Theory of the Properties of Quantum Paraelectrics and Ferroelectrics of $SrTiO_3$-type

P. Konsin[1], B. Sorkin[1]

[1]Institute of Physics, University of Tartu, Riia 142, 51014 Tartu, Estonia

e-mail: konsin@fi.tartu.ee

A semi-microscopic electron-phonon (vibronic) mechanism of the structural ferroelectric phase transitions in oxide perovskites of $BaTiO_3$ –type has been proposed [1,2]. At this, some properties in the paraelectric cubic, ferroelectric rombohedral phases are described and explained (for the tetragonal phase spontaneous polarization is calculated in $BaTiO_3$ [1]). In this report the semi-microscopic vibronic theory of quantum paraelectrics and ferroelectrics of oxide perovskites ($SrTi^{16}O_3$, $CaTiO_3$, $SrTi(^{18}O_x{}^{16}O_{1-x})_3$, $KTaO_3$, TiO_2) has been developed further. It is shown that the electron-lattice couplings of the filled A_{1g} and empty F_{1u} electronic states of the BO_6 cluster in ABO_3 perovskite oxides lead to the renormalization of these electronic states by the potential ferroelectric soft mode with the F_{1u} (Γ_{15}) symmetry at the Γ point and the F_{2u} (Γ_{25}) zone-boundary phonon mode (at the R point). At this, the interband vibronic interactions-hybridizations with the F_{2u} mode cause the antiferrodistortive phase transition at T_a=105K from the cubic O_h to the D_{4h} phase in incipient ferroelectric $SrTiO_3$. The electron-acoustic phonon interactions lead to the superelasticity properties of $SrTiO_3$ –type systems. The Helmholtz free energies of the quantum paraelectrics and ferroelectrics for these cases are obtained in which also the strain and stress terms are derived. For the explanation of the temperature dependence of the staggered rotation of oxygen octahedra Φ_i also the deviation from the mean field approximation is considered. The antiferrodistortive structural transition in $SrTiO_3$ is due to static oxygen octahedra rotations around one cubic axis, the rotations alternating from cell to cell in all three cubic directions (see also [3]). The generalized Barrett formulae for the dielectric constants $\varepsilon_{a,c}$ are derived. At this, the effects of the zero-point motion are taken into account, which are connected also with the vibronic couplings. The oxygen isotope effects are studied in $SrTi(^{18}O_x{}^{16}O_{1-x})_3$. The pressure effects in quantum paraelectrics at the quantum critical point are also investigated.

Acknowledgment

The research was supported by the Estonian Research Council (project IUT2-27) and by the European Union (projects 3.2.0101.11-0029 and SF0180013s07AP).

References

1. P. J. Konsin and N. N. Kristoffel, (1987). In: Interband model of ferroelectrics. Ed. E. V. Bursian, Hertzen Pedagogical Institute, Leningrad, p.32.
2. I. B. Bersuker, The Jahn-Teller Effect, Cambridge: Cambridge University Press (2006).
3. K. A. Müller, W. Berlinger, and F. Waldner, Phys. Rev. Lett. **21**, 814 (1968).

R-8

New Piezoelectric Materials and Transducer Designs for Energy Harvesting Devices

A. Rybyanets, A. Naumenko, M. Lugovaya, N. Shvetsova

Institute of Physics, Southern Federal University, Russia

e-mail: arybyanets@gmail.com

In this paper a comprehensive review and critical comparison of different piezoelectric materials and devices designs for energy harvesting applications were presented. Various types of energy harvesting piezoelement and transducer designs including multilayer stacks, cantilevers, flex-tensional elements, and shear-mode elements and stacks were examined. Empirical criteria of piezoelectric materials efficiency for energy harvesting devices were discussed. Several types of hot-pressed and conventionally sintered PZT piezoceramics, porous PZT piezoceramics, and multilayer PZT/PZT ceramic piezocomposites with diverse ferroelectric "hardness" were fabricated, optimized and tested.

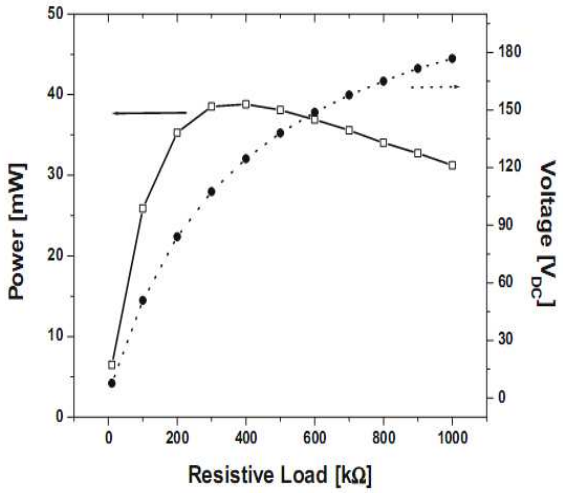

Fig.1 Output power P_{out} and voltage V_{load} as a function of resistive load R_{load} for piezoelectric generator with $|Z_{int}|$ = 300 kOhm.

Systematical experimental results comprising electric impedance and capacitance measurements, cyclic loading at different load resistances, frequencies, and mechanical stresses for various types of piezoelements were presented. Original design concept for energy harvesting devices with higher overall efficiency, stability, life-time and low self-cost, based on both new materials (piezoelectric, pyroelectric and electret ceramics and composites) and new physical principles (giant field-induced piezoelectric and pyroelectric responses, multimode vibrations and complex deformations) were discussed.

References

1. A.N. Rybyanets and A.A. Rybyanets, IEEE Trans. UFFC. **58**, 1757, (2011),
2. A.N. Rybyanets, IEEE Trans. UFFC. **58**, 1492, (2011),
3. A.N. Rybianets and R. Tasker, Ferroelectrics, **360**, 90, (2007).

R-9

Surface Relief and Domain Structure of Ferromagnetic Shape Memory Alloys

R.M. Grechishkin[1], O.V. Gasanov[1], E.T. Kalimullina[2], S.E. Ilyashenko[3], O.M. Korpusov[4], A.B. Zalyotov[1,4]

[1]Tver State University, Russia

[2]Kotel'nikov Institute of Radio Ingineering and Electronics of RAS, Moscow, Russia

[3]Tver State Technical University, Russia

[4]Tver State Medical Academy

e-mail: rostislav.grechishkin@tversu.ru

In recent studies [1-2] it was shown that the structural, thermal, magnetomechanical and mechanical properties of ferromagnetic shape memory (FSMA) alloys may be substantially affected by defects at or near the surface introduced by different surface treatments such as abrasive grinding, spark eroding, wire cutting. In the present work we examine another type of surface effects manifesting themselves in surface corrugation during thermal cycling of initially planar FSMA samples [3]. This specific feature is inherent to FSMA alloys and is basically a consequence of martensitic phase transformation not necessarily connected with surface defects of the material. The key experiments were performed by examination of the surface relief structure and magnetic domain structure during thermal cycling with the aid of optical profilometry, differential polarized light microscopy and SEM. The analysis was facilitated making use of auxiliary reference grids applied to the surface of the samples. An example of this technique is given in Fig. 1.

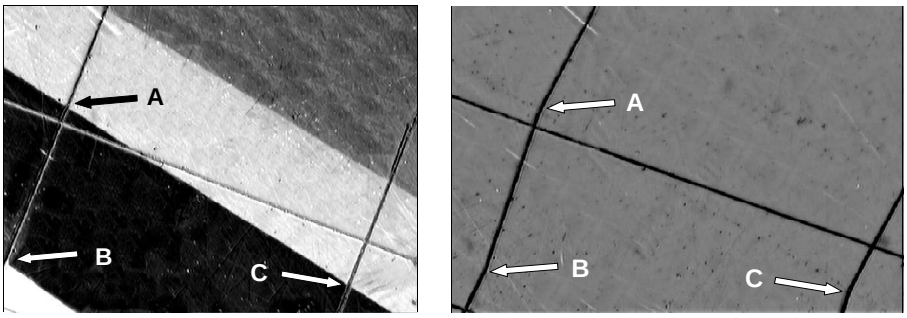

(a) (b)

Fig.1. Microstructure of $Ni_{2.16}Mn_{0.84}Ga$ FSMA alloy observed at RT (martensite state) (a) and after transformation into the austenite state at T = 370 K (b). The arrows show the points of martensite twin boundary intersections with a square grid of scratches in (a) and the points of the grid inflection in (b)

References

1. M. Chmelius, K. Rolfs, R. Wimpory, W. Reimers, P. Mullner, R. Schneider, Acta Materialia **58**, 3952 (2010).
2. M. Chmelius, C. Witherspoon, K. Ullakko, P. Mullner, R. Schneider, Acta Materialia **59**, 2948 (2011).
3. S.J. Murray, Magneto-mechanical properties and application of Ni-Mn-Ga FSMA, MIT Theses, 2000.

R-10

Dielectric Behavior in *A*-site Ordered Perovskite $CaCu_3Ti_4O_{12}$: Effect of *A*'-Site Doping

N. Hasegawa[1], A. Onodera[1], M. Sasaki[1], T. Hattori[1], H. Satoh[2], M. Takesada[1]

[1]Department of Physics, Faculty of Science, Hokkaido University, Sapporo 060-0810, Japan

[2]Hakodate National College of Technology, Hakodate 042-8501, Japan

e-mail: n70-h@ec.hokudai.ac.jp

A huge dielectric constant has been found in $CaCu_3Ti_4O_{12}$ in the wide temperature region from 100 K to 600 K, although it drops drastically to about 100 below 100 K [1,2]. $CaCu_3Ti_4O_{12}$ is a complex perovskite where *A*-site ion and *A'*-site ion order in a chemical formula $AA'_3Ti_4O_{12}$. This compound is consisted of eight TiO_6 octahedra and six CuO_4 planer molecules in the cubic unit cell [3]. The characteristic feature of this crystal structure is that all TiO_6 octahedra are linked tightly by CuO_4 due to Cu3*d* - O2*p* hybridization, in contrast to a typical $ATiO_3$ perovskite. In this paper, we will report the effect of doping with small Be ion (ionic radius 0.27 Å) instead of Cu ion (ionic radius 0.57 Å). Furthermore Be ion has no *d*-electrons, which modifies the nature of Cu-O bonds and may produce an extra space in the tightly-packed crystal structure.

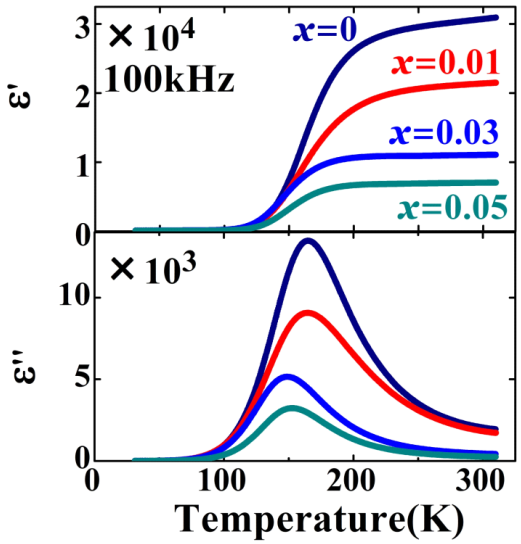

Fig.1 Dopant dependence of dielectric constant of Be-doped $CaCu_{3(1-x)}Be_{3x}Ti_4O_{12}$ (x=0, 0.01, 0.03 and 0.05).

Figure 1 shows the Be-dopant dependence of dielectric constant of $CaCu_{3(1-x)}Be_{3x}Ti_4O_{12}$ in the low-temperature region, where the real part of dielectric constant (ε') decreases exponentially with increasing Be-dopants . The relaxation time and activation energy show 50% of decrease and 8% decrease by Be-doping respectively, which suggests some structural relaxation in crystal. We will report also the effect of stress on the high dielectric behavior in $CaCu_3Ti_4O_{12}$.

References

1. M. A. Subramanian, D. Li, N. Duan, B. A. Reisner, and A. W. Sleight, J. Solid State Chem. **151**, 323 (2000).
2. A. P. Ramirez, M. A. Subramanian, M. Gardel, G. Blumberg, D. Li. T. Vogt, and S. M. Shapiro, Solid State Commun. **115**, 217 (2000).
3. Y. Liu, R. Withers, and X. Y. Wei, Phys. Rev. B **72**, 134104 (2005).

R-11

Multicaloric Efficiency of Ferroelectric-Ferromagnetic Volume Composites $(x)La_{0.7}Pb_{0.3}MnO_3$ - $(1-x)PbTiO_3$

E. Mikhaleva, I. Flerov, A. Kartashev, M. Gorev, K. Sablina, N. Mihashenok

Kirensky Institute of Physics, Siberian Department of RAS, Krasnoyarsk 660036, Russia

e-mail: katerina@iph.krasn.ru

In the recent studies of magneto(MCE)- and baro(BCE)-caloric effects in ferromagnet $La_{0.7}Pb_{0.3}MnO_3$ [1] and electrocaloric effect (ECE) and BCE in ferroelectric $PbTiO_3$ [2] we have shown that caloric efficiency of monoferroic materials can be elevated using two from three distinct external fields (electric, magnetic, mechanical stress). Such a way is promising also for multiferroic materials involving two or even three subsystems characterized by different ferroic nature (ferroelectric, ferromagnetic, ferroelastic). In single-phase materials, magnetoelectric, magnetoelastic or electroelastic coupling arises directly between the two order parameters. On the other hand, the interaction between two monoferroic phases can be enhanced through their strain-mediated indirect coupling in composites. In such materials, the electric, magnetic and elastic order parameters arise in separate but intimately connected phases.

In the present paper, volumetric ferromagnet - ferroelectric composites $(x)La_{0.7}Pb_{0.3}MnO_3$ - $(1–x)PbTiO_3$ with x=0.85 and x=0.18 were prepared. For all samples there was obtained the detailed experimental information on MCE, BCE, magnetization, heat capacity, entropy, thermal dilatation, susceptibility to hydrostatic pressure. Multicaloric efficiency of composites is discussed and compared with that of initial $La_{0.7}Pb_{0.3}MnO_3$ and $PbTiO_3$ compounds. Variation of a relationship between components can significantly increase both barocaloric and magnetocaloric efficiency of compositional material due to the mechanical stress appearing between grains of different ferroic phases under magnetic field.

The results obtained allow us to suppose that ferromagnetic–ferroelectric composites are really promising materials for their use as effective solid-state refrigerants in magnetic as well as multicaloric cooling cycles built on MCE and BCE.

References:

1. Kartashev A.V., Mikhaleva E.A. et al. J. Appl. Phys. **113**, 073901 (2013).
2. Mikhaleva E.A., Flerov I.N et al. Physics of the Solid State. **54**, 1832 (2012).

R-12

The Nickel and Cobalt Ferrite Nanopowders and it Composites with Polycarbonate

I. Bockovs[1], I. Zalite[2], M. Kodols[2], G. Heidemane[2], J. Grabis[2], J. Zicans[1], R. Merijs-Meri[1], A.K. Bledzki[3]

[1]Institute of Polymer Materials, Riga Technical University, Latvia

[2]Institute of Inorganic Chemistry, Riga Technical University, Latvia

[3]Institute of Material Engineering, University of Kassel, German

e-mail: ilmars@nki.lv

The materials, containing ferrites, are widely applied in life sciences, biochemical processes (magnetic liquids, hyperthermia etc.) and special coatings (antistatic, electro-magnetic interference shielding). In the current research attention is devoted to the synthesis of nanostructured ferrites by sol-gel auto-combustion method and by high frequency plasma route. Structure of the synthesized ferrites is analyzed by X-ray diffraction method. Magnetic properties of the synthesized ferrites are analyzed by vibrating sample magnetometry (VSM). It is found that all the synthesized ferrites are nanocrystalline single phase materials with specific surface area of 30–40 m^2/g and calculated particle size of 30–40 nm. Ni and Co ferrites synthesized by high-temperature plasma route are characterized by saturation magnetization M_S of 44,2 emu/g and 75,4 emu/g, remanent magnetization M_r of 10,0 and 32,0 emu/g and coercivity H_c of 74 Oe and 780 Oe, respectively. Magnetic properties of the samples obtained with sol-gel self-combustion method differ from which the plasma products have. Selected nanopowders (2 - 10 wt. %) are introduced in a polycarbonate matrix by melt compounding. The effects of the nanofiller type and concentration on structural, mechanical and magnetic characteristics of the polycarbonate based composites are investigated. By SEM-EDX investigations it is shown that desirable dispersion of the investigated nanocrystalline ferrites in the polymer matrix has been achieved by the thermoplastic compounding technique used. By VSM investigations it is demonstrated that certain magnetic traits are assigned to the investigated polycarbonate nanocomposites already at ferrite content of 2 wt. %. By tensile investigations it is shown that considerable increase (by 26 %) in tensile modulus of the investigated polycarbonate nanocomposites is observed at ferrite content of 10 wt. %, although gain in tensile modulus decreases by rising ferrite content above 2 wt. %. Considering previously mentioned, one can conclude that polycarbonate composites are successfully modified with ferrite nanopowders and have enhanced elastic, thermal and magnetic properties in respect to neat polycarbonate.

R-13

Dielectric Properties of Diammonium Hypodiphosphate $(NH_4)_2H_2P_2O_6$

R. Mackeviciute[1], J. Banys[1], P. Szklarz[2]

[1]Vilnius University, Faculty of Physics, Lithuania

[2]Faculty of Chemistry, University of Wroclaw, Poland

e-mail: ruta.mackeviciute@ff.vu.lt

The connection between ferroelectricity and organic molecules started in 1920 with the discovery of the first ferroelectric crystal, Rochelle salt, containing organic tartrate ions [1]. Organic ferroelectrics, such as diammonium hypodiphosphate (ADhP) [2], could be important not only for fundamental approach but also for versatile technical applications.

Dielectric measurements were performed in 100 — 300 K temperature and 20 – 1 GHz frequency range. Frequency dependence of the real and imaginary parts of dielectric permittivity could be divided into three frequency ranges: the high frequency range (10^6 Hz – 10^9 Hz), the mid-frequency range (400 Hz – 10^6 Hz) and the low frequency range (20 Hz – 400 Hz) (see Fig. 1).

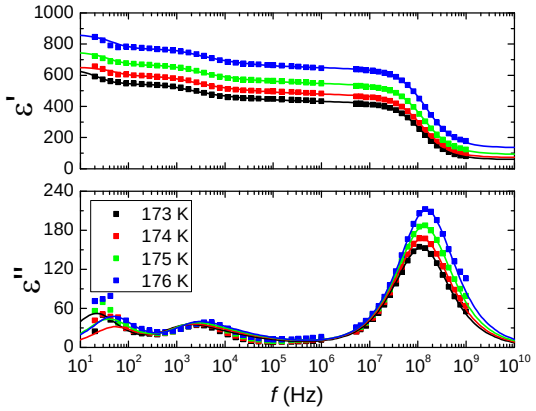

Fig. 1. Frequency dependence of the real and imaginary parts of dielectric permittivity of ADhP crystal.

The Cole – Cole equation perfectly describes the relaxation process which is observed in the high frequency range and this process could be related to the ordering of NH_4 cations. The Cole – Davidson equation describes the dispersion at the mid-frequency range, which is related to the domain wall formation and motion. Despite the fact that we can only observe the end of the low frequency process, it is necessary to describe that process, due to the fact that all of the observed processes are overlapped together and they influence each other considerably in the whole frequency range. This process is described by the Debye equation and could be related to the other type of the domain wall motion.

References

1. J. Valasek, Phys. Rev, Vol: 17, 475-481, (1921)
2. P. Szklarz, M. Chanski, K. Slepokura, T. Lis, Chem. Mater,; 23; 1082-1084, (2011)

R-14

Influence of Powder Milling On Properties of Barium Strontium Titanate Particles and the Ferroelectric Ceramic-Polymer Composites

E. Pawlikowska[1], K. Gorziszewski[2], Y. Yashchyshyn[2], M. Szafran[1]

[1]Faculty of Chemistry, Warsaw University of Technology, Warsaw, Poland

[2]Institute of Radioelectronics, Warsaw University of Technology, Warsaw, Poland

e-mail: epawlikowska@ch.pw.edu.pl

Ceramic-polymer composites based on ferroelectric Barium Strontium Titanate (BST) have a correspondingly low dielectric constant allowing for effective tunability by changing the intensity of the polarization. The electrical behavior of BST is extremely dependent upon its material properties, including its stoichiometry and crystal structure. Ceramic powder obtained by the solid-phase synthesis requires the mechanical milling treatment. Its effect was tested as well as reducing the stress generated in the crystal lattice as a result of relaxation during the annealing BST powder. Use of a combination of ceramic powder with the polymer allows to obtain a tunable thin film having a thickness of between 0.2-1mm, and low loss tangent values by tape-cating method[1]. Additionally, obtained tapes are flexible and have high mechanical strength parameters(Fig.1).

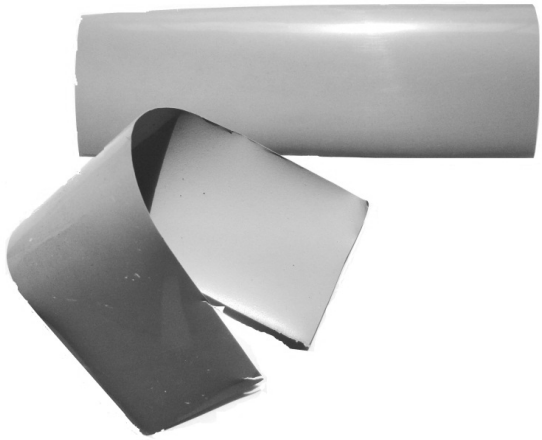

Fig.1 Flexible ceramic-polymer composite tape based on ferroelectric Barium Strontium Titanate.

Several methods were used for characterization ferrolectric BST and based on it ceramic-polymer composite: XRF for stoichiometry, XRD for structure, SEM for film thickness and characterizations of solid phase concentration gradient in the composite.

Acknowledgment

This work has been partially supported by the National Science Center of Poland (Grant No. 2011/01/B/ST05/06295) and by Warsaw University of Technology.

References

1. Y. Yashchyshyn, “Low-cost ferroelectric ceramic-polymer scan antenna”, International Microwave and Optoelectronics Conference, 20-23 September 2003, Foz do Igacu, Brazil, pp. 401-405
2. D. L. Huber, D. S. Hamilton and B. Barnet, Phys. Rev. B **16**, 4642 (1977)

R-15

Losses and Dispersion in Ceramic Matrix Composites

A. Naumenko, M. Lugovaya, E. Petrova, A. Rybyanets

Institute of Physics, Southern Federal University, Russia

e-mail: arybyanets@gmail.com

The multiphase ceramic composites are very complex objects for theoretical modelling NDT inspection, and ultrasonic measurements. Changes in chemical composition on the phase interfaces as well as microporosity appearance during co-firing of composite components can alter elastic, electric and mechanical properties of composites. Spatial dispersion can distort ultrasonic pulse characteristics and make ultrasonic measurements ambiguous [1]. Therefore, a comprehensive study of different composites structures with strong spatial dispersion and high losses (porous piezoceramics, composites ceramics/ceramics and ceramics/crystals) including finite difference 3D simulations, impedance spectroscopy characterization and ultrasonic measurements were carried out in this paper. The Wave 3000 Pro computer software package based on finite differences method was used for full time-domain solution of the 3D viscoelastic wave equations. Complex sets of elastic, dielectric, and piezoelectric parameters of the porous piezoceramics and ceramic matrix piezocomposites were determined by impedance spectroscopy method using Piezoelectric Resonance Analysis (PRAP) software [3]. This software uses a generalized form of Smits' method to determine material properties for any common resonance mode, and a generalized ratio method for the radial mode valid for all material Q_M's. By analyzing on each harmonic, complex material properties as a function of frequency can be determined.Microstructure of polished, chemically etched, and chipped surfaces of porous ceramics and piezocomposite samples was observed with optical and scanning electron microcopies. The simulation results were compared with the experimental data obtained by ultrasonic pulse-echo and through-transmit methods.

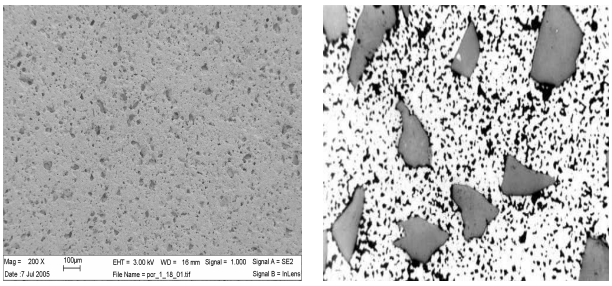

Fig.1 Optical and SEM micrographs of porous PZT piezoceramics (a,b) and PZT/α-Al2O3 composites (c,d) samples.

It was shown that pulse-echo measurements of frequency dependencies of elastic properties for dispersive and lossy ceramic composites are inaccurate and ambiguous. In its turn, piezoelectric resonance measurements (PRAP) give accurate and reproducible results that well agree with the results of 3D finite-difference simulations. Anomalies of sound velocities and attenuation near corresponding elastic percolation thresholds were found out. Microstructural and physical mechanisms of elastic, piezoelectric and dielectric losses and spatial dispersion in ceramic matrix piezocomposites were considered and discussed.

References

1. A.N. Rybyanets and A.A. Rybyanets, IEEE Trans. UFFC. **58**, 1757, (2011),

2. A.N. Rybyanets, A.A. Naumenko, N.A. Shvetsova. In.: " Nano- and Piezoelectric Technologies, Materials and Devices", Ivan A. Parinov Ed. Nova Science Publishers Inc., 2013. Chapter 1. – P. 275-308.

R-16

Porous PZT Films Prepared by PVP Assisted Sol-Gel Process

A. Sigov, K. Vorotilov, and D. Seregin

Moscow State Technical University of Radioengineering, Electronics and Automation, Russia

e-mail: sigov@mirea.ru

Sol-gel process of porous $PbZr_{0.48}Ti_{0.52}O_3$ film formation on $Pt/TiO_2/SiO_2/Si$ substrates is studied. Polyvinylpyrrolidone (PVP) is used as a porogen agent destroyed after annealing.

The films were prepared from PZT film-forming solution with 0 – 20 wt.% PVP (the average molecular weight of 29000) by spin on deposition. Each layer was dried after deposition at 170°C and 400°C, after deposition of each five layers the film was annealed for 20 min at 650°C. Maximum layers number is 30.

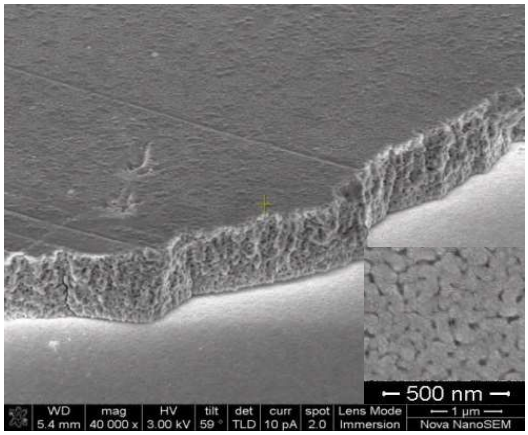

Figure 1. SEM image of PZT film (6.6 % PVP, 20 layers)

Ellipsometric data, dielectric hysteresis behavior, and the capacitance–voltage (CV) dependencies using mercury probe were obtained after deposition of each five layers. X-ray diffraction and microstructure were studied after formation of final film thickness.

Porous structure of the PZT film with the 6.6 % PVP is shown in Figure 1. Volume porosity reaches 33 % at 20 % PVP content. Grain size is decreased and voids are observed in the films structure at higher PVP content. An increase of annealing temperature (up to 750-800°C) leads to intensive shrinkage and formation of dense fine-grained structure.

Despite dramatic changes in the film structure, the value of remanent polarization practically does not depend on PVP content, but the hysteresis loop shape is changed in porous films. These loops have specific saturation region as a result of domain pinning by defects. At the same time, the dielectric constant reduces with increasing film porosity as a result of film density decrease. Other properties of the films with different thickness and PVP content are discussed as well.

R-17

Magnetodielectric Properties of $Bi_{1-x}La_xFeO_3$ Films

S.S. Aplesnin[1], A.A. Ostapenko[1], V.V. Kretinin[1], A.M. Panasevich[1,2], A.I. Galyas[2] and K.I. Yanushkevich[2]

[1]Siberian State Aerospace University, Krasnoyarsk, 660014 Russia

[2]GO NPTs Materials Science Center, National Academy of Sciences of Belarus, 220072 Minsk, Belarus

e-mail: apl@iph.krasn.ru

Discovery of high polarization, magnetization, piezoelectric coupling, magneto-electric and photovoltaic and exchange bias make $BiFeO_3$ one of the widely investigated materials. The ground state of $BiFeO_3$ can best be represented as cycloidal spiral with a period of approximately λ =62 nm[1]. The thin of films $La_xBi_{1-x}FeO_3$ is 160 nm and is equal to 2.5 λ. Small magnetization at the film surface leads to the domain walls as result of magnetostatic interaction. Under an external electric field the domain structure of an epitaxial film is reconstructed and lead to the ferroelectric switching. The influence of La ions substitution for Bi and action of the external electric field on the magnetodielectric effect of thin films were investigated. Real and imaginary parts of the permittivity were measured in the 90 K < T < 1000 K temperature range at frequencies of 1, 10 and 100 kHz in magnetic fields H=0.8 T and without of field for $La_xBi_{1-x}FeO_3$ films. Magnetocapacity has maximum at T=350 K and small drop at 400 K under external field 5 V/cm in the region of 300 K < T < 420 K (Fig.1). Thegrows of magnetocapacity is observed at frequency decreasing. Dielectric loss is increased in magnetic and decreased in electric fields particularly at low temperatures. The anomalies in the $\varepsilon(T)$ *и* $tg\delta$ temperature dependences are observed at high temperature and the origin of these anomalies is associated with magnetic phase transition in LaxBi1-xFeO3.

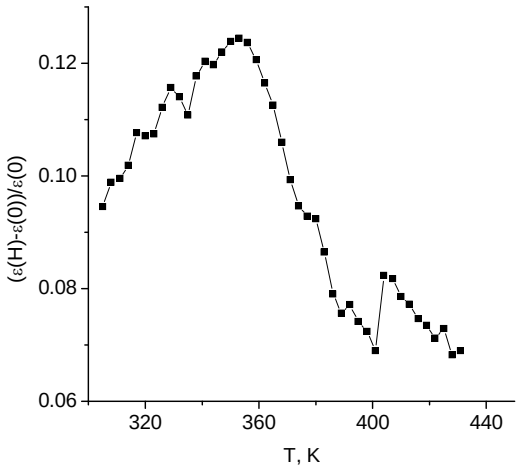

Fig.1 The magnetocapacitance Bi_{1-x} La_xFeO_3 for X=0.1 at a frequency $\omega=10^5$ Hz , H=0.8 T in bias voltage U=0.5 V as a function on temperature.

Reference

1. A.P. Pyatakov, A. K, Zvezdin , Phys. Usp. **55,** 557–581 (2012) .

R-18

Microwave Dielectric Measurements of Mn-Doped Perovskite-Type $SrTiO_3$ Nanopowders

D. Jablonskas[1], M. Ivanov[1], J. Banys[1], V. Trepakov[2,3], M. Makarova[2,4], A. Dejneka[2]

[1]Faculty of Physics, Vilnius University, Lithuania

[2]Institute of Physics AS CR, Czech Republic

[3]Ioffe Physico-Technical Institute RAS, Russia

[4]WPI-MANA NIMS, Japan

e-mail: maksim.ivanov@ff.vu.lt

The Mn-doped $SrTiO_3$ (STO) is in attention of material researchers for its intriguing polarization response, low-temperature dielectric relaxation, polar behavior and magnetoelctric multiglass properties in lightly Mn-doped STO [1]. There is technological interest in moderately doped STO:Mn as new magnetic, semiconducting, multiferroic and "spintronic" material [2]. Heavily Mn-doped STO deserved a special interest as one of the materials, with which Matthias formulated rule, is circumvented by showing that in ABO_3 perovskite magnetic B-site ions can be forced offcenter [3].

The aim of this work is to characterize the dielectric properties of STO:Mn nanopowders. The nanopowder form of the material allows to avoid the technological difficulties, which occur making bulk heavily Mn-doped STO. The sizes of particles of the powders are 10 – 80 nm. The method of production and structural analysis of STO:Mn are discussed in [4]. The dielectric measurements at room temperature in 100 MHz – 40 GHz frequency range of $SrTi_{1-x}Mn_xO_3$ (x = 0, 0.3, 0.4, 0.5) are shown in fig. 1. strengthening of charge relaxation-related dispersion with increase of Mn is observed. The analysis and further measurements will be presented.

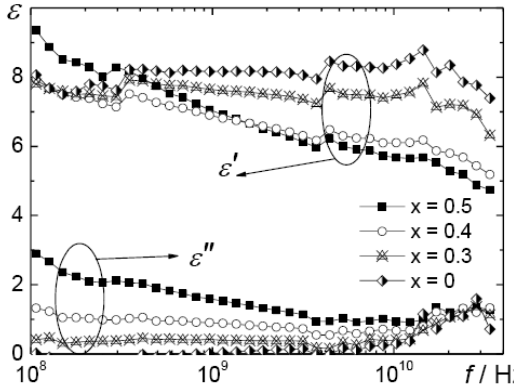

Fig.1 Frequency dependency of complex dielectric permittivity of $SrTi_{1-x}Mn_xO_3$ (x = 0, 0.3, 0.4, 0.5) at room temperature

References

1. V.A. Trepakov, M. Savinov, V. Železný, J. Pokorný, et. al, J. Phys. Conf. Ser. 93 (2007)
2. P. Galinetto, A. Casiraghi, M.C. Mozzati, C.B. Azzoni, et.al, Ferroelectrics 368 (2008)
3. J.M. Rondinelli, A.S. Eidelson, N.A. Spaldin, Phys. Rev. B 79 (2009)
4. V. Trepakov, M.Makarovaa, O. Stupakova, E.A. Tereshina, et.al., Mater. Chem. and Phys. 143 (2014)

R-19

Effects of Long Term Annealing on the Nanostructures Formed in CdI_2 Crystals

I. Bolesta[1], I. Karbovnyk[2], I. Rovetsky[3], S. Velgosh, I. Kityk, A.I. Popov[2]

[1]Department of Electronics, National University of Lviv, Ukraine

[3]Institute of Solid State Physics, University of Latvia, Latvia

e-mail: popov@ill.fr

Layered cadmium iodide (CdI_2) crystals [1] are known to be good scintillators, UV photochromic materials and efficient phosphors [2]. These crystals are highly anisotropic and exhibit ferroelectricity under certain conditions (for example, see [3]). Structural anisotropy also gives a motivation to study the mechanism of impurity introduction into the crystal lattice. It has been shown that upon crystal growth various nanocluster formations are likely to be created in CdI_2 [4]. These nanoclusters have influence on many physical properties, including optical absorption and luminescence [5]. However the reliable model of the light-cluster interaction in CdI_2 is still under development.

In this report the effect of aging (or long term annealing at room temperature) on the structure and optical properties of nanoclusters in cadmium iodide anisotropic crystals is reported. Modification of 3D topology of cleaved crystal surface and respective changes in luminescence from CdI2 crystalline samples due to aging are discussed

References

1. R. Bozorth, *J. Am. Chem. Soc.* **44**, 1922, 2232
2. S. Kawabata, H. Nakagawa, *Journal of Luminescence* **126**, 2007, 48.
3. I. Kityk, S. Pyroha, T. Mydlarz, J. Kasperczyk, M. Czerwiński, *Ferroelectrics* **205**, 1998, 107.

R-20

Cathodoluminescence Characterization of Polystyrene–$BaZrO_3$ Hybrid Composites

V.P. Savchyn[1], O.I. Aksimentyeva[1], Yu.Yu. Horbenko[1], I.Karbovnyk[1], V. Pankratov[2] and A.I. Popov[2]

[1]Ivan Franko National University of Lviv, Ukraine

[2]Institute of Solid State Physics, University of Latvia, Latvia

e-mail: popov@ill.fr

The luminescence properties and structure of hybrid composites based on suspension of polystyrene (PS) and nanocrystals of $BaZrO_3$ (BZO) ($d < 50$ nm) has been studied using cathodoluminescent spectroscopy and X-ray diffraction. It was found that for BZO-nanocrystals a strong cathodoluminescence (CL) is developed. For the BZO-PS composites a modification of CL spectra is observed: the low energy bands and a high energy band (near 4 eV) are appearance together with significant reduction of the CL intensity. The decrease of the lattice parameter a for BZO phase in the composite and the modification of CL spectra indicate a change in the structure of nanocrystals under the influence of polymer.

R-21

An Observation of Nano Sized Effect on EPR of Mn^{4+} and Cr^{3+} in $SrTiO_3$ Powders

A.G. Badalyan[1], D.V. Azamat[2], V.A. Trepakov[1,2], M. Makarova[1], J.Rosa[1], A. Dejneka[1] and L. Jastrabik[1]

[1]Ioffe Physical-Technical Institute, RAS, 194021, St. Petersburg, Russia

[2]Institute of Physics AS CR, 182 21, Prague 8, Czech Republic

e-mail: andrey.badalyan@mail.ioffe.ru

The studies of size effects on ferroelectric properties have great significance because of Curie temperature, electrical polarization, coercive field, switching time etc. depend on particle size or, generally, correlational length [1].

The method of electron paramagnetic resonance (EPR) has been applied to the study dimensional properties of $SrTiO_3$ fine powders which were doped by Mn^{4+} and Cr^{3+} ions. Previously, this method was used for research of $BaTiO_3$ and $PbTiO_3$ ultra fine powders, activated by manganese and chromium [2, 3].

The $SrTiO_3$:Mn:Cr powders of 100, 50, 20 nm have been studied. Doping the fine $SrTiO_3$ powders by manganese ions appears appropriate because manganese substitutes for Ti^{4+} without any charge compensation. Mn^{4+} ions on Ti^{4+} lattice sites were identified, with spin-Hamiltonian parameters (*g* factor and hyper fine structure constant *A*).

The broadening effect of linewidth has been observed. When the particle size decreases the linewidths increase and line amplitudes decrease accordingly. The broadening effect may be traced back to changes of the small parameter of fine structure *D* due to its dependence on the particle size of the individual nanocrystallite. The critical size of the particles, which can be carried out phase transition during 105K, is discussed.

References

1. S . Wada, T. Suzuki and T. Noma, Jpn. J. Appl. Phys. **34** (1995) 5368.
2. R. B ¨Ottcher, H.-C. Semmelhack, G. Voelkel, H.-J. Gloesel and E. Hartmann, Phys. Rev. B **62** (2000) 2085.
3. E. Erdem, R. Boettcher, H.-C. Semmelhack, H.-J. Gloesel, E. Hartmann, D. Hirsch. J. of Materials Science **38** (2003) 3211.

R-22

Phase Transitions in Li-Doped $KSc(MoO_4)_2$

W. Zapart[1], M.B. Zapart[1] , N.M. Nesterenko[2]

[1]Institute of Physics, Technical University, Czestochowa, Poland

[2]B.Verkin Institute for Low Temperature & Engineering of Ukrainian NASc, Kharkov, Ukraine

e-mail: wzapart@wip.pcz.pl

Ferroelastics belonging to the family of trigonal double molybdates are characterized by a two-dimensional structure [1] and at the high-temperature phase they have a common trigonal structure with the P-3m1 space group. These materials are of great interest because of the existence in them the sequences of ferroelastic phase transitions.

This paper presents the results of electron paramagnetic resonance (EPR) studies of structural phase transitions in case of isostructural replacement of K^+ ions by Li^+ ions in $KSc(MoO_4)_2$. Earlier microscopic observations in the polarized light have revealed the occurrence of three ferroelastic phase transitions in $K_{1-x}Li_xSc(MoO_4)_2$ crystals with a low lithium concentration ($x=0.05$) [2]. As the paramagnetic sonda in EPR investigations of $K_{0.95}Li_{0.05}Sc(MoO_4)_2$ the trace amounts of Cr^{3+} and Fe^{3+} were used, which occupy the positions of Sc^{3+}. The behaviour of the EPR spectra versus temperature confirms the existence of three ferroelastic phase transitions in this crystal. Temperature measurements of the positions of the split resonance lines show that the separation between the edge EPR lines can be described by a relation $(T_1-T)^{\beta}$ where the value of β is bigger than the one in pure $KSc(MoO_4)_2$.

References

1. R.F Klevtsova and P.V. Klevtsov, Kristallografiya **15**, 953 (1970)
2. W. Zapart, M.B. Zapart and N.M. Nesterenko, Ferroelectrics **462**, 1 (2014)

R-23

X-ray Diffraction Intensity Influenced by Transverse Electric Field in TGS

S. Tsuge, T. Kikuta, and T. Yamazaki

Graduate School of Science and Engineering, University of Toyama, Japan

e-mail: tkikuta@eng.u-toyama.ac.jp

Triglycine sulfate, abbreviated as TGS, is a ferroelectric with spontaneous polarization along the *b*-axis. The amount of the remanent polarization decreases by prolonged application of the electric field along the direction which is not parallel to the *b*-axis. Furthermore, the reduced value is maintained even if the transverse electric field has been removed [1]. The original properties will not be restored unless the sample is annealed above the phase transition temperature. Since the reduction process significantly depends on temperature [2], free electric charges flowing into the sample by the application of the transverse electric field seem to play an important role for the reduction process.

Because X-ray diffraction intensity includes information about positions of atoms in the unit cell of the sample crystal, a direction of the dipoles which quantify the polarization can be distinguished [3]. To get the reason why the remanent polarization decreases, the direction of the dipoles which are influenced by the transverse electric field has been investigated by X-ray diffraction. Three kinds of diffraction intensity under electric fields along the *b*-axis, which are an AC electric field, a positive and a negative DC electric fields, were observed before the application of the transverse electric field and after the remanent polarization becomes sufficiently small, respectively. The intensity under the AC electric field shows average one of that by positive domains and that by negative domains which are frequently switched. The intensity under the DC electric field shows one by positive or negative single domain which is oriented by the DC electric field. Table 1 shows an example of the observation. Two kinds of intensity under the DC electric field become same value when the remanent polarization is small. This implies that there are no mobile dipoles in the sample.

Table 1. X-ray diffraction intensity before application of transverse electric field and after prolonged application under different electric fields.

(k counts)

Electric Field	Before	Influenced
AC	132752	124438
Positive	123384	124003
Negative	141430	124795

References

1. K. Ćwikiel, B. Fugiel, M. Mierzwa, *J. Phys.: Condens. Matter* **12**, 5033-5041 (2000).
2. T. Kikuta, H. Nishizuka, T. Yamazaki, N. Nakatani, *Ferroelectrics* **336**, 91-100 (2006).
3. T. Kikuta, T. Yamazaki, N. Nakatani, *Ferroelectrics* **403**, 111-118 (2010).

R-24

Optical Studies and Birefringence of $K_{1-x}Rb_xSc(MoO_4)_2$

M.B. Zapart[1], W. Zapart[1], M. Maczka [2]

[1]Institute of Physics, Technical University of Czestochowa, Czestochowa, Poland

[2]Institute of Low Temperature and Structure Research, Polish Academy of Science, Wroclaw, Poland

e-mail: zapart@wip.pcz.pl

Mixed $K_{1-x}Rb_xSc(MoO_4)_2$ crystals belong to a family of the trigonal double molybdates, compounds which have attracted a great deal of interest in recent years because of their simple structure and ability to undergo ferroelastic phase transitions. In $KSc(MoO_4)_2$ three structural phase transitions leading to ferroelastic phases of monoclinic symmetry are observed [1,2]. For the low concentration of rubidium (x=0.03) the sequence of phase transitions resembles that revealed in pure $KSc(MoO_4)_2$ [3,4]. However for x=0.1 and 0.2 only one phase transition is observed down to the liquid nitrogen temperature [3,4]. Optical microscopic observation has revealed that the phase transition in mixed crystals is characterized by a change from uniaxial to biaxial upon cooling and appearance of ferroelastic domains.

The contribution presents results of the spontaneous birefringence measurements in the $K_{1-x}Rb_xSc(MoO_4)_2$ crystals using the Senarmont method. The temperature dependence of the birefringence Δn has been measured for the light propagation direction along the c-axis between 77 and 300 K. The disposition of optical indicatrix principal axes has been determined in the ferroelastic phases of all crystals under investigation. It has been shown that $\Delta n(T)$ is given by a relation $(Tc-T)^{\alpha}$ where the value of α changes with the concentration x. The last results are compared with the temperature dependence of the splitting of the EPR lines as found upon transition to the ferroelastic phase in these crystals [4].

References

1. A. I. Otko, N. M. Nesterenko and L. V. Povstyanyi, Phys. Stat. Sol. (a) **46**, 577 (1978)
2. W. Zapart and M. B. Zapart, Phys. Stat. Sol. (a) **121**, K43 (1990)
3. W. Zapart, M. B. Zapart, K. Maternicki, R. Kowalczyk, M. Maczka and A. Winiarski, Phase Transitions, **83**, 884 (2010)
4. W. Zapart, M. B. Zapart, R. Kowalczyk, K. Maternicki and M. Maczka, Ferroelectrics **418**, 164 (2011)

R-25

Optical Anisotropy and Domain Structure of Multiferroic Ni-Mn-Based Heusler Alloys

A.I. Ivanova[1], O.V. Gasanov,[1] E.I. Kaplunova[1], E.T. Kalimullina[2], A.B. Zalyotov[3]
R.M. Grechishkin[1]

[1]Tver State University, Russia

[2]Kotel'nikov Institute of Radio Engineering and Electronics of RAS, Russia

[3]Tver State Medical Academy, Russia

e-mail: alex.ivanova33@yandex.ru

A study is made of the optical anisotropy and magnetic domain structure of martensite twins of ferromagnetic shape-memory alloys (FSMA) on the base of Ni and Mn making use of polarized light microscopy in the visual range. Observations in the reflected polarized light turned out to be very convenient for studying the martensite twin structure of multiferroic materials [1]. In the present work we study the mechanisms of polarized light image formation by an example of some Ni-Mn-based FSMA. It is shown that polarization-optical method has a number of advantages for studying both the crystal twin structure and magnetic domain structure in comparison with electron microscopy or AFM.

Fig. 1 illustrates the dependence of the reflected light intensity on the angle of sample stage rotation. The measurements were made in a localized field of view separately for two adjacent martensite twins. It is seen that the optical contrast $C = (I_1 - I_2) /(I_1 + I_2)$ may be set to zero, be maximized or inverted simply by rotation of the sample on the microscope stage. It is also evident that the symmetry of this optical effect differs from that of the magnetooptic polar Kerr effect which is invariant to sample rotation. This feature opens the way of enhancing the conditions for both martensite and magnetic domain structure observations by the digital methods of differential polarized microscopy [2].

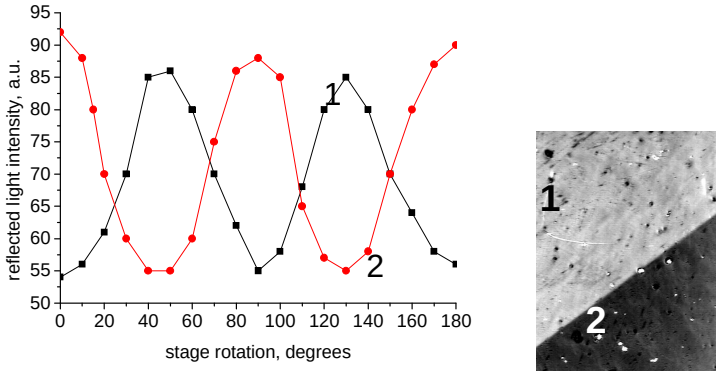

Fig.1. Dependence of the reflected light intensity for two adjacent martensite twins of $Ni_{2.16}Mn_{084}Ga$ alloy (micrograph at the right) on the angle of sample stage rotation in crossed polarizers.

References

1. L. Dorosinsky, B. Farber, M. Indenbom, et al. Ferroelectrics **111**, 321 (1990).
2. R.M. Grechishkin, O.V. Malyshkina and S.S. Soshin, Ferroelectrics, **222**, 215 (1999).

R-26

Dielectric Behavior of Monoclinic $Rb(H_{0.7}D_{0.3})_2PO_4$ Under Constant Hydrostatic Pressure

M. Fukunaga, M. Nomura, K. Tsukahara, M. Komukae

Department of Applied Physics, Tokyo University of Science, Japan

e-mail: fukunaga@rs.tus.ac.jp

Measurement of the dielectric constants of monoclinic $Rb(H_{0.7}D_{0.3})_2PO_4$ under various hydrostatic pressure was carried out at a frequency of 1 MHz. The temperature dependence of dielectric constant was measured in a temperature range covering the ferrielectric transition temperature T_C at various pressures below 0.45 GPa. The pressure derivative of the transition temperature dT_C/dp was estimated to be -22.3 ± 0.4 K/GPa. All dielectric constants at various pressures of $Rb(H_{0.7}D_{0.3})_2PO_4$ show a pronounced deviation from the Curie-Weiss law. The dielectric property of $Rb(H_{0.7}D_{0.3})_2PO_4$ is consistent with those of RbD_2PO_4 and CsH_2PO_4, and is explained by the quasi-one-dimensional nature[1-2]. The dielectric constant is given by the following the quasi-one-dimensional Ising model for the antiferroelectric case except the vicinity of the T_C; $\varepsilon=\varepsilon_\infty+A/(Te^{-\Gamma/T}-B)$ where Γ and B are related to the intrachain interaction energy of the nearest neighbor electric dipole moments and the interchain coupling energy as the long range interaction, respectively. The ratio $\xi=\Gamma/B$ represents the relative strength of one-dimensionality. The characteristic parameters Γ, B and ξ were estimated to be 977 K, 4.92 K and 199 at ambient pressure, respectively. The pressure derivative of characteristic parameters ξ, Γ and B can be obtained in the present study for $Rb(H_{0.7}D_{0.3})_2PO_4$. The values of $d\Gamma/dp$, dB/dp and $d\xi/dp$ near zero pressure were estimated to be -311 K/GPa, -0.4 K/GPa and -48 $(GPa)^{-1}$, respectively.

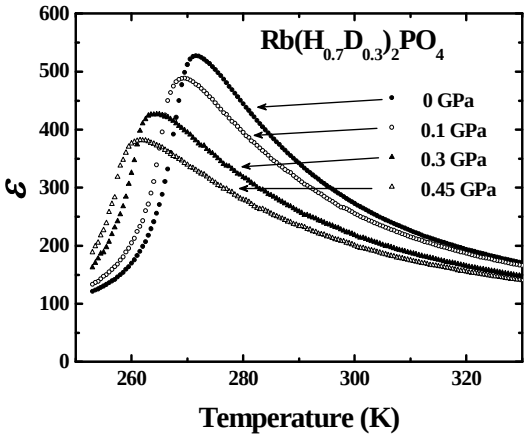

Figure. Temperature dependence of dielectric constant in $Rb(H_{0.7}D_{0.3})_2PO_4$ under various hydrostatic pressures.

References

1. R. Blinc, *et al.*, Phys. Rev. Lett. **43**, 231 (1979)
2. M. Komukae and Y. Makita, J. Phys. Soc. Jpn. **54**, 4359 (1985)

R-27

Thermal Diffusion and Heat Conductivity of $BiFeO_3$ and $Bi_{0.95}La_{0.05}FeO_3$ Multiferroics at High Temperatures

S.N. Kallaev[1], A.G. Bakmaev[1], L.A. Reznichenko[2], R.M. Ferzilaev[1]

[1]Institute of Physics, Dagestan Scientific Center, Russian Academy of Sciences, ul. 26 Bakinskikh komissarov 94, Makhachkala, 367003 Russia

[2]Research Institute of Physics, Southern Federal University, Rostov-on-Don, 344006Russi

e-mail: kallaev-s@rambler.ru

In this work, the thermal diffusion (phonon diffusion coefficients) and heat conductivity of $BiFeO_3$ and $Bi_{095}La_{0\ 05}FeO_3$ multiferroics are studied in a wide temperature range of 300—1200 K, including the regions of high-temperature phase transitions. As far as we know, the heat transport properties of these materials have not yet been studied.

The thermal diffusion and heat conductivity were studied using the laser flash method on an LFA-457 MicroFlash setup (NETZSCH, Germany).

The dominant mechanisms of phonon heat transfer in the region of ferroelectric and antiferromagnetic phase transitions have been revealed. The temperature dependence of the mean free path of phonons has been determined. The analysis of the results obtained in this work together with the structural and acoustic data indicates that local distortions of the crystal lattice, which are caused by the distortions of oxygen octahedra of FeO_6 and polar shifts of Bi^3+ and Fe^3+ ions from their initial positions, constitute the main mechanism of the scattering of phonons in $BiFeO_3$ and $Bi_{0.95}La_{0.05}FeO_3$ multiferroics. It has been found that doping with lanthanum, which is a rare-earth element, leads to a significant change in the temperature anomalies of the thermal diffusion and heat conductivity near phase transitions, namely, to the smearing of the ferroelectric transition T_c and the appearance of a minimum in the region of the antiferromagnetic transition T_N.

R-28

Local Structure and Oxidation State of 3*d* Impurities in Cubic (Ba,Sr)TiO_3

I.A. Sluchinskaya, A.I. Lebedev, V.F. Kozlovskii

Moscow State University, Moscow, Russia

e-mail: irinasluch@nm.ru

In recent years, doped ferroelectric perovskite oxides have attracted much attention due to the developing of a new type of solar energy converters based on the bulk photovoltaic effect. Recent theoretical studies have shown that the substitution of Ti at the *B* site of $PbTiO_3$ by vacancy-compensated divalent impurities with the d^8 electron configuration reduces the band gap to the levels optimal for effective energy conversion [1].

The aim of this work was the study of Fe-, Co- and Ni-doped $BaTiO_3$ using X-ray, XAFS and optical techniques in order to understand the mechanisms on the influence of 3*d* elements on the optical properties of $BaTiO_3$. To prevent the formation of the hexagonal phase of $BaTiO_3$ when doping with 3*d* elements, Ba atoms were partially substituted by Sr atoms.

Samples $Ba_{0.8}Sr_{0.2}TiO_3$ with the impurity concentration of 3% were prepared by solid-phase synthesis at 1500°C and additionally annealed at 1100°C. Since the impurities can enter both the *A* and *B* sites of the perovskite structure and stay in them in different oxidation states [2], XAFS spectroscopy was used to determine their local structure and oxidation state. XAFS spectra were measured at the KMC-2 station at the BESSY synchrotron radiation source at the *K* edges of Fe, Co and Ni in the fluorescence mode at 300 K.

All the samples had the cubic perovskite structure at 300 K. Analysis of XANES spectra showed that Fe and Co impurities in $Ba_{0.8}Sr_{0.2}TiO_3$ are in the 3+ oxidation state. The Ni impurity in $Ba_{0.8}Sr_{0.2}TiO_3$ is in the oxidation state intermediate between 2+ and 3+. To determine the local structure of impurities, EXAFS spectra were analyzed. The best agreement between the experimental and calculated spectra was obtained in the model in which the impurity atoms form complexes with oxygen vacancies and are shifted from the Ti sites. The parameters of the local structure were determined in this work. Optical studies showed that the doping of $Ba_{0.8}Sr_{0.2}TiO_3$ samples with 3*d* impurities improves the overlap of their absorption spectra and the spectrum of solar radiation.

Acknowledgment

This work was supported by RFBR grant № 13-02-00724.

References

1. W. Bennett, I. Grinberg, A.M. Rappe. J. Am. Chem. Soc. **130**, 17409 (2008).
2. A.I. Lebedev, I.A. Sluchinskaya, A. Erko, V.F. Kozlovskii. JETP Lett. **89**, 457 (2009).

R-29

Photoelectric Current and Dielectric Properties of Barium-Strontium Niobate Ceramics under UV and Visible Irradiation

K. Bormanis[1], A.I. Burkhanov[2], L.T. Nhan[3], S.V. Mednikov[3], and M. Antonova[1]

[1]Institute of Solid State Physics, University of Latvia, Riga, LV-1063, Latvia

[2]Volgograd State Architectural and Engineering University, Volgograd, Russia

[3]Volgograd State Technical University, Volgograd, Russia

e-mail: bormanis@cfi.lu.lv

The study is focused on the photocurrent kinetics and dielectric response to infra-low frequencies in $Sr_{0.75}Ba_{0.25}Nb_2O_6$ (SBN-75) relaxor ceramics under visible and shortwave radiation in the vicinity of the broad phase transition. The compound, either in ceramic or single crystal form has a heterogeneous structure containing polar and nonpolar phases coexisting over a wide range of temperature determining its high sensitivity to external agitations. An amorphous phase might also be present on grain boundaries in ceramics determining a difference in reaction to light between ceramics and single crystals.

Since there is a number of processes contributing to photocurrent (pyroelectric current, formation of space charge, anomalous photovoltaic current, and other), the ratio of $\Delta J = (J_{max} - J_{st})/J_{max}$ (where J_{max} is the maximum value of the photocurrent and J_{st} – the stationary value upon the end of the transition about 50—60 s after a rapid drop) is chosen in the present study to assess the behaviour of the photocurrent and the different contributions over the range of the broad phase transition in SBN-75 ceramics.

The photocurrent as a function of time excited by UV (400 nm) and visible (white) along with the dependence of ΔJ on temperature – $\Delta J(T)$, are examined. Kinetics of the photocurrent in ceramics is found to be similar to what is observed in crystal (particularly at UV irradiation) the $\Delta J(T)$ deviating from a monotonous pattern. The maximum of the $\Delta J(T)$ curve shifts to a considerably lower temperature under UV.

Results of the study of the kinetics of photocurrent and the infra-low frequency dielectric response at different temperatures are discussed as the effects of the defected structure of ceramics and non-equilibrium carriers on relaxation of polarisation in the range of the broad phase transition.

R-30

Preparation and Electric Properties of Barium Zirconium Titanate Ceramics

B. Garbarz-Glos[1], W. Bąk[2], M. Antonova[3], A. Budziak[4], K. Bormanis[3], C. Kajtoch[1]

[1]Institute of Technology, Pedagogical University of Cracow, Poland

[2]Institute of Physics, Pedagogical University of Cracow, Poland

[3]Institute of Solid State Physics, University of Latvia, Latvia

[4]The H.Niewodniczanski Institute of Nuclear Physics PAN, Cracow, Poland

e-mail: maija@cfi.lu.lv

Barium titanate is a well-known, intensively studied and technologically important ferroelectric material with a perovskite structure. Barium zirconium titanate - has attracted considerable attention both as bulk ceramics and thin films, due to its potential applications for various devices in particular as piezoelectric transducers, tunable filters, phase shifters, terrestrial and satellite communications (operating in the microwave frequency range), the GPS system and radiolocation. Substitution of Ti^{4+} with Zr^{4+} in $BaTiO_3$ exhibits an interesting behavior in the dielectric study. All the three phase transitions corresponding to pure $BaTiO_3$ are merged or pinched into single phase transition depending on the content of zirconium. Therefore, in this study the structure and dielectric properties of pure barium titanate and selected compositions barium zirconate titanate ceramics of were investigated. These ceramics were prepared by solid-state reaction from oxides and carbonates using the conventional method. The structure and morphology of sintered samples were characterised by X-ray diffraction (XRD) and scanning electron microscopy (SEM). The dielectric measurements, in the frequency range between 20 Hz and 1 MHz, were performed by means of QUATRO KRIO 4.0 temperature system together with precise LCR Agilent 4284A meter, BDS 1100 cryostat and WINData 5.62 Novocontrol software. The data were taken at stabilized temperature points within the range from 500 K to 140 K with 5 K step. The application of dielectric spectroscopy made possible to determine independently both real and imaginary parts of the response function of various excitations related to polarization in solids in particular the study of quantitatively ferroelectric dispersion.

R-31

Characterization of Ferroelectric Ceramic-Polymer Composites in Sub-Terahertz Frequency Range

K. Godziszewski[1], Y. Yashchyshyn[1], E. Pawlikowska[2], M. Szafran[2]

[1]Institute of Radioelectronics, Warsaw University of Technology, Poland

[2]Faculty of Chemistry, Warsaw University of Technology, Poland

e-mail: K.Godziszewski@ire.pw.edu.pl

Ferroelectric ceramic-polymer composites are emerging materials that can be used to design tunable and flexible electronic devices operating at sub-terahertz frequency range. However, to be able to use developed materials their electromagnetic properties have to be known. For this purpose appropriate quasi-optical measurement setup has been created. It is based on Vector Network Analyzer with six pairs of Frequency Extenders. This set is completed by horn antennas and Teflon lenses used to focus the beam of electromagnetic radiation. The setup allows to measure complex permittivity of materials in the frequency range up to 500 GHz. Competitive method – Time Domain Spectroscopy (TDS) widely used in terahertz and sub-THz frequencies does not enable to obtain accurate results below 300 GHz due to low dynamic range. The proposed measurement setup and methods of extraction of electromagnetic properties do not have this limitation [1].

The research team from Institute of Radioelectronics and Faculty of Chemistry, Warsaw University of Technology is working on developing new ferroelectric composites for sub-THz applications [2]. The composites are consisted of barium strontium titanate (BST) and appropriate polymeric binder. Many different samples of developed materials were fabricated and characterized. Measurement results showed that it is possible to obtain flexible, high tunable and low loss materials that can be an alternative to other commonly used tunable materials.

References

1. K. Godziszewski, Y. Yashchyshyn, E. Pawlikowska, E. Bobryk and M. Szafran, Proc. of European Conference on Antennas and Propagation, 3857 (2013)
2. Y. Yashchyshyn, J. Modelski, K. Godziszewski, P. Bajurko, E. Pawlikowska, B. Bogdanska, E. Bobryk and M. Szafran, Proc. of Asia-Pacific Microwave Conference, 206 (2013)

R-32

Electrical Characterization of Fe Doped $BaTiO_3$ Ceramic by Impedance Spectroscopy

D. Sitko[1], W. Bąk[1], B. Garbarz-Glos[2], M. Livinsh[3], I. Smeltere[3], C. Kajtoch[2]

[1]Institute of Physics, Pedagogical University of Cracow, Poland

[2]Institute of Technology, Pedagogical University of Cracow, Poland

[3]Institute of Solid State Physics, University of Latvia, Latvia

e-mail: mlivins@cfi.lu.lv

The ABO_3-type compounds with perovskite structure are one of the most interesting group of materials. Among them, the titanates are of great interest from the point of view of fundamental research as well as regarding their possible applications. Barium titanate $BaTiO_3$, (BT) was the first developed piezoelectric ceramic material and even now due to its excellent ferroelectric properties and the high electric permittivity at room temperature it is still widely used as capacitors, thermistors, chemical sensors, and piezoelectric devices.

The electric behavior of the Fe-doped and undoped $BaTiO_3$ was investigated as a function of frequency and temperature. The ceramics were prepared by solid state reaction. Scanning electron microscopy (SEM) Hitachi S4700 with a field emission and a Noran Vantage EDS system was used to observe the microstructure of the polycrystalline sample surface. The performed EDS investigations revealed that the all investigated specimens were perfectly sintered. They contained a little glassy phase and their grains were well shaped. The impedance measurements were carried out in the temperature range from 150K to 600K, and in the frequency range from 0.1Hz to 10MHz. All the electric measurements of the samples were performed using an Alfa - AN modular measurement system with a temperature control system Quatro Krio 4.0. Based on these parameters the electrical properties of the grains and grains boundaries were described. The grain and grain boundaries relaxation frequencies were shifted to higher frequency with increasing temperature. Bulk resistance of ceramics and the thermal activation energies were determined.

R-33

AC Impedance Spectroscopy Study of Barium Titanate Based Electroceramics

B. Garbarz-Glos

Institute of Technology, Pedagogical University of Cracow, Poland

e-mail: barbaraglos@gmail.com

Ferroelectric ceramic materials belonging to the vast family of perovskite-type structure, are characterized by the extreme values of physical parameters sensitive to external factors (temperature, pressure, electric field strength) and the conditions of preparation. The correlation between the chemical composition of the solution and its crystal structure, and the domain structure and electrophysical properties has a significant impact on the optimization of the properties of ferroelectric ceramics. Not without significance is the fact that its electrical properties can be controlled within a wide range by means of various elemental additions, what results in enhanced control over dielectric characteristics. These characteristics depend on the type of the substitution, isovalent or heterovalent ions and its location in the crystal sublattice: for Ba (A-site) or for Ti (B-site). Ferroelectric ceramics based on barium titanate were prepared by solid-phase reaction of simple oxides and carbonates using the conventional ceramic method (CMO). This method is considered to be a very economical and therefore it is constantly modified. Phase composition and crystal structure of the samples was studied by X-ray diffraction. The experiments was performed using X-ray diffractometer with X'Pert PRO (Pananalytical) with CuKα radiation and a graphite monochromator, at various temperatures in the temperature range between 140K and 500K. Impedance spectroscopy (IS) method was used for probing the relaxation processes during the charge transport in the prepared electroceramics. The equivalent circuits were applied as a series of lumped elements (i.e. resistance and capacitance) corresponding to the grain boundaries or the within grains. IS measurements were performed by means of a Alpha-AN modular measurement system together with cryogenic temperature control system - Quatro Cryosystem and WinDETA Novocontrol software, at frequency varying from 0.1 Hz to 10 MHz and at temperature range from 140 K to 600 K.

R-34

Study of Dielectric Properties of Europium Doped Barium Titanate Ceramics by Impedance Spectroscopy

D. Sitko[1], W. Bąk[1], B. Garbarz-Glos[2], M. Antonova[3] and J. Suchanicz[2]

[1]Institute of Physics, Pedagogical University of Cracow, Poland

[2]Institute of Technology, Pedagogical University of Cracow, Poland

[3]Institute of Solid State Physics, University of Latvia

e-mail: sitko.dorota@gmail.com

A small change of the dopant concentration can significantly change the microstructure, thus influencing electrical properties of the specimens. In this work the differences between the physical properties of barium titanate ($BaTiO_3$) and the $BaTiO_3$+ 0.1wt.% Eu_2O_3 were identified. The $BaTiO_3$ and $BaTiO_3$+ 0.1wt.% Eu_2O_3 ceramics were prepared by a two-stage hot-pressing technology in the Institute of Solid State Physics at the University of Latvia. The structural studies were carried out by an X-ray diffraction technique. The dielectric behaviour were investigated in a wide range of temperatures and frequencies. The measurements of dielectric permittivity were performed during cooling cycle. Investigations of dielectric properties were performed by means of a Alpha-AN modular measurement system together with cryogenic temperature control system - Quatro Cryosystem and WinDETA Novocontrol software in the frequency range from 0.1Hz to 10MHz and at temperature ranging from 150K to 600K. The results of measurements show frequency and temperature dependencies. The conductivity processes were determined by the Arrhenius behaviour of relaxation time (τ) and a possible cause of the processes was discussed. The dielectric data suggest that the incorporation of europium ions has a significant influence on the dielectric characteristic of the investigated material.

References

1. M. E. Lines and A. M. Glass, Principles and applications of ferroelectrics and related materials, Oxford University Press, New York, (2001).
2. Y. Tsur, T. D. Dunbar and C. A. Randall, Journal of Electroceramics, **7**, 25 (2001).

R-35

Heat Losses and Thermal Imaging of Piezoelectric Elements

S.E. Ilyashenko[1], O.V. Malyshkina[2], A.I. Ivanova[2], A.Yu. Eliseev[2], A.V. Bodrov[2], R.M. Grechishkin[2]

[1]Tver State Technical University, Russia

[2]Tver State University, Russia

e-mail: SvIlyashenko@yandex.ru

Piezoelectric actuators are finding their use in a great variety of devices. In order to obtain maximum displacement of the actuator an applied electric field of the order of 1 to 3 kV/mm and working frequency up to several kHz is usually required. Such conditions lead to large heat generation affecting the reliability and limiting the applications [1-2]. In the present work we study the heat generation produced by typical piezoceramic elements including multilayer thin-film actuators, piezoelectric macro-fiber composites (MFC) and experimental samples with varying porosity. Different from the previous studies in the present work we complemented the measurements of the sample temperature with direct observation of its distribution over the sample surface (Fig.1). For the latter purpose a thermovision infrared videocamera (FLIR Research IR MAX) was exploited. In addition these measurements were accompanied by the observation of dielectric hysteresis loops evolutions with the aid of Sawyer-Tower scheme.

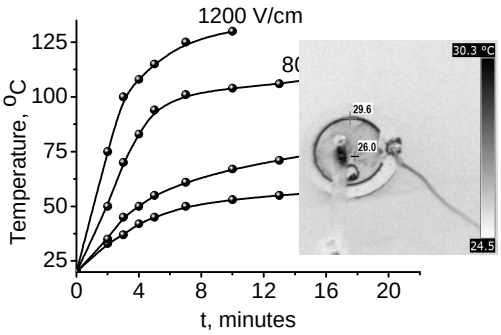

Fig.1. Effect of the AC electric field on the heating and temperature distribution of the piezoceramic PZT disk sample

The results of the study show that typically the main contribution to the heat losses in piezoceramics is that associated with the domain wall motion [3]. Among the main sources of nonuniform heating is the piezoceramics porosity.

References

1. K. Uchino, IEEE Trans. Ultrasonics, Ferroelectrics and Freq. Control, **48**, 307 (2001).
2. J.A. VanGordon, S.D. Kovaleski, P. Norgard, B.B. Gall, Rev. Sci. Instr. **85**, 023101 (2014).
3. K.H. Hardtl, Ceram. Intern. **8**, 121 (1982).

R-36

Interpretation of the Electrocaloric Effect in NBT-ST-PT Solid Solutions

M. Dunce[1], E. Birks[1], J. Peräntie[2], J. Hagberg[2], M. Antonova[1], A. Sternberg[1]

[1]Institute of Solid State Physics, University of Latvia, Latvia

[2]Microelectronics and Material Physics Laboratories, University of Oulu, Finland

e-mail: marija.dunce@cfi.lu.lv

The relationship between polarization and electrocaloric effect is analysed in $0.4Na_{1/2}Bi_{1/2}TiO_3$-$(0.6-x)SrTiO_3$-$xPbTiO_3$ (NBT-ST-PT) solid solutions. Earlier a wide stability range of the relaxor state depending on $PbTiO_3$ concentration was found in these solid solutions. The pronounced electrocaloric effect at high concentrations of $PbTiO_3$, as well as extremely low values of the electrocaloric effect at low concentrations of $PbTiO_3$ were observed, which does not correspond to the variation of polarization depending on $PbTiO_3$ concentration. The measured values of the electrocaloric effect do not correspond to the values, calculated from frequently used thermodynamic equations. It is shown that, in the relaxor state, the observed temperature change of the electrocaloric effect as a function of polarization $\Delta T(P)$ and the measured values can not be explained by reorientation of polar nanoregions, and the role of the surrounding media in the physical properties should be reconsidered. In the ferroelectric state $\Delta T(P)$ has rather unique dependence independently of temperature, indicating that the measured polarization is solely responsible for the observed electrocaloric effect.

R-37

Polarization Reversal and Domain Kinetics in MgO Doped Congruent and Stoichiometric Lithium Tantalate Crystals

A. Akhmatkhanov[1,2], V. Shur[1,2], M. Chuvakova[1], I. Baturin[1,2]

[1]Ferroelectrics Laboratory, Institute of Natural Science, Ural Federal University, Russia

[2]Labfer Ltd., Russia

e-mail: Andrey.Akhmatkhanov@urfu.ru

The domain kinetics was studied during polarization reversal in 1 mol.% MgO doped stoichiometric lithium tantalate (MgOSLT) and 8 mol.% MgO doped congruent lithium tantalate (MgOCLT) single crystals. These representatives of lithium tantalate family are the most promising candidates for high-power second harmonic generation devices.

All samples were z-cut and optical grade polished. The sample's dimensions were 10x15x1 mm. The liquid (saturated aqueous solution of LiCl) and metal (chromium) electrodes with diameter 2-3 mm were used. The experimental setup allowed to apply the external field pulse of arbitrary shape with simultaneous *in situ* recording of the domain kinetics and the switching current.

The hexagonal isolated domains with Y oriented domain walls appeared in MgOSLT in contrast to triangular domains with X oriented walls in MgOCLT [1]. The analysis of the switching current data by modified Kolmogorov-Avrami approach [2] based on the visualization of domain kinetics has allowed to reveal the main stages of domain structures evolution and to extract the parameters of domain kinetics. The dependence of the coercive field on the field ramp rate for polarization reversal by triangular field pulses demonstrated the power-law growth with factor about 0.18 for both crystals. The limiting lowest value of coercive field for quasi-static switching (for dE_{ex}/dt approaching to zero) is equal to 1.2 kV/mm for MgOCLT and 0.15 kV/mm for MgOSLT.

The equipment of the Ural Center for Shared Use “Modern Nanotechnology”, Institute of Natural Sciences, Ural Federal University has been used. The research was made possible in part by RFBR and the Government of Sverdlovsk region (Grant 13-02-96041-r-Ural-a), by RFBR (Grants 13-02-01391-a, 14-02-01160-a) and with the financial support of young scientists in terms of Ural Federal University development program.

References

1. V.Y. Shur, A.R. Akhmatkhanov, D.S. Chezganov, A.I. Lobov, I.S. Baturin, and M.M. Smirnov, Appl. Phys. Lett. **103**, 242903 (2013).
2. V. Shur, E. Rumyantsev, and S. Makarov, J. Appl. Phys. **84**, 445 (1998).

R-38

Time-Dependent Conductivity and Dielectric Permittivity in Lithium Niobate Crystals with Charged Domain Walls

A. Akhmatkhanov[1,2], V. Shur[1,2], A. Esin[1], D. Chezganov[1], I. Baturin[1,2]

[1]Ferroelectrics Laboratory, Institute of Natural Science, Ural Federal University, Russia

[2]Labfer Ltd., Russia

e-mail: Andrey.Akhmatkhanov@urfu.ru

We present the experimental study of time dependence of the abnormal conduction current appeared during polarization reversal in stoichiometric and MgO doped lithium niobate single crystals with charged domain walls in temperature range from 120 to 250°C.

Recently, much attention is given to study of the conductivity along the charged domain walls (CDW) in thin film multiferroics and ferroelectrics due to possible applications in memory storage devices [1-3]. The conductivity increase and decrease have been studied by partial polarization reversal by high field (creation of multi-domain state with CDW) and subsequent immediate measurement of the conduction current in low field using the setup equipped with software-controlled relays.

It was shown that the arising of abnormally high conduction current correlates with appearance of the through CDW and its maximal value is of 4–5 orders of magnitude higher than in initial single domain state. Two stages of current changes have been revealed: increase and subsequent slower decrease. The analysis of the temperature dependence of the time constants for conduction current increase and decrease allowed to extract the activation energy 1.1 eV [4]. The strong increase (above 100 times) of the low-frequency dielectric permittivity has been revealed in the crystals with CDW. The obtained effects have been attributed to bulk screening of the depolarization field produced by bound charges.

The equipment of the Ural Center for Shared Use “Modern Nanotechnology”, Institute of Natural Sciences, Ural Federal University has been used. The research was made possible in part by RFBR and the Government of Sverdlovsk region (Grant 13-02-96041-r-Ural-a), by RFBR (Grants 13-02-01391-a, 14-02-01160-a) and with the financial support of young scientists in terms of Ural Federal University development program.

References

1. J. Seidel, L.W. Martin, Q. He et al., Nature Materials **8,** 229 (2009).
2. P. Maksymovych et al., Nano Letters **12**, 209 (2012).
3. H. Ishizuki, I. Shoji and T. Taira, Appl. Phys. Lett. **82**, 4062 (2003).
4. V.Y. Shur, I.S. Baturin, A.R. Akhmatkhanov, D.S. Chezganov, and A.A. Esin, Appl. Phys. Lett. **103**, 102905 (2013).

R-39

Relaxor Behavior of the Surface Layer of $BaTiO_3$ Crystals, Grown by Remeika Nethod

E. Dul'kin, M. Roth

Department of Applied Physics, The Hebrew University of Jerusalem, Israel

e-mail: evgeniy.dulkin@mail.huji.ac.il

Remeika method provides the $BaTiO_3$ crystals grow over a very wide temperature interval (from 1180 to 900ºC). As temperature decreases the KF flux viscosity changes and the impurities concentration varies in the crystals volume so, that in the surface layer the K ions concentration is 5-8 times greater than in the bulk [1]. While $Ba_{1-x}K_{x/2}La_{x/2}TiO_3$ compound is well-known to be a relaxor [2], one could expect the presence of relaxor features in the surface layer of $BaTiO_3$ crystals, grown by Remeika method.

Earlier such the $BaTiO_3$ crystals were scrupulously studied using the dielectric and acoustic emission (AE) methods [3]. It was established that the Curie temperature of the surface layer (T_c^s) occurs on some degrees below than the Curie temperature of the bulk (T_c^b). In the present work the surface layer of $BaTiO_3$ crystals are studied in dependence on frequency.

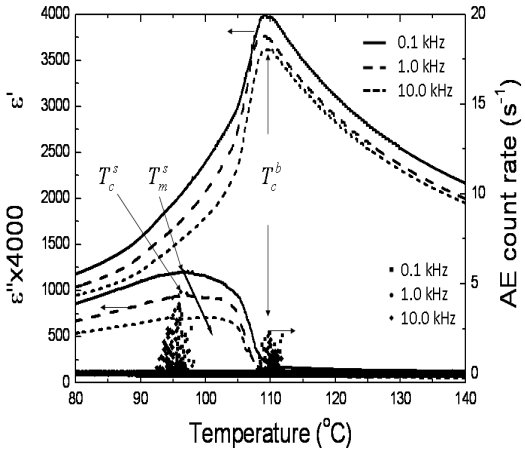

Fig. 1 The dependences of both ε' and ε'' as well as AE count rate of both surface T_c^s and bulk T_c^b of $BaTiO_3$ crystals, grown by Remeika method.

It is established, that the structural phase transition in T_c^s, detected by AE, occurs on 13ºC below in comparing with T_c^b and independent on frequency. In contrast, the maximum of imaginary part ε'' of dielectric permittivity of the surface layer T_m^s slightly shifts to higher temperature as frequency increases. Thus, the surface layer of $BaTiO_3$ crystals, grown by Remeika method, demonstrates the relaxor behavior.

References

1. A. Yu. Kudzin, E. P. Guenok, Yu. V. Zabara, Sov. Phys. Journal **16**, 533 (1973)
2. J. Ravez and A. Simon, Solid State Sciences **2**, 525 (2000)
3. E. Dul'kin, Ferroelectrics Letters **20**, 157 (1996)

R-40

Critical Slowing Down and Elastic Anomaly in Relaxor-Based Ferroelectric PMN-53PT Crystals Proved by Broadband Brillouin Scattering

M.A. Helal and S. Kojima

Graduate School of Pure and Applied Sciences, University of Tsukuba, Tsukuba, Ibaraki 305-8573, Japan

e-mail:kojima@ims.tsukuba.ac.jp

Dynamical properties of $PbTiO_3$ rich relaxors were studied by high resolution broadband Brillouin scattering technique. The temperature dependence of quasielastic central peak (CP) of relaxor ferroelectric $0.47Pb(Mg_{1/3}Nb_{2/3})O_3–0.53PbTiO_3$ (PMN-53PT) crystals have been measured over a wide temperature range of 25-500ºC. The temperature evolution of CP in both VV and VH scattering geometries are shown in Figs.1 and 2. We observed that below 350ºC, both the components of the CP become narrower significantly indicating marked slowing down of the dynamics of the relevant polarization fluctuation. The Debye-relaxation time (τ_d) estimated from the CP with comparable orders of magnitude indicates the dynamical slowing down (DSD) near the Curie temperature (T_c). The quantitative analysis of the DSD with Vogel-Fulcher law gives us the reasonable values of τ_0, U and T_{VF} in comparison with other relaxor and relaxor-based ferroelectrics [1].Further using the empirical equation of stretched slowing down given by S.Kojima *et.al.* [2] with stretched index $\beta = 1.0$, critical slowing down in the vicinity of T_c is clearly observed. These finding strongly suggests that the physical origin of the observed CP is polar nanoregions (PNRs).It is also observed that CP appears mainly in the VH scattering geometry due to the spectral selection rule.

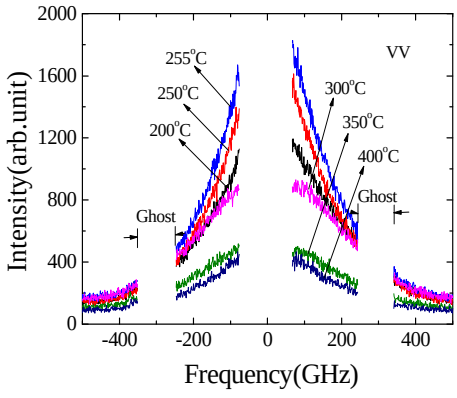

Fig.1. Polarized (VV) Brillouins cattering spectra of a PMN-53PT single crystal

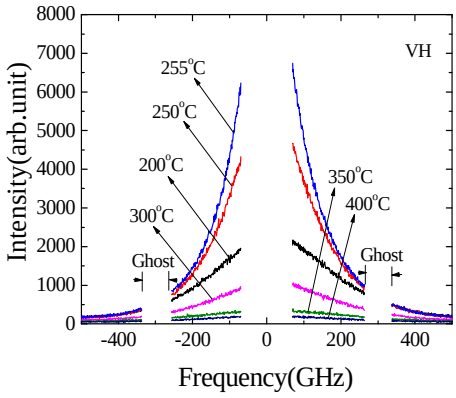

Fig.2. Depolarized (VH) Brillouin scattering spectra of a PMN-53PT single crystal.

References

1. Y.Nakata*et al.*, Appl.Phys.Lett. **89**, 022903 (2006).
2. S.Kojima *et al.*, Ferroelectrics **405**, 32(2010).

R-41

The Pyroelectric Properties of Calcium Barium Niobate Crystals of Different Composition

O. Malyshkina[1], V. Lisitsin[1], J. Dec[2], T. Lukasiewicz[3]

[1]Tver State University, Tver, Russia

[2]University of Silesia, Institute of Materials Science, Katowice

[3]Institute of Electronic Materials Technology, Warsaw

e-mail: Olga.Malyskina@mail.ru

The calcium-barium niobate $Ca_xBa_{1-x}Nb_2O_6$ (CBN) crystals are allied to strontium barium niobate $Sr_xBa_{1-x}Nb_2O_6$ (SBN). In contrast to SBN crystals, which may be grown in a wide range of *x*, the CBN materials exist in a crystalline form in a rather narrow interval of $0.2 < x < 0.4$ [1]. In the present work we studied the pyroelectric properties of the Czochralski grown single crystals of CBN with nominal concentrations of calcium in the solution 28% (CBN28), 30% (CBN30) and 32% (CBN32). The measurements of pyroelectric response were carried out in a broad temperature range using a dynamic method (Fig. 1) (the heat flux modulation was 10 Hz).

It is found, that above of the maximum of the pyroelectric current and only in the vicinity of the negatively charged surface of the poled samples of CBN32 and CBN30, a change in the direction of the polarization takes place. After cooling from the paraelectric phase a system of antiparallel domains arises in the crystals of CBN30 and CBN32. Very similar effect has hitherto been observed in SBN61 crystals [2]. The occurrence of the surface depolarization layer is confirmed by the fact that the pyroelectric current maximum temperature appears below the maximum of the dielectric permittivity of these materials (~ 9 K for CBN32 and CBN30; and ~ 75 K for CBN28). After cooling the CBN28 crystal becomes completely depolarized.

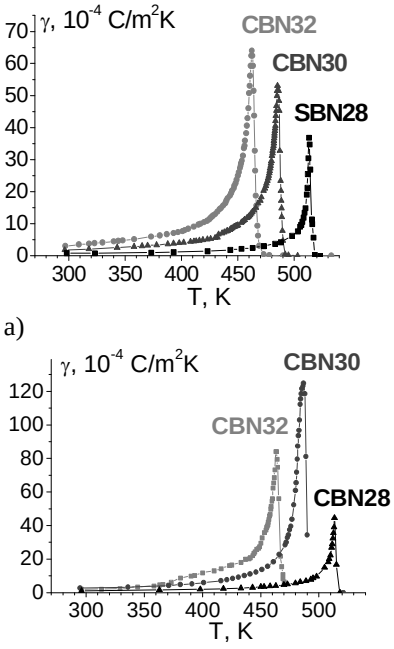

Fig.1 Temperature dependence of the pyroelectric coefficient for CBN crystals with various Ca concentration. The side corresponding to the positive (a) and negative (b) ends of the polarization vector was heated.

References

1. M. Esser, M. Burianek, D. Klimm, M. Muhlberg, J. Crystal Growth. **240**, 1 (2002).
2. O.V. Malyshkina, A.A. Movchikova, Phys. of the Solid State. **51**, 1381 (2009).

R-42

Conductivity Investigations of PMT-PT Single Crystals

E. Palaimiene[1], J. Macutkevic[1], A. Kania[2], J. Banys[1]

[1]Vilnius University, Faculty of physics, Saulėtekio av. 9, III b., LT-10222 Vilnius, Lithuania

[2]A. Chelkowski Institute of Physics, University of Silesia, Uniwersytecka 4, 40-007 Katowice, Poland

e-mail: edita.palaimiene@ff.vu.lt

The (1-x)$PbMg_{1/3}Ta_{2/3}O_3$ – $xPbTiO_3$ ((1-x)PMT-xPT or PMT-PT) single crystals were grown of the perovskite structure by the flux method. The nature of the phase transition in these crystals is highly dependent on the composition. With the increase in the Ti content the dielectric anomaly gradually changes from the typical relaxor behaviour to the normal ferroelectric phase transition and moves to the higher temperatures [1].

In this work we present broadband dielectric spectroscopy results of 0.9PMT-0.1PT single crystals. Dielectric measurements were performed in wide temperature region (25 K – 800 K) at 20 Hz – 1 GHz frequencies. We will discuss results in terms of conductivity, and electrical modulus (Fig.1). At high temperatures (above 650 K) the electrical transport is dominated by two conduction mechanisms, which are most probably caused by oxygen vacancies diffusion in the material. The relaxor related dielectric anomaly (which is observed below 650 K in our frequency range) will be also discussed in the presentation.

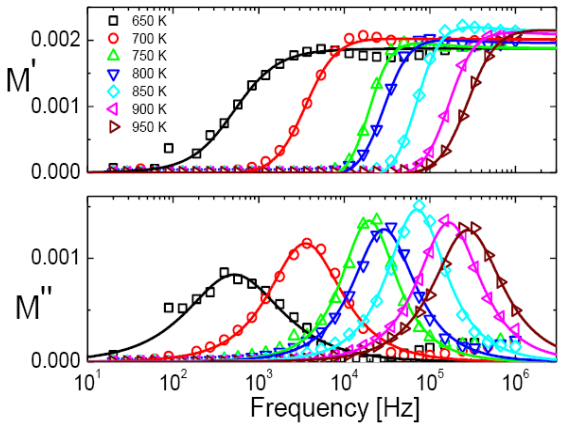

Fig.1 Frequency dependencies of the real (M′) and imaginary (M″) parts of electrical modulus at different temperatures for 0.9PMT–0.1PT single crystals.

Acknowledgment

This research is funded by the European Social Fund under the Global Grant measure.

References

1. A. Kania. Flux Growth and Dielectric Studies of (1-x) $PbMg_{1/3}Nb_{2/3}O_3$-xPbTiO3 Single Crystals, Ferroelectrics, 369, 141-148 (2008).

R-43

Phenomenological Model of Phase Transitions in $[N(C_2H_5)_4]_2MnCl_4$ Crystals

S. Pavlov

Lomonosov Moscow State University, Russia

e-mail: swcusp@mail.ru

$[N(C_2H_5)_4]_2MnCl_4$ crystals undergoes two first-order phase transitions at T_1=224 K and T_2=200 K [1]. The aim of the present work is to construct and investigate a structurally stable phenomenological model that describe the temperature dependence of anomalies of calorimetric properties of $[N(C_2H_5)_4]_2MnCl_4$ crystals near the points of both phase transitions. Group-theoretical analysis shows that the phase transitions from tetragonal phase into orthorhombic one are induced by two-dimensional irreducible representation. The rational basis of invariants consists of two invariants: $I_1=\eta_1^2+\eta_2^2$ и $I_2=\eta_1^2\eta_2^2$, where η_1 and η_2 are the components of the order parameter. A structurally stable thermodynamic potential is determined by the catastrophe theory methods [2]. It has the form:

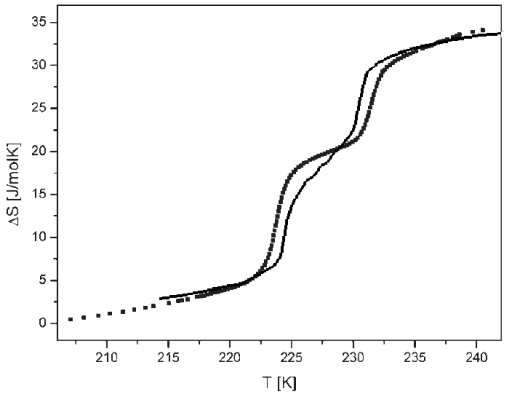

Fig.1 The temperature dependence of the entropy change ΔS for $[N(C_2H_5)_4]_2MnCl_4$ crystals. Solid line is the theoretical curve of the model; squares are the experimental data of [1].

$$\Phi=a_1I_1+a_2I_1^2+a_3I_1^3+a_4I_1^4+a_5I_1^5+a_6I_1^6+b_1I_2+b_2I_2^2+b_3I_2^3+c_1I_1I_2+c_2I_1^2I_2+c_3I_1I_2^2+c_4I_1^2I_2^2,$$

where $a_1=a_1'(T-T_0)$, $a_6>0$ and $c_4>0$. Phase diagram of the model has the regions of isomorphic phase transitions and the liquid-vapor critical points. When thermodynamic path passes near these regions, on the temperature dependence of physical properties appear anomalies, characteristic for overcritical behavior. Such a situation is apparently occurs in $[N(C_2H_5)_4]_2MnCl_4$ crystals. Fig. 1 shows the theoretical and experimental dependence of the entropy. Low-temperature anomaly one can be interpreted as the supercritical behavior, but not as a first-order phase transition.

References

1. A. Cizman, R. Poprawski and A. Sieradzki, Ferroelectrics, **363:1**, 209 (2008)
2. E. I. Kut'in, V. L. Lorman and S. V. Pavlov, Sov. Phys.-Uspekhi, **34**, 497 (1991)

R-44

Raman Studies of Stoichiometric and Congruent Lithium Niobate Crystals at Temperatures within the 100 – 450 K Range

N.V. Sidorov[1], M.N. Palatnikov[1], A.A. Kruk[1], A.A. Yanichev[1], K. Bormanis[2]

[1]I.V. Tananaev Institute of Chemistry and Technology of Rare Elements and Mineral Raw Materials of Kola Science Centre of RAS, Apatity, Russia

[2]Institute of Solid State Physics, University of Latvia, Latvia,

e-mail: sidorov@chemy.kolasc.net.ru, bormanis@cfi.lu.lv

Raman spectra of congruent and stoichiometric lithium niobate crystals studied within the temperature range of 100 ÷ 450 K are presented. The bands of fundamental vibrations of the crystal lattice only are observed in the spectrum of the stoichiometric crystal. In the case of congruent crystal, apart from the bands of fundamental lattice vibrations allowed by selection rules for the C_{3V}^6 (R3c), Z=2 space group, the Raman spectrum contains an "extra" band of low intensity corresponding to oscillations of "forbidden" A_2 type of symmetry and bands belonging to acoustic phonons of two-particle states with total wave vector equal to zero. A linear dependence of frequency and bandwidth on temperature is observed in the 100 ÷ 450 K range. However, the width of the band corresponding to oscillations of A_1(TO) symmetry of the Li^+ ions is much less dependent on temperature as compared with bands related to oscillations of Nb^{5+} ions of the same symmetry indicating to a quite unusual substantial anharmonicity of the heavier Nb^{5+} ions along the polar axis. Anharmonicity of the vibrations of Nb^{5+} ions is shown to have a significant contribution from O^{2-} ions characterized by anharmonic potential fluctuations which, according to calculations from the first principles, mix with vibrations of the Nb^{5+} ions. Anharmonicity of O^{2-} ions is confirmed by a strong dependence on temperature of the A_1(TO) bandwidth of O^{2-} ions vibrations perpendicular to the polar axis. This result is also indicative to some insignificant contribution to ionic conductivity of Li^+ cations at T < 450 K and the dominant role of protons and small polarons. At a significant contribution of "hopping" Li^+ cations to the ionic conductivity within the temperatures of 100 ÷ 450 K the temperature dependence of the width of the Li^+ A_1(TO) band would be close to exponential. Intensity of the bands of fundamental vibrations is not a monotonous function of temperature while the intensity of the "extra" bands has a strictly linear dependence. It is such a behavior of the fundamental vibration band intensities the is possibly related to presence of clusters and microstructures in the crystal.

R-45

Structural and Optical Homogeneity in Lithium Niobate Crystals of Low Photorefractivity

N.V. Sidorov[1], M.N. Palatnikov[1], N.A. Teplyakova[1], A.A. Yanichev[1], O.V. Makarova[1], O.Yu. Pikoul[2], and K. Bormanis[3]

[1]I.V. Tananaev Institute of Chemistry and Technology of Rare Elements and Mineral Raw Materials of Kola Scientific Centre of RAS, Apatity, Russia

[2]Far Eastern State University of Transportation, Khabarovsk, Russia

[3]Institute of Solid State Physics, University of Latvia, Latvia

e-mail: bormanis@cfi.lu.lv

The structural and optical homogeneity of lithium niobate crystals ($LiNbO_3$) of stoichiometric, congruent ($LiNbO_{3cong.}$), and single-crystals of $LiNbO_3$ containing cation admixtures of Mg (0.078, 0.89 wt .%), Zn (0.03, 0.52, 0.62 wt .%), Cu (0.015 wt .%), B (0.12 wt .%), Gd (0.51 wt .%), Y (0.46 wt .%), Gd (0.23 wt .%): Mg (0.75 wt .%), Mg (0.86 wt .%): Fe(0.0036 wt .%), Ta (1.13 wt .%): Mg (0.011 wt .%), and Y (0.24 wt .%): Mg (0.63 wt .%) was studied by Raman scattering, photo-induced light scattering (PILS), laser conoscopy and optical spectroscopy. Having a low photorefractivity the crystals are promising materials for frequency and broadband converters of coherent optical radiation. Position of the optical absorption edge in modified crystals $LiNbO_3$: Y (0.46 wt. %) and $LiNbO_3$: Y (0.24 wt. %): Mg (0.63 wt. %) is found to match the absorption edge of congruent crystals. Disclosure of the PILS indicatrix of these crystals proceeds very fast - during the first second of laser irradiation, qualifying them as potential materials for holography, electro-optic modulators, and optical switches. A noticeable influence of the photorefractive effect on the conoscopic patterns is observed along with a smaller angle of the transmission curve in the $LiNbO_3$:Y(0.46 wt.%) and $LiNbO_3$:Y(0.24 wt.%):Mg(0.63 wt.%) crystals, as compared with a congruent crystal. indicates of a significantly lower optical homogeneity.

The asymmetry of the PILS indicatrix of $LiNbO_3$ crystal is shown to be the result of birefringence of the exciting laser radiation propagating perpendicular to the polar axis of the crystal, and the asymmetry of the Raman spectrum is the result of the presence of spontaneous polarization and birefringence. The shape of the PILS pattern depends on the difference between the values of refractive indices $\Delta n = n_o - n_e$ and the ratio of the energies E of the ordinary (n_o) and extraordinary (n_e) rays. If $En_o >> En_e$, the PILS picture is a round three-layer spot. With approximately equal energies the shape being a symmetrical number eight. At $En_o < En_e$ the PILS pattern is asymmetric.

R-46

As-Grown Domain Structure of β-Glycine Single Crystal

D.S. Petukhova[1], S.G. Vasilev[1], A.S. Nuraeva[1], P.S. Zelenovskiy[1], E. Seyedhosseini[2], D. Isakov[3], V.Ya. Shur[1], A.L. Kholkin[1,2]

[1]Institute of Natural Sciences, Ural Federal University, Russia

[2]Department of Materials and Ceramic Engineering & CICECO, University of Aveiro, Portugal

[3]Center of Physics, Campus de Gualtar, University of Minho, Portugal

e-mail: daria.petuhova@gmail.com

The domain structure geometry with neutral and charged domain boundaries has been systematically studied by high-resolution method in β-glycine single crystals.

Glycine is the simplest amino acid crystallizes at ambient conditions in three polymorphic phases: α, β and γ [1]. Piezoelectric response, domain switching and hysteresis loops in β-phase of glycine has been demonstrated recently [2]. The domain structures in β-glycine have been visualized by piezoresponse force microscopy (PFM) using probe laboratory Ntegra Aura (NT-MDT, Russia). The faceted crystals with in plane polar axis (typical thickness about 20 μm and area about 200x50 μm) were grown from aqueous solution by drop drying on Pt/SiO/Si substrate at ambient conditions with controlled relative humidity. The polymorphic phase and orientation of the polar axis of the crystal were confirmed by confocal Raman microscope Alpha300AR (WiTec GmbH, Germany).

The obtained PFM images on non-polar crystal surface allowed to reveal the as-grown domain structure consisted of domains extended along the polar axis separated by neutral and two types of charged domain walls. The steps existing on the charged domain wall allowed us to determine the direction of domain growth. Detailed study revealed the topographic features at the charged walls - shallow wells of 0.2-1 nm-depth and about 150 nm-width. PFM response perpendicular to the polar axis at the boundary indicated its complex structure. In contrast the topographic features near neutral walls were absent. The results are discussed in terms of phenomenological theory.

Acknowledgment

The research was made possible in part by RFBR (research project 13-02-01391-a) and in terms of Ural Federal University development program with the financial support of young scientists. The equipment of the Ural Center for Shared Use “Modern Nanotechnology” (Institute of Natural Sciences, Ural Federal University) has been used.

References:

1. E. V. Boldyreva, V. A. Drebushchak, T. N. Drebushchak et al., J. Therm. Anal. Calorim. **73**, 419 (2003)
2. A. Heredia, V. Meunier, I. K. Bdikin et al., Adv. Funct. Mater. **22**, 2996 (2012)

R-47

In Situ Observation of Polymorphic Phase Transformation in Glycine Crystal

P.S. Zelenovskiy[1], D.S. Petukhova[1], S.G. Vasilev[1], A.S. Nuraeva[1], T.A. Khazamov[1], D.V. Isakov[2], V.Ya. Shur[1], A.L. Kholkin[1,3]

[1]Institute of Natural Sciences, Ural Federal University, Russia

[2]Center of Physics, Campus de Gualtar, University of Minho, Portugal

[3]Department of Materials and Ceramic Engineering & CICECO, University of Aveiro, Portugal

e-mail: zelenovskiy@labfer.usu.ru

In the present work we demonstrate the β→γ polymorphic transformation in glycine single crystal *in situ* visualized by piezoresponse force microscopy (PFM).

Glycine amino acid (NH_2CH_2COOH) is considered as an advanced material for ferroelectric [1], nonlinear optical and piezoelectric applications [2]. At ambient conditions glycine crystallizes in three polymorphic phases: α, β and γ [3]. Metastable β-phase can irreversibly transform into the α or γ-phases under the presence of moisture [3]. The microscopic mechanism of such transformation still requires detailed investigations.

Scanning probe microscope Ntegra Aura (NT-MDT, Russia) with a Ti/Pt-coated tip was used for PFM measurements. Polymorphic phases before and after the transformation were confirmed by confocal Raman microscope Alpha300AR (WiTec GmbH, Germany) equipped by 488 nm solid state laser in backscattering geometry.

β-glycine crystal was grown by evaporation of aqueous solution on $Pt/Ti/SiO_2/Si$ substrate at ambient conditions with relative humidity of about 24%. Transformation into γ-phase was visualized during gradual decreasing of relative humidity from 30 down to 25%. It was shown that the transformation occurs for relative humidity above 25%. Analysis of the time dependence of ratio β to γ phase area obtained from PFM images allowed to reveal the averaged velocity of the phase boundary motion. Raman analysis of the phase boundary allowed to provide a microscopic model of the process.

Acknowledgment

The research was made possible in part by RFBR (research project 13-02-01391-a) and in terms of Ural Federal University development program with the financial support of young scientists. The equipment of the Ural Center for Shared Use “Modern Nanotechnology” (Institute of Natural Sciences, Ural Federal University) has been used.

References

1. A. Heredia, V. Meunier, I. K. Bdikin et al., Adv. Funct. Mater. **22**, 2996 (2012)
2. D. Isakov, E. d. M. Gomes, I. Bdikin et al., Cryst. Growth Des. **11**, 4288 (2011)
3. E. V. Boldyreva, V. A. Drebushchak, T. N. Drebushchak et al., J. Therm. Anal. Calorim. **73**, 419 (2003)

R-48

Electrical Properties of Congruent $LiTaO_3$ Single Crystals

A.V. Yatsenko[1], M.N. Palatnikov [2], N.V. Sidorov[2], S.V. Yevdokimov[1], and K. Bormanis[3]

[1]Taurida National V.I. Vernadsky University, Simferopol, Ukraine

[2]I.V. Tananaev Institute of Chemistry and Technology of Rare Elements and Mineral Raw Materials of Kola Science Centre of RAS, Apatity, Russia

[3]Institute of Solid State Physics, University of Latvia, Latvia

e-mail: bormanis@cfi.lu.lv

The study is focused on the dependence of dark conductivity on temperature in virgin and vacuum-reduced congruent single crystals of $LiTaO_3$ (LT). Detailed experimental data obtained after the samples of either kind are heated up to 454 K can be simulated by assuming existence of at least two types of charge carriers: $\sigma(T) = \left[\frac{A}{T}\cdot\exp\left(-\frac{E_1}{k_0T}\right)+\frac{B}{T}\exp\left(-\frac{E_2}{k_0T}\right)\right]$. The temperature dependence of the conductivity of the reduced samples is characterized by activation energies E_1=(1.25 ± 0.05) eV and E_2=(0.48 ± 0.04) eV, in virgin samples the activation energies are equal to E_1=(1.01 ± 0.02) eV and E_2=(0.29 ± 0.04) eV. Since no information is available concerning the effect reducing in vacuum has on electrical properties of LT crystals, the data from $LiNbO_3$ (LN) crystal reduced in vacuum are analyzed instead. The data demonstrates the well-known fact that the reducing in vacuum increases the conductivity of LN crystals at T=293 K by some orders. Nevertheless, the value of σ at T=293 K in virgin LT samples exceeds that of reduced samples and is equal to $(12\pm2)\times10^{-17}(\Omega\cdot\mathrm{cm})^{-1}$. The values of activation energies of electric conductivity in reduced LT samples at low temperatures demonstrate a polaronic conductivity the highest value E_1 being close to activation energy of the diffusion of oxygen vacancies V_O. On the other hand, the highest value E_1 in virgin crystals is typical for proton conductivity in LT and LN crystals, while the value of E_2 indicates to hopping electron conductivity. Our data confirms a strong diffusion and volatility of hydrogen reducing LT in vacuum at 830 K. In addition, a partial loss of oxygen caused by reducing is observed leading to recharging transition metal impurities to the lowest valence state and blocking the hopping electronic conductivity. After filling of electron traps, the process of small polaron formation Ta_{Li}^{4+} starts. So the increase of the activation energy of σ(T) at high temperature in reduced LT samples is a result of increased bulk concentration of V_O and decreased content of hydrogen.

R-49

Synthesis, Structure, Electrical and Mechanical Characteristics of Ceramic $Nb_{2(1-y)}Ta_{2y}O_5$

M.N. Palatnikov[1], O.B. Shcherbina[1], V.V. Efremov[1], N.V. Sidorov[1], and K. Bormanis[2]

[1]I.V. Tananaev Institute of Chemistry and Technology of Rare Elements and Mineral Raw Materials of Kola Science Centre of RAS, Apatity, Russia

[2]Institute of Solid State Physics, University of Latvia, Latvia

e-mail: sidorov@chemy.kolasc.net.ru, bormanis@cfi.lu.lv

Optimization of the physical properties of ceramic oxides Nb_2O_5 and Ta_2O_5 and their solid solutions ($Nb_{2(1-y)}Ta_{2y}O_5$) is of current interest due to usage as construction materials of high heat resistance and as functional materials in microelectronics. Results of a comprehensive study of ceramic $Nb_{2(1-y)}Ta_{2y}O_5$ obtained from co-precipitated oxides including probing microscopy, Raman scattering, impedance spectroscopy, and treatment by concentrated light flux (CLF) are reported.

The modulus of elasticity, micro-hardness, dielectric permittivity, and features of self-conductivity of the microstructure in the series of ceramic $Nb_{2(1-y)}Ta_{2y}O_5$ solid solutions are affected by the change of the polycrystalline structure with the content of tantalum. A serious change of structure manifested in spectral characteristics of the $Nb_{2(1-y)}Ta_{2y}O_5$ ceramics is revealed after treatment by CLF.

Most strongly affected by CLF treatment is the $Nb_{2(1-0.363)}Ta_{2\cdot(0.363)}O_5$ compound, the least – Nb_2O_5. Perhaps the effect is due to a higher degree of dissociation in the $Nb_{2(1-y)}Ta_{2y}O_5$ structure under CLF. The melting temperature of mixed $Nb_{2(1-y)}Ta_{2y}O_5$ oxides rises with the tantalum concentration being the reason why after melting under CLF the crystallization proceeds much faster compared with Nb_2O_5.

R-50

Thermal Properties of Relaxor $PbNi_{1/3}Nb_{2/3}O_3$ Solid Solution Ceramics

K. Bormanis[1], S.N. Kallaev[2], Z.M. Omarov[2], A.R. Bilalov[2], S.A. Sadykov[3], and R.G. Mitarov[3]

[1]Institute of Solid State Physics, University of Latvia, Riga, Latvia

[2]Institute of Physics, Dagestan Science Centre, RAS, Makhachkala, Russia

[3]Dagestan State Technical University, Makhachkala, Russia

e-mail: bormanis@cfi.lu.lv

Ceramic ferroelectric relaxors of specific crystal structure and unique physical properties make a promising class of functional ferroelectric materials the multicomponent perovskite solid solutions of mixed oxides, such as $PbNi_{1/3}Nb_{2/3}O_3$, being special interest. The studies of the behavior of heat capacity and dielectric permittivity of $PbNi_{1/3}Nb_{2/3}O_3$-$PbTiO_3$ (PNN-PT) solid solutions over a wide temperature range from 150 to 800 K are reported.

The temperatures characterizing the anomalies of dielectric permittivity ε(T) and of heat capacity $C_p(T)$ are found for the (1-x)PNN-xPT system at x = 0.3, 0.4, 0.5, the temperatures T_m of the maximums of dielectric permittivity of which are around 315, 385, and 455 K, respectively. The 0.7PNN-0.3PT composition has a noticeable frequency-dependence of the broad phase transition peak of dielectric permittivity not being observed in compositions of x = 0.4 and 0.5. The extended shape of the anomaly of heat capacity at $T_m \approx 315$ K in the 0.7PNN-0.3PT composition is typical to ferroelectric relaxors.

The temperature dependence of the heat capacity $C_p(T)$ of the 0.7PNN-0.3PT ceramics has an λ anomaly at T≈225 K another anomaly being discovered extending from 250 to 650 K around T≈520 K. A quantitative analysis of the temperature dependence of heat capacity and separation of the anomalous contribution from phonon contribution, as in most cases, is made by estimating the phonon heat capacity of the compounds as the sum of the Debye and Einstein functions the anomalous component being found as the difference between the measured and calculated phonon heat capacities $\Delta C = C_p - C_p^o$. Local distortions of the structure revealed in the Brillouin scattering spectra are found in two regions of the ΔC(T) anomaly: 250-450 K coinciding with the ε(T) and within 450-650 K. The temperature dependence on temperature of the ΔC anomaly separated from the phonon contribution is described by expression for the Schottky heat capacity of two-level states separated by an energy barrier.

R-51

The Slow Relaxation of Polarization in $(K_{0,5}Na_{0,5})(Nb_{1-x}Sb_x)O_3$+ 0,5mol%$MnO_2$ Ferroelectric Ceramics

K. Bormanis[1], I. Smeltere[1], A.V. Sopit[2], and A.I. Burkhanov[2]

[1]Institute of Solid State Physics, University of Latvia, Riga, LV-1063, Latvia;

[2]Volgograd State Architectural and Engineering University, Volgograd, Russia

e-mail: bormanis@cfi.lu.lv

Solid solutions of niobate compounds near the morphotropic boundary are known to be the most appropriate ferroelectric materials without lead competing in electrical properties with the PZT systems. However, particularly the niobate systems have multiple phase transitions at which phenomena of slow relaxation are manifested. The presented study of dielectric response to low and infra-low frequencies under DC bias field ($E_=$) is aimed at the slow relaxation processes of polarization.

The samples of hot-pressed $(K_{0.5}Na_{0.5})(Nb_{1-x}Sb_x)O_3$+0.5mol%$MnO_2$ ferroelectric ceramics made for dielectric measurements of the size of 5x3x0.9 mm^3 were furnished with silver electrodes to study dielectric permittivity $\varepsilon'(E_=)$ under reversing the bias field over a wide range of temperature including the structural phase transition. A considerable rise of the dispersion of ε' is observed at increasing $E_=$ after the samples are held at constant temperature and constant bias (Fig. 1a) possibly pointing to increased number of relaxators at repealing the phase (not domain) boundaries since the maximum applied bias fields have been below the the coercive field value.

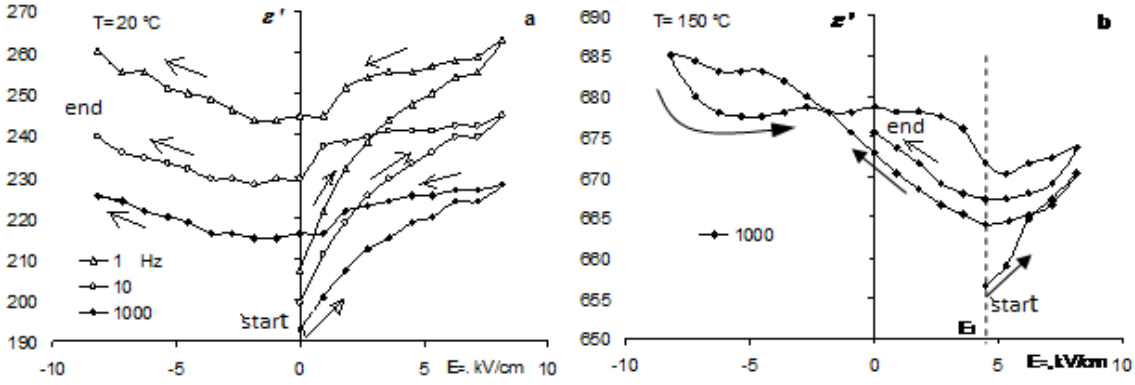

Fig. 1. $\varepsilon'(E_=)$ curves of KNN-5 at different frequencies (a) and exposure to constant bias field before the measurements (b).

A minimum on the $\varepsilon'(E_=)$ curve is observed at the bias field intensity the value of which is equal to that applied to the sample at the temperature of the $\varepsilon'(T)$ anomaly of $(K_{0.5}Na_{0.5})(Nb_{0.95}Sb_{0.05})O_3$+0.5mol%$MnO_2$ (KNN-5) (Fig. 1b). Appearance of the minimum at repeating the cycle (Fig. 1b) is an evidence of the field memory effect specific to ultra-slow relaxation processes of polarization in ferroelectrics of broad phase transitions.

R-52

Electronic Properties of Hexagonal $SrMnO_3$ Ceramic

R. Bujakiewicz-Korońska[1], D.M. Nalecz[1], E. Markiewicz[2], A. Kalvane[3], A. Budziak[4]

[1]Institute of Physics, Pedagogical University, Podchorążych 2, 30-084 Krakow, Poland

[2]Institute of Molecular Physics, Polish Academy of Science, Smoluchowskiego 17, 60-179 Poznan, Poland

[3]Institute of Solid State Physics, University of Latvia, Latvia

[4]The H.Niewodniczanski Institute of Nuclear Physics PAN, Radzikowskiego 152, 31-342 Kraków, Poland

e-mail: kalvane@cfi.lu.lv

The strontium manganite ($SrMnO_3$) shows a lot of interesting magnetodielectric properties [1,2]. Recently, we prepared the $SrMnO_3$ ceramic using the conventional sintering method. The XRD tests and dielectric measurements were performed which confirmed the hexagonal structure at room temperature (Fig.1) and two contributions in the complex impedance originating from grains and grain boundaries. The electronic and magnetic structures were investigated by Siesta 3.2 code [3] in the formalism of the density functional theory. The calculations showed an existence of a band gap about 0.5 eV at 0 K. Contribution of exchange-correlation energy in the total energy is about 30%.

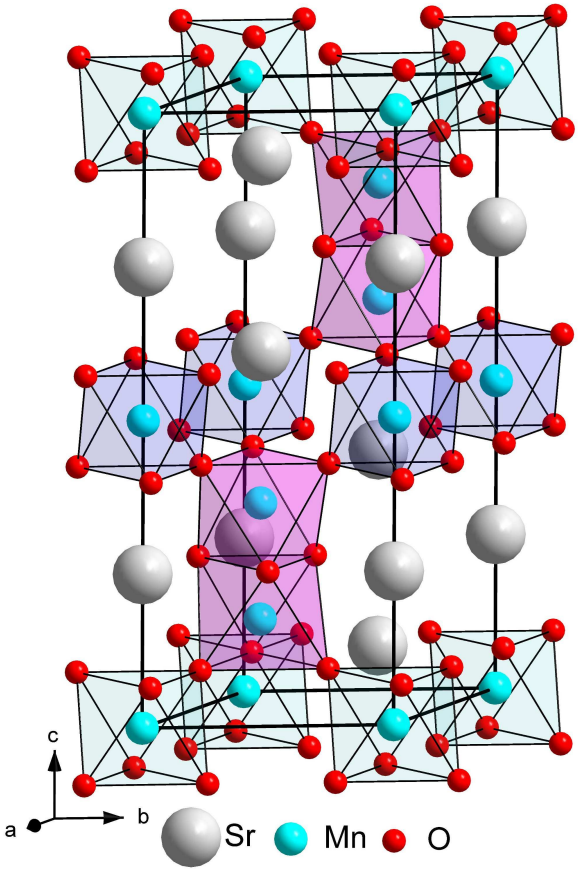

Fig.1 Relaxed unit cell of the hexagonal 6H-$SrMnO_3$

Acknowledgments

The authors acknowledge the CPU time allocation at Academic Computer Centre CYFRONET AGH in Cracow. This work was supported in part by PL-Grid Infrastructure.

References

1. R. Søndenå, P. Ravindran, S. Stølen, T. Grande, M. Hanfland, Phys. Rev. B 74, 144102 (2006)
2. S. Kamba, V. Goian, V. Skoromets, J. Hejtmanek, V. Bovtun, M. Kempa, F. Borodavka, P. Vanek, A.A. Belik, J.H. Lee, O. Pacherova, K.M. Rabe, arXiv:1402.2165
3. J. Soler, E. Artacho, J.D. Gale, A. García, J. Junquera, P. Ordejón, D. Sánchez-Portal, J. Phys. Condens. Matter. 14, 2745 (2002)

R-53

Phase Coexistence in $Bi_{1-x}Pr_xFeO_3$ Ceramics

D.V. Karpinsky[1,2], I.O. Troyanchuk[2], A.L. Kholkin[1]

[1]CICECO & Department of Materials and Ceramics Engineering, University of Aveiro, 3810-193 Aveiro, Portugal

[2]Scientific-Practical Materials Research Centre of NAS of Belarus, P. Brovka str. 19, 220072 Minsk, Belarus

e-mail: karpinski@ua.pt

$Bi_{1-x}Pr_xFeO_3$ ceramics across the rhombohedral-orthorhombic phase boundary have been studied by X-ray diffraction, transmission electron microscopy and differential scanning calorimetry. The structural phase transitions in $Bi_{1-x}Pr_xFeO_3$ driven by doping concentration and temperature are significantly different from those in $BiFeO_3$ compounds doped with other rare-earth elements [1, 2]. The detailed study of the crystal structure evolution clarified the ranges of both single phase and phase coexistence regions at different temperatures and dopant concentrations. For x = 0.125 compound extraordinary three-phase coexistence state has been observed in the narrow temperature range about 400 ºC. The three phase coexistence state stable in the temperature range is thermodynamically self-consistent if one will consider non-equilibrium character of the antipolar (O_2-) orthorhombic phase. It is assumed that specific character of the structural transitions observed in the *Pr*-doped $BiFeO_3$ ceramics is caused by significant covalent component of the *Pr – O* chemical bonds and low structural stability of the dominant rhombohedral (*R*-) phase. High mechanical compliance of the rhombohedral phase estimated for the compounds near the *R* - O_2 structural transition results in the enhanced electromechanical properties.

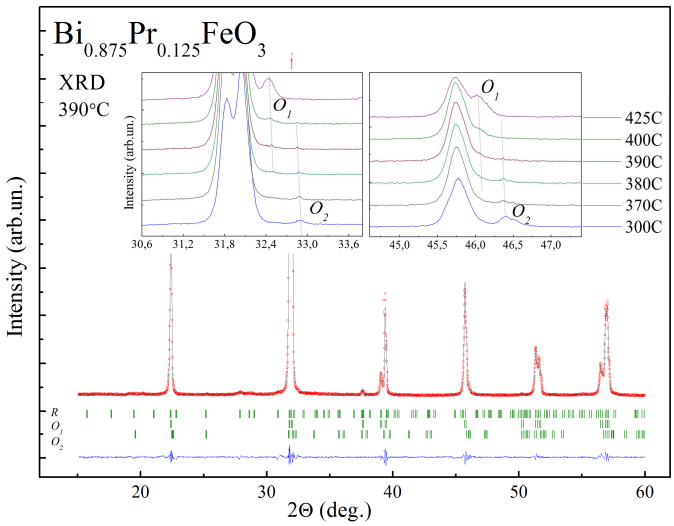

Fig. The XRD pattern of the $Bi_{0.875}Pr_{0.125}FeO_3$ compound at 390 °C. The insets show thermal evolution of the structural peaks characteristic for O_2- and O_1- phases.

References

1. I. O. Troyanchuk, D. V. Karpinsky, M. V. Bushinsky, O. S. Mantytskaya, N. V. Tereshko, V. N. Shut (2011) J. Am. Ceram. Soc. 94: 4502

2. D. V. Karpinsky, I. O. Troyanchuk, O. S. Mantytskaya, V. A. Khomchenko, A. L. Kholkin (2011) Solid State Commun. 151: 1686

R-54

Development of Ceramics for High Temperature Applications

E.D. Politova[1], G.M. Kaleva[1], N.V. Golubko, A.V. Mosunov[1], V.S. Akinfiev[2],
S. Yu. Stefanovich[1,2], A.H. Segalla[3]

[1]L.Ya.Karpov Institute of Physical Chemistry, Obukha s.-st., 3-1/12, b.6, 105064, Moscow, Russia

[2]Lomonosov Moscow State University, Leninskie gory, 1, Moscow, 119992, Russia

[2]ELPA Company, Panfilovsky pr. 10, Zelenograd, 124460, Moscow, Russia

e-mail: politova@cc.nifhi.ac.ru

Demands of various industries simulate search for new piezoelectric materials for high temperature applications. In this work, dielectric and piezoelectric properties of perovskite oxides based on (1-x)BiScO3 – xPbTiO3 (BSPT) with x = 0.63 - 0.65 and K0.5Na0.5NbO3 (KNN) compositions close to the MPB were studied. To compensate Bi3+, Pb2+, K1+ and Na1+ cations loss and to regulate functional properties of BSPT- and KNN-based ceramics complex approach was used that included modification of compositions by cation substitutions and overstoichiometric additives (various oxides and clorides).

The samples were prepared by the solid state reaction method. Structure, microstructure, and functional properties were studied using the X-ray diffraction, SEM, SHG, and Dielectric Spectroscopy methods. Piezoelectric parameters d33 and kt were determined.

Dense single-phase ceramic samples with different grain size were obtained, the influence of additives on dielectric properties and TC values was revealed.

The changes of the TC values observed correlated with the phase content and unit lattice parameters regulated by doping of the BSPT- and KNN-based ceramics.

Effects of dielectric relaxation were observed in samples prepared at high sintering temperatures due to the presence of vacancies in A- and oxygen sublattices. Suppression of relaxation effects was observed in modified samples characterized by decreased to more than one order of total conductivity. High piezoelectric coefficients d33 up to ~ 500 pC/N and kt ~ 0.65 values were measured in the BSPT ceramics prepared. Enhancement of piezoelectric properties will be discussed in relation to the preparation conditions, type and content of dopants.

Acknowledgment

The work was supported by the Russian Fund for Basic Research (Grant 12-03-00388).

R-55

Influence of Compressive Stress and Aging on Dielectric Properties of $BiFeO_3$ Ceramics

J. Suchanicz[1], R. Bujakiewicz-Koronska[1], M. Dziubaniuk[2], A. Kalvane[3], A. Sternberg[3]

[1]Institute of Physics, Pedagogical University, ul. Podchorazych 2, 30-084 Kraków, Poland

[2]Faculty of Materials Science and Ceramic, University of Science and Technology, 30-059 Krakow, al. Mickiewicza 30, Poland

[3]Institute of Solid State Physics, University of Latvia, Kengaraga 8, LV-1063 Riga, Latvia

e-mail: sfsuchan@up.krakow.pl

Multiferroic materials usually possess the ferroelectric, ferromagnetic and ferroelastic properties simultaneously. These materials have attracted much attention, because of its potential applications in sensors, transducers, magnetic recording media and spintronic. Among a few multiferroics, $BiFeO_3$ exhibited both ferroelectric and antiferromagnetic properties at room temperature. The external stress (0-1500 bar) dependence of dielectric properties and aging effect of $BiFeO_3$ ceramics have been investigated. The electric permittivity and dielectric losses first increased and then decreased with uniaxial pressure applied parallel to the *ac* field direction, while increased with the stress applied perpendicularly. It was suggested that hopping conductivity can be mainly responsible for these changes. The aging effect followed a logarithmic law and can be explained by migration of defects, which influences the electric conductivity and by the relaxation of the domain structure towards an equilibrium configuration. The aging rate was found to decrease with increasing frequency and can be a result of effect the electric conductivity and the pinning of polarization components by defects field.

R-56

Dielectric Behaviour of $(Ba_{1-x}Na_x)(Ti_{1-x}Nb_x)O_3$ Ceramics Obtained by Conventional and Mechanochemical Synthesis

W. Bąk[1], P. Dulian[2], B. Garbarz-Glos[3], C. Kajtoch[3], K. Wieczorek-Ciurowa[2],

[1]Institute of Physics, Pedagogical University, Cracow, Poland

[2]Faculty of Chemical Engineering and Technology, Cracow University of Technology, Poland

[3]Institute of Technology, Pedagogical University, Cracow, Poland

e-mail: wbak@up.krakow.pl

The $(Ba_{1-x}Na_x)(Ti_{1-x}Nb_x)O_3$ (BNTN) ferroelectric ceramics have been prepared by solid state reaction using the conventional method. Mechanochemical treatment based on the high-energy planetary ball milling has been used as an alternative method of synthesizing of the ceramics. The structure and morphology of the investigated samples were characterized by an X-ray diffraction (XRD) and scanning electron microscopy (SEM). Phase transitions parameters of investigated ceramics were described. In order to better understand of the phase transitions character in BNTN ceramics the calorimetric measurements were also performed. Characterization of electrical properties of BNTN samples within the temperature range $130\ K \div 600\ K$ were performed by means of dielectric spectroscopy method within the frequencies from 0.1 Hz to 10 MHz. Analysis of temperature and frequency dependences of real and imaginary parts of dielectric permittivity, electric modulus as well as impedance, provided the new details about specific features of physical properties of ceramic samples. According to complex impedance/electric modulus analysis, the grain's interior dominates the electrical response at high frequencies ($\sim 10^6$ Hz), but dielectric behaviour in all the frequency range is related to interfacial relaxation phenomena (Maxwell – Wagner type). This relaxation is due to displacement of the trapped charge in the interfaces that is development in heterogeneous ferroelectric ceramics associated with grain boundaries.

Acknowledgement

This study was supported by the National Science Centre Poland, Project DEC-2012/05/N/ST8/03764.

R-57

Dielectric Relaxation Processes in $Ba_2NdFeNb_4O_{15}$ and $Ba_2EuFeNb_4O_{15}$ Ceramics

D. Gabrielaitis[1], M. Albino[2], M. Josse[2], M. Kinka[1], V. Samulionis[1], R. Grigalaitis[1], M. Maglione[2], J. Banys[1]

[1]Vilnius University, Faculty of Physics, Lithuania

[2]CNRS, Université de Bordeaux, ICMCB-CNRS, France

e-mail: dainius.gabrielaitis@ff.stud.vu.lt

The tetragonal tungsten bronze (TTB) ferroelectric family attracted much attention in recent years. It is a promising material with many appealing properties that make it a good candidate in search of relaxors, ferroelectrics and even multiferroics. TTB structure is based on interconnected octahedra, leaving three open channels of different pseudo-symmetry [1]. This offers a more open crystalline network allowing multiple substitutions of various cations, thus opening up a wide range of interesting compositions [2, 3].

Dielectric measurements of $Ba_2NdFeNb_4O_{15}$ and $Ba_2EuFeNb_4O_{15}$ ceramics were carried in a frequency range from 20 Hz to 37 GHz, upon heating and cooling. Temperature dependencies of complex dielectric permittivity for both ceramics exhibit unusual shifts of permittivity maxima (ranging over 50 K) associated with ferroelectric phase transition. Both compound also have a second „relaxor like" permittivity dispersion region at lower temperatures, which might indicate an appearance of a second phase. Two separate, temperature dependent dielectric relaxation processes were distinguished by examining measured frequency dependences of complex permittivity. Further investigation of these temperature dependent processes might give an explanation for observed cooling-heating hysteresis loop formation and permittivity maxima shifts.

References

1. E. Castel, M.Josse, D. Michau and M. Maglione, J. Phys.: Condens. Matter **21,** (2009)
2. A. Magneli, Ark. Kem. **24,** 213 (1949)
3. M. Pouchard, J-P. Chaminade, A. Perron, J. Ravez and P. Hagenmuller, J. Solid State Chem. **14,** 274 (1975)

R-58

Dielectric Properties of Cromium-Containing Bismuth Titanate Ceramics with the Layered Perovskite Type Structure

M.S. Shashkov[1], O.V. Malyshkina[1], I.V. Piyr[2], M.S. Korolyova[2]

[1]Tver State University, Tver, Russia

[2]Komi Institute of Chemistry of Ural branch of Russian Academy of Sciences, Syktyvkar, Russia

e-mail: maksim.shashkov69@gmail.com

Complex oxides of bismuth titanate with a structure of layered perovskite doped by Cr in accordance with the stoichiometric formulas $Bi_4Ti_{2.98}Cr_{0.02}O_{11.99}$, $Bi_4Ti_{2.5}Cr_{0.5}O_{11.75}$, $Bi_4Ti_{1.8}Cr_{1.2}O_{11.4}$ were measured in the frequency range from 30 Hz to 10^6 Hz at the temperature of 296 K. The polycrystalline samples were prepared by the procedure of solid phase synthesis in air using Bi_2O_3 (99.99%), TiO_2 (99.999%) and Cr_2O_3 (99.9%), in stoichiometric ratios.

In paper were obtained the spectra of the dielectric permittivity (ε) (Fig. 1), the dielectric loss ($tg\delta$), the complex conductivity (σ') and the diagrams of $\varepsilon''(\varepsilon')$. Analysis of the experimental data was performed using the fractal-power universal law for the dielectric response [1]. It is shown that the type of the dispersion curve depends on the concentration of substitutional atoms. The difference of the dielectric permittivity between sample with $x = 1.2$ and compositions with $x = 0.02$ and 0.5 depends on a different number of Bi_2O_3 layers.

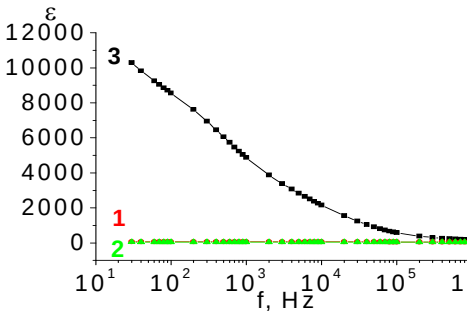

Fig.1 Frequency dependence of the dielectric permittivity for compounds: 1 - $Bi_4Ti_{2.98}Cr_{0.02}O_{11.99}$, 2 - $Bi_4Ti_{2.5}Cr_{0.5}O_{11.75}$, 3 - $Bi_4Ti_{1.8}Cr_{1.2}O_{11.4}$

The surface microstructure of bismuth titanate ceramics was investigated by AFM method (Fig. 2). The tendency to the formation of the conglomerates of grains and a large concentration of pores was shown. The average grain size was measured on the obtained images. It was found that the pore density of the compound correlates with the concentration of substitutional atoms (Cr).

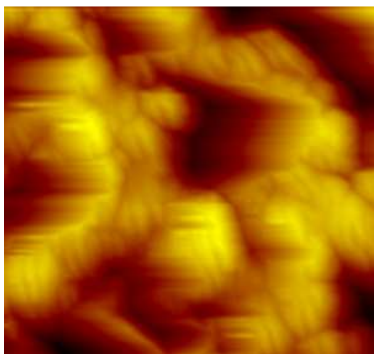

Fig. 2 Microstructure of $Bi_4Ti_{1.8}Cr_{1.2}O_{11.4}$ ceramics. The image size is 20x20 μm.

References:

1. Jonscher A.K. Universal relaxation law. London. Chelsea Dielectrics Press Ltd. 415 p. (1996).

R-59

Effect of Bismuth Oxide Dispersivity on the Dielectric Properties of Zinc Oxide Ceramics

O. Malyshkina[1], A. Ivanova[1], S. Pugachev[2], E. Rytov[2]

[1]Tver State University, Tver, Russia

[2]State Marine Technical University of St. Petersburg, St.- Peterburg, Russia

e-mail: Olga.Malyshkina@mail.ru

Bismuth oxide (Bi_2O_3) is an important additive necessary for the production of zinc oxide (ZnO) varistors. In the present work we study the effect of Bi_2O_3 dispersivity on the dielectric properties of zinc oxide ceramics. The structure and element composition were studied with the aid of scanning electron microscope JEOL JSM-6610LV. The distinctions due to different Bi_2O_3 dispersivity are clearly revealed by the images of lateral cleavages of ZnO ceramics obtained in the regime of back scattered electrons (BEC) (Fig. 1).

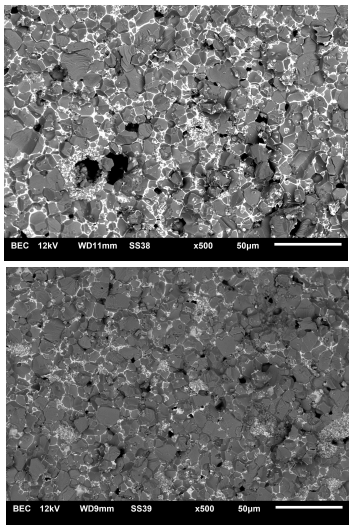

Fig.1 Lateral cleavage images ZnO ceramics for ordinary (a) and finely dispersed Bi_2O_3 (b). Scale mark length 50 μm

In spite of the decrease of both dielectric permittivity and dielectric loss tangent values which are observed when finely dispersed Bi_2O_3 is used for the preparation of the samples instead of standard ingredient, the shape of the corresponding frequency dependences remains unchanged. Two regions having different behaviour of the complex dielectric permittivity may be distinguished at the dispersion diagrams ε″(ε′). The frequency of ~ 8 kHz corresponding to the change of the dispersion type is independent of the Bi_2O_3 dispersivity. In the low frequency region a linear dependence of the imaginary component on the real part of dielectric permittivity is observed, while in the high frequency region this dependence may be approximated by a circular arc (Fig. 2).

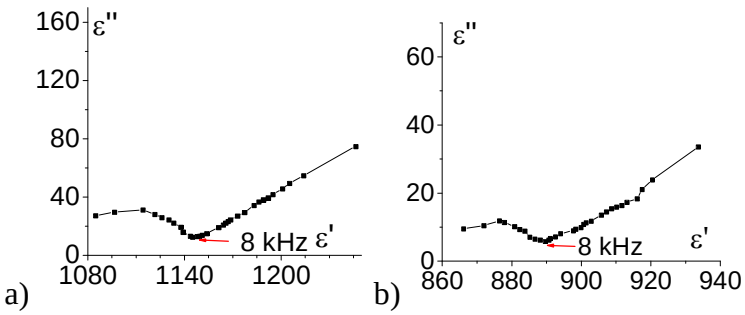

Fig. 2. Dielectric permittivity dispersion diagrams for ordinary (a) and finely dispersed Bi_2O_3 (b)

R-60

Pore Effect on the Switching Processes in PZT Ceramics

E.V. Barabanova[1], O.V. Malyshkina[1], A.Y. Eliseev[1], A V Daineko[2]

[1]Tver State University, Tver, Russia

[2]Research Institute "ELPA", Zelenograd, Russia

e-mail: pechenkin_kat@mail.ru

Comparative study was made of pore-free PZT-19 ceramic samples and those containing specified volume of pores (25%). Earlier it was found [1] that dielectric hysteresis loops of PZT ceramics with varying porosity differ significantly in their values of coercive fields and remanent polarization. In comparison with pore-free samples the porous ones possess lower remanent polarization and higher coercive field values. At the same time in porous samples the hysteresis loop itself is more rectangular, i.e. the remanent polarization P_r is close to spontaneous polarization P_s.

In addition, the heating and aging effects occuring during the exposure of the samples in AC fields of constant amplitud were studied. The sample temperature was rnonitored with the aid of thermal imager Testo–875-1. The sample heating takes place with the enlargement of the hysteresis loop and attains a maximum when the hysteresis loop becomes satrurated. It is important to note that the dielectric loop saturation occurs at different ratios between the applied and coercive fields E_a/E_c of a given sample. So it was possible to obtain a saturated loop of the porous sample at E_a = 1,6 E_c, while the saturation of the pore-free sample is reached at $E_a = 2\ E_c$. In the latter case the sample heating is more intensive and the maximal temperature of heating is twice as high as that of the porous sample for the same time of exposure. In theory the area of the dielectric hystesis loop is related to the energy losses during one cycle of field changing [2]. So far as both the hysteresis loop area and heating temperature of the porous sample are lower than in the pore-free one it may be inferred that the losses in pore-free samples are higher than in porous ones.

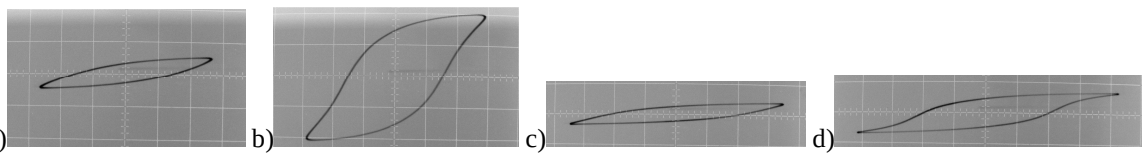

Figure 1. Dielectric loops of PZT pore-free ceramics (a, b) and that with porosity of 25% (c, d). At the initial moment (a, c) and 3 minutes later (b, d) after applying a field. Scale OX: 200 V/div; OY: 5 V/div.

References

1. E V Barabanova, O V Malyshkina, A I Ivanova, E M Posadova, K M Zaborovskiy and A V Daineko , IOP Conf. Ser.: Mater. Sci. Eng. **49**, 012026 (2013)

2. K. Uchino, IEEE Trans. Ultrasonics, Ferroelectrics and Freq. Control, **48**, 307 (2001).

R-61

Porous Piezoelectric Ceramics: Complex Representation of Material Properties

M. Lugovaya, A. Naumenko, A. Rybyanets, E. Petrova

Institute of Physics, Southern Federal University, Russia

e-mail: lugovaya_maria@mail.ru

Demands on medical and NDT ultrasonic transducer performance have increased in recent years. Low-Q piezoceramics and piezocomposite materials are widely used for wide-band NDT ultrasonic transducers with high sensitivity and resolution. Some of these advanced materials are lossy, and direct use of IEEE Standard for material constants determination leads to significant errors. The accurate description of piezoceramics must include the evaluation of the dielectric, piezoelectric and mechanical losses, accounting for the out-of-phase material response to the input signal.

Numerous techniques using complex material constants have been proposed to take into account losses in low-Q_M materials and to overcome limitations in the IEEE Standard. Iterative methods provide a means to accurately determine the complex coefficients in the linear range of poled piezoceramics from complex impedance resonance measurements.

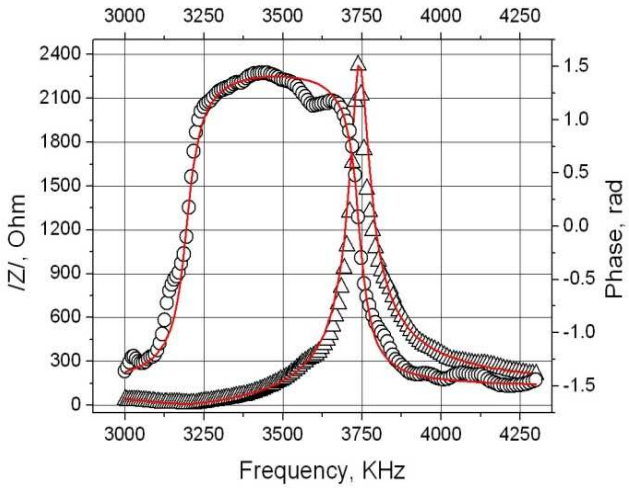

Fig.1. Impedance spectrum and PRAP approximation for thickness extensional mode of porousPCR-1 disk.

The piezoelectric resonance analysis method and program (PRAP) has been proposed for the full set of standard geometries and resonance modes needed to complete complex characterization in a wide range of materials with very high and moderate losses [1].

In this paper a line of porous PZT piezoelectric ceramics with 3-0/3-3 connectivity types and relative porosity up to 60% was systematically studied. Both the IEEE Standards and the piezoelectric resonance analysis method (PRAP) were used to determine material constants [2]. Complex sets of elastic, dielectric and piezoelectric coefficients of the porous piezoelectric ceramics were measured by impedance spectroscopy methods using (PRAP) software. The PRAP iterative method enables complete automatic analysis of resonance impedance spectra to derive complex elastic, dielectric, and piezoelectric properties of the piezoresonator. Material constants obtained by the different methods were compared.

The results show that the PRAP method gives results that are more accurate and allow taking into account elastic, piezoelectric, and dielectric losses.

References

1. PRAP (Piezoelectric Resonance Analysis Program). TASI Technical Software Inc. www.tasitechnical.com.
2. A.N. Rybyanets, A.A. Naumenko, N.A. Shvetsova. In.: " Nano- and Piezoelectric Technologies, Materials and Devices", Ivan A. Parinov Ed. Nova Science Publishers Inc., 2013. Chapter 1. – P. 275-308.

R-62

Mechanical and Electrical Properties of Li Doped Sodium Niobate Ceramic System

W. Śmiga[1], B. Garbarz-Glos[1], W. Piekarczyk[2], M. Livinsh[3], M. Krawczyk[4]

[1]Institute of Technology, Pedagogical University of Cracow, Poland

[2]Faculty of Materials Science and Ceramics, AGH-University of Science and Technology, Cracow, Poland

[3]Institute of Solid State Physics, University of Latvia

[4]Institute of Physics, Pedagogical University of Cracow, Poland

e-mail: w.smiga@gmail.com

The perovskite niobates constitute a very interesting group of functional materials, because of their extreme physical parameters sensitive to external factors. Some solid solutions based on a sodium niobate have i.a. a very good piezoelectric properties, moreover, they contain no lead and so they fulfil a very important demand of high technology industry concerning a reduction of the environmental pollution. One of the most interesting and extensively studied system is a lithium niobate -sodium niobate solid solution ($LiNbO_3$-$NaNbO_3$).

Pure and 4 mol% Li-added sodium niobate ceramics were prepared by a two-stage hot-pressing technology in the Institute of Solid State Physics at the University of Latvia. The preliminary structural studies were carried out by X-ray diffraction technique showed the formation of single perovskite phase in the investigated compositions. The effect of Li doping on a microstructure and mechanical properties of the $Li_{0.04}Na_{0.96}NbO_3$ solid solution was investigated at room temperature. The microstructure and EDS measurements were performed by means of scanning electron microscope with field emission Hitachi S4700 and microanalyses system Noran-Vantage. To determine the elastic constants (the Young′s modulus E, the shear modulus G, bulk modulus K and the Poisson′s ratio v) of $Li_{0.04}Na_{0.96}NbO_3$ a method of measurement of the longitudinal (V_L) and transverse (V_T) ultrasonic wave velocities for this type of material was developed. The electric properties of $NaNbO_3$ and $Li_{0.04}Na_{0.96}NbO_3$ ceramics were investigated in the frequency range from 100 Hz to 200 kHz and from room temperature up to 750 K, both in the process of heating and cooling. Both electric permittivity and conductivity exhibit an anomaly as a function of the temperature and frequency. The a.c. electric conductivity as a function of angular frequency $\sigma(\omega)$ follows the relation $\sigma(\omega) = A\omega^s$. The local minima of electrical conductivity σ were observed, which are probably associated with a polaronic transport mechanism.

R-63

Aging and Memory Effects in Electro-Optical PLZT 8/65/35 Ceramics Modified with 3d Transition-Metal Ions

V. Dimza[1], L. Kundziņa[2], M. Kundziņš[1], K. Kundziņš[1], A. Plaude[1]

[1]Institute of Solid State Physics, University of Latvia, Latvia

[2]Riga Technical University, Latvia

e-mail: Vilnis.Dimza@cfi.lu.lv

Most of ferroelectric materials exhibit aging effect (a time-dependent gradual change of physical properties) in their ferroelectric state.

The effects of aging and memory have been studied in a number of jobs, for example, PLZT without admixture - [1-3], PLZT with Mn - [4], the proposed interpretation of effects is controversial.

The aging process of relaxor electro-optical PLZT 8/65/35 (La 8) ceramics modified with Mn, Fe, Co, Cu (Me) additives was studied in this work.

Specific details were investigated in the aging process changes for PLZT 8/65/35 (La 8) ceramics doped with different concentration of Mn additive (Mn = 0.01, 0.1, 0.3, 1.0 and 3.0 wt. %) and Cu admixture.

Cu additive is interesting because the Cu^{2+} ions are both Jahn-Teller ions and ions, sensitive to EPR.

The sample with additives structure changes were controlled by SEM and XRD methods.

Aging effects were studied by measuring the complex dielectric permeability $\varepsilon^*=\varepsilon'-i\varepsilon''$ temperature and frequency dependencies (the frequency range 130 Hz to 1 MHz) and polarization loops P(E).

It was found that aging is significantly reduced at Me = 1 wt.%.

The mechanisms of the phenomena are discussed, such as: migration of oxygen vacancies V_O, reorientation of dipoles like Me^{2+}-V_O, polar nano region growth and their merger in clusters (domains), interfacial space charge polarization. Jahn-Teller ions (Mn^{3+}, Fe^{4+}, Co^{2+}, Cu^{2+}) role in aging process is discussed.

References

1. W. A. Schulze, J. V. Biggers, and L. E. Cross, Journ of the American Ceramic Society **61**, 46(1979)
2. . E. Birks, M. Kundzinsh, A. Sternberg and H. Shmitt, Ferroelectrics **234**(1-4) 263 (1999)
3. F. Cordero, F. Cracuin, A. Franco and C. Galassi Ferroelectrics, **353**, 78 (2007)
4. A. I. Burkhanov, A. V. Shilnikov and V. Dimza, Ferroelectrics **131**, 267(1992)

R-64

p,T,x – Diagram Ferrielectric Crystals $CuInP_2(Se_xS_{1-x})_6$ in the Range $0 \le x \le 1.0$

E.I. Gerzanych, V.Yu. Bihanych, I.Yu. Kuritsa

Uzhhorod National University, Ukraine

e-mail: vanja_k@mail.ru

The influence of hydrostatic pressure on the ferrielectric phase transition crystals $CuInP_2(Se_xS_{1-x})_6$ in the range $0 \le x \le 1.0$. A *p,T,x*-diagram is constructed and the limits of the existence of para- and ferrielectric phases are defined. It is shown that in the region $0.8 \le x \le 1.0$ baric coefficient shift the Curie temperature – is negative, and it is positive in the region $0 \le x \le 0.7$. There is inversion of the sign of the coefficient dT_c / dp at $x \simeq 0{,}75$.

It is established that phase transitions in ferroelectric crystals $CuInP_2S_6$ and $CuInP_2Se_6$ are the transitions of the first type. Isovalent replacement of S↔Se atoms leads to the formation of solid solutions $CuInP_2(Se_xS_{1-x})_6$. Thus, the Curie temperature decreases, both from the sulphide so selenide compounds, while blurring the phase transition. In the area of concentration of I - $(0.75 \le x \le 1.0)$ $dT_c / dx < 0$, and in II - $(0.35 \le x \le 0.75)$ and III - $(0 \le x \le 0.35)$ $dT_c / dx > 0$. Under the influence of high pressure, Curie temperature changes so that in the area of I - $dT_c / dp < 0$, and in II and III - $dT_c / dp > 0$. Concentration change of coefficient of the pressure shift of T_c is equal in the area of concentrations II $\frac{dT_c}{dp \cdot dx} = 130 \frac{K}{GPa \cdot \text{ml.fate}}$. In papers [1,2] it was shown that in the areas III and I corresponding coefficients are equal to 170 and 110.

References

1. Phase transitions in crystals $CuInP_2(Se_xS_{1-x})_6$ in the area $0 \le x \le 0.3$ with compression and *p,T,x*- diagram./ V.Yu. Bihanych, I.Yu. Kuritsa, V.S. Shust , E.I. Gerzanych // Vysnik UzhNU. series physics. - 2010.- v.27. p. 21-28.

2. Phase p, T , x- diagram and inversion of sign the pressure shift the Curie temperature in ferrielectric $CuInP_2(Se_xS_{1-x})_6$./ V.Yu. Bihanych, E.I. Gerzanych // Vysnik UzhNU. series physics. - 2012.- v.32 . p. 7-13.

R-65

Dynamics of Incommensurate Phase Transformation in *C* and 2*C* Polytypes of $TlInS_2$ Ferroelectric

A. Salnik[1], Yu.P. Gololobov[2], R.M. Ischenko[2], N.A. Borovoy[1]

[1]Faculty of Physics, Taras Shevchenko National University of Kyiv, Ukraine

[2]Department of Physics, National Transport University, Ukraine

e-mail: alina.salnik@gmail.com

In present work the crystal structure of *C* and 2*C* TlInS2 polytypes was investigated by single-crystal four-circle X-ray diffraction method in the temperature range 190–250 K. The scanning of reciprocal space of *C* and 2*C* polytypes was performed in directions [*H*0*L*] and [*HHL*] under quasistatic cooling. It was found for C-polytype the existence of satellite reflections with scattering vector $\vec{q}(4\pm\delta;0;5\pm0.25)$ (δ=0.04±0.01) which correspond to incommensurate phase (IP) [1]. These satellites arise as weak lines at temperatures 242–244 K which is much higher than 214 K (avowed temperature of IP creation). Furthermore, the active formation of IP in polytype *C* does not occur at a fixed temperature of 214 K, but in the temperature range of 212–217 K. Measurements of temperature dependences of the incommensurability parameter *δ(T)* shows that below 201 K there occurs an incommensurate phase transformation, at which the modulation wavelength increases in the *H*-direction.

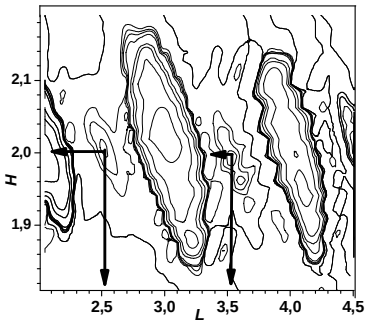

Fig.1 2D-intensity distribution in direction [*H2L*] of reciprocal space. The satellites $\vec{q}(2;2;3\pm0.5)$ are shown

Unlike polytype *C*, IP satellites were not observed at temperature 190–240 K in 2*C* polytype. But an additional maxima $\vec{q}(4;0;5\pm0.5)$ and $\vec{q}(2;2;3\pm0.5)$ were observed at all temperature for this polytype (Fig.1). They are typical for doubling of the unit cell parameter *c*. At the same time, the anomalies on a dependences *c(T)* testify about existence of IP in 2*C*-polytype in a range of 190–230 K. The model of incommensurate phase formation in *C* and 2*C* polytypes was proposed.

References

1. S Kashida, Y Kobayashi, J. Phys. C.: Condens. Matter **11**, 1027 (1999).

R-66

On Photoinduced Phase Transition in Ferroelectric Ag_3AsS_3

A. Salnik[1], Yu.P. Gololobov[2], N.B. Stepanischev[1], N.A. Borovoy[1]

[1]Faculty of Physics, Taras Shevchenko National University of Kyiv, Ukraine

[2]Department of Physics, National Transport University, Ukraine

e-mail: alina.salnik@gmail.com

Proustite Ag_3AsS_3 crystals are well-known materials for nonlinear optics, but the effect of optical irradiation on physical properties of these crystals is rather contradictory. That is why the temperature dependences of the unit cell parameters *a(T)* and *c(T)* of Ag_3AsS_3 were measured by X-ray dilatometry method with high precision in temperature range 100 – 300 K in dark mode and during laser irradiation (λ = 532 nm). It was revealed that the *c* value increased on Δc=(0,002–0,003) Å at T_p=(145–147) K at the cooling under laser irradiation (Fig.1). Such an anomaly may indicate the existence of a first order phase transition (PT) in Ag_3AsS_3 at laser irradiation.

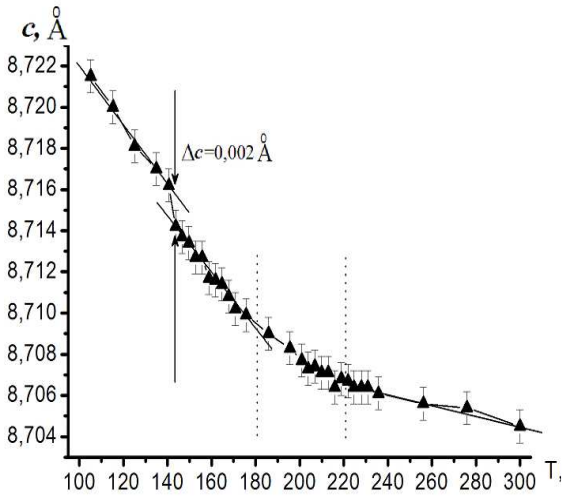

Fig. 1. The dependence *c(T)* under laser irradiation

Also it was investigated the temperature dependences of relative intensity *I(T)* some X-ray structure maxima. In particular, for (312) reflex it was established miscellaneous character of *I(T)* dependences at laser irradiation and in dark mode. Moreover, experimental dependences *I(T)* and *c(T)* demonstrate anomalies at the same temperature range T = 145 ÷ 160 K, so these results confirm the possibility of existence photoinduced PT in Ag_3AsS_3. Observed effects are explained in terms of the redistribution of silver ions on the two groups of vacant crystallographic positions in the unit cell.

R-67

Investigation of $CuInP_2S_6$ Family Layered Crystals under High Hydrostatic Pressure

O.V. Shusta, A.G. Slivka, V.S. Shusta

Department of Physics, Uzhhorod National University, Ukraine

e-mail: sasha.shusta@gmail.com

The investigation of $CuInP_2S_6$ crystals has showed that at T=310K the first-order phase transition occurs, which is connected with the hopping motion of the Cu ions [1]. The enrichment of the crystal by indium $CuIn_{1+d}P_2S_6$ increases the phase transition temperature to T=330 K [2], and the replacement of copper to argentum in $Ag_{0,05}Cu_{0,95}InP_2S_6$ crystals leads to a change in the phase transition temperature to T=300 K.

The influence of the high hydrostatic pressure on the dielectric properties of $CuInP_2S_6$, $CuIn_{1+d}P_2S_6$ and $Ag_{0,05}Cu_{0,95}InP_2S_6$ crystals was investigated. It was found that the phase transition temperature of each of these crystals is increased under pressure, this is typical for order disorder type of phase transition. We also investigated the influence of pressure on the relaxation behavior of dielectric permittivity at low temperatures T<180 K and the pressure behavior of Curie-Weiss constant and Curie-Weiss temperature.

The p,T phase diagram for $CuInP_2S_6$ family crystals was built and its peculiarities were defined. It was established that the deviation of the phase diagrams of the linear law could be connected with the influence of free charge carriers at high temperatures.

References

1. V. Maisonneuve, C. Payen, V. Cajipe, Chem. Matter 5, 783 (1993)
2. A. Dziaugis, J. Banys and Yu. Vysochanskii , Z. Kristallogr. 226, 171 (2011)

R-68

The Influence of an External Electric Field and Uniaxial Pressure on the Dielectric Properties of Co- and Cu-Doped TGS Crystals

A.I. Susla, A.M. Guivan, O.G. Slivka, V.M. Kedyulich, M.S. Zelenyuk

Uzhhorod National University, Faculty of Physics 32 Voloshin Str., UA-88000 Uzhhorod, Ukraine

e-mail: kaf-optics@uzhnu.edu.ua

To change the properties of the Triglycine sulfate (TGS) crystals they are doped by metallic or organic impurities. There are relatively few data on research of Co- and Cu-doped TGS crystals. Therefore, the aim of this paper is to study the dielectric properties of TGS+Co and TGS+Cu crystals under the influence of an external electric field and uniaxial pressure.

In both types of crystals the applying of an external electric field and mechanical stress reduces the maximum value of the dielectric constant. Herewith, the temperature of this maximum increases under the influence of an external electric field whereas it – decreases under the influence of uniaxial pressure. The field dependences of the maximum temperature of the dielectric constant, the values of this maximum and phase σ_2,*T*-diagrams of the crystals under consideration were constructed.

If was shown that the increase in the atomic mass of doped impurities leads to the increase in the phase transition temperature. Thus, for TGS, TGS+Co and TGS+Cu crystals it was, respectively, 321,9 K, 322,9 K and 323,6 K.

The displacement of the phase transition temperature under the influence of uniaxial pressure along the ferroelectric axis of doped crystals was less than for the undoped ones. The pressure coefficients of the shift the phase transition temperature for TGS, TGS+Co and TGS+Cu crystals were, respectively, –7,5, –5,2 and –5,3 K/kbar.

This effect can be accounted for by the existence of internal electric fields in doped crystals, the value of which is determined by the presence of impurities [1, 2]. Therefore, the macroscopic field, which emerges due to the piezoelectric effect, under the mechanical compression inside the crystal is smaller. The presence of such internal field leads to a change in the temperature of the maximum of the dielectric constant even in the absence of external fields, mechanical stresses and blurring dependencies $\varepsilon(T)$.

References

1. Influence of spatially inhomogeneous electric fields on dielectric constant in ferroelectrics / V. M. Kedyulich, E. I. Gerzanich, A. G. Slivka, P. M. Lukach // Scientific Bulletin of the Uzhhorod University, ser. Physics (*in Ukrainian*). – 1999. – № 3. – P. 79-81.

2. Influence of electric field on the ferroelectric phase transition in $Sn_2P_2S_6$ / A. G. Slivka, V. M. Kedyulich, E. I. Gerzanich, V. S. Shusta, P. P. Guranich // Ukr. fiz. z (*in Ukrainian*). – 2000. – V. 45, № 3. – P. 328-331.

R-69

Ab Initio Characterization of Pressure-Induced Metallic State in Ferroelectric $Sn_2P_2S_6$

K.Z. Rushchanskii[1], V. Haborets[2], Y.M. Vysochanskii[2]

[1]Peter Grünberg Institut, Forschungszentrum Jülich and JARA, 52428 Jülich, Germany

[2]Institute for Physics and Chemistry of Solid State, Uzhgorod National University, 88000, Uzhgorod, Ukraine

e-mail: vysochanskii@gmail.com

The second-order ferroelectric instability in the $Sn_2P_2S_6$ (SPS) is driven by non-linear interaction of the low-energy polar B_u mode with full-symmetry mode A_g [1]. The relaxation of lone-pair electrons on Sn^{2+} cations leads to the three-well potential energy surface [1]. A*b inito* derived effective Hamiltonian [1] was used in Metropolis Monte Carlo simulations of the temperature—pressure phase diagram. Modeling revealed chaotic phases as well as phases with quadrupolar ordering in addition to experimentally known tricritical point on the transitions line between paraelectric and ferroelectric phases. Recent neutron and X-ray scattering experiments [2,3] testifies appearance of weak first order nature of the phase transition, which is induced by hydrostatic pressure. *Ab inito* band structure and phonon spectra for both phases of $Sn_2P_2S_6$ are in good agreement with available experimental data at ambient conditions. Calculated spontaneous polarization fits well with experimental value of 16 $\mu C/cm^2$.

Calculated athermal equations of state reveal first-order phase transition from polar Pn to non-polar $P2_1/n$ phase, which occurs near 0.7 GPa. For ambient pressure energy gap is about 2.2 eV. For pressure above 37 GPa energy gap is closed, i.e. monoclinic non-polar phase is in metallic state, in accordance with experimental observation [4]. For the pressure above 37 GPa calculated phonon spectra point out on drastic changes in high-energy phonons. This is result of increasing covalency in S-S interactions. For pressure above 52 GPa transition to triclinic P-1 phase of $Sn_2P_2S_6$ with one formula unit in the cell was revealed. Band structure calculations and phonon structure for this new phase point on significant decrease of covalent P-P bonding in molecular P_2S_6 anions. Metallic behavior of this phase occurs already for pressure above 11 GPa, while at ambient conditions this metastable phase is semiconductor with energy gap about 1.6 eV.

References

1. K.Z. Rushchanskii *et al*., Phys. Rev. Lett. **99**, 207601 (2007)
2. P. Ondrejkovic *et al*, Phys. Rev. B **86**, 224106 (2012)
3. P. Ondrejkovic *et al*, J. Phys.: Condens. Matter **25**, 115901 (2013)
4. S.V. Ovsyannikov *et al*, J. Appl. Phys. **113**, 013511 (2013)

R-70

Tricritical Point and Virtual Ferroelectricity in $(Pb_ySn_{1-y})_2P_2S_6$

R. Bilanych[1], A. Molnar[1], M. Medulych[1], V. Shvalia[1], A. Kohutych[1], R. Yevych[1], A. Dziaugys[2], V. Samulionis[2], J. Banys[2], Yu. Vysochanskii[1]

[1]Uzhgorod National University, 88000 Uzhgorod, Ukraine

[2]Vilnius University, LT-10222 Vilnius, Lithuania

e-mail: vysochanskii@gmail.com

In $Sn_2P_2S_6$ family crystals the ferroelectric ordering is determined by stereochemical activity of tin lone pair electrons [1]. The local three-well potential in ground state could be related to the Blume-Emery-Griffiths model with dipolar and quadrupolar order parameters that predict coexistence of metastable paraelectric phase with ferroelectric ground state [2]. At this, the tricritical point and discontinuity of the ferroelectric transition appear at their temperature lowering by compression or by variation of composition. Under hydrostatic pressure, which suppresses the stereoactivity of tin ions, the tricritical point for $Sn_2P_2S_6$ was found [3,4]. Similar influence on the ferroelectric transition is expected at tin by lead substitution that also lowers covalence of chemical bonds. By dielectric, ultrasound and Brillouin scattering investigations the change from continuous to first order transition was found in $(Pb_ySn_{1-y})_2P_2S_6$ mixed crystals at growth of lead concentration more than $y \approx 0.2$, when the phase transition temperature lowers below 250 K. For composition with $y = 0.45$ clear first order phase transition is observed with wide temperature range (near 30 K) of the phases coexistence. At lead concentration above $y = 0.61$ the centersymmetric state exists till 4.2 K. At low temperatures, the dipole glassy could be obviously presented [5]. For the end $Pb_2P_2S_6$ compound some evidences of possible virtual ferroelectricity were found. For this crystal the lowest energy Raman scattering spectral lines lower their frequencies at cooling. Here it have been also found a growth of the lattice anharmonicity according both Raman and Brillouin scattering data. Moreover, the most important fact is that dielectric susceptibility of $Pb_2P_2S_6$ crystals increases at temperature lowering.

References

1. K.Z. Rushchanskii *et al*., Phys. Rev. Lett. **99**, 207601 (2007)
2. C. Ekiz *et al*., Physica A **293**, 215 (2001)
3. P. Ondrejkovic *et al.*, Phys. Rev. B **86**, 224106 (2012)
4. P. Ondrejkovic *et al.*, J. Phys.: Condens. Matter **25**, 115901 (2013)
5. K. Moriya *et al.*, J. Phys. Soc. Japan **64**, 1775 (1995)

FM&NT-2014 Oral Presentation Abstracts

Fabrication of Bismuth Chalcogenide Nanoribbons by Catalyst-Free Solid-Vapor Technique

J. Andzane[1], G. Kunakova[1], D. Jevdokimovs[1], F. Lombardi[2], D. Erts[1]

[1]Institute of Chemical Physics, University of Latvia, Latvia

[2]Chalmers University of Technology, Gothenburg, Sweden

e-mail: jana.andzane@lu.lv

Bismuth chalcogenides (Bi_2Te_3 and Bi_2Se_3) are narrow band gap layered semiconductors with room temperature thermoelectric properties. The synthesis and physical properties of these materials have been widely studied for more than half a century because of their applications as active elements in thermoelectric micro-generation, local micro-cooling and infrared detectors [1].

The efficiency of thermoelectric materials can be improved by creating structures where one or more dimensions are reduced, such as nanowires, nanoribbons or thin films. Such nanostructured materials show better thermoelectric properties due to reduction of their thermal conductivity and at the same time enhancement of electron conductivity [2].

Previously, high crystalline bismuth chalcogenide nanoribbons were fabricated by Au-catalysed vapor-liquid-solid synthesis [3], but catalyst-free vapor-solid synthesis process was developed only for ultra-thin bismuth chalcogenide nanoplates [4].

Here we present simple catalyst-free vapor-solid synthesis method for fabrication of bismuth telluride and bismuth selenide nanoribbons. 99,999% Bi_2Te_3 and Bi_2Se_3 powders are used as source materials. The synthesis process occurs under low (0.1 Torr) pressure and does not require constant gas flow. Fabricated nanoribbons had high-crystalline structure proved by investigation under transmission electron microscope. Nanoribbons were up to 50 μm long and 20-500 nm wide. Their thicknesses varied in the range from 20 up to 100 nm. Electroconductive and thermoelectrical properties of fabricated nanoribbons were investigated under IR illumination, showing potential perspective application as IR detectors.

References

1. S. Li, M.S. Torpak, H.M.A. Soliman, J. Zhou, M. Muhammed, D. Platzek and E. Muller, Chem. Mater. **18**, 3627 (2006)
2. M. Saleemi, M. S. Torpak, S. Li, M. Johnsson and M. Muhammed, J. Mater. Chem. **22**, 725 (2012)
3. D. Kong, J.C. Randel, H. Peng, J.J. Cha, S. Meister, K. Lai, Y. Chen, Z.-X. Shen, H.C. Manoharan and Y. Cui, *Nano Lett.* **10**, 329 (2010)
4. D. Kong, W. Dang, J.J. Cha, H. Li, S. Meister, H. Peng, Z. Liu, Y. Cui, Nano Lett. **10**, 2245 (2010)

FM&NT Or-2

In-operando XAFS Analysis of Li-sulfur Batteries

G. Aquilanti[1], I. Arčon[2,3], M. Patel[4], L. Stievano[5] and R. Dominko[4]

[1]Elettra - Sincrotrone Trieste s. S. 14 , km 163.5 34149 Basovizza, Trieste,Italy

[2]University of Nova Gorica, Vipavska 13, POB 301, Nova Gorica, Slovenia

[3]J. Stefan Institute, Jamova 39, P. P. 3000, Ljubljana, Slovenia

[4]National institute of Chemistry, P.O.B. 660, SI-1001 Ljubljana, Slovenia

[5]Univeriste Montpellier II, 2 Place Eugene Bataillon–CC 1502, 34095 Montpellier (France)

e-mail: giuliana.aquilanti@elettra.eu

Rechargeable Li-S batteries are most promising solution for automotive applications. Advanced lithium sulphur cell for automotive use with high energy density, charge efficiency and durability, meeting or exceed the safety and low cost standards are being developed within the EU project EUROLIS (www.eurolis.eu). The principle of Li-S battery operation has been known for several decades [1], however, it has not been successfully commercialized yet, mainly due to fast capacity fading and very low columbic efficiency.

One of the key points for a better understanding of the mechanisms of battery operation, which can lead to the technical solutions to optimize the battery performance and design of Li-S cathode materials with superior properties, is the knowledge of the nano-structuration and electrochemical processes in the cathode material and in the electrolyte during battery operation.

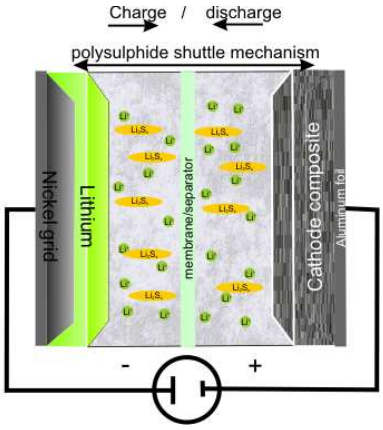

In this work we demonstrate that in operando sulphur K-edge XANES and EXAFS analysis are powerful and indispensable tools for the characterization of the redox chemistry and to monitor the formation of Li-polysulphides and unwanted byproducts in the cathode and those diffused away from cathode material during charging and discharging of the battery [2]. Different sulphur compounds that coexist in the battery (elemental sulphur, sulphur-polysulphides and suphur bound in electrolyte) can be efficiently distinguished, and their relative amount in the cathode can be monitored precisely during the battery operation with sulphur XANES analysis. Additionally, sulfur K-edge EXAFS analysis gives direct insight in the environment and coordination of sulphur atom and allows identification of sulphur byproducs.

The methodological approaches for efficient in-operando XAS experiments at sulphur K-edge (2472 eV) in fluorescence detection mode are presented, the limitations and sources of potential systematic errors in sulphur K-edge XANES and EXAFS analysis due to small and strongly energy dependent penetration depth of X-ray beam and self-absorption effects in the sample are discussed.

Acknowledgement

This work was supported by the European Union Seventh Framework Programme under grant agreement No. 314515 (EUROLIS).

References

1. J.M. Tarascon & M. Armand, Nature, 414 (2001) 359.
2. M. Patel, I. Arcon, G. Aquilanti, L.Stievano, G.Mali, R.Dominko, ChemPhysChem 15 (2014) 894

FM&NT Or-3

Spin-Phonon Relaxation Processes of Transition Metal Ions in ZnO

D.V. Azamat[1], A.G. Badalyan[2], L. Jastrabik [1], J. Lančok[1], M. Fanciulli [3, 4], A. Dejneka[1]

[1]Institute of Physics AS CR, 182 21, Prague 8, Czech Republic

[2]Ioffe Physical-Technical Institute, RAS, 194021, St. Petersburg, Russia

[3]Laboratorio MDM, IMM-CNR, 20041 Agrate Brianza (MB), Italy

[4]Dipartimento di Scienza dei Materiali, Università degli studi di Milano-Bicocca, 20125 Milano, Italy

e-mail: azamat@fzu.cz

Diluted magnetic semiconductors based on ZnO with transition metal ions are widely used nowadays as model objects for testing concepts for spintronics applications. The $3d^5$ transition metal ions such as Fe^{3+} and Mn^{2+} with electron spin S=5/2 potentially provide a spin multiplet for use in the implementation of quantum algorithms. Recently, systems with the same ground state electron configuration as Mn^{2+} in single-crystal MgO [1, 2] and in colloidal ZnO quantum dots [3] have been suggested for quantum computing applications. Here, we report the spin dynamics of transition metal ions in ZnO investigated by the Pulse-Electron Paramagnetic Resonance (Pulse-EPR) technique.

Inversion recovery with electron spin echo detection has been used in order to measure the spin-lattice relaxation time T_1 for Fe^{3+} and Mn^{2+} ions in hydrothermal grown ZnO single crystals. The relaxation of longitudinal magnetization was dominated by the sum of two exponentials with two time constants. To estimate the relaxation rates, we consider direct (one-phonon) and a two-phonon Raman processes. The fitting of these data revealed a Debye temperature for Fe^{3+} and Mn^{2+} significantly lower than the value known for the host matrix. The presence of a second fast time constant in inversion recovery data indicates that cross relaxation transitions between Fe^{3+} and Mn^{2+} ions provide an essential contribution to the relaxation at low temperatures.

References

1. S. Bertaina, L. Chen, N. Groll, J. Van Tol, N. S. Dalal and I. Chiorescu, Phys. Rev. Lett. **102**, 050501 (2009)
2. H. De Raedt, B. Barbara, S. Miyashita, K. Michielsen, S. Bertaina and S. Gambarelli, Phys. Rev. B **85**, 014408 (2012)
3. S. T. Ochsenbein and D. R. Gamelin, Nat. Nanotechnol.**6**, 112 (2011)

FM&NT Or-4

Phonon Spectra of Single-Walled TiO_2 Nanotubes

A. Bandura, R. Evarestov

Institute of Chemistry, Quantum Chemistry Division, St. Petersburg State University, Russia

e-mail: andrei@ab1955.spb.edu

The ab initio quantum mechanical methods have successfully been applied to study of the structure and physical properties of oxide nanotubes (NTs) [1, 2]. The first stage of NT theoretical calculations provides the properties based on the ground state energy and its first derivative on atomic positions and cell dimensions. The next stage of NT simulations should provide more detailed information about the properties defined by the second energy derivatives. These are the quantities which govern the mechanical and thermodynamic stability of nanoobjects. Vibrational frequencies are the first and foremost of them.

In this work we present the first-principles results for the phonon frequencies in the selected TiO_2 nanotubes obtained for the first time. We have considered the two NT morphologies: (1) hexagonal generated by folding of (111) layers of the fluorite TiO_2 phase with chiralities (*n*, *n*) and (*n*, 0), and (2) rectangular generated by folding of (101) anatase layers with chiralities (*n*, *n*) and (*n*, -*n*). Calculations have been made within the density functional theory using the hybrid exchange-correlation functional and localized atomic basis set and a direct (frozen phonons) method for estimating frequencies. Comparative classical force-field [3] simulations allow us to extend the scope of treatable NT periods and diameters. The symmetry analysis of the calculated frequencies has been made via the induced representations of line symmetry groups in two **k**-points (Γ and X) of 1D Brillouin Zone.

The results obtained indicate that NT stability depends on its morphology, diameters and chirality. Thus, the presence of imaginary frequencies indicates the structural instability of (*n*, 0) NT with hexagonal morphology at low diameters (~10 Å). In stable cases the lowest (doubly degenerated) frequency gradually decreases to zero when the NT diameter rising.

Acknowledgements

Authors wish to acknowledge the assistance of the Saint-Petersburg State University Computer Center and financial support from the Russian Foundation for Basic Research (grant 14-03-00107 a).

References

1. R. A. Evarestov, Yu. F. Zhukovskii, A. V. Bandura, S. Piskunov, J. Phys. Chem. C **114**, 21061 (2010)
2. R. A. Evarestov, A. V. Bandura, M. V. Losev, S. Piskunov, Yu. F. Zhukovskii, Physica E **43**, 266 (2010)
3. M. Matsui, M. Akaogi, Mol. Simul. **6**, 239 (1991)

FM&NT Or-5

Defect Thermodynamics of $BaZrO_3$ from First Principles Phonon Calculations

T.S. Bjørheim[1], R. Haugsrud[1], J. Maier[2], E. Kotomin[2]

[1]FASE, Department of Chemistry, University of Oslo, Norway

[2]Max-Planck Institute for Solid State Research, Stuttgart, Germany

e-mail: torsb@kjemi.uio.no

Y-doped $BaZrO_3$ (BZY) is a state-of-the-art high temperature proton conductor with potential application in for instance intermediate temperature solid oxide fuel cells. In BZY, effectively positive oxygen vacancies ($v_O^{\bullet\bullet}$) and protons ($OH_O^{\bullet}$) constitute the dominating charge-compensating defects, with hydration proceeding according to

$$H_2O(g) + O_O^{\times} + v_O^{\bullet\bullet} = 2OH_O^{\bullet}$$

The corresponding hydration enthalpy and entropy, $\Delta_{Hydr}H^{\circ}$ and $\Delta_{Hydr}S^{\circ}$, depend both on dopant concentration and type [1, 2, 3]. Trends in $\Delta_{Hydr}H^{\circ}$ with dopant type are usually rationalized by higher charge density on oxide ions in the vicinity of the dopant [1, 2]. Understanding trends in $\Delta_{Hydr}S^{\circ}$ with dopant type is, however, more intricate as it contains vibrational contributions from both $OH_O^{\bullet}$ and $v_O^{\bullet\bullet}$. In this contribution, we investigate the defect thermodynamics, including vibrational contributions, of undoped and acceptor doped (Sc, Y, In, and rare-earths) $BaZrO_3$ from first principles phonon calculations.

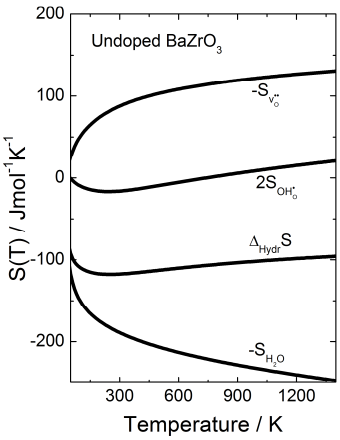

Fig. 1 Calculated $\Delta_{Hydr}S$ of undoped $BaZrO_3$, including the individual contributions from loss of $H_2O(g)$, formation of $2OH_O^{\bullet}$ and consumption of $v_O^{\bullet\bullet}$

All calculations are performed using Density Functional Theory (GGA-PBE) within the VASP code. Phonon spectra are obtained from force calculations using the finite displacement method, from which vibrational contributions to the thermodynamic properties are derived. The calculations are performed under both constant volume and pressure conditions.

The calculated electronic $\Delta_{Hydr}H$ amounts to -74 kJ/mol for undoped $BaZrO_3$ and becomes more exothermic in the order Gd→Y→Sc due to trapping of both $OH_O^{\bullet}$ and $v_O^{\bullet\bullet}$, in line with previous experimental and computational studies [1, 3]. Further, the calculated $\Delta_{Hydr}S$ of undoped $BaZrO_3$ (Fig.1) is also in good agreement with experimental results [1, 2]. The calculations show that the largest contributions to $\Delta_{Hydr}S$ are loss of $H_2O(g)$ and filling of $v_O^{\bullet\bullet}$. The large vibrational contribution from $v_O^{\bullet\bullet}$ is related both to local structural changes and its large negative formation volume (-20 Å/$v_O^{\bullet\bullet}$). Finally, we discuss the effect of dopant choice on the vibrational properties of $OH_O^{\bullet}$ and $v_O^{\bullet\bullet}$.

References

1. K.D. Kreuer *et al*. Solid State Ionics, 2001, 145
2. K.D. Kreuer, Annu. Rev. Mater. Res., 2003, 33
3. M. Björketun *et al*, Faraday Discussions, 2008, 134

FM&NT Or-6

Water-Like Anomaly of Elastic Properties of Inorganic Glasses and Their Melts

V. Bogdanov[1], E. Lähderanta[2], L. Maksimov[3]

[1]St Petersburg State University, St Petersburg, Russia

[2]Lappeenranta University of Technology, Lappeenranta, Finland

[3]Research and Technological Institute of Optical Material Science, St Petersburg, Russia

e-mail: v.n.bogdanov@mail.ru

The present paper is devoted to three questions: on the anomalous ("water – like") temperature dependence of sound velocity in SiO_2, GeO_2, B_2O_3 and in silicate, germanate and borate glasses and melts with the rich content of SiO_2, GeO_2, B_2O_3; on the similarity of elastic properties of water and water solutions with the silicate, germanate and borate glass melts, and on the nature of the frozen-in nano scale inhomogeneities in oxide glasses.

What means water – like anomaly (WLA)? Well known that sound velocity decreases with the temperature practically in all solids and liquids. Exclusions are H_2O, liquid B_2O_3, Al_2O_3, liquid Te, Sb, glassy GeO_2, SiO_2 where velocity increases with the temperature. SiO_2, GeO_2, B_2O_3 glass melts at high (Brillouin) frequencies and at high viscosity range also show WLA. How to explain anomaly? What about this anomaly in other glasses and melts?

Measurements of temperature coefficients of ultrasound velocities (TCV) as a function of modifier concentration in B_2O_3, SiO_2, GeO_2, in a number of binary and ternary germanate, silicate, borate glasses and melts, where glassformer exhibits water - like anomaly (positive TCV), are reported.

WLA is found in pure glassformers of "long" or "strong" type where the existence of a network structure is usually assumed. In these substances WLA is found both in liquid and glassy states. WLA or, at least, tendency to it, is seen in both longitudinal and shear elasticity of such glasses. Adding ionic modifiers to the glassformer (which is supposed to break up the network) diminishes and eventually destroys WLA. It is not yet clear whether it is possible to separate a common for all systems main mechanism of the anomaly. It is assumed that with raising temperature T a structural rearrangement (often modeled as the increasing content of the second structure) takes place leading to a denser packing and higher instantaneous rigidity. These effects must be sufficiently strong to show against the background of "normal" temperature dependence — decreasing v with raising T. Increasing the content of metallic oxides-modifiers in the glass destroys the network by substituting ionic bonds for covalent ones, and then WLA is weaken.

FM&NT Or-7

New Materials for Nanobiophotonics Based on Photonic Crystals

G. Dovbeshko[1], O. Fesenko[1], V. Boiko[1], L. Dolgov[2], V. Kiisk[2], I. Sildos[2], V. Gorelik[3], V. Moiseyenko[4]

[1]Institute of Physics, Natl. Acad. of Sci. of Ukraine. Ukraine

[2]Institute of Physics, University of Tartu, Estonia

[3]P.N. Lebedev Physical Institute of the Russian Academy of Sciences, Russia

[4]Dnipropetrovsk National University, Prospect Gagarina 72, Dnipropetrovsk 49050, Ukraine

e-mail: vb@iop.kiev.ua

Photonic crystals (PC) are nanostructured materials, which posses a periodicity on the length scale comparable with the wavelength of light. Probability of spontaneous fluorescent emission in the PC is defined by the matrix element of the corresponding two-state transition $|\langle m|\hat{H}_{int}|n\rangle|$ and the density of optical states available to the photon emitted g(ω) [1]

$W_{nm} = (2\pi/\hbar)\cdot|\langle m|\hat{H}_{int}|n\rangle|^2\cdot g(\omega)$.

The spectrum of spontaneous emission S(ω) is determined completely by the spectral distribution of frequencies of molecular transitions ω_{nm} and the density of optical states g(ω). In the case of frequencies ω_{nm} lying in the area of photonic band gap, where g(ω) = 0, the spontaneous emission is absent. We registered the maximum of reflectance and minimum of transmittance, respectively, in this case because the light can not escape from PC being localized in the cavities of PC. If the frequency of optical transition of an atom or molecule ω_{nm} is near the edge of photonic band gap, the efficiency of the process of interaction of light and atom (molecules) inside PC could be increased significantly. In this case the bound state of the photon and an atom or molecule forms and emitted photon is kept inside the crystal by means of Bragg reflection and re-absorption.

Described effects were used for amplification of luminescence of the molecules introduced into the cavities of PC. The luminescence of biological objects (DNA, bases, cells) were located near the edge of the band gap of PC. That is why we could enhance the luminescence signal from DNA in 100 or more times. Possible applications of this effect include creation of optical materials, based on the PC and creation of highly sensitive sensors of biological molecules.

Acknowledgement

We thank Nanotwinning FP7 (project ID 294952), Marie Curie ILSES project No. 612620 and Russian-Ukrainian project 27-02-14.

References

1. N. Vats, S. John, K. Busch, *Physical Review A*, **65**, No043808 (2002).

FM&NT Or-8

Nonpolar ZnO Epilayers and ZnO/$Zn_{1-x}Mg_xO$ Multiple Quantum Wells Grown on $LiGaO_2$ by Molecular Beam Epitaxy

T. Yan[1], C.Y.J. Lu[1], L. Trinkler[2], B. Berzina[2], V. Korsaks[2], L. Chang[1], M.M.C. Chou[1] and K.H. Ploog[1]

[1]Department of Materials and Optoelectronic Science/Center for Nanoscience and Nanotechnology, National Sun Yat-Sen University, Kaohsiung 80424, Taiwan, R.O.C.

[2]Institute of Solid State Physics, University of Latvia, Kengaraga 8, 1063 Riga, Latvia

e-mail: lwchang@mail.nsysu.edu.tw

$LiGaO_2$ (LGO) (100) and (010) substrates have demonstrated the potential for growing nonpolar ZnO epilayers [1-2]. The lattice mismatch is 4.2% in $[10\bar{1}0]_{ZnO}$ //$[100]_{LGO}$, 2.0% in $[\bar{1}2\bar{1}0]_{ZnO}$ //$[010]_{LGO}$ and 4.0% in $[0001]_{ZnO}$//$[001]_{LGO}$, respectively, which are low compared to those of sapphire. For $Zn_{1-x}Mg_xO$ (ZMO) epilayers in which 45% Zn is substituted by Mg, the lattice mismatch will change to similar values of ~2.6% in both directions. In this work, m-plane ZnO epilayer and multiple quantum wells (QWs) having $(10\bar{1}0)$ and $(\bar{1}2\bar{1}0)$ azimuth orientation, respectively, were grown on $LiGaO_2$ substrates by plasma-assisted molecular beam epitaxy. For the growth of QWs, a ZnO buffer layer of 30 nm was first deposited on the substrate followed by a layer of 40 nm $Zn_{1-x}Mg_xO$, where x=0.45 for the m-plane QWs and x=0.16 for the a-plane ones. Subsequently, multiple QWs were grown with the well width thickness of 1.1 nm. A 10 nm $Zn_{1-x}Mg_xO$ cap layer was finally deposited on top of the structure.

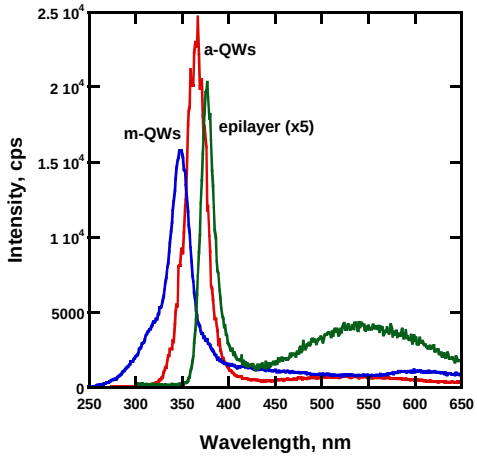

Fig. 1 Room temperature cathodoluminescence spectrum of the epilayer and the QWs samples

Room temperature cathodoluminescence spectrum of the epilayer and the QWs samples are shown in Fig. 1. It indicates that both QWs samples exhibit a strong near band-gap emission peak with different blue shifts of 0.10 eV for the a-QWs and 0.27 eV for the m-QWs. The shift is probably due to effects combining the positive quantum confinement effect and the residual strains.

Acknowledgement

The work was supported by Taiwan-Latvia-Lithuania Cooperation project “Nonpolar ZnO thin films: growth-related structural and optical properties”.

References

1 M. M. C. Chou, D. -R. Hang, C. L. Chen, and Y. -H. Liao, *Thin Solid Films*, **519** (2011) 3627.
2 J. -Y. Yu, T. -H. Huang, L. Chang, Y. -H. Liao, M. M. C. Chou, and D. Gan, *J. Electrochem. Soc.*, 158 (2011) 1166.

FM&NT Or-9

Graphene Sheets versus Carbon Nanotubes: Synthesis, Property, Application

G. Dovbeshko[1], T. Isaeva[1], D. Pidgirnyi[1], Y. Sementsov[2]

[1] Institute of Physics, Nat. Acad. of Sci. of Ukraine, Ukraine

[2]Chuiko Institute of Surface Chemistry, Nat .Acad. Sci. of Ukraine, Ukraine

e-mail: gd@iop.kiev.ua

A discovery of carbon nanostructures namely, fullerenes, carbon nanotubes and graphene, has opened up a new era in scientific research and industrial applications. In this work we present the data on cheap production, certification and comparative analysis of the multi-wall carbon nanotubes (CNTs), graphene nanoparticles (GNPs), graphene flakes and graphene oxide for different application with the emphasis on bionanotechnology. The carbon nanostructures were characterised by conventional Raman spectroscopy, electronic microscopy, Fourie-Transform Infrared (FTIR) spectroscopy and atomic fourth microscopy (AFM). Mechanical property study and quantum-chemical calculation were also used.

We discuss the following points: 1) Which kind of support, CNT or graphene, is better for SEIRA and SERS spectroscopy for analysis of extremely small quantity of molecules [1,2]; 2) The suitability of graphene and CNT/CexOy, CNT/CexOy/AgO complexes as catalytic agents for converting alcohol-containing materials (primary alcohols, aldehydes, esters) to ketones; 3) Applications of CNT/DNA/protein complexes as the tissue implants; 4) Usage of CNTs and graphene as interceptors of biologically active compounds [3]; 5) Usage of CNTs and graphene as anticancer agents; 6) Usage of CNT-based black absorbing coatings for pyroelectric and other thermal detector application [4].

Acknowledgment

Acknowledgment to Nanotwinning FP7 (project ID 294952), Ukrainian-Polish Joint Research Project (2012-2014), FP7 project PIRSES-2012-318617 FAEMCAR for financial support.

References

1. G. Dovbeshko, O. Fesenko, O. Gnatyuk, A. Rynder, O. Posudievsky. J. Nanophoton. **6**(1), 061711(2013)
2. G. Dovbeshko, O. Fesenko, K. Yakovkin, S.Bertrione, A. Damin, D. Scarano, A.Zecchina and E. Obraztsova. MCLC.**496,** 170 (2008)
3. A. Buchelnikov, G. Dovbeshko, D. Voronin, V. Trachevsky, V. Kostjukov, M. Evstigneev, Applied spectroscopy.**68,** 232 (2014)
4. S. Bravina, N. Morozovsky, G. Dovbeshko, O. Fesenko, and E. Obraztsova, Nanosystems, nanomaterials, nanotechnology,**4,** 112 (2008)

FM&NT Or-10

Towards a Practical Rechargeable 5 V Li Ion Battery

R.I. Eglitis[1]

[1]Institute of Solid State Physics, University of Latvia, Latvia

e-mail: rieglitis@gmail.com

Current Li-ion batteries are the state-of-the-art power sources for consumer electronics operating mainly in the 4 V regime. One frequently discussed direction to improve the performance of such batteries is the development of a family of 5 V cathode materials. I report here a Full Potential Liniarized Augmented Plane Wave (FP-LAPW) calculation for $Li_2Co_1Mn_3O_8$ in the F_{d3m} spinel structure [1]. My calculated battery voltage for this material is around 5 V. This result is stable against interchange of positions of Mn and Co atoms as well as the choice of the position of the Li vacancy.

References

1. R. I. Eglitis and G. Borstel, Phys. Stat. Sol. A **202**, R13 (2005)

FM&NT Or-11

Space Charge Limited Current in Bi_2S_3 Nanowires

G. Kunakova[1], R. Viter[2], T. Bauch[3], F. Lombardi[3], J.D. Holmes[4], D. Erts[1]

[1]Institute of Chemical Physics, University of Latvia, Latvia

[2]Experimental physics department, Odessa National I.I. Mechnikov University, Ukraine

[3]Chalmers University of Technology, Gothenburg, Sweden

[4]National University of Ireland, Cork, Ireland

e-mail: Donats.Erts@lu.lv

Semiconductor nanowires have been studied intensively for applications in electronic devices as field effect transistors, chemical sensors and optoelectronics requiring well established contact properties and nanowire electrical characterisation. Frequently, obtained data show nonlinear characteristics often attributed to Schottky barriers. Previous works aimed to electrical characterization of nonohmic semiconductor nanowire devices draw attention on space charge limited currents (SCLC). Reducing the wire size to nanoscale, causes large surface to volume ratio of the nanowires and presence of charge traps enhance their sensitivity to SCLC [1].

There have been several reports on SCLC regime in semiconducting nanowires having nonlinear I(V) behaviour at higher applied voltages and deviation from Ohm`s law. Information of the trap energy distribution and trap density can be derived from nonlinear I(V) characteristics. Here we report on SCLC conduction of Bi_2S_3 nanowires.

Individual Bi_2S_3 nanowires were transferred to the substrate and for electrode fabrication electron beam lithography was used. Electrical measurements were performed in a ^{3}He refrigerator to measure temperature dependent I(V) characteristics.

At temperature of 300 K all nanowire devices showed Ohmic behaviour. Transition from Ohmic to SCLC conduction was observed in range from 200 to 140 K and calculated characteristic trap energy is 0.1 eV. I(V) curves at fixed temperature for several distances between contacts leading to different radius to length ratio were analysed. Well pronounced voltage steps were observed for distances 300 nm and shorter which indicates presence of discrete trap levels or impact of surface states.

References

1. A. Talin, F. Léonard, B. Swartzentruber, X. Wang, and S. Hersee, Phys. Rev. Lett., **101**, 7, 076802, (2008)

FM&NT Or-12

Nanostructural Properties of Holmium Oxide Prepared by the Thermal Decomposition of Organic and Inorganic Precursors

P. Fursikov[1], I. Khodos[2], I. Kovalev[3], M. Abdusalyamova[4], Y. Shulga[1]

[1]Institute of Problems of Chemical Physics RAS, Chernogolovka, Russia

[2]Institute of Microelectronics Technology and High-Purity Materials RAS, Chernogolovka, Russia

[3]Institute of Structural Macrokinetics and Materials Science RAS, Chernogolovka, Russia

[4]Institute of Chemistry of Tajik Academy of Science, Dushanbe, Tajikistan

e-mail: fpv@icp.ac.ru

Like other lanthanide sesquioxides (Ln_2O_3), holmium oxide of the *C*-form, *C*-Ho_2O_3, finds its use in various optical, ceramic, and chemical applications. Nanocrystalline microstructure in this solid is of particular interest, because when the crystallite size decreases down to nanometer scale, the ratio of surface to bulk atoms increases substantially to endow Ho_2O_3 based materials with novel features. Ln_2O_3 can be prepared by a variety of techniques, including the thermal decomposition of various precursors, and low decomposition temperatures being favorable for the formation of nanocrystalline solids. However, the preparation and study of nanocrystalline Ho_2O_3 have been given small attention from researchers.

This work aimed at studying the effect of the nature of precursors and synthesis conditions on structural properties of holmium oxide. Powders of holmium oxide were prepared in bulk from the thermal decomposition of holmium nitrate, chloride, acetate and, first, carbamide-containing complex of Ho [1] as precursors at 600 and 700°C. The powders obtained were investigated by X-ray diffraction, elemental analysis, thermogravimetry, TEM, IR- and Raman spectroscopy. The crystal phase of the solids corresponds to bcc crystal structure of *C*-Ho_2O_3 and consists of nano-sized crystallites, except for the case of holmium chloride which was a well-crystallized powder. XRD analysis and Raman spectroscopy consistently indicate that the bcc lattice parameter of nanocrystalline *C*-Ho_2O_3 exceeds that of the well-crystallized holmium oxide. Main impurities in the nanocrystalline powders of holmium oxide are water and surface adsorbed carbonate species. With the use of HRTEM observations other microstructural features of the powders of Ho_2O_3 are also discussed.

Acknowledgement

The authors are grateful for the support to Russian Foundation for Basic Research (grant No 13-03-01208) and International Science & Technology Center (grant T-1882).

References

1. M.N. Abdusalyamova, F.A. Makhmudov, E.N. Shairmardanov, I.D. Kovalev, P.V. Fursikov, I.I. Khodos, and Y.M. Shulga, J. Alloys Compd. **601C**, 31 (2014).

FM&NT Or-13

Impact of Nanotechnology on Green and Sustainable Growth: Micro- and Nanofibrillated Cellulose. A Nordic Case Study to the OECD

D. Høvik[1], M. Lämsä[2], U. Holmgren[3], E.P. Vico[3]

[1]The Research Council of Norway, Norway

[2]The Finnish Funding Agency for Innovation - TEKES, Finland

[3]Sweden's Innovation Agency - VINNOVA, Sweden

e-mail: dah@rcn.no

Nanotechnology and cellulose fiber can be key factors to speed up forest industry again. It shows a new Nordic study to be included in an OECD report. The point to unique industrial opportunities presented by the Nordic Countries' major raw materials from the forest. This case study was prepared as a part of a wider OECD project presenting Countries Initiatives for Nanotechnology in Green Growth. It is describing the environment, especially the policy environment, in which Micro- and Nanofibrillated cellulose (MFC/NFC) are being developed to contribute to green and sustainable growth in Finland, Norway and Sweden.

From trunk to micro- and nanoscale fibers and chemical components [1]

Fibre structures in wood [2]

Structural element	Size	Approximate number of fibrils per fibre cross-section
Complete fibre diameter	13 micrometer	1 (one)
Macrofibril	0.75 micrometer	236
Microfibril	0.15 micrometer	5902
Nanofibril	10 nanometer	1,330,000

Figure 1. Structure and relationship between fibres in a wood log

The potential and the main applications of nanotechnology for green growth is discussed, - how nanotechnology is being included in the broader green growth policy agenda, and finally developing "good practices" and tools for policy makers to evaluate the impact of the technology on green growth in socio economic and environmental terms.

The financing of the necessary steps from pilot scale up to the production scale is a pervasive problem in all three Nordic countries, according to this study.

References

1. Copyright University of Canterbury, 1996. Artwork by Mark Harrington

2. E.*C.* Homonoff, R.E. Evans, C.D. Weaver. Engineered Fibers: Nanofibrillated Cellulose Fibers Presentation to 2008 TAPPI Nanotechnology Conference. June 25-27, 2008. St Louis, MO

An Innovative Electron Beam Lithography Writing Strategy for High Speed and Precision Lithography of Large Circle Arrays for Microfiltration and Photonics in Solar Cells

M. Kahl[1], A. Rudzinski[1], M. Kirchner[1], K.E. Burcham[2], J.E. Sanabia[2], O. Humbach[3], M. Fleger[3]

[1]Raith GmbH, Dortmund, Germany

[2]Raith America, Inc., Ronkonkoma, NY, USA

[3]temicon GmbH, Dortmund, Germany

e-mail: sales@raith.de

With a growing world population, nanotechnology is one approach to address the rising demands for improving the quality of food and for green energy.

Nano sieves for micro-filtration are proposed to serve a growing demand for filtration, e.g. for beer or milk production. Many groups have already indicated that perforated membranes with sharply defined cylindrical pore diameters will have a broad range of applications, such as sterile filtration (particle and bacteria) and size exclusion-based separation.

In green energy, solar cells are seen as a promising method for energy generation; but their cost and efficiencies would need to be drastically improved in order for them to become a viable option. Controlling the scattering of photons in the absorbing material by adding photonic crystal arrays or other periodic nanostructures can potentially enhance the efficiency of these devices.

In both applications, the large circle arrays can cover significant areas (over several square centimeters), and writing times by patterning with conventional Electron Beam Lithography (EBL), “stitching errors”, and pitch control between adjacent “stitched” fields could be issues, especially for photonic crystal arrays.

To meet the needs of these applications, we present and discuss the differences between two EBL patterning modes, one being the conventional stitching EBL, and the other being a new and unique “stitch-error-free” EBL writing strategy called “Modulated Beam and Moving Stage”. We demonstrate that this technique can produce large circle arrays for nano sieves and photonic crystals with uniform pore size distributions, fast EBL patterning times, and with virtually no stitching boundaries and high pitch accuracy.

FM&NT Or-15

Challenges in Energy Applications of Non-stoichiometric Complex Perovskites

E.A. Kotomin[1,2], M.M. Kuklja[3], Yu.A. Mastrikov[1], R. Merkle[2], J. Maier[3]

[1]Institute for Solid State Physics, University of Latvia, Kengaraga str. 8, Riga, Latvia

[2]Max Planck Institute for Solid State Research, Heisenbergstr. 1, Stuttgart, Germany

[3]Materials Science and Engineering Dept, University of Maryland, College Park, USA

e-mail: kotomin@fkf.mpg.de

Two ABO_3-type perovskite solid solutions (BSCF: $Ba_{1-x}Sr_xCo_{1-y}Fe_yO_{3-\delta}$ and LSCF: $La_{1-x}Sr_xCo_{1-y}Fe_yO_{3-\delta}$), mixed ionic – electronic conductors, recently have attracted a lot of attention because of a wide range of potential applications in modern technologies, e.g. gas separation membranes, solid oxide fuel cells (SOFC), etc. The structural defects, first of all oxygen vacancies and antisite defects in perovskites, affect many properties and worsen performance of the perovskite materials in specific applications.

In this study, we present results of first principles calculations of the perfect BSCF and LSCF crystals, the crystals containing basic point defects (cation and anion vacancies, cation exchange, and antisite defects), disorder (Frenkel and Schottky), and a set of relevant solid-solid solution reactions [1,2]. Our DFT modeling reveals that oxygen Frenkel defects, full Schottky disorder and partial Schottky disorder accompanied by the growth of a new phase (e.g. a parent perovskite) all have relatively low formation energies and are favorable. The obtained cation exchange energies are very low for both the A- and B- sublattices of the perovskite structure; this leads to a formation of new phases or interphases.

We explored and analyzed in great detail the oxygen vacancy formation energies in the cubic and hexagonal phases of BSCF and demonstrated that a high concentration of vacancies (oxygen non-stoichiometry), in fact, serves as a stabilizing factor that governs the preference of the cubic phase over the hexagonal phase. We also discuss peculiarities of the oxygen vacancy diffusion in BSCF and LSCF. We established that the *A*/*B*-site cation size mismatch in BSCF leads to the unusually low oxygen vacancy formation energy, which causes a considerable non-stoichiometry, and facilitates vacancy migration with a prominent charge transfer at the transition state. The smaller mismatch between *A*- and *B*-site cations in LSCF results in twice higher vacancy formation energy and higher migration activation barrier, which give rise to a smaller oxygen vacancy concentration and thus a slower oxidation reaction, as compared to BSCF.

Based on the above-discussed results of first principles calculations of the defect formation and migration energies, as well as oxygen atom and molecule adsorption on perovskite surfaces, we calculated the diffusion-controlled kinetics of oxygen reduction reaction (ORR) as a function of adsorbed oxygen and surface vacancy concentrations [3]. This allowed us to determine *the rate-determining steps* (which is important for improvement of fuel cell and permeation membrane performances) and suggest interpretation of available experimental data.

References

1. M. M. Kuklja, Yu. A. Mastrikov, B. Jansang, and E.A. Kotomin, *J. Phys. Chem. C* **116** (2012) 18605−18611
2. M. M. Kuklja, E.A. Kotomin, R.Merkle, Yu. A. Mastrikov, J. Maier, *Phys. Chem. Chem. Phys.* **15** (2013) 5443 (a review article).
3. Yu. A. Mastrikov, R. Merkle, E. Heifets, E.A. Kotomin, J. Maier, J. Maier, J. *Phys. Chem. C* **114** (2010) 3017.

FM&NT Or-16

Transition Metal Doped Indium Sulfide Films by Chemical Spray Method

A. Katerski[1], I. Oja Acik[1], K. Otto[1], A. Mere[1], M. Krunks[1]

[1]Department of Materials Science, Tallinn University of Technology, Estonia

e-mail: Malle.Krunks@ttu.ee

Indium sulfide films prepared by several chemical and physical methods are recognized buffer layers for chalcopyrite absorber solar cells. According to quantum calculations, β-In_2S_3 where In atoms are partially substituted by transition metals (TM) is able to sustain the two-photon absorption processes [1]. In_2S_3:TM is a likely absorber material for an intermediate band solar cell. It has been shown that single-phase β-In_2S_3 films can be deposited by low-cost chemical spray pyrolysis (CSP) method considering the formation chemistry introduced in [2].

In this paper we study the deposition of Ti-doped In_2S_3 thin films by CSP method. In_2S_3:Ti films were prepared using $InCl_3$ as Indium source, titanium alkoxide complexes and titanium terachloride as Titaniun source and $SC(NH_2)_2$ as Sulfur source. We studied the effect of the titanium source type and concentration and the film growth temperature on film properties. The films are characterised by means of XRD, SEM/EDX, Raman and optical spectroscopies. Spraying of the solutions containing stabilised titanium acetylacetonate or chloride reduces unit cell volume of In_2S_3 films and decreases width of the band gap (indirect transitions, Fig.1). Phase composition, structural and optical properties of the sprayed films depending on the titanium source is discussed.

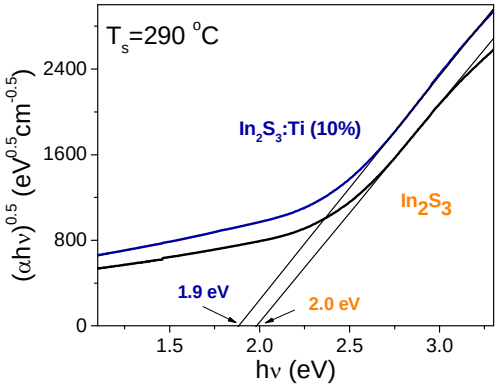

Fig.1 Determination of Eg for In_2S_3 and In_2S_3:Ti films deposited by CSP method at 290 °C .

References

1. P. Palacios, et al., Phys. Rev. Lett. **101**, 046403 (2008)
2. K. Otto, et al., J. Therm. Anal. Cal., **105**, 615 (2011)

FM&NT Or-17

High-pressure X-ray Absorption Spectroscopy Study of Tin Tungstates

A. Kuzmin[1], A. Anspoks[1], A. Kalinko[2], J. Timoshenko[1], R. Kalendarev[1], L. Nataf[2], F. Baudelet[2]

[1]Institute of Solid State Physics, University of Latvia, Latvia

[2]Synchrotron SOLEIL, l'Orme des Merisiers, Saint-Aubin, France

e-mail: a.kuzmin@cfi.lu.lv

Tin tungstate ($SnWO_4$) has two polymorphs, the low-temperature orthorhombic α-phase and high-temperature cubic β-phase, which transform into each other by a diffusion-controlled phase transition mechanism at ~670°C [1]. At the same time, β-$SnWO_4$ can be stabilized at room temperature by rapid cooling that makes its investigation more practical. The two phases have small band gaps (E_g=1.7 (2.6) eV in α-$SnWO_4$ (β-$SnWO_4$)) and unique band structures, strongly influenced by the second-order Jahn-Teller effect (SOJT) due to the W-O partially covalent bonding and the presence of the lone pair of Sn 5s electrons [2,3].

In this study we have conducted room-temperature pressure-dependent (0-25 GPa) x-ray absorption spectroscopy at the W L_1 and L_3 edges of α-$SnWO_4$ and β-$SnWO_4$ using the dispersive set-up of the bending-magnet SOLEIL ODE beamline and high-pressure nano-diamond anvil cell. The detailed analysis of experimental data suggests that upon increasing pressure a displacement of tungsten atoms by about 0.2 Å towards the center of the WO_6 octahedra occurs in α-$SnWO_4$, whereas the coordination of tungsten atoms changes from tetrahedral to distorted octahedral in β-$SnWO_4$ (Fig. 1). The obtained results will be discussed based on the results of our first-principles calculations [3].

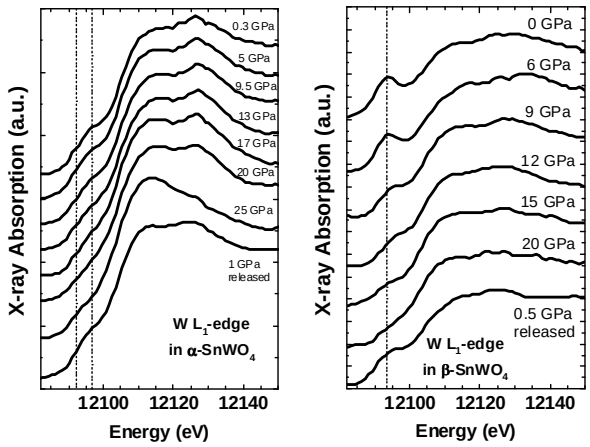

Fig.1. Pressure dependence of the W L_1-edge x-ray absorption spectra in α-$SnWO_4$ and β-$SnWO_4$.

References

1. W. Jeitschko and A. W. Sleight, Acta Cryst. B **28**, 3174 (1972); **30**, 2088 (1974).
2. I.-S. Cho, In-Sun Cho , C. H. Kwak, D. W. Kim, S. Lee, K. S. Hong, J. Phys. Chem. C **113**, 10647 (2009).
3. A. Kuzmin, A. Anspoks, A. Kalinko, J. Timoshenko, R. Kalendarev, Phys. Scripta **89**, 044005 (2014).

FM&NT Or-18

Electrical Properties and Redox Stability of Nb-substituted $SrVO_3$ as Prospective SOFC Anode Material

J. Macías, A. Yaremchenko, J. Frade

Department of Materials and Ceramic Engineering, CICECO, University of Aveiro, 3810-193 Aveiro, Portugal

e-mail: jmacias@ua.pt

Perovskite-like $SrVO_{3-\delta}$ exhibits high electrical conductivity under reducing conditions and good resistance to sulfur poisoning and carbon deposition, and can be considered, therefore, as a promising parent material for solid oxide fuel cell (SOFC) anodes [1-3]. Its applicability is however limited due to a rather narrow $p(O_2)$-stability domain of the perovskite phase coincident with fuel atmospheres. Under oxidizing conditions, $SrVO_3$ transforms into insulating V^{5+}-based compounds; this transformation is not fully reversible at T < 1000C and is accompanied with significant dimensional changes. The present work was focused on the effect of Nb substitution into vanadium sublattice on the stability domain, electrical conductivity and thermal expansion of $SrVO_{3-\delta}$.

$SrV_{1-y}Nb_yO_{3-\delta}$ ceramics were prepared by solid-state reaction route assisted with high-energy milling, and sintered at 1500ºC in 10%H_2-N_2 atmosphere. XRD analysis in combination with microstructural studies (SEM/EDS) confirmed that the solid solubility range of Nb cations in $SrVO_{3-\delta}$ cubic perovskite lattice under applied conditions corresponds to ~ 25% of vanadium sites. The characterization of ceramic materials included measurements of electrical conductivity as function of temperature, $p(O_2)$ and time (in redox cycles), and controlled-atmosphere thermogravimetry and dilatometry. Substitution with niobium was found to result in a moderate decrease of electrical conductivity, but also suppresses to some extent high thermal expansion, characteristic for $SrVO_{3-\delta}$, and shifts the perovskite phase stability boundary to higher oxygen partial pressures.

References

1. S. Hui, A Petric, Solid State Ionics **143**, 275 (2001)
2. C. Peng, J. Luo, A.R. Sanger, K.T. Chuang, Chem. Mater. **22**, 1032 (2010)
3. Z. Cheng, S. Zha, L. Aguilar, M. Liu, Solid State Ionics **176**, 1921 (2005)

XPS Depth Profiling of Organic and Organic/Inorganic Multilayer Systems

M. Mannsberger[1], T.S. Nunney[2], A.E. Wright[2] and P. Mack[2]

[1]Thermo Fisher Scientific, Austria

[2]Thermo Fisher Scientific, United Kingdom

e-mail: michael.mannsberger@thermofisher.com

Devices based on thin organic or polymer layers are becoming increasingly important in a wide variety of applications; from OLEDs, touchscreens and electronics, to medical implants and consumer products. These devices are typically composed of complex stacks of thin/ultrathin layers of novel organic or organometallic compounds, together with inorganic materials. There is an increasing requirement for compositional profiling of these devices.

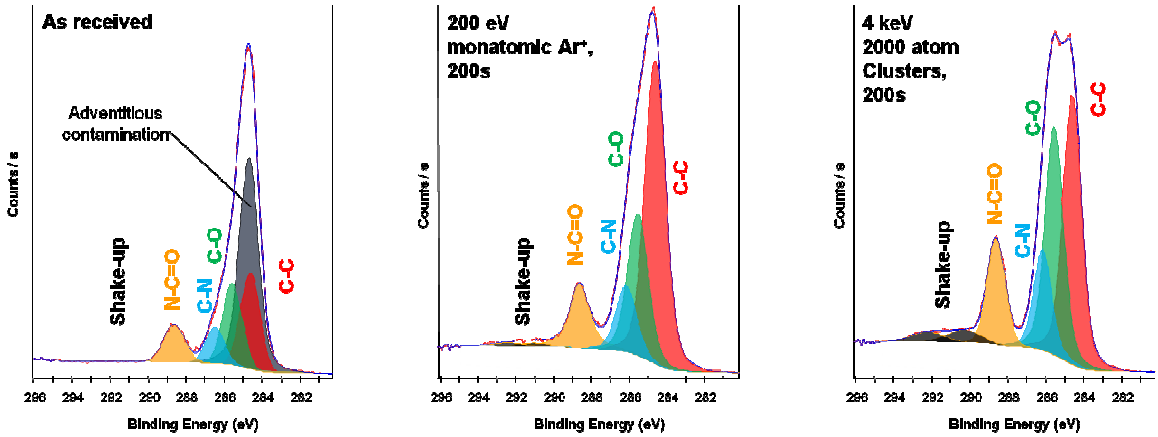

Fig.1 C1s spectra of polyimide. (a) as received, (b) after 200s sputtering in mono mode, (c) after 200s sputtering in cluster mode

Traditional methods using argon monomer ion profiling results in a high degree of damage to the underlying chemistry of the surface and near-surface region which contributes to the XPS spectra, as shown in figure 1. The Thermo Scientific™ MAGCIS dual mode source (www.xps-simplified.com), capable of operating in both monatomic and cluster ion modes, overcomes those deficits and allows depth profiling of polymer-based structures, cleaning metal oxides without change of the oxidation state, and analysis of complex multilayer devices. In this presentation we will illustrate with examples, how MAGCIS enables these types of analyses.

References

1. Cumpson, P. J., Portoles, J. F., Barlow, A. J., Sano, N. and Birch, M. (2013), Surf. Interface Anal., 45: 1859–1868.
2. Cumpson, P. J., Portoles, J. F., and Sano, N. (2013) J. Vac. Sci. Technol. A 31, 020605;

FM&NT Or-20

Plasmonic Solar Cells by Low-Cost Chemical Spray Method

A. Mere[1], A. Katerski[1], E. Kärber[1] I. Oja Acik[1], T. Dedova[1], I. Sildos[2], R. Land[3], M. Krunks[1]

[1]Department of Materials Science, Tallinn University of Technology, Estonia

[2]Institute of Physics, University of Tartu, Estonia

[3]Thomas Johann Seebeck Department of Electronics, Tallinn University of Technology, Estonia

e-mail: arvo.mere@gmail.com

The surfice plasmon resonance effect could be attracted for the incresing absorption ability of the thin film absorber layer in thin film solar cells [1]. Plasmonic solar cells were grown entirely by chemical spray pyrolysis using an extremely thin $In_2S_3/CuInS_2$ as buffer/absorber to uniformly cover either planar ZnO or ZnO nanorod layer. Gold(III) chloride trihydrate ($HAuCl_4 \cdot 3H_2O$) was used as precursor for the synthesis of gold nanoparticles [2]. Au-nanoparticles were formed via thermal decomposition of $HAuCl_4 \cdot 3H_2O$ solution at 0.01-0.1 mol/L concentrations. Current-voltage characteristics and external quantum efficiency were used to evaluate the cell output. A relative increase of 20% in short circuit current density is achieved using plasmonic particles in the cell with planar layers, while 15% relative increase is obtained for cell on ZnO nanorods. EQE spectra (Fig.1) show increased carriers collection in long wavelength region due to plasmon resonance effect caused by gold nanoparticles.

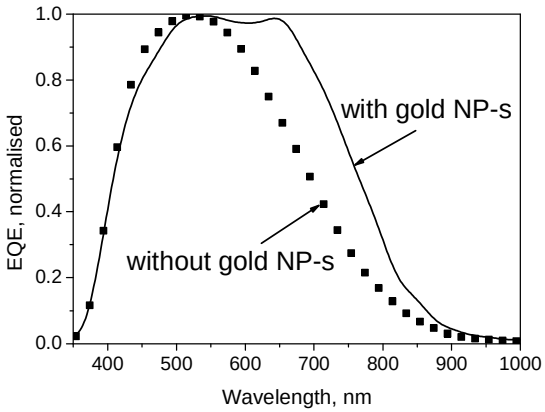

Fig.1 External quantum efficiency spectra of sprayed $ZnO/In_2S_3/CuInS_2$ solar cells with and without gold nanoparticles in $CuInS_2$ absorber layer

References

1. H.A. Atwater, A. Polman, Nature Materials, **9**, 205 (2010)
2. I.Oja Acik, L. Dolgov, M. Krunks, A. Mere, V. Mikli, S. Pikker, A. Loot, I. Sildos, Thin Solid Films, **553,** 144 (2014)

Optimization of Optical Parameters for Qubit Operation in Photonic Crystals

H. Nihei[1], A. Okamoto[2]

[1]Health Sciences University of Hokkaido, Japan

[2]Hokkaido University, Japan

e-mail: nihei@hoku-iryo-u.ac.jp

The realization of quantum bit (qubit) using two excited states of an atom (or a quantum dot) embedded in photonic crystals is one of the challenging goals in the area of physics and the theory of nanostructures [1]. A significant issue for carrying out qubit operation is to cause a strong oscillation between the excited states. The strength of oscillation depends on two optical parameters: the detuning (δ) of the atomic transition frequency from a photonic band edge and the strength (Ω) of the control laser for coupling the excited states. A strong oscillation requires a high laser strength ($\Omega >> 0$) and the atomic transition frequency to be deep inside the PBG ($\delta << 0$). However, a high laser strength causes a wide Rabi splitting leading to $\delta \to 0$, so that we should optimize δ and Ω [2, 3]. Figure 1 shows the time-averaged probability of finding the atom on excited states as a function of the laser strength Ω for various values of the detuning δ. Furthermore, Figure 2 shows a contour plot of the time-averaged probability for δ and Ω. It also shows that the time-averaged probability has a ridge fitting to a line *L*. The fitting line *L* maximizes the time-averaged probability, which provides the optimum value of a pair of δ and Ω for causing strong oscillation between the excited states. These results are useful for determining the designs of a qubit based on solid-state photonic crystal systems.

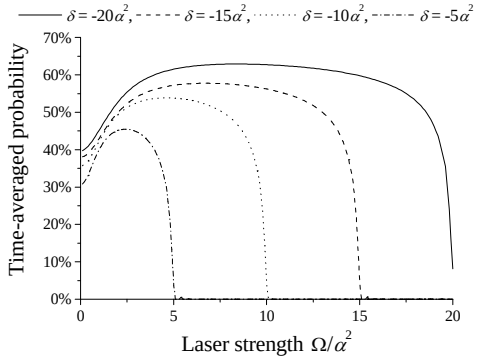

Fig. 1 Time-averaged probability. α is a scaled parameter [3].

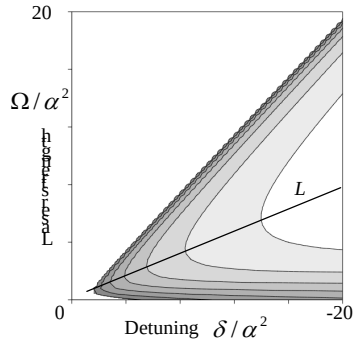

Fig. 2 Contour plot of the time-averaged probability.

References

1. S. John, Nature, vol. 460, p. 337, 2009.
2. H. Nihei and A. Okamoto, J. Mod. Opt., vol. 55, pp. 2391-2399, 2008.
3. H. Nihei and A. Okamoto, J. Opt. and Quant. Electron., 44, 3-5, pp. 265-271, 2012.

FM&NT Or-22

Electrochemical Measurements of the Electronic Density of States

G.A. Niklasson

Department of Engineering Sciences, The Ångström Laboratory, Uppsala University P.O. Box 534, SE-75121 Uppsala, Sweden

e-mail: gunnar.niklasson@angstrom.uu.se

The electronic density of states of metal oxides can in many cases be measured by electrochemical techniques [1], such as chronopotentiometry or impedance spectroscopy. When small ions such as protons or Li ions are intercalated into a material, which is used as the working electrode in an electrochemical cell, electrons must be inserted from the back contact to maintain charge neutrality. These electrons will enter into previously unoccupied states and the Fermi level will shift upwards in energy as intercalation proceeds. Provided that the rigid band approximation holds, measuring the inserted charge during this process will give an image of the electronic density of states over 1 to 2 eV from the band edge.

We have compared the so called electrochemical density of states obtained by this method to density functional calculations for a number of oxides. The electrochemical technique is able to give results in qualitative agreement with calculations. We have studied a number of metal oxides such as WO_3, TiO_2, V_2O_5, Sb:SnO_2, In:SnO_2, IrO_2 as well as some NiO based coatings.

There are a number of questions that need to be better understood in order to make the technique fully quantitative, though. A limitation is that the number of ions that can be intercalated in a given material is restricted. In addition, the ions do not distribute uniformly in the coating but probably exhibit a gradient in concentration, due to slow kinetics of the process. In addition, the validity of the rigid band approximation is largely an open question.

The technique will be useful for screening the density of states of a large amount of coatings in the laboratory. Then interesting materials and specimen can be selected for further studies by advanced techniques, such as photoelectron or X-ray spectroscopies at synchrotron facilities.

References

1. M. Strömme, R. Ahuja and G.A. Niklasson, Phys. Rev. Lett. 93 (2004) 206403.

FM&NT Or-23

Manipulation of Nanoparticles with Different Morphology Inside a Scanning Electron Microscope

B. Polyakov[1], S. Vlassov[1,2,3], L.M. Dorogin[2,3], J. Butikova[1], M. Antsov[2,3], S. Oras[2,3], R. Saar[2,3], I. Kink[2] and R. Lõhmus[2,3]

[1]Institute of Solid State Physics, University of Latvia

[2]Institute of Physics, University of Tartu, Riia 142, 51014, Tartu, Estonia

[3]Estonian Nanotechnology Competence Center, Riia 142, 51014, Tartu, Estonia

e-mail: sven.oras@ut.ee

Polyhedron-like gold nanoparticles (NP) and sphere-like silver NPs on an oxidized Si substrate were manipulated with a XYZ nanomanipulator to analyze the dependence of static friction and contact area on particle geometry. The experiments were carried out inside a scanning electron microscope thus providing visual guidance for the experiment while force was simultaneously measured with a QTF based force sensor with a sharp tip glued to it. This allows for the correlation of particle trajectory with the interaction force between tip and NP and enables to distinguish between continuous and abrupt motion. The general behavior of Ag and Au NPs during manipulation is very similar.

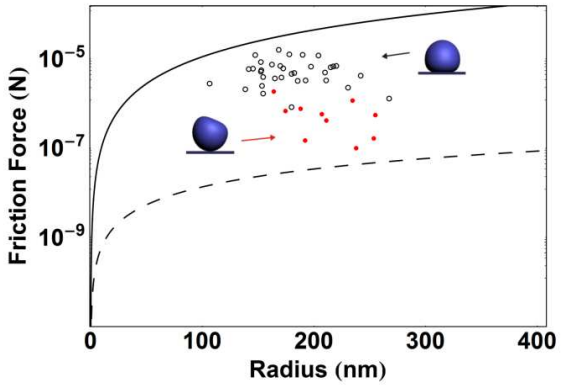

Fig. 1 The static friction forces of Ag NPs on a Si wafer as a function of particle radius. It can be seen that the friction forces determined by different methods (dots and circles) are between theoretically curves calculated by DMT-M model (dashed curve) and frozen droplet model (solid curve).

The theoretical static friction forces were calculated by various methods. For Ag NPs contact areas were calculated using both Frozen droplet model and DMT-M[1] model while for Au NPs the contact areas were determined by applying geometrical considerations on the polyhedron-like particles. The theoretical friction force was then compared with experimentally measured friction force. It was shown that experimental and theoretical data was in good agreement with each other both in case of Au and Ag NPs[2].

References

1. B.V. Derjaguin et al, *J. Colloid Interface Sci.* 1975, *53* , 314-326.
2. B. Polyakov et al, *Beilstein Journal of Nanotechnology.* 2014, *5*, 133-140

Precise Tuning of the Photonic Band Gap Using Multilayered Inverse Opals

L. Österlund[1], D. T. Lebrun[1], V. Kaplaklis[2], G. Niklasson[1], P. K. Sahoo[3], and S. Anand[3]

[1]Dep. Engineering Sciences, The Ångström laboratory, Uppsala University, SE-751 21 Uppsala, Sweden

[2]Dep. Physics and Astronomy, The Ångström laboratory, Uppsala University, SE-751 21 Uppsala, Sweden

[3]School of Information and Communication Technology, KTH-Royal Institute of Technology, Electrum 229 SE-16440 Kista, Sweden

e-mail: lars.osterlund@angstrom.uu.se

Inverse opals are photonic band gap (PBG) structures with a periodic arrangement of voids with low refractive index (air) in a high-refractive index dielectric media with sub-wavelength periodicity. Inverse opals have recently been suggested in photocatalysis applications. Here the idea is to match the edge of the PBG with the electronic band gap of a semiconductor to allow for efficient light absorption. Here we present a novel approach to tune the position and shape of the PBG by purposefully deposit multilayers of oxides with controlled thicknesses on the inside walls of the inverse opals. This avoids technical problems of changing diameter and materials of the opals. The fabrication involves a three-step process: Self-assembly of polystyrene (PS) particles by volume dip coating; atomic layer deposition (ALD) of metal oxides (Al_2O_3) to fill the voids between PS particles; and subsequent Ar+ ion etching and calcination to crystallize and develop the inverse opal structure. ALD is then repeated to make multi-layer structures of TiO_2 with controlled thickness. The inverse opals were characterized by optical spectroscopy, XRD, electron microscopy, and profilometry. In addition, band structure calculations of the inverse opals were made by the plane-wave expansion method together with finite-difference time-domain simulations of the transmission spectra (Fig. 1). Our method is versatile and can be used to fabricate multilayer inverse opals with e.g. reactive nanoparticles on the inside walls; as well as plasmonic nanoparticles embedded in the layers to efficiently absorb slow light.

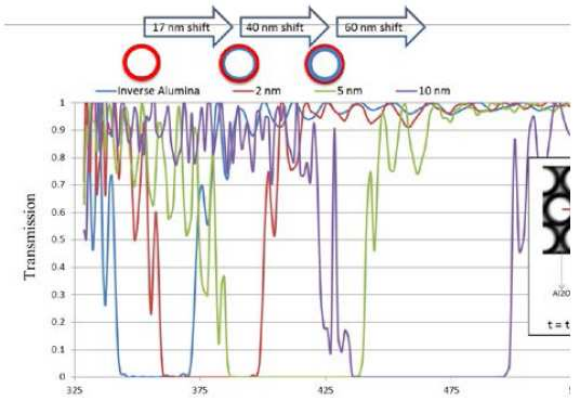

Fig.1 Finite-difference time-domain numerical electromagnetic simulations of inverse opal Al_2O_3/TiO_2 multilayer structures for different TiO_2 layer thicknesses. The experimental results are reproduced with a TiO_2 layer thickness t = 2 nm, lattice spacing D = 190 nm.

FM&NT Or-25

Dark Relaxation of Holographic Gratings in Azobenzene and Chalcogenide Films

A. Ozols, P. Augustovs, K. Kenins, V. Kokars, E. Zarins, K. Traskovskis, D. Saharov

Faculty of Material Science and Applied Chemistry, Riga Technical University, Latvia

e-mail: aozols@latnet.lv

Studies of transmission holographic grating (HG) relaxation (recorded with *s-s*, *p-p*, *s-p*, *L-L*, *L-R* laser beam polarizations) have been carried out in organic molecular azobenzene glassy films W-50, W-75, K-RJ-9 and chalcogenide glassy film a-As_2S_3 film. HG with the periods of 0.50, 2.0 and 8.6 μm were studied in these films. It is found that recording efficiency in the same sample depends on both recording polarizations and HG period. The HG stability in the course of relaxation also depends on these factors. In almost all cases the maximum recording efficiency was achieved with *p-p* or *L-R* polarizations at 2.0 μm period. The HG stability did not correlate with the recording efficiency, and in most cases corresponded to *s-s* or *L-L* polarizations at 8.6 μm period. It was higher in the samples with higher glass transition temperature, T_g . In other experiments, whose co-authors were V.Kokars and K.Traskovskis, Kleinman's second-order nonlinear coefficient d_{33} was also more stable during the relaxation in the case of the films with higher T_g values.

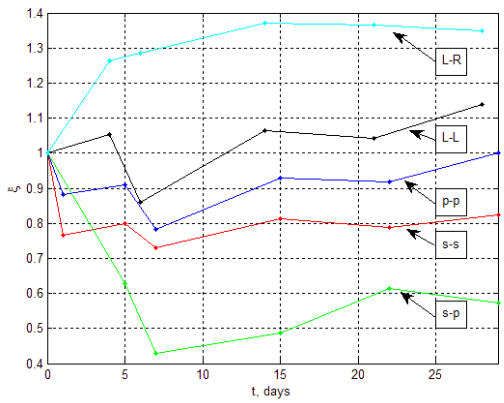

Fig.1 The dark relaxation time dependences of relative diffraction efficiency ξ of HG recorded with different recording beam polarizations in azobenzene film W-75 with the period of 0.50 μm. The ξ=1 value corresponds to the initial diffraction efficiency. Similar oscillating time dependences were observed also in other cases.

The HG dark (relaxational) self-enhancement of HG was observed in the case of W-75 [*L-R* polarizations, 0.50μm (Fig.1); *s-s* polarizations, 2.0μm] and K-RJ-9 (*p-p* polarizations, 8.6μm) samples. In the latter case the dark self-enhancement of HG was also observed in reflection mode. Relaxational effects are explained in terms of post-recording mass transfer.

Acknowledgment

The financial support of the Latvian State Research Program on Multifunctional Materials is greatly acknowledged.

FM&NT Or-26

Electronic and Optical Properties of Magnesium and Calcium Hydroxides: The Role of Covalency and Many-body Effects

A. Pishtshev[1], S.Zh. Karazhanov[2], M. Klopov[3]

[1]Institute of Physics, University of Tartu, Tartu, Estonia

[2]Institute for Energy Technology, Kjeller, Norway

[3]Tallinn University of Technology, Tallinn, Estonia

e-mail: aleksandr.pishtshev@ut.ee

In the present work, within PBE-GGA and range-separated hybrid functional schemes we have carried out DFT electronic structure calculations on magnesium and calcium hydroxides $X(OH)_2$ (X = Mg and Ca). Concerning the overall bonding picture, it was shown that a crystal-chemical integrity of the hydroxides is governed by the oxygen via a bridging combination of the strong covalent bonding in the hydroxyl anion and the X-O ionic connection. This feature is a principal component of the multifunctionality of $X(OH)_2$ compounds because it provides the equal utilization of electronic characteristics such as large band gap and low refractive index (relevant to purely ionic systems) and the covalent contributions from the oxygen. Electronic structure analysis shows that (i) the $X(OH)_2$ hydroxides are direct band gap insulators; (ii) the calculated fundamental band gaps are in the range of 7.7 - 8.3 eV for $Mg(OH)_2$ and 7.3 - 7.6 eV for $Ca(OH)_2$; (iii) effective masses of carriers in vicinity of the band extreme are strongly anisotropic, and for the electrons are similar to those in ZnO. Optical properties of the bulk crystalline $X(OH)_2$ hydroxides have been studied by using the many-body Hedin's GW approximation combined with the numerical solution of BSE. The existence of excitonic states possessing large binding energies of 0.46 eV for $Mg(OH)_2$ and 0.85 eV for $Ca(OH)_2$ has been predicted for the first time. Our analysis indicates that the origin of the excitons is attributed to the strong localization of the hole to oxygen $2p_x$, $2p_y$ occupied states and the electron to oxygen and metal *s* empty states. The potential of applicability of the crystalline $X(OH)_2$ compounds in semiconductor device engineering and optoelectronics is discussed.

Acknowledgment

This work was supported by the European Union through the European Regional Development Fund (Centre of Excellence “Mesosystems: Theory and Applications”, TK114) as well as by the Research Council of Norway within the FME and ISP NANOMAT projects.

FM&NT Or-27

Electromagnetics of Tannin-based Carbon Foams

M. Letellier[1], J. Macutkevic[2], A. Paddubskaya[3], A. Plyushch[3], P. Kuzhir[3], S. Maksimenko[3], M. Ivanov[2], J. Banys[2], A. Pizzi[4], V. Fierro[1], A.Celzard[1]

[1]IJL-UMR Université de Lorraine – CNRS 7198, ENSTIB, France

[2]Vilnius university, Lithuania

[3]Research Institute for Nuclear problems of Belarusian State University, Belarus

[4]LERMAB – EA Université de Lorraine 4370, ENSTIB, France

e-mail: polina.kuzhir@gmail.com

Tannin-based rigid foams and their carbonaceous counterparts are new, easily fabricated, cellular solids based on renewable resources [1]. Prepared from raw, commercial, mimosa bark extracts as a major component, and being cheap and lightweight, they are able to compete with more expensive synthetic polymer foams [2]. Broadband dielectric analysis of tannin-based carbon foams produced at 7 different densities, ranging from 0.048 to 0.114 g/cm^3, was carried out in wide frequency (20 Hz – 35 GHz) and temperature (25 – 300 K) ranges.

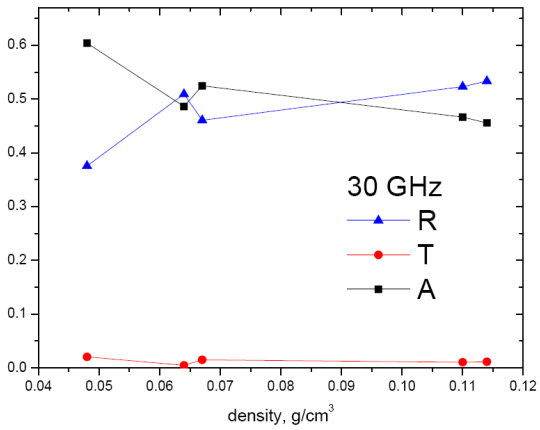

Fig.1 Absorption/transmission/reflection (A/T/R) coefficients measured and calculated at 30 GHz for 2 mm thick carbon foams vs their density.

The average values of electromagnetic (EM) attenuation at 30 GHz for 2 mm thick carbon foam was -18 – -20 dB (see Fig.1). Such absolute values are higher than those presented by polymer composites containing high concentrations (5-20 wt.%) of nanocarbons [3]. Dielectric permittivity (and therefore EM interference shielding ability) has been observed to be almost temperature independent in the range 200-400K.

To conclude, being environment-friendly, cheap, extremely lightweight, chemically inert, thermally stable and at the same time highly conductive in static regime and providing very good EMI shielding ability in microwaves and in wide temperature range, tannin-based carbon foams should be an interesting alternative to various commercialized EM shields and filters.

References

1. W. Zhao, A. Pizzi, V. Fierro, G. Du, A. Celzard, Material Chemistry and Physics **122**, 175 (2010).
2. G. Tondi, W. Zhao, A. Pizzi, G. Du, V. Fierro, A. Celzard, Bioresource Technology **100**, 5162 (2009).
3. F. Qin and C. Brosseau, J. Appl. Phys. **111**, 061301 (2012)

FM&NT Or-28

Silver and Gold Nanodumbbells for Tribological Experiments

B. Polyakov[1], S. Vlassov[1], L. Dorogin[2,3], M. Antsov[2,3], R. Zabels[1], J. Butikova[1], K. Smits[1], and R. Lohmus[2,3]

[1]Institute of Solid State Physics, University of Latvia, Latvia

[2]Estonian Nanotechnology Competence Centre, Estonia

[3]Institute of Physics, University of Tartu, Estonia

e-mail: boris.polyakov@cfi.lu.lv

In this work, metal nanodumbbells (NDs) have been formed by laser-induced melting of Ag or Au nanowires (NWs) on an oxidized silicon substrate, and their tribological properties have been investigated [1]. ND formation is a complicated dynamic process, which involves extreme temperature gradients, and includes rapid heating and melting of the ends of NWs, contraction of liquid droplets into spheroidal bulbs followed by rapid solidification. The mechanism of ND formation is proposed and illustrated with Finite Element Method simulations.

Nanodumbbells (ND) are highly attractive objects for nanomanipulations and tribological experiments. ND can be roughly considered as two spheroid NPs connected by a NW. NDs can be produced by pulsed laser processing of metal NWs. If the distance between the rounded ends of NW is short enough, the dumbbell rests on the rounded ends mainly. Thus, ND ends ensure relatively small contact area, reduced adhesion and static friction. Therefore, NDs can be easily manipulated, and different types of motion can be distinguished: rolling (fig. 1a), rotation (fig. 1b-d).

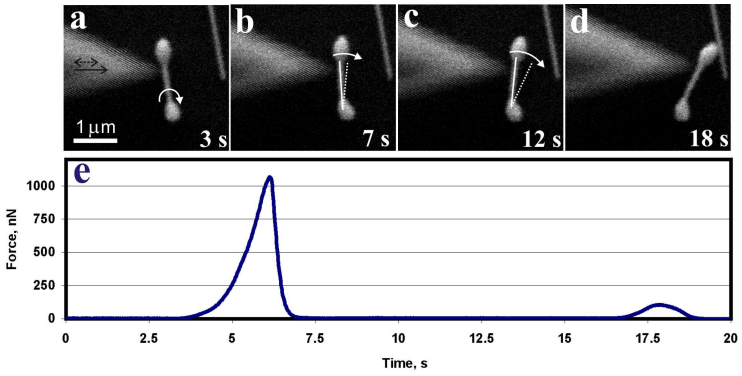

Fig. 1. Example of Ag ND Nanomanipulation inside SEM.

Tribological measurements consist of controllable real time manipulation of NDs inside a scanning electron microscope (SEM) with simultaneous force registration. More information on experimental technique can be found in our previous work [2]. The geometry of NDs enables to distinguish between different types of motion, i.e. rolling, sliding, and rotation. Real contact areas are calculated from the traces left after the displacement of NDs, and compared to the contact areas predicted by the contact mechanics and frozen droplet models.

References

1. B.Polyakov, S.Vlassov, L.Dorogin, N.Novoselska, J.Butikova, M.Antsov, S.Oras, I.Kink, R.Lõhmus. Nanoscale Research Letters 9, 186 (2014)
2. B.Polyakov, S.Vlassov, L.Dorogin, J.Butikova, M.Antsov, S.Oras, I.Kink, R.Lõhmus. Beilstein Journal of Nanotechnology 5, 133–140 (2014)

FM&NT Or-29

First-Principles Calculations of V_2O_5 Nanotubes

V.V. Porsev, A.V. Bandura, R.A. Evarestov

Institute of Chemistry, Quantum Chemistry Division, St. Petersburg State University, Russia

e-mail: vporsev@gmail.com

Nanotubes (NT) of divanadium pentoxide (or VO_x in general case) are the subject of an intensive research due to their promising physical and chemical applications. The reported syntheses of the VO_x NTs and experimental studies of their properties are numerous. However the theoretical studies of V_2O_5 NTs are restricted to a few publications (see [1] and references therein), where the extended Hückel theory has been used.

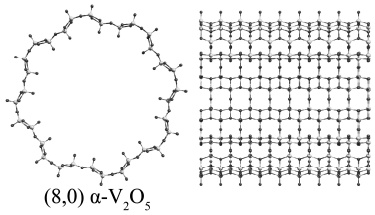

(8,0) α-V_2O_5

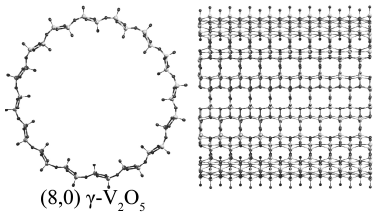

(8,0) γ-V_2O_5

In this work we present the results of hybrid DFT-HF calculations with PBE0 exchange-correlation functional of the structure and energetics of V_2O_5 nanotubes. The basis of atomic orbitals implemented in CRYSTAL09 computer code [2] has been used in our simulations.

We have calculated the nanotubes rolled up from both the layers of α-V_2O_5 (α-NT) and layers of γ-V_2O_5 (γ-NT) with (*n*,0) and (0,*n*) chiralities. The simulations have been performed for the chiralities from (4,0) to (16,0) and from (0,9) to (0,25), correspondingly.

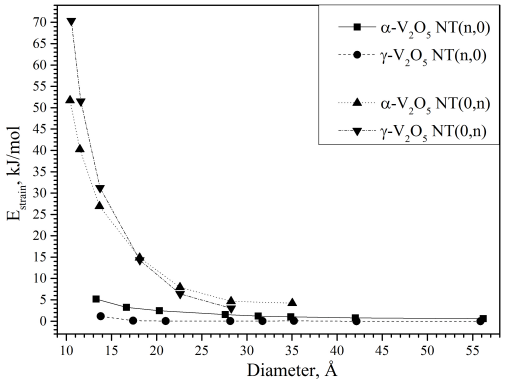

The obtained data show that the strain energy E_{str} of NT with (*n*,0) chiralities are close to zero for the both phases due to unique flexibility of the considered layers. E_{str} of NTs with (0,*n*) chiralities are considerably larger. It should be noted, that the E_{str} values of the relaxed α-NTs are larger than those of the γ-NTs.

Acknowledgements

Authors are grateful to St. Petersburg State University for the financial support and computer center facilities.

References

1. A. N. Enyashin, at al., Chem. Phys. Lett., **392**, 555 (2004).
2. R. Dovesi, at al., Z. Kristallogr., **220**, 571 (2005).

FM&NT Or-30

GaAs and $Ga_{1-x}Al_xAs$ Overlayer Formation on GaAs (111) Substrate Plane by Organometallic Vapor Phase Epitaxy

S. Larkin[1], A. Avksentyev[1], M. Vakiv[2], R. Krukovsky[1], Y. Kost[2], S. Krukovsky[2], I. Saldan[3]

[1]Scientific & Industrial Concern "Nauka", 20 Dovnar-Zapolskogo St., 01314, Kiev, Ukraine

[2]Scientific Research Company "Carat", 202 Stryiska St., 79031, Lviv, Ukraine

[3]Department of Physical and Colloid Chemistry, Ivan Franko National University of Lviv, 6 Kyryla and Mefodiya St., 79005, Lviv, Ukraine

e-mail: ivan_saldan@yahoo.com, horo56@i.ua

The mechanisms of GaAs overlayer growth with crystallographic orientation (111) by MOCVD at low pressure have not been fully clarified [1,2]. Therefore the aim of the research was to study the temperature and element (A^{III} and B^{V}) ratio influences on the structural and electrical properties of the deposited overlayer.

The GaAs and $Ga_{1-x}Al_xAs$ epitaxial growth on GaAs (111A) substrate plane was carried out by organometallic vapor phase epitaxy at pressure ~70 Torr. The regime of a quantitative modulation of trimethylgallium, $Ga(CH_3)_3$, gas flow was applied to optimize the atomic ratio between A^{III} and B^{V} on the substrate surface while the tangential and normal components of the growth rate were comparable. Deposited GaAs and $Ga_{1-x}Al_xAs$ overlayers with crystallographic orientation of (111A/B) were obtained at ~0.1-0.2 Torr pressures of arsine, AsH_3, gas and low crystallization temperature ~570-620 ºC. Their observed morphology and proposed mechanism of the defect-free GaAs and $Ga_{1-x}Al_xAs$ surface crystallization was discussed in details. Physical and electrical properties of the obtained epitaxial materials were studied experimentally.

Technological approach to form structurally perfect overlayer with high-quality morphology and good electrical properties is proposed based on the experiments. The results can provide valuable data to perform GaAs and $Ga_{1-x}Al_xAs$ epitaxial growth on the substrates with crystallographic orientation (111) in practice.

References

1. M. Umenura, K. Kuvahara, S. Fuke, J. App. Phys. **68**, 97 (1990)
2. S. Fuke, V. Umenura, N. Yamada, J. App. Phys. **72**, 313 (1992)

FM&NT Or-31

Luminescence, Energy Migration and Energy Transfer Processes in Gd_2SiO_5 and $(LuGd)_2SiO_5$ Single Crystals Doped with Ce^{3+}, Eu^{3+} and Tb^{3+} Ions

V. Bondar[1], A. Krasnikov[2], M. Nikl[3], T. Shalapska[2], O. Sidletskiy[1], S. Zazubovich[2]

[1]Institute for Scintillation Materials NAS of Ukraine, 60 Lenin Ave. 61001 Kharkiv, Ukraine

[2]Institute of Physics, University of Tartu, 51014 Riia 142, Tartu, Estonia

[3]Institute of Physics AS CR, Cukrovarnicka 10, 162 53 Prague, Czech Republic

e-mail: tetiana.shalapska@ut.ee

Rare earth oxyorthosilicate single crystals are well established commercial scintillator materials which have found a number of important applications in high energy physics, nuclear physics, tomographic medical X-ray imaging, etc. owning to their high light yield, high density, effective atomic number and fast decay time. The studies of gadolinium containing oxyorthosilicates have shown that a strong overlap of the absorption and emission bands of Gd^{3+} leads to an effective energy migration through the Gd^{3+} sub-lattice with the subsequent energy transfer from a Gd^{3+} ion towards an adjacent impurity ion. In Ce^{3+}-doped gadolinium oxyorthosilicates, these processes result in the enhancement of the scintillation efficiency, but lead to the appearance of an undesirable slow component in the decay kinetics of the Ce^{3+}-related emission [1, 2]. Similar phenomenon is found also in Eu^{3+}- and Tb^{3+}-doped gadolinium oxyorthosilicates, which can be considered as good candidates for lighting applications [3, 4]. The aim of this work is the investigation of peculiarities of the energy migration and transfer processes in Gd_2SiO_5 and $(LuGd)_2SiO_5$ crystals doped with Ce^{3+} and Eu^{3+} or Tb^{3+} ions having different outer electron shells *(5d* and 4*f*, respectively). For that, the steady-state and time-resolved emission and excitation spectra as well as the luminescence decay kinetics are studied at 4.2-300 K in the μs-s time range. It is concluded that the $Gd^{3+} \rightarrow Eu^{3+}$ and $Gd^{3+} \rightarrow Tb^{3+}$ energy transfer occur only in the closest pairs through a short-range exchange interaction, while the $Gd^{3+} \rightarrow Ce^{3+}$ energy transfer is possible also in more separated pairs mainly due to the long-range multipolar interaction.

References

1. H. Suzuki, T.A. Tombrello, C.L. Melcher, C.A. Peterson, and J.S. Schweitzer, Nucl. Instrum. Methods Phys. Res. A **346**, 510 (1994)

2. I. Kamenskikh, A.N. Belsky, A.V. Gektin, M.V. Limonova, S. Neicheva, and O. Sidletskiy, IEEE Trans. Nucl. Sci. **61**, 1 (2014)

3. Y. Chen, B. Lui, Ch. Shi, M. Kirm, M. True, S. Vielhauer and G. Zimmerer, J. Phys.: Condens. Matter **17**, 1217 (2005)

4. M. J. J. Lammers and G. Blasse J. Electrochem. Soc. **134**, 2068 (1987)

FM&NT Or-32

Electromechanics and Electromagnetics of CNT- and Graphene-Based Nanoporous Materials: *Interconnects and Nanosensoring*

Y. Shunin[1,2], Yu. Zhukovskii[1], V. Gopeyenko[2], N. Burluckaya[2], T. Lobanova-Shunina[3] and S. Bellucci[4]

[1]Institute of Solid State Physics, University of Latvia, Latvia

[2]Information Systems Management Institute, Latvia

[3]Riga Technical University, Aviation Institute, Latvia

[4]INFN - Laboratori Nazionali di Frascati, Frascati (Rome), Italy

e-mail: yu_shunin@inbox.lv

Electromechanical and electromagnetic properties of CNTs and graphene-based nanoporous materials are essential for various nanotechnology applications, e.g. for engineering new classes of ultra-light, highly conductive nanomaterials with exceptional mechanical strength, flexibility, and elasticity. We pay major attention to CNTs, graphene nanoribbons and nanofibers (GNR and GNF), CNT- and graphene-based aerogels (CNTBA, GBA), CNT- and grapheme-based 3D-nanofoams and carbon-based polymer nanocomposites, as to the basis for the unique nanoelectronic devices, revolutionary membrane materials (due to their strength and atomic thickness) and nanosensors. Particular properties of carbon-based nanoporous systems in dependence on porosity extent, morphology and fractal dimension allow finding practically useful correlations between their mechanical and electrical properties.

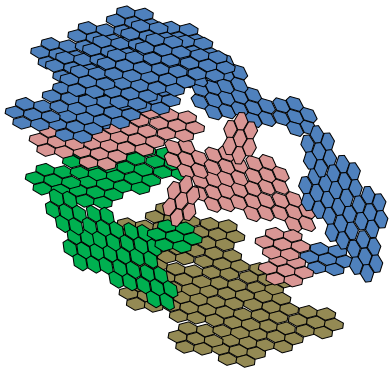

Fig. 1. Structural model of GBA: covalent bonding in interconnects between statistically parametrized GNR and van der Vaalse type bonding of GNR layers.

Nanoporous systems are considered as complicated ensembles of basic nanocarbon interconnected elements (e.g., CNTs or GNRs with possible defects and dangling boundary bonds) within the effective media type environment (see Fig.1). Interconnects are essentially local quantum objects and are evaluated in the framework of the developed cluster approach based on the multiple scattering theory formalism as well as effective medium approximation[1], which allows calculating the above mentioned nanosized systems' local electronic densities of states, conductivity, force interaction constants, etc. Technological interest in contacts of CNTs or GNRs with other conducting elements in nanocircuits [2], FET-type nanodevices, CNTBA and GBA, carbon-based nanofoams constitutes the reason for estimating their electromagnetic properties including interconnect impedances, which depend on chirality effects and electromechanical properties as some integrated effect of macroscopic structural deformations.

References

1. Yu. N. Shunin, Yu. F. Zhukovskii, V. I. Gopejenko, N. Burlutskaya, S. Bellucci. In: Nanodevices and Nanomaterials for Ecological Security, Yu. Shunin and A. Kiv, Eds. Series: Nato Science for Peace Series B - Physics and Biophysics, Springer Verlag, 237-262 (2012)

2. Yu. N. Shunin, Yu. F. Zhukovskii, V. I. Gopejenko, N. Burlutskaya, T. Lobanova-Shunina and S. Bellucci, Journal of Nanophotonics **6**(1), 061706-1-16 (2012)

FM&NT Or-33

Praseodymium Luminescence in Zirconia Nanocrystals and Single Crystals

K. Smits[1], J. Xu[2], J. Grabis[3], D. Millers[1], L. Grigorjeva[1]

[1]Institute of Solid State Physics, University of Latvia, Latvia

[2]Shanghai Institute of Technology, China

[3]Institute of Inorganic Chemistry, Riga Technical University, Latvia

e-mail: smits@cfi.lu.lv

The study of time-resolved luminescence of Y stabilized as well as Pr ion activated zirconia single crystals and free standing nanocrystals (with the same contamination) was carried out. Zirconis single crystals were grown by skull melting process, the nanocrystals were synthesized with the same contamination of activators by Sol- Gel and microwave driven hydrothermal methods. To exclude the Y impact on Pr luminescence also Ca stabilized and Pr codoped nanocrystal samples were prepared.

The different excitation sources (e-beam, x-ray, lasers 6,42eV, 4.66eV and 3.67eV) were used in experiments. The previous research shows that intrinsic defects in nanocrystals and in single crystal are the same, however the defect concentration and distribution is various [1]. The comparison of Pr doped nanocrystals and single crystals gives additional information about the defect type and distribution. The RE ions are used as luminescent probes to analyze the local symmetry and energy transfer.

The intrinsic defects related and activator luminescence bands were observed. The RE ion luminescence showed that this luminescence decay kinetics depends on both activator and intrinsic defects concentration in nanocrystals. The intrinsic defect affected Pr ion luminescnece were studied using Pr line fine structure at low temperatures. Different Pr sites were found and defect impact on dopand luminescence will be discused.

References

1. K. Smits, J. Lumin. **131**, 2058–2062 (2011)

FM&NT Or-34

Shape Restoration Effect and Enhanced Fracture Resistance of Ag/SiO_2 Core-Shell Nanowires

S. Vlassov[1], B. Polyakov[1], L.M Dorogin[2,3], M. Vahtrus[2,3], M. Antsov[2,3], M. Mets[2,3], R. Saar[2,3], R. Lõhmus[2,3]

[1]Institute of Solid State Physics, University of Latvia, Kengaraga 8, LV-1063, Riga, Latvia

[2]Institute of Physics, University of Tartu, Riia 142, 51014, Tartu, Estonia

[3]Estonian Nanotechnology Competence Centre, Riia 142, 51014, Tartu, Estonia

e-mail: vahtrus@ut.ee

Silver nanowires (Ag NWs) are promising material for nanoscale systems due to their excellent electrical and thermal properties, perfect structure and easy syntheses. Potential applications of Ag NWs include waveguides, sensors, solar cells and transparent, flexible and conductive films. As Ag NWs are subjected to mechanical stresses and deformation in many of these applications, improvement of mechanical properties is essential for performance and reliability of the devices. One possible way to significantly enhance properties is by combing Ag NWs with oxide materials in one core-shell heterostructures.

In the present work core-shell structures were synthesized by covering commercially available Ag NWs (BlueNano) with SiO_2 shells by sol-gel method. Cantilevered beam-bending technique was used for mechanical characterization of obtained heterostructures. In plane bending of single core-shell nanowires were carried out by 3D nanomanipulator (SLC-1720-S, SmarAct) equipped with a self-made force sensor installed inside a SEM (Vega-II SBU, TESCAN). The force sensor was made by gluing an AFM cantilever with a sharp tip (ATEC- CONT) to one prong of a commercially available quartz tuning fork [1]. Additional bending tests were conducted inside a high resolution FEI Helios Nanolab SEM using polar coordinate manipulator (Kleindiek MM3A-EM) without force sensor. Remarkable mechanical properties of Ag/SiO2 core-shell nanowires were demonstrated. Strong dependence of deformation type on deformation rate, shape restoration effect promoted by electron beam, as well as superior durability was noted.

References

1. S. Vlassov, B. Polyakov, L. Dorogin, M. Antsov, M. Mets, M. Umalas, R. Saar, R. Lõhmus, I. Kink, Mater. Chem. Phys., 134, 1026-1031

FM&NT Or-35

Energy Levels of Glass Forming Low Molecular Weight Organic Compounds in Thin Amorphous Film

A. Vembris, J. Latvels, R. Grzibovskis, K. Pudzs

Institute of Solid State Physics, University of Latvia, Latvia

e-mail: aivars.vembris@cfi.lu.lv

Energy levels of molecule in molecular crystals have been intensively investigated few decades ago by E. Silinsh, V. Capek and others [1, 2]. Experimental methods for energy level determination were developed at that time. Nowadays in organic optoelectronic devises mostly use polycrystalline or amorphous thin films where no ordered structure is. This is especially true for amorphous films where molecules are aligned in all passible directions.

In the work energy levels of glass forming pyranyliden and indandion derivatives in thin films was measured and analyzed. Two types of samples were made. Spin coated thin film with the thickness of 300 nm on ITO substrate were made for photoelectron emission measurements. Sandwich type samples (ITO/ organic compound/ Al) were prepared for photoconductivity and temperature modulated space charge limited current (TM-SCLC) measurements. Organic layer about 600 nm was spin coated on ITO substrate and semi-transparent Al layer was thermally evaporated in vacuum.

Ionization energy of molecule in thin film was obtained from threshold value of photoelectron emission spectral dependence. The difference between molecular ionization energy and electron affinity energy is adiabatic energy gap which could be obtained from threshold energy of photoconductivity spectral dependence. These two measurements give possibility to obtain hole conductivity (molecule ionization energy) and electron conductivity (electron affinity energy) levels of thin films. TM-SCLC method provides information about local trap states between hole and electron conductivity levels. Energy level correlation on molecular structure and its made thin film will be discussed.

Acknowledgment:

This work has been supported by the European Social Fund within the Project No. 2013/0045/1DP/1.1.1.2.0/13/APIA/VIAA/018

References:

1. E. A. Silinsh, Organic Molecular Crysrtals: Their Electronic States. New York: Springer-Verlag Berlin Heidelberg, 1980,
2. E. A. Silinsh, V. Capek, Organic Molecular Crystals: Interacton Localization, and Transport Phenomena, American Institute of Physics, New York, 1994

Phase Stability and Thermochemical Expansion of $Ba_{0.5}Sr_{0.5}Co_{0.8}Fe_{0.2}O_{3-\delta}$ Mixed-Conducting Ceramics under Oxidizing Conditions

A.A. Yaremchenko, A. Davarpanah, J.M. Pérez, J.R. Frade

Department of Materials and Ceramic Engineering, CICECO, University of Aveiro, 3810-193 Aveiro, Portugal

e-mail: ayaremchenko@ua.pt

Perovskite-like $Ba_{0.5}Sr_{0.5}Co_{0.8}Fe_{0.2}O_{3-\delta}$ (BSCF) attracted attention in the last decade as a prospective material for dense ceramic oxygen separation membranes and solid oxide fuel cell cathodes. This work addresses the thermochemical expansion behavior of this material, which determines the compatibility with other solid oxide cell materials as well as dimensional stability under gradients of oxygen partial pressure or under electrode polarization, and stability of BSCF perovskite structure at elevated oxygen partial pressures.

Thermal and chemical expansion were evaluated in the $p(O_2)$ range 10^{-4}-1.00 atm in combination with the data on oxygen nonstoichiometry (δ). BSCF exhibits rather high thermal expansion coefficients – $(24.1\text{-}24.5)\times10^{-6}$ K^{-1} at 773-1273 K and $p(O_2)$ = 0.21-1.00 atm. This puts constrains on applicability of BSCF in single-phase porous electrodes as well as planar mixed-conducting membranes. On the other hand, BSCF demonstrates favorably small chemical expansion compared to many other mixed conductors, originating from the smaller δ variations with $p(O_2)$, and larger unit cell less sensitive to temperature and nonstoichiometry changes.

Another limitation of BSCF is the stability of perovskite lattice at oxygen pressures $\geq$ 1 atm. Apart from well-known issues of BSCF lattice instability at temperatures close to 1073 K, this mixed conductor was demonstrated to undergo a partial transformation to additional oxygen-rich phase at elevated $p(O_2)$. On heating in pure oxygen at ambient pressure, this transformation occurs at 410-470°C; once formed, the oxygen-rich phase is stable up to ~950°C. As formation of this phase seems to be limited mainly to the surface, this may affect the surface exchange kinetics and therefore may result in degradation of performance of mixed-conducting membrane or SOFC cathode.

The effect of partial substitution with zirconium or niobium into B sublattice of BSCF on thermochemical expansion and perovskite lattice stability is also evaluated.

FM&NT-2014 Poster Presentation Abstracts

F-1

Technet_nano: the Cooperation Network of Clean Room Facilities in BSR

T. Plank, M. Kodu, R. Rammula, N. Austa, A. Tarre

Institute of Physics, University of Tartu, Estonia

e-mail: toomas.plank@ut.ee

A Baltic Sea Region (BSR) programme [1] project "Technet_nano – Transnational network of public clean rooms and research facilities in nanotechnology making accessible innovation resources and services to SMEs in the BSR" – was running from autumn 2011 till June 2014 [2]. With the help of the project, the SMEs got the opportunity to access the clean rooms and related scientific facilities for their business. Estonian partner in Technet_nano project was Institute of Physics, University of Tartu (IPUT).

Fig.1 New building of the Institute of Physics. The inauguration of the building is scheduled on 25. August 2014.

What IPUT learned from Technet_nano project?

1. Our own clean room in the new building of IPUT (Fig.1) is in the process of state tender at the moment. Experience and knowhow of partners helps us to build that clean room to fully respond the present and possibly also the future needs of IPUT avoiding the mistakes the partners made building their clean rooms.
2. After the end of EU financing, five Technet_nano partners continue the cooperation in the field of clean rooms. At the final conference of Technet_nano in March 2014, the memorandum of understanding was signed between University of Latvia, Kaunas University of Technology, University of Tartu, Acreo Swedish ICT and University of Southern Denmark, Mads Clausen Institute.
3. Processes/objects we are unable to investigate in our small clean room, we can investigate in partner's clean rooms. The same is valid for Estonian SMEs who ask us for clean room service.

References

1. The Baltic Sea Region Programme 2007-2013 http://eu.baltic.net/
2. Technet_nano http://www.technet-nano.eu

F-2

Ab Initio Modelling of Ag Adsorption on the MnO_2- and LaO-terminated LMO[001] Surfaces

A.U. Abuova[1], T.M. Inerbaev[1], E.A. Kotomin[2,4], A.T. Akilbekov[1], Yu.A. Mastrikov[2,3]

[1]L.N. Gumilyov Eurasian National University,Mirzoyan str.2, Astana, Kazakhstan

[2]Institute of Solid State Physics, University of Latvia, Kengaraga str. 8, Riga, Latvia

[3]Materials Science and Engineering Dept., University of Maryland, College Park, USA

[4]Max Planck Institute for Solid State Research, Heisenbergstr.1, Stuttgart, Germany

e-mail: fatika_82@mail.ru

The flexibility of the perovskite structure provides significant technological advantages for making fuels cell cathodes and permeation membranes. The perovskite ABO_3 lattice allows for a large variety of chemical elements to be used in designing the material and hence crafts a playground for achieving targeted mass and charge transport properties by manipulating chemical compositions.

Metallic silver is a potential component for the SOFC cathode operated at less than 800°C because of its good catalytic activity, high electrical conductivity, and relatively low cost. Different methods have been used to prepare functionalized composite cathodes with improved electrochemical performance and long term stability at reduced operating temperature. [1] In addition, even far below its melting point, silver is relatively mobile. Therefore, these concerns should be addressed prior to a long-term application of silver-based cathodes in SOFCs.

To overcome this problem Zhou *et. al.* presented $(La_{0.8}Sr_{0.2})_{0.95}Ag_{0.05}MnO_{3-\delta}$ as a high performance intermediate temperature cathode material, in which the contained Ag functions as an effective catalyst through an intercalation/deintercalation mechanism. [2] Under cathodic polarization, Ag moves out of cathode to be deposited as small nanoclusters of Ag metal, leaving the remaining $(La_{0.8}Sr_{0.2})_{0.95}MnO_{3-\delta}$ as a catalyst carrier. The Ag nanoclusters which are 5–15 nm are very active and stable in catalyzing the cathode reaction even at a reduced temperature. Under anodic polarization, the Ag moves back into the deficient sites of the LSM. This permits an easy regeneration method to restore Ag nanoclusters which may become degraded over time by fusing together, thereby losing the activity.

We present results of *ab-initio* calculations of Ag adsorption on the LMO [001] polar surface. The most energetically favourable adsorption sites on both MnO_2- and LaO-terminations have been determined. Electron charge transfer between the adsorbate and the adsorbent has been analyzed. Optimized interatomic distances have been measured.

References

1. S. Uhlenbruck, F. Tietz, V. Haanappel, D. Sebold, H.P. Buchkremer, and D. Stover, Journal of Solid State Electrochemistry 8 (2004) 923-927.
2. W. Zhou, Z. Shao, F. Liang, Z.-G. Chen, Z. Zhu, W. Jin, and N. Xu, Journal of Materials Chemistry **21** 15343-15351.
1. The Baltic Sea Region Programme 2007-2013 http://eu.baltic.net/
2. Technet_nano http://www.technet-nano.eu

F-3

Ab Initio Simulations on N and S Co-doped Titania Nanotubes for Photocatalytic Applications

A. Chesnokov[1], O. Lisovskii[1], D. Bocharov[1,2], S. Piskunov[1], Yu.F. Zhukovskii[1], M. Wessel[3] and E. Spohr[3]

[1]Institute of Solid State Physics, University of Latvia, Latvia

[2]Transport and Telecommunication Institute, Latvia

[3]University of Duisburg-Essen, Germany

e-mail:. Andrew.Cesnokov@gmail.com

Titania (TiO_2, band gap ~3 eV) is the most attractive photocatalyst proposed for water-splitting applications. To dissociate water and to obtain hydrogen under visible light irradiation, the band gap ($\Delta\varepsilon_g$) of an efficient photocatalyst must be adjusted into the range of $1.23 < \Delta\varepsilon_g < 2.5$ eV. In comparison with conventional catalysts, titania nanotubes (NTs), which morphology corresponds to anatase phase, possess a larger specific surface area and, consequently, have a better adsorption capacity and a higher photocatalytic activity.

Using hybrid exchange-correlation functional within the density functional theory (DFT), we have predicted that both S- and N-doped TiO_2 NTs (Fig. 1) may enhance their photocatalytical properties with respect to pristine titania nanotube. In this study, we have carried out calculations on real band structures of titania nanotubes co-doped with both nitrogen and sulfur as a substitute for oxygen atoms. Based on the results of our simulations, we conclude that sulfur and nitrogen co-doped titania NT with the bottom of conduction bands positioned slightly above standard hydrogen electrode level can be the most suitable catalyst for photocatalytic hydrogen generation under influence of visible light.

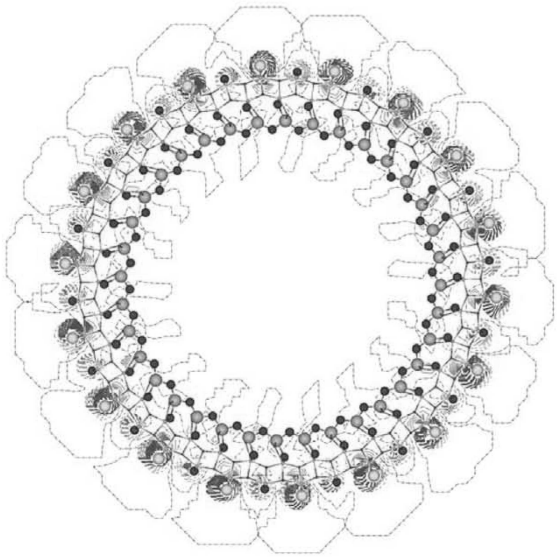

Fig.1 Electronic charge redistribution in S-doped titania nanotube leads to enhancement of its photocatalytical properties [1].

References

1. Yu. F. Zhukovskii, S. Piskunov, J. Begens, J. Kazerovskis and O. Lisovski, Phys. Status Solidi B **250**, 793 (2013) 1. The Baltic Sea Region Programme 2007-2013 http://eu.baltic.net/
2. Technet_nano http://www.technet-nano.eu

F-4

Numerical Simulation of Thermo-Magneto-Osmotic Flow of Ferrocolloid through Ordered and Disordered Permeable Structures

D. Zablotsky[1], E. Blums[1]

[1]Institute of Physics, University of Latvia, Latvia

e-mail: dmitrijs.zablockis@gmail.com

Fluidic actuation, mobilization of particles and mixing are important problems on micro-scale, especially in microfluidic applications. Pressure driven actuation is challenging in high surface-to-volume ratio microsystems and methods of bulk forcing (for example, electroosmosis) attract great interest.

We show by numerical simulations that colloidal solution of magnetic nanoparticles can be actuated in a system of fixed non-magnetic microscopic inclusions by simultaneous application of temperature gradient and homogeneous magnetic field. In such conditions, the temperature gradient creates a stratification of the colloid concentration through strong colloidal thermophoresis. In turn, the application of magnetic field induces a complicated pattern of internal demagnetizing fields in the vicinity of the inclusions. The combination of imbalance of concentration of magnetic nanoparticles and internal gradients of magnetic field creates magnetic force and convective flow of solution through the porous structure. This effect is similar to osmotic phenomena.

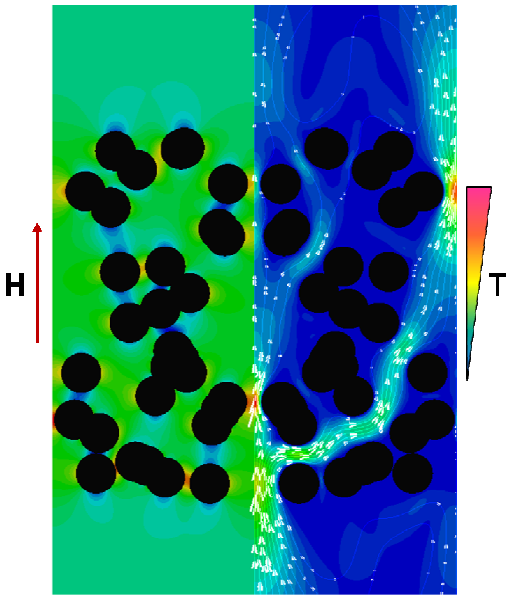

Fig.1. Demagnetizing field (left) within the disordered permeable structure and streamlines of thermo-magneto-osmotic flow (right).

We report results of pore-scale numerical simulations of ferrocolloid thermo-magneto-osmosis in generated ordered and disordered permeable structures and membranes with different porosity.

Acknowledgements

The work has been supported by the European Social Fund, Project 2013/0018/1DP/1.1.1.2.0/13/APIA/VIAA/061 The Baltic Sea Region Programme 2007-2013 http://eu.baltic.net/
2. Technet_nano http://www.technet-nano.eu

F-5

The Consideration of Virial Corrections in the Diffusion Equations

D. Levin[1], E. Trutnev[1]

[1]Tula State University, Russia

e-mail: levin@physics.tsu.tula.ru, trutnevs@mail.ru

Diffusion is one the most general physical processes and phenomena underlying a lot of transformations and processes in solids. The ordinary diffusion theory does not explain a number of effects during the diffusion of the interstitial atoms with high solution energy, causing a considerable deformation of the crystal lattice in the first coordination spheres. Such atoms strongly interact with the nearby atoms of the solvent crystal lattice and each other, that becomes considerably apparent in a number of special effects, particularly, these are anomalies of atom redistribution within the diffused zone, a special character of the influence of lattice defects on the diffusion kinetics, stress diffusion and so on.

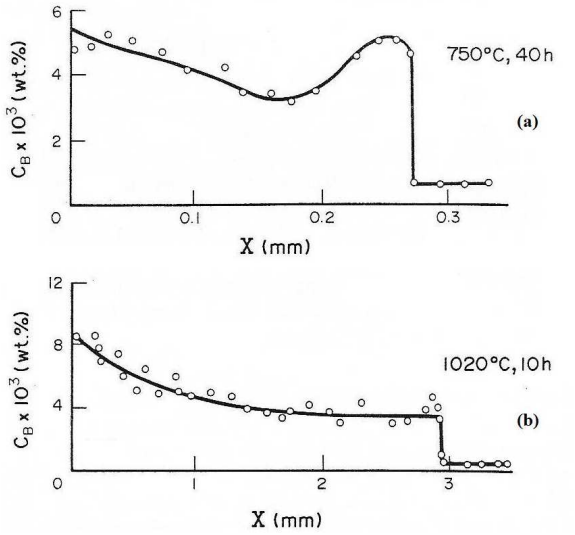

Fig.1. The boron distribution as a function of the diffusion layer depth in iron after annealing in the temperature ranges α-Fe (a) and γ-Fe (b) [1]

In our research we took an attempt to pass from phenomenological description of diffusion processes to microscopic (i.e. if we speak about interatom interaction). The aim of this work is to specify the impurity diffusion model, strongly interacting with the lattice, as well as the connection of the diffusion coefficient with the interatom interaction force law by means of configuration integral. The results of the theoretical calculations will be used to explain the anomalies observed in concentration-penetration diffusion, in iron-boron system, in particular.

Acknowledgment

This work was supported by the grant of RFBR № 13_08_97545_r_center_a

References

1. E.M. Grinberg. Nucl. Tracks Radiat. Meas., **20**, No. 2: 273-276 (1992)
2. E.M. Grinberg. Metal science of structural boron steel (Moscow: MISIS; 1997), P. 198

F-6

Electronic Effects on Hydrogen-Adsorbed Surfaces of ZnO: First Principles Study

A. Usseinov[1], E.A. Kotomin[2], Yu.F. Zhukovskii[2], J. Purans[2], A. Akilbekov[1], A.K. Dauletbekova[1]

[1]L.N. Gumilyov Eurasian National University, Kazakhstan

[2]Institute of Solid State Physics, University of Latvia, Latvia

e-mail: useinov_85@mail.ru

Understanding of the atomic and electronic structure of defective/doped ZnO is of great importance for improving performance of electrodes in optoelectronic devices based on transparent conducting oxides, *e.g.*, light-emitting diode (LED). Particular interest in this case is connected with clarification of a role of hydrogen impurities penetrating into ZnO thin films from plasma.

We report results of *ab initio* modeling of atomic hydrogen adsorption onto the two nonpolar $(10\bar{1}0)$ and $(11\bar{2}0)$ surfaces of ZnO positioned into two sites: *i*) atop surface O atom; *ii*) atop surface Zn atom. Our calculations of the corresponding 2D supercells have been performed using the hybrid DFT method (using PBE0 exchange-correlation functional) within the formalism of linear combination of atomic orbitals (LCAO) as incorporated into the CRYSTAL-2009 computer code [1]. This approach allows us to obtain very accurate calculations of the optical gap and defect level positions therein. The defect-induced electronic charge redistribution, lattice distortion, adsorption energy as well as the density of electronic states (DOS) and band structure have been calculated for both $(10\bar{1}0)$ and $(11\bar{2}0)$ surfaces of ZnO.

As a result, we have shown that energetically favorable position of hydrogen atom on both surfaces is atop the surface oxygen with similarly adsorption energies, whereas hydrogen locations atop the surface Zn is unstable. It should be noted also that hydrogen incorporation induces the defect states, which contribute below and within the surface conduction band. Thus, it is characterized as a shallow donor. Analysis of the charge redistribution has shown that hydrogen atom forms strong chemical bond with surface oxygen atom, unlike that in bulk. Based on our calculations, we have shown that hydrogen adsorption leads to decrease of both $(10\bar{1}0)$ and $(11\bar{2}0)$ surface relaxations and reduces the surface energy, in consistence with results of other DFT calculations [2].

References

1. Dovesi R, Saunders V R, Roetti R, Orlando R, Zicovich-Wilson C M, Pascale F, Civalleri B, Doll K, Harrison N M, Bush I J, D'Arco P and Llunell M 2009 *CRYSTAL09 User's Manual* University of Torino, Torino.
2. Siao Y I, Liu P L and Wu Y T 2011 *Appl. Phys. Express* **4** 125601

Calculation of the Excess Current and the Pseudogap in Cuprate High-Temperature Superconductors by the Monte Carlo Method

D. Sergeyev[1,2], K. Shunkeyev[1], S. Shunkeyev[1], N. Zhanturina[1]

[1]Zhubanov Aktobe Regional State University, Kazakhstan

[2]Military Institute of Air Defense Forces, Kazakhstan

e-mail: serdau@rambler.ru

Within the model of local pairs [1] using the Monte Carlo method, the dependences of the normalized pseudogap (PG) Δ^*_{norm} and the excess current I_{exc} of cuprate high-temperature superconductors (HTSC) YBCO and Bi2223 on temperature were determined. PG quantity was calculated by the expression: $\Delta^*(T) \approx T \cdot \ln\left(\frac{\Delta\sigma}{A \cdot n_{FCP}}\right)$, where $\Delta\sigma$ – the excess conductivity, $n_{FCP} \approx 1 - T/T^*$ – concentration of fluctuation Cooper pairs (PCP), T – temperature, T^* – the temperature at which tightly bosons are produced and the pseudogap appears, A – coefficient.

In considered formula excess conductivity was calculated using the Monte Carlo method as a pseudo-random process. It is known that the excess current is directly proportional to the PG: $I_{exc}(T) \infty \frac{\Delta^*(T)}{k_B T} + \exp\left(\frac{\Delta^*(T)}{k_B T}\right)$, where k_B – the Boltzmann constant.

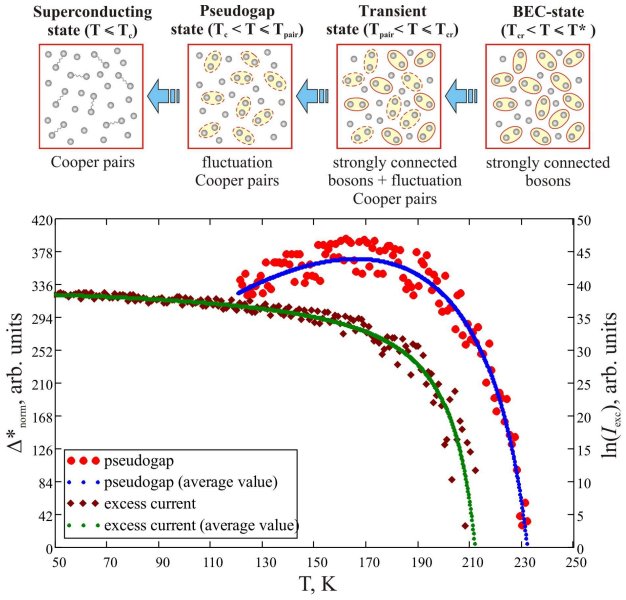

Fig.1 Transformation «Tightly Bosons ⇒ Fluctuation Cooper Pairs ⇒ Cooper Pairs» in HTSC in the temperature range $T_c < T \leq T^*$ and the dependence of the pseudogap and the excess current on temperature.

As can be seen, the maximum value of the PG corresponding to T_{pair} coincides with the deviation of $I_{exc}(T)$ from linearity (Fig. 1). The results of the modeling are in good agreement with the experimental data [1,2].

References

1. A. L. Solovjov and V. M. Dmitriev, Low Temp. Phys. **35**, 227 (2009)
2. T. Kondo, Y. Hamaya, A. D. Palczewski, et. all, Nature Phys. **7**, 21 (2011)

F-8

Theoretical Modeling of Nanodevices Using Embedded Molecular Cluster Method

E.K. Shidlovskaya[1,2]

[1]Information Systems Management Institute, Latvia

[2]Institute of Chemical Physics, University of Latvia, Latvia

e-mail: shidlovska@inbox.lv

When we theoretically describe nanodevice we have to treat the whole quantum system as two subsystems: small finite fragment of the system containing nanodevice (cluster) and the rest of the system containing electrodes. Problem "cluster in the field of the rest of system" is successfully solved in the frameworks of embedded molecular cluster (EMC) model with *orthogonal* wave functions. We have modified EMC model treating cluster embedding problem in the frameworks of one-electron approximation with *non-orthogonal* wave functions. We have proposed new cluster embedding scheme based on our approach [1].

Our present aim is application of our cluster embedding method for quantum-chemical modeling of processes in nanosystems and calculation of electrical properties of nanodevices. One of the approaches for theoretical description of nanodevices is quantum transport theory developed by Gross with co-workers [2]. We study possibility to combine our approach with approach of Gross et al [2] based on time-dependent DFT (TDDFT). We demonstrate [3] that our cluster embedding method is compatible with DFT Kohn-Sham method. We conclude that our embedding scheme may be combined with TDDFT if electron transitions are described correctly: occupied and vacant cluster states are localized in the cluster region in the same manner. To get occupied and vacant states of the same localization degree, we have modified [4] our initial cluster embedding equations [1]. We demonstrate that our cluster embedding method is compatible with electric current calculation method based on TDFT [2] and propose approach for calculation of electric parameters of nanodevices. Possibilities of our approach for theoretical modeling of nanodevices from the first principles are discussed.

References

1. E.K. Shidlovskaya, *Int. J. Quantum Chem.* **89**, 349 (2002)
2. S. Kurth, G. Stefanucci, C.-O. Almbladh, A. Rubio, and E.K.U. Gross, doi: 10.1103/PhysRevB.72.035308, Phys. Rev. **B72** (2005)
3. E.K. Shidlovskaya, in *Nanodevices and Nanomaterials for Ecological Security*, *NATO Science for Peace and Security Series B: Physics and Biophysics*, eds. Y.N. Shunin and A.E. Kiv, Springer, pp. 191-202 (2012)
4. E.K. Shidlovskaya, *Computer Modelling and New Technologies* **10,** No 4, 17 (2006)

F-9

Ab Initio Simulations on Frenkel Pairs of Radiation Defects in Corundum

A. Platonenko, S. Piskunov, Yu.F. Zhukovskii, E.A. Kotomin

Institute of Solid State Physics, University of Latvia, Latvia

e-mail: alexander.platonenko@gmail.com

Corundum is a wide band gap (8.8eV) insulator widely used in optical devices being also alternative dielectric for complementary metal oxide (CMOS) gate stacks. Due to high radiation-resistance, α-Al_2O_3 is also considered as a perspective material for high-energy nuclear applications [1].

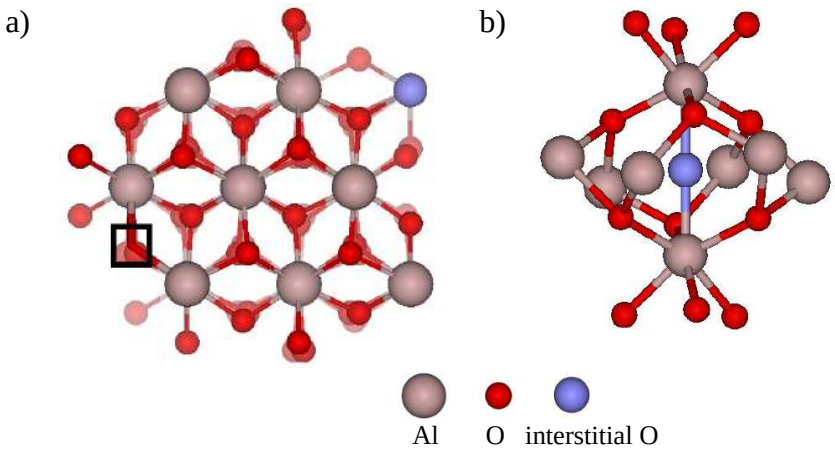

Fig.1 Atop and across images of either Frenkel pair (a) or O interstitial in regards to selected fragments of α-Al_2O_3 (0001) crystallographic plane, respectively. O vacancy is shown as a black-line-terminated square.

Radiation-induced changes in structural and optical properties of exposed corundum are mainly associated with oxygen vacancies and complementary Frenkel pairs of defects (vacancy + interstitial atom) [2] as shown in Fig. 1.

In this study, we have performed DFT-LCAO calculations of Frenkel pairs of radiation defects in α-Al_2O_3 within the hybrid B3PW exchange-correlation functional using the CRYSTAL14 code [3]. The basis sets of Al and O were selected and optimized, toachieve a reasonable compromise between the size of supercell and computational time.

As a result, good agreement has been achieved between the calculated and experimental data for parameters of a pure corundum lattice, its elastic constants and band gap. The most stable position for interstitial O atom has been found simultaneously with the defect formation energy and lattice distortion. Lastly, the calculations of Frenkel pairs at different mutual separations have been performed, accompanied with the determination of the energy barrier for back recombination, in order to suggest interpretation of experimental data.

Reference

1. D. Liu, J. Robertson, *Microelectron.Eng*, **86**, 1668-1671 (2009)
2. P. W. M. Jacobs, E. A. Kotomin, *J. Amer .Ceram. Soc.* **77**, 2505-2508 (1994)
3. R. Dovesi, V. R. Saunders, C. Roetti, R. Orlando, C. M. Zicovich-Wilson, F. Pascale, B. Civalleri, K. Doll, N. M. Harrison, I. J. Bush, Ph. D'Arco, *et al*. *CRYSTAL14 User's Manual* (University of Torino, Torino, 2014).

F-10

First-Principles Calculations of TiO_2-Based Consolidated Single-Walled Nanotubes

S. Lukyanov, A. Bandura, R. Evarestov

Institute of Chemistry, Quantum Chemistry Division, St. Petersburg State University, Russia

e-mail: lsiq80@hotmail.com

A new method of theoretical modelling of the polyhedral single-walled (SW) nanotubes (NTs) based on consolidation of walls in the rolled-up multi-wall (MW) nanotubes is proposed. The molecular mechanics and ab initio quantum mechanics methods are applied to investigate the merging of walls in nanotubes constructed from the different phases of titania with anatase, rutile, fluorite and lepidocrocite morphology. Quantum mechanical calculations have been performed using the density functional theory and hybrid exchange-correlation functional PBE0, as implemented in CRYSTAL09 code [1]. The GULP computer code [2] has been used for the molecular mechanics simulations.

It is shown that the SW constituents of the MW NTs are inclined to merge together when the interwall distances become sufficiently small. The symmetry of the resulting consolidated single-wall (CSW) nanotubes is significantly lower than the symmetry of initial coaxial cylindrical double- or triple-wall nanotubes. The wall thickness of the merged nanotubes exceeds 1 nm and approaches the thickness of the experimental patterns. Consolidated single-walled nanotubes acquire greater stability in comparison with the initial multi-wall NTs. Moreover, in many cases the merged CSW NTs prove to be more stable nanostructures than the layers which they are folded from.

The obtained results indicate that the CSW NTs can integrate the two different crystalline phases forming a new wall arrangement. Thus, the relaxed wall structure of the individually merged fluorite and rutile based multi-walled NTs includes the structural elements of both the rutile and fluorite crystals.

Acknowledgements

Authors wish to acknowledge the assistance of the Saint-Petersburg State University Computer Center and the financial support of the Russian Foundation for Basic Research (grant 14-03-00107 a).

References

1. R. Dovesi at al., CRYSTAL09 User's Manual, University of Torino, Torino, 2009
2. J. D. Gale, Z. Kristallogr. **220**, 552 (2005)

F-11

The Peculiarities of Halogens Adsorption on A^3B^5(001) Surface

A. Bakulin[1,2], A. Shaposhnikov[2], I. Smolin[1], S. Eremeev[1], S. Kulkova[1,2]

[1]Institute of Strength Physics and Materials Science of Siberian Branch Russian Academy of Science

[2]National Research Tomsk State University, Russia

e-mail: kulkova@ispms.tsc.ru

For modern nanotechnologies, it is important to develop an atomic-layer ("digital") etching. In binary A^3B^5 semiconductors, atomic layer etching can be realized by adsorbates selectively reacting with cation or anion atoms. In general, halogens and halogen-containing molecules are used for this goal. Despite the intensive implementation of atomic–layer etching, the microscopic mechanisms of the halogen interaction with semiconductor surfaces are still under debate. We present a comparative study of halogen (F, Cl, Br, I) adsorption on the cation enriched A^3B^5(001) surface for the series of semiconductors (GaAs, InAs, InP, GaP, etc.) in dependence on the halogen concentration. The energy stability of the surface reconstructions for semiconductors were re-examined by the projector augmented wave method within generalized gradient approximation for exchange-correlation functional (GGA-91). The estimation of charge transfer from semiconductor substrate to halogens was performed. Our study reveals a strong ionic bonding between halogen and dimerized cation atom in the surface layer at low coverage by halogens. It was shown that irrespective of the surface reconstructions halogens prefer to be bounded with cation dimerized atoms. A weakening of the cation-anion bonds in the surface layer is discussed. The influence of the halogen coverage (up to one monolayer) on the atomic and electronic structures of semiconductor surface with $\zeta(4\times2)$ reconstruction was studied in details in case of GaAs(001) and InAs(001). It was found that two halogen atoms (F or Cl) can be bonded with one cation atom of the surface dimer. The most preferential sites for halogens with increase of their concentration were determined. It was shown that the monohalides can be formed up to halogen coverage of 0.75 ML but the formation of dihalides is possible if the coverage reaches to 1 ML. It was shown that the breaking of cation dimers with increase of the halogen concentration is observed. The change of the binding energies of surface atoms with substrate upon halogen adsorption is discussed.

Acknowledgment

This work is partially supported by the Russian Foundation for Basic Research (N 13-02-98017_r_a). The calculations were performed using SKIF-Cyberia supercomputer of TSU.

F-12

Relativistic Time-resolved Approach for Phonon Assisted Interaction between Electron and Intensive Radiation Field

E. Klotins

Institute of Solid State Physics, University of Latvia, Latvia

e-mail: klotins@cfi.lu.lv

This work is addressed to the dynamics of electron-hole pair in a dielectric excited by strong time-dependent laser field. Motivation of this work is based on modern understanding of the Diracs point-like particle model revealing that electron-hole pairs are expected to be important within the Compton wavelength at which the concept of a single point-like particle breaks down completely. It is the case of dielectrics with electrons and holes at short distances obeying relativistic conditions and the formalism of quantum field theory (QFT). The mathematical tool used here to describe electron-hole pair without resorting to perturbation theory is the QFT based oscillator representation formally given by complex scalar Klein-Gordon equation [1]. This equation is derived from dispersion relations for electron and hole (considered as an antiparticle to the electron) and the band gap as input entities either computed or found experimentally. Recent solution is defined on hypersurfaces formed by dispersion relations and allows including the electromagnetic radiation in the distribution function for electron and hole quasiparticles. The resulting observables are the conductivity and polarization currents constituting QFT background for optical properties: susceptibility, absorption and relevant physical quantities far from equilibrium.

We report here on the phonon assisted kinetics of electrons and holes as an improvement addressed to more realistic models. Unlike the electromagnetic radiation which is an extrinsic entity, this kind of the quasiparticle-phonon interaction is intrinsic and heavy depends on the properties of ionic subsystem. Nevertheless, we will show that both the electromagnetic radiation and the quasiparticle-phonon interaction contribute in the kinetic energy on equal footing, thus extending the QFT based oscillator representation for indirect optical transitions.

Acknowledgment

This work was supported by National Research Program of Latvia Nr. 2014. 10-4/VPP-2/ and Grant Nr.237/2012.

References

1. S. A. Smolyansky, M. Bonitz, A. V. Tarakanov, Physics of Particles and Nuclei **41**, 1075 (2010)

F-13

Ab Initio Calculations of Interactions between Y and O Impurity Atoms and Vacancies in *bcc*- and *fcc*-iron Lattices

A. Gopejenko[1], Yu.F. Zhukovskii[1], P.V. Vladimirov[2], E.A. Kotomin[1], Yu.A. Mastrikov[1], V.A. Borodin[3] and A. Möslang[2]

[1]Latvijas Universitātes Cietvielu Fizikas Institūts, Rīga, Latvija

[2]Karlsruhe Institut für Technologie, Institut für Angewandte Materialen, Karlsruhe, Germany

[3]NRC "Kurchatov Institute", Kurchatov sq. 1, 123182 Moscow, Russian Federation

e-mail: agopejen@inbox.lv

Oxide dispersion strengthened (ODS) structures of reduced activation ferritic-martensitic (RAFM) steels are found to be promising construction materials for fusion reactor applications. Development of the ODS steels strengthened by Y_2O_3 precipitates as more suitable materials for reactors instead of non-modified RAFM steels permits to increase the operating temperatures of blanket structures by 100°C. Both size and spatial distribution of oxide particles significantly affect mechanical properties and radiation resistance of ODS steels which are produced by mechanical alloying, followed by a hot isostatic pressing (hipping) at temperature around 1000-1200°C and pressure ~100 MPa. On the other hand, the mechanism of the ODS particle formation is not completely understood yet.

Theoretical approach for atomistic simulations of this process is performed in the two steps. Firstly, *ab initio* calculations on different complexes of Y and O impurity atoms and vacancies have been are performed [1,2]. Calculations performed for 5×5×5 Fe supercells (SCs) have reproduced both qualitatively and semi-quantitatively the results received for 4×4×4 SC. The results of these calculations have been used in the lattice kinetic Monte Carlo (LKMC) simulations of Y_2O_3 particle growth inside Fe lattices of both phases. Binding energies between defects and diffusion barrier energies are important parameters in the LKMC modeling of the ODS particle formation. To perform diffusion barrier calculations, the nudge elastic band (NEB) method have been used (as implemented within the VASP computer code). The calculations of different Y diffusion trajectories have been performed. The lowest calculated energy of the diffusion barrier is about 1.75eV. The high values of diffusion energies prove that the increased concentration of vacancies is required for Y diffusion and the increased size of the supercell is required for this purpose.

References

1. A. Gopejenko, Yu. F. Zhukovskii, P. V. Vladimirov, E. A. Kotomin, A. Möslang, *J. Nucl. Mater*, 416, 40-44 (2011).
2. A. Gopejenko, Yu.F. Zhukovskii, P.V. Vladimirov, E.A. Kotomin, A. Möslang, *Proc. NATO ARW Meeting* (Eds. Yuri N. Shunin and Arnold E. Kiv; Springer: Dordrecht, 2012), p. 149-160.

F-14

R and *M* Mode Softness in Cubic ScF_3: Predictions from First Principles

D. Bocharov[1,2,3], S. Piskunov[1], P. Zhgun, J. Purans[1], A. Kuzmin[1]

[1]Institute of Solid State Physics, University of Latvia

[2]Transport and Telecommunication Institute, Riga, Latvia

[3]Faculty of Physics and Mathematics, University of Latvia

e-mail: bocharov@latnet.lv

ScF_3 is a perovskite-type material with a cubic ReO_3-type structure (space group *Pm-3m*). Recently it was found that ScF_3 undergoes strong negative thermal expansion (NTE) over a wide range of temperatures from 10 to 1100 K [1], therefore an understanding of its electronic structure and lattice dynamics is of key importance to shed light on the NTE origin.

In the current activity the electronic structure (band structure, DOS, charges analysis), lattice dynamics, and phonon anharmonicity of ScF_3 were studied within the framework of the first-principles approaches (LCAO and PAW, HF-DFT) using Crystal14 and VASP programs. Our results predict that the Sc-F bond has considerable covalent nature due to a hybridization of the F 2*p* and Sc 3*d* states. The band gap obtained in HF-DFT calculations is equal to 8-10 eV and is in good agreement with that experimentally observed.

It has been found that the position of scandium atoms in the middle of regular ScF_6 octahedron is stable, and that the modes at the Γ and *X* points of the Brillouin zone are harmonic, whereas whose at the *R* and *M* points are soft modes. Grüneisen parameters of soft modes and coefficients describing mode's anharmonic potentials are found to be strongly dependent upon calculation technique used. Simple model that accounts for static lattice energy and a contribution of oscillator (*R* soft mode) is capable to describe NTE at low temperatures. This suggests that NTE occurs due to *R* and *M* mode softness. In order to prove this conclusion the changes in the phonon DOS calculated for *Pm-3m* and hypothetical *Im-3* phases of ScF_3 will be compared in discussed.

References

1. B.K. Greve, K.L. Martin, P.L. Lee, P.J. Chupas, K.W. Chapman and A .P. Wilkinson J. Am. Chem. Soc. **132** 154962 (2010).

F-15

Ab-initio Study of Cation-rich InP(001) and GaP(001) Surface Reconstructions and Iodine Adsorption

A. Bakulin[1,2], A. Ponomarev[1], K. Tarasov[2], S. Kulkova[1,2]

[1]Institute of Strength Physics and Materials Science of Siberian Branch Russian Academy of Science, Russia

[2]National Research Tomsk State University, Russia

e-mail: bakulin@ispms.tsc.ru

It is well-known that A^3B^5 semiconductors are widely used for modern nanotechnologies. The A^3B^5(001) surface exhibits a large number of surface reconstructions depending on surface treatment. The cation-rich surface geometry attracts special attention, because it is preferable for deposition of ferromagnetic metals and may be used in spin electronics devices. For this goal it is desirable to keep an atomically smooth surface morphology. In the etch-based techniques halogens and halogen-containing molecules are used. In this work we reexamine the stability of surface reconstructions of both semiconductors and study new possible ones. The results of comparative study of iodine adsorption on InP(001) and GaP(001) surfaces are presented also. Atomic structure of about 20 surface reconstructions were calculated by the projector augmented wave method implemented in program code VASP. An analysis of the electronic characteristics allowed us to identify the iodine bonding mechanisms on the considered reconstructions. It is shown that on the ζ-(4×2) surface the largest adsorption energy corresponds to iodine M1-position over one of dimerized cation atoms (Fig. 1). In the case of β2-(4×2) and (2×4) mixed dimer surface the preferential positions for iodine are H3 and T2a (Fig. 1), respectively. In general, independently of the surface reconstruction, iodine prefers to be bonded with In or Ga in on-top or bridge positions above dimerized cation atoms due to large charge transfer from substrate surface atoms to the adsorbate and rather strong hybridization of I and cation states. A weakening of the chemical bonds between surface atoms is important condition in the initial stage of dry etching process.

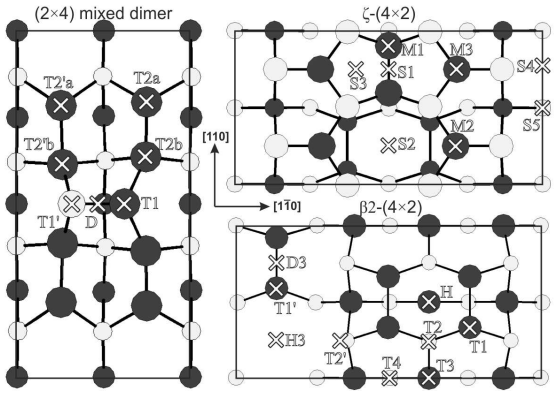

Fig.1 Equilibrium atomic structure and considered adsorption sites marked by crosses.

Acknowledgment

This work is partially supported by the Russian Foundation for Basic research (grant N 13-02-98017_r_a).

F-16

Quantum Chemical Investigations of Oxide Nanostructures for Energy Conversion in Aqueous Solution

M. Wessel, E. Spohr

Faculty of Chemistry, University Duisburg-Essen, Essen, Germany

e-mail: michael.wessel@uni-due.de

The recent years exhibited a rising interest in the design of efficient photocatalysts for the conversion of sunlight to hydrogen from water. TiO_2 performs as an electrode in such a process with high efficiency under ultraviolet irradiation, but lacks performance under visible light. One approach to overcome this is the introduction of a dopant, but this often leads to the problem of electron and hole trapping. The synthesis of nanostructured electrodes offers a solution to this problem as the charge transport and the photon propagation are orthogonalized.

In our previous works, we studied [1] the bandgap of $SrTiO_3$ nanotubes in comparison to the bulk and we investigated [2] the effect of doping TiO_2 and $SrTiO_3$ nanotubes with both cations and anions.

Now, these oxide nanotubes are investigated under more realistic conditions using density functional theory calculations. We study the behaviour of the $SrTiO_3$ nanotube in water and furthermore we investigate possible pathways of proton migration on the TiO_2 nanotube.

References

1. S. Piskunov, E. Spohr, J. Phys. Chem. Lett. **2**, 2566 (2011)
2. S. Piskunov, D. Bocharov, O. Lisovski, J. Begens, Z. F. Zhukovskii, M. Wessel, E. Spohr, submitted to PCCP.

F-19

Plasmonic Photoluminescence Enhancement by Silver Nanowires

B. Polyakov, R. Zabels, A. Sarakovskis, S. Vlassov, A. Kuzmin

Institute of Solid State Physics, University of Latvia, Latvia

e-mail: boris.polyakov@cfi.lu.lv

The collective excitation of the electron gas in the conduction band of the metal nanoparticles/nanowires can result in strong optical response known as localized surface plasmon resonance (LSPR) and representing considerable interest in the field of nanophotonics and plasmonics [1]. Coupling of LSPRs can create regions of concentrated electric fields, “hot-spots”, in the gaps between metal nanoparticles/nanowires, leading to the photoluminescence enhancement from nearby quantum dots (QDs) or dye molecules [2,3].

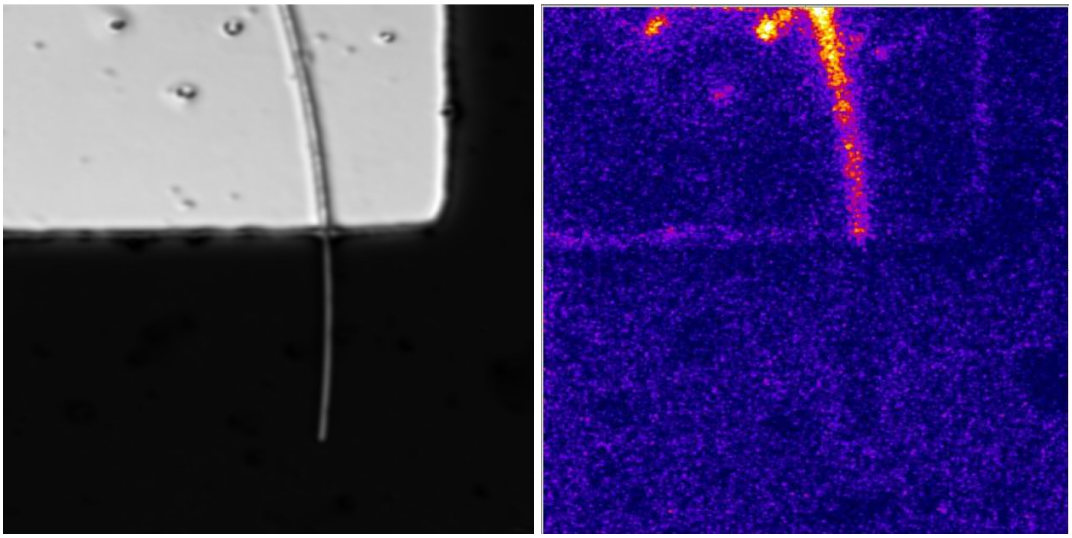

Fig.1. Confocal (left) and spectral (right, at 750 nm) images (size 24x29 µm) of Ag nanowire placed above the silver film on glass substrate and uniformly covered with CdS nanocrystals.

In this study we report on the investigation of photoluminescence enhancement phenomenon for CdS nanocrystals and Ruthenizer 535-bisTBA (N719) dyes caused by silver nanowires. Samples were prepared by depositing nanowires on a glass substrate with square patterned silver film, and then coated by a thin layer of nanocrystals or dyes. Maximal enhancement effect was detected on nanowires placed on the silver film (Fig. 1), and in the region of crossing nanowires.

References

1. E. Fort and S. Gresillon, J. Phys. D: Appl. Phys. **41**, 013001 (2008).
2. D. J. Anderson and M. Moskovits, J. Phys. Chem. B **110**, 13722 (2006).
3. T. Ming, H. Chen, R. Jiang, et al., J. Phys. Chem. Lett. **3**, 191 (2012).

F-21

Silver Nanoprisms Self-Assembly on Differently Functionalized Silica Surface

A. Chodosovskaja, J. Pilipavicius, A. Beganskiene, A. Kareiva

Department of Inorganic Chemistry, Faculty of Chemistry, Vilnius University, Lithuania

e-mail: alachodosovskaja@gmail.com

Silver nanoprisms (NPRs) are one of the most interesting nanoparticle type, because of wide tuneability and high intensity of surface plasmon resonance (SPR) band [1, 2]. Manipulating particle thickness and edge length, possible to obtain SPR peak position in 400 – 1300 nm range. These properties opens the gateway for application in near infrared working technologies [3], or surface enhanced Raman spectroscopy (SERS) [4].

In this work we have made colloidal Silica/Silver nanoprisms (NPRs) composite coatings. We synthesized porous silica coatings by Sol-gel method and silanised by (3-Aminopropyl)triethoxysilane (APTES), N-[3-(Trimethoxysilyl)propyl]ethylenediamine(AEAPTMS), (3-Mercaptopropyl)trimethoxysilane (MPDMS). Nanoparticles where synthesized via seed-mediated method, and high yield of 94 nm average edge length silver NPRs were obtained. Composite coatings formed by self-assembly on silica coated-functionalized surface. Coatings were characterized by scanning electron microscopy, dynamic light scattering, water contact angle and surface free energy methods. Results have sowed that most homogeneous, even distribution composite coatings obtained on APTES functionalized silica coatings (fig. 1).

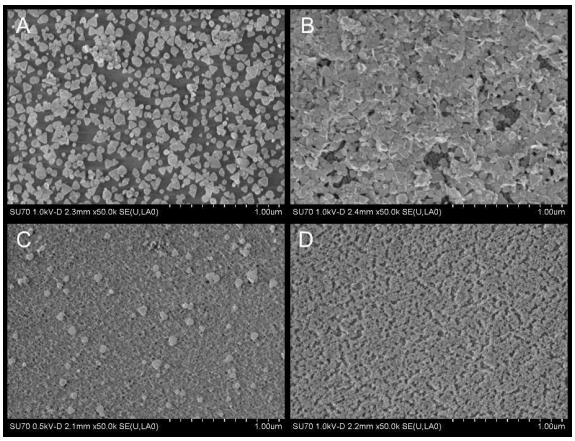

Fig.1 SEM images of silanised composite coatings: A- APTES, B- AEAPTMS, C- MPDMS, D- nonsilanised coating

Acknowledgement

The financial support to A.Ch. from the Research Council of Lithuania under project "Postdoctoral Fellowship Implementation in Lithuania" (No. SF-PD-2012-12-31-0397) is acknowleged**.**

References

1. Aherne, D., D.M. Ledwith, M. Gara, and J.M. Kelly, Adv Funct Mater, **18,** 2005 (2008)
2. Métraux, G.S. and C.A. Mirkin, Adv. Mater., **17,** 412-415 (2005)
3. Bastys, V., I. Pastoriza-Santos, B. Rodríguez-González, R. Vaisnoras, and L.M. Liz-Marzán, Adv Funct Mater, **16,** 766 (2006)
4. Yi, Z., X. Xu, X. Wu, C. Chen, X. Li, B. Luo, J. Luo, X. Jiang, W. Wu, Y. Yi, and Y. Tang, Appl. Phys. A, **110,** 335 (2013)

F-22

A New Preparation Method of Size Controllable Gold Nanoparticles Using Hydrogen

E.V. Abkhalimov, R.D. Solovov, B.G. Ershov

Institution of Russian Academy of Sciences - A.N. Frumkin Institute of Physical Chemistry and Electrochemistry of RAS, Russian Federation

e-mail: abkhalimov@ipc.rssi.ru

In the absence of gold nanoparticles, molecular hydrogen cannot reduce $AuCl_4^-$ ions in aqueous solution [1]. It is established that the presence of 3 nm gold NPs in solution catalyzes the reduction of $AuCl_4^-$ ions by hydrogen. The rate of the catalytic reaction is proportional to concentration of gold NPs. Figure 1 illustrates the kinetic of this process.

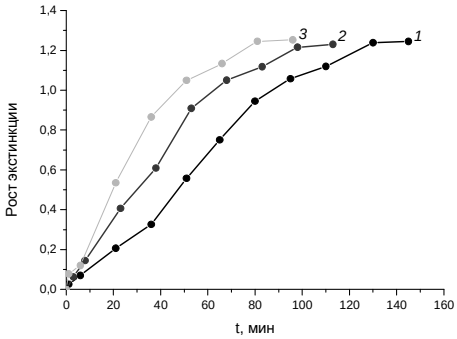

Fig.1. Kinetic curves of the process of the reduction, $AuCl_4^-$ ions by hydrogen in the presence of gold NPs with different concentration: 1 – 1×10^{-4}, *2* – 2×10^{-4}, *3* – 3×10^{-4}, *4* – 4×10^{-4} M. Solution content: Au(III) – 4×10^{-4} M, Sodium citrate – 1×10^{-3} M.

The TEM and DLS data are shown that the reduction of $AuCl_4^-$ ions is accompanied with a growth of size of gold nanoparticles. Thus, nanoparticles can act as «nanoelectrodes», at first taking electrons in the process of hydrogen ionization, and then giving them for the reduction of AuCl4- ions. There is a typical electrochemical reaction of charging/ionization. The feature of the reaction is that it is realized on the cathode and on the anode which are «belonging» the same gold NP.

Acknowledgment

This work was supported by the Russian Found of Basic Research (Project Grant Nos. 12-03-00449-a).

References

1. B. G. Ershov, V. I. Roldugin, E. V. Abkhalimov, R. D. Solovov, V. M. Rudoy, O. V. Dement'eva, Coll. J. **76**, (In press 2014)

F-23

Self-Assembly of Gold Nanoparticles and Poly(diphenylamine): A Versatile Approach to One-Step Synthesis of Poly(diphenylamine) and Gold Nanoparticles

D.W. Kim[1], A.M. Showkat[1], X.T. Cao[1], Y.H. Kim[1], C. Oh[2], and K.T. Lim[1]

[1]Department of Imaging System Engineering, Pukyong National University, Busan 608-737, Republic of Korea

[2]Department of Marine Biology, Pukyong National University, Busan 608-737, Republic of Korea

e-mail: ktlim@pknu.ac.kr.

Composites of polydiphenylamine and gold nanoparticles were chemically prepared from solutions which containing methane sulfonic acid (MSA) with the addition of gold chloride trihydrate as the oxidant by a one - step synthesis as source for initiation of polymerization and generation of Au nanoparticles. Gold was subsequently anchored onto the host matrix by reducing the respective metal salts with the amine sites in the monomer. Polydiphenylamine decorated with noble-metal gold nanoparticles were synthesized successfully and exposure of the solutions to caused polymerization of diphenylamine to polymerize with gold salt. The nanocomposites were characterized for the structure, morphology and electronic properties through X-ray diffraction analysis (XRD), Fourier transform infrared spectroscopy (FT-IR), transmission electron microscopy (TEM) and UV–visible spectroscopy.

F-24

The Novel Au/TiO_2 and Au/CeO_2 Nanocomposites Synthesis. The *S*tudy of Their Physical Properties and Catalytic Activity

S. Chornaja[1], S. Zhizhkuna[1], D. Jankovica[2], D. Karashanova[3], K. Dubencovs[1], O. Stepanova[1], V. Kampars[1], G. Poikane[1]

[1]Institute of Applied Chemistry, Riga Technical University, Latvia

[2]Institute of Inorganic Chemistry, Riga Technical University, Latvia

[3]Institute of Optical Materials and Technologies Bulgarian Academy of Sciences, Bulgaria

e-mail: Svetlana@ktf.rtu.lv

The work is devoted to the synthesis and the study of the physical properties of the novel Au/TiO_2, Au/CeO_2 nanocomposites, as well as testing their catalytic activity in the reaction of glycerol oxidation. Glycerol is a major by-product of bio-fuel production. A number of important products can be obtained in the process of glycerol catalytic oxidation by molecular oxygen. Typical TEM microphotography and the corresponding histograms of the synthesized nanocomposites are presented in Figure 1 and 2. Electronic microscopy revealed that the Au nanoparticles posses higher contrast and are spherically shaped. The Au nanoparticles could be distributed in the interval of 2 to 26 nm. Coalescence between metal particles occurs in all of the samples, and bigger particles (50 – 100 nm) or clusters of metal particles were found in separate regions of the catalysts. The effect of novel nanocomposites synthesis parameters on their catalytic activity and selectivity was studied in this work. The effect of the gold nanoparticle size (d_{Au}), nature of support, composites' specific surfaces (S_{sc}), and gold load in the composite on its activity and selectivity was studied as well. According to the data presented in the Table glycerol conversion increased from 61% to 83% in the presence of the novel nanocomposites when Au particle size decreased from 26 to 9 nm. Glyceric acid was obtained as a main product with high selectivity.

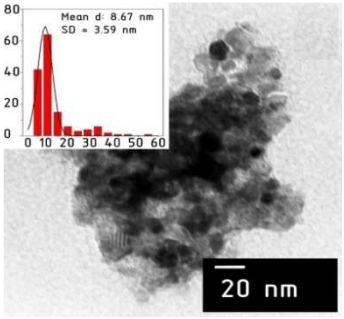

Fig. 1. *TEM of 1%Au/CeO₂*

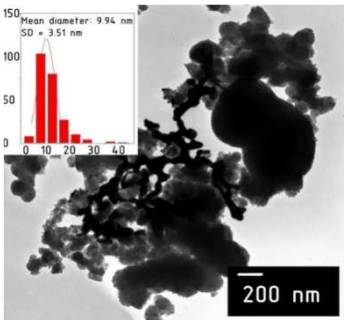

Fig. 2. *TEM of 5%Au/TiO₂*

Catalyst	d_{Au} by TEM nm	d_{Au} by XRD nm	Glycerol conv. mol%	Glyceric acid select mol%
1%Au/CeO_2	9	20-23	83	61
5%Au/TiO_2	10	10-15	78	68
5%Au/TiO_2	26	22-25	61	73

F-25

Microwave Synthesis of Nanocomposites in ZnO-Zn_2SnO_4/Ag System and Their Photocatalytic Activity

J. Grabis, A. Letlena, Dz. Rašmane, A. Krūmiņa

Institute of Inorganic Chemistry, Riga Technical University

e-mail: grabis@nki.lv

Zinc oxide and zinc stannate nanoparticles as well as their composites due to their attractive electrical and optical parameters are promising candidates for a wide range of application in solar cells, sensors, photocatalysis for the degradation of organic pollutants. The photocatalytic activity of oxides depends on their particle size and morphology, crystallinity and used dopants.

The aim of the present work was to prepare particulate nanocomposites with different content of the components in the ZnO-Zr_2SnO_4/Ag system by using microwave synthesis and to compare their photocatalytic activity in degradation of methylene blue solution.

ZnO, ZnO-Zn_2SnO_4/Ag system nanoparticles were prepared by heating mixtures of the salt solutions in the presence of the citric acid, urea, NH_4OH or NH_4HCO_3 in microwave reactor (Masterwave BTR, Anton Paar) at 160–180 ^oC for 2–10 min. Doped with Ag nanocomposite were prepared by adding silver nitrate water solution to mixture of oxides in ethanol with following Ag reduction by formaldehyde.

The specific surface area of the prepared nanocomposites was in the range of 19–28 m^2/g in the dependence on the phase composition. Crystallite size of the oxide and Ag particles was in the range of 30–60 nm and 30-70 nm, respectively. The powders were composed of tetra-pode shaped or rod-like particles of ZnO and cubic particles of Zn_2SnO_4. The silver particles were situated on the surface of oxides.

The photocatalytic activity depended on ratio of the components, content and crystallite size of Ag. The highest photoactivity showed ZnO/Ag, ZnO-Zn_2SnO_4/Ag.

F-26

Layers of Two and Three Dimensional Metal Nanoparticle Assemblies for Plasmonic Sensor Applications

T. Tamulevičius, G. Bergs, D. Erts, J. Prikulis

Institute of Chemical Physics, University of Latvia, Latvia

e-mail: juris.prikulis@lu.lv

Metal nanostructures support resonant modes of charge density oscillations or localized surface plasmons (LSP), which redistribute the incident radiation and can produce high electric field near surface. In particular silver and gold nanoparticles have LSP resonances in visible frequency region. Plasmonic refractive index sensors can be built by utilization of resonance frequency shift depending on effective dielectric function of surrounding medium.

In this work we analyze interaction between particles in dense assemblies in two (2D) and three dimensional (3D) layers. Gold and silver 2D arrays were obtained by masked deposition through anodized aluminum membrane [1], whereas silver nanoparticles embedded in diamond like carbon (DLC) films [2] were used as 3D structures. In all cases the particle size is in 20 nm range. The thickness of 3D layers is few hundred nm. The layer structure is of short range ordered nature with center separation ~50 nm. The 3D samples have somewhat broader size distribution and individual particles have different orientation in space.

Due to strong near-field interaction, mentioned nanoparticle layers produce complex interference patterns, which change rapidly with small variations in experiment conditions. We utilize this sensitivity to develop a new type of refractive index sensor. Coupled dipole model calculations produce results, which are consistent with experimental observations [3]. We compare various aspects of 2D and 3D nanoparticle layers for sensor applications, e.g. the DLC film protects the silver nanoparticles from chemical reactions and allows sensor regeneration for repetitive use.

Acknowledgment

This work was done within ESF project 1DP/1.1.1.2.0/13/APIA/VIAA/054.

References

1. U. Malinovskis, et al., J. Phys. Chem. C. *in press* (2014) doi:10.1021/jp412689y
2. T. Tamulevičius, et al., Nucl. Instr. Meth. Phys. B. *in press* (2014) doi:10.1016/j.nimb.2013.09.052
3. J. Prikulis, et al., Plasmonics *in press* (2013) doi:10.1007/s11468-013-9639-2

F-27

Polarization Effects in Layers of Dense Short-Range Ordered Plasmonic Nanoparticles

J. Prikulis, R. Popļausks, I. Apsīte, G. Bergs, U. Maļinovskis, D. Erts

Institute of Chemical Physics, University of Latvia, Latvia

e-mail: juris.prikulis@lu.lv

We report on optical properties of dense short-range ordered nanoparticle arrays produced by masked deposition through anodized aluminum oxide membranes [1]. Depending on membrane synthesis process parameters, mainly electrolyte and anodization voltage, the achievable particle diameters can be below 20 nanometers and center separation in 50-100 nm range. Silver and gold nanoparticles are particularly interesting since they are strong light scatterers in visible spectral range.

The obtained nanoparticles have similar size (standard deviation approximately 10%) and are assembled in non periodic short-range ordered arrays. For simulation of optical properties we use coupled dipole, model, where each particle is characterized by ellipsoid polarizability and responds to incident radiation and dipole fields of all other particles [2]. Experimentally the optical scattering is measured using dark-field microscope setup using either white light or laser source.

The simulation results are consistent with experimental observations. Most importantly, there is a significant change of polarization, which would be absent in non-interacting particles. Far-field imaging of depolarized scattered light from the arrays shows a granular structure, which changes rapidly with wavelength and is sensitive to minute changes in refractive index of sample surrounding medium. This effect can be used for development of sensor applications. In comparison to earlier work by our group [1,2] we extend the study to systems, where nanoparticle arrays are stacked on top of each other forming multilayer structures.

Acknowlwedgment

This work was done within ESF project 1DP/1.1.1.2.0/13/APIA/VIAA/054.

References

1. U. Malinovskis, et al., J. Phys. Chem. C. in press (2014) doi:10.1021/jp412689y
2. J. Prikulis, et al., Plasmonics in press (2013) doi:10.1007/s11468-013-9639-2

F-28

Dense Arrays of Nanometer Holes in Thin Metal Films on Anodized Aluminum Oxide Membranes

R. Poplausks, I. Apsite, J. Prikulis, D. Erts

Institute of Chemical Physics, University of Latvia, Latvia

e-mail: raimonds.poplausks@lu.lv

Nanoporous anodized aluminum membranes are used for production of dense hole arrays in thin Au films. The membranes are prepared using two step anodization in sulfuric acid. DC voltage of 20 V is used for pore formation, resulting membrane thickness using sulfuric acid is 60-100 nm [1]. AAO membrane thickness is reduced using ion etching. 20 nm Au layer is deposited on anodized aluminum oxide (Fig. 1.).

Tiny holes, similarly to nanoparticles, support localized surface plasmon resonances. Depending on membrane thickness, hole diameter, hole density and gold layer thickness, the resulting structure reflects light in different intense colors. This indicates strong coupling to incident radiation. Theoretical treatment of hole arrays in thin metal film is more complex than for similar size nanoparticle arrays since propagating plasmon modes provide additional means of interaction between individual scatterers. Moreover, interaction with aluminum substrate must be taken into account. The pore ordering is also expected to influence the optical properties, in particular, angular distribution of scattered field.

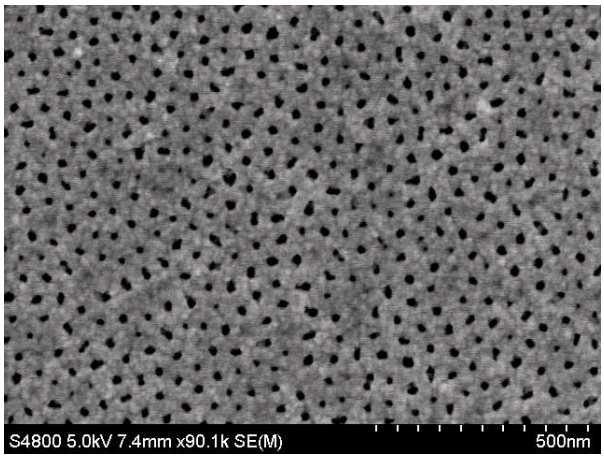

Fig.1 SEM image of a gold film on anodized aluminum oxide membrane.

In this work we characterize the multilayer structure consisting of hole array in metal (Au) film, aluminum oxide, and bulk aluminum and test the usability for plasmonic device applications, e.g. sensors or field enhancing substrates.

Acknowledgment

This work was done within ESF project 1DP/1.1.1.2.0/13/APIA/VIAA/054.

F-29

Colloid of Metal Nanoparticles Produced by Laser Ablation in Liquid

V.Ya. Shur, A.E. Tyurnina, R.V. Kozin, V.I. Pryakhina, G.V. Burban

Ferroelectrics Laboratory, Institute of Natural Sciences, Ural Federal University,

51 Lenin Ave., 620000, Ekaterinburg, Russia

e-mail: vladimir.shur@urfu.ru

Over the last decade, the major effort has been on the production of stable colloids of small nanoparticles (NP) with narrow size distributions and controlled surface chemistry by laser ablation in liquid [1]. The size dependence of the NP properties opens their wide application in microelectronics, optics, catalysis and medicine.

We have produced the stable colloids with different concentrations and sizes of metal NP by pulse laser ablation of metal target (Ag, Au, Cu) in deionized water. The Yb fiber laser with 1064 nm wavelength and 100 ns pulse duration has been used [2].

The NP size distribution function and colloid ζ-potential have been measured by dynamic light scattering (DLS) using Zetasizer Nano ZS. Analysis of size and morphology was carried out by scanning electron microscope CrossBeam Workstation Auriga.

The effect of the target surface treatment by laser scanning on NP sizes have been studied. The obtained essential size decrease during first scanning cycles has been attributed to removement of the amorphous surface layer of the target produced during polishing. It was shown that the proper number of treatment cycles prepared the target for production of the spherical NP with diameter 40±10 nm for Ag, 50±10 nm for Au, and 100 nm for Cu NP.

The morphology of NP after ablation has been changed by laser irradiation of the colloid without metal target (fragmentation). The two stage fragmentation have been used for Au NP. The first stage was applied for termination of the aggregation and essential increase of ζ-potential value. Thus the subsequent increase of the colloid concentration by partial drying did not change the sizes of NP. The second stage allowed to produce the stable colloid with the spherical Au NP of required sizes. The variation of technological parameters allowed to change the NP sizes in wide range. The application of the optimized parameters allowed to produce the Au colloid with concentration of 0.5 g/l with narrow size distribution and stability over several months.

Currently, much attention is paid to synthesis of CuO NP of various shapes. We have studied the evolution of CuO NP parameters during heating. DLS measurements showed that at elevated temperatures (above 50°C) the average sizes of NP increased, whereas the ζ-potential decrease. The detail study allowed to reveal the growth of CuO nanocrystals (“nanospindles”) at the temperature about 68°C. The composition was confirmed by energy dispersive X-ray analysis.

It was shown that short-time fragmentation (about 10 min) of CuO NP colloid reduced niticably the NP sizes and increased the colloid stability (ζ-potential above 40 mV), whereas the long-time fragmentation (about 30 min) leads to increase the NP sizes accompanied by change of the colloid color due to formation of “nanospindles”. This effect can be attributed to increase of the colloid temperature.

Acknowledgement.

The equipment of the Ural Center for Shared Use “Modern Nanotechnology”, Institute of Natural Sciences, Ural Federal University has been used. The research was made possible in part by RFBR and Government of Sverdlovsk region (Grant 13-02-96041-r-Ural-a), by RFBR (Grant 13-02-01391-a).

References

1. A. Moores, F. Goettmann, New J. Chem, **30**, 1121 (2006)
2. A.E. Tyurnina, V.Ya. Shur, R.V. Kozin, D.K. Kuznetsov, E.A. Mingaliev, Proc. of SPIE 9065, 90650D (2013)

F-30

Ultra Thin TiO_2 Films with Gold Nanoparticles by the Chemical Spray Pyrolysis Method

I. Oja Acik[1], G.N. Oyekoya[1], T. Dedova[1], V. Mikli[1], A. Mere[1], M. Krunks[1], L. Dolgov[2], I. Sildos[2]

[1]Department of Materials Science, Tallinn University of Technology, Estonia

[2]Institute of Physics, University of Tartu, Estonia

e-mail: ilona.oja@ttu.ee

Noble metal nanoparticles are perspective for modification of light absorption and scattering in optical materials. Optical films doped with noble metal nanoparticles have been used for more effective light harvesting in solar cells.

In the present study, the chemical spray pyrolysis method was used to deposit ultra thin TiO_2 films with gold nanoparticles (Au-NP). The TiO_2 spray solution was composed of titanium(IV) isopropoxide (0.2 mol/L) and acetylacetone in a molar ratio of 1:2 in ethanol. Gold(III) chloride trihydrate ($HAuCl_4 \cdot 3H_2O$) was used as precursor for the synthesis of Au-NP. $HAuCl_4 \cdot 3H_2O$ (0 or 5.4 mol%) was added into the spray solution for incorporation of Au-NP into TiO_2 films. Ultra thin TiO_2 films with Au-NP (Au:TiO_2) were deposited onto glass and ZnO nanorod layers at substrate temperatures in the range of 260-400 °C using pulsed spray solution feed (pulse consisting of 1 s of spray and 1 s of pause).

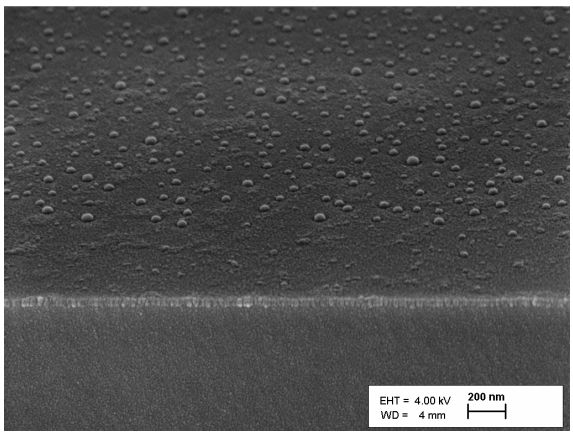

Fig.1 SEM image of the ultra thin Au:TiO_2 films deposited at Tsn= 300°C by the chemical spray pyrolysis method

The effect of the deposition temperature on the morphology, optical and structural properties of the ultra thin Au:TiO_2 films was characterized. According to XRD, TiO_2 films are amorphous at temperatures below 400 °C. According to SEM study, the size of the Au nanoparticles varies from 20 to 50 nm. The growth of the ultra thin Au:TiO_2 films on glass and ZnO nanorod layers are discussed. It is planned to adapt ZnO nanorod layer coverd with ultra thin Au:TiO_2 films in the generation solar cells.

F-31

Microwave Assisted Synthesis and Photocatalytic Properties of Sulfur and Platinum Modified TiO_2 Nanofibers

R. Drunka, J. Grabis

Institute of Inorganic chemistry, Riga Technical University

e-mail: reinis_drunka@inbox.lv

Photocatalytic activity of TiO_2 nanoparticles strongly depends on its crystallity, specific surface area, morphology of the particles and used dopants. Promising are materials with high specific surface area and with modified composition. In the present work formation of active TiO_2 nanoparticles in microwave synthesis and their modification with sulfur and platinum were studied. Anatase nanopowder and 10M KOH solution were used as raw materials. Microwave assisted synthesis method permited to obtain TiO_2 nanofibres and nanowires with a diameter of 10 nm and a specific surface area in the range of 70- 150m^2 / g. In order to improve the photocatalytic activity of nanofibers under visible and UV light, the samples were modified by their treatment at 380^{o}C in hydrogen sulfide gas streams for different time intervals. In order to modified TiO_2 nanofibers with platinum it was stirred in H_2PtCl_6 solution under UV irradiation. Photocatalytic activity was determined by degradation of the methylene blue solution under UV and visible light irradiation. The obtained samples showed higher photocatalytic activity with respect to pure TiO_2 nanofibers. The doped TiO_2 nanofibers were appropriate for degradation of harmful organic compounds as well as for hydrogen production by water splitting.

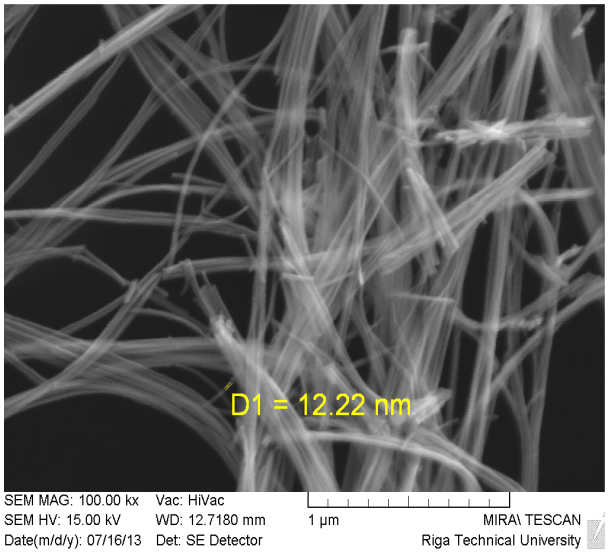

Fig.1 SEM micrograph of TiO_2 nanofibers.

Acknowledgment

The financial support of government research program LATENERGI is greatly acknowledged.

References:

1. L.Li, X.Qin, G. Wang, L. Qi, G.Du. J.Appl.Surf.Sci. **257**, 18 (2011)

F-32

Synthesis and Photocatalytic Activity of TiO_2 Nanotubes

A. Knoks, J. Kleperis, L. Grīnberga

Institute of Solid State Physics, University of Latvia, Latvia

e-mail: ainars.knoks@gmail.com, kleperis@latnet.lv

TiO_2 is commonly used material with a wide range of usage. It is also known that under irradiation of solar light TiO_2 nanostructures show photocatalytic activity. Therefore such kind of structures can be used for purification of air and water and hydrogen generation.

Different TiO_2 nanostructures can be made by vacuum evaporation, sol-gel and electrochemical methods, spraying, and others. Electrochemical anodization is one of the most efficient and cost-effective method for the preparation of nanostructured TiO_2 layers on titanium substrate. Moreover the surface morphology of nanostructures can be easily varied by changing temperature, applied voltage, composition and other chemical and physical parameters.

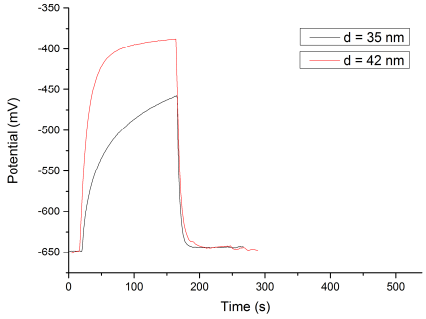

Fig.1 Open circuit potential dependence of NTs diameter.

In this work TiO_2 nanotubes were grown on Ti foils using electrochemical anodization process. Before the anodization samples were mechanically treated with polishing paste and then chemical cleaning in $HF:HNO_3:H_2O$ were performed. Nanotubes were grown in 0.14M NaF and 0.5M H_3PO_4 electrolyte applying different voltage for different samples.

Obtained TiO_2 nanotube structures were investigated with X-ray diffractometer, Raman scattering spectrometer and scanning electron microscope. Photoactivity of samples was defined using UV and VIS irradiation and potentiostat. Open circuit potential and current density measurements were studied and hydrogen production rate were determined.

Acknowledgement

Authors acknowledge State research program IMIS-2 for the financial support.

F-33

Water Adsorption on $SrTiO_3$ Single-Walled Nanotubes

A. Bandura, R. Evarestov, D. Kuruch

Institute of Chemistry, Quantum Chemistry Division, St. Petersburg State University, Russia

e-mail: di_ma_rex@front.ru

A low-temperature hydrothermal treatment is one of the main techniques of oxide-based nanotubes (NTs) synthesizing. This method has been successfully applied to generate strontium titanate NTs with relatively thin walls. As it can be supposed, the presence of water molecules is an important factor which can govern the inorganic NT structure and stability.

In this work we consider the results of the first ab initio calculations of water adsorption on the surface of the NTs rolled up from the strontium titanate layers. The structure and properties of bare perovskite-based NTs have been considered in our previous works [1] using the density functional theory and hybrid exchange-correlation functional. Similar computer modeling techniques have previously addressed to the adsorption of water molecules at the flat surfaces of perovskite-type strontium titanates [2]. For our present study we have chosen the relatively thin NTs folded from stoichiometric 4-layer $SrTiO_3$ slab with chirality (12, 12). Water molecules have been placed on the internal and external surfaces of the NTs, corresponding to both SrO and TiO_2 termination compositions. The full optimization of all atomic positions in the considered systems has been performed.

Our calculations revealed that the structure of NTs with adsorbed water molecules differs significantly from that of the non-hydrated NTs. The presence of water molecules promotes a disappearance of cylindrical symmetry and formation of tubular polyhedral objects. In all cases, the adsorption of molecules is accompanied by exothermic effect and leads to lowering of the NT formation energy. We have found that the adsorption energy of the water molecules depends on the curvature of surface in the vicinity of the adsorption centers. Obtained data confirm a significant role of aqueous environment in stabilizing the oxide NTs. It has been proved that the water molecules adsorbed on the SrO-terminated surfaces of NTs are more inclined to dissociation than the molecules adsorbed on thin flat layers.

References

1. R. A. Evarestov and A. V. Bandura, IOP Conf. Series: Mater. Sci. Eng. **23**, 012013 (2011)
2. R. A. Evarestov, A. V. Bandura and V. E. Alexandrov, Surf. Sci. **601**, 1844 (2007)

F-34

Hydrothermal Synthesis of Cobalt Ferrite Nanosized Powders

I. Zalite[1], G. Heidemane[1], L. Kuznetsova[1], M. Maiorov[2]

[1]Institute of Inorganic Chemistry of Riga Technical University, Latvia

[2]Institute of Physics of University of Latvia, Latvia

e-mail: ilmars@nki.lv

Recently ferrites have an increased scientific interest and demand for the material in different ways. The most significant usage of ferrites is in optic, electronic, mechanic and other fields [1]. Ferrites are of great importance in medicine, for biomedical purposes and in chemical catalysis.

In this research the cobalt ferrite nanopowders synthesis, prepared by hydrothermal method and their mechanical and magnetic properties has been studied.

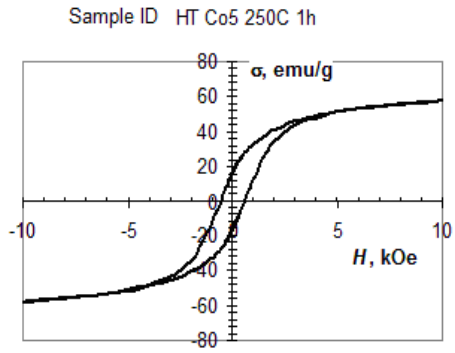

Fig.1. Magnetic properties of the cobalt ferrite nanopowder, prepared by hydrothermal synthesis.

Synthesis of cobalt ferrite nanoparticles was performed by co-precipitation technology, combined with the hydrothermal synthesis method. Firstly the precursor was prepared by hydrolysis of $FeCl_3$ and by co-precipitation of Fe and Co hydroxides. Then the obtained mixture of hydroxides was treated by hydrothermal way at different temperatures. After hydrothermal treatment, the suspension was washed and dried at 40 ^oC.

All samples were analyzed with X-ray diffractometer Advance 8 (Bruker AXS). Crystallite size determined using Scherer's equation. Magnetic properties analyzed with Vibrating Sample Magnetometer (Lake Shore Cryotronics, Inc., model 7404 VSM). Specific surface area (SSA) determined with BET method.

The all samples of cobalt ferrite obtained by hydrothermal synthesis have the same results of XRD and BET data, except sample No 1. This sample was synthesized at 200 ^oC of temperature by hydrothermal method and on the XRD pattern shows FeOOH phase.

However, the mode of synthesis influence on the magnetic properties and a coercive force of samples. Thus, the magnetization force of the samples is in the range of 50-60 emu/g.

References

1. B. Xue. *et al*. Chemistry Letters (2008), 37, 10, 1058-1059

F-35

ZnO Nanorods Grown Electrochemically on Different Metal Oxide Underlays

I. Gromyko, T. Dedova, M. Krunks, V. Mikli, T. Unt, I. Oja Acik, A. Mere

Tallinn University of Technology, Estonia

e-mail: inga.gromyko@gmail.com

For hybrid organic/inorganic solar cells with “ITO/blocking layer/ZnO nanorod/absorber layer” structure, it is highly important to synthesize series of ITO/blocking layer/ZnO nanorod structures by simple, inexpensive and low temperature technique. In order to increase the solar cell performance, it is desired to obtain high aspect ratio relatively conductive ZnO nanorods. In this study we present results on growth of ZnO nanorod on different seed layers, such as ZnO with different morphologies, ZnS, TiO2 compact thin films produced by spray pyrolysis on TCO substrates. Also blocking layer could be deposited on a top of ZnO nanorods grown onto TCO (transparent conductive oxide) directly, therefore in this work we also deposited ZnO nanorods by electrochemical deposition method directly on some chosen TCO substrates. All ZnO nanorod layers were grown electrochemically using ZnCl2 aqueous solutions (c=2 mmol/l) at the bath temperature of 80oC during one hour. Depending on the seed layer morphology, ZnO rods with different dimension, density were obtained. The structural, optical properties and morphology of seed layers and ZnO nanorod layers grown on them were studied by scanning electron microscopy (SEM), x-ray diffraction spectroscopy (XRD).

The dimensions, orientation, shape and density of the rods depends strongly on the properties of the used substrate or seed layer on a substrate.

Morphology and conductivity of the initial substrate plays an important role in ZnO nanorods dimensions, orientations and shape. For instance, larger rods (d=170, L=700 nm) were obtained on conductive substrates, such as ITO and ZnO:In substrates/ITO glass substrates and FTO substrates (d=250 nm, L=600 nm). Smaller rods (d=ca. 60 nm, L=400 nm) were obtained on nonconductive smooth, uniform and fined-grained substrates, such as ZnS and TiO2. Various ZnO seed layers resulted in ZnO nanorods with different shapes, sizes and distribution on the substrate.

F-36

Structure and Stability of WC Nanorods

V. Teil, A. Bandura, R. Evarestov

Institute of Chemistry, Quantum Chemistry Division, St. Petersburg State University, Russia

e-mail: tejlvitalij@gmail.com

Tungsten carbide (WC) exhibits an excellent combination of unique physical and chemical properties, such as low electrical resistivity, very high hardness and melting point, high bulk and Young's modulus, and good corrosion resistance. The nanosized forms of WC can provide further improving of physical properties and the generation of new materials with promising applications.

In this work we present for the first time the results of ab initio calculations of the atomic and electronic structure of WC nanorods (NR) fabricated from the cubic and hexagonal phases of WC. All calculations in this work were performed by first-principles method based on density functional theory (DFT) with using of a hybrid exchange-correlation functional PBE0, as implemented in CRYSTAL09 code [1]. Prior to study of NR structure, the bulk and surface properties of cubic and hexagonal WC polymorphs have been examined. Obtained structural, energetic and elastic properties of both the bulk phases agree well with the available experimental and theoretical estimations. The values of surface energies calculated for thin layers parallel to (100) crystallographic plane in cubic phase and parallel to (100), (110), (101), and (001) planes in hexagonal phase are close to those obtained in recent theoretical work [2]. In accordance with experimental observations, both the bulk and nanosized forms of WC possess the conductive capacity. It has been found that accounting of the spin-polarized states may be important for specific nanolayers and NRs.

The obtained results indicate that NR stability depends on its morphology, translational axis direction, and facet indices. The lowest formation energy was found for six-facet NRs cut from the hexagonal phase along the [001] direction by {100}, {010}, and $\{\bar{1}10\}$ crystallographic planes. The symmetry of these NRs is described by $P\bar{6}m2$ rod group.

Acknowledgements

Authors wish to acknowledge the assistance of the Saint-Petersburg State University Computer Center.

References

1. R. Dovesi at al., CRYSTAL09 User's Manual, University of Torino, Torino, 2009
2. Y. Li, Y. Gao, B. Xiao, T. Min, Z. Fan, S. Ma, D. Yi, Comput. Mater. Sci. **50**, 939 (2011)

F-37

Graphene Nanosheets Grown on Ni Particles

V. Grehov[1], J. Kalnacs[1], A. Vilken[1], A. Mishnev[2], G. Chikvaidze[3], M. Knite[4], D. Saharov[4]

[1]Institute of Physical Energetics, Latvia

[2]Latvian Institute of Organic Synthesis, Latvia

[3]Institute of Solid State Physics, University of Latvia, Latvia

[4]Riga Technical University, Latvia

e-mail: jkalnacs@edi.lv

Ultrathin graphite sheets or/and graphene nanosheets were obtained on the surface of particles of Ni powder. The new method based on well known dissolution and precipitation mechanism of graphene formation on catalyst surface is reported. Fig.1a presents the Ni powder particles with as prepared graphene sheets. Graphene nanosheets can be seen on the surface of Ni beads as grey coating on light beads. Freestanding graphene sheets were obtained after dissolution of Ni. Upon dissolution of the Ni powder is possible disintegration of the coating into the individual graphene sheets or the graphene sheets are formed the carbon body in the form of the original ingot sintered powder of Ni. In the first case graphene samples were obtained by vacuum filtration, in the second after drying of carbon body. SEM images (Fig. 1b) revealed that surface of the bodies consist of randomly aggregated, crumpled sheets closely associated with each other. The thickness of these sheets was determined with XRD by (002) diffraction peak broadening (Fig. 3). The quality of the sheets was estimated by Raman scattering spectra. Obtained by us layers can be defined as a graphene nanosheets. Number of graphene monolayers in these nanosheets controllably varied from 7 to 40.

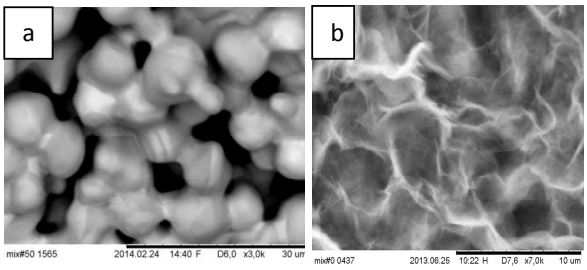

Fig. 1. SEM images of the particles of Ni powder after annealing with appropriate conditions (a). Surface of the carbon sample after Ni dissolution.

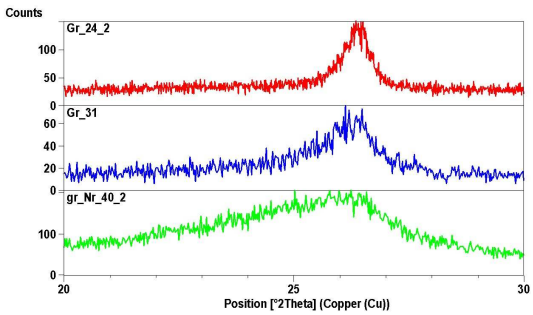

Fig. 3. XRD patterns of the graphene nanosheets samples, with different (002) diffraction peak broadening.

F-38

Structure and Properties of Functionalized Carbon Nanotube/Polypropylene Composites

I. Reinholds[1], V. Kalkis[1], J. Zicans[2], R. Merijs Meri[2], J. Bitenieks[2]

[1]Faculty of Chemistry, University of Latvia, Latvia

[2]Institute of Polymer Materials, Riga Technical University, Latvia

e-mail: ingars.reinholds@lu.lv

Structure, thermal, and mechanical properties were investigated for composite materials of polypropylene (PP) and acetic group functionalized multi-walled nanotubes (FCNT) at FCNT concentrations of 0.1%, 0.5% and 1.0% by weight. Part of the composites were compatibilized with maleic acid anhydride grafted polypropylene (PP-g-MA) at concentration of compatibilizer of 3 wt.%. Researched compositions were laboratory made from masterbatches of PP/FCNT and PP/PP-g-MA/FCNT solutions in o-xylene, which were sonificated, precipitated in methanol, dried and melt mixed with the same matrix of PP. The compositions were compression moulded in to film samples. Structure changes and the properties of composites were researched by the methods of tensile tests, differential scanning calorimetry (DSC), X-ray diffraction (XRD), Fourier infrared spectrometry (FTIR), and the measurements of dielectric characteristics. Effect of FCNT concentration in compositions as well as the effect of PP-g-MA compatibilizer was researched in detail.

The present study by structure changes confirmed that PP-g-MA compatibilizer served as an adhesive and affected improvement of FCNT dispersion in PP matrix greatly improving the mechanical properties. The stress–strain characteristics of PP/PP-g-MA/FCNT compositions revealed remarkable effects of the FCNT additions already at 0.1 wt.%. At this FCNT concentration, the Young's modulus and tensile yield stress increased by 13.5 and 17% that is by 1.5-fold greater increase of tensile yield stress compared to that of PP/FCNT. It should be noted that PP-g-MA compatibilized PP/FCNT compositions remained by 5-fold higher elongation at break even at FCNT content of 1.0% compared to unmodified PP/FCNT. XRD data showed formation of ordered crystals consistent with the monoclinic alpha phase of PP for all the compositions. The changes of DSC measurements indicated a reduced decrease of crystal ordering of PP with increase of FCNT in the presence of PP-g-MA. The changes of FTIR spectra for PP-g-MA containing composites indicated the interaction of FCNT carboxyl groups with maleic anhydride functional groups and their influence on the interfacial adhesion between FCNT and polypropylene, that confirmed increase of mechanical properties.

F-39

Investigation of Hard Wear Resistant Nanostructured Carbonitride Coatings Based on Ti-(Nb,Hf)-C-N Quarternary System Deposited by DC Magnetron Sputtering

V. Mitin[1], U. Kanders[1], V. Kovalenko[1], P. Nazarovs[1], D. Erts[2], J. Maniks[3]

[1]High-Tech Company Naco Technologies; Riga, Latvia

[2]Institute of Chemical Physics, University of Latvia, Riga, Latvia

[3]Institute of Solid State Physics, University of Latvia, Riga, Latvia

e-mail: ukanders@nacotechnologies.com

Ti-based nanostructured coatings such as Ti-Nb-C-N and Ti-Hf-C-N have been deposited by dc reactive magnetron sputtering in [Ar]/[N_2] gaseous mixture on a variety of steel substrates. Novel mosaic type sputter targets have been designed of titanium matrix and Nb/Graphite or Hf/Graphite inserts to generate 3-component Ti-Nb-C or Ti-Hf-C high energetic sputtered vapor flux during reactive deposition process. Sputtering resp. deposition rate and energetics of sputtered particles affect strongly film growing conditions, its structure, mechanical and tribological properties. Using conventional DC magnetron sputtering techniques without direct target cooling system discharge power density could not be raised higher than 10 W/cm^2. However, recently high power ion-plasma magnetron sputtering (HiPIPMS) sources have been designed allowing increase discharge power considerably higher than 60 W/cm^2 in average but reaching even 200 W/cm^2 within race track maximum [1]. In turn, mechanisms of formation and properties of Ti-(Nb,Hf)-C-N films got at high deposition rate are not investigated sufficient enough until now.

Within this investigation sputter deposited Ti-(Nb,Hf)-C-N film structure, mechanical and tribological properties have been modified by means of changing reactive DC HiPIPMS technological parameters. Mechanical and tribological properties such as adhesion to substrate, toughness, hardness, stiffness, friction coefficient (COF) and wear rate (W_r) of deposited Ti-(Nb,Hf)-C-N films have been studied by Vickers hardness testers HVS-50, HVS-1000B, nano-indenter G200, Teer Co Ltd thickness tester BC-2, scratch tester ST-30, and tribotester POD-2. 1,5÷5,4 um thick Ti-(Nb,Hf)-C-N films as hard coatings for cutting tools deposited at appropriate sputtering and growing conditions on high speed steel and cemented carbide substrates demonstrated excellent adhesion, hardness up to 38 GPa and Young modulus up to 520 GPa. In humid air, COF and W_r values dropped down as low as 0,21 and 0,18E-17 m^3/(Nm) respectively even at long friction path, > 1500 m.

References

1. V. Mitin, E. Sharipov, A. Mitin. High deposition rate magnetrons – innovative coating technology: key elements and advantages. // Surface Engineering, vol. 22, № 1, 1-6 (2006)

F-40

Tribological and Mechanical Properties of Sputter Deposited Carbon-Copper Composite Films and Their Structure

V. Mitin[1], U. Kanders[1], V. Kovalenko[1], P. Nazarov[1], J. Maniks[2], R. Meija[3], D. Erts[3]

[1]High-Tech Company Naco Technologies; Riga, Latvia

[2]Institute of Solid State Physics, University of Latvia, Riga, Latvia

[3]Institute of Chemical Physics, University of Latvia, Riga, Latvia

e-mail: ukanders@nacotechnologies.com

Sputter deposited amorphous carbon-copper composite (a-C/Cu) films on a variety of different steel substrates have been investigated with respect to their tribological and mechanical properties. Deposition rate affects film growth conditions, its structure and tribological properties. Using conventional DC magnetron sputtering technique discharge power density usually does not exceed 10 W/cm^2 thresholds. However, recently high power ion-plasma magnetron sputtering (HiPIPMS) sources have been designed allowing increase of discharge power considerably higher than 60 W/cm^2 in average [1]. In turn, mechanisms of formation and properties of a-C/Cu films obtained at high deposition rate are investigated insufficient until now.

In this work various parameters for deposition of films by HiPIPMS were applied. Pressure of sputtering gas mixture with Ar, Ar/H_2 and Ar/N_2 was varied in the interval p=0,1-0,7 Pa, electrical glow discharge voltage was U_d,=400-680 V, and current, I_d=1-3,5 A. Novel mosaic type sputter targets designed of copper matrix and carbon inserts has been used for deposited a-C/Cu films. The a-C/Cu films have been deposited onto faceted and polished plain steel discs made of cast iron, bearing steel, 100Cr6 and cemented carbides.

Mechanical and tribological properties of a-C/Cu films have been matched with their nano-structural features in order to understand mechanisms how amorphous carbon matrix interact with copper nanoparticles (Cu-NP) and how they determine film tribological properties such as coefficient of friction (COF), wear rate, W, and wear resistance or durability as wear distance, S, at low COF until Pin-On-Disk testing ball penetrates the film and COF jumps up. a-C/Cu films deposited at appropriate sputtering and growing conditions manifest low COF (<0,1) and W (<0,3E-15 m^3/(Nm)), but wear durability, S, reaches 1450 m. a-C/Cu film nanohardness, H, and Young's modulus, E, demonstrate such values as about 4 GPa and 80 GPa respectively.

References

1. V. Mitin, E. Sharipov, A. Mitin. High deposition rate magnetrons – innovative coating technology: key elements and advantages. // Surface Engineering, vol. 22, № 1, 1-6 (2006)

F-41

Humidity Induced Resistive Response Behavior of Bismuth Sulfide Nanowires

G. Kunakova[1], I. Bite[1], R. Meija[1], J. Prikulis[1], J.D. Holmes[2], D. Erts[1]

[1]Institute of Chemical Physics, University of Latvia

[2]National University of Ireland, Cork, Ireland

e-mail: Raimonds.Meija@lu.lv

During last decade semiconductor nanowires have been investigated as structural elements in relative humidity (RH) sensor devices [1]. In most cases the demonstrated nanowire sensors react by change of their surface properties. Due to large nanowire surface to volume ratio, this factor determines the advantage for application in sensors and influences the transport properties.

In previously reported studies, relative humidity nanowire sensing devices convincingly show linear response to RH in a broad measurement range [2]. However, this linearity fails in some specific conditions indicating an unusually strong surface impact to electrical transport. So far, bismuth sulfide (Bi_2S_3) nanowires have been studied for application in oxygen and hydrogen sensors [3,4], but relative humidity impact was not analyzed. Here we focus on humidity controlled Bi_2S_3 nanowire electrical properties.

Individual Bi_2S_3 nanowires were drop-casted to a pre-patterned substrate and electron beam lithography was used to fabricate contacts. RH sensing behavior was measured in the range from 5-90% in inert atmosphere and constant temperature.

Measured devices show nonlinear resistance dependence of the nanowire changing RH from 5 to 90%. In specific RH region from 40-50% reversible resistive behavior change is observed. Therefore resistance of the Bi_2S_3 nanowire and type of the major charge carriers can be tuned using appropriate relative humidity level.

References

1. S. Wang, C. Hsiao, S. Chang, and K. Lam, IEEE Sens. J., **12**, 1884 (2012)
2. Y. P. Leung, W. C. H. Choy, and T. I. Yuk, Chem. Phys. Lett, **457**, 189 (2008)
3. A. D. Schricker, M. B. Sigman, and B. A. Korgel, Nanotechnology, **16**, S508 (2005)
4. K. Yao, Z. Y. Zhang, X. L. Liang, Q. Chen, L.-M. Peng, and Y. Yu, J. Phys. Chem. B, **110**, 21408 (2006)

F-42

Synthesis and Properties of Magnetic Iron Oxide/Platinum Nanocomposites

V. Serga[1], M. Maiorov[2], L. Kulikova[1], A. Krumina[1], D. Karashanova[3]

[1]Institute of Inorganic Chemistry, Riga Technical University, Latvia

[2]Institute of Physics, University of Latvia

[3]Institute of Optical Materials and Technologies, Bulgarian Academy of Sciences

e-mail: vera_serga@inbox.lv

Magnetic composite nanoparticles produced on the base of ferromagnetic iron oxides with noble metals are of particular interest for applications in catalysis, sensor materials and biomedicine [1].

In this work, an iron oxide nanopowder was synthesized by the extractive-pyrolytic method (EPM) and used as a carrier for the further synthesis of Pt-containing nanocomposites by the EPM. The Pt content in the composites was 1.2 wt%, 2.4wt% and 4.8 wt%. The phase composition, morphology and magnetic properties of the produced materials were investigated. XRD analysis and magnetic measurements showed the dominance of the magnetic phase - Fe_3O_4 magnetite – in a carrier sample produced by the pyrolysis of iron carboxylate, but hematite α-Fe_2O_3 was present as an admixture. It is found that at the production of Pt-containing composites, the phase composition of the carrier has not practically changed, but the metal particle size there varies from 3 to 9 nm. Fig. 1 illustrates the TEM results for a composite with the 2.4 wt% Pt content.

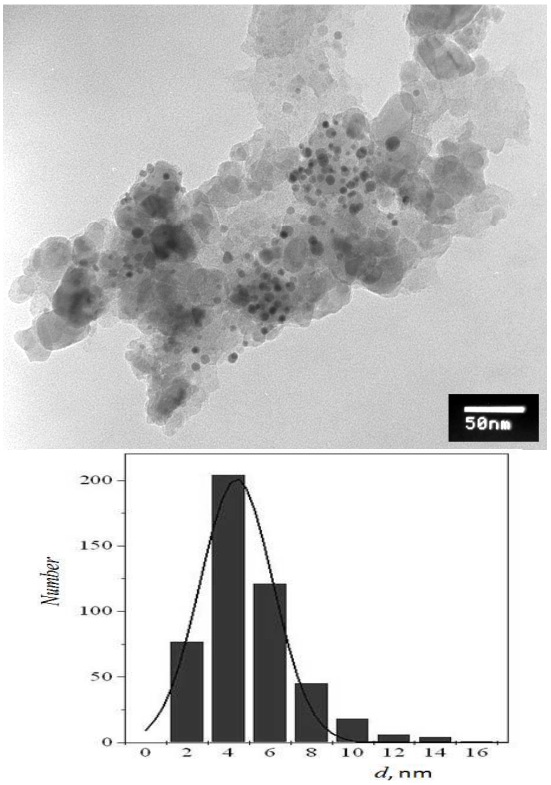

Fig. 1. TEM image of iron oxide/2.4 wt% Pt composite and the size distribution of Pt nanoparticles.

References

1. A.-H. Lu, E.L. Salabas and F. Schuth, Angew. Chem. Int. Ed. **46**, 8, 1222 (2007).

F-43

Magnetite Based Nanoparticles with Immobilized Heterocyclic Choline Derivatives as Potential Anti-Infective Agents

I. Segal[1], A. Zablotskaya[1], M. Maiorov[2], D. Zablotsky[2], E. Blums[2], V. Nikolajeva[3], D. Eze[3]

[2]Latvian Institute of Organic Synthesis, Latvia

[1]Institute of Physics, University of Latvia, Latvia

[3]Biological Department, University of Latvia, Latvia

e-mail: seg@osi.lv

The aim of the present study is synthesis and investigation of nanoparticles based on natural components: magnetite, oleic acid, and biologically active heterocyclic alkanolamine derivatives, structural analogues of choline**.**

The parent alkanolamine, 2-hydroxy-1-[3,4-dihydroisoquinolin-2(1*H*)-yl]ethane, was modified by introduction of undecyl substituent and further quaternization of the modified substance. Magnetic particles were obtained by wet synthesis. The method of magnetogranulometry and DLS measurements were used for determination of size and magnetic properties of nanoparticles prepared. The water-soluble magnetic nanoparticles synthesized were screened for *in vitro* antimicrobial properties against Gram-positive, Gram-negative bacterial and fungal strains using the agar dish diffusion method.

New water-soluble nanoparticles, containing biologically active derivatives of heterocyclic alkanolamines, which are immobilized on the surface of biocompatible, pre-coated with oleic acid iron oxide magnetite nanocarriers, have been prepared, and evaluation of efficacy of these nanostructures as antimicrobial agents has been studied. It was found that diameter of iron oxide core ranges within 6.2–10.5 nm, and magnetic fluids obtained possess antimicrobial effect.

Introduction of long chain alkyl substituent into the molecule of the second surfactant is an attractive and original approach to the lipophilicity increase and better interaction with lipophilic chains of the first coating. The wide possibility for variation of alkyl substituent in the alkanolamine can promote finer selection of perspective biologically active iron oxide based nanoparticles.

F-44

Optical Forcing of Magnetostatic Patterns in Ferrofluid Layers

L. Pukina, A. Mezulis, D. Zablotsky

Institute of Physics, Latvian University, Miera str. 32, Salaspils LV-2169, Latvia

e-mail: lasma.pukina@gmail.com

Colloidal solutions of magnetic nanoparticles – ferrofluids – are systems capable of unique pattern forming behavior. Spontaneous phase separation and formation of ordered and disordered patterns in layers of magnetic colloid may occur under the influence of external magnetic fields [1]. These patterns are the consequence of magnetic dipole-dipole interactions and the reversible agglomeration of the magnetic nanoparticles. Here we demonstrate experimentally how certain patterns can be selected through optical forcing and sustained by magnetostatic interactions.

The experiment was carried out with the continuous laser forced scattering setup in combined scattering mode. The sample is put into a solenoid so that its magnetic field is oriented normally to the walls of the ferrofluid layer. The low power reading He-Ne laser beam has the same direction through the sample- all reading optics is adjusted to see aggregated structures in the sample. Our ferrofluid contains Fe_2CoO_4 particles, the mean magnetic diameter of which 8…10 nm.

Ferrofluid layers with different thickness (10μm, 100μm, 200μm, and 500μm) were initially exposed to the external magnetic field. If the magnetic field is applied, the magnetostatic interaction occurs, tending to create a hexagonal pattern of ferroparticle agglomerates (Fig. 1, left).

In turn, the optical forcing is created by Nd:Yag laser beam, which transmits the sample layer from above in order to exclude the thermogravitation convection. The beam forms a periodic temperature grid within the sample, which also induces a corresponding particle concentration grid through colloidal thermophoresis. The achieved amplitude of the concentration modulation is less than 1%.

If the temperature grid by the Nd:Yag laser is induced after the magnetic field is switched on the Soret effect is too weak to alter the created hexagonal structures. On the other hand, if the temperature grid is induced first, the created concentration grid shapes the pattern of aggregation when the magnetic field is applied afterwards (Fig. 2, right). If the optical forcing is now switched off, the aggregation pattern remains in place, supported just by the magnetostatic interaction. Thus, in this way magnetostatic patterns, which have not been observed before can be created.

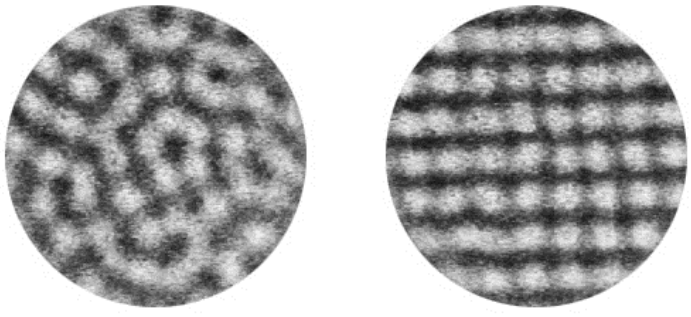

Fig. 1. Phase separation patterns: left – magnetic field prior, right – optical illumination prior

References

1. E. Blums, A. Cebers, M. M. Maiorov, Magnetic Fluids. Walter de Gruyter & Co., Berlin, New-York, 1997.
2. A. Cebers, J. Magnetohydrodynamics, 35 No.4, 1999, 278-296 pp.

F-45

Enhancement of the Optical Signal from Nitrogen-Vacancy Centers by Coupling to Surface Plasmons in Nanostructures

A. Jarmola[1], F.H. Gahbauer[1], J. Prikulis[2], D. Budker[3], D. Erts[2], R. Ferbers[1]

[1]Faculty of Physics and Mathematics, University of Latvia, Latvia

[2]Institute of Chemical Physics, University of Latvia, Latvia

[3]Department of Physics, University of California, Berkeley, USA

e-mail: jarmola@latnet.lv

Nitrogen-vacancy (NV) centers in diamond have received intensive interest in recent years because of their potential applications to quantum information [1] as well as magnetic field measurements with high spatial resolution [2,3]. The triplet ground state of NV centers can be polarized by optically pumping the spins into the m_s=0 level. The intensity of the red fluorescence observed after excitation with green light depends on the spin state of the center. The m_s=±1 levels in the ground state are separated from the m_s=0 level by 2.87 GHz, and undergo Zeeman splitting in a magnetic field. As a result, probing the NV centers with microwave radiation while observing the optical fluorescence allows the NV centers to be used as magnetic field sensors.

The optical output of these NV centers can be increased by coupling to plasmon-active nanostructures, which enhance the field of the incident radiation and reduce the lifetime of the excited state by coupling the fluorescence light to surface plasmons that propagate in metal nanostructures [4]. Layers of gold and silver nanostructures with plasmon resonances in the visible spectral range were produced by metal deposition through porous anodized aluminum oxide [5]. We will present the results of the study of the effect of different nanostructure parameters on the fluorescence of the NV centers in diamond.

Acknowledgment

Support from the ESF project 1DP/1.1.1.2.0/13/APIA/VIAA/054 is gratefully acknowledged.

References

1. M. V. G. Dutt et al., Science 316, 1312 (2007)
2. J. R. Maze et al., Nature 455, 644 (2008)
3. G. Balasubramanian et al. Nature 455, 648 (2008)
4. A. Huck et al. Phys. Rev. Lett. 106, 096801 (2011)
5. U. Malinovskis, et al., J. Phys. Chem. C. *in press* (2014) doi:10.1021/jp412689y

F-47

Structure, Nanohardness and Photoluminiscence of ZnN Ceramics Based on Nanopowders

F. Muktepavela[1], L. Grigorjeva[1], K. Chernenko[3], E. Gorokhova[4], P. Rodnyi[3]

[1]Institute of Solid State Physics, University of Latvia

[3]Saint-Petersburg State Polytechnic University

[4]Vavilov State Optical Institute, St. Petersburg

e-mail:famuk@latnet.lv

Properties and applications of ZnO ceramics as functional material for optoelectronics largely are determined by the structural state: grain size, porosity and quality of grain boundaries. Moreover, for ceramics based on nanopowders the formation process of structure due to aggregation and initial GB formation depends on the type, and morphology of powders [1,2]. Present work shows that the problem of aggregation can be solved by using uniaxial hot pressing (UHP) of grained powders or high temperature sintering (HTS) at 0.4-0.6T_m of powders with 3D tetrapod morphology. The UHP is very energy-intensive method which allows to obtain transparent ZnO ceramics [1]. Nanoindentation, SEM, AFM and PL studies were carried out on the obtained ZnO ceramics. Comparative analysis of results showed that all ceramics have recrystallized grains with sizes for UHP d=5-30 μm and for HTS d=2-4 μm. Within grains at depth range 50-500 nm hardness size effect was observed. Influence of GBs has softening character and at depth range 0.5-2μm hardness decreases from 5 GPa to 2-3 GPa without brittleness for both ceramics. Young's modulus was 100-120 GPa for HTS ceramic and 150 GPa for UHP and the latter coincides with ZnO single crystal. In HTS ceramics the photoluminescence (PL) spectrum at 12 K revealed a narrow exitonic band with LO phonon satellite peaks (1LO_Ex states) and almost negligible “green” luminescence. However, in UHP ceramics the main PL is in “green” spectral region and is due to point defect states. Results are discussed in terms of defects distribution during recrystallization processes. The differences in optical and structural properties define different fields of ZnO ceramics applications. Transparency of UHP ceramics allows it to be used as scintillators, and HTS ceramics as sensors.

References

1. E I Gorokhova et al J. Opt. Technology **78,** 753 (2011)
2. F Muktepavela at all IOP Conf. Ser.: Mater. Sci. Eng. **38** 012016(2012)

F-48

Cathodoluminescence Studies of Nanostructured AlN and AlN/CsI

V. Savchyn[1], C. Balasubramanian[2], A. Moskina[3] , I. Karbovnyk[1] and A.I. Popov[3]

[1]Ivan Franko National University of Lviv, 107 Tarnavskogo str., 79017 Lviv, Ukraine

[2]Institute for Plasma Research, Bhat, Gandhinagar, 382 044. India

[3]Institute for Solid State Physics, University of Latvia, Kengaraga 8, LV-1063 Riga, Latvia

e-mail: popov@ill,fr

Cathodoluminescence (CL) spectra of the aluminum nitride nanotubes and nanoparticles, synthesized by using a highly nonequilibrium dc-arc plasma method have been measured at 80 K and room temperature (RT) under electron irradition with 9 keV energy. Low-temperature CL spectra of nanostructured AlN have been compared with those of the commercially available AlN powder. The significant difference between emission spectra of the three investigated samples has been established. Commercial AlN has been found to emit a band peaked at 3.47 eV which is commonly ascribed to oxygen impurities. Emission of the AlN nanoparticles is centered around 3.66 eV while CL spectrum of AlN nanotubes show complex character with at least three peaks at 2.2, 3.0 and 3.5 eV in the photon energy range of 1.8 – 3.8 eV. CL intensity of the nanostructured samples has been found to decrease significantly at RT, most probably due to a combination of non-irradiative relaxations at the surface, electron-phonon interactions and the reabsorption of the emitted light. CL of AlN-nanotube/CsI-scintillator composites has been also studied. Energy transfer from CsI scintillator to AlN nanotube is demonstrated

F-49

Induction Heat Treatment and Technique of Nano-Bioceramic Coatings Production on Titanium

A. Fomin[1], I. Rodionov[1], M. Fomina[1], N. Petrova[2]

[1]Institute of Electronic Technology and Engineering, Yuri Gagarin State Technical University of Saratov, Russia

[2]Institute of Nanostructures and Biosystems, Saratov State University, Russia

e-mail: afominalex@rambler.ru

In medical practice, titanium and its alloys are widely used when intraosseous implants are manufactured [1]. It is important to obtain biocompatible coatings improving osseointegration on medical items. The substrate of implants has resistance to mechanical loads of distributed type. When installed with an interference fit into the prepared bone bed there is significant shear force causing coating delamination. Hence, biocompatible coatings should have high morphological heterogeneity of micro- and nanostructure [2,3].

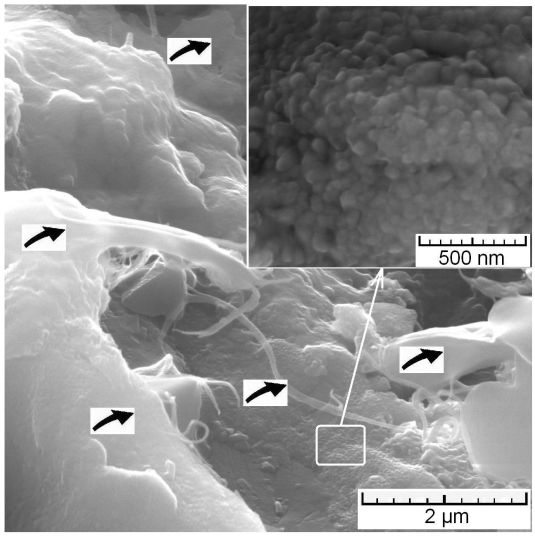

Fig.1 Titania coating and in vivo testing result (cell structure are shown by arrows)

The surface structure of titanium medical alloy after induction heat treatment (IHT) has high morphological heterogeneity and mechanical properties. The optimal parameters of morphology and hardness (10…15 GPa) are achieved at 800…1000 ºC and holding for 30…120 s. Titania coatings with nanocrystals are highly biocompatible, that is established *in vivo* (Fig.1). Oxidation at IHT and colloidal modification with hydroxyapatite nanoparticles form mechanically strong structure of porous titania matrix and bioceramic filler [2].

The research was carried out with financial support: grant RFBR 13-03-00898 “a”, 13-03-248 “a”, SP-1051.2012.4, project No. 1189 (basic part of the state educational task for institutions of higher education; Ministry of Education of the Russian Federation).

References

1. S. R. Paital, N. B. Dahotre, Mater. Sc. and Eng.: R, **66**, 1 (2009)
2. A. A. Fomin, I. V. Rodionov, et al., Adv. Mater. Res., **787**, 376 (2013)
3. A. A. Fomin, A. B. Steinhauer, et al., J. Frict. Wear, **35**, 32 (2014)

F-50

Dielectric and Mechanical Relaxation in the Modified Carbon Nanofillers Containing Polyvinyl Alcohol Composites

J. Zicāns[1], R. Merijs Meri[1], R. Bērziņa[1], J. Bitenieks[1], V. Kokars[2], V. Peipiņš[2], A. Rudušs[2]

[1]Institute of Polymer Materials, Riga Technical University, Latvia

[2]Chair of Chemistry, Riga Technical University, Latvia

e-mail: zicans@ktf.rtu.lv

Allotropes of carbon, such as graphite, graphene and carbon nanotubes, are one of the most promising materials for development of functional fillers for advanced composites, particularly polymer composites [1-3]. By modifying carbon nanostructures it is possible to tailor it electromagnetic, electrical, thermal, mechanical, and other properties according to the needs of the customer. Modification of carbon nanofillers aids also in improving of it compatibility with polymer matrix, being the most important prerequisite for development of successful polymer based nanomaterials.

Consequently in the current research carbon nanofiller (polyvinylpyrrolidone treated graphite, graphite oxide, reduced graphite oxide) containing polyvinyl alcohol composites have been obtained via solvent casting route. The content of carbon nanofillers in the polyvinyl alcohol matrix has been changed within the borders between 0 and 5 wt. %. Technological parameters of the method for manufacturing of polyvinyl alcohol composites with aforementioned carbon nanofillers have been optimized. The effect of the concentration of polyvinylpirrolidone on the dispersion ability of the carbon nanofillers in the polyvinyl alcohol matrix has been evaluated. Besides it structure, as well as dielectric and mechanical relaxation properties of polyvinyl alcohol – carbon nanofiller composites have been investigated.

References

1. P.J.F. Harris. Carbon Nanotubes and Related Structures. New Materials for the Twenty-first Century. Cambridge University Press. 2004.
2. Carbon Nanotubes - Polymer Nanocomposites. Ed. S. Yellampalli, InTech, 2011.
3. Polymer-Graphene Nanocomposites. Ed. V. Mittal, Royal Society of Chemistry, 2013.

F-51

Structure, Rheological and Mechanical Properties of Melt Compounded Polypropylene Nanocomposites

R. Merijs Meri[1], J. Zicans[1], T. Ivanova[1], A. Kokins[1], V. Kalkis[2], I. Reinholds[2]

[1]Institute of Polymer Materials, Riga Technical University, Latvia

[2]Department of Chemistry, University of Latvia, Latvia

e-mail: remo.merijs-meri@rtu.lv

Melt compounded polymer nanocomposites have certain advantages (such as commercial viability, mass production capacity and ease of integration in the existing recycling schemes) over the nanocomposites, obtained by solvent casting, latex and *in situ* polymerization routes. For manufacturing of perspective thermoplastics based nanocomposites, one of the most important tasks is assurance of excellent dispersion of the nanostructured filler in the polymer matrix. In the case of thermoplastics based carbon nanocomposites throughout qualitative dispersion of the nanofiller in the polymer matrix is hindered due to high viscosity of the polymer matrix, as well as strong Van der Waals interaction between the nanofiller particles.

Consequently in the current research the effects of surface functionalization of carbon nanofillers as well as addition of specific processing aids to the polypropylene matrix during melt compounding by means of various manufacturing methods (internal mixer, twin screw extruder, twin roll mills) are evaluated. The effect of modification of polypropylene matrix by neat and functionalized carbon nanofillers has been evaluated by means of direct and undirect methods, such as electron microscopy, rheometry, stress-strain characterization, dynamic mechanical thermal analysis, thermogravimetric analysis and broadband dielectric spectroscopy.

F-52

Dielectric Properties of Graphene Like/Polyurethane Composites

J. Macutkevic[1], J. Banys[2], H. Muller[3]

[1]Vilnius University, Sauletekio al. 9, LT-00122 Vilnius, Lithuania

[2]IJL–UMR Universite de Lorraine–CNRS 7198, ENSTIB, 27 rue Philippe Seguin, CS 60036, 88026 Epinal Cedex, France

e-mail: jan.macutkevic@gmail.com

Graphene, a monolayer of sp^2-hybridized carbon atoms arranged in a two-dimensional lattice, has attracted tremendous attention in recent years owing to its exceptional thermal, mechanical, and electrical properties [1]. One of the most promising applications of this material is in polymer nanocomposites, polymer matrix composites which incorporate nanoscale filler materials. In this work broadband dielectric/electric properties of graphene like particles/poyurethane composites are presented in wide temperature range (25 - 450 K). Graphene like particles there are consitituted of single crystal particles of graphite made through exfoliation. They were characterized by scanning electron microscopy which showed that their thickness is of the order of 0.1 mm. Laser counting furnished a particle size distribution histogram with an average diameter of 10 mm. It was established that percolation threshold in investigated systme is between 1 and 2 vol% (Fig.1). On heating both dielectric permittivity and electrical conductivity of all composites increases. However, the most pronouncend increasing occurs above glass transition temperature in pure poliurethane (390 K). Above this temperature all composites, including those are below percolation threshold, are electrically conductive due finite polymer matrix conductivity and tunneling from graphene particles to poyurethane matrix. Potential barrier for currier tunneling increases below percolation threshold and decreases above. This can be explained by non-omic contact of graphene particles and polyurethane matrix below percolation threshold. The electrical transport at low temperatures, as well microwave dielectric properties of composites will be discussed in the presentation.

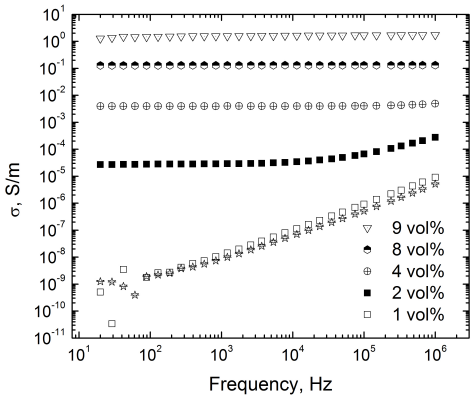

Fig.1 Frequency dependence of electrical conductivity of graphene/polyurethane composites at room temperature.

Acknowledgment

This research is funded by the European Social Fund under the Global Grant measure.

References

1. A. K. Geim, K. S. Novoselov, The rise of graphene, 6, 183-191 (2007).

F-53

Dielectric Properties of Composites with Carbon Nanotubes in PMMA Matrix

I. Kranauskaite[1], J. Macutkevic[1], J. Banys[1], D. Krasnikov[2], S. Moseenkov[2], V. Kuznetsov[2]

[1]Vilnius university, Sauletekio al. 9 Vilnius, Lithuania

[2]Boreskov institute of Catalysis SB RAS, Novosibirsk, Russia

e-mail: i.kranauskaite@ff.vu.lt

Dielectric properties of carbon nanotubes (CNT) composites were investigated very often, mainly in order to find an electrical percolation [1]. Indeed, above percolation threshold the values of dielectric permittivity and electrical conductivity for composites with CNT are very high in wide frequency range, including microwave and terahertz frequencies [2]. However, the relation between CNT microscopic parameters (like length or diameter), polymer matrix and percolation threshold in composites up to now is not clear [1]. Therefore, before experiment it rather impossible to predict dielectric properties of CNT composites. Generally, it is expected that percolation threshold (f_c) is directly proportional to CNT aspect ratio, however this relation experimentally was never observed and more complicated formula were used in order to establish influence of aspect ratio on percolation threshold in composites.

In this presentation results of dielectric investigations of composites with CNT in Polymethylmethacrylate (PMMA) matrix are presented in wide (20 Hz – 3 THz) frequency range. The mean diameter of all CNT used for composite preparation was 9 nm, while four different length CNT groups where used: 1) CNT with mean length about several tens micrometers, 2) CNT after oxidation with nitric acid, mean length 335 nm, 3) CNT after grinding in mill, mean length 438 nm, 4) CNT after grinding in mill, mean length 428 nm. It was establish that electrical percolation threshold in the first and second groups was 2 wt%, in the third 1 wt% and in the fourth 0.5 wt%.

The influence of CNT length on composite dielectric properties and DC conductivity will be discussed in the presentation.

Acknowledgment

This research is funded by the European Social Fund under Global Grand measure.

References:

1. W. Bauhofer, J. Z. Kovacs, A review and analysis of electrical percolation in carbon nanotube polymer composite, Composite Science and Technology 69, 1486 (2009).
2. D. Nuzhnyy, M. Savinov, V. Bovtun, M. Kempa, J. Petzelt, B. Mayoral, T McNally, Broad-band conductivity and dielectric spectroscopy of composites of multiwalled carbon nanotubes and poly(ethylene terephtalate) around their low percolation treshold, Nanotechnology 24, 055707 (2013).

F-54

Detecting VOC with Diferent Polymer-Nanostructured Carbon Composites

S. Stepina, G. Sakale, M. Knite

Institute of Technical Physics, Riga Technical University, Latvia

e-mail:Santa.Stepina@rtu.lv

Newest researches shows large amount of volatile organic compounds (VOC) used in manufacturing. Mostly workers can't detect VOC as soon as it's needed, creating more health problems and if VOC concentration in air is high enough it can be letal. Therefore advanced polymer - nanostructured carbon composites has been developed, where ethylene vinylacetate (EVA) copolymer (content of vinylacetate (VA) is 40%; Sigma Aldrich) have been used as matrix. Graphitesed nanoparticles (carbon black - CB) PRINTEX XE-2 with average particle size 30nm were used as conductive filler in one part of samples. Particles specific surface: 950m^2/g and DBP (dibutyl phthalate) adsorption: 380ml/100g. In other samples as conductive filler was used short multiwalled carbon nanotubes (SMWCNT). SMWCNTs were obtained from CheapTubes; outer diameter is 50-80 nm, inner diameter is 5-15 nm, length 0.5-2 μm. The SMWCNT specific surface area is 40 m^2/g, electrical conductance 100 S/cm.

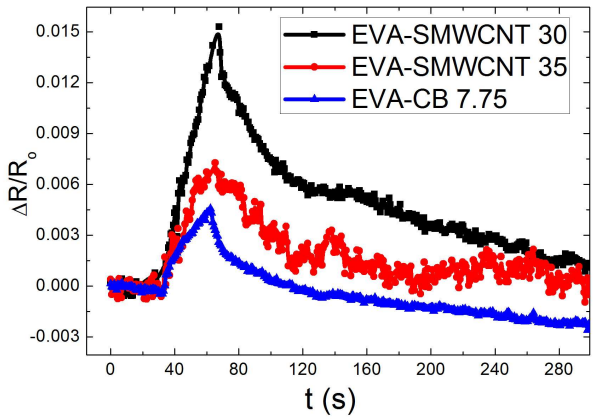

Fig.1 Relative electric resistance change in ethanol vapours (2000ppm) versus time (sample thickness is 70 μm). Sample exposed in vapours 30 seconds.

Both composite types were exposed to ethanol vapour (see Fig. 1). Results shows that the best of the EVA-SMWCNT composites has higer sensitivity to vapours than the best of the EVA-CB composite. that can be explained by specific character of conductive SMWCNT grid inside composite.

Additionaly EVA-CB composite, where exposed to fuel vapour. It was found that EVA-CB is able to distinguish different oil based products – petrol (with octane number 95) an diesel. When EVA-CB was exposed to petrol vapour, the composite relative electric resistance change was much larger comaring to diesel vapour. Observed difference in the composite response is explained by volatiliy of different fuel type.

F-55

Highly Porous Wood Based Carbon Materials for Supercapacitors

A. Volperts[1], G. Dobele[1], A. Zhurinsh[1], D. Vervikishko[2], E. Shkolnikov[2], N. Mironova-Ulmane[3]

[1]Latvian State Institute of Wood Chemistry, Latvia

[2]Scientific Association for High Temperatures, Russian Academy of Sciences, Russia

[3]Institute of Solid State Physics, University of Latvia, Latvia

e-mail: gdobele@edi.lv

Wood based activated carbons (AC) belong to micro- and mesoporous amorphous carbon materials. Chemical activation is a widely used method for activated carbons production – its advantage is the fact that it leads to synthesis of carbon materials with higher specific surface which is close to theoretical limits for the carbonaceous materials. Alkali metals hydroxides are one of the most effective activating agents allowing production of carbon adsorbents with specific surface over 3000 m^2/g when evaluated according BET theory. Variation in raw materials and activation conditions allow controlling total porosity, pore size distribution and properties of inner volume. This leads to alterations in activated carbons chemical and physical properties depending on precursor and synthesis conditions.

The topical area of research is AC their application as electrodes in supercapacitors. The main problem in this area is matching of carbonaceous material pore sizes with hydrodinamical radii of electrolytes molecules, elucidation of oxygen surface groups role, decrease of electrodes resistance. Low cost of AC is a necessary requirement as well.

This research is devoted to the propertis of nanoporous wood-based activated carbons for the application as electrodes in supercapacitors with inorganic and organic electrolytes. The main factors defining properties of carbonaceous material thermocatalytical synthesis are shown: specific surface, pores volume and width, particles dispersity, ash content, and electrical conductivity, as well as their relation to capacity and working properties of supercapacitors. It was found that electrical capacity is practically independent from catalyst addition ratio at the given mode of thermocatalytical synthesis. On of the main factors is temperature of activation which leads to formation of micropores with narrow size distribution in carbonaceous material structure.

Acknowledgment

This research was supported by LV PP 5,2;2,4 program and cooperation project 666/2014.2.

F-56

Nanostructure Characterization of Fatigued IN738LC Superalloy at Elevated Temperature

M. Petrenec[1], P. Strunz[2], U. Gasser[3], M. Heczko[4], J. Zálešák[5], J. Polák[6]

[1]TESCAN ORSAY HOLDING, Czech Republic

[2]Nuclear Physics Institute of the Academy of Sciences of the Czech Republic, Czech Republic

[3]Laboratory for Neutron Scattering, PSI, Switzerland.

[4]Institute of Physics of Materials of the Academy of Sciences of the Czech Republic, Czech Republic

[5]Erich Schmid Institute of Materials Science, Austria

[6]CEITEC IPM AS CR, Czech Republic

e-mail: martin.petrenec@tescan.cz

The nanocrostructure characterized by trimodal distribution of strengthening γ' precipitates in Inconel 738LC nickel based superalloy after Low Cycle Fatigued (LCF) at temperature 700°C was observed. Different microscopic techniques and detectors as Scanning Electron Microscope (SEM) equipped STEM detector, transmission Kikuchi diffraction in the SEM, transmission electron microscope (TEM) in the bright field mode and high resolution transmission electron microscopes (HRTEM) with STEM mode were used for characterization and comparison of the superalloy nanostructure. The characteristic morphology of γ' precipitates in the γ matrix was examined by ex-situ and in-situ Small Angle Neutron Scattering (SANS) at high temperatures. From all used microscopic techniques, it was observed that the microstructure in the original material consisted of γ' precipitates from two distribution of different morphology: cuboid-like shape, with size around 670nm, and the spherical shape with diameter 52nm. After the LCF tests at temperature of 700°C (and not at other tested temperatures), the ex-situ SANS exhibited additional scattering intensity coming from another small γ' precipitates of up to 10 nm size. It was confirmed using the standardly prepared foils examined by STEM detector in SEM, TEM and HRTEM. Evolution of size and distribution of these precipitates was studied by in-situ SANS at elevated temperatures. It revealed that the smallest γ' precipitates arise regardless the application of the mechanical load. Main effect of these precipitates is that they influence the low-cycle fatigue resistance at 700°C: the dislocations pinning by the smallest γ' precipitates was observed by STEM detector in SEM and by TEM in STEM mode.

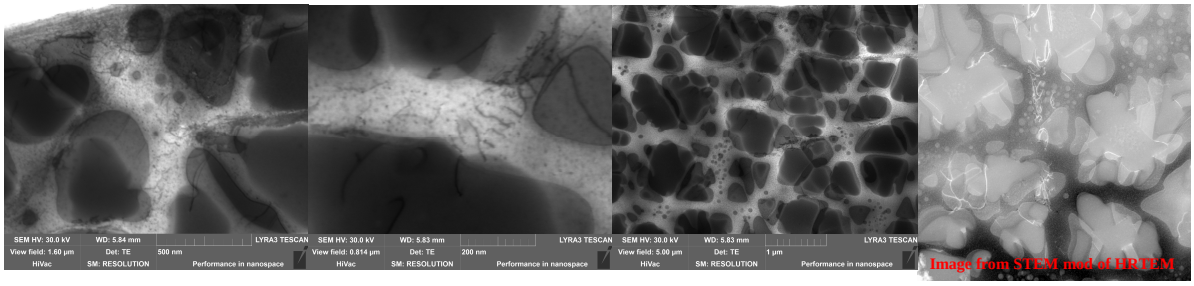

F-57

Control of Thickness and Residual Deformation in Lead Selenide Nanolayers

A.M. Pashaev[1], O.I. Davarashvili[2], M.I. Enukashvili[2], Z.G. Akhvlediani[2,3], R.G. Gulyaev[2] and M.A. Dzagania[2]

[1]National Aviation Academy, Baku, Azerbaijan

[2]Iv. Javakhishvili Tbilisi State University, Tbilisi, Georgia

[3]E.Andronikashvili Institute of Physics, Tbilisi, Georgia

e-mail: omardavar@yahoo.com, zairaak@yahoo.com

Recently we have proposed to use strained lead selenide layers grown on KCL substrates as the base for high-temperature and high-sensitivity photodetectors [1]. In thin PbSe layers ≤ 200nm thick, "negative" pressure is realized (the lead selenide layers are stretched at a_{PbSe}=6.126Å, a_{KCl}= 6.290Å) and the forbidden gap width increases. At appropriate doping of lead selenide with such impurities as Cr, In and Yb, the quasi-dielectric state can be realized, and the impurity level shifts deeply into the forbidden gap. According to the estimates, the concentration of current carriers decreases by 5-6 orders of magnitude as a result of compensation of electrically active nonstoichiometric defects. As the critical thickness of lead selenide layers on the KCl substrates made up 2 nm, for formation of the supercritical unrelaxed state, natural barriers were used for retarding the dislocations - placement of nonstoichiometric defects in dislocation nuclei at high concentration of defects, $>10^{18}cm^{-3}$ [2]. During the two-stage growth of layers by molecular epitaxy with a "hot" wall, when at the first stage the islands emerged and merged, the basic growth took place at the second stage, and residual deformations at the level ~0.01 was realized at the layer thickness ≤ 100nm, i.e. in the nanolayers [3]. It should be noted that these results were obtained at the growth rate < 5 nm/s at the second stage and the temperature of epitaxy ~300°C. For achieving two goals: to increase the level of residual deformations in the layers and the corresponding layers thickness, the production process was carried out in a complex way. The level of residual deformations increased with the increasing temperature of epitaxy when the migration of nonctoichiometric defects accelerated and their more efficient placement in the dislocation nuclei was achieved. For preventing the decrease in the growth rate and the thickness of layers, the epitaxy source temperature was somewhat increased, and the distance between the open end of the ampoule with the source of epitaxy and the substrate was reduced. When the growth of the layers at the second stage made up a few nm/s, the layers thickness and residual deformations in the layers were controlled by changing the growth time. As a result, at the thickness of the strained PbSe layer ~ 100nm, the increase in the forbidden gap made up ≥100meV as compared with the PbSe monocrystal. The realization of the quasi-dielectric state in a wider set of solid solutions of lead selenide with tin selenide will allow spanning a wider spectrum range in corresponding IR photodetectors.

References

1 A.M. Pashaev, O.I. Davarashvili, Z. G. Akhvlediani, M. I. Enukashvili, L. P. Bychkova, M.A. Dzagania. *J. Mat. Sci. Eng.*, 2012, 2, 2, 142-150.

2 A.M. Pashaev, O.I. Davarashvili, Z. G. Akhvlediani, M. I. Enukashvili, R. G. Gulyaev, V. P. Zlomanov. *J. Mod. Phys.*, 2012, 3, 6, 502-510.

3 A.M. Pashaev, O.I. Davarashvili, M. I. Enukashvili, R. G. Gulyaev, M.A. Dzagania, V. P. Zlomanov. *Georg. Eng. News*, 2012, 2, 109-112.

F-58

Multifunctional Properties of KI Crystal at Lattice Symmetry Lowering by Low Temperature Elastic Stress

K. Shunkeyev[1], N. Zhanturina[1], A. Barmina[1], L. Myasnikova[1], S. Sagymbaeva[1]

[1]Zhubanov Aktobe Regional State University, Kazakhstan

e-mail: shunkeev@rambler.ru

By the method of stationary absorption and luminescence spectroscopy the efficiency of radiation defects formation of (I_3^-- and F- centers) and the nature of luminescence in KI crystal at lattice symmetry lowering by low temperature (100K) elastic stress were investigated. The main mechanism of radiation creation of X_3^-- centers in alkali halide crystals (AHC) is a result of the interaction between interstitial halogen atoms in a regular lattice sites[1]. Unitization process of halogen atoms in NaCl crystal with different configurations of - Cl_3^-, Cl_5^- and Cl_7^- centers, which appear at ultrahigh pressures, were shown in [2] that is a proven phenomenon in AHC.

Intrinsic luminescence of AHC is interpreted by the radiative relaxation of self-trapped electronic excitations (excitons, electron-hole pairs) in regular lattice sites. Thus, on the example of KI crystal, where there is a sufficient length of the path of free excitons to self-trapping (at 80K is 350a, where a - the lattice constant), experimentally was demonstrated the influence of low temperature stress on the non-radiative (I_3^-- and F- centers) and radiative relaxation of self-trapped excitons. At KI crystal lattice symmetry lowering by low temperature (90K) elastic stress were established the following physical effects:

• increase in the intensity of exciton-like emission due to the increased probability of excitons self-trapping, caused by the weakening of the exciton-phonon interaction;

• decrease in the concentration of radiation defects I_3^-- and F- centers, which are an indicator of the efficiency of generation of anion Frenkel pairs.

In conclusion, the increase in the yield of intrinsic luminescence of crystals is interpreted by the growth of the potential barrier height, reducing the probability of radiation defect formation at self-trapped excitons decay.

References

1. Ch. Lushchik, A. Lushchik, Decay of Electronic Excitons with Defect Formation in Solids, Moscow, Nauka (1989)
2. W. Zhang, A. Oganov, A. Goncharov, Q. Zhu, S. Boulfelfel, A. Lyakhov, E. Stavrou, M. Somayazulu, V. Prakapenka, Z. Konopkova, Science, **342**, 1502 (2013)

F-59

Sheet Resistance Parameter Optimization of Light Transmitting Welding Electrodes Made of Indium Tin Oxide

K.D. Vanyukhin, A.A Voronova, E.M. Evseeva, R.V. Zakharchenko, L.A. Seidman

National Research Nuclear University "MEPhI", Russia

e-mail: kirivan@list.ru

Stoichiometric composition of indium tin oxide (ITO) is a n-type semiconductor with low sheet resistance $(5\text{-}10)\cdot10^{-4}$Ohm·cm. Due to its properties, ITO film forms an ohmic contact to p-GaN, and provides a good spreading of the electric current over the contact window area.

Previously [1], various technological modes of formation of a transparent conductive ITO films have been discussed, its interrelation with the parameters of the films after heat treatment has been observed and the optimization of a post-deposition annealing was performed to use them as a contact to p-type conduction areas in GaN LEDs. Films annealed at 500°C in air become transparent with a sheet resistance of 45ohm/sq. Subsequent annealing of this film in nitrogen with the same parameters does not change its transparency, but reduces its surface resistance to 27ohm/sq. As we can see, by choosing an annealing atmosphere (nitrogen or air) we can affect on the film resistance value which can be changed in both directions. In this paper we show that the same trends are applicable to the ITO films, which were obtained without an oxygen inlet under a multistage annealing in different environments. ITO films were deposited by e-beam evaporation that eliminates the negative impact of plasma on a crystal structure of a semiconductor. It was found that the deposition process and the environment have only slight effect on the electrical and optical properties of the ITO film. It was found that annealing in nitrogen environment reduces sheet resistance of the film, but does not provide its transparency. Specified optical transmittance is about 80-90% can only be achieved by annealing in the air at 500-600°C with a sufficiently low resistivity of the film around $(5,5\text{-}7,0)\bullet10^{-4}$ohm•cm.

This method allows to vary the surface resistance of the ITO layers in a wide range (from 20÷100ohm/sq.) and to reach values specified for LED structures. This provides a homogeneous current spreading in the LED window and uniform illumination at the entire surface of the window, which prevents overheating of a selected diode areas and increases the diode light output.

References

1. K.D. Vanyukhin, R.V. Zakharchenko, N.I. Kargin, L.A. Seidman (2013). Peculiarity of forming Transparent Conducting films on basis of Oxides Indium-Tin for contacts on GaN-Based Light Emitting Diodes. Izvestiya Vysshikh Uchebnykh Zavedenii. Materialy Elektronnoi Tekhniki, 2013, No. 2, pp. 60–65.

F-60

Comparative Studies of Alumina Coatings on Aluminum Prepared with Electrochemical and Plasma Electrochemical Oxidation Routes

K. Smits[1,2], D. Millers[1,2], J. Maniks[1,2], A. Zolotarjovs[1,4], R. Drunka[3,4]

[1]Institute of Solid State Physics, University of Latvia, Latvia

[2]Applied Electronics Labs, Latvia

[3]Institute of Inorganic Chemistry, Riga Technical University, Latvia

[4]Elgoo Tech, Latvia

e-mail: smits@cfi.lu.lv

In past centuries the aluminum protective coatings are very important objectives in different industries. By coating of aluminum with alumina the designed materials combines the lightness of aluminum and the hardness of alumina. Alumina coating increases performance and an extends service life.

Alumina plasma electrolytic oxide (PEO) and electrochemical oxide coatings under various conditions were prepared for comparative studies. The PEO coatings were prepared by new time correlated profile route. The coating thickness were varied by preparation modes (current intensity in peaks and peak profiles) and also overall process time. In this first research stage the electrolyte composition was kept the same, however the parameters of PEO regime was varied.

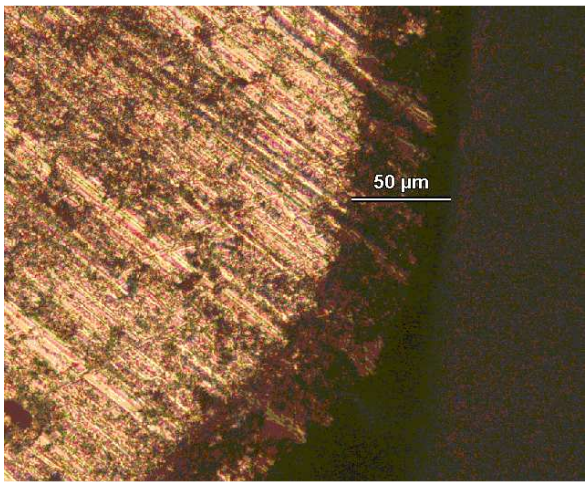

The samples covered by alumina were subsequently annealed and studied by a number of methods usually applied for solid state. These methods were optical microscopy, scanning electron microscopy, x-ray diffraction, x-ray energy disperse spectroscopy, optical spectroscopy and also surface roughness and hardness tests.

It was shown that the alumina morphology, structure, and hardness strongly depends on the selected preparation mode profiles.

F-61

SbSI Based Photonic Crystal Superlattices: Band Structure and Optics

S. Simsek[1], S. Palaz[2], O. Oltulu[2] A.M. Mamedov[3,4], E. Ozbay[3]

[1]Department of Material Science and Engineering, Hakkari University, Hakkari Turkey

[2]Department of Physics, Harran University, Urfa Turkey

[3]Nanotechnology Research Center, Bilkent University, Ankara Turkey

[4]International Scientific Center, Baku State University, Baku, Azerbaijan

e-mail: mamedov@bilkent.edu.tr

In present paper we have studied the optical properties and band structure in ferroelectric based aperiodic photonic structures, namely the Fibonacci lattices, combining ordinary positive index materials and dispersive metamaterials. The structure present new band gap which in contrast with the usual photonic band gap and do not based on interference mechanisms.

We also find that the width of the gap will be maximum at an optimum filling factor. The gap will vanish if the filling factor is greater than a critical value. Moreover, for a given filling factor and a metamaterial, it is interesting that the gap will be enlarged as the refractive index of the traditional layer increases. Some distinctive aspects of these gaps are outlined and the impact on the photonic spectra produced by the level of the generation of the aperiodic structure is analyzed.

Futhermore, we extend this result to other aperiodic systems.

F-62

Comparative Study of Nanoscaled Fluctuation Inhomogeneities in Main Glass Forming Oxides

L. Maksimov[1], A. Anan'ev[1], V. Bogdanov[2], N. Ovcharenko[1], V. Rusan[1]

[1]Research and Technological Institute of Optical Material Science, Russia

[2]Saint Petersburg State University, Russia

e-mail: inter_glass@inbox.ru

"Frozen-in" density, anisotropy, and concentration fluctuations of undoped and doped glassy SiO_2, B_2O_3, GeO_2, P_2O_5, TeO_2 and their combinations were studied by joint application of Rayleigh and Mandel'shtam-Brillouin scattering (RMBS) spectroscopy and high temperature acoustic (HTA) measurements. Analysis of the data is based on Schroeder's formulation [1]:

$$R_{L-P} = \frac{I^R}{2 \cdot I^{MB}} = R_\rho + R_C + R_{anis}$$

where I^R, I^{MB} are the intensities of components of RMBS spectrum, $R_{L\text{-}P}$ is the Landau-Placzek ratio, R_ϱ, R_C, R_{anis} are the contributions of density, concentration, and anisotropy in $R_{L\text{-}P}$.

$$R_\rho \approx \frac{T_g}{T}[(v/v_{0,Tg})^2 - 1]$$

where T_g, T are the glass transition and room temperatures, v and $v_{0,Tg}$ are the extremely high and low frequency sonic velocities, correspondingly Measurement procedures is described elsewhere [2].

$R_{L\text{-}P}$ of glassy P_2O_5 and TeO_2 are found from the RMBS spectra of La_2O_3-P_2O_5 glasses and HTA data of R_2O-TeO_2 glass melts [3]. It allowed to outline the composition range of well-developed index fluctuations and, consequently, light scattering losses of TeO_2-P_2O_5 glasses. RMBS and HTA data for glassy B_2O_3 with various amounts of OH groups evidencies that OH groups causes the growth of light scattering losses while discrepance of $R_{L\text{-}P}$ of various samples of glassy GeO_2 originates from dependence of GeO_2/GeO ratio on synthesis conditions. It was found that clustering of Nd^{3+} ions in silica glasses causes both the growth of $R_{L\text{-}P}$ and lowering lifetime and quantum yield of luminesnce. This effect can be reduced by addition of third component in the system.

References

1. J. Schroeder, 'Light Scattering of Glass" in Treatise on Material Science and Technology. Glass I. Academic, New York, N.Y., **12**, 157 (1977)

2. A. Anan'ev, V. Bogdanov, B. Champagnon, M. Ferrari, G. Karapetyan, L. Maksimov, S. Smerdin, V. Solovyev, Journal Non-Cryst. Solids, **354**, n 26, 3049 (2008)

3. J. Kieffer, L.E.Masnik, O.Nikolayev Phys.Rev.B, **58**, N2, 694 (1998)

F-63

Electrooptical Fibers

L. Maksimov, A. Anan'ev, V. Ivanov, B. Tatarintsev

Research and Technological Institute of Optical Material Science, Russia

e-mail: inter_glass@inbox.ru

Electro optical fibers (EO) seem promising as EO modulators in communication lines [1]. Inorganic glass compositions, drawing technology, and parameters of EO fibers are presented. Groups with stoichiometry of EO crystal $NaNbO_3$ in an alkali silicate glass led the dramatic increase in its Kerr coefficient. Optimal concentration of Nb_2O_5 in a glass batch was determined that ensured the growth of Kerr coefficient, B, from $0.5 \cdot 10^{-16}$ m/V^2 (silica glass) to $10 \cdot 10^{-16}$ m/V^2 [2]. Usage of the so-called bundle technology made the manufacturing the trial single mode EO fiber possible [3].

Parameters of EO fibers made of inorganic and organic glass are listed below.

Material of a core	Inorganic niobate glass	Organic glass PMMA [1]
Diameter of a core, μm	3	5
Glass transition temperature T_g, °C	655	< 230
Poling	No	at the drawing
EO effect	Quadratic (Kerr)	Linear (Pockels)
Half wave voltage $U_{\lambda/2}/d$, V/μm	5	5
Half wave length $l_{\lambda/2}$, m	20	384
Optical losses, dB/m (λ = 0.64 μm)	4	< 30
Depth of modulation, %	4.5×10^{-2}	4.5×10^{-2}

The bundle technology was used for manufacturing trial photonic crystal fiber (PCF) from EO multicomponent glasses. It was evidenced that PCF could keep polarization of propagating light. Two optical modes propagated in the PCF within the transparency range breaking down to photonic band-gaps shown in Fig. The metal alloy was chosen for forming buried electrodes at fiber drawing. [4]

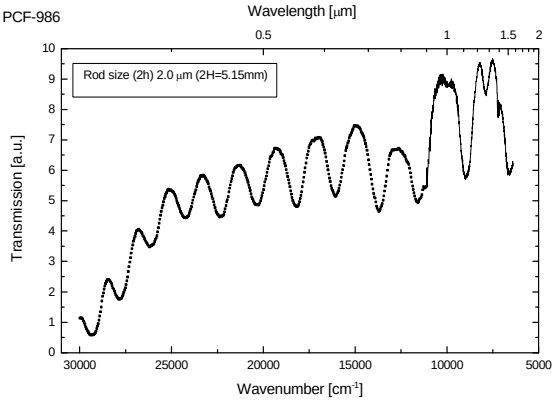

Fig.1 Transmission spectra measured along PCF fiber

References

1. D.J.Welker, J.Tostenrude, D.W.Garvey, B.K.Canfield and M.G.Kusyk Optics Letters **23**, 1826 (1998)

2. A.Anan'ev, G. Karapetyan, A. Lipovskii, L. Maksimov, V. Polukhin , D. Tagantsev, B. Tatarintsev, A. Vetrov and O.Yanush, Journal Non-Cryst. Solids **351**, 1046 (2005)

3. V.N.Polukhin, V.N.Ivanov, B.V.Tatarintsev, A.A.Vetrov, H.Bartelt and J.Kobelke Patent RU 2247414. Bull. **6 (**2005) (in Russian)

4. A.V.Anan'ev, V.B.Zheltov, V.N.Ivanov, A.A.Lipovskii, V.N.Polukhin, D.K.Tagantsev, B.V.Tatarintsev, H.Bartelt and J.Kobelke Patent RU 2397516. Bull. **23 (**2010) (in Russian)

F-64

Fabrication and Properties of Graphene/Bismuth Chalcogenide Layered Structures

M. Baitimirova[1], D. Jevdokimovs[1], D. Erts[1], J. Andzane[1]

[1]University of Latvia, Latvia

e-mail: margarita.baitimirova@lu.lv

During past half-century, bismuth chalcogenides (Bi_2Se_3 and Bi_2Te_3) were widely investigated due to their pronounced room-temperature thermoelectric properties. Application of these materials include thermoelectric generation, cooling and infrared detectors. Nanostructuring these materials became a challenging task because it is believed that the efficiency of thermoelectric materials can be improved by creating structures where one or more dimensions are reduced, such as nanowires, nanoribbons or thin films [1].

In our research, we combined bismuth chalcogenide thermoelectric materials and graphene in layered structures. Graphene – 2D crystalline allotrope of carbon – is perspective candidate to be used as a substrate for nanostructured bismuth chalcogenide synthesis due to its lattice geometry, allowing epitaxial growth of bismuth telluride and bismuth selenide [2, 3]. Also, graphene is perfect candidate for use as a top electrode in optoelectronic devices due to unique combination of properties – mechanical strength, excellent heat and electrical conductivity and transparency for visible and near-infrared spectrum.

Graphene/bismuth chalcogenide nanostructures were synthesized by combination of chemical vapor deposition (CVD) and catalysis-free vapor-solid deposition methods. Quality of structure components was inspected by scanning electron microscope, Raman and energy dispersive X-ray spectroscopy. Thermo- and optoelectrical properties of fabricated layered structures with different bismuth chalcogenide compounds were investigated under ambient conditions, compared and discussed. The presented combination of graphene with bismuth chalcogenides in layered structures may have applications in flexible infrared sensors, thermo-power and local cooling microdevices as well as in Li-ion batteries anodes.

References

1. S. Li, M.S. Torpak, H.M.A. Soliman, J. Zhou, M. Muhammed, D. Platzek and E. Muller, Chem. Mater. **18**, 3627 (2006)
2. C.-L. Song, Y.-L. Wang, Y.-P. Jiang, Y. Zhang, C.-Z. Chang, L. Wang, K. He, X. Chen, J.-F. Jia, Y. Wang, Z. Frang, X. Dai, X.-C. Xie, X.-L. Qi and X. Ma, Appl. Phys. Lett. **97**, 143118 (2010)
3. F. Tu, J. Xie, G. Cao and X. Zhao, Materials **5**, 1275 (2012)

F-65

Optical Properties of the Low-molecular Amorphous Azochromophores

A. Gerbreders[1], J.Aleksejeva[1], A. Bulanovs[2], E. Potanina[1]

[1]Institute of Solid State Physics, University of Latvia, Latvia

[2]G.Liberts' Innovative Microscopy Centre, Daugavpils University, Latvia

e-mail: andrejmah@gmail.com

The films based on the different type of the low-molecular amorphous azochromophores were prepared. The optical properties of the materials, such as transmittance and reflection spectra of the films, sensitivity to polarization holographic recording by two wavelengths (405 and 532 nm) were studied and compared.

The direct relief formation during the polarization holographic recording was explored, relief depth dependence on exposure and record beam intensity was investigated.

The holographic matrix on these materials base was produced without chemical etching process; the replication of holographic image was performed.

F-66

Kinetics of Diffraction Efficiency During the Holographic Recording of Surface Relief Gratings

M. Reinfelde, J. Teteris

Institute of Solid State Physics, University of Latvia, Latvia

e-mail: mara.reinfelde@cfi.lu.lv

Phenomenon of direct surface structure formation by holographic recording is provoked by photoinduced mass transport under polarized light illumination. Efficiency of recording is defined by distribution of electric field vector of resulting interference pattern inside the recording media [1, 2]. More profound studies showed the dependencies on film thickness and grating period. As factors affecting the manifestation of given effect, we should take into account the interaction between surface tension and surface relief grating formation forces created by light intensity gradient perpendicularly as well parallel to grating vector. The light propagation inside the films volume - inner reflection and diffraction by surface relief modifying the structure of electric field could be a factor affecting the surface relief formation process too. In presented study we consider the kinetics of diffracted light for different grating periods with the aim to evaluate the possible impact on distribution of electric field inside the samples volume by appearance of diffracted beams of higher orders.

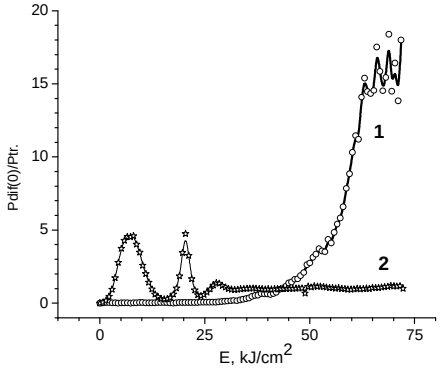

Fig.1. Dependence of ratio for diffracted 1-st and 0-orders light beam intensities on illumination doses: As_2S_3 sample thickness d = 1,3μm, recording light intensities I1≈I2=4W/cm^2; grating period Λ=1μm (curve 1) and Λ=5μm (curve 2)

References

1. M. Reinfelde, R. Grants and J. Teteris, J. Non-Cryst. Solids **377,** 162–164, (2013)
2. J. Teteris, U. Gertners and M. Reinfelde, Phys. Stat. Solidi (c) **8**, 2780-2784, (2011)

F-67

Recording of Surface Relief in Azobenzene Containing Low Molecular Weight Organic Glasses

K. Klismeta[1], J. Teteris[1]

[1]Institute of Solid State Physics, University of Latvia, Latvia

e-mail: k.klismeta@gmail.com

It was firstly shown by P. Rochon *et al.* [1] that stable, highly efficient surface relief gratings can be optically induced on surface of azopolymer films. One of the used methods to induce mass motion is holographic recording using wavelength corresponding to the absorption band of the azo compound. The sinusoidal light interference pattern on the surface of the sample leads to a sinusoidal surface patterning - a surface relief grating (SRG). As confirmed by atomic force microscopy (AFM), these gratings are found to be very large, with depth up to hundreds of nanometres and they diffract light very efficiently. [2]

In this work azobenzene containing low molecular weight organic glasses were experimentally studied. All of the studied samples absorb at the visible spectrum. Holographic recording with different wavelengths in the spectrum range of 375 – 671 nm and different polarization states of the recording beams (s-s, p-p and $+45^0$:-45^0) was used. Diffraction efficiency was measured during the recording of the SRG. Formation of the SRG was observed in all of the studied samples with depth determined by AFM to be up to 600 nm. The relationship between formation of SRG and photoinduced birefringence is discussed.

References

1. P. Rochon, E. Batalla and A. Natansohn, Appl. Phys. Lett. 66 (2), 136 (1995)
2. K. G. Yager and C. J. Barret, Smart Light-Responsive Materials, 145 (2009)

F-68

Analysis of Excitonic Mechanism of Defect Formation in Insulating Materials - Generalization of Rabin-Klick Diagram for a whole Family of Alkali Halides

A.I. Popov[1], A. Lushchik[2], Ch. Lushchik[2] and E.A. Kotomin[1,3]

[1]Institute for Solid State Physics, University of Latvia, 8 Kengaraga Str., Riga LV-1063, Latvia

[2]Institute of Physics, University of Tartu, Riia 142, 51014 Tartu, Estonia

[3]Max Planck Institute for Solid State Research, Heisenbergstr. 1, D-70569 Stuttgart, Germany

e-mail: popov@ill.fr

In this presentation, the efficiency of excitonic mechanism of radiation-induced defects formation in insulating solids is discussed. We analyze the condition of nonradiative exciton decay into stable Frenkel point defects and compare experimental and theoretical values of primary defect formation energies, band gap and absorption energies including wide class of materials (halides, binary and ternary oxides etc).

In materials, containing F centers, the relation between the stable F center (anion vacancy with trapped electron) formation yield vs material structural parameters under irradiation (known as Rabin-Klick diagram) is widely used. We demonstrate in this talk, how this diagram could be generalized for a whole family of alkali halides (both NaCl and CsCl –type structures). For this reason experimental data on the F center production efficiency (eV/center) vs. S/D parameter (the ratio of the separation between halogen ions and diameter of the halogen ion) for cesium halides are collected and analysed. We discuss also current understanding of the F-type center formation process in alkali halides and oxides with a special attention to self-trapping of electron/holes.

F-69

Integrating Sphere Produced by 3D Printing and CNC Milling

R. Trukša[1], S. Fomins[2], J. Dzenis[1]

[1]Optometry and Vision Science Department, University of Latvia, Ķengaraga 8, Rīga, LV-1063

[2]Institute of Solid State Physics, University of Latvia, Ķengaraga 8, Rīga, LV-1063

e-mail: reenaars@inbox.lv

To provide total amount of the irradiated light or luminous flux, integrating spheres are used [1]. Application of integrating sphere is helpful also for design of light source consisting of many light emitting elements like LEDs. It is very important to know irradiance spectra and total irradiance in photometric units of each source. This knowledge enables us to predict light colour of mixture when we change voltage on few LEDs apart and all at once. Also we can predict colour of objects illuminated by our light source, because objects in our environment doesn't appear coloured till they are illuminated by proper light source. Excellent light mixing properties are useful in colour vision science where ability to change light source spectral properties is essential in order to get more inside in nature of person colour perception.

In this study we design and produce integrating sphere by 3D printing and CNC milling techniques. We have designed integrated sphere 50 mm in diameter with 4 openings – 3 of them are meant for light sources and 1 of them is for spectrometer or other sensors.

The inside surface of the sphere is covered with non-fluorescent white ink. Spectral reflectance was tested with calibrated *USB4000 Ocean Optics* spectrometer and fibre optics in the visible and near infrared wavelengths range. The surface structure produced by 3D printing provides more scattering comparing to absolute surface, but this does not influence the reflection properties. Device is suitable for photometric evaluation of small size light sources (2x2x4 cm) and provides excellent light mixing for vision science and colorimetry.

References:

1. R.W.G. Hunt. Measuring colour. pp:114-117.

F-70

Study of Performance of Hybrid Fiber (Hemp/ Polypropylene/ Glass) Woven Reinforcements

M. Manins, A. Bernava, G. Strazds

Forest Industry Competence Centre, Riga, Latvia

e-mail:audejs@inbox.lv

With increased strain on petroleum resources textiles are replacing traditional materials in various industries. Textile fibers and fabrics are increasingly being used to create fiber-reinforced plastic composites that have the fabric structure and surface density suitable for the future use of the particular composite and in which fiber materials are compatible with the matrix.

Woven composites are superior to conventional materials due to their stiffness, strength, stability, weight, cost, manufacturing, corrosion resistance, insulation purposes, taking shape, etc...The main factors to evaluate when deciding whether to use a textile composite or a conventional tape laminate are mechanical properties and the ease and cost of manufacture [1]. Textile-reinforced thermoplastic composites have huge application potential in rapid manufacturing of components with versatile possibilities of integrating functions. In structural applications, textile composites are usually used as reinforcement due to the possibility to tailor the load bearing capacity through the fibre architecture. As a result of their growing potential for lightweight applications, textile-reinforced thermoplastic composites are becoming of greater interest for the industry. Thermoplastic composites show a number of advantages compared to classical composites based on thermoset matrices, among which the possibility of low-cost, rapid production has to be mentioned first [2].

The aim of the research is to look for a rapid manufacturing of components with versatile possibilities of integrating functions. The hemp fibers and polypropylene fibers were used for reinforcement production. To ensure better mechanical properties of reinforcement, 25% or 50% of glass roving in warp direction was added. The performance of woven reinforcements was tested.

References

1. D. Derakhshan, F.Pourfakharan, Proc. Eng.**14,** 2830(2011)
2. W. Hufenbach, R.Böhma, M.Thieme, A Winkler, E.Mäder, J.Rausch, M.Schade, Mat &Des.**32** 1468 (2011)

F-71

Properties of Carbonized Na-Al-Si Glass Fiber Fabrics

E. Pentjuss, A. Lusis, J. Gabrusenoks, G. Bajars

Institute of Solid State Physics, University of Latvia

e-mail: pentjuss@cfi.lu.lv

Object of research is industrially produced Na-Al-Si glass fiber fabrics having diffusion of Na^+ ions to surface of elementary fibers that react with CO_2 and humidity from atmosphere and create the shell of mixture of hydrated carbonates on glass fibers [1]. It is known that trona ($Na_2CO_3 \cdot NaH(CO_3) \cdot 2H_2O$) heating over 56 ºC and hydrated sodium carbonate ($Na_2CO_3 \cdot H_2O$) heating over 100 ºC leads to its decomposition to sodium carbonate (Na_2CO_3) and weight loss by evolving H_2O and CO_2 to atmosphere. There are experimentally investigated the samples weight retrieval at room conditions and in elevated relative humidity environment. The weight increase is analyzed by regression technique. In the first 0.2-0.4 h after heating the weight increases with high degree ($R^2>0.99$) follows to regression

$$\Delta M(t) = A_0 - A_1 \exp(-t/t_1) - A_2 \exp(-t/t_2), \quad (1)$$

where A_0, A_1, A_2 are weight constants, t_1, t_2 - time constants ($t_1 \leq t_2$). $\lim \Delta M(t)=A_0$ if $t\to\infty$. $\lim \Delta M_1(t) =A_1\exp(-t/t_1)= A_1$ and $\lim \Delta M_2(t)=A_2$, if $t\to 0$. $A_0=A_1+A_2$ and $t_1 \leq t_2$ [2]. The short time (t_1) exponent (1) of weight increase is associated predictable with water and CO_2 absorption on the shell surface and second exponent with water and CO_2 diffusion inside the shell, allowing its additional absorption. As a rule are $t_1 << t_2$ and initial weight absorption velocity $v_1 >> v_2$. Some hours later appears the fabric thickness growth, associated with irreversible water and CO_2 incorporation into carbonate molecules. Weight recovery velocity and level are determined by environmental humidity level. At the low humidity levels (15-20 %) the weight relation after/before heating reach 1.0 after some thousands hours. Later there are observed some decrease of fabric thickness indicating to compacting structure of shell. In a case of high humidity (65-70 %) relation attains its maximal value (above 1.0) after tenths hours and then slowly decreases to a stable value (above 1.0) that may be determined by increased equilibrium content of free water of fabrics. Decrease of weight could be caused by changes in weights of mixture components at unchanged number of Na atoms

Acknowledgment

We are grateful to financial support of National program of Material Science “IMIS”

References

1. B. W.Veal, D. J. Lam and D. P. Karim, Nuclear Technology **51,** 136 (1980)
2. E. Pentjuss, A. Lusis, G. Bajars and J. Gabrusenoks, IOP Conf. Series: Materials Science and Engineering **49** (2013) 012044 doi:10.1088/1757-899X/49/1/012044

F-72

A Comparative Study of Natural Fiber and Glass Fiber Fabrics Properties with Metal or Oxide Coatings

A. Lusis, E. Pentjuss, G. Bajars, J. Gabrusenoks, U. Sidorovicha

Institute of Solid State Physics, University of Latvia, Kengaraga Street 8, Riga, LV-1063, Latvia

e-mail: lusis@latnet.lv

Sustainable development issues and rapidly growing global demand for technical textiles (woven and non-woven) for a variety of applications in the energy, automotive, aerospace and defense industries is stimulated to develop new materials based on hybrid textiles materials (fibers, yarns, fabrics) – woven and nonwoven. We are doing complex research on such new material based on natural and glass fibers. In these hybrid fabrics we benefit from the advantages of particular fibers which, when combined, may satisfy specific customer requirements for hybrid hemp-glass fiber yarns. For that we have to investigate some general features related to such fibers and fabrics, which are porous.

Recently many researchers recognized there is strong interest in new nanostructured porous materials based on fabrics or textiles for the application electrochemical technologies and devices. The fabrics have wide application as support material or substrate for functional species. Nanostructured textiles where conducting substances coated on porous textile fibers, are serving as conductive three-dimensional frameworks for electrodeposition of functional species. The actual for textiles are topics which textiles are used both as functional construction material and as a support of functional species for electrochemical devices.

A comparative study had been done of flax, hemp and glass fiber fabrics coated with Ni, Cu, NiO and CuO. The fabric samples before coating had been treated (etched) in argon plasma and after that in the DC magnetron sputtering process had been coated with metal or metal oxide.

The microscopy (OM, AFM), sorptometry, TGA-DTA, Raman and electrical impedance spectroscopy data are used for characterization of coated fabrics.

The impedance $Z(\omega)$ spectra and their components (ε, σ) versus of metal, oxide and water content are going over percolation threshold. The model for description of electrical properties will be presented.

Acknowledgment

Authors are grateful to financial support of National program of Material Science “IMIS”

F-73

Durable Hydrophobic Sol-Gel Finishing for Textiles

S.Vihodceva[1], S. Kukle[2], J. Bitenieks[3]

[1]Institute of Textile Materials Technology and Design, Riga Technical University, Latvia

[2]Institute of Polymer Materials, Riga Technical University, Latvia

e-mail: Svetlana.Vihodceva@rtu.lv

Incorporation of the additional functionality into traditional textiles allows adding new valuable functional properties, finding new application areas, solving ecological problems and enhancing the quality of the consumer life, as a result of that the added value and marketability of the product shall increase. Technical and special use textiles often need a finishing coat ensuring water-repellence i.e. hydrophobic features. Natural - cellulose fibers have the highest content of active hydroxyl groups (-OH) thus providing most effective moisture binding properties. Furthermore, the ability to repel water also enables a surface self-cleaning [1-2] effect and together with water-repellence, this provides important additional functions in clothing as well as these features be well in demand across different textile products for outdoor use.

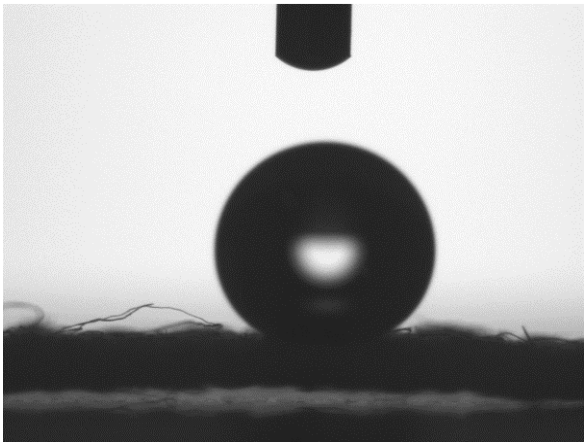

Fig.1 Treated cotton textile surface wettability process (drop 5 µl)

Cotton textile treatment by sol-gel technology for the obtaining of ZnO/SiO_2 coating is providing to cotton textiles water-repellent properties (Fig. 1) even after 50 cycles of intensive hydrothermal treatment of the treated material that also is providing a surface self-cleaning.

References

1. S. Hanumansetty, J. Maitey, R. Foster and E. A. O'Rear App. sc.. **2**, 192 (2012)
2. E. S. Namligor, M. I. Bahtiyari, E. Hosaf and S. Coban, Fibres&Textiles in East. Europe. **17**, 76 (2009)

F-74

Mechanical Pressure Induced Capacitance Changes of Polyisoprene/Nanostructured Carbon Black Composite Samples

K. Ozols, M. Knite

Institute of Technical Physics, Riga Technical University, Latvia

e-mail: kozols@ktf.rtu.lv

Electroconductive polyisoprene/nanostructured carbon black (PNCB) composites show pronounced piezoresistance effect when subjected to mechanical deformation [1]. This effect has been used to elaborate flexible mechanical pressure sensors [2].

To study changes in PNCB composites, which are induced by mechanical pressure, capacitance measurements of PNCB samples were conducted while applying mechanical pressure.

Relative capacitance changes depending on frequency and applied different values of mechanical pressure for PNCB sample containing 6 phr of carbon black (6 mass parts of the filler per 100 mass parts of polyisoprene) are shown in Fig.1. It can be seen that mechanical pressure reduces capacitance of the sample, but values of relative capacitance change are different at all frequencies measured (20 Hz - 2 MHz). Maximum absolute $\Delta C/C_0$ value (the maximum effect) for the sample is around 3 kHz. PNCB samples containing different amount of CB showed different values of maximum effect at different frequencies. Samples with extremely small CB filler content (3 phr CB) or extremely large CB filler content (10 phr CB) showed a decrease of capacitance change effect.

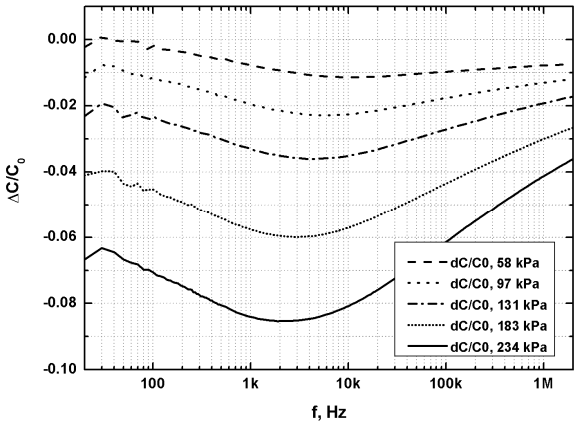

Fig.1 Frequency dependence of pressure induced relative capacitance change of PNCB composite, containing 6 phr of CB.

References

1. M. Knite, V. Teteris, A. Ķiploka, J. Kaupuzs, Sensors and Actuators A 110, p142–149 (2004)
2. J. Zavickis, M. Knite, G. Podins, A. Linarts, R. Orlovs, Sensors and Actuators A: Physical A171-1, p38 (2011)

F-75

Research of Interaction Fluorine-Doped Co_3O_4 (100) and (111) Surfaces with Water

G. Kaptagay[1], T.M. Inerbaev[1], E.A. Kotomin[2,4], A.T.Akilbekov[1], Yu.A. Mastrikov[2,3], F.U. Abuova[1]

[1]L.N. Gumilyov Eurasian National University, Mirzoyan str. 2, Astana, Kazakhstan

[2]Institute of Solid State Physics, University of Latvia, Kengaraga str. 8, Riga, Latvia

[3]Materials Science and Engineering Dept., University of Maryland, College Park, USA

[4]Max Plank Institute for Solid State Research, Heisenberg str. 1, Stuttgart, Germany

e-mail:gulbanu.kaptagai@mail.ru

Electrochemical water splitting has attracted substantial interest in the recent years as a key process in hydrogen production from sunlight and other sources of electricity. Recent experimental studies have demonstrated that Co_3O_4 is high-promising anode material for electrochemical water splitting due to its high catalytic activity in the oxygen evolution reaction (OER) [1]. In this context, understanding the interaction of Co_3O_4 surfaces with water is an essential preliminary step that can help to shed light on the atomic scale reaction mechanisms. Our attention is focused on investigation of Co_3O_4 (100) and (111) surfaces which are the most abundantly presented in Co_3O_4 nanoparticles [2]. Density functional method is applied to describe thermodynamics of electrocatalytic water splitting on the Co_3O_4 (100) and (111) surfaces. We calculated free energy changes along the reaction pathway using the computational standard hydrogen electrode (SHE) allowing us to replace a proton and an electron with half a hydrogen molecule at U = 0 V vs SHE. The analysis performed for the free energies is at standard conditions (pH = 0, T = 298.15 K) and U = 0.

Using accurate DFT+U calculations, we shown that water adsorbs dissociatively on Co_3O_4 on the (100) and intactly on the (111) surfaces. From the computed free-energy changes along the OER, we found that the (100) surface is catalytically inactive while (111) surface demonstrates some electrocatalytic activity on its threefold coordinated surface cobalt ions. In this case free energy changes along the OER is the same to corresponding value for the most stable termination of (110) Co_3O_4 surface. Fluorine doping of Co_3O_4 nanoparticles drastically changes their interaction with water. In our investigations solvent effects are generally expected to be small for neutral species, the neglect of the water environment is a rather drastic approximation, for which the main justifications are that it provides a qualitative description of experimentally observed trends, and it is the first step toward more complete treatments that include the solvent.

References

1. I. C. Man, H.-Y. Su, F. Calle-Vallejo, H. A. Hansen, J. I. Martínez, N. G. Inoglu, J. Kitchin, T. F. Jaramillo, J. K. Nørskov, and J. Rossmeisl, ChemCatChem. **3**, 1159 – 1165 (2011).
2. F. Zasada, W. Piskorz, S. Cristol, J.-F. Paul, A. Kotarba, and Z. Sojka, J. Phys. Chem. C. **114**, 22245–22253 (2010).

F-76

Insulator-Metal Transition in $FeAs_2$ Caused by Substitutions

P. Rubin, A. Pishtshev

Institute of Physics, University of Tartu, Tartu, Estonia

e-mail: rubin@fi.tartu.ee

In the present work, in the context of the physics of cation substitutions we have carried out DFT electronic structure calculations on the system $FeAs_2$. Of the main interest were the studies of the possible insulator–metal transition caused by different types of defects as well as the testing of a number of relevant sustitutional impurities in order to change smoothly the value of the forbidden electronic gap. In particular, special attention was dedicated to the effects of partial Ni and Mg substitutions for Fe atoms. It was found that the insulator-metal transition occurs at 6% concentration of impurity. The closing of the forbidden gap is caused mainly either due to 3d-states of Ni or due to 2p-states of Mg. The significance of the hybridization effects is demonstrated.

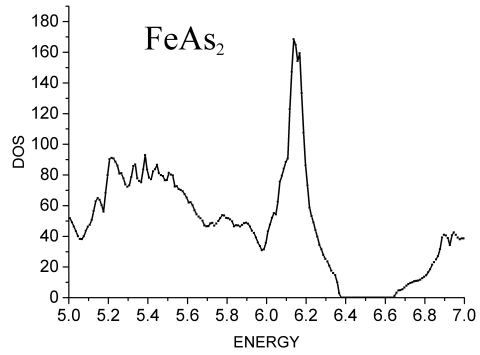

Fig.1 Calculated total density of states (DOS) o $FeAs_2$. The valence band top locates at 6.38 eV.

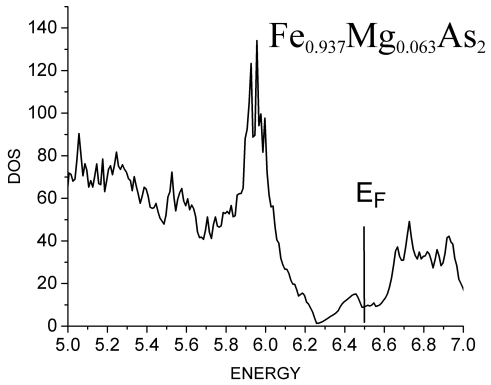

Fig.2 Calculated total density of states (DOS) of $Fe_{0.937}Mg_{0.063}As_2$ The Fermi level (E_F) locates at 6.49 eV.

Acknowledgment

This work was supported by the European Union through the European Regional Development Fund (Centre of Excellence ``Mesosystems: Theory and Applications", TK114).

F-77

Low-Temperature Delayed Recombination in Y_2SiO_5:Ce and Lu_2SiO_5:Ce

A. Krasnikov[1], M. Nikl[2], S. Zazubovich[1]

[1]Institute of Physics, University of Tartu, Riia 142, 51014 Tartu, Estonia

[2]Institute of Physics AS CR, Cukrovarnicka 10, 162 53 Prague, Czech Republic

e-mail: svet@fi.tartu.ee

Single crystals of Lu_2SiO_5:Ce and Y_2SiO_5:Ce can be used for fast detection of γ- or X-rays in many applications such as medical imaging, high-energy physics, environmental monitoring, etc. However, the presence in the luminescence decay kinetics, besides the Ce^{3+}-related fast (ns) component, of slow (μs-s) components negatively influences the scintillation characteristics. The aim of our work was to clarify the origin of the defects and the mechanisms of the delayed recombination processes resulting in the slow low-temperature luminescence decay of these crystals. For that, time-resolved emission and excitation spectra and luminescence decay kinetics are studied in the 10 μs - 10 s time range. In the luminescence decay kinetics, both the multiexponential (at t<50 μs) and the nonexponential (at t>60 μs) decay stages are found at 4.2-80 K. Mainly the Ce^{3+} emission is observed at the first stage, and both the intrinsic (≈2.6 eV) and the Ce^{3+} emission, at the second stage. At t>60 μs, tunneling recombinations in the pairs of spatially correlated and randomly distributed electron and hole centers are responsible for the nonexponential luminescence decay.

The appearance of electron and hole centers in the crystals studied has been explained in [1] by the photostimulated electron transfer from the valence band (VB) to an oxygen-vacancy-related electron traps. The mobile holes, appearing in the VB as a result of this process, can migrate along the crystal lattice and be self-trapped or trapped at oxygen ions, located near intrinsic and/or impurity defects, producing various O^--type hole centers, or at Ce^{3+} ions, producing Ce^{4+} centers. Tunneling recombinations in these electron-hole pairs are accompanied with the slow intrinsic and Ce^{3+}-related emissions, respectively. Recombinations of electrons, optically released from different traps, with the hole Ce^{4+} centers result in the multiexponential decay of the Ce^{3+} emission at t<50 μs. According to [1], the $5d^{1,2}$ excited states of Ce^{3+} ions are not involved into the low-temperature delay recombination processes.

References

1. V. V. Laguta, M. Nikl and S. Zazubovich, Optical Materials, http://dx.doi.org/10/1016/j.optmat.2013.12.018

F-78

Depth Profiles of Indentation Hardness and Dislocation Mobility in MgO Single Crystals Irradiated with Swift Kr and N Ions

R. Zabels[1], I. Manika[1], K. Schwartz[2], J. Maniks[1], M. Sorokin[3], A. Dauletbekova[4], M. Zdorovets[5]

[1]Institute of Solid State Physics, University of Latvia, Latvia

[2]GSI Helmholtzzentrum für Schwerionenforschung, Darmstadt, Germany

[3]National Research Centre Kurchatov Institute, Moscow, Russia

[4]L. N. Gumilyov Eurasian National University, Astana, Kazakhstan

[5]Institute of Nuclear Physics, Almaty, Kazakhstan

e-mail: rzabels@gmail.com

MgO single crystals have an energy gap below the critical energy for the creation of Frenkel defects, and are highly resistant to radiation. MgO is a promising material for application in nuclear fusion reactors and nuclear technique. A study of the role of electronic excitations and elastic collisions in structural damage and modification of micromechanical properties of MgO single crystals irradiated with swift ions is presented. Irradiation was performed with 150 MeV ^{84}Kr and 24.5 MeV ^{14}N ions at fluences up to 10^{15} ions.cm^{-2}. Complex investigations with AFM, optical absorption spectroscopy, nanoindentation, and dislocation mobility methods were conducted. Optical absorption spectroscopy confirms ion-induced formation of single and complex color centers. Irradiation leads to an increase of hardness associated with formation of ion-induced dislocations and interstitial clusters. The depth profiles of indentation hardness and dislocation mobility along the ion path confirm joint contribution of electronic excitations and atomic displacements by elastic collisions (increasing with the depth) in structural damage of MgO. The impact mechanism becomes dominant in the tail part of the ion range where ion energy losses caused by elastic collisions reach considerable values (Fig.1).

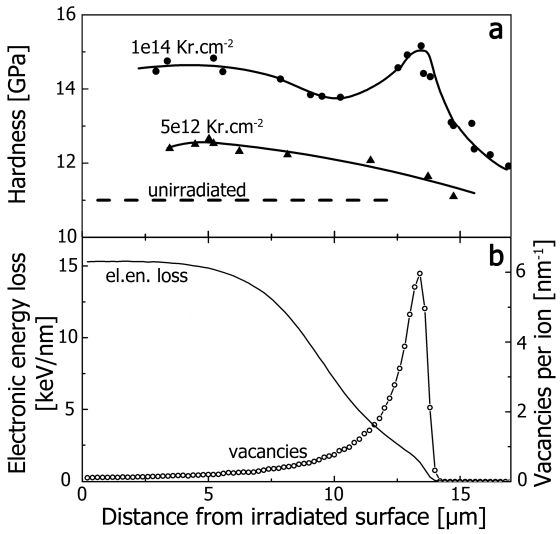

Fig.1 Depth profiles of (a) hardness of MgO irradiated with 150 MeV Kr ions at fluences 10^{14} and 5×10^{12} ions.cm^{-2} and (b) electronic and nuclear energy loss, calculated using SRIM-2008.04 Hardness measurements obtained on cross-sections.

F-79

New Insights into Charge Transfer Transitions in $CdWO_4$: Covalency, Polarizability and Charge Effects on Energy Positions

L. Wang, H.M. Noh, S.W. Park, B.C. Choi, J. Hong, J.H. Jeong*

Department of Physics, Pukyong National University, Busan 608-737, Republic of Korea

e-mail: qauwanglili@126.com

Blue-emitting phosphors CdWO4 were prepared by hydrothermal route, precipitation method and high temperature solid-state reaction. The broad and asymmetrical excitation and emission spectra were related to the particle size of the product and were investigated deeply. Three charge transfer bands were obtained in the excitation spectra through Gaussian fitting.

According to the dielectric theory of the chemical bond for complex crystals, a new factor H corresponding to chemical parameters of every W-O bond was calculated.1 Thus every charge transfer band was assigned to be from one kind of W-O bond within WO6 group. The emission for the tungstate groups originate from the charge transfer from excited 2p orbits of O2- to the empty 5d0 orbits of the central W6+ ions. Possible energy transfer process was given to illustrate the photoluminescence process. The thorough study on charge transfer transitions of CdWO4 will be helpful for understanding the energy transfer between charge transfer band and the activator in CdWO4 and will be useful for the applications of the photoluminescence of tungstates.

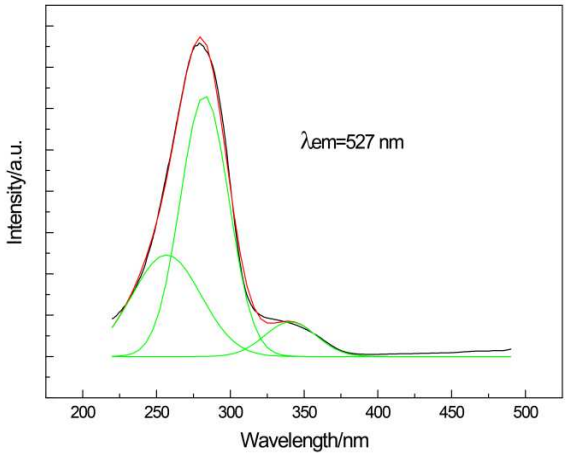

Fig.1 The excitation spectra of $CdWO_4$ and Gaussian fitting results.

References

1. J. S. Shi and S. Y. Zhang, J. Phys. Chem. B, 108, 18845 (2004).

F-80

Template-Based Synthesis of Nickel Oxide

N. Mironova-Ulmane[1], A. Kuzmin[1], I. Sildos[2]

[1]Institute of Solid State Physics, University of Latvia, Latvia

[2]Institute of Physics, University of Tartu, Tartu, Estonia

e-mail: ulman@latnet.lv

Materials synthesis using various template techniques becomes popular during last years due to simplicity and often low costs [1]. Such approach involves fabrication of the desired material within the pores or channels of a template.

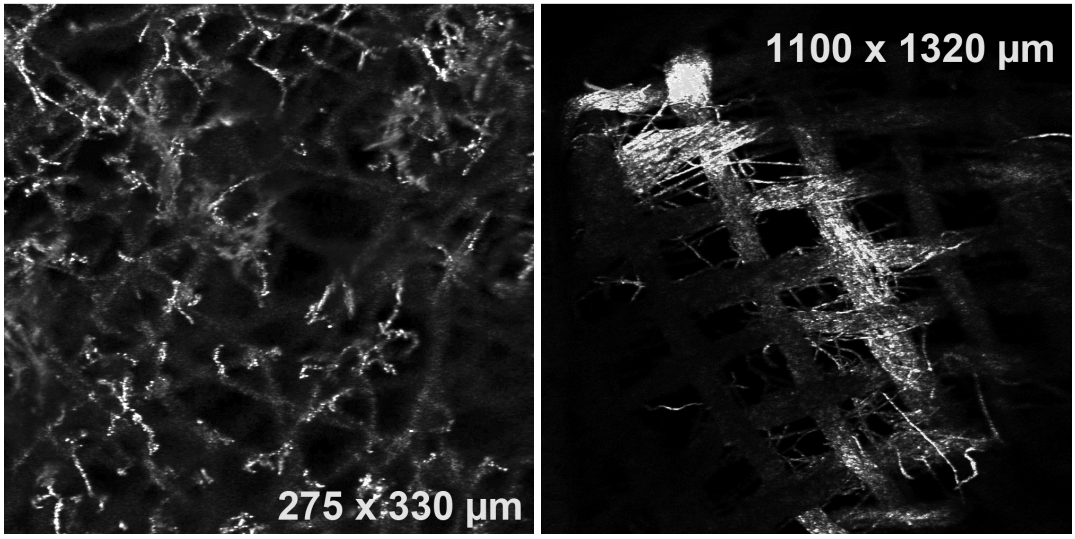

Fig.1 Confocal images of NiO produced by template synthesis based on cellulose (left) and cotton (right).

In this study we report on a facile template-based synthesis of nickel oxide from nickel nitrate solutions using cellulose and cotton templates (Fig. 1). We have found that thus obtained NiO samples retain the morphology of the templates, and their properties can be easily controlled by modifying the solution concentration. In particular, we will focus on the lattice dynamics, antiferromagnetic ordering and visible (red) photoluminescence of templated nickel oxide in comparison with micro- and nanocrystalline NiO produced by other methods [2-4].

References

1. M.R. Jones, K.D. Osberg, R.J. Macfarlane, M.R. Langille and C.A. Mirkin, Chem. Rev. **111**, 3736 (2011).
2. N. Mironova-Ulmane, A. Kuzmin, J. Grabis, I. Sildos, V.I. Voronin, I.F. Berger and V.A. Kazantsev, Solid State Phenom. **168-169**, 341 (2011).
3. A. Kuzmin, N. Mironova-Ulmane and S. Ronchin, Proc. SPIE **5122**, 61 (2003).
4. E. Cazzanelli, A. Kuzmin, G. Mariotto and N. Mironova-Ulmane, J. Phys.: Condens. Matter **15**, 2045 (2003).

F-81

Synthesis, Structure and Electrical Properties of $Li_{4x}Ti_{1-x}P_2O_7$ (x = 0; 0.1) Pyrophosphates

A. Dindune[1], Z. Kanepe[1], J. Ronis[1], D. Valdniece[1], V. Venckutė[2], A. Orliukas[2]

[1]Institute of Inorganic Chemistry, Riga Technical University, Salaspils, Latvia

[2]Faculty of Physics, Vilnius University, Vilnius, Lithuania

e-mail: tonija@nki.lv

Electrochemical properties investigation of TiP_2O_7 compound shows that it has a theoretical capacity of 121 mAh/g and is an attractive cathode material for Li-ion secondary batteries [1,2].TiP_2O_7 has a cubic superstructure (3×3×3) (space group $Pa\bar{3}$) with Z = 108 formula units in the supercell [2].In such superstructures cells Li can be insert down to 2.2 V vs Li^+/Li corresponding to the reduction of Ti^{4+} to Ti^{3+} [3]. According to [4] TiP_2O_7 compound is proton conductor. The dielectric permittivity of TiP_2O_7 ceramic was investigated in the frequency range between 20 Hz and 1 MHz from room temperature to 973 K. In the temperature range 473 – 573 K and at temperature 873 K the anomalies of dielectric constant and loss were found and conclude that anomalies are caused by phase transitions in TiP_2O_7 [5]. The peculiarities of solid electrolyte properties at Li insertion into TiP_2O_7 and phase transitions phenomenon stimulate the investigation of some members of pyrophosphate family. In the present work we synthesized the powder of $Li_{4x}Ti_{1-x}P_2O_7$ (x=0; 0.1) by solid state reaction and structural studies of the powder were conducted by X-ray diffraction (XRD). For investigation of electrical properties of the compounds the ceramic samples were sintered. The results of the investigation on electrical properties of the ceramics in the frequency range ($10 – 3\cdot10^9$) Hz and in the temperature range (400-720) K by impedance spectroscopy are presented in the paper.

Acknowledgements

This work was supported by Research cooperation project of Latvian Council of Sciences N666/2014 and Research Council of Lithuania (Project No TAP LLT 03/2012).

References

1. Y. Uebou, S. Okada, M. Egashira, J.-I. Yamaki, *Solid State Ionics***148**, 323 (2002)
2. J. Sanz, J.E. Iglesias, J. Soria, E.R. Losilla, M.A.G. Aranda, S. Bruque, *Chem Mater***9**, 996 (1997)
3. S. Patoux, C. Masquelier,Chem. Mater. **14**, 5057 (2002).
4. V. Nalini, R. Haugsrud, T. Norby, High – temperature proton conductivity and defect structure of TiP_2O_7, Solid State Ionics**, 181**, 510 (2010)
5. C.H. Kim, H.S. Yim, Solid State Commun. 110, 137 (1999)

F-82

Production of Glycolic Acid from Glycerol Using Novel Fine-Disperse Platinum Catalysts

E. Sproge[1], S. Chornaja[1], K. Dubencovs[1], V. Kampars[1], L. Kulikova[2], V. Serga[2]

[1]Institute of Applied Chemistry, Riga Technical University, Latvia

[2]Institute of Inorganic Chemistry, Riga Technical University, Latvia

e-mail: Elina.Sproge@rtu.lv

Selective heterogeneous oxidation of glycerol is one of the most frequently glycerol transformation methods studied today. Fine-disperse composites consisting of noble metal and its support are found their application as effective catalysts in the glycerol oxidation. In the glycerol oxidation number of valuable products can be obtained and one of these products is glycolic acid. Glycolic acid has a broad application field – it is used in textile, food, pharmaceutical and plastics industries. Unfortunately in the literature there is poor information about glycolic acid production from glycerol.

Using extractive-pyrolytic method, we have synthesized several fine-disperse platinum catalysts, supported on different carriers. It was shown that all catalysts except with iron materials as carriers were mostly selective to glyceric acid – glyceric acid formed as the main product. Only in the case of iron containing nanocomposites glycolic acid formed as the main product with good selectivity (Table 1). Glycerol oxidation was carried out in mild conditions – atmospheric pressure, low temperature. In the literature under similar conditions glycolic acid was obtained only as by-product with low selectivity (< 20%) [1].

Catalyst	d_{Pt} by XRD nm	Glycerol conversion mol%	Glycolic acid selectivity mol%
5%Pt/Fe_2O_3 [a]	8	56	53
2.5%Pt/Fe_2O_3 [a]	-	31	60
71%Pt/Fe_2O_3 [b]	11-35	47	55
5.8%Pt/Fe [c]	-	48	60

Table 1. Selective oxidation of glycerol to glycolic acid. Reaction conditions: $c_o(C_3H_8O_3)$ = 0.3 M, c_o(NaOH) = 1.5 M, $n(C_3H_8O_3)/n(Pt)$ = [a, c]300 mol/mol; [b]211 mol/mol, 60 °C, P(O2) = 1 atm, reaction time 7 h. Catalyst calcination temperature: [a]–300 °C, [b]–500 °C, [c]–600 °C; catalyst calcination time: [a, b]–5 min, [c]–30 min.

References

1. D. Liang, J. Gao, H. Sun, P. Chen, Z. Hou and X. Zheng, Appl. Catal. B **106**, 423–432 (2011)

F-83

Fabrication and Electrical Characteristics of P(VDF-TrFE) Films on Si(100) Substrates using Cyanoethyl Pullulan Buffer Layers

B.E. Park, B. Jin

School of Electrical and Computer Engineering, University of Seoul, Seoul 130-743, Korea

e-mail: pbe@uos.ac.kr

In this work, we applied a cyanoethyl pullulan (CEP) thin film as a buffer layer and a ploy(vinylidene fluoride trifluorethylene) (P(VDF/TrFE)) film as a ferroelectric layer. The C-V characteristics of the Au/CEP/p-Si(100) MIS (Metal-Insulator-Silicon) structure revealed that the 5wt%-CEP thin film had good electrical properties and was suitable for a buffer layer in a MFIS (Metal-Ferroelectric-Insulator-Silicon) structure. We estimated the EOT (equivalent oxide thickness) value of the CEP film as about 11nm.

For the Au/P(VDF-TrFE)/CEP/p-Si MFIS structures, the memory window width increased as the bias sweep voltage increased. The memory window width of MFIS structures is over 6V at a bias sweep range of ±7V. The value of the leakage current density is about 3.6×10^{-7} A/cm^2 for a P(VDF-TrFE) (5wt%) thick film.

Acknowledgement:

This research was supported by Basic Science Research Program through the National Research Foundation of Korea (NRF) funded by the Ministry of Education, Science and Technology (2010-0021507).

F-84

Method for Purifying Silicon Using Electron Beam Technology

G. Chikvaidze[1], A. Kalle[2]

[1]Institute of Solid State Physics, University of Latvia, Latvia

[2]XERON ESK AG, Switzerland

e-mail: georgc@cfi.lu.lv

A method for refining silicon is developed, which comprises electron-beam melting of silicon using an electron beam gun, followed by vacuum and then oxidative purification of low-grade silicon from impurities, such as phosphorus, arsenic, antimony, boron, then crystallization of the molten mass of silicon.

The method provides evidence of the possibility to produce solar elements from relatively low grade and low-cost silicon through vacuum electron beam purification and forming quantum dots arrays, using crystallization under the directed influence of an electronic beam (scanning the surface of the silicon melt under a specially developed program) and applying additional treatment. The material containing three dimensional quantum dots arrays has a higher efficiency compared to a commercial silicon solar and may provide a basis for improving the construction of a solar cell with increased photo effect derived from absorbing of infrared radiation.

The method involves the usage of electron beam technology for obtaining highly purified basic material containing nano-clusters where the remaining metal impurities concentrated upon completion of silicon purification procedure. Purified basic silicon has the impurity level of less than 0.5 ppm. Due to the high content of quantum dots clusters, being small traps in the silicon obtained through the use of the described method, IR-light releases charge carriers from these traps, which leads to an increase in photoelectric current and thus increases the efficiency of a solar element.

Solar cells made from such silicon show increased efficiency in the wavelength range of 1-2 microns and the degradation period of solar cells using the quantum dots cluster effect is considerably longer than that of regular solar cells made of commercial solar silicon.

F-85

Importance of FTIR Spectra Deconvolution in Amorphous Calcium Phosphate Analysis

A. Brangule[1,2], K.A. Gross[1]

[1]Institute of Biomaterials and Biomechanics, Riga Technical University, Latvia

[2]Riga Stradiņš University, Latvia

e-mail: agnese.brangule@rsu.lv, kgross@rtu.lv

Amorphous calcium phosphate (ACP) plays an important role in the formation of biominerals. More crystalline analogues form more stable configurations of biological apatites [1]. The diversity of possible arrangements within the apatite structure requires sensitive tools to detect changes. Tracking the bond type provides atomic level sensitivity through various spectroscopy techniques. This work will consider Fourier transform infra-red spectroscopy – diffuse reflectance induced reflection (FTIR-DRIFT) for collecting the spectra and deconvolution to identify changes in bonding as a means of more powerful detection. Spectra were recorded from poorly crystalline apatites synthesized by wet precipitation. FTIR-DRIFT was used to study the chemical environments of PO_4, CO_3, OH ions and water molecules. Deconvolution of spectra separated overlapping bands in the υ_4PO_4, υ_2CO_3, υ_3CO_3 and OH region allowing a closer analysis of changes within the material at the atomic level. Poorly crystalline apatites showed additional bands which do not appear in well-crystallized apatites signifying greater variability at low structural order. Additional peaks have been designated as "nonapatitic" for υ_4PO_4, υ_2CO_3 bands (Figure 1). FTIR DRIFT spectrometry in combination with deconvolution should be used as an advanced tool for qualitative and quantitative determination of "nonapatitic" CO_3, apatitic CO_3, PO_4 and HPO_4 bands, as well as chemical analysis and a measure of crystallinity.

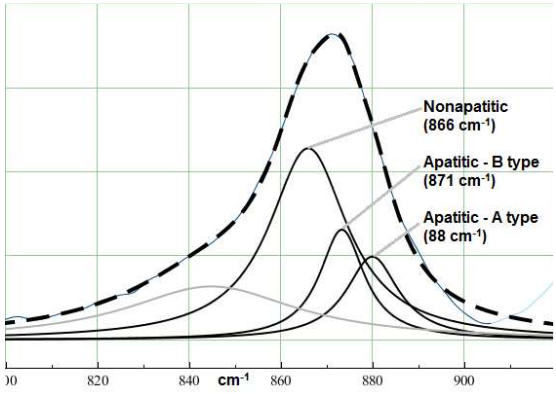

Fig.1 Separated peaks from deconvolution of the v_2 CO_3 band with Magic Plot.

References

1. Legeros R.Z. In P.W. Brown, B.Constantz (Eds.) Hydroxyapatite and Related Materials, 3-28 (1994).
2. Rey C., et.a, Calcif Tissue Int, **45**, 157-164 (1989).
3. Rey C., et.a, Calcif. Tissue Int., **46**, 384-394 (1990).

F-86

Ultrasonic Wave Propagation in PDMS with ZnO Nanoparticles

J. Belovickis[1], J. Macutkevic[1], Š. Svirskas[1], V. Samulionis[1], J. Banys[1], O. Shenderova[2]

[1]Faculty of Physics, Vilnius University, Sauletekio 9/3, LT-10222 Vilnius, Lithuania

[2]International Technology Center, Raleigh, NC 27715, USA

e-mail: jaroslavas.belovickis@ff.vu.lt

The integration of nanoparticles within a polymer is widely used to create nanocomposites with enhanced material properties. Polymer based nanocomposites have attracted increasing attention because of their unique properties emerging from the combination of organic and inorganic materials [1]. Our nanocomposite includes polydimethylsiloxane (PDMS) which distinquishes from other organic silicones for its lowest glass-transition temperature (168 K) and good thermal stability, ZnO - a semiconductor with a relatively high longitudinal acoustic wave velocity (6027 m/s).

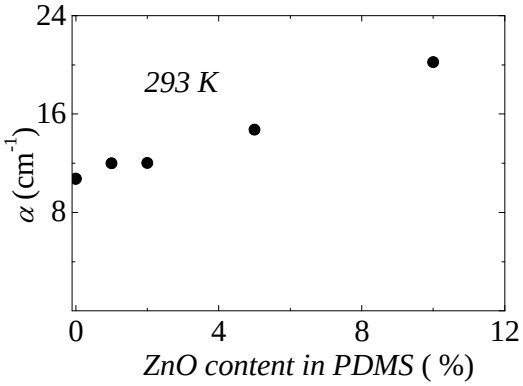

Fig.1. Experimental dependency of ultrasonic attenuation on ZnO content in PDMS nanocomposites

Investigation of mechanical relaxation over a wide range of temperature in PDMS-ZnO nanocomposites with different concentrations of ZnO nanoparticles (30 nm) (0, 1, 2, 5, 10 %) was performed in order to determine the interaction between the ZnO nanoparticles and PDMS polymer.

Figure 1 shows dependency of acoustic wave attenuation on the concentration of ZnO in the nanocomposite at room temperature. It can be observed from the figure that the height of the loss increases with addition of ZnO. We attribute this dependency to the additional elastic energy dissipation due to wave scattering from the dispersed ZnO particles similarly as it was observed in styrene-butadiene rubber with rigid polystyrene particles [2].

Acknowledgment

This research is funded by the European Social Fund under the Global Grant measure.

References

1. L. Bistricic, V. Borjanovic, L. Mikac, V. Dananic, Vib. Spectrosc. **68**, 1-10 (2013)
2. F. Faghihi, N. Mohammadi, M. Haghgoo, J. Polym. Sci., Part B: Polym. Phys. **48**, 82-88 (2010)

F-87

Angular Dependence of Recombination Luminescence Detected EPR in ZnO Crystal

A. Fedotovs[1], Dz. Brezins[1], U.Rogulis[1], K. Smits[1], G. Doke[1], A. Medvids[2], P. Onufrijevs[2]

[1]Institute of Solid State Physics, University of Latvia, Latvia

[2]Institute of Technical Physics, Riga Technical University, Latvia

e-mail: andris.fedotovs@lu.lv

Zinc oxide is known as a promising semiconductor material for production of transparent electronic and opto-electronic devices. It is possible to obtain structural changes in ZnO and other semiconductors samples using laser-treatment [1]. It has been observed that in the laser-treated ZnO sample the recombination luminescence (RL) spectra consist of two bands (630nm and 740nm) with different decay times. All bands detected in the RL-EPR belong to the RL band with slower decay time. Using modulation of microwaves (PL-EPR), it is possible to observe one donor band which does not appear in the RL-EPR spectra. The detected RL-EPR spectrum has a pronounced angular dependence. The EPR measurements show presence of some transition elements in the investigated samples. The mechanisms of the RL in the laser-treated samples will be discussed.

References

1. A. Medvid, P. Onufrijevs, R. Jarimaviciute-Gudaitiene, E. Dauksta, I. Prosycevas, Nanoscale Research Letters, **8**, 264 (2013)

F-88

EPR Spectra of ScF_3

A. Antuzevics, U. Rogulis, J. Purans, A. Fedotovs, Dz. Berzins

Institute of Solid State Physics, University of Latvia, Latvia

e-mail: andris.antuzevics@gmail.com

Extensive experimental and theoretical studies have been reported on scandium trifluoride (ScF_3) cubic structure due to its distinct property of negative thermal expansion (NTE) over a temperature range of 10-1100 K. Our electron paramagnetic resonance (EPR) studies at room and liquid nitrogen temperatures show presence of several structural defects.

Observed angular dependences with $g = 1.992$ and $S = 7/2$ in the single crystal ScF_3 are caused by the Gd^{3+} impurity ion embedded into Sc^{3+} position. Previous zero field splitting (ZFS) parameter values of ScF_3:Gd^{3+} at 77 and 290 K [1] are swapped in [2], therefore we reinspect ZFS parameters and investigate, what effect NTE has on them. Parameter b_4 superposition model analysis is in good agreement with studies made for other cubic perovskite fluorides. [3].

EPR signals of powder samples could be explained by two overlapping spectra with $g = 2.002$. Defect models with $S = 1/2$ and superhyperfine interaction non-equivalence and anisotropy with six neighbouring fluorine ions will be discussed.

References

1. L. S. Starostina, B. N. Grechushnikov and V. F. Koryagin, Fiz. Tverd. Tela **14**, 3480 (1972)
2. M. Arakawa, H. Aoki, H. Takeuchi, T. Yosida and K. Horai, J. Phys. Soc. Japan **51**, 2459 (1982)
3. J. Y. Buzare, M. Fayet-Bonnel and J. C. Fayet, J. Phys. C: Solid State Phys. **14**, 67 (1981)

F-89

Gallstones Studies by Raman, EPR and EDX Spectroscopes

D. Jakovlevs[1], M. Polakovs[2], N. Mironova-Ulmane[2], V. Skvortsova [2], L. Berzina-Cimdina[2], I. Sildos[3]

[1]Riga Technical University, Latvia, Riga, Kalku Str. 1, LV-1048

[2]Institute of Solid State Physics, University of Latvia, Kengaraga street 8, LV-1063, Riga, Latvia

[3]Institute of Physics, University of Tartu, Tartu, Estonia

e-mail: dmitrijs.jakovlevs@inbox.lv

In the present work we report results of spectroscopic investigations of gallstones.

Gallstones could be divided on three main types: cholesterol, brown pigment, black pigment and white pigment stones [1].

The each gallstones was separated in different samples by gallstone's component color. EPR and EDX observed spectra show differences for studied components. We received information about composition of gallstones by EDX spectroscopy (C, O, Na, Mg, Si, Cl, Ca, Fe, Cu, Al. S, K, Ba, I, Zn). EPR spectroscopy let us to reiceve information about electronic states of transition metal ions (Fe3+). EPR spectra obtained for black pigment have two EPR signals with g-factor = 4.8 (high spin state S= 5/2 of Fe3+) and EPR signal with g-factor = 2.003 (low spin state S=1/2 of Fe3+). Micro-Raman spectroscopy also used for the characterization of gallstones particularly carefully researched gallstone with a white pigment, as there assumed the presence of calcium carbonate. Calcium carbonates, are to exist in different polymorphs: calcite, aragonite, vaterite, and amorphous CaCO3. There are numerous examples of biogenic calcite and aragonite, as well as a growing list of discoveries of biogenic CaCO3 formation via transient amorphous calcium carbonate [2-3]. We observed Raman spectra of calcite and aragonite in the gallstone with white pigment.

References

1. E.N. Chikvaidze, T.V. Gogoladze, I.N. Kirikashvili, G.I. Mamniashvili. Georgian Medical News, ISSN 1512-0112, No3(168) (2009).
2. T. Tu Anthony. Journal of the Chinese Chemical Society, , 50, 1-10 (**2003)**
3. O.A.Golovanova, N.F.Palchik, N.Eu.Berezina, N.N.Yudina. Chemistry for Sustainable Development 14 (2006) 125 - 131.

F-90

EPR Spectroscopy of C3A

M. Oja, E. Tõldsepp, T. Kärner, E. Feldbach, M. Kirm

Institute of Physics, University of Tartu, Estonia

e-mail: marek.oja@ut.ee

$Ca_3Al_2O_6$ (C3A) belongs to a rich family of $CaO\text{-}Al_2O_3$ compounds being a wide gap (~6.5 eV) insulator. It has been shown to be a promising material for doping with rare-earth ions [1]. C3A has a cubic crystal structure and 6 non-equivalent positions for Ca^{2+} atoms. Only a few reports have been published about EPR active centres in pure C3A and doped with various rare-earth ions. In previous EPR studies lines belonging to Mn^{2+} centre [2] in undoped C3A and lines with g-factor around 2 belonging to O^- and F^+ centre in Eu doped C3A have been found at temperatures above room temperature [3]. In this work we present results of EPR, thermo-stimulated luminescence (TL) and photoluminescence (PL) studies for undoped and Eu^{3+} and Pr^{3+} doped C3A, which cover temperature range of 5 – 300 K.

C3A powders were prepared by self-propagating combustion synthesis, followed by thermal post-treatment. Phase purity of resulted samples was confirmed by XRD. TL measurements were performed at the cathodoluminescence setup and EPR measurements on the Magnettech MiniScope MS400 X-band (9.3 GHz) spectrometer at the Institute of Physics in Tartu. 6 lines belonging to Mn^{2+} centre with g-factor ~2 and hyperfine coupling constant ~85 G were detected in non-irradiated samples. The splitting of these lines can be caused by different non-equivalent positions of Mn^{2+} while substituting Ca^{2+} ions. Irradiation of samples at 77 K with X-rays gives rise to extra lines around broad central line with g-factor ~2. Analysis of TL glow curves, PL temperature quenching and EPR spectra at different temperatures enable us to propose some interpretations for the origin of the revealed g~2 lines in pure and doped C3A. The electronic properties of pure C3A, luminescence and defect centres will be discussed.

References

1. E. Tõldsepp, E. Feldbach, M. Kirm, *Journal of Ceramic Science and Technology* **4**, 77-84 (2013).
2. M.C. Ball, C. M. Marsh, M. C. R. Symons, et al, *Journal of Materials Science* **22**, 4121-4124 (1987).
3. V.Singh, S. Watanabe, T.K. Gundu Rao, et al, *Applied Physics B* **104**, 1019-1027 (2011).

F-91

Determination of Methemoglobin in Human Blood after Ionising Radiation by EPR

M. Polakovs[1], N. Mironova-Ulmane[1], A. Pavlenko[1] A. Aboltinš[2]

[1]Institute of Solid State Physics, University of Latvia, Riga, Latvia

[2]Nuclear Medicine Dep. P.Stradins Clinical University Hospital, Riga, Latvia

e-mail: maksims.polakovs@gmail.com

The study of blood and hemoglobin radiation damage is very important in order to understand the biological effects of ionizing radiation. Various physical techniques are used to determine structural damages of blood and hemoglobin after irradiation. The new data on structural changes of oxyhemoglobin under irradiation by Mossbauer parameters to estimate the probability of protein degradation products and proposed scheme oxyhemoglobin radiolysis processes [1,2]. Confocal micro-Raman and FT-IR spectroscopies have been used for detection of radiation influence of hemoglobin of patients examined by radio-isotopes diagnosis (Tc99m). After irradiation we observed some little changes of the Raman scattering bands which connected with out of plane porphyrine bending vibrations, also we observed additional band due to methemoglobin [3]. Radiation of blood leads to the transition from hemoglobin (Fe2+) to methemoglobin (Fe3+) with a delocalization of iron from porphyrine plane. We have chosen the EPR method to study the effect of radiation on blood. It is a sensitive method for detecting the valence state of iron and copper ions.

In the present work we report results of investigations of radiation influence on blood of patients examined by radio-isotopes diagnosis (Tc^{99m}), Chernobyl clean-up workers blood, human blood before and after radioisotope Tc^{99m} diagnosis and irradiated blood in vitro using electron paramagnetic resonance (EPR). EPR spectroscopy let us to reiceve information about electronic states of transition metal ions (Fe^{3+}). It is shown that EPR spectra of blood of patients after examination by radio-isotopes diagnosis has signal of the ion Fe^{3+} (methemaglobin) in low-spin state with g = 2.0 and in the high spin state with g=6.0. We can also detect EPR signals from the metal-protein transferrin (g=4.3) that contains the non-haem rhombic iron. The EPR signal of human blood mixed with Tc^{99m} has signal Fe^{3+} (methemaglobin) in low-spin state with g = 2.003 only.

References

1. Oshtrakh M.I., Nucl. Instr. and Meth. in Phys. Res. B 185 129–135 (2001)
2. Chevalier, A., Kellershohn, C., Rimbert, J.N., 1983, Radiat. Res 94, 51
3. M. Polakovs, N. Mironova-Ulmane, N.Kurjane, E.Reinholds, M. Grube, Proc. SPIE 7142 (2008) 714214:1-8.

F-92

Color Center Creation in LiF Irradiated with ^{12}C and ^{130}Xe MeV Ions: Dependence on Energy Loss and Absorbed Energy

A. Dauletbekova[1], M. Sorokin[2], K. Schwartz[3], M. Baizhumanov[1], A. Akilbekov[1]

[1]L.N. Gumilyov Eurasian University, 5 Munaitpassov Str., 0100087 Astana, Kazakhstan

[2]National research Centre 'Kurchatov Institute', Kurchatov Square 1, 123182 Moscow, Russia

[3]GSI Helmholtzzentrum für Schwerionenforschung, Planckstr. 1, 64291 Darmstadt, Germany

e-mail: baijumanov.muratbek@yandex.ru

Our former studies on color center creation in LiF crystals demonstrate a strong influence of both the ion energy loss (<S_e>) and the applied fluence (absorbed energy) [1, 2]. The present study compares the process in the crystals irradiated with 21 MeV ^{12}C (<S_e>=1.17 keV/nm) and 221 MeV ^{130}Xe (11.8 keV/nm) ions. Besides the lower energy loss, ^{12}C ions have some peculiarities of interaction with the LiF target (see [3] and references within). Irradiation with Xe ions leads to saturation of single F centers (at $N_F \sim 10^{19}$ cm^{-3}) at the absorbed energy of 1.3×10^{23} eV/cm^2 (Fig. 1) and at higher absorbed energy no decrease was observed both for single F centers and F_2/F_3^+ centers (the absorption of F_2 and F_3^+ centers overlaps, and their concentrations cannot be extracted [2]). In LiF irradiated with 21 MeV ^{12}C ions the saturation of single F centers ($N_F \sim 2.3\times10^{19}$ cm^{-3}) occurs at the higher absorbed energy of ~5×10^{24} eV/cm^3. Further irradiation decreases concentrations of both single F and F_2/F_3^+ centers due to the active formation of larger defect aggregates (colloids, vacancy clusters, etc.). Peculiarities of the color center accumulation under irradiation with ^{12}C and ^{130}Xe ions are analyzed in the framworks of the model developed in [4].

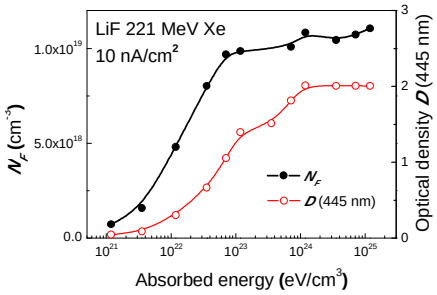

Fig. 1. Volume concentration of F centers and the optical density at 445 nm of F_2/F_3^+ centers vs the absorbed energy in LiF crystals irradiated with 221 MeV Xe ions at the beam current density of 10 nA/cm^2.

References

1. K. Schwartz, A. E. Volkov, M. V. Sorokin et al., Phys. Rev. B **78**, 024120 (2008)
2. A. Dauletbekova, K. Schwartz, M. V. Sorokin et al., Nucl. Instr. Meth. B **313**, 21 (2013)
3. M. V. Sorokin, K. Schwartz, K.-O. Voss et al., Nucl. Instr. Meth. B **285**, 24 (2012)
4. A. Russakova, M. V. Sorokin, K. Schwartz et al., Nucl. Instr. Meth. B **295**, 21 (2013)

F-93

EXAFS Study of the Local Structure of Crystalline and Nanocrystalline Y_2O_3 Using Evolutionary Algorithm Method

I. Jonane, J. Timoshenko, A. Kuzmin

Institute of Solid State Physics, University of Latvia, Latvia

e-mail: ingajonaane@gmail.com

Crystalline Y_2O_3 has body-centered cubic structure (space group Ia3, Z=16) with the unit cell consisting of 80 atoms, where the Y^{3+} ions occupy two non-equivalent (8(b) and 24(d)) Wyckoff positions with different local environment [1]. In this study we have investigated the local structure of crystalline and nanocrystalline Y_2O_3 using the Y K-edge x-ray absorption spectroscopy.

The extended x-ray absorption fine structure (EXAFS) has been interpreted using the recently developed reverse Monte Carlo and evolutionary algorithm (RMC/EA) approach [2]. The method is based on the random changes of atomic coordinates within 3D structure model of the material with the aim to minimize the difference between experimental and theoretically calculated EXAFS spectra (Fig.1). This approach allowed us to analyze the temperature-dependent Y K-edge EXAFS spectra from Y_2O_3 considering the influence of multiple-scattering effects and contributions of outer coordination shells, as well as structural and thermal disorder.

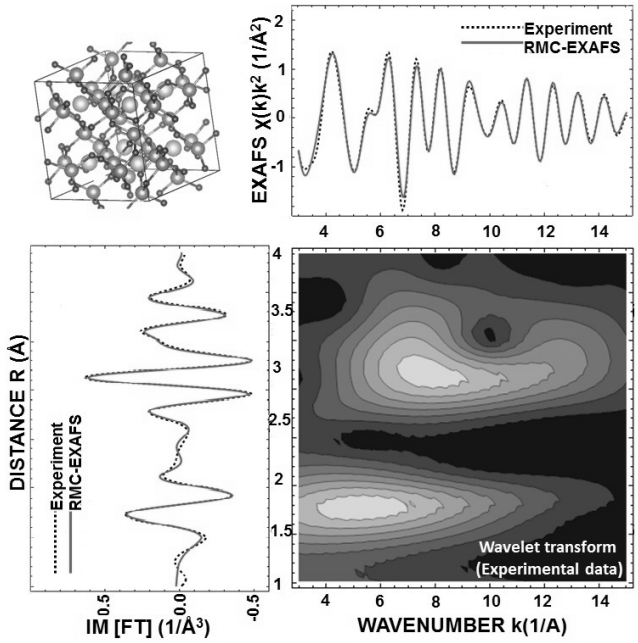

Fig.1 Unit cell of crystalline Y_2O_3 (upper left panel) and the results of RMC/EA EXAFS calculations for crystalline Y_2O_3 at room temperature: Y K-edge EXAFS spectra (upper right panel), their Fourier transforms (FT, left panel) and the wavelet transform (bottom right panel).

References

1. F. Hanic, M. Hartmanova, G.G. Knab, et al., Acta Cryst. B **40**, 76 (1984).
2. J. Timoshenko, A. Kuzmin, J. Purans, J. Phys.: Condens. Matter **26**, 055401 (2014).

F-94

Local Structure and Lattice Dynamics of Cubic Y_2O_3: an X-ray Absorption Spectroscopy Study

K. Lazdins and A. Kuzmin

Institute of Solid State Physics, University of Latvia, Latvia

e-mail: klazdins@inbox.lv

Cubic Y_2O_3 (space group *I*a3, *Z*=16) is technologically important material with complex crystallographic structure, composed of two types (regular and distorted) of YO_6 octahedra [1]. Recently, the lattice dynamics of yittrium oxide has been studied in details as a function of pressure in three phases: cubic, monoclinic and hexagonal [2]. It was shown that some Y-O bonds show large compression upon increasing pressure and are responsible for the change of coordination around Y atoms in the monoclinic phase [2]. The transition to the hexagonal phase is displacive in nature [2].

In this study we decided to take a closer look at material behaviour in a wide range of temperatures from 300 K to 1300 K at atmospheric pressure. The local structure and lattice dynamics of cubic Y_2O_3 were studied experimentally using the Y K-edge x-ray absorption spectroscopy and theoretically using classical molecular dynamics and lattice dynamics simulations [3]. Several force-field (FF) models were choosen and validated comparing experimental and calculated Y K-edge extended x-ray absorption fine structure (EXAFS) spectra. The obtained results on the structural and thermal disorder in cubic Y_2O_3 will be discussed.

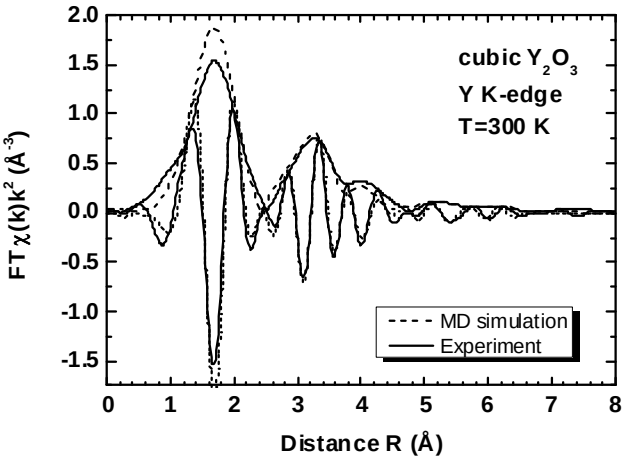

Fig. 1. Fourier transforms of the experimental (solid line) and simulated (dashed line) Y K-edge x-ray absorption spectra for cubic Y_2O_3 at the temperature T=300 K.

References

1. F. Hanic, M. Hartmanova, G.G. Knab, et al., Acta Cryst. B **40**, 76 (1984).
2. P. P. Bose, M. K. Gupta, R. Mittal, et al, Phys. Rev. B **84**, 094301 (2011).
3. A. Kuzmin, R.A. Evarestov, J. Phys.: Condens. Matter **21**, 055401 (2009).

F-95

ODS Steel Raw Material Local Structure Analysis Using X-ray Absorption Spectroscopy

A. Cintins[1], A. Anspoks[1], J. Purans[1], P. Vladimirov[2]

[1]Institute of Solid State Physics, University of Latvia, Latvia

[2]Karlsruhe Institut für Technologie, Institut für Materialforschung-I, Germany

e-mail: Cintinsarturs@gmail.com

Oxide dispersion strengthened (ODS) steels are promising materials for fusion reactors[1]. In this work we have studied local structure of ODS steel raw materials with X-ray absorption spectroscopy using analysis of X-ray absorption near edge structure (XANES) and extended X-ray absorption fine structure (EXAFS).

Analysis of XANES revealed information about dependency of iron matrix phase on temperature and duration of mechanical processing. From EXAFS we reconstructed radial distribution function and obtained local structure parameters.

We have revealed that mechanical processing of ODS raw materials influences the local structure of the material, and that heating of the materials causes phase transition in the iron matrix from α-Fe to γ-Fe.

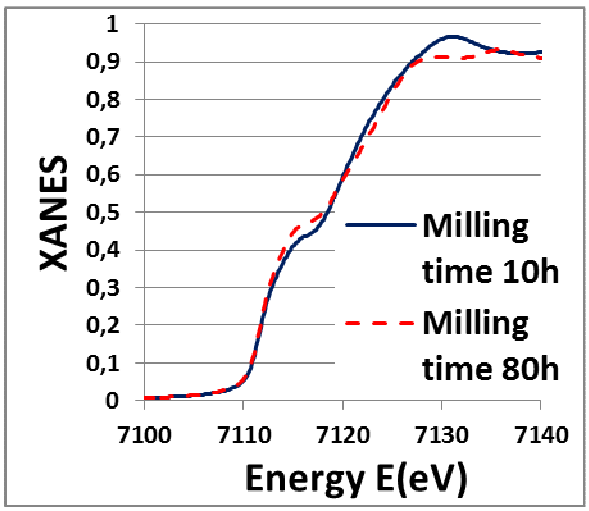

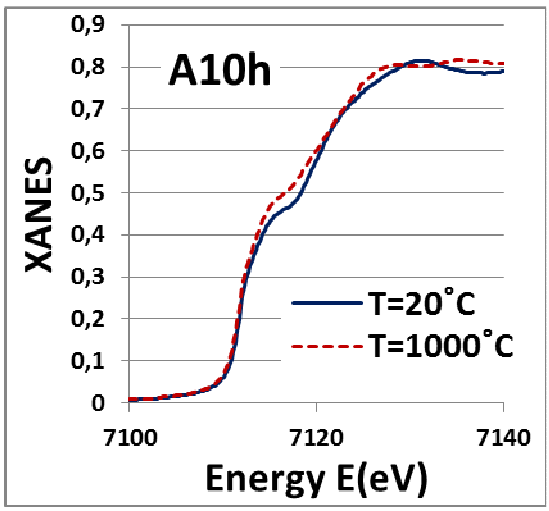

References

1. N.Baluc, J.L. Boutard, S.L. Dudarev, M. Reith, J. Brito Correia, B. Fournier, J. Henry, F. Legendre, T. Leguey, M. Lewandowska, R. Lindau, E. Marquis, A. Mucoz, B. Radiguet, Z. Oksiuta, J. Nucl. Mater. **417** (2011) 149-153.

F-96

Vibrational Spectra of Tungsten Oxytetrachloride

J. Gabrusenoks

Institute of Solid State Physics, University of Latvia, Latvia

e-mail: gabrusen@latnet.lv

The tungsten-oxygen compounds have crystalline lattices with different topology of W-O network. It determines dynamic behaviour of crystal lattice. Theoretical and experimental investigations of the lattice vibrations of tungsten oxytetrachloride ($WOCl_4$) have been carried out in the work. The structure of $WOCl_4$ consists of six-co-ordinate tungsten containing an approximately planar WCl_4 units and linear -W--O---W--O---W- chains.

Group theoretical analysis of the symmetry of lattice vibrations has been carried out. Symmetry correlation of vibrations for different possible structures have been determined. Group theory predicts four A vibrations, three B vibrations and four E vibrations. The B vibrations are active only in the Raman.

Calculations have been performed by using hybrid exchange density functional theory as implemented within the CRYSTAL09 program to determine the equilibrium geometries and phonon frequencies.

The Raman linewidth and the frequency of the q=0 optical phonons over the temperature range of 80-450°K have been measured. The results of symmetry and numerical calculations have been compared with Raman spectra.

F-97

Kinetic Properties of Grain Boundary with Ridges in Zn Bicrystal

R. Grants[1], V. Sursaeva[2], F. Muktepavela[1]

[1]Institute of Solid State Physics University of Latvia

[2]Institute of Solid State Physics, Russian Academy of Sciences, Chernogolovka

e-mail: phys.rolands.grants@gmail.com

Internal interfaces, both homogeneous and heterogeneous, often play a critical and determinant role on the properties of polycrystalline metals, ceramics and semiconductors. Structural elements of grain boundaries (GB): GB micropores, GB facets, triple joints (TJ) and GB ridges are especially important for nanomaterials. Their role increases during annealing when the GB migration processes occur (at the sintering stages of nanopowders or grain growth during recrystallization). Evolution of polycrystalline system is motion of two-dimensional (facets) and one-dimensional crystal defects (TJ, GB ridges) each of which has its own mobility. Bicrystals are well suited for the study of these little known GBs migration processes. In this paper the behaviour of the special tilt $[10\bar{1}0]$ GB system with facets and ridges was investigated in the temperature range 380-410^{0}C on bicrystals of zinc which have been grown using a modified Bridgman technique [1]. The temperatures of faceting-roughening transition were experimentally defined in AFM and *in situ* in optical microscope using polarized light. For the first time we observed transition from the “rough-to-rough” GB ridge to “facet-to-facet” state. The theory of the steady-state motion of the GB half-loop with ridges is presented. The expanded picture of change of the shape and properties of a moving GB half-loop with GB ridges is given. Activation enthalpy of GB motion with the “rough-to-rough” (1.27eV) and “facet-to-facet” (0.2eV) GB ridges of the first order have been measured. The values of activation enthalpy are defined by the mechanism of motion for curved and facet grain boundary segments of ridges. It has been shown that GB ridges can control and slow dawn the motion of GB.

The obtained results can be successfully applied to explain the sintering and recrystallization processes in the hexagonal or wurtzite-type materials, where faceting of GBs occurs.

References

1.V G Sursaeva, G Gottstein, L S Shvindlermann Acta Mater **41,**7725 (2010)

F-98

Preparation and Characterization of Tin Tungstate Thin Films

A. Kuzmin, M. Zubkins, R. Kalendarev

Institute of Solid State Physics, University of Latvia, Latvia

e-mail: a.kuzmin@cfi.lu.lv

Tin tungstate exists at low-temperatures (below 670°C) in α-$SnWO_4$ phase, having orthorhombic crystal structure and dark-red color [1]. It is a promising gas-sensing and photocatalytic material [2,3], also suggested for the use as an anode material in Li-ion batteries [4]. Thin films of tin tungstate are of significant interest because of their possible use in transparent electronics [5].

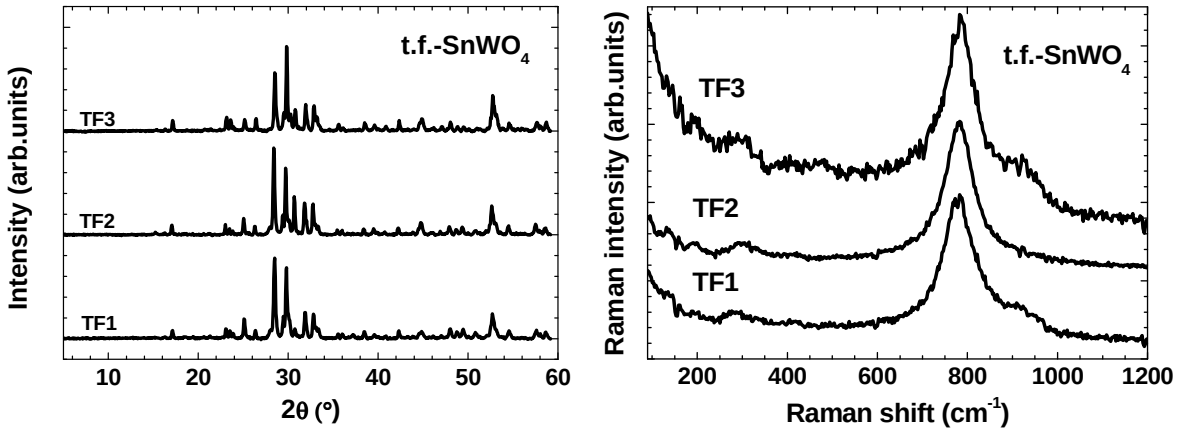

Fig.1. Typical x-ray diffraction patterns and micro-Raman spectra of tin tungstate thin films deposited on glass substrate at different O_2/Ar gas ratios and post-annealed at 450°C in vacuum.

In this study we report on the preparation of tin tungstate thin films by dc magnetron sputtering method. The morphology and phase composition of the films have been studied using several techniques (x-ray diffraction, confocal microscopy and Raman spectroscopy) as a function of the O_2/Ar gas ratio, substrate temperature and post-annealing treatment. The obtained results suggest the formation of nanocrystalline α-$SnWO_4$ phase (Fig. 1). The possibility to use these films as optical recording media will be demonstrated.

References

1. J.L. Solis and V. Lantto, Sensor. Actuat. B **24-25**, 591 (1995).
2. J.L. Solis and V. Lantto, Phys. Scripta **T69**, 281 (1997).
3. J. L. Solis, J. Frantti, V. Lantto, L. Häggström, M. Wikner, Phys. Scripta **T79**, 216 (1999).
4. R. Huang, H. Ge, X. Lin, Y. Guo, R. Yuan, X. Fua, Z. Li, RSC Adv. **3**, 1235 (2013).
5. H. Odaka, U.S. Patent 7,514,023 B2 (2009).
6. A. Kuzmin, R. Kalendarev, A. Kursitis, J. Purans, J. Non-Cryst. Solids **353**, 1840 (2007).

F-99

Electronic Properties of Polar and Nonpolar ZnO Films on $LiGaO_2$

P. Ščajev[1], R. Nedzinskas[1], S. Tumėnas[1], L. Trinkler[2], B. Berzina[2], V. Korsaks[2], M.M.C. Chou[3], L.W. Chang[3], and L.C. Chen[4], K.H. Chen[4]

[1]Optoelectronics department, Center for Physical Sciences and Technology, A. Goštauto 11, Vilnius, Lithuania

[2]Institute of Solid State Physics, University of Latvia, Kengaraga 8, 1063 Riga, Latvia

[3]Department of Materials and Optoelectronic Science, National Sun Yat-Sen University, Kaohsiung, Taiwan

[4]Center for Condensed Matter Sciences, National Taiwan University, Taipei 106, Taiwan

e-mail: patrik.scajev@ff.vu.lt

Hexagonal ZnO grows preferentially along the [0001] c-axis direction. However, it exhibits a strong lattice polarization effect along the c-axis leading to build-in electric fields. This is called Quantum Confined Stark Effect (QCSE). It is proposed to grow ZnO along nonpolar directions, such as (11-20) (a-plane), and (10-10) (m-plane) to overcome QCSE. For characterization of MBE ZnO films, grown on a-, m-, and c- planes of lattice-matched $LiGaO_2$ substrates, we have applied photoluminescence (PL) spectroscopy, time resolved differential reflectivity (TRDR) and light-induced transient grating (LITG) techniques for characterization of spontaneous and stimulated emission, as well as recombination processes. Picosecond laser pulses at 355 nm wavelength were used for interband carrier injection, while the delayed pulse at 1064 nm for probing their relaxation. TRDR technique provided carrier density $\Delta N(t)$ near the surface and carrier lifetime. Similarly, diffraction of the probe beam on the LITG monitored lifetime integrated over the photoexcited layer thickness and excess carrier diffusivity in wide range of injected carrier densities (from ~10^{18} cm^{-3} to 10^{20} cm^{-3}).

Optical absorption spectra of c-ZnO are red-shifted in the band-edge region compared to a- and m-ZnO. PL spectra of all samples measured at RT contain a sharp exciton peak at ~380 nm and a broad defect-band peaking at 600 nm. Near band edge emission is red-shifted in the c-plane layer with respect to nonpolar ones due to presence of polarization field along the polar c-axis. A fine structure of near band edge emission due to excitons and phonon replicas was observed at 10 K.

The TRDR and LITG measurements revealed the longest electron-hole pair lifetimes in the c-plane ZnO (up to 100 ps at lowest injections) versus few times shorter ones in the a- and m- plane layers. Tendency of shorter lifetime correlated well with larger DR decay tail amplitude. The dacay tails were attributed to defects (i. e. carrier traps, which were found more abundant in a-plane sample).

Acknowledgment

The work was supported by Taiwan-Latvia-Lithuania Cooperation project “Nonpolar ZnO thin films: growth-related structural and optical properties” (No. TAP-LLT-02/2014).

F-100

Optical Properties of Polar and Nonpolar ZnO Thin Films Grown on $LiGaO_2$ Substrate

R. Nedzinskas[1], A. Rimkus[1], A. Balčiūnas[1], S. Tumėnas[1], P. Ščajev[1], L. Trinkler[2], B. Berzina[2], V. Korsaks[2], M. M. C. Chou[3], L. W. Chang[3], L. C. Chen[4], and K. H. Chen[4]

[1]Optoelectronics department, Center for Physical Sciences and Technology, A. Goštauto 11, Vilnius, Lithuania

[2]Institute of Solid State Physics, University of Latvia, Kengaraga 8, 1063 Riga, Latvia

[3]Department of Materials and Optoelectronic Science, National Sun Yat-Sen University, Kaohsiung, Taiwan

[4]Center for Condensed Matter Sciences, National Taiwan University, Taipei 106, Taiwan

e-mail: ramunas@pfi.lt

Zinc oxide (ZnO) is a promising material for short-wavelength light emitting applications. The wurtzite crystal structure of ZnO grows preferentially in the polar (0001) direction. Strong spontaneous and piezoelectric lattice polarization along the c-axis leads to an undesirable built-in electric field, which separates electrons and holes in a real space (quantum-confined Stark effect, QCSE) and red-shifts emission peak of multiple-quantum well devices. In this work, an effective approach to supress QCSE is proposed by growing epitaxial ZnO in nonpolar directions along the a-plane $(11\bar{2}0)$ and the m-plane $(10\bar{1}0)$.

Two nonpolar a- and m-plane ZnO thin films together with polar c-plane (0001) film were grown by chemical vapor deposition on a lattice-matched (100) $LiGaO_2$ substrate. We have used temperature-dependent photoluminescence (PL) and photoreflectance (PR) spectroscopy to study optical properties of ZnO films in 3-300 K temperature range. Additionally, we have examined polarization properties of nonpolar ZnO thin films using an ultraviolet rotatable polarizer and achromatic depolarizer in front of a monochromator. Pulsed 266 nm laser was used as an excitation and modulation source for PL and PR experiments. PR measurements were carried out in the so called bright configuration mode using two monochromators and lock-in detection system.

Room temperature PL and PR spectra exhibited main ZnO excitonic peak at 380 nm (c-plane) and at 375 nm (a-, m-planes) together with a broad defect-induced band centered at 550 nm. A red-shift of near band edge emission in the c-plane ZnO was attributed to polarization field along the polar c-axis. A fine structure of near band edge emission due to excitons and their phonon replicas was observed and discussed in detail. Moreover, optical data from polarized PL and PR measurements revealed the in-plane optical anisotropy of nonpolar a- and m-plane ZnO thin films.

Acknowledgment

This research was funded by a grant (No. TAP-LLT-02/2014) for Lithuania-Latvia-Taiwan project: “Nonpolar ZnO thin films: growth-related structural and optical properties”.

F-101

Measuring the Brightness of the Retinal Reflex to Study the Accommodative Response of Stimuli with Various Spectral Distribution

V. Karitans[1], N. Lesina[2], G. Krumina[2]

[1]Institute of Solid State Physics, University of Latvia, Latvia

[2]Department of Optometry and Vision Science, University of Latvia, Latvia

e-mail: variskaritans@gmail.com

It is known that that the retinal brightness depends on the refractive state of an eye. Therefore, the retinal brightness is a function of the accommodative state of an eye. Infrared photorefraction method [1] measures the intensity gradient across the pupil of an eye. In this study, we describe a method using the brightness of the retinal reflex to measure the accommodative response.

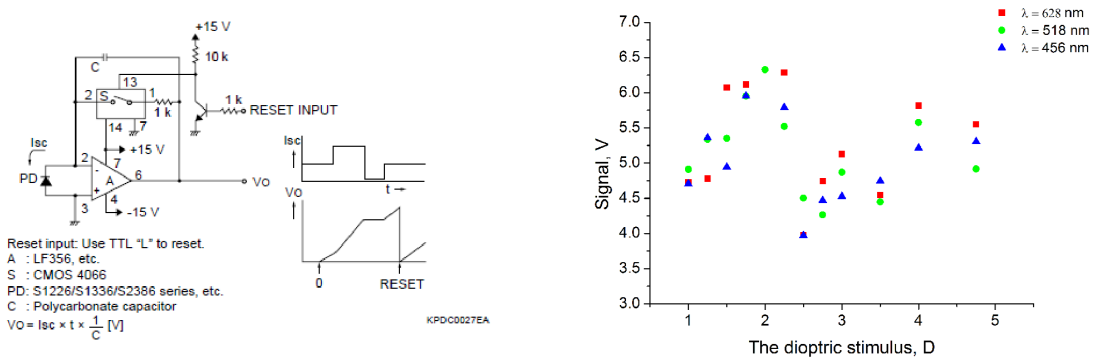

Fig.1 Left - the electronic circuit of the light integrator. Right - the accommodative response to stimuli in three primary colors.

As the retina reflects only 4 % of the incident light we designed a light integrator [2] to measure the light reflected from the retina. The light integrator is schematically shown in Figure 1 (left). A light coming out of an eye falls onto a photodiode charging a capacitor. The used integration time is 60 [ms].

Initial results show that there are differences in response to accommodative stimuli in three primary colors (see Figure 1 right). The value of the dioptric stimulus corresponding to the peak in the response may be somewhat shifted for stimuli of different colors. This difference may be due to chromatic aberration in the human eye equal to about 1.5 [D].

Acknowledgment

The authors are thankful to the European Social Fund project 2013/0021/1DP/ 1.1.1.2.0/13/APIA/VIAA/001

References

1. M. Erdurmus and R. Yagci, Journal of AAPOS. **11**, 606 (2007).
2. Hamamatsu, Si Photodiodes, (2014)

ESF EIROPAS SOCIĀLAIS FONDS
EIROPAS SAVIENĪBA
IEGULDĪJUMS TAVĀ NĀKOTNĒ

F-102

Adaption of Liquid Crystal Shutters for Infrared Binocular Eye Pupil Tracking

S. Fomins[1], R. Trukša[2], G. Krūmiņa[2] M. Ozoliņš[1]

[1]Institute of Solid State Physics, University of Latvia, Latvia

[2]Optometry and Vision Science Department, University of Latvia, Latvia

e-mail: sergejs.fomins@gmail.com

Eye pupil is a relatively slow acting system, which is a part of neural system and can be used as indicator of neural load and visual fatigue. To study the eye pupil cooperation we developed the system incorporating high frame rate CCD equipped with IR band pass filter and narrow angle optical objective. Band pass filter is chosen to transmit the light other 850 nm wavelength. The sensitivity of CCD to infrared illumination is shown in fig1. Our system consists of two capturing cameras for each eye and electronic ferroelectric shutters [1], which separate the stimuli for each eye. Studying illumination influence on visual fatigue it is prevalent to block the specific spectral signal by shutter, in cases then cannot control directly. Liquid crystal shutter holds also beneficial light polarization properties. Signal separation allows tracking the eye pupil latencies in fellow eye while stimulating other. Real time tracking and analysis of pupil parameters is provided to reduce the amount of data.

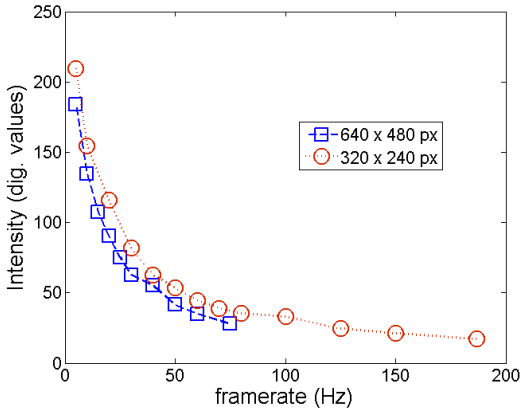

Fig.1 Sensitivity of IR band pass filter equipped camera to infrared (850 nm) light source.

Acknowledgement

Research is supported by ESF 2013/0021/1DP/1.1.1.2/13/APIA/VIAA/001.

References

1. M. Ozolinsh, G. Andersson, G. Krumina, S. Fomins. Spectral and temporal characteristics of liquid crystal goggles for vision research. Integr. Ferroelectrics 103, 1-9 (2008).

F-103

Smart Model Eye on Base of PDLC for Continued Stage Cataract Studies

M. Ozolinsh[1], P. Paulins[2], V. Karitans[1], G. Krumina[3]

[1]Institute of Solid State Physics, University of Latvia, Latvia

[2]Department Physics and Mathematics, University of Latvia, Latvia

[3]Department of Optometry and Vision Sciences, University of Latvia, Latvia

e-mail: ozoma@latnet.lv

We report on developed model eye for studies of deterioration of image quality, optical system resolution, modulation transfer function in cataract eye lens using a polymer dispersed liquid crystal (PDLC) cell as smart media allowing the electrical field inducing of scattering that corresponds to various levels of cataract. Since now different media are used for alternating of scattering efficiency (i.e., no smart media, but model with alternate scattering – (Donnelly, 2005) in model eyes[1]. Previously we have demonstrated[2] the controlling of "cataract" scattering efficiency in visible by applying the AC electric field to a thin PDLC layer (Bueno et al., 2008).

The model eye is built using a plano-convex 50D glass lens, glued on a sandwich element comprised of two glass plates with a light scattering PDLC layer filled between them. Applying the electric field up to 30V continuously diminishes scattering efficiency. The lens (effective f-number F = 3.3) module is mounted on the platform of digital photocamera with Samsung 14Mpix CMOS sensor 1/2.3' – sensor pixel pitch 1.4 μm. Software allows to ignore camera built-in autofocusing function and allows to select exposure 1/2000 to 4 s. Model eye properties were tested regarding to image point spread function and image line resolution, eye „contrast vision function" in presence *vs.* absence of simulated in PDLC light scattering, Light scattering effect on detectability of model eye lens aberrations using Shack-Hartman sensor is in progress.

References

1. W. J. Donnelly (2005); voi.opt.uh.edu/VOI/WavefrontCongress/2005/presentations/19-Donnelly-Scatter.pdf
2. J. M. Bueno, M. Ozolinsh and G. Ikaunieks, Ferroelectrics **370**, 18 (2008)

F-104

HOPG Patterning Methods for Graphene Transferring Onto the Substrate

E. Butanovs, J. Butikova, B. Polyakov, G. Marcins, R. Zabels, I. Tale

Institute of Solid State Physics, University of Latvia

e-mail: edgarsbutanovs@gmail.com

Different patterning methods of highly oriented pyrolytic graphite (HOPG) were investigated. Micropatterning of HOPG surface facilitates the detachment of graphene layers during contact stamp printing. Direct pulsed laser beam scribing in air and water, nanoindenter scribing were used to produce square patterns (with square size down to approx. 35x35 μm). Raman spectroscopy, optical profilometer, scanning electron and optical microscopy were used to determine quality of scribed graphite surface and size of pattern elements depending on the method used.

Two methods of the graphene transfer onto the substrate were examined. Silicone glue and polydimethylsiloxane (PDMS) epoxy were used for stamp preparation by mechanical lift-off of thin layer of patterned graphite and following contact printing of graphene onto an oxidized silicon wafer [1]. Electrostatic deposition of freshly cleaved HOPG uppermost layers [2] was applied to transfer graphene sheets directly onto the substrate.

Both presented methods of graphene placement into a substrate are a more flexible and convenient alternative to the conventional methods, allowing transferring of relatively large-surface graphene sheets with thickness from a single to several layers.

References

1. J. Butikova, B. Polyakov, L. Dimitrocenko, E. Butanovs, I. Tale. Central European Journal of Physics. **11**, 580 (2013)
2. A. N. Sidorov, M. M. Yazdanpanah, R. Jalilian, P. J. Ouseph, R. W. Cohn and G. U. Sumanasekera, Nanotechnology **18**, 135301 (2007)

F-105

Optimization of Deposition and Characterization of Graphene Oxide Monolayers and Films Obtained by Langmuir-Blodgett Technique

A. Dravniece[1], L. Gerca[1], K. Kundzins[1], K. Piterane[2], M. Rutkis[1]

[1]Institute of Solid State Physics, University of Latvia, Latvia

[2]Riga Technical University, Latvia

e-mail: agnese.dravniece@lu.lv

In last decade particular interest has been shown in using graphene materials in optoelectronic devices. Graphene has high optical transmittance and electrical conductivity therefore it is considered as an innovative and alternative material to produce transparent conductive films. Single – sheet graphene (SG) covered substrates could be used in a wide variety of optoelectronic devices, such as solar cells, optical communication devices and solid state lightning.

In this study single – sheet graphene oxide (SGO), two – dimensional multifunctional material, is used for producing graphene - based materials. SGO has been obtained by modified Hummer`s method followed by SGO – water gel lyophilization. Langmuir – Blodgett technique has been used for transferring SGO from suspension to substrate. Deposition parameters and conditions have been chosen and characterized; nevertheless careful and thoughtful optimization of deposition process has to be carried out. Obtained SGO thin films have been characterized by scanning electron microscopy.

Benzene and benzene/methanol mixtures were chosen as suspension and spreading solvents in order to avoid loss of material in water subphase. SGO sheet size was regulated by sonication and centrifugation with careful attention to sonication time and centrifugation speed; deposition was carried out in a variety of pressures. The effect of variously treated glass substrate surface (hydrophilized, ozonated) was observed and analyzed. The work to improve the quality of obtained SGO layers is continued.

Acknowledgment

This work has been supported by National Research Program No. 2. “Development of Innovative Multifunctional Materials, Signal Processing and Information Technologies for Competitive Science Intensive Products", Project No. 6. "Graphene, modified graphene and graphene containing composites for surface coatings, nanodevices, sensors and energy conversion”.

F-106

Thermal Deoxygenation of Graphite Oxide at Low Temperature

V. Kampars[1], M. Legzdina[1]

[1]Institute of Applied Chemistry, Riga Technical University, Latvia

e-mail: kampars@ktf.rtu.lv

Thermal exfoliation of graphite oxide (GO) is considered to be a promising strategy for realizing mass production of graphene materials at low cost and high quality [1]. If the temperature is low the thermal deoxygenation of GO is less complicated and more easily controllable method than chemical reduction. In order to lower the deoxygenation temperature we have made additionally treatment of GO, synthesized accordingly to the modified Hummer's method [2], with acetone by ultrasonification. From Fig.1 it is seen that during the thermogravimetric investigation under nitrogen atmosphere by heating rates exceeding 1 ^{o}C/min an explosion like mass loss at 130 ^{o}C has been arisen, indicating the deoxygenation and spontaneous defoliation of graphite oxide at low temperature. The FTIR spectra of products do not show the presence of oxygen atom containing bond absorption in infrared spectra and the characteristic XRD pattern at 2θ ~ 10^{o}. Thermogravimetric investigation of GO with heating rate of 1 ^{o}C/min allows to register the mass loss curve of the synthesised graphite oxide until its full decomposition (800 ^{o}C). The mass loss curve consists at least of four stages of anticipated H_2O, CO and CO_2 release. The investigation of the composition of evolved gases by hyphenated Pyr/GC/MS method at different experimental conditions under helium atmosphere shows that without the expected H_2O, CO and CO_2 also sulphur dioxide and acetone has been released.

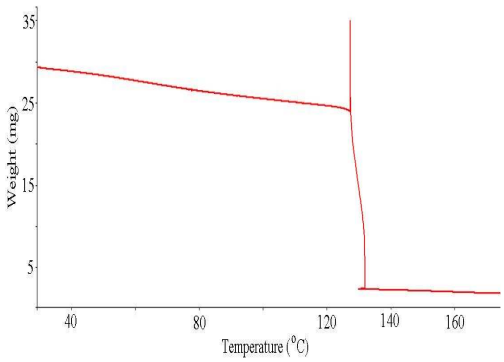

Fig.1 Weight loss curve obtained for synthesized graphite oxide at 1 ^{o}C/min.

Acknowledgement

The financial support from the Program "IMIS" is gratefully acknowledged.

References

1 C. Zhang, W .Lv, X. Xie, D. Tang, C. Liu and Q.-H.Yang, Carbon. **62**, 11 (2013)
2. X. Wang and W. Dou, Thermochimica Acta. **259**, 25 (2012)

F-107

TTT Thin Film Morphology and Electrical Properties

K. Pudzs, A. Vembris, M. Rutkis

Institute of Solid State Physics, University of Latvia, Latvia

e-mail: kaspars.pudzs@cfi.lu.lv

Mankind wastes a lot of energy as low level heat (<200°C). Low-cost organic thermoelectric devices would allow direct heat-to-electrical energy from this vast. New organic materials are necessary to create such devices. Tetra-thio-tetracene is one of the candidates for this application. This leads to the necessity to study thin films of TTT morphology and electrical properties.

In this work morphology of TTT thin films obtained at different conditions like substrate temperature and evaporation rate was studied. The organic thin films were made by thermal evaporation in vacuum technique. Optical microscopy and scanning electron microscopy were used to study thin film morphology. Charge carrier mobility was determined by carrier extraction by linearly increasing voltage method[1]. Space charge limited current methods [2,3] were used to determine charge carrier local trapping states. Electrical conductivity was measured by four probe technique.

The morphology of thin film dependence on substrate temperature and evaporation rate will be shown. Electrical properties dependence on morphology will be discussed.

Acknowledgment

This work has been supported by European Commission 7th Framework Programme project "Waste Heat to Electrical Energy via Sustainable Organic Thermoelectric Devices".

References

1. G. Juska, K. Arlauskas, M. Viliunas, J. Kocka, Phys. Rev. Lett. 84 (2000) 4946.
2. F. Schauer, J. Phys. C Solid State Phys. 19 (1986) 7231.
3. F. Schauer, S. Nešpůrek, H. Valerián, J. Appl. Phys. 80 (1996) 880.

F-108

Optical Properties of Natural and Synthetic Beryl Crystals

V. Skvortsova[1], N. Mironova-Ulmane[1], L. Trinkler[1], V. Merkulov[2]

[1]Institute of Solid State Physics, University of Latvia, Latvia

[2]Institute of Solid State and Semiconductor Physics NASB, Minsk, Belarus

e-mail: vera@cfi.lu.lv

Beryl is a silicate mineral with a general chemical formula of $Be_3Al_2Si_6O_{18}$. Natural and synthetic minerals of beryl are used not only as gemstone but have also practical industrial application. Beryl crystals find application as laser and dosimetry materials. Small amount of impurities and structural defects have a significant effect on the physical properties of crystals, chemical and radiation resistance of products and devices manufactured on the basis of beryl crystals. We present a study of optical properties of natural and synthetic beryl crystals before and after irradiation.

Absorption spectra of synthetic beryl crystals include three bands with maxima 270, 430 and 630 nm. Bands 430 and 630 nm are associated with electronic transitions $^4A_{2g}(F) \rightarrow {}^4T_{1g}(F)$ and $^4A_{2g}(F) \rightarrow {}^4T_{2g}(F)$ of chromium ions. If chromium concentration is about 0.1% or more the absorption spectra is characterized by sharp R-lines (zero phonon transition $^4A_{2g}(F) \rightarrow {}^2E_g(G)$ in Cr^{3+}ion). Natural beryl crystals have wide absorption band at 820 nm. The band is generally ascribed to internal electron transition of $^5T_2$ (^5D) $\rightarrow$ ^5E (^5D) of Fe^{2+} ions localized in octahedral aluminum sites of beryl. Fast neutron irradiation produces additional bands with maxima 286, 370, 500 and 667 nm. Most probably these bands are due to intrinsic anion defects (F^+, F, F_2, F_2^+ and F_2^+ centers) similar to those observed in Al_2O_3 [1, 2]. Under increase of the fast neutron fluence the intensity of the 820 nm band reduces and there appears a series of narrow bands in the 500 - 700 nm region. We suppose that these narrow bands belong to the complex center, which consists of Cr^{3+} ions and radiation defects.

Wide band at 740 nm observed in the photoluminescence spectra of beryl crystals at T= 300 K is connected with Fe^{2+} ions. Narrow lines in region from 680 to 720 nm at T= 8 K belong to single Cr^{3+} ions (R- lines) and Cr^{3+}- pairs (N- lines).

References

1. K. Atobe, N. Nishimoto, M. Nakagawa, Phys. Stat. Sol. (a) **89**, 155 (1985)
2. K. H. Lee and J. H. Crawford Jr., Phys. Rev. **15**, 4065 (1977)

F-109

Optical and Structural Studies of Zn-Ir-O Thin Films Deposited by Reactive DC Magnetron Sputtering

M. Zubkins, R. Kalendarevs, J. Gabrusenoks, A. Azens, K. Vilnis, J. Purans

Institute of Solid State Physics, University of Latvia, Latvia

e-mail: zubkins@cfi.lu.lv

One of the obstacles to further developments of transparent electronics based on transparent conductive oxide thin films is lack of p-type conductors [1].

Amorphous ZnO-IrO_2 thin films deposited by pulsed laser deposition at room temperature are reported to be potential p-type TCOs [2]. In the present study, we have investigated optical and vibrational properties of Zn-Ir-O thin films deposited by reactive DC magnetron sputtering.

Zn-Ir-O thin films were deposited on glass, Si and Ti substrates by reactive DC magnetron sputtering from a metallic Zn (99.95 %) target with Ir pieces on the target surface in an Ar+O_2 atmosphere. A set of samples was deposited at different oxygen to argon gas ratios (1/4, 1/2/, 1/1) and at different fractions of iridium on the zinc target erosion zone (1, 3, 5, 7, 10, 13, 15 %). Structural, optical and vibrational properties of the Zn-Ir-O thin films were studied by XRD, Raman, FTIR techniques, as well as two beam optical spectrophotometry.

Pure ZnO films are crystalline with the grain size of approximately 50 nm. Iridium concentration in the range between 0 and 7 at. % alters structure to amorphous and shifts the absorption edge toward to the shorter wavelength compared to the c-ZnO. Increase in iridium concentration changes the form of transmittance curve and leads to higher absorption coefficient in the visible range [3]. In the Raman spectrum a band at 712 cm^{-1} appears after doping with iridium and disappears when iridium concentration reaches 24 at. %.

References

1. L. Castaneda, Materials Science and Applications **2**, 1233-1242 (2011)
2. J. M. Dekkers, Transparent Conductive Oxides on Polymeric Substrates by Pulsed Laser Deposition (Ph. D. thesis University of Twente, Enschede, Netherland 2007)
3. M. Zubkins, R. Kalendarev, J. Gabrusenoks, K. Vilnis, A. Azens, J. Purans, Physica Status Solidi C (in press)

F-110

Examining Temperature Influence on Er^{3+} Luminescence in $NaLaF_4$ Matrix

J. Grube, G. Doke, G. Krieke, A. Sarakovskis, M. Springis

Institute of Solid State Physics, University of Latvia, Latvia

e-mail: Jurgis.Grube@cfi.lu.lv

Different kinds of materials doped with rare-earth (RE) elements often serve as up-conversion (UC) luminescence sources where photons with lower energy (usually IR) are converted into higher energy photons (VIS, and UV). One of the requirements for the high UC luminescence efficiency is low material phonon energy, other – existence of sites where RE ions can freely incorporate within the lattice. Previous studies have shown that $NaLaF_4$ meets these requirements [1]. Different green luminescence spectra under various excitation wavelength are observed at low temperature (15K) clearly indicating multisite nature of $NaLaF_4$. At room temperature (300K) such significant differences in luminescence spectra are not observed. Therfore in this work we will show temperature influence on $NaLaF_4$:Er^{3+} luminescence.

In this report spectroscopic measurements at different temperatures (15K-300K) for $NaLaF_4$ doped with Er^{3+} (0.1 and 2 mol%) will be shown. Variations of the shape of the green luminescence (origin from $^4S_{3/2}$ to $^4I_{15/2}$ transition) were observed when temperature was increased. In addition, variation in green luminescence decay kinetics at different temperatures depends on Er^{3+} concentration. For the low Er^{3+} concentration (0.1 mol%) green luminescence decay kinetics remains nearly unchanged at different temperatures (15K-300K), but at higher Er^{3+} concentration (2 mol%) significant variations in the kinetics of the green luminescence decay are observed.

Based on the experimental results temperature impact on Er^{3+} spectroscopic properties in $NaLaF_4$ will be discussed.

Acknowledgements:

This work has been supported by the European Social Fund within the project „Support for Doctoral Studies at University of Latvia" (No. 2009/0138/1DP/1.1.2.1.2/09/IPIA/VIAA/004) as well as State Research Program IMIS (project 1).

References

1. A. Sarakovskis, J. Grube, A. Mishnev, M. Springis, Optical Materials **31**, 1517-1524 (2009)

F-111

Influence of Different Crystal Field Environments on the Luminescence of $NaLaF_4:Er^{3+}$

A. Sarakovskis, G. Krieke, G. Doke, J. Grube, L. Grinberga and M. Springis

Institute of Solid State Physics, University of Latvia, Latvia

e-mail: anatolijs.sarakovskis@cfi.lu.lv

Low phonon energy of the matrices and multisite nature of the crystalline lattice make complex fluoride materials attractive for the upconversion luminescence. The aim of this work has been to study multisite formation in $NaLaF_4:Er^{3+}$ and the influence of the multisite structure on the luminescence processes in the material.

The results of low-temperature site-selective spectroscopy measurements in hexagonal $NaLaF_4:Er^{3+}$ will be shown. Three distinct luminescence spectra in the green spectral region associated with $^4S_{3/2} \rightarrow {}^4I_{15/2}$ electronic transition could be extracted under the photoexcitation at different positions corresponding to the excitation of $^4F_{7/2}$ level of Er^{3+}. It was possible to model the experimentally obtained luminescence spectra at any excitation wavelength by a linear combination of the extracted spectra with a tolerance better than 5%.

The results of the site-selective spectroscopy suggest the presence of three different crystalline field environments where Er^{3+} ions incorporate. The analysis of the structure of the material and time-resolved luminescence have been used to differentiate between cationic sites with C_3 and C_{3h} symmetries in the structure of $NaLaF_4$ available for Er^{3+} incorporation. Site-selective excitation of Er^{3+} located at a specific site induced energy transfer to erbium ions located at other sites has been observed in both the upconversion and traditional luminescence processes.

The enhanced energy transfer between the different sites in $NaLaF_4:Er^{3+}$ signifies the importance of multisite nature of the structure, which is a key factor for an efficient upconversion luminescence.

F-112

Synthesis and Luminescent Properties of Blue Emitting $CaAl_2Si_2O_8:Eu^{2+}$ Phosphor

S.H. Kwon, B.K. Moon, B.C. Choi, J.H. Jeong*

Department of Physics, Pukyung National University, Busan 608-737, Republic of Korea

e-mail: ksh014@nate.com

The alkaline earth feldspars of $MAl_2Si_2O_8$ (M = Ca, Sr, Ba) phosphor have drawn much attention for their excellent luminescence properties. In alkaline earth feldspars, the framework structures are formed from an array of interlinked corner-sharing SiO_4, AlO_4 tetrahedra, with Al charge-compensating cations Ca, Sr, Ba occupying the large cavities with in the structure. A solid solution series of isostructural members with slightly different sized cations as hosts, would be an ideal system to study the effect of crystal chemical variation on the luminescence of Eu^{2+} ions. It is well known that Eu^{2+} have been widely used as activators in phosphor materials. The Eu^{2+} ions show broad emission bands ranging from UV to red spectral region arising from $4f^6\ 5d^1 - 4f^7$ allowed transition. This is strongly dependent on the crystal fields of the host lattices since 5d orbitals are more sensitive to the ligand field. Accordingly, the Eu^{2+} becomes a very useful activator in phosphors for applications in displays, lamps and luminescent paintings.

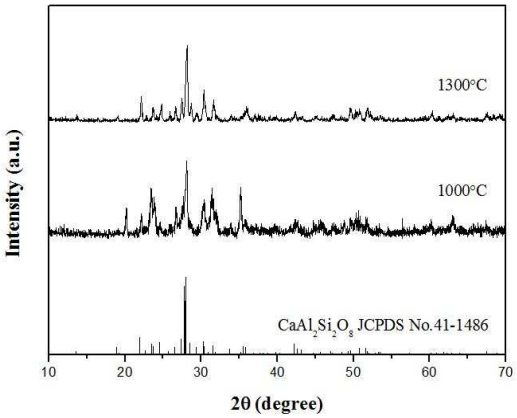

Fig.1 X-ray diffraction patterns of $CaAl_2Si_2O_8:Eu^{2+}$

In this study, Eu^{2+} doped $CaAl_2Si_2O_8$ phosphors were prepared by mean of solid state reaction method. The structural and luminescence properties of $CaAl_2Si_2O_8:Eu^{2+}$ phosphors have been confirmed by the measurements of their X-ray diffraction (XRD) and photo luminescence (PL).

References

1. A.E.R. Malins, N.R.J. Poolton, F.M. Quinn, O. Johnsen, P.M. Denby, J. Phys. D Appl. Phys. **37** 1439–1450 (2004).
2. W.J. Yang, L. Luo, T.M. Chen, N.S. Wang, Chem. Mater. **17** 3883–3888 (2005).

F-113

Thermally Stimulated Luminescence of Undoped and Ce^{3+}-Doped Gd_2SiO_5 and $(LuGd)_2SiO_5$ Single Crystals

V. Bondar[1], L. Grigorjeva[2], T. Kärner[3], O. Sidletskiy[1], K. Smits[2], S. Zazubovich[3], A. Zolotarjovs[2]

[1]Institute for Scintillation Materials, NAS of Ukraine, 60 Lenin Ave. 61001 Kharkiv, Ukraine

[2]Institute of Solid State Physics, University of Latvia, 8 Kengaraga Str., Riga, LV-1063, Latvia

[3]Institute of Physics, University of Tartu, 142 Riia Str., 51014 Tartu, Estonia

e-mail: alexeyzolotarjov@gmail.com

Single crystals of Gd_2SiO_5:Ce (GSO:Ce) and $(LuGd)_2SiO_5$:Ce (LGSO:Ce) are extensively studied as promising scintillation materials. For their successful applications, the origin of crystal lattice defects and their thermal stability parameters must be defined. This information can be obtained by the thermally stimulated luminescence (TSL) method. In this paper, TSL glow curves and TSL spectra are studied in the 4-520 K temperature range for the nominally undoped GSO and LGSO crystals, containing traces of Ce^{3+}, Tb^{3+}, and Eu^{3+} ions, and for Ce^{3+}-doped GSO and LGSO crystals. For the first time, the TSL glow curves of the X-ray irradiated crystals are measured separately for the electron (Ce^{3+}-, Tb^{3+}-related) and hole (Eu^{3+}-related) recombination luminescence, which allows the identification of the TSL glow curve peaks arising from the thermal destruction of electron and hole centers, respectively.

The TSL glow curves measured for the Tb^{3+}-, Ce^{3+}-related 2.8-3.2 eV emission and for the Eu^{3+}-related 1.8-2.0 eV emission are found to be different. From the comparison of these curves and the analysis of the TSL spectra corresponding to each TSL peak, the electron or hole origin of the TSL peak is defined. The intense peaks located in the 40-110 K and 320-365 K temperature ranges are mainly of an electron origin. They are suggested to arise from thermal release of the electrons, trapped at various oxygen-vacancy-related defects, and their subsequent recombination with the hole Tb^{4+} or Ce^{4+} centers accompanied with the Tb^{3+}- or Ce^{3+}-related emission. The peaks located in the 115-280 K temperature range are mainly of a hole origin. They can arise from thermal release of holes trapped at the regular oxygen ions (the self-trapped holes) or at the oxygen ions located close to intrinsic or impurity crystal lattice defects and their subsequent recombination with the electron Eu^{2+} centers accompanied with the Eu^{3+}-related emission. From the TSL data, thermal stability parameters (the trap depths and frequency factors) are calculated for various electron and hole traps. The values of these parameters for hole traps are found to be smaller than those obtained for electron traps.

F-114

Luminescent Properties of Tb^{3+}-Doped $SrLaMgTaO_6$ Phosphor for White Light-Emitting Diodes

G. Yue[1], B.K. Moon[1], J.W. Jang[1], J.H. Jeong[1,*], J.H. Kim[2]

[1]Department of Physics, Pukyong National University, Busan 608-737, Republic of Korea

[2]Department of Physics, Dong-eui University, Busan 614-714, Republic of Korea

e-mail: 1216069619@qq.com

Rare earth (RE) doped materials have been paid great attention in the field of lighting, lasers, displays and structural analysis because of their unique intra-configurational f–f transitions, which can occur as sharp and intense emission lines. Generally, the green-emitting emission can be achieved by the 4f-4f transitions of Tb^{3+} ions doped in a host.

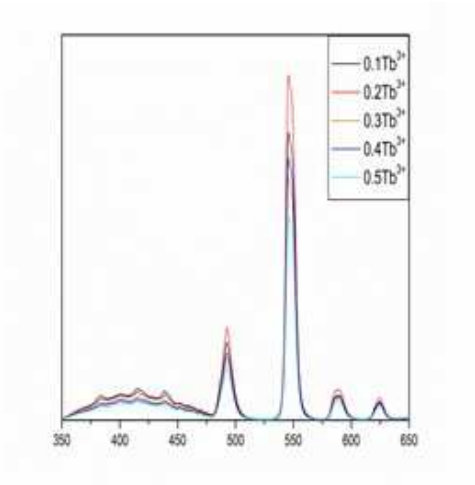

Fig1: The luminescence spectra of $SrLaMgTaO_6$: Tb^{3+} under the excitation of 256nm

In this work, the perovskite phosphors Tb^{3+}-doped $SrLaMgTaO_6$ were synthesized by a solid-state reaction. The X-ray powder diffraction (XRD), photoluminescence excitation, emission spectra, concentration quenching, and luminescence decay curves and lifetime were applied to characterize the samples. The CIE chromaticity coordinates of the phosphors were located in the green region. So the phosphors may be potentially used for white light-emitting diodes.

References:

1. Ren ZY, Tao CY, Yang H, Feng SH. Mater Lett 2007;61:1654–7.
2. Wang R, Xu J, Chen C. Mater Lett 2012;68:307–9.

F-115

Luminescence of Coesite

A.N. Trukhin[1], K. Smits[1], J. Jansons[1], G. Chikvaidze[1], T.I. Dyuzheva[2], L.M. Lityagina[2]

[1]Institute of Solid State Physics, University of Latvia, Latvia

[2]Institute of High pressure Physics of RAS, Troitsk, Russia

e-mail: truhins@latnet.lv

Coesite is dense (2.92 g·cm^{-3}) polymorph tetrahedron structured modification of crystalline silicon dioxide. Tetrahedral structured are α-quartz (2.65 g·cm^{-3}), cristobalite (2.35 g·cm^{-3}), tridymite (2.26 g·cm^{-3}). The coesite single-crystals were grown under hydrothermal conditions natural quartz powder and distilled water. Studied samples were 0.5·0.5·0.3 mm^3. Luminescence of synthetic coesite was studied under excitation of x-ray, electron beam, KrF (248 nm), ArF (193 nm) and F2 (157 nm) excimer lasers. It was found that under all these excitations two luminescence bands at about 2.5 eV and 4.4 eV appear. The blue band exhibits compose decay kinetics and three main decay times are revealed. One is in ns range of time. Two others decay times are in 10 µs and 700 µs. First of these components is also seen under KrF excitation whereas both are seen under ArF excitation. Time resolved spectra mutually similar and they are corresponding to spectra under x-ray and cathodoexcitation.

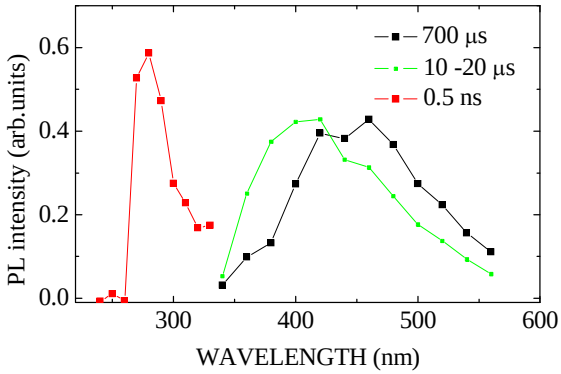

Fig. 1. Time resolved photo luminescence spectra of coesite at 9 K under pulses of ArF laser (193 nm).

The UV band is fast with time constant about 0.5 ns independent on temperature. Under KrF laser excitation only component 2 ns and 10 µs are revealed for blue band. Spectrally fast and slow components are resolved (Figure 1). Blue Luminescence thermal quenching takes place for temperature above 50 K with good correspondence between intensity thermal dependences under different excitation and that of decay time constant.The parameters of quenching are 0.05 eV for energy and 6·10^5 s^{-1} for frequency factor. The UV band is practically independent on temperature in the range 10- 290 K. The nature of luminescence could be determined as host defect similar to known oxygen deficient luminescence center in pure silica glass [1].

References

1. L. N. Skuja J. Non-Cryst. Solids, **239(**1998) 16-48.

F-116

Luminescence and Energy Transfer in $RE(Nb_xTa_{1-x})O_4$, RE = Y or Gd

D. Spassky[1,2], O. Sidletskiy[3], O. Voloshyna[3]

[1]Institute of Physics, University of Tartu, Tartu, Estonia

[2]Skobeltsyn Institute of Nuclear Physics, Moscow State University, Moscow, Russia

[3]Institute for scintillation materials NAS of Ukraine, Kharkiv, Ukraine

e-mail: deris2002@mail.ru

Requirements for the functional materials with efficient conversion of high-energy radiation into luminescence are determined by the demands of new experiments in fundamental physics, necessity for the decrease of radiation dose for patients in medical imaging, new security control systems, etc. Crystals doped with rare-earth elements are usually used nowadays, however some applications require searching for the novel materials with intensive intrinsic luminescence. New experiments in high-energy physics require materials with high scintillation performance at ultra-low temperatures for cryogenic scintillating bolometers [1]. In such conditions compounds with the intrinsic emission are the most perspective while the well - known scintillation materials with activator's emission becomes inefficient due to the self-trapping of charge carriers at the host. Here we present the study of luminescence properties and energy transfer in solid solutions of tantalo-niobates with cations of yttrium or gadolinium. Samples of undoped yttrium and gadolinium tantalo-niobates with common formulae $RE(Nb_xTa_{1-x})O_4$, where RE = Y or Gd, and x=0, 0.2, 0.4, 0.6, 0.8, 1, have been obtained by solid-state reaction. The luminescence characteristics of the samples were measured using synchrotron radiation at the branch-line FINEST at MAX-lab, Lund and at laboratory set-up. The substituted cation of oxyanionic group participates in the formation of intrinsic emission centers, which arise due to radiative annihilation of excitons, self-trapped at TaO_4 (or NbO_4) group. The competition between these intrinsic emission centers in the mixed crystals was studied. As it has been shown recently an enhancement of the scintillation light yield can be achieved for the solid solutions of inorganic crystals [2]. We have observed this effect in the tantalo-niobate solid solutions. The modification of exciton creation efficiency, which arise due of the effects of limitation of charge carriers mean path in solid solutions and might be responsible for the effect, will be analyzed.

References

1. F.A. Danevich, IEEE Trans. Nucl. Sc.**59**, 2207 (2012)
2. A.V. Gektin, A.N. Belsky and A.N. Vasilev, IEEE Trans. Nucl. Sc.**61**, 262 (2014)

F-117

Luminescence of Eu Ions in Oxyfluoride Glasses and Glass-Ceramics

U. Rogulis, I. Brice, E. Elsts, J. Grube, D. Millers

Institute of Solid State Physics, University of Latvia, Latvia

e-mail: uldis.rogulis@lu.lv

The luminescence intensity of several oxyfluoride glasses and glass-ceramics is comparable with the intensity of commercial white LED phosphors [1]. In the present work, we investigated the luminescence spectra of oxyfluoride glasses and glass-ceramics of the composition SiO_2-Al_2O_3-ZnF_2-SrF_2 doped with 2 mol.% Eu.

In the oxyfluoride glasses, initially only the Eu^{3+} luminescence lines in the red spectral region could be observed. After the creating of the glass-ceramics by a heat treatment at a temperature of 800^0C, the broad UV luminescence band of the Eu^{2+} becomes dominant, and the Eu^{3+} lines change their relative intensities. Therefore, for the investigated oxyfluorides the europium in the Eu^{3+} charge state in the glass could be nearly completely transformed to the Eu^{2+} state by creating of the glass-ceramics.

In the Eu^{3+} luminescence spectrum of the glass sample, the lines attributed to the electric dipole transition $^5D_0$ - $^7F_2$ [2] are more intense than the lines of the magnetic dipole transition $^5D_0$ - $^7F_1$. For the glass-ceramics on the contrary, the magnetic dipoles lines are more intense than the electric dipole lines. These changes in the Eu^{3+} line intensities indicate that Eu^{3+} in the glass is embedded in the low symmetry vicinity, and in the glass-ceramics comes over to the higher symmetry vicinity.

References

1. I. Brice, U. Rogulis, E. Elsts, J. Grube, Latv. J. Phys. Techn. Sci. **6(I)**, 44 (2012)
2. T. Montini, A. Speghini, P. Fornasiero, M. Bettinelli, M. Grazini, J. Alloys Compounds 451, 617 (2008)

F-118

Luminescence of Er/Yb Doped HAp-FAp Nanocrystals and Ceramics

L. Pukina[1], L. Grigorjeva[1], K. Šmits[1], D. Millers[2], Dz. Jankoviča[2]

[1]Institute of Solid State Physics, University of Latvia, Latvia

[2]Institute of Inorganic Chemistry, Latvia

e-mail: lgrig@latnet.lv

The hydroxylapatite (HAp) and fluorapatite (FAp) are bio-compability materials and the interest to these materials is due to its biomedical applications, for example as coating material for metallic implants, dental implantology, drug delivery and deep tissue bio-imaging [1,2]. The rare-earth doped HAp and FAp are prospective luminescent biomarkers, especially if the high efficiency of up-conversion luminescence in nanoparticles (NP) will be achieved. The NP of HAp, FAp and HAp-FAp were synthesized and analyzed by FTIR, XRD, scanning electron microscopy (SEM, TEM). The results of up-conversion luminescence studies under 980 nm diode laser excitation of Er/Yb doped HAp-FAp NP and ceramics were presented.

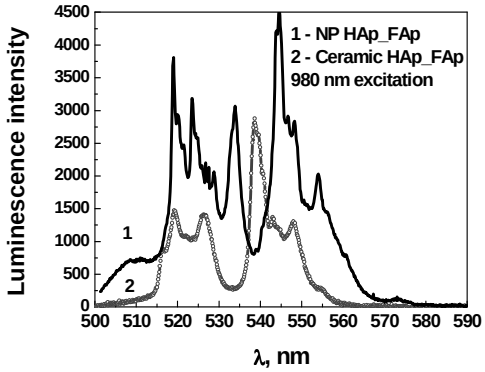

Fig.1. The up-conversion luminescence of HAp-FAp NP and ceramic sintered from the same powder at 800°C 24h

The up-conversion luminescence spectra (Fig.1) shows intensive luminescence of Er ion and energy transfer from Yb to Er ions were observed. The efficiency of up-conversion process in HAp NP is low and the substitution of OH groups to fluorine enhanced luminescence intensity. The dependence of luminescence intensity and spectra on OH/F relations and grain sizes were studied and analyzed.

Acknowledgment

Reserch is supported by Latvian State Program for development of novel multifunctional materials and LZP grant 2013.10-5/014.

References

1. V. J. Shirtliff and L.L.Hench, J.of Mater.Sci. **38**, 4697 (2003)
2. Can T. Xue, Q. Zhan, H. Liu, G. Somesfalean, J. Qian, S. He and S. Andersson-Engels, Laser Photonics Rev. **7**, N5, 663 (2013)

F-119

Synthesis and Photoluminescence Properties of $Sr_3Y(PO_4)_3$: Dy^{3+}

Y.W. Seo[1], J.H. Jeong[1*], Y.C. Suh[2], D.S. Shin[3], K. Jang[4]

[1]Department of Physics, Pukyong National University, Busan 608-737, Republic of Korea

[2]Department of Spatial Information Engineering, Pukyong National University, Busan 608-737, Republic of Korea

[3]Department of Chemistry, Changwon National University, Changwon 641-773, Republic of Korea

[4]Department of Physics, Changwon National University, Changwon 641-773, Republic of Korea

e-mail: nouvellesini@naver.com

In recent years, Dy^{3+} doped phosphors have been extensively studied due to its two dominant emission bands. Dy^{3+} ions have emission bands in the blue region owing to the $^4F_{9/2} \rightarrow {}^6H_{13/2}$ transition and in the yellow region owing to the $^4F_{9/2} \rightarrow {}^6H_{15/2}$ transition. It is possible to achieve near white light emission by adjusting the yellow to blue intensity ratio value [1]. Single-component white-light phosphors have attracted much attention for solid-state lighting. The single-phase full-color emitting phosphors have been elucidated and investigated for many hosts such as borates, phosphates, aluminates, and silicates [2]. Among these hosts, phosphates are good candidates due to easy synthesis, chemical/thermal stabilities over a wide range of temperatures, and low cost.

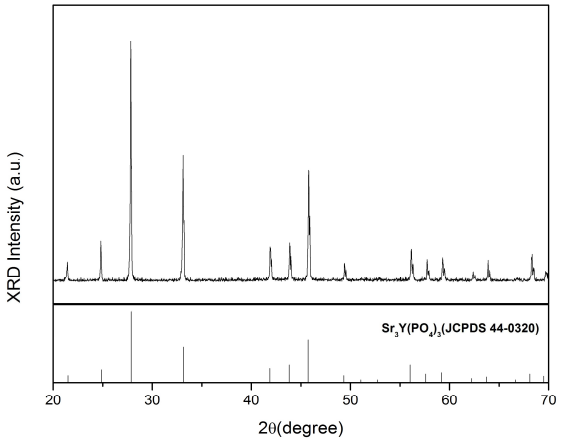

Fig.1 XRD pattern of $Sr_3Y(PO_4)_3$:0.14 mol% Dy^{3+} phosphor.

In this paper, white emitting phosphor Dy^{3+} doped $Sr_3Y(PO_4)_3$ powder samples by solid-state reaction method. The structural and luminescence properties of the phosphors were investigated by X-ray diffraction (XRD), field-emission scanning electron microscopy (FE-SEM), photoluminescence (PL) excitation and emission spectra. Fig. 1 shows the XRD pattern of $Sr_3Y(PO_4)_3$:0.14Dy^{3+} phosphor sintered at 1300 ℃. The XRD study confirms that the structure of the system is cubic phase (JCPDS 44-0320).

References

1. J. Wang, J. Wang, and P. Duan, Mater. Lett. **107**, 96 (2013)
2. X. H. Zhang, Z. M. Lu, F. B. Meng, and et al, Mater. Lett. **79**, 292 (2012)

F-120

Excitation Luminescence Spectroscopy of Rare-Earth Doped $NaLaF_4$

V. Pankratov[1,2], G. Doke[1], A. Sarakovskis[1]

[1]Institute of Solid State Physics, University of Latvia, Latvia

[2]Department of Physics, University of Oulu, Finland

e-mail: vpankratovs@gmail.com

Wide band gap materials such as fluoride compounds are excellent matrices to be doped by rare-earth ions. Such materials have a high potential from the point of view of abundant luminescence applications. Recently it was shown that $NaLaF_4$ has relatively small effective phonon energy ($E_{ph} \sim 290$ cm^{-1}) and, therefore, can be a prospective host material to be doped by rare-earth ions and utilized for up-conversion luminescence purposes [1].

In the current study we apply vacuum ultraviolet luminescence spectroscopy for the investigation of Er^{3+} as well as Eu^{3+} doped $NaLaF_4$. This method was successfully employed before for a study of wide band gap fluorides [2, 3], oxides [4] and even semiconductors [5].

The luminescence emission and excitation measurements were carried out under pulsed synchrotron radiation (5.5 – 45 eV) emitted from Max III storage ring by means of luminescence endstation located at FinEst (I3) beamline of the MaxIV laboratory (Lund, Sweden). Special attention was paid to the vacuum ultraviolet spectral range, which is not reachable in standard commercial spectrometers and “in house” equipment. Peculiarities in the emission and excitation spectra of Eu^{3+} and/or Er^{3+} doped $NaLaF_4$ as well as the influence of oxygen impurities on luminescence properties and energy transfer processes in the materials in question will be demonstrated and discussed.

References

1. A. Sarakovskis et al., Opt. Mater., **31,** 1517 (2009)
2. V. Pankratov, M. Kirm, H. von Seggern, J. Lumin. **113,** 143 (2005)
3. J. C. Krupa, M. Queffelec, J. All. Comp. **250**, 287 (1997)
4. V. Pankratov et al., J. Appl. Phys. **110,** 053522 (2011)
5. V. Pankratov et al., Phys. Rev. B **83,** 045308 (2011)

F-121

Enhanced Up-Conversion Emission of Core-Shell Structured α-$NaYF_4:Yb^{3+}/Er^{3+}@SiO_2$

J.H. Oh[1], S.H. Park[1], J.H. Jeong[1,*], C.W. Oh[2]

[1]Department of Physics, Pukyong National University, Busan 608-737, Republic of Korea

[2]Department of Marine Biology, Pukyong National University, Busan 608-737, Republic of Korea

email: jhoh0713@nate.com

PL imaging plays an improtant role in biomedical research, being extremely useful for early detection, screening, and image-guided therapy of life-threatening diseases. Recently, lanthanide-doped UC materials have attracted much attention due to their applications such as biological labels, carrier. Among various kinds of host materials for lanthanide doped up-conversion emission, fluorides have many advantage such as low phonon energies and long life-times, which promote an efficient up-conversion [1-2].

In the study, core-shell structured $NaYF_4:Yb^{3+}/Er^{3+}@SiO_2$ was prepared via the Stöber sol-gel method by coating a layer of silica on the surface of $NaYF_4:Yb^{3+}/Er^{3+}$ particles derived from a solvothermal process.

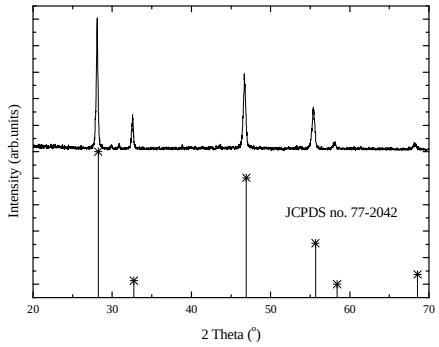

Fig.1 The XRD pattern of $NaYF_4:Yb^{3+}/Er^{3+}$ (black line), and standard pattern (JCPDS no. 77-0242).

References

1. Rumin Li, Hongfeng Ji, Zhanshuang Li, Jun Wang, Qi Liu and Lianhe Liu, New J. Chem. **38**, 611(2014)
2. Guanying Chen, Hailong Qiu, Paras N. Prasad and Xiaoyuan Chen, Chem. Rev. In Press

F-122

Luminescence of Terbium Activated $NaLaF_4$ in Oxyfluoride Ceramics

E. Elsts, G. Krieke, U. Rogulis, K. Smits, R. Ignatans, A. Sarakovskis

Institute of Solid State Physics, University of Latvia, Latvia

e-mail: eelsts@cfi.lu.lv

Sodium lanthanide fluorides ($NaLnF_4$) are prospective materials due to their luminescence properties, high refractive indexes and optical stability [1].

Glass samples with nominal composition $16Na_2O$-9NaF-$5LaF_3$-$7Al_2O_3$-$63SiO_2$ (mol%) doped with 3 mol% TbF_3 were prepared by melting the appropriate batch materials (Na_2CO_3, NaF, LaF_3, Al_2O_3, SiO_2, TbF_3). The batches of 10 g were melted in covered corundum crucibles at ambient atmosphere at 1500° C for 30 min. The melts were casted in stainless steel moulds. The glasses were subjected to different heat treatment: at 600° C, 700° C, 800° C for 30 min. The temperatures for this heat treatment were estimated from differential thermal analysis.

The properties of glass and glass-ceramics were investigated by X-ray diffraction and X-ray excited luminescence spectroscopy. We will analyze formation of $NaLaF_4$ as well as formation of other crystalline phases (LaOF and LaF_3) in the samples and its influence on the luminescence properties.

New technology will be developed in framework of the ESF project “Experimental and theoretical investigation of technologically important materials”.

Acknowledgements

E. Elsts thanks the ESF (project No. 2013/0046/1DP/1.1.1.2.0/13/APIA/VIAA/021) for financial support. A. Sarakovskis thanks VPP IMIS program for financial support.

References

1. Z. Wang, L.Wang, Z. Li, Materials Letters, 65, 3516 (2011)

F-123

The Radioluminescence and Cathotodoluminescence of TlCl:Bi Crystals

D. Millers[1], L. Grigorjeva[1], I.S. Lisitskij[2], M.S. Kouznetsov[2], K. Zaramenskikh[2]

[1]Institute of Solid State Physics, University of Latvia, Latvia

[2]State Scientific-Research and Design Institute of Rare-Metal Industry "Giredmet" JSC, Russia

e-mail: dmillers@latnet.lv

The Bi centers in crystals and glasses were studied due to interest for fast scintillators, NIR solid state lasers, including optical fiber amplifiers [1,2]. The photoluminescence (PL) of Bi^+ centers luminescence were early studied experimentally and theoretically [1], however the cathodoluminescence (CL) and radioluminescence (RL) are not studied in details. It will be noted that the energy and/or charge transfer is important for RL and CL since the electron and hole creation is main process during excitation, whereas in PL direct excitation of luminescence centers could take place.

TlCl:Bi single crystals of 22 mm diameter and 80–100 mm length were grown by the Bridgman–Stockbarger method as described in [1] varying the Bi concentration and Bi incorporation method ($BiCl_3$ or Bi in melt).

The RL was measured under steady state x-ray excitation (30 kV, 15 mA); registration system includes the monochromator SHAMROC303 coupled with CCD camera ANDOR iDUS DU401A-BV. The CL was excited by pulsed electron beam and detected by PMT through monohromator.

The results of CL and RL studies as well as the time-resolved CL studies of TlCl: Bi single crystals were presented. The broad luminescence band in spectral range 950-1200 nm (due to $^3P_1 \rightarrow {}^3P_0$ transitions of Bi^+ centers) was observed in RL spectrum and its intensity correlated with Bi concentration up to ~0.4 mol% $BiCl_3$. At higher doping concentration probably the Bi dimer centers probably was created. The luminescence intensity is lower for TlCl samples doped with Bi or Bi+$BiCl_3$ during sample growth.

References

1. V.G. Plotnichenko, V.O. Sokolov, D.V. Philippovski, I.S. Lisitsky, M.S. Kouznetsov, K.S. Zaramenskikh and E.M. Dianov, Optics letters. **38**, № 3, 362 (2013)
2. X.Meng, J.Qiu, M.Peng, D.Chen, Q.Zhao, X.Jiang, and C.Zhu, Opt.Express, **13**, Iss.5, 1628 (2005)

F-124

AlN Based Composite – White Light Emitter

B. Berzina[1], V. Korsaks[1], L. Trinkler[1], R. Kirsteins[1], M. Knite[2], and J. Grabis[3]

[1]Institute of Solid State Physics, University of Latvia, Latvia

[2]Institute of Technical Physics, Riga Technical University, Latvia

[3]Institute of Inorganic Chemistry, Riga Technical University, Latvia

e-mail: baiber@latnet.lv

At present after intensive withdrawal of incandescent lamps from usage the main lighting elements available for users are luminescent lamps (LL) and light emitting diodes (LEDs). Therefore, a development of advanced light sources and elaboration of new prospective luminescent materials is actual.

The aim of this study is elaboration of composite material based on mixture of pure and doped AlN nano-powders inserted into the polymethyl methacrylate (PMMA) matrix emitting white light under UV irradiation within a spectral range 250-280 nm including 254 nm line of Hg emission used in the LL.

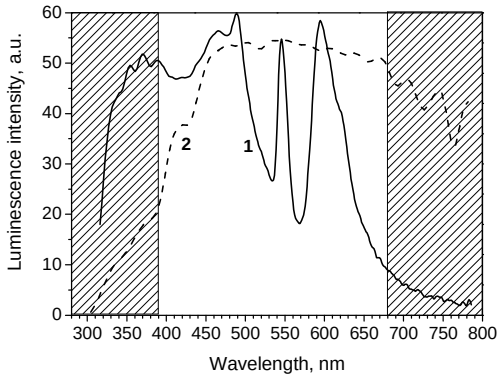

Fig.1. Luminescence spectrum under 263 nm UV excitation of AlN based composite material (1) and the Sun emission spectrum at sea level (2). The white square demonstrates a spectral region detectable for human eye.

AlN powders with average grain size of 60 nm produced from raw material and doped with Mn or Tb ions were used. Photoluminescence and excitation spectra of AlN, AlN:Mn, AlN:Tb nanopowders and PMMA material were studied. It was observed that under the 250 – 270 nm UV light excitation the AlN nanopowder emits blue light (480 nm), AlN:Mn – red light (600 nm), AlN:Tb – green light (550 nm), but the PMMA emits a blue light around 400 nm. It allows production of the white light emitter by mixing the nanopowders at definite concentrations of single components.

Luminescence spectrum of final resulting composite material is shown in Fig. 1. It is seen that within the spectral range detectable by human eye the composite material emits white light with spectrum being close to that of the Sun emission.

F-125

Photoluminescence Properties of Bi^{3+} Centers in Yttrium Oxide

K. Chernenko[1], L. Lipińska[2], T. Shalapska[1], A. Suchocki[3,4], S. Zazubovich[1], Y. Zhydachevskii [3,5]

[1]Institute of Physics, University of Tartu, Estonia

[2]Institute of Electronic Materials Technology, Poland

[3]Institute of Physics, Polish Academy of Science, Poland

[4]Institute of Physics, University of Bydgoszcz, Poland

[5]Lviv Polytechnic National University, Ukraine

e-mail: nuclearphys@yandex.ru

Luminescence properties of Bi^{3+} centers have been intensively studied in various materials (alkali halides, sulphates, phosphates, rare-earth aluminate and gallate garnets, oxyorthosilicates, perovskites, etc). Yttrium complex oxides, where luminescence arises from Bi^{3+} ions substituting for trivalent yttrium ions, have been considered as perspective materials for scintillators and luminescence screens due to a fast and intense Bi^{3+}-related emission.

In this work, the X-ray diffraction and luminescence properties of Bi^{3+}-doped yttrium oxide (Y_2O_3) powder are studied. Temperature evolution of the emission and excitation spectra of Y_2O_3:Bi as well as of the luminescence decay kinetics are measured at 4.2–400 K.

In yttrium oxide, the Bi^{3+} ion occupies two cation positions with different symmetry (S_6 and C_2). It causes the presence of two bands in the luminescence spectrum located at 3.03 eV and 2.35 eV, respectively. The 3.03 eV emission is excited at 3.33 eV and 4.95 eV, whereas the 2.35 eV emission has excitation bands at 3.6-3.8 eV, 4.74 eV and ~5.5 eV, arising from transitions to the triplet and singlet excited states of Bi^{3+} centers. Luminescence decay kinetics and temperature dependences of decay times and maxima positions of the emission bands are shown to be characteristic for the triplet emission of Bi^{3+} centers.

With the use of the phenomenological model of relaxed excited states, proposed before for the description of temperature evolution of luminescence spectra and decay kinetics, characteristic parameters of excited states structure are evaluated. The comparison of the obtained results with the luminescence characteristics of other Bi^{3+}-doped materials (see, e.g., [1] and references therein) is presented.

References

1. A. Krasnikov, L. Lipińska, E. Mihokova, M. Nikl, T. Shalapska, A. Suchocki, S. Zazubovich and Ya. Zhydachevskii, Optical Materials (2014), doi: 10.1016/j.optmat.2014.01.030.

F-126

Improved Optical Photoluminescence by Bi^{3+} Co-Doped in $CaMoO_4:Eu^{3+}$

E.O. Kim[1], J.H. Jeong[1*], J.H. Park[2], D.S. Shin[3], K. Jang[4], S.S. Yi[5]

[1]Department of Physics, Pukyong National University, Busan 608-737, Republic of Korea

[2]Department of Applied Mathematics, Pukyong National University, Busan 608-737, Republic of Korea

[3]Department of Chemistry, Changwon National University, Changwon 641-773, Republic of Korea

[4]Department of Physics, Changwon National University, Changwon 641-773, Republic of Korea

[5]Department of Electronic Material Engineering, Silla University, Busan 617-736, Republic of Korea

e-mail: zzangkeo@naver.com

Common commercial green phosphors are faced serious problems of stability and efficiency [1]. Therefore, new green phosphors of produce of improved stability and efficiency are needed urgently. The crystal structure of $CaMoO_4$ has good thermal stability and chemical stability, and it is also good host for luminescent metals under UV and X-ray excitation due to its luminescent center-MoO_4 tetrahedron unit. Using excitation through this, the emission intensity of rare-earth doped ions can be enhanced significantly because of energy transfer from Mo-O charge transfer to RE [2]. In order to improve the optical property, many efforts have been made. It has been discussed that different trivalent ion co-doped with Tb^{3+} in molybdate phosphors can improve the luminescence property.

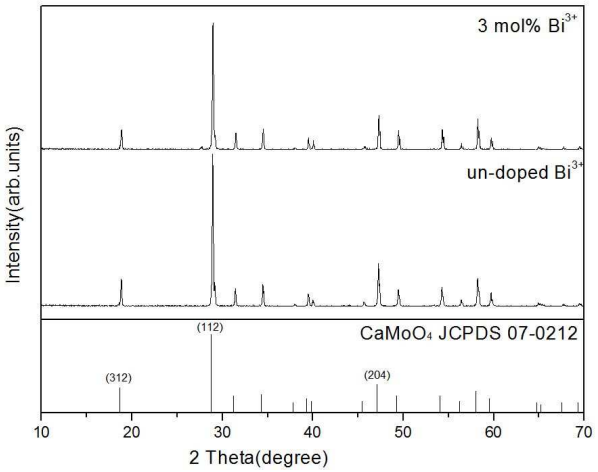

Fig.1 XRD pattern of $Ca_{0.88}MoO4$: $Tb_{0.05}{}^{3+}$, $Bi_{0.03}{}^{3+}$ phosphor.

In this study, Bi^{3+} and Tb^{3+} co-doped $CaMoO_4$ phosphor were synthesized by sol-gel method. X-ray diffraction (XRD), field emission scanning electron microscope (FE-SEM) and photoluminescence excitation and emission spectra were used to characterize the resulting samples.

References

1. Z. Xianju and Y. Xiaodong, J. Rare Earths. **31**, 655 (2013).
2. Z. J. Zhang and H. H. Chen, Mater. Sci. Eng. B. **145**, 34 (2007)

F-127

Luminescence of Complex Terbium Centres in $CaSO_4$

I. Kudryavtseva[1], A.Maaroos[1], S. Pazylbek[2], A. Tussupbekova[3]

[1]Institute of Physics, University of Tartu, Estonia

[2]L.N.Gumilyov Eurasian National University, Astana, Kazakhstan

[3]E.A. Buketov Karaganda State University,Karaganda, Kazakhstan

e-mail: irina@fi.tartu.ee

An interest to the luminescence of Tb^{3+} centres in $CaSO_4$:Tb is connected with the elaboration of efficient spectral transformation of VUV radiation into visible light with quantum yield QY > 1 (see, e.g. [1]). In the present study, the investigation of complex (four-component) luminescence terbium centres as well as the analysis of technological features of the synthesis of small-grained wide-gap $CaSO_4$:Tb^{3+} anhydrite phosphors containing 0.3–4% of Tb^{3+} and some amount of additional impurity ions and radicals (Na^+, K^+, Rb^+, NH_4^+, F^-, Cl^-, Br^-) have been continued (see also [1, 2] and references therein) using the methods of optical and thermoactivation spectroscopy. Highly pure $(NH_4)_2SO_4$ (99.999%) and $CaSO_4$ (99.993%) were used as starting materials for a successful synthesis, which was performed in an extra dry air atmosphere at an optimal temperature of 1023 K for the solid-state reactions route. Of particular interest was a contribution of calcium ions into formation of complex luminescence centres. Ca causes efficient dynamic hybridization of electronic states and influence on the formation of terbium and near-terbium electronic excitations (see also [2]).

The excitation spectra of Tb^{3+}-centre emission have been measured in the VUV spectral range at 77 or 300 K. The excitation band related to the lowest *f–d* transition of Tb^{3+} ions at ~5.9 eV in $CaSO_4$ undergoes broadening toward the long-wavelength side, when the radius of a charge compensator increases ($K^+ \rightarrow Rb^+$). The band at 8–9 eV ascribed to the excitation of oxyanions has a different shape in CaSO4:Tb,K and CaSO4:Tb,Rb. Thermally stimulated luminescence (77–700 K) have been analyzed for a set of anhydrite phosphors previously irradiated by VUV photons selectively forming different intrinsic electronic excitations or X-rays at 77 and 300 K.

Acknowledgment

We are grateful for the support from Estonian Research Council – Institutional Research Funding IUT02-26.

References

1. A.Lushchik, Ch.Lushchik, I.Kudryavtseva, A.Maaroos, V.Nagirnyi,F.Savikhin, Radiat. Meas. **56**, 139 (2013).
2. I.Kudryavtseva, M.Klopov, A.Lushchik, Ch.Lushchik, A.Maaroos, A.Pishtshev, Phys. Scr. **89**, 044013 (2014).

F-128

Thermally Stimulated Luminescence of KPO_3-NO_3^- Doped Tl^+ Ions

T. Koketai[1], B. Tagayeva[1], E. Mussenova[1], E. Turmukhambetova[2], A. Tussupbekova[1], G. Mussina[1]

[1]E.A.Buketov Karaganda State University, Kazakhstan

[2]Kazakh National Technical University after K.I.Satpayev, Kazakhstan

e-mail: katkargu@mail.ru

This article presents results of the study of the recombination luminescence of potassium metaphosphate doped by Tl^+ ions. To this the potassium nitrate addition to the initial solution in an amount of 0.1 mol%.

Fig. 1 shows the spectrum of the thermally stimulated luminescence (TSL) of potassium metaphosphate doped ions NO_3^-. We observed a new TSL peak at 175 K in the spectrum of KPO_3-NO_3^-. It confirms the incorporation of the nitrate anions into the lattice of the potassium metaphosphate salts.

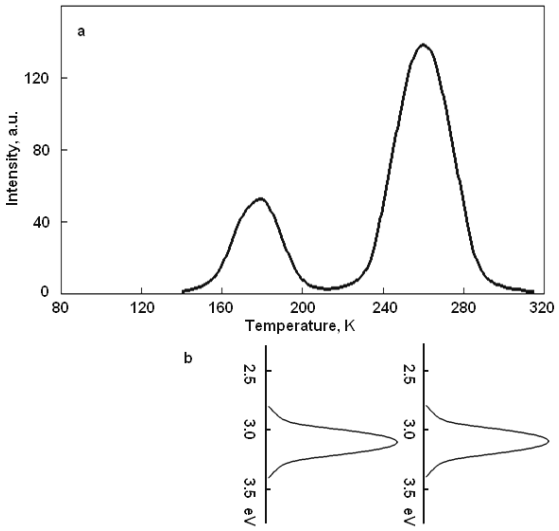

Fig.1 TSL curves of (a) KPO_3-NO_3^- at 80K (300 kGy) and (b) spectral composition of the TSL peaks.

TSL peak at 175 K may be associated with changes of the level of thermal stability of radiation defects, localized near the impurity Tl^+ ions. We observed that two peaks (at 175 K and at 260 K) have the same recombination luminescence. Hence, the peak at 260 K has an electronic mechanism of recombination.

References

1. A. Otani and S. Makishima, J. Phys. Soc. Jap. **26**, 85 – 87 (1969)

F-129

Thermostimulated Luminescence (TSL) and Temperature Studies of the $Lu_xY_{1-x}PO_4:Ce^{3+}$ Solid Solutions

V.S. Levushkina[1,2], D.A. Spassky[1,3], E.M. Aleksanyan[1,5], M.G. Brik[1], M.S. Tretyakova[4], B.I. Zadneprovski[4]

[1]University of Tartu, Institute of Physics, Tartu, Estonia

[2]Physics Faculty, Moscow State University, Moscow, Russia

[3]Skobeltsyn Institute of Nuclear Physics, Moscow State University, Moscow, Russia

[4]Central Research and Development Institute of Chemistry and Mechanics, Moscow, Russia

[5]A. Alikhanyan National Science Laboratory, Yerevan, Armenia

e-mail: viktoriia.levushkina@ut.ee

Phosphates doped with rare-earth ions are well known phosphors with a broad range of applications. The mixed crystals on the base of phosphates such as $Lu_xY_{1-x}PO_4:Ce^{3+}$ may demonstrate enhanced luminous characteristics (e.g. light output under high energy excitation) in comparison with the characteristics of their constituents, as it has been demonstrated for several solid solutions of complex oxides [1]. The physical origin of such enhancement is connected with the limitation of free mean path of the separated charge carriers at the thermalization stage of energy relaxation. Other effects (modification of the electronic structure as a result of the cation substitution, appearance of the additional electronic states within the host's band gap, shift of the electronic bands etc) strongly affect the emission centers efficiency as well. In order to reveal the influence of these effects on the emission efficiency we have performed the study of the TSL curves and temperature dependencies of steady emission in a set of the $Lu_xY_{1-x}PO_4:0.5\%Ce^{3+}$ solid solutions, synthesized by the sol-gel method. The TSL curves were analyzed; modification of the conduction band's bottom was determined from the experiments; the electronic structure of the considered compounds was calculated to facilitate the experimental data analysis.

References

1. A.V. Gektin, A.N. Belsky and A.N. Vasilev, IEEE Trans. Nucl. Sc.**61**, 262 (2014)

F-130

Hexagonal Boron Nitride Luminescence Intensity Dependent on Ambient Vacuum Level

V. Korsaks, B. Berzina

Institute of Solid State Physics, University of Latvia, 8 Kengaraga Str., LV-1063 Riga

e-mail: vkorsaks@cfi.lu.lv

Hexagonal boron nitride (a bulk material, nanotubes and single crystals) have been widely investigated experimentally and theoretically. The main interests are paid to exciton luminescence around 215 nm and phonon assisted defect luminescence around 318 nm. Our attention is paid to 400 nm photoluminescence (PL).

Dependence of PL integral intensity on vacuum level ambient the hBN powder with various particle sizes was studied. The materials were excited with 270 nm light from a deuterium lamp under continuous irradiation. Luminescence spectra are complex including the well observable phonon structured 400 nm band. The 400 nm luminescence excitation spectrum (PLE) shows two main bands at 265 nm and 340 nm.

It was found that the intensity of the 400 nm PL is sensitive to vacuum level ambient the hBN for all studied materials (Fig 1.). Experimental results (luminescence spectra when sample is situated in vacuum at different levels or oxygen gas together with the mass spectrometry measurements) were analysed. It allows conclusion that the observed 400 nm luminescence of hBN is sensitive to concentration of surrounding oxygen gas.

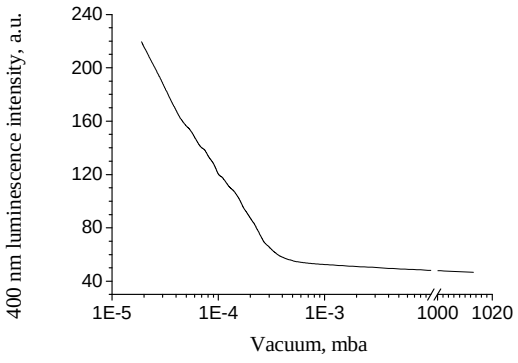

Fig. 1. 400 nm luminescence integral intensity dependent on vacuum level surrounding hBN

Acknowledgment

This study was supported by ESF project Nr 2013/0046/1DP/1.1.1.2.0/13/APIA/VIAA/021

F-131

The Study of the High-Pressure Phase of $TlInS_2$ Crystal

P.P. Guranich[1], R.R. Rosul[1], O.O. Gomonnai[1], A.G. Slivka[1], I.Yu. Roman[2], A.V. Gomonnai[2]

[1]Uzhhorod National University, Ukraine

[2]Institute of Electron Physics, Ukr. Nat. Acad. Sci, Ukraine

e-mail: pguranich@gmail.com

A considerable interest towards $TlInS_2$ type crystals is related to the fact that these materials with ferroelectric and semiconductor properties possess a quasi-two-dimensional structure where a series of structural phase transformations from paraelectric to incommensurate and ferroelectric phases occurs. Besides, $TlInS_2$ studies at elevated pressures [1-3] revealed that at pressures $p > 550$ MPa a transition to a high-pressure phase is observed. However, until now this transition and the high-pressure phase properties have not been sufficiently studied.

The studies of dielectric and optical properties of $TlInS_2$ single crystal were carried out in the temperature interval 150–400 K and in the hydrostatic pressure range up to 700 MPa. The presence of the structure of ferroelastic domains at high pressures enables us to claim that the high-pressure phase in the $TlInS_2$ crystal is a ferroelastic one. The transition to this phase with increasing pressure is achieved via a sequence of two first-order phase transitions with an intermediate phase. A number of features is revealed in the polycritical region in the range of pressures 550–650 MPa and temperatures 180–220 K. Thus, the (p, T) phase diagram of the $TlInS_2$ crystal is redetermined.

References

1. O.O. Gomonnai, P.P. Guranich, M.Y. Rigan, I.Y. Roman, A.G. Slivka, High Press. Research. **28**, 615 (2008)
2. W. Henkel, H.D. Hochheimer, C. Carlone, A. Werner, S. Ves, H.G.v. Schnering, Phys. Rev. B. **26**, 3211 (1982)
3. O.O. Gomonnai, R.R. Rosul, P.P. Guranich, A.G. Slivka, I.Yu. Roman, M.Yu. Rigan, High Pressure Research. **32**,39 (2012)

F-132

Novel Method for Feedstock Production for High Efficiency FZ c-Si PV

An. Kravtsov

SIA "KEPP EU", Latvia

e-mail: doc@keppeu.lv

Efficiency of solar cells manufactured from FZ wafers, thanks to their purity and structure perfection is significantly higher than if CZ or multicrystalline wafers are used. High cost of FZ silicon limits applicability of such wafers because of a) high deprecation costs, due to expensive FZ pullers, and b) high price of polycrystalline silicon rods – FZ feedstock. The aim of present work was a creation of rather price-efficient way of FZ feedstock production. It requires obtaining of crystal of cylindrical shape from raw material applicable for PV applications without further contamination during pulling.

We used electron beam monocrystals growing[1] and skull process[2] as a basis. Electron beam guns with cooled cathode were used. During pulling process two electron beam heaters were used. Each beam was moved less an 180 degrees arc with variable radius. Growth was conducted with use of seed, which was pulled upwards while rotating. Crucible with raw material stayed motionless.

Next, new generation of an experimental furnace was created. It consists of melting and pulling (crystal) chamber, flap gate valve in between, pulling mechanism and two electron beam guns, each equipped with its own power systems. The process is conducted under residual pressure not more than 0,05 mbar. Batchload is placed in a copper water cooled mold equipped with elements designed for thermal field management.

Using this equipment we have shown a possibility of manually growing crystals of diameter up to 240 mm and purification of heavily doped silicon in this kind of process. Thus, we successfully created basis for technologies of production of competitive FZ feedstock from recycled materials in arbitrary form like chunks, etc; and recycling of leftovers of FZ process.

References

1. B. Movchan and A. Zlotin, "Electron beam radial heater for furnaces for pulling monocrystals by Czochralsky method," Author’s certificate N159293, Class 40d 1/36 MPK C22F, Bulletin N24, 07.12.1963.
2. A.D. Zumbrunnen, "High Frequency Resistance Melting Furnace," US Patent 4133969, 09.01.1979.

F-133

New Feedstock for c-Si Photovoltaics

Al. Kravtsov[1], A. Shagun[2], An. Kravtsov[2]

[1]KEPP-service, Ltd, Russia

[2]SIA "KEPP EU", Latvia

e-mail: alexeykravtsov@gmail.com

Purpose of the work was to study applicability of new feedstock obtained by heavily doped electron-grade silicon rectification with electron beam for use in standard CZ and FZ processes in order to obtain PV-grade materials.

The rectification furnace consists of chamber with cooled base plate in it. Graphite crucible with quartz crucible inside are placed on the base plate. Electron beam gun is mounted on the top of the furnace to provide heating. Scheme is described in [1]. Basic principle of technology were described previously at [2].

Three different companies tested rectified material and pulled CZ monocrystals from it. Each company used its standard process of obtaining CZ monocrystals for semiconductor or photovoltaic application. One 8" and two 6" CZ full length monocrystals were obtained and demonstrated reasonable quality in terms of resistivity, lifetime; no defects were revealed by standard surface tests such as Sirtl and Secco baths.

For FZ tests two silicon rods were pulled from crucible during rectification process. Rods had volatile diameter in 100..130mm range and weight ca 15kg. Mechanical and following chemical treatment was used in order to bring rods to a constant diameter for further use in standard FZ process. Subsequently, two FZ monocrystals of 65 and 100 mm diameters were grown. Both crystals demonstrated very high lifetime and adequate for photovoltaic applications resistivity levels.

Electron beam rectification of heavily doped electronic grade material enables one to receive feedstock which can be used directly without blending for successful production of solar grade silicon by well-known methods such as CZ and FZ without any modifications. Said methods applied to given feedstock yield in dislocation free crystals with reasonable resistivity and lifetime levels.

References

1. Kravtsov A., "Method of vacuum refinement of silicon", Patent of Russia 2381990, 20.02.2010, bulletin N5
2. Kravtsov A., Kravtsov A., "Electron Beam Silicon Purification", 26th EU PVSEC 2011, pp. 1814-1816

F-134

Sequentially Deposited Perovskite Solar Cell Employing $CH_3NH_3PbI_{3-x}Cl_x$ Light Absorber

I. Kaulachs[1], A. Ivanova[1], G. Shlihta[1], J. Grabis[2], P. Shipkovs[1], M. Roze[3], K. Pudzhs[4], J. Kalnachs[1]

[1]Institute of Physical Energetics, Latvia

[2]RTU Institute of Inorganic Chemistry, Latvia

[3]Riga Technical University, Latvia

[4]Institute of Solid State Physics, University of Latvia, Latvia

e-mail: kaulacs@edi.lv

Recently it was shown by J.Burshka et.al. (doi:10.1038/nature12340) that by growing perovskite pigment directly in mesoporous metal oxide film by two step sequential deposition of perovskite building solutions it is possible to achieve 15% power conversion efficiency by using $CH_3NH_3PbI_3$ perovskite as light absorber; mesoporous TiO_2 as electron receiver and spiro-MeOTAD as hole conducting layer. In this work we will present solar cell where spiro-MeOTAD is replaced by more cost-efficient material – CuSCN.

So our cell is build in following way: 30-40 nm thick dense TiO_2 underlayer was built by aerosol spray pyrolysis on patterned FTO–coated glass substrate, then 400-500 nm thick mesoporous anatase layer was deposited by spin coating using commercial paste Dyesol 18NRT diluted in ethanol. After baking this layer at 500°C and cooling it, mesoporous TiO_2 layer was infiltrated by $PbCl_2$ solution in dimethylformamide and dried at 70°C. After cooling it to room temperature, the film was dipped in solution of CH_3NH_3I in 2-propanol for 20-30 sec, rinsed and dried at 70°C. As the hole transporter CuSCN was deposited by thermal deposition in vacuum. For top electrode Au was evaporated in a vacuum chamber at pressure ~ 10^{-6} mbar. All photoelectric measurement has been made in the same home made vacuum cryostat where electrode was deposited at p~10^{-6} mbar without breaking the vacuum and moving the cell.

The spectral dependences of short circuit photocurrent external quantum efficiency (EQE), fill factor (FF) and open circuit voltage (V_{OC}) has been investigated in spectral range 370-1100 nm, using synhro-detection technique and PC controlled data storage equipment.

F-135

Research on Controlled Porosity Composite Thin Layers and Systems for Energy Storage and Conversion Applications

J. Kleperis[1], I. Dimanta[2], G. Bajars[1], G. Dobele[3], A. Dindune[4], G. Vaivars[5]

[1]Institute of Solid State Physics, University of Latvia, Riga, Latvia

[2]Faculty of Biology, University of Latvia, Riga, Latvia

[3]Latvian Institute of Wood Chemistry, Riga, Latvia

[4]Institute of Inorganic Chemistry, Riga Technical University, Riga, Latvia

[5]Faculty of Chemistry, University of Latvia, Riga, Latvia

e-mail: kleperis@latnet.lv

The report will be given about the planned goals and objectives of just begun collaborative project that focuses on obtaining and investigating thin layers of composites from controlled porosity carbon and lithium insertion compounds for electrodes in lithium/hybrid batteries (LIB) and in microbial fuel cells (MBFC) for energy storage and conversion applications. Objectives of the project are associated with synthesis and investigation of separate materials to be used for composites to obtain electrodes for LIB and MBFC: carbonaceous materials from Latvian wood with controllable pore size, lithium insertion materials (LiFePO4, etc.), lithium solid electrolyte materials and ionic liquids with lithium salts; hydrogen insertion materials (hydride-forming metals, some transition metal oxides); selected microorganisms and substrates for hydrogen evolution and energy harvesting in fermentation process. Different methods will be used: structural, morphological, physical-chemical properties, porosity of synthesized materials and composites; investigation of their electrochemical and impedance characteristics in the form of bulk material; development of methodology to obtain a thin layers from elaborated composites, using DC and AC magnetron sputtering, pulsed laser deposition methods. Project work will include synthesis and research of new materials, as well as the selection and modification of microorganisms, as well usage of resources available in Latvia - wood, sludge from waste water tanks and organic waste from agricultural industry. The project will result in new knowledge about carbon materials with the necessary properties for electrodes to obtain all-solid-state and thin/thick film lithium ion batteries, hybrid batteries; lithium liquid solution electrolyte and hydrogen insertion electrodes for fermentation reactors.

Acknowledgment

All authors acknowledge Latvian Council of Science Cooperation Project COPOCO No 666/2014 for financial support.

F-136

Bacteria Produced Hydrogen Storage Possibilities in Metal Hydride Alloy

I. Dimanta[1,2], Z. Rutkovska[1,2], J. Kleperis[1], V. Nikolajeva[2] and I. Muiznieks[2]

[1]Institute of Solid State Physics, University of Latvia, Latvia

[2]Faculty of Biology, University of Latvia, Latvia

e-mail: ilze.dimanta@gmail.com

Biological production of hydrogen using bacteria is a perspective way for alternative energy production and it noticeably decreases the raw material cost. Bacteria produce hydrogen in liquid medium under anaerobic conditions and when thermodynamic equilibrium concentration is reached, hydrogen from the liquid phase moves to the gaseous phase [1-2]. From the gaseous phase hydrogen may be collected using a variety of gas separation methods. We have previously shown [3] that in a bacterial culture medium during the fermentation process oversaturated hydrogen solution forms and because of that it is necessary to collect hydrogen from the liquid phase. This can be done by using selective hydrogen-absorbing materials (such as metals to form hydrides) or selectively permeable membranes. Experiments were performed with powdered metals and alloys (Pd, LaNi5, AB5, AB2) forming hydrides to test for their facility to remove hydrogen from liquid phase in dark fermentation process. Differential thermogravimetric method was used to measure amount of adsorbed hydrogen in alloy – before and after the contact with microorganisms. The study aims to find an optimal method / materials for hydrogen release from the liquid phase and to build a bioreactor prototype for more efficient bacterial production of hydrogen gas extraction and usage.

Acknowledgment

All authors acknowledge Latvian Council of Science Cooperation Project No. 666/2014 for financial support and the European Social Fund for the scholarship to Ilze Dimanta.

References

1. Holladay, J.D., HU, J., King, D.L., Wang, Y. 2009. An overview of hydrogen production Technologies, Catalysis Today, 139, 244–260
2. I. Dimanta., A.Gruduls, V. Nikolajeva, J. Kleperis, I. Muiznieks Assessment of bio-hydrogen production from glycerol and glucose by fermentative bacteria. , Power Engineering 2013. ISSN 0235-7208
3. I Klepere, I Muiznieks, J Kleperis. Latvian J. Physics and Technical Sciences 2 (2010) 60-68.

F-137

Structural Studies of Graphite-Containing Divertor Materials by Raman Spectroscopy and by Quantum Chemical Calculations

I. Rundāne[1], Ģ. Barinovs[1], G. Ķizāne[1], L. Avotiņa[1]

[1]Institute of Chemical Physics, University of Latvia, Latvia

e-mail: ineta.rundane@lu.lv

Carbon-containing, especially graphite-containing, materials has been used in the fusion devices as divertor materials because of the low Z and good thermal conductivity. However there are some disadvantages - fusion fuel components tritium and deuterium, accumulate in materials and decrease the efficiency of the reaction. The accumulation of the fuel in the graphite crystal can be promoted by defects being in initial material structure and created by neutron irradiation taking place during fusion reaction. To investigate the nano-scale structure of carbon-based materials a theoretical model could allowing to estimate what kinds of defects have been formed in the materials used in the plasma chamber has to be developed.

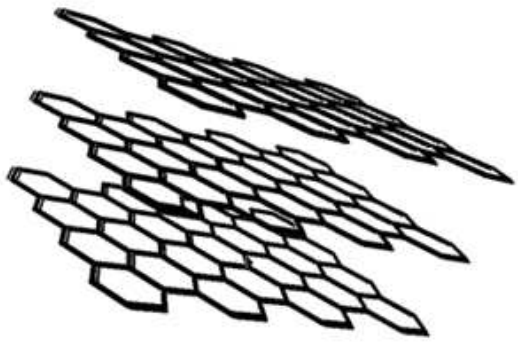

Fig. 1. Ideal graphite plates configuration with Gamess US software

The aim of this research is to create a model allowing comparing the structure of damaged graphite structures to a pe rfect one. For the comparison the difference between theoretical Raman spectrum and experimental results of Raman spectroscopy and are analyzed. The Gamess US program enables to model ideal graphite with plates are in ABAB configuration. In the Raman spectrum of ideal graphite only one maximum at 1582cm^{-1} is observable [1]. Therefore it will be possible to estimate the disorder of graphite-like structures. By developing the theoretical model it could be possible even to detect the types of defects in the graphite containing materials which are used in the plasma chamber. The obtained results will point to bond transitions as well as to the formation of disordered structures on the surface and bulk of the material. From the obtained results it will be possible to propose the possible ways of the transport of fuel of fusion reaction in the substance.

References

1. S.Reich and C.Thomsen, *Phil. Trans. R. Soc. Lond. A Nov 15, 2004, 362, 1824 2271-2288*

F-138

Floor Tile Tritium Accumulation at Various JET Fusion Device Divertor Configurations

M. Halitovs[1], G. Kizane[1], L. Avotina[1], J. Likonen[2], N. Bekris[3], C. Stan-Sion[4] and JET-EFDA contributors[5]*

[1]Institute of Chemical Physics, University of Latvia, Latvia

[2]VTT Technical Research Centre of Finland, Finland

[3]Karlsruhe Institute of Technology, Germany

[4]H. Hulubei National Institute of Physics and Nuclear Engineering, Romania

[5]JET-EFDA, Culham Science Centre, Abingdon, OX14 3DB, UK

e-mail: mihails.halitovs@lu.lv

Post mortem analyses of JET divertor tiles have shown that fuel retention is particularly important in co-deposits found on divertor tiles, especially in the inner divertor (Tiles 1 and 3) and on the divertor floor (Tile 4 and Tile 6) [1, 2]. In this work we present the measurement of the tritium in divertor tiles used for various divertor configurations at JET

Carbon fibre composite (CFC) samples from three divertor configuration divertors – Tile 4 of MkII-SRP (2001-2004), Tiles 4 and 6 of MkII-HD (2007-2009) and Tile 6 of MkII-HD ILW (2010-2012) – were analysed (see Fig. 1). Samples of MkII-SRP and MkII-HD type divertor tiles had no additional coating, while MkII-HD ILW divertor type tile had ~ 25 μm tungsten coating with ~ 3 μm molybdenum interlayer [3].

Examined samples of Tile 4 (MkII-SRP divertor, no coating) have tritium surface activity from $1.2 \cdot 10^6$ $Bq \cdot g^{-1}$ on the plasma exposed surface (closer to central dome) to $1.6 \cdot 10^8$ $Bq \cdot g^{-1}$ on "shadowed side" (closer to inner louvre). Bulk activity is at a level of $1 \cdot 10^4$ $Bq \cdot g^{-1}$ for the whole tile. Samples of Tile 4 (MkII-HD divertor, no coating) have rather constant tritium surface activity of $(0.7 \div 6.7) \cdot 10^6$ $Bq \cdot g^{-1}$ and bulk activity at $(2 \div 4) \cdot 10^3$ $Bq \cdot g^{-1}$ for the whole tile. Tile 6 (MkII-HD divertor, no coating) samples have tritium surface activity from $4.6 \cdot 10^4$ $Bq \cdot g^{-1}$ to $1.5 \cdot 10^6$ $Bq \cdot g^{-1}$ at varying surface positions while bulk tritium activity is at $2 \cdot 10^3$ $Bq \cdot g^{-1}$. Samples of Tile 6 (MkII-HD ILW divertor, W coating) show clear decrease in tritium surface activity and have at an average only $4.6 \cdot 10^4$ $Bq \cdot g^{-1}$. Bulk activity has mostly remained the same at a level of $4 \cdot 10^3$ $Bq \cdot g^{-1}$.

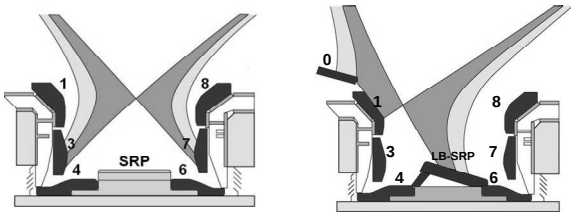

MkII-SRP (*Septum Replacement Plate*) (2001– 2004)

MkII-HD, MkII-HD ILW *(High Delta)* (2007– 2012)

Fig. 1. Schemes of JET divertor configurations

The divertor layout and plasma geometry has gradually changed and plasma x-point was shifted closer to divertor inner wall, plasma surface interaction of base tiles has been significantly transformed. Comparing surface activity of samples from Tile 4 in campaigns of 2001-2004 and 2007-2009, since then surface tritium activity has become more homogeneous and by a factor of 100 smaller for $Bq \cdot g^{-1}$ activity. As can be seen in [4], amount of deuterium (corresponding to amounts of tritium) trapped in different areas of JET MkII-HD divertor in 2007-2009 of base tiles contains by a factor of 10 to 55 more deuterium than any other divertor tile. The same can be referred to amounts of tritium. As can be seen in the results of Tile 6 samples, the average surface activity has remained roughly the same after divertor upgrade. This is both due to geometric screening by other tiles and less plasma interaction on the surface and fusion fuel diffusion from the erosion material layer [5] on the surface of divertor tiles.

References:

* See the Appendix of *F. Romanelli et al., Proceedings of 24th IAEA Fusion Energy Conference 2012, San Diego, USA*
1. E. Pajuste et al. / Journal of Nuclear Materials 415 (2011) S765–S768
2. J. Likonen et al. / Journal of Nuclear Materials 390–391 (2009) 631–634
3. C. Ruset et al. / Fusion Engineering and Design 86 (2011) 1677–1680
4. S. Koivuranta et al. / Journal of Nuclear Materials 438 (2013) S735–S737
5. A. Widdowson et al. / Journal of Nuclear Materials 438 (2013) S827–S832

F-139

Thermal Treatment of JET Carbon Dust Mixtures Containing Long-Chain Hhydrocarbons

L. Avotina[1], G. Kizane[1], M. Halitovs[1], E.Pajuste[1], J. Lapins[1], S. Romanelli[2], EFDA-JET contributors[3]

[1]Institute of Chemical Physics, University of Latvia, Latvia

[2]EURATOM / CCFE Fusion Association, Culham Science Centre, Abingdon, Oxon, OX14 3DB, UK

[3]JET-EFDA, Culham Science Centre, Abingdon, OX14 3DB, UK

e-mail: liga.avotina@lu.lv

Carbon fibre composites (CFC) have been used in the Joint European Torus (JET) until 2009 as plasma facing material. Plasma erosion of wall materials, transport and re-deposition cause the formation of co-deposits which can subsequently give rise to the formation of flakes and dust that might contain fullerenes and long-chain hydrocarbons.

The aim of research was to analyse and compare the oxidation and sublimation processes of mixtures with different composition (≤5 wt.% of additions), in order to analyse dust and flakes from JET. Artificially made mixtures containing dust material from plasma non-exposed JET CFC tile, hexacontane ($C_{60}H_{122}$), pentaconatane ($C_{50}H_{102}$) and fullerene C_{60}, were analysed by both, spectroscopic and thermal methods. Samples were heated in air and inert atmosphere.

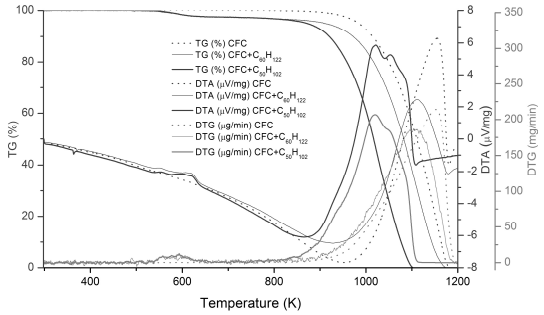

Fig.1. TG/DTA curves of CFC (dotted line) and mixtures with $C_{60}H_{122}$ (thin solid line), $C_{50}H_{102}$ (thick solid line) addition

Analysis of changes was done for melting temperatures and enthalpies of separate and mixed materials. It was obtained, that it is possible to detect the presence of the added long-chain hydrocarbons by appearance of melting effects in DTA curves and decrease of decomposition temperature of mixture. The results will be used as references for analysis of dust and flakes collected from vacuum vessel of JET tokamak.

* See the Appendix of F. Romanelli et al., Proceedings of the 24th IAEA Fusion Energy Conference 2012, San Diego, US

F-140

Structure and Photocatalytic Properties of TiO_2-WO_3 Composites Prepared by Electrophoretic Deposition

I. Liepina[1], G. Bajars[1], M. Rublans[2], A. Lusis[1], E. Pentjuss[1]

[1]Institute of Solid State Physics, University of Latvia, Latvia

[2]Faculty of Physics and Mathematics, University of Latvia, Latvia

e-mail: liepina.ineta@gmail.com

Due to its photocatalytic capability, low cost and chemically inert properties, TiO_2 is a promising material for water and air contamination treatment technologies. In this work bi-component WO_3 is used as a photo-electron storing material, since the electrophoretic deposition was carried out on steel substrates that might suffer from corrosion [1, 2].

TiO_2-WO_3 coatings were prepared by electrophoretic deposition (EPD) on 3x3 cm steel substrates (316 mark) using working electric field ranges from 50 to 100 V/cm. Dispersion medium was prepared from either HCl or charging additive (benzoic acid) solution in isopropanol. After the metal oxides were added, the dispersion was ultrasonificated for 30 min. Deposition was carried out for 5 to 20 min.

Among other traditional deposition methods (physical vapour deposition, electrochemical vapour deposition, plasma technologies etc.), EPD doesn't require vacuum environment and has the advantages of obtaining coatings with homogenous surface [1]. As-deposited films were heated in 60 ^oC for 2 h and then annealed at 500 ^oC for 2 h. The phases and crystalline sizes of obtained TiO_2 thin films were determinate by X-ray diffraction. X-ray fluorescence was used to establish WO_3 content in thin films. Surface morphologies were analysed by scanning electron microscopy. Photoacatalytic properties of obtained coatings were assessed in dependence on TiO_2/ WO_3 content ratio.

Acknowledgments

The present work has been supported by National Research Program IMIS.

References

1. J. H. Park, J. S. Kim and J. M. Park, Surf. Coating Tech. **236**, 172 (2013)
2. J. Georgieva, E. Valova, S. Armyanov, N. Philippides, I. Poulios and S. Sotiropoulos, J. Hazard. Mater. **211- 212**, 30 (2012)

F-141

Yttrium Doped Hematite Nanograin Thin Films as Anode Material for Solar Water Splitting

M. Vanags[1], A. Šutka[2], P. Onufrijevs[2], J. Kleperis[1]

[1]Institute of Solid State Physics, University of Latvia, Riga, Latvia

[2]Institute of Silicate Materials, Riga Technical University, Riga, Latvia

e-mail: sf11053@gmail.com

From all transition metal oxides the hematite (α-Fe_2O_3) has band gap at 2.0 eV, absorbing light in the visible spectra region where solar radiation spectrum is maximal. Doping of hematite is necessary, to increase the number of charge carriers, and rare-earth metals particularly interesting due their chemical stability and high number of valence electrons. Yttrium iron garnet $Y_3Fe_5O_{12}$ has been widely as material for microwave filters and magneto-optical devices, less as photo-electrode. Photo-electrochemical cell based on semiconductor electrode anode is converting light energy directly to chemical energy, for example, splitting water into H_2 and O_2. Anode material must posses the semiconductor properties, only than the light can excite electrons from valence to conduction band, leaving holes in valence band. Interface electrode/electrolyte typically has flat-band potential region where separation between excited electrons and holes occurs, giving them chance to participate in ox-red reactions - electrons are participating in reduction reaction, while holes – in oxidation reaction. Spray pyrolysis method is used to prepare Y-doped $Fe_{2-x}Y_xO_3$ (x = 0, 0.05, 0.10, 0.2, 0.3) thin films (thickness 300-400 nm) on glass and ITO covered glass slides. Raman spectroscopy, scanning electron microscopy, UV-visible absorption and photo-electrochemical measurements where used to characterize Y-doped α-Fe_2O_3 thin films. From all samples the photo-current shows highest value for $Fe_{1.9}Y_{0.1}O_3$ and decreases for lower and higher concentrations of yttrium. Mott-Schottky plot indicates more negative flat-band potential value for $Fe_{1.9}Y_{0.1}O_3$ comparing other compounds; therefore charge transfer between semiconductor electrode and electrolyte occurs more easily, only calculated concentration of charge carriers is lower particularly for this compound.

Acknowledgments

Authors gratefully acknowledge the financial support from European Social Fund project “Elaboration of Innovative Functional Materials and Nanomaterials for Application in Environment Control Technologies” No 1DP/1.1.1.2.0/13/APIA/VIAA/30.

F-142

Possibility of the Doping of Electrochemical Systems with Deuterium

A. Zvyagintseva

Voronezh State Technical University, Faculty of Physics and Engineering, Voronezh, Russia

e-mail: zvygincevaav@mail.ru

The aim of this work is to study the possible application of electrochemical systems (ES) for hydrogen accumulation. The hydrogenation of ES differs from hydrogen reaction with metallurgical metals. First of all, the evolution of hydrogen gas on the cathode is accompanied with the formation of metal atoms, according to equations: $Me^{n+} + ne \rightarrow Me^0$ (1); $H^+ + e \rightarrow H^0$ (2); $H^0 + H^0 \rightarrow H_2$ (3). Secondly, the formation of H atoms (2) favors the reaction of hydrogen with metals. Lastly, the formation of structural defects with potentials higher than those of atoms becomes possible during the electrocrystallization of metals. Once the defects exist the H atoms can be trapped in them, and the hydrogenation proceeds most readily. Therefore, the investigations were performed in two directions: 1. preparation of metals and alloys with defect structure; and 2. doping of the defect metal matrix with H or D (to take away the influence of background hydrogen in the experiments). For example, an optimal defect structure in Ni has been obtained by doping the metal with boron atoms, and the hydrogenation behavior of the system Ni-B-H has been studied successfully [1] with the use of structural and electrochemical kinetic measurements.

Another interesting system for doping with H(D), namely Ni–In, has been first investigated in [2]. The composites were prepared by the electrolytic codeposition and ion implantation techniques, and the kinetics of deuterium desorption from the doped materials has been studied by thermodesorption mass spectrometry (TDMS) depending on the Ni/In ratio and the dose of implanted D (D_i). A highest value of the content of D in the composite (D/M = 2) can be attained for composites $Ni_{70}In_{30}$ by the doping at T~100 K. The shape of TDMS spectrum strongly depends on D_i: at low values of D_i it exhibits a single peak at ~530 K attributed to the solid solution of D in $Ni_{70}In_{30}$ being decomposed. At $D_i > 3\times10^{17}$ ions/cm^2 a second TDMS peak occurs initially at ~420 K, and as D_i further increases it shifts toward lower temperatures, seemingly due to the formation of the deuteride phase in $Ni_{70}In_{30}$ starting to decompose at room temperature with a peak on the temperature-decomposition profile at ~350 K.

References

1. N.M.Vlasov, A.V.Zvyginceva. Mathematical Modeling of the Hydrogen Permeability of Metals. Monograph. Voronezh State University, 2012 (in Russian).
2. A.V.Zvyginceva, O.M. Morozov, V.I. Zhurba, V.O. Progolaieva. Proc. Int. Conference Nanomaterials: Applications and Properties. **2(1)**, 01NTF37(3pp) (2013).

F-143

Effects of Concentration Ti, Zr, V, Fe on Deuterium Desorption Temperature Range from Mg-based Composite

O.M. Morozov, I.M. Neklyudov, V.I. Zhurba, V.O. Progolaieva, A.S. Kuprin, N.S. Lomino, V.D. Ovcharenko

National Science Center "Kharkov Institute of Physics and Technology", Ukraine

e-mail: morozov@kipt.kharkov.ua

One of ways of reception of materials in nanocrystalline state is introduction of chemical elements which have low solubility or do not co-interaction at all with components. According to the phase state diagrams of systems Mg-Ti, Mg-V, Mg-Zr and Mg-Fe of interaction of these components do not exist.

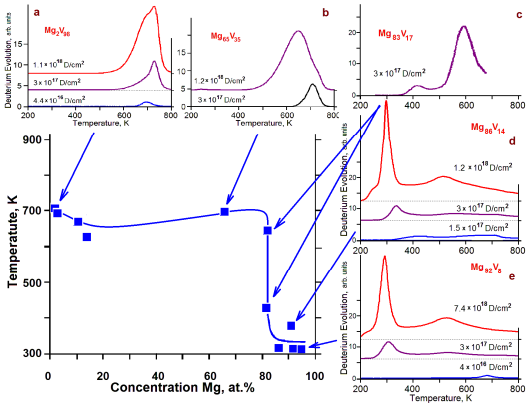

Fig.1 Deuterium desorption temperature versus the Mg-V composition (■) for a deuterium dose of ~3×10^{17} D/cm^2 (T_{irr}.~100 K) and thermodesorption spectra of deuterium from composites: (a) $Mg_{02}V_{98}$; (b) $Mg_{65}V_{35}$; (c) $Mg_{83}V_{17}$; (d) $Mg_{86}V_{14}$; (e) $Mg_{92}V_{08}$

To manufacture Mg-based composites the plasma evaporation-sputtering method was used enabling the atom-by-atom component growth. Thus, the composites with a wide range of the ratios of insoluble components were obtained [1]. Deuterium introduction into the samples was performed by the ion implantation method. The deuterium desorption temperature ranges and the deuterium storage levels were determined by the thermo-desorption spectroscopy.

It has been established that the introduction of V impurity to magnesium leads to the significant decrease of the deuterium desorption temperature (-350 K) as compared to the release from Mg samples (fig. 1).

A step-like form of the curve of the deuterium desorption temperature testifies to presence of two various structural conditions at composites Mg-V, Mg-Zr, Mg-Ti and Mg-Fe depending on the relation of components. The hydrogen desorption data obtained using Mg-based composites can be used for the further investigations into the hydrogen storage materials containing chemical elements with a low solubility in the alloy components.

References

1. I.M. Neklyudov, O.M. Morozov, V.G. Kulish, V.I. Zhurba, N.S. Lomino, V.D. Ovcharenko, O.S. Kuprin. IOP Conf. Ser.: Mater. Sci. Eng. 23 (2011) 012028.

F-144

Synthesis of $Mg(BH_4)_2$–TMO (TMO=TiO_2; ZrO_2; Nb_2O_5; MoO_3) Composites and Their Hydrogen Desorption

I. Saldan[1,2], I. Llamas-Jansa[1], S. Hino[1,3], C. Frommen[1], and B.C. Hauback[1]

[1]Physics Department, Institute for Energy Technology, Box 40, 2027 Kjeller, Norway

[2]Department of Physical and Colloid Chemistry, Ivan Franko National University of Lviv, 6 Kyryla and Mefodiya St., 79005, Lviv, Ukraine

[3]Graduate School of Engineering, Hokkaido University, N-13, W-8, Sapporo, 060-8278, Japan

e-mail: ivan_saldan@yahoo.com

Magnesium borohydride is one of the most promising hydrogen storage materials though its kinetics and reversibility are still main challenges. The decomposition of $Mg(BH_4)_2$ occurs via several stages [1]. The most stable intermediate is magnesium dodecaborane, $MgB_{12}H_{12}$, which eventually transforms into MgB_2. The geometrical similarity of the boron icosahedral frame-work in $MgB_{12}H_{12}$ and that of bulk boron can be a reason for the kinetic stability of the dodecaborane [2], which in turn may hamper rehydrogenation. The synthesis of $Mg(BH_4)_2$ from lower polyboranes might be possible at reasonable hydrogen pressure and temperature [3]. An additive that prevents the dodecaborane formation may be one of the possibilities to improve the reversibility of $Mg(BH_4)_2$ dehydrogenation. Therefore development of the effective additive for the improved decomposition/formation of $Mg(BH_4)_2$ is one of the most important problems to solve before its practical application. High valence transition metal (TM) compounds with carbon, nitrogen, oxygen or halogenide ligands have the ability to form bonds to hydrogen with varying stoichiometries. This encourages the fast dissociation into atomic hydrogen or its recombination to hydrogen molecules [4].

In the present paper TM oxides are studied as the additive to improve hydrogen desorption in the prepared $Mg(BH_4)_2$–TMO (TMO=TiO_2; ZrO_2; Nb_2O_5; MoO_3) composites.

References

1. K. Chłopek, C. Frommen, A. Leon, O. Zabara, M. Fichtner, J. Mater. Chem . **17**, 1396 (2007)
2. H. W. Li, K. Miwa, N. Ohba, T. Fujita, T. Sato, Y. Yan, S. Towata, M. W. Chen, S. Orimo, Nanotech. **20**, 204013 (2009)
3. M. Chong , A. Karkamkar, T. Autrey, S. Orimo, S. Jalisatgi, C. M. Jensen, Chem. Comm. **47**, 1330 (2011)
4. G. Barkhordarian, T. Klassen, R. Borman, J. Phys. Chem. C **110**, 11020 (2006)

F-145

Electrophoretic Graphene Film Electrode for Lithium Ion Battery

K. Kaprans[1], G. Bajars[1], A. Dorondo[2], J.Mateuss[3], G. Kucinskis[1], J. Gabrusenoks[1], J. Kleperis[1], A. Lusis[1]

[1]Institute of Solid State Physics, University of Latvia, Latvia

[2]Faculty of Chemistry, University of Latvia, Latvia

[3]Faculty of Physics and Mathematics, University of Latvia, Latvia

e-mail: k.kaprans@gmail.com

Recent advances in the technology of microelectronics demand micro power sources. Thin film technology offer an option of miniaturizing power sources. Most of the thin film electrode materials used in current batteries are deposited by RF or/and DC magnetron sputtering. Other methods include a variety of physical and chemical vapor deposition processes, such as aerosol spray coating and pulsed laser deposition. However above mentioned methods demand high material or energy consumption or they are relatively slow processes and require expensive equipment.

This work addresses the feasibility of an electrophoretic deposition (EPD) method for the preparation of graphene film electrode for lithium ion batteries. EPD technique has many advantages such as low deposition temperature, low consumption of energy as well as low cost and simplicity of equipment. Graphene is a new class of two dimensional carbon nanostructure owing exceptional high electric and thermal conductivity and mechanical stiffness. New electrode is made from sheets of graphene which is capable of accommodating more lithium ions and therefore delivers higher energy density than traditional carbon or graphite materials.

Graphene oxide nanosheet film was electrophoretically deposited on steel substrate from a stable ethanol suspension using potenciostatic mode with the electric field 150 V/cm. The deposition time was varied in order to obtain films with different thickness. Graphene oxide thermal reduction was performed by heating at 700 ºC in argon/hydrogen flow. Obtained graphene layers were analyzed by scanning electron microscopy, X-ray diffraction and Raman spectroscopy. These methods confirm the formation of homogeneous graphene sheet films. The application of these films as an electrode for lithium ion batteries was tested by various electrochemical methods.

Acknowledgment

The financial support of Latvian project of scientific cooperation 666/2014 is greatly acknowledged.

F-146

Deposition and In-Depth Electrochemical Analysis of $LiFePO_4$ Thin Films

G. Kucinskis[1], K. Bikova[1], G. Bajars[1], A. Orliukas[2], K.Z. Fung[3], J. Kleperis[1]

[1]Institute of Solid State Physics, University of Latvia, Latvia

[2]Faculty of Physics, Vilnius University, Lithuania

[3]Department of Material Science and Engineering, National Cheng Kung University, Taiwan

e-mail: gints.kucinskis@cfi.lu.lv

Since its first mention in 1997 [1], $LiFePO_4$ has been one of the most intensively studied lithium ion battery cathode materials. Nevertheless, the material itself is not fully understood [2]. In a standard bulk $LiFePO_4$ electrode preparation a binder and, due to inherently low electronic conductivity, also electronically conductive additive is used. The use of additives can be avoided in thin films because of significantly increased surface/mass ratio and better adhesion to the substrate.

$LiFePO_4$ thin films were deposited by RF magnetron sputtering, followed by high-temperature annealing step. Thin films were then characterized by scanning electron microscopy and x-ray diffraction. Various electrochemical measurements were carried out, including extremely slow nA-rate chronopotentiometry. The fit of Butler-Volmer equation to the results at high rate charge/discharge was very good. However, the Butler-Volmer equation describing electrochemical kinetics did not fit the low-rate experimental results. Possible explanations for such behavior were analyzed, including parasitic electrochemical side-reactions and thermodynamic aspects, such as the multi-particle charge-discharge model described by Dreyer and Gaberscek [3].

Acknowlwdgment

Authors acknowledge Taiwan – Latvia – Lithuania cooperation project “Materials and processing development for advanced lithium ion batteries” and Latvian Council of Science (project 666/2014). Gints Kucinskis acknowledges ESF project “Support for Ph.D. studies”.

References

1. A. Padhi, K. Nanjundaswarny, J. Goodenough, J. Electrochem. Soc. **144**, 1188 (1997)
2. R. Malik, A. Abdellahi, G. Ceder, J. Electrochem. Soc. **160**, A3179 (2013)
3. W. Dreyer, J. Jamnik, C. Guhlke, R. Huth, J. Moskon, M. Gaberscek, Nat. Mater. **9**, 448 (2010)

F-147

Investigation of Electrochemical Noise in the Cells with Advanced Superionic

A. Ukshe, A. Chub, E. Astafiev, Y. Dobrovolsky

Institute of Problems of Chemical Physics, Russian Academy of science, Russia

e-mail: ukshe@mail.ru

For electrochemical devices there is a problem of analysis of a degrading changes as the thermodynamic and chemical stability of the structure of advanced materials, especially those using the nanotechnology. This problem exists at the level of a single element (electrode) and at the level of the entire device.

One way to study changes in the structure of the material may be an analysis of self noise generated by the electrochemical system. Accordingly, the object of the work was to determine the possibility of measuring the noise of electrochemical cells with advanced materials and the possibility of obtaining information on the basis of the analysis of this noise.

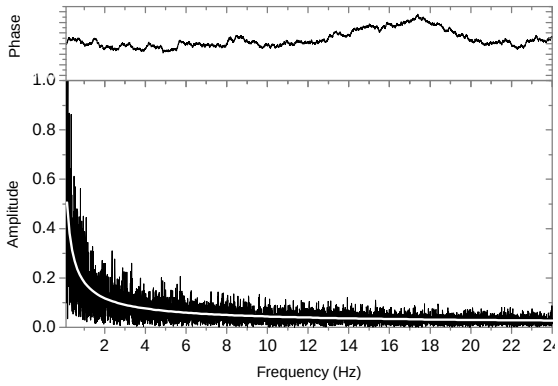

Fig.1 Range of electrochemical noise model cell with platinum electrodes and solid Superprotoh conductor (phosphotungstic getero(poly)acid).

For noise analysis, we used two approaches: measurement of the spectral characteristics of electrochemical noise (Fig. 1) that allows to determine the integral characteristics of the electrode [1-2], and the analysis of correlation functions low-frequency flicker noise, allowing you to analyze the processes of degradation [3]. Noise characteristics of the solid-state electrochemical cell with a proton conductor, and self noise of platinized platinum electrodes in a liquid electrolyte were measured and evaluated using both methods.

Acknovledgment

The work was supported by the Ministry of Education and Science of the Russian Federation (agreement #14.604.21.0087)

References

1. B. M. Grafov, L. S. Kanevskii, M. G. Astafiev, J. Appl. Electrochem. **35**, 1271 (2006.)
2. M. G. Astaf`ev, L. C. Kanevskii, B. M. Grafov, Russ. J. Electrochem. **43**, 17-24 (2007)
3. S. F. Timashev, Fluctuation and Noise Letters. **7**, R15-R47 (2007)

F-148

Experiment and Quantum Chemical Calculations in Studying the H Sorption Behavior of Nanostructured Composites and Light Metal Clusters

P. Fursikov[1], O. Charkin[1], B. Tarasov[1]

[1]Institute of Problems of Chemical Physics RAS, Chernogolovka, Russia

e-mail: fpv@icp.ac.ru

This study is aimed at establishing a correlation between experimental results on the reaction of hydrogen with nanostructured alloys and compounds based on light metals (LM), namely, Mg, Al, Ti, and the results of precise quantum chemical calculations (QCC), the subject of which are clusters of LMs, including those doped with atoms of transition metals (TM). It is suggested that such a combine approach enables an optimizing search of novel materials based on LMs with improved H storage performances.

The experimental studies involved the measurements of hydrogen sorption and desorption by modified (by intensive plastic deformation) eutectic alloys of Mg with La, Mm and Ni using *in-situ* high temperature X-ray diffractometry, programmed thermodesorption, metallography, etc. It was shown how the modified microstructure, phase composition, catalytic additives, and crystallite sizes of the materials substantially improve their hydrogen sorption and desorption performances. Metal hydride composites based on the ternary eutectic Mg-Mm-Ni alloys with nano-carbon additives were modeled using an Avrami-Erofeev approach. The additives were shown to alter the mechanism of H release from the MgH_2 phase in the composites at $T \leq 300$°C.

Precise QCC were employed to study the hydrides of light metals and elementary hydrogenation reactions. The Møller-Plesset perturbation theory was used to calculate structure and properties of low-lying isomers of the elementary and hydrided forms of doped aluminides with icosahedral [Al_{12}] cage and endohedral *closo*-alanes with the light cations inside *closo*-alane and related dianions $Al_{12}X_{12}^{2-}$ were predicted to be stable. The potential energy surfaces (PES) of the elementary catalytic cycle of early stages of the $H_2 + MAl_{12}$ reaction of dissociative addition of H_2 to Al clusters MAl_{12} doped with Sc, Y, Ti, Zr, V, and Nb in the states of different multiplicity have been calculated by DFT method. The effect of the dopant nature and the electronic state multiplicity of the cluster on the energies and activation barriers of hydrogenation reactions of Al clusters were considered. The calculated PES corresponding to the early stages of the $H_2 + TiAl_{12}$ show no significant preference of Ti dopant as compared with other TMs like Zr or V.

Acknowledgment

The work is supported by RFBR (grants № 13-08-00642 and 14-03-01060).

F-149

Studies of Hydrogen Bonding to Graphitic Nanosheet Structures

P. Lesnicenoks[1], J. Zemitis[1], L. Grinberga[2], G. Chikvaidze[2], J. Kleperis[2]

[1]Faculty of Material Science and Applied Chemistry, Riga Technical University, Riga, Latvia

[2]Institute of Solid State Physics, University of Latvia, Latvia

e-mail: peteris.lesnicenoks@rtu.lv

In our work the graphite waste as raw source material for obtaining graphitic structure materials of few layer thicknesses is examined. Nanosheet material is obtained with plasma and electrochemical exfoliation methods (Figure 1). The hydrogen bonding mechanism to graphitic structures is examined with FTIR–RAMAN spectroscopy, gravimetric and volumetric adsorption methods as well as characterized by SEM. There are at least three ways how hydrogen can bond with nanosize graphitic materials that are built from stacked sheets of graphene. The physical sorption of hydrogen molecules on the active surface of graphene is reported far below room temperature (typically at 77 K), nevertheless the stacks of graphitic sheets are new material with increased surface area and different results are expected. Other possibility is chemisorption of hydrogen – it can be achieved by doping the graphitic material with catalyst, for example - with platinum nanoparticles, on which hydrogen molecules disassociate and atomic hydrogen can easier fill the pores of the material. Third way is to adjust hydrogen adsorption enthalpy, introducing hydride-forming material nano-grains between the sheets of graphene in stacks, for example, lithium or magnesium. All three possibilities are tested and results reported.

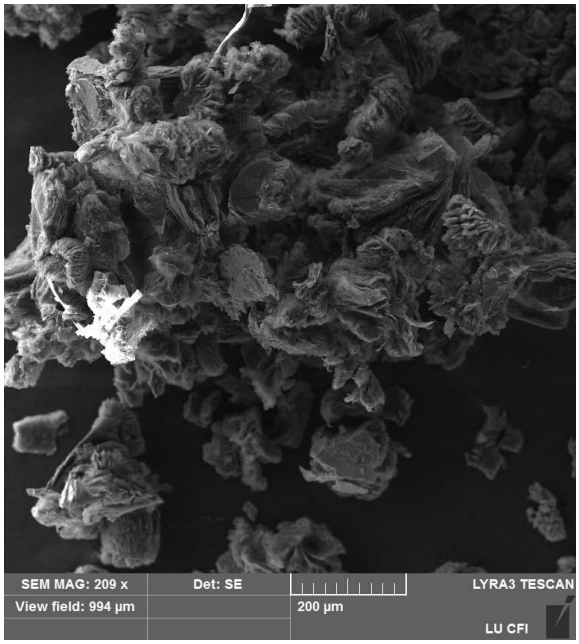

Fig.1 SEM image showing graphitic structure obtained from base material.

Acknowledgment

Authors acknowledge National Research Program in Material science.

F-150

Composite Organic-Inorganic Membranes for Fuel Cells

J. Hodakovska and J. Kleperis

Institute of Solid State Physics, University of Latvia, Latvia

e-mail: julia_h_lv@yahoo.co.uk

A fuel cell technology has been paid a lot of attention as a part of hydrogen economy during recent years, but even though it has a great potential – and also need – for improvement to become widely used. Polymer electrolyte fuel cells have advantage of comparably low working temperature, which makes this type of fuel cells possible candidate for portable use or any other applications, where significant thermal isolation would be a disadvantage. There are a lot of works which focus on possible ways to improve different parts of fuel cell indicating significant interest to the technology.

One of the most important parts of fuel cells is electrolyte: proton conductive polymer (or polymer-based composite) membrane. Though polymers have huge variety of possible compound's compositions, there are only several types with the proton conductivity. In this work attention is paid to sulfonated polymers, concentrating on sulfonated poly(ether-ether-ketone) (SPEEK) and commercially available Nafion-like polymers for comparison. To improve membrane's characteristics inorganic components are used as dopant and inorganic oxide nanopowder is added to SPEEK and reference membranes in our research. Conductivity dependence on temperature and related parameters are measured to compare concentration's and treatment's effect on membrane.

Acknowledgement

Author (JH) would like to thank ESF project Nr.2013/0046/1DP/1.1.1.2.0/13/APIA/VIAA/021 for financial support.

F-151

SPEEK Polymer Composites with 1-butyl-2,3-dimethyl-imidazolium dimethylphosphate Ionic Liquids for Fuel Cell Membranes

G. Vaivars[1,2], J. Kleperis[2], E. Priede[1], E. Sprugis[1], A. Zharova[1], A. Zicmanis[1]

[1]Department of Chemistry, University of Latvia, Latvia

[2]Institute of Solid State Physics, University of Latvia, Latvia

e-mail: Guntars.Vaivars@cfi.lu.lv

In this work, the sulphonated poly (ether ether ketone) (SPEEK) membrane composites with 1-butyl-2,3-dimethyl-imidazolium dimethylphosphate ionic liquid have been investigated as an example of acidic ionic liquid. 1-butyl-2,3-dimethyl-imidazolium dimethylphosphate ionic liquid was synthesized as follows. Equivalent amount of an amine was weighed into a dry Schlenk flask and equivalent amount of tributhylphosphate was added dropwise to ensure isothermal reaction conditions. The reaction mixture was stirred for 3 days at 160^{o}C under an argon atmosphere. SPEEK was dissolved in DMF and mixed with ionic liquid. The membrane was prepared with different ionic liquid content by mixture casting and drying [1-2].

Conductivity was obtained from impedance measurements using Autolab set-up in temperature range 20-150^{o}C. XRD, IR spectroscopy and thermal analysis was used for structure characterization. The impact of the ionic liquid content and casting conditions will be discussed.

References

1. G. Vaivars, L. Lasmane, E. Ausekle, E. Sprugis, A. Avotins and A. Priksane. In: Abstr. 18th Int. Conf. EcoBalt 2013. Vilnius, Lithuania. 25-27 October 2013.
2. L. Lasmane, E. Ausekle, A. Priksane and G.Vaivars, IOP Conf. Ser.: Mat. Sci. Eng. 49, 012039 (2013)

F-152

Mechanical Properties and XRD of Composite SPEEK Polymer Membranes Modified by Acidic Ionic Liquids

E. Sprugis[1], I. Reinholds[1], G. Vaivars[1,2]

[1]Department of Chemistry, University of Latvia, Latvia

[2]Institute of Solid State Physics, University of Latvia, Latvia

e-mail: Guntars.Vaivars@cfi.lu.lv

In this work, the sulphonated poly (ether ether ketone) (SPEEK) membrane composites with 1-butyl-2,3-dimethyl-imidazolium dimethylphosphate ionic liquid have been investigated. Prepared composite membrane (SPEEK/ionic liquid) is characterized by mechanical testing, such as tensile test and creep test [1]. The impact of ionic liquid on elastic modulus, the creep compliance and the tensile strength will be discussed. Those membranes are designed for application in fuel cells and other alternative energy devices. For optimal performance, the temperature range should be between 100 and 200^{o}C. At the same time, the mechanical strength should be maintained. Large variety of ionic liquids is suitable to provide high conductivity and temperature stability [2]. However, the ionic liquids are also polymer plastificators and the impact on mechanical strength is less studied.

Also, composite membranes were studied by wide angle X-ray diffraction. The shift of the peak maximum to the lower angle is used to characterize the polymer interaction with ionic liquid. In this work, the biodegradable ionic liquids were used for composite preparation.

References

1. V. Garaev, S. Pavlovica, I. Reinholds and G. Vaivars, IOP Conf. Ser.: Mat. Sci. Eng. 49, 012058 (2013)
2. V. Garaev, J. Kleperis, S. Pavlovica and G. Vaivars, IOP Conf. Ser.: Mat. Sci. Eng. 38 (2012)

F-153

Function of Titanium Oxide Coated on Carbon Nanotubes as Support for Platinum Catalysts

Q. Ying[1], S. Naidoo[1], L. Petrik[2], G. Vaivars [3,4]

[1]Bioanalytical Laboratory, Division of Clinical Pharmacology, Faculty of Medicine and Health Sciences, University of Stellenbosch, South Africa

[2]Environmental and Nanosciences Research Group, University of the Western Cape, South Africa

[3]Department of Chemistry, University of Latvia, Latvia

[4]Institute of Solid State Physics, University of Latvia, Latvia

e-mail: Guntars.Vaivars@cfi.lu.lv

Recently, organic-inorganic hybrid nanocomposite materials have attracted considerable research interests in fundamental and application studies. TiO_2 is a well-known substrate material due to the superior properties such as large specific surface area, high uniformity, and excellent biocompatibility and has been applied in a variety of fields including highly efficient photocatalysis [1-2], fuel cells [3-4], biosensors [5], hydrogen sensor [6-7] and hydrogen evolution [8]. It has been reported that Pt [9] or PtRu [10] catalysts supported on TiO_2 exhibited excellent catalytic activity for methanol electro-oxidation because of the synergetic interaction between Pt and TiO_2.

The study here describes the outcome of the synthesis of Pt monometallic, binary and ternary catalysts supported on TiO_2/CNT and based on the use dry-mix method of OMCVD. These multicomponent catalysts were investigated and compared with commercial Johnson Matthey 40 % Pt/C catalyst. The results then enabled a profile for the catalysts with regards to their synthesis route, characteristics and EC activity.

References

1. L. Yang, D. He, Q. Y. Cai, J. Phys. Chem. C 111, 8214 (2007)
2. Y. Chen, J. C. Crittenden, S. Hackney, L. Sutter, D. W. Hand, Environ. Sci. Technol. 39, 1201 (2005)
3. H. Q. Song, P. Xiao, X. P. Qiu, W. T. Zhu, J. Power Sources 195, 1610 (2010)
4. Z. Y. Wang, G. Chen, D. G. Xia, L. J. Zhang, J. Alloy and Compounds 450, 148 (2008)
5. S. Q. Liu, A. C. Chen, Langmuir 21, 8409 (2005)
6. O. Varghese, X. Yang, J. Kendig, M. Paulose, K. Zeng, C. Palmer, K. Ong, C. A.Grimes, SensorLett. 4, 120 (2006)
7. O. Varghese, D. Gong, M. Paulose, K. Ong, C. A. Grimes, Sens. Actuators B 93, 338 (2003)
8. P. Paunovic, A. T. Dimitrov, O. Popovski, D. Slavkov, Macedonian J. Chem. Chem. Eng. 26 (2), 87 (2007)
9. K. W. Park, S. B. Han, J. M. Leger, Electrochem. Commun. 9, 1578 (2007)
10. M. Hepel, I. Dela, T. Hepel, J. Luo, C. J. Zhong, Electrochim. Acta 52, 5529 (2007)

F-154

Investigation of Activities for Pt_3-M Bimetallic Nanoparticles Catalysts on the Oxygen Reduction Reaction

Q. Ying[1], S. Naidoo[1], G. Vaivars[2,3]

[1]Bioanalytical Laboratory, Division of Clinical Pharmacology, Faculty of Medicine and Health Sciences, University of Stellenbosch, South Africa

[2]Department of Chemistry, University of Latvia, Latvia

[3]Institute of Solid State Physics, University of Latvia, Latvia

e-mail: Guntars.Vaivars@cfi.lu.lv

Hydrogen fed polymer electrolyte membrane fuel cell (PEMFC) provides zero-emission power sources for stationary and portable power generation as well as in transportation [1]. The origin of the sluggish kinetics of the oxygen reduction reaction (ORR) has been extensively studied for PEMFCs. To enhance the ORR activity and reduce operational costs of platinum electrocatalyst, advanced electro-catalyst design by alloying Pt with Ni and Co have been investigated. Pt-Ni and Pt-Co catalysts with high ORR activities were successfully synthesized by Organometallic Chemical Vapour Deposition (OMCVD) method, which is fast and the stages of impregnation, washing, drying, calcinations, and activation, surface poisoning and material transformations activated during drying are avoided and characterized by XRD, TEM, EDS and CV.

References

1. Proton exchange membrane fuel cell, [Online], Available: http://en.wikipedia.org/wiki/Proton_exchange_membrane_fuel_cell, 2006

F-155

New Proton Conductors: the Calix(aren)sulfonic Acids

L. Shmygleva, A. Pisareva, A. Ukshe, Y. Dobrovolsky

Institute of Problems of Chemical Physics, Russian Academy of Science, Russia

e-mail: dobr@icp.ac.ru

The proton conductivity of crystalline calix [4] arene-p-sulfonic acids: 5,11,17,23-tetra-sulfo-25,26,27,28-tetra-hydroxy-Calix [4] arene (**I**) and 5.11 , 17,23-tetra-sulfo-25,26,27,28-(ethoxy carbonyl methoxy) -Caliks [4] arene (**II**), was studied. The high proton conductivity at normal temperatures in a wide range of ambient humidity and, consequently, the water content in the crystal hydrateis founded. At a relative humidity of 10% rel the conductivity of compounds is 10^{-4}-10^{-3} Sm/cm, reaching values of 10^{-2}-10^{-1} Sm/cm with increasing of humidity to 70% rel. The conductivity is more, then Nafion® conductivity and less dependent on the of humidity/

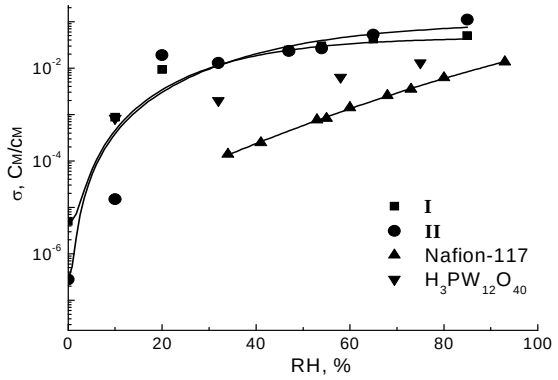

Fig.1 Dependence of the conductivity on humidity for Nafion®117 and Calix [4] arene-p-sulfonic acids at 298 K.

Features of the transport properties of the investigated compounds with changes in humidity, probably related to the distance between the molecules in the anion layer planar structure: a greater distance between the molecules in the compound II with additional chains of substituents results in significantly greater (2 times) the value of the proton conductivity at high humidity, but and a sharper drop in it at a low of humidity (conductivity compound II at humidities below 10 rel.% less than that of compound I in order).

High conductivity of these compounds makes it possible to use them as precursors for the preparation of proton membrane.

Authors Index

C

D

E

F

G

H

I

J

K

L

M

N

O

Ö

O

P

R

S

T

U

V

W

X

Y

Z